

Catalytic Enantioselective Transformations with Chiral Cyclopentadienyl Ruthenium(II) Complexes

Présentée le 3 avril 2020

à la Faculté des sciences de base
Laboratoire de catalyse et synthèse asymétriques
Programme doctoral en chimie et génie chimique

pour l'obtention du grade de Docteur ès Sciences

par

Sung Hwan PARK

Acceptée sur proposition du jury

Prof. J. Waser, président du jury
Prof. N. Cramer, directeur de thèse
Dr C. Bruneau, rapporteur
Prof. C. Valdés, rapporteur
Prof. J. Zhu, rapporteur

Acknowledgement

First, I would like to cordially thank *Prof. Nicolai Cramer* for supervising my PhD studies and allowing me to work on a very innovative field. I appreciate that he is always open to discussion and gave me his insightful advice that helps find the right direction for the progress of my work. Moreover, he granted me freedom regarding my work, which gave me a chance to improve my chemistry knowledge and learn about managing a project. Additionally, I am grateful for his efforts to organize our cooperative group culture that allows learning with each other.

I would like to thank *Prof. Jérôme Waser* for taking the duty of being the jury president of my PhD exam. Also, I thank *Prof. Jieping Zhu* for kindly accepting to become the internal examiner. Furthermore, I would like to express my gratitude to external examiners, *Dr. Christian Bruneau* and *Prof. Carlos Valdés*, accepting the invitation for evaluating my thesis manuscript.

I am grateful to *Dr. Alissa Götzinger* and *John Reed* for proofreading of my thesis, and to *Philipp Seeberger* for helpful discussions for preparing my thesis draft.

I sincerely appreciate help from *Dr. David Kossler*. At the beginning of my PhD, he taught me everything related to lab work in here and share his experience in ruthenium chemistry. I am very thankful to *Dr. Yun-Suk Jang* for productive discussions and kind help for settling in Switzerland and understanding European cultures. Without his help, it would be more difficult for me living in a foreign country, which is far away from South Korea. In addition, *Dr. Johannes Diesel* and I were newbies of BCH4412. I appreciated his help and his warm-hearted advice. Working with postdocs in BCH4412, *Dr. Michael Dieckmann*, *Dr. Caio Oliveira* and *Dr. Alissa Götzinger* was enjoyable, and they made a good atmosphere in our lab. *Dr. Caio Oliveira* made me unforgettable and pleasant memories when we met again in Brazil. I was grateful to work with *Qui-Hien Nguyen* and *Kristers Ozols*. I have no doubt that they will keep Vietnamese music in our lab and the hard-working environment as our tradition. Our lovely postdoc *Dr. Shou-Guo Wang* was warm-hearted and willing to give me kind help and advice. I appreciated all his support for me. I would like to thank *Dr. Daria Grosheva*, who is a passionate chemist, for helping me whenever I exhausted from teaching courses. I am thankful to *Dr. Marcus Brauns*, *Dr. Gints Smits*, *Dr. Julia Pedroni*, and *Dr. Yang Sun*, for the time we spent together.

I am grateful for all the former and current group members. They don't hesitate to share their knowledge and skills with other group members. Under the cooperative atmosphere of LCSA, I was able to learn many things from chemistry knowledge to small tips for everyday lives. I would like to thank *Dr. Joachim Ahlin*, *Dr. Christopher Kourra*, *Dr. Chris Newton*, *Dr. Chistoph Heinz*, *Dr. Manh Van Pam*, *Dr. Laetitia Souillart* and *Dr. Baihua Ye*. Among them, I especially appreciated *Dr. Joachim Ahlin* for participating in Christmas dinners and shares his experience in the chemical industry. It was a great fortune to work with highly talented colleagues. Discussion with them gave me opportunities for broadening my perspective and having more knowledge. Thus, I am thankful to *Dr. Chris Newton*, *Dr. Solène Miaskiewicz*, *Dr. Josep Roselló*, *Dr. Łukasz Wozniak*, *Dr. Ana Escudero*, *Coralie Duchemin*, *Benoît Audic*, *Elena Braconi*, *Jin Fay Tan*, *Vitalii Smal*, *Aragorn Laverny*, *Yixuan Cao* and *Adrien Madron Du Vigné*.

Moreover, I appreciated *Fabienne Rudin* for all her support for administrative works. Thanks to her help, I was able to escape from a bureaucracy swamp. I am thankful to NMR team members, *Emily Baudat*, *Anto Barisic* and *Dr. Aurélien Bornet*, for their supports on maintain our NMRs and resolving issues related to NMR. Furthermore, I would like to thank to our X-ray team, *Dr. Rosario Scopelliti*, *Dr. Euro Solari* and *Dr. Farzaneh Fadaei Tirani*.

Lastly, I would like to thank my family for their unconditional supports. Without their support, I would not move forward for finishing my PhD.

Table of Contents

Abstract IV

Abstract VI

List of Abbreviations VIII

Chapter 1 Introduction..... 11

1.1 Ruthenium in Catalysis 12

1.1.1 Ruthenium catalyzed reactions without Cp ligands..... 12

1.1.2 CpRu and Cp^{*}Ru catalyzed reactions 17

1.2 Precedents of Chiral Cyclopentadienyl Ligands and Complexes..... 22

1.2.1 General properties of the cyclopentadienyl ligand 22

1.2.2 Early stage of development of chiral cyclopentadienyl ligands 23

1.2.3 The advancement of chiral cyclopentadienyl ligand development 27

1.2.4 Precedents of chiral cyclopentadienyl ruthenium complexes 36

1.3 Aims of the thesis 40

Chapter 2 Synthesis of Chiral Cp^x Ligands and Cp^xRu (II) Complexes 43

2.1 Cyclopentane Fused Cp^x Ligands..... 44

2.1.1 Ligand Synthesis and Complexation 44

2.1.2 Aryl Group Derivatives 46

2.1.3 Synthesis of Neutral Complexes 49

2.2 Synthesis of Atropchiral Binaphthyl-Derived Cp^x Ligands 51

Chapter 3 Enantioselective Ruthenium(II)-Catalyzed Synthesis of Benzonorcaradienes 55

3.1 Introduction..... 56

3.2 Optimization Studies for Asymmetric Benzonorcaradiene Synthesis..... 58

3.3 Reaction Scope 67

3.4 Reaction Mechanism Study 72

3.4.1 Control Experiments..... 73

3.4.2 Computational Studies 74

Chapter 4 Enantioselective Ruthenium(II)-Catalyzed Alkylative Cycloetherification..... 77

4.1 Introduction..... 78

4.2 Optimization Studies for Enantioselective Ruthenium(II)-Catalyzed Alkylative Cycloetherification 81

4.3 Outlook for Enantioselective Ruthenium (II)-Catalyzed Alkylative Cycloetherification.. 88

Chapter 5 Preliminary Results for Developing Enantioselective Ru(II)-catalyzed [2+1] Cycloaddition of Ruthenium Vinyl Carbenes..... 89

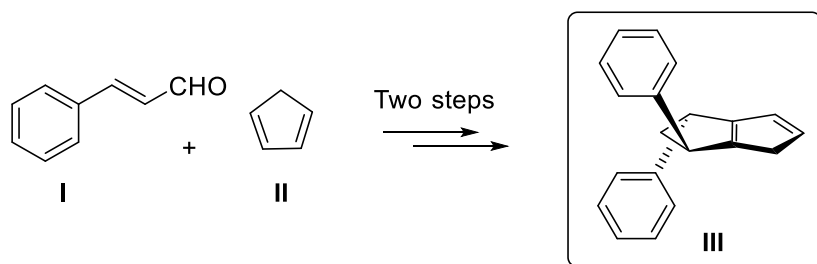
5.1 Introduction..... 90

5.2 Optimization Studies for the Enantioselective [2+1] Cycloaddition of Catalytic Ruthenium Vinyl Carbenes	92
5.3 Outlook for Enantioselective [2+1] Cycloaddition of Catalytically Generated Ruthenium Vinyl Carbenes	100
Chapter 6 Summary	101
Chapter 7 Outlook.....	107
Chapter 8 Experimental Part	109
8.1 General Methods	110
8.2 Synthesis of Chiral Cp ^x Ligands and Cp ^x Ru (II) Complexes	111
8.3 Enantioselective Ruthenium(II)-Catalyzed Synthesis of Benzonorcaradienes	130
8.4 Enantioselective Ruthenium(II)-Catalyzed Alkylative Cycloetherification.....	170
8.5 Enantioselective Ru(II)-catalyzed [2+1] Cycloaddition of Ruthenium Vinyl Carbene..	172
Curriculum Vitae	181
Chapter 9 Appendix	185
9.2 Optimized Geometry	186
9.3 NMR spectra.....	196
Chapter 10 Bibliography	275

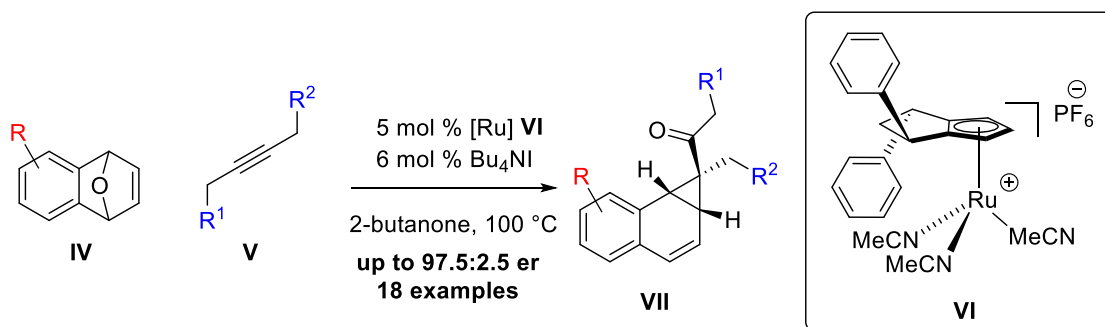
Abstract

The chemistry of cyclopentadienyl ruthenium(II) complexes plays an important role in ruthenium catalysis because of its high potential for various transformations. However, asymmetric catalysis with chiral cyclopentadienyl ruthenium(II) complexes is still at an infant stage, but rapidly developing because of its expected impact on multiple enantioselective applications.

This thesis discusses the synthesis of a novel class of chiral cyclopentadienyl ligands **III**, which can be readily accessed by a two-step process from α,β -unsaturated aldehydes **I** and cyclopentadiene **II**. The novel C_2 -symmetric chiral cyclopentadienyl ligands were complexed with ruthenium(II) and successfully applied in asymmetric catalysis.

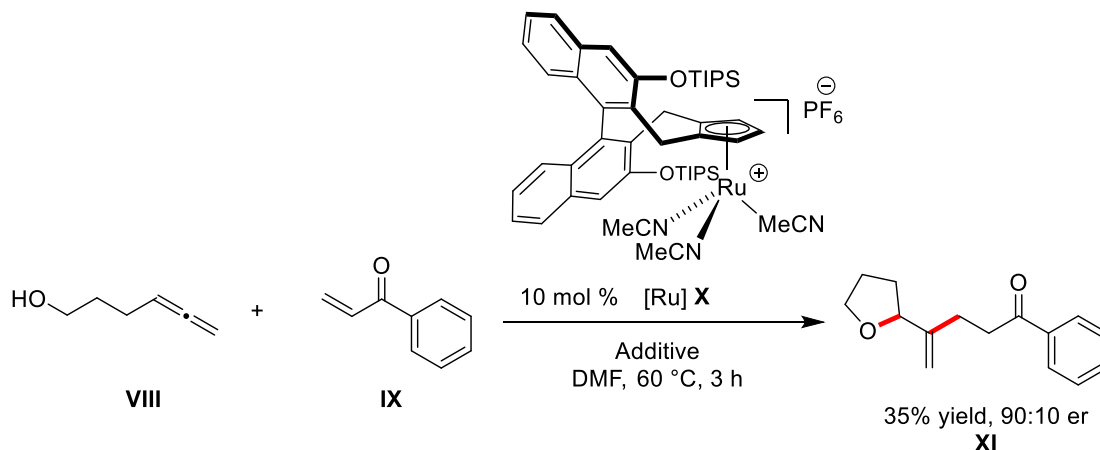


The cyclopentane-fused Cp^*Ru complex **VI** enables the enantioselective synthesis of benzonorcaradienes by coupling of oxa-benzonorbornadienes **IV** with internal alkynes **V** in high enantioselectivity (up to 97.5:2.5 er). The reaction mechanism was investigated by computational studies and control experiments.

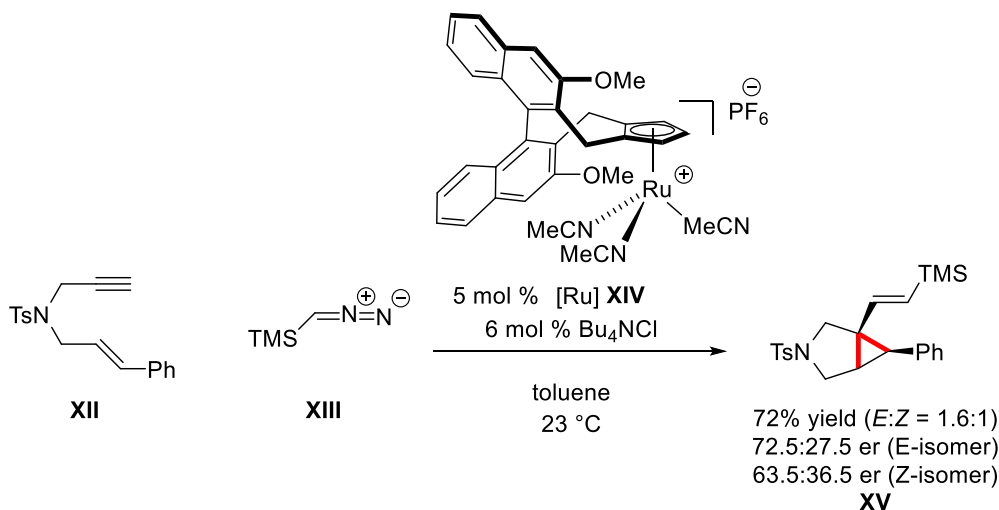


The chiral cyclopentadienyl ruthenium(II) complexes show promising results for other transformations. An alkylative cycloetherification of allenols and aryl vinyl ketones was investigated

using binaphthyl-derived chiral cyclopentadienyl ruthenium(II) complex **X**. After an initial optimization study, allenol **VIII** and phenyl vinyl ketone **IX** gave the desired enantio-enriched cyclic ether with a promising enantioselective ratio of 90:10.



Furthermore, preliminary studies were undertaken for the [2+1] cycloaddition of enynes *via* ruthenium vinyl carbenes. Model substrate **XII** delivered the desired enantio-enriched bicyclo[3.1.0]hexane **XV** in a good yield of 72% (*E*:*Z* = 1.6:1), with enantiomeric ratios of 72.5:27.5 and 63.5:36.5 for the *E*- and *Z*-isomer, respectively.



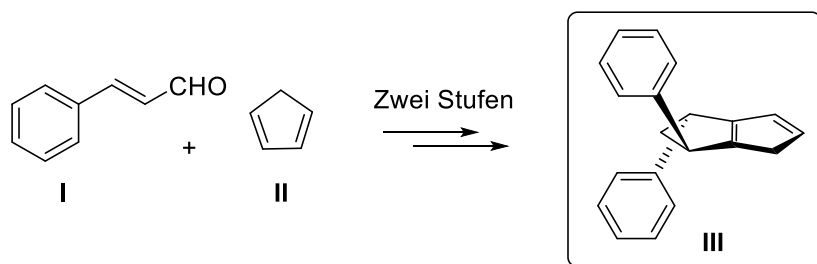
Keywords: ruthenium, cyclopentadienyl ligand, asymmetric catalysis

Abstract

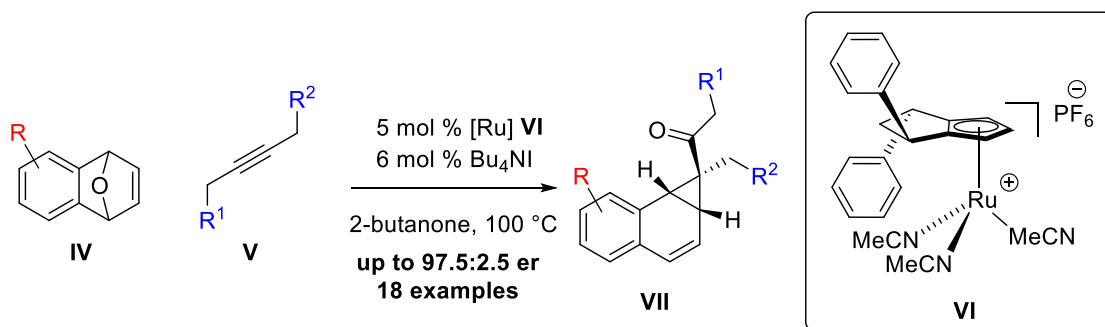
Cyclopentadienylruthenium(II)-Komplexe spielen eine wichtige Rolle in der Rutheniumkatalyse aufgrund ihres grossen Potentials für eine Vielfalt an Transformationen. Ihr Einsatz in der asymmetrischen Katalyse befindet sich noch in den Kinderschuhen. Sie entwickelt sich jedoch rapide, da eine grosse Bedeutung für enantioselektive Anwendungen zu erwarten ist.

Die Arbeit befasst sich mit der Synthese einer neuen Klasse von chiralen Cyclopentadienylliganden **III**, die in zwei Schritten einfach zugänglich sind, ausgehend von α,β -ungesättigten Aldehyden **I** und Cyclopentadien **II**.

Diese neue, C_2 -symmetrische dritte Generation von Cp^x -Liganden wurden mit Ruthenium(II) komplexiert und erfolgreich in katalytischen asymmetrischen Anwendungen eingesetzt.

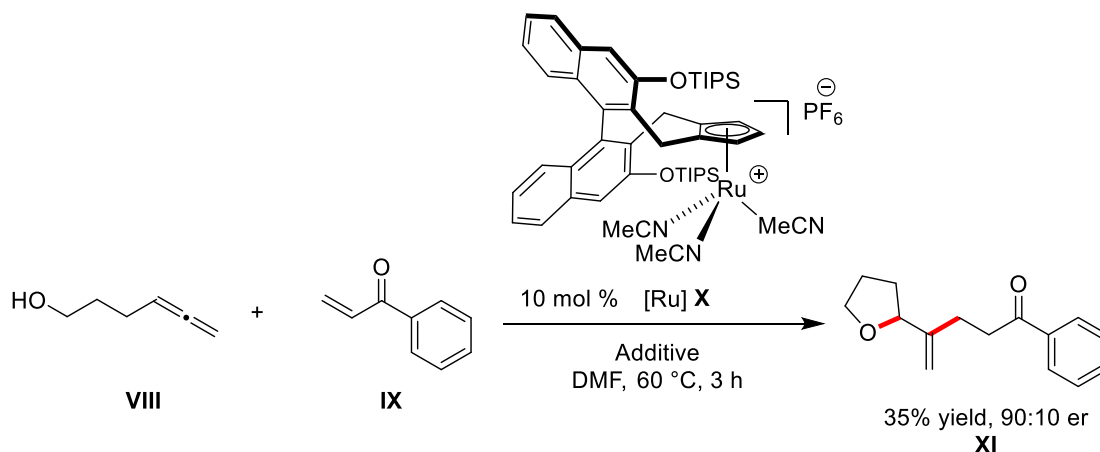


Die chiralen Cyclopentadienylruthenium(II) -Komplexe ermöglichen die enantioselektive Synthese von Benzonorcaradienen durch Kupplung von Oxabenzonorbonadienen **IV** mit internen Alkinen **V** mit einer hohen Enantioselektivität von bis zu 97.5: 2.5 er. Der Reaktionsmechanismus wurde mithilfe von DFT-Rechnungen und Kontrollexperimenten untersucht.

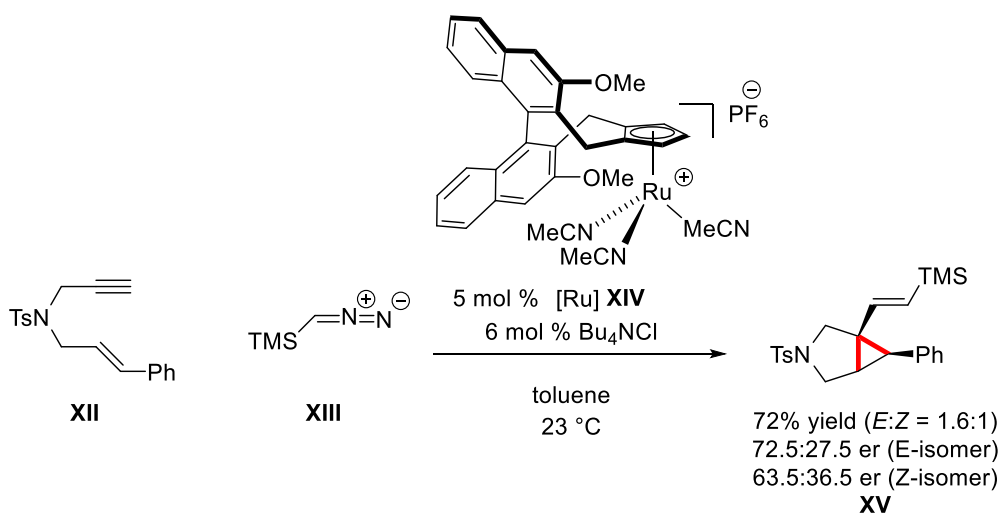


Chirale Cyclopentadienylruthenium(II)Komplexe zeigten ausserdem vielversprechende Ergebnisse für andere Transformationen. Eine alkylierende Cycloveretherung von Allenolen und

Phenylvinylketonen wurde mit dem binaphthyl-basierten chiralen Cyclopentadienylruthenium(II)-Komplex **X** untersucht. Nach einer anfänglichen Optimierung ergab die Reaktion von Allenol **VIII** und Phenylvinylketon **IX** den gewünschten cyclischen Ether im mit einem vielversprechenden Enantiomerenverhältnis von 90:10.



Weitere vorläufige Studien befassten sich mit der [2+1]-Cycloaddition von Eninen **XII** über Rutheniumvinylcarbene. Das Modells substrat **XII** ergab enantiomerenangereichertes Bicyclo[3.1.0]hexan in einer guten Ausbeute von 72% mit Enantiomerenverhältnissen von 72.5:27.5 und 63.5:36.5 für das *E*- bzw. *Z*-isomer.



List of Abbreviations

$[\alpha]_{\text{D}}$	specific rotation at 25 °C at the sodium D line
°	degree
°C	degree Celsius
Ac	acetyl
Ar	aryl
Bn	benzyl
cat.	catalyst
COD	1,5-cyclooctadiene
conc.	concentration
Cp	cyclopentadienyl
Cp*	1,2,3,4,5-pentamethylcyclopentadienyl
Cy	cyclohexyl
DCE	1,2-dichloroethane
DCM	dichloromethane
DMF	dimethylformamide
dr	diastereomeric ratio
<i>ee</i>	enantiomeric excess
EPFL	École polytechnique fédérale de Lausanne
equiv.	equivalent
er	enantiomeric ratio
ESI	electron spray ionisation
h	hour
HMBC	heteronuclear multiple bond correlation
HPLC	high performance liquid chromatography
HRMS	high resolution mass spectroscopy
HSQC	heteronuclear single quantum coherence
Hz	hertz
<i>i</i> Pr	isopropyl
Ir	iridium
IR	infrared
<i>J</i>	coupling constant
M	mega
m.p.	melting point

m/z	mass-to-charge ratio
Me	methyl
MeCN	acetonitrile
MeOH	methanol
mg	milligram
mL	milliliter
mmol	millimole
Ms	methanesulfonyl
MS	mass spectroscopy
NBD	norbornadiene
nm	nanometer
NMR	nuclear magnetic resonance
Ns	nitrobenzenesulfonyl
<i>o</i>	ortho
<i>p</i>	para
Ph	phenyl
Piv	pivaloyl
ppm	parts per million
quant.	quantitative
rac	racemic
R_f	retention factor
Rh	rhodium
Ru	ruthenium
t	triplet
T	temperature
TBAF	tetra- <i>n</i> -butylammonium fluoride
<i>t</i> Bu	<i>tert</i> -butyl
Tf	trifluoromethanesulfonic
TFE	2,2,2-trifluoroethanol
THF	tetrahydrofuran
TLC	thin layer chromatography
Ts	4-toluenesulfonyl
δ	chemical shifts
μ	micro

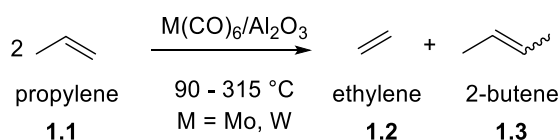
Chapter 1 Introduction

1.1 Ruthenium in Catalysis

Ruthenium is a transition metal that exhibits abundant reactivity. Its electron configuration is [Kr] 4d⁷ 5s¹. It can have oxidation states from -2 to +8, with +2, +3 and +4 the most common.¹ It is more abundant than other platinum group metals, such as iridium and rhodium.² Ruthenium compounds, such as tetra-*n*-propylammonium perruthenate (TPAP) and ruthenium tetroxide have been used widely for oxidation reactions.³ However, they have been utilized not only for oxidation reactions but also for a variety of different transformations. Especially in combination with ligands such as carbonyl, phosphines, cyclopentadienyls, arenes, dienes, and carbenes, ruthenium complexes show versatile reactivities for organometallic reactions.⁴

1.1.1 Ruthenium catalyzed reactions without Cp ligands

Olefin metathesis is one of the most representative applications of ruthenium in catalysis. Transition-metal catalyzed olefin metathesis was discovered in the 1950s, as a process forming ethylene **1.2** and 2-butene **1.3** from propylene **1.1** (Scheme 1-1).⁵



Scheme 1-1: The first reported example of olefin metathesis.

Grubbs and coworkers found that an active catalytic species is Ru(II) by examining ring-opening metathesis of 7-oxanorbornene in 1988.⁶ In 1995, his student SonBinh Nguyen developed an air-stable and the first well-defined ruthenium carbene **1.4** (Figure 1-1).⁷ In the same year, Grubbs reported a simplified ruthenium carbene, which is commercially available and known as the first generation Grubbs catalyst **1.5**.⁸ Introducing an *N*-heterocyclic carbene (NHC), a strong σ -donating ligand, gave what is now known as the second generation Grubbs catalyst **1.6**.⁹ Hoveyda reported that a chelating oxygen ligand improves the stability of the ruthenium carbene in 1999,¹⁰ which allows for recycling of the catalyst. Subsequently, the oxygen chelating ligand was combined with the NHC. That novel class of ruthenium carbene, now called the second generation Hoveyda-Grubbs catalyst **1.7**, promotes olefin metathesis in a highly efficient manner, and makes the formation of tri- and tetra-substituted olefins feasible.¹¹ Most examples of olefin metathesis result in a predominant formation of *E*-olefins,¹² due to the high reversibility of the transformation. Accessing *Z*-olefin

selectively by olefin metathesis was a challenging topic. Grubbs reported ruthenium catalyst **1.8**, which enables a *Z*-selective olefin metathesis.¹³

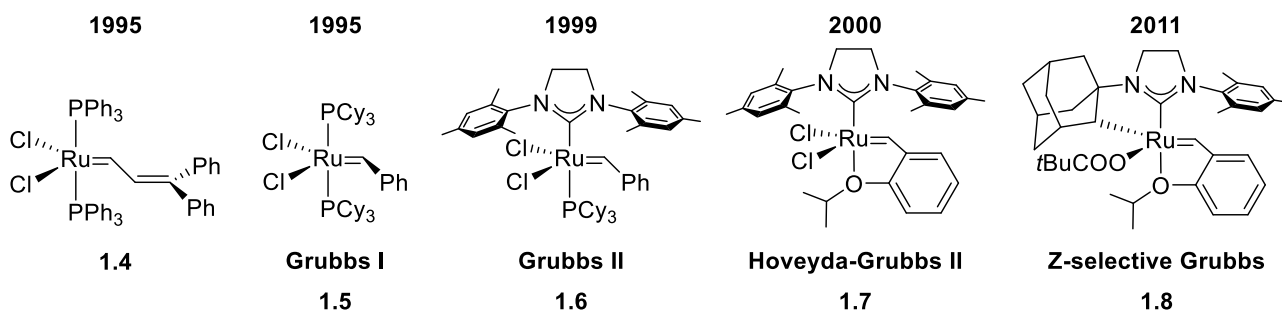
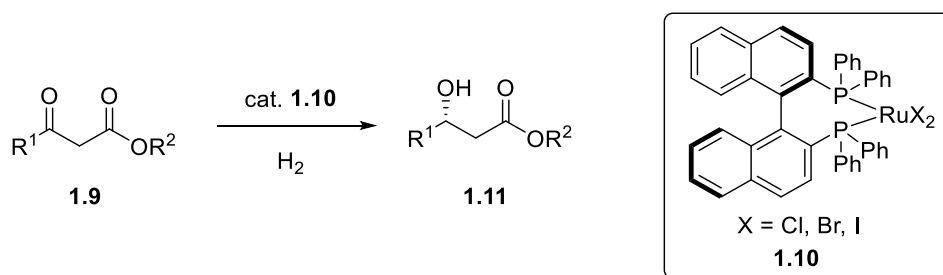


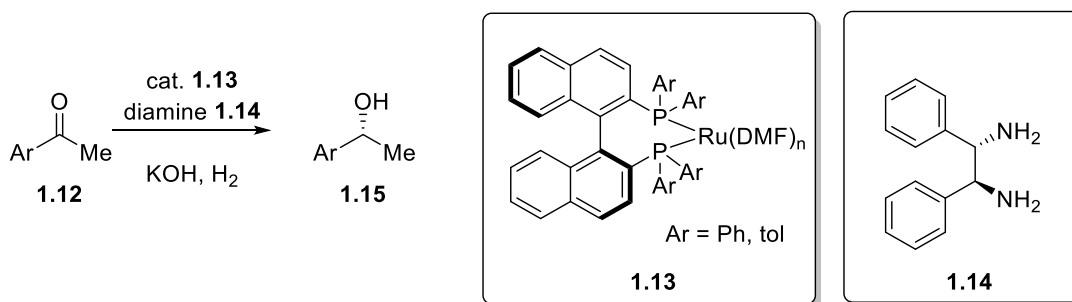
Figure 1-1: The development of the Grubbs catalysts.

Ruthenium catalyzed asymmetric hydrogenation has also made a huge impact on both academy and the chemical industry. Noyori and coworkers made huge contributions to this field.¹⁴ In 1987, they reported the asymmetric hydrogenation of β -keto esters **1.9** catalyzed by BINAP/ruthenium halide complex **1.10** (Scheme 1-2).¹⁵



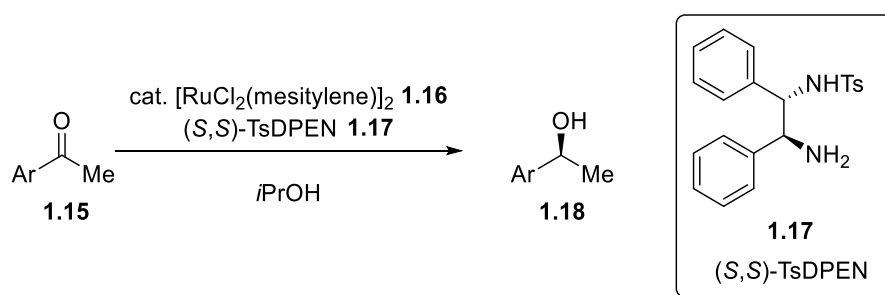
Scheme 1-2: Ruthenium catalyzed asymmetric hydrogenation of β -keto ester.

The limitation of asymmetric hydrogenation using BINAP ruthenium halides **1.10** (Scheme 1-2) is that unfunctionalized and simple ketones **1.12** cannot be converted. This issue was resolved by development of BINAP/diamine ruthenium systems (**1.13** and **1.14**) (Scheme 1-3).¹⁶



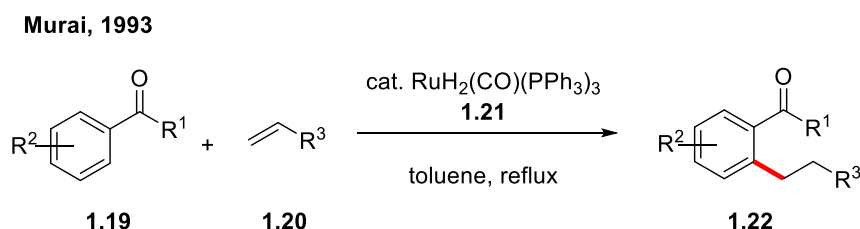
Scheme 1-3: Ruthenium catalyzed asymmetric hydrogenation of unfunctionalized ketone.

Noyori expanded his ruthenium chiral diamine system to transfer hydrogenation. Instead of using hydrogen gas, transfer hydrogenation using ruthenium diamine complex (**1.16** and **1.17**) allows the reduction of unfunctionalized ketones **1.15** using isopropanol as a hydrogen source (Scheme 1-4).¹⁷



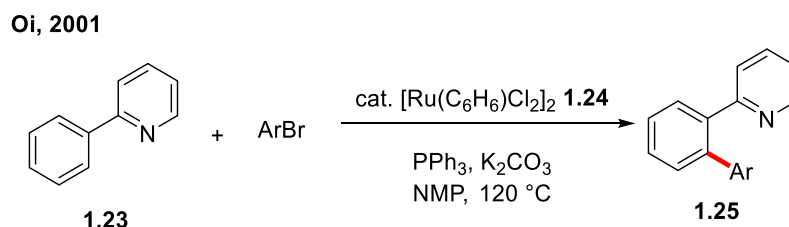
Scheme 1-4: Ruthenium catalyzed transfer hydrogenation of unfunctionalized ketone.

Catalytic C–H functionalization makes a profound impact on synthetic organic chemistry by enabling step-economic and atom-economic approaches to the synthesis of pharmaceuticals and natural products. Initially C–H functionalization for C–C bond formation was examined mostly using palladium or rhodium catalysts, but ruthenium complexes were also investigated.¹⁸ Murai and coworkers reported sp^2 C–H functionalization using a ruthenium(0) precursor in 1993¹⁹, in which the aromatic C–H bond in the *ortho*-position of **1.19** added to an olefin **1.20** (Scheme 1-5).



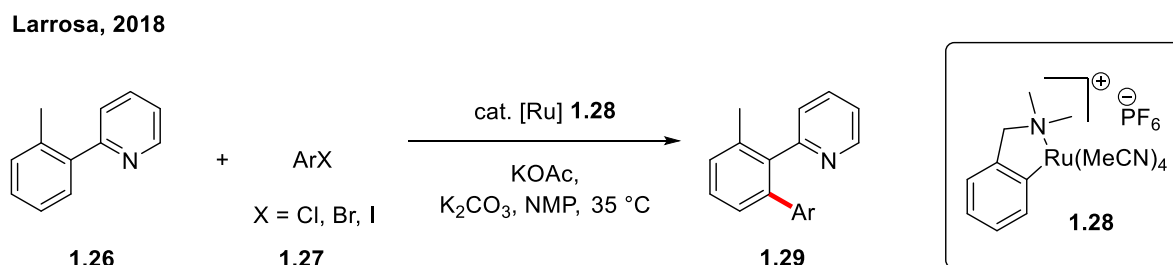
Scheme 1-5: Ruthenium(0) catalyzed sp^2 C–H functionalization.

Later, Oi's pioneering work enabled C–H functionalizations using a ruthenium(II) catalyst **1.24**, which is more convenient to prepare and more stable than ruthenium(0) complexes. The authors showed that the pyridyl group of **1.23** performs well as a directing group for the *ortho*-position of **1.23** in a ruthenium(II) catalyzed C–H arylation (Scheme 1-6).²⁰



Scheme 1-6: Ruthenium(II) catalyzed sp²C–H functionalization with a pyridyl directing group.

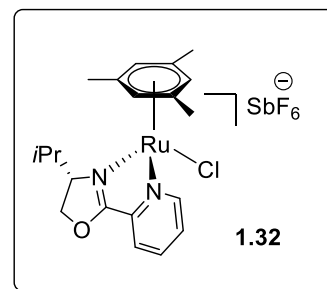
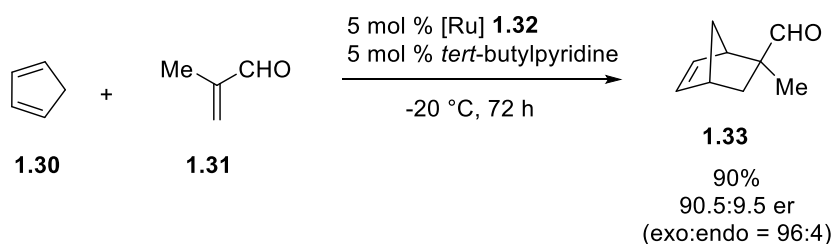
Recently, the Larrosa group investigated the mechanistic details of ruthenium(II) catalyzed C–H functionalization. They revised the previously proposed Ru(II)/Ru(IV) cycle by suggesting a bis-cyclometallated ruthenium(II) species as an intermediate. Based on their revised mechanistic proposal, they applied cyclometallated ruthenium complex **1.28** as a catalyst for C–H arylation of arylpyridine **1.26** (Scheme 1-7).²¹



Scheme 1-7: sp² C–H functionalization with a cyclometallated ruthenium catalyst.

Enantioselective Diels–Alder reactions have been realized using Cp*Rh(I) or CpFe(II) complexes in combination with chiral bi-dentate phosphine ligands.²² A similar reactivity was observed for (η⁶-arene)Ru(II) complexes. Davies and coworkers showed that (η⁶-arene)Ru(II) complex **1.32** can be used as a chiral Lewis acid for enantioselective Diels–Alder reaction (Scheme 1-8).²³ This reaction provides norbornene **1.33** in an excellent yield of 90%, and with high enantioselectivity (90.5:9.5 er).

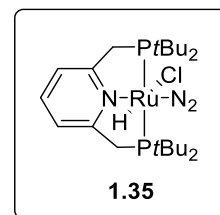
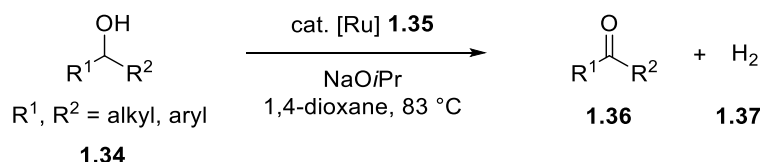
Davies, 1997



Scheme 1-8: Enantioselective Diels-Alder reaction catalyzed by the (η⁶-arene)Ru(II) complex **1.32**

The application of ruthenium pincer complexes **1.35** was extensively explored on hydrogenation/dehydrogenation and dehydrogenative functionalization reactions, which are highly valuable as eco-friendly transformations for the chemical industry.²⁴ Milstein and coworkers explored homogeneous catalysis using ruthenium pincer complexes **1.35**. Early on in their investigation of ruthenium pincer complexes, they reported the dehydrogenation of secondary alcohols **1.34**, forming the corresponding ketone **1.36** and hydrogen gas **1.37** (Scheme 1-9).²⁵

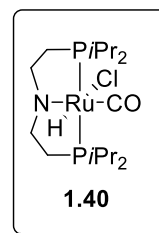
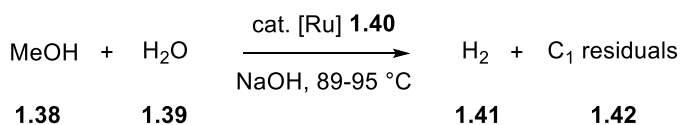
Milstein, 2004



Scheme 1-9: Dehydrogenation of secondary alcohol by ruthenium pincer complex **1.35**.

Beller and coworkers developed a highly efficient process for the evolution of hydrogen gas (**1.41**) from methanol **1.38**.²⁶ The state-of-the-art heterogeneous system for methanol (**1.38**) reforming requires high temperatures (above 200 °C) and high pressure (25-50 bar). In contrast to the heterogeneous system, Beller's conditions only need 89–95 °C and ambient pressure. Furthermore, this process can be used in aqueous methanol.

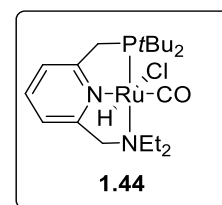
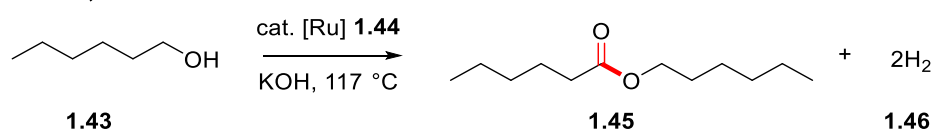
Beller, 2013



Scheme 1-10: Dehydrogenation of methanol by ruthenium pincer complex **1.40**.

The Milstein group also reported the dehydrogenative coupling of alcohols, which is an environmentally benign method for accessing esters **1.45** (Scheme 1-11).²⁵ Other dehydrogenative functionalizations for the synthesis of fundamental materials such as acetals and amides were investigated as well.²⁴

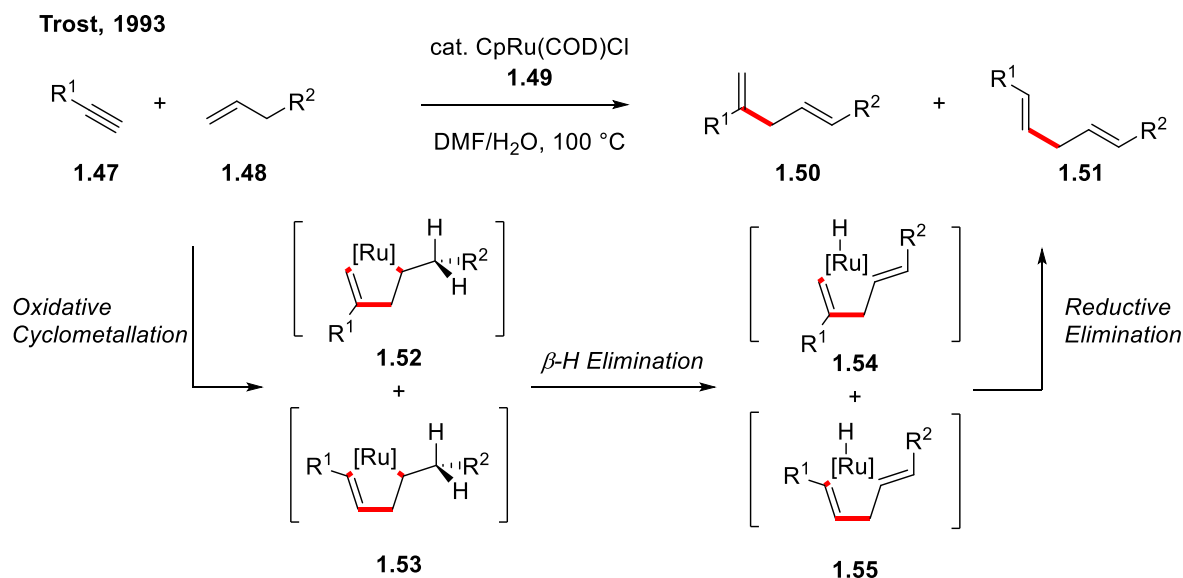
Milstein, 2005



Scheme 1-11: Dehydrogenative coupling of alcohols forming ester and hydrogen gas

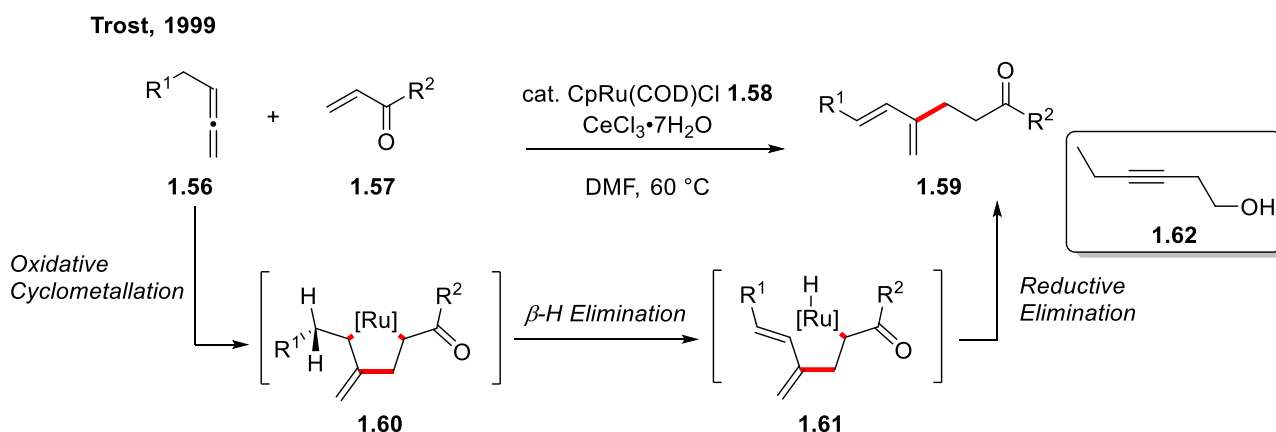
1.1.2 CpRu and Cp*Ru catalyzed reactions

The Trost group has explored various transformations catalyzed by CpRu(II) and Cp*Ru(II) complexes. Their pioneering work has made extensive and profound impact on this field.²⁷ Their contribution lies not only in the development of novel transformations, but also mechanistic proposals and studies, which became the ground for new discoveries.²⁸ An early examples of CpRu(II) catalyzed transformation is the addition of alkenes to alkynes (Scheme 1-12).²⁹ The coupling between alkenes and alkynes forms 1,4-dienes. This transformation can be seen as a metallo-ene reaction using alkynes as enophiles. In this reaction, a ruthenacyclopentene was proposed as a key intermediate.^{27a} Oxidative cyclometallation forms ruthenacyclopentenenes **1.52** and **1.53**, is followed by *syn* β -hydride elimination. The β -hydride elimination occurs on the exocyclic hydrogen because of geometrical constraints for a *syn* elimination on an endocyclic hydrogen. Reductive elimination of the resulting ruthenium hydride complexes **1.54** and **1.55** delivers the 1,4-dienes **1.50** and **1.51**.



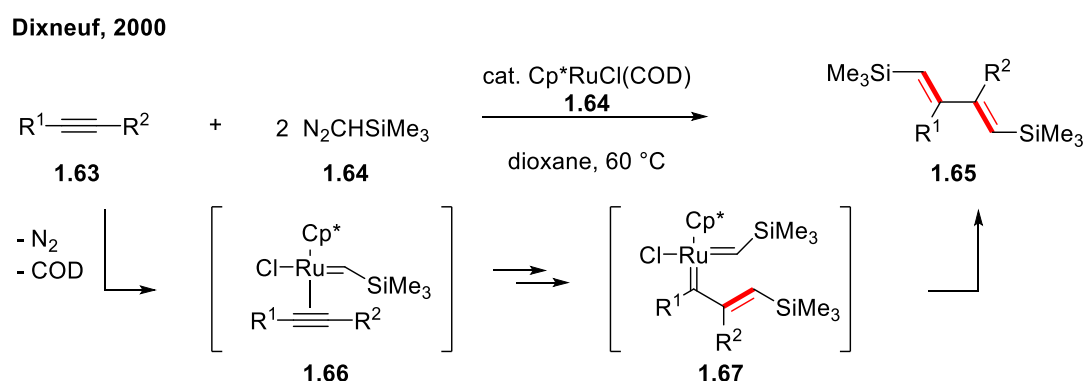
Scheme 1-12: Ruthenium catalyzed alkene-alkyne coupling, forming 1,4-diene.

In an analogous fashion, the coupling of allenes and alkenes to form 1,3-dienes was also investigated. 1,3-Dienes are formed by the addition of allenes **1.56** to Michael acceptors **1.57** (Scheme 1-13).³⁰ As for the coupling of alkenes and alkynes, the proposed mechanism is initiated by the formation of a 5-membered ruthenacycle **1.60** by oxidative cyclometallation. Subsequent β -hydride elimination gives ruthenium hydride **1.61**, which undergoes reductive elimination, regenerating the active CpRu(II) complex and releasing the 1,3-diene product. A catalytic amount of alkynol **1.62** was added as an activator, which enhances the removal of COD for generating a coordinatively unsaturated CpRu(II) species.



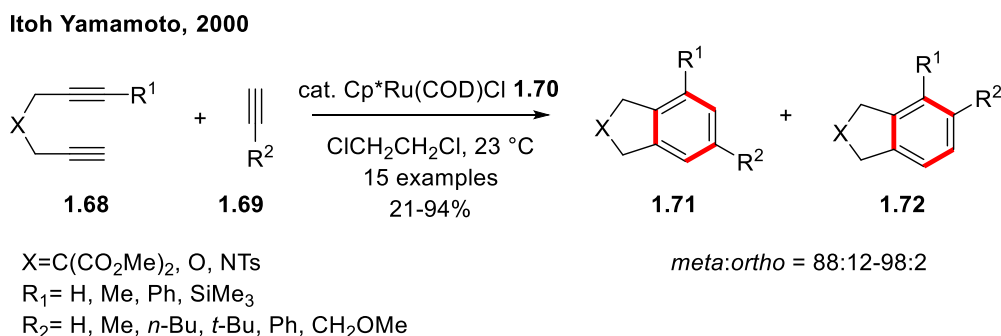
Scheme 1-13: Ruthenium catalyzed allene-alkyne coupling, forming 1,3-diene.

The Dixneuf group showed that alkynes have a potential bis-carbene character by demonstrating a double addition of carbenes to a triple bond (Scheme 1-14).³¹ The results of the reaction suggested that the key intermediate is ruthenium vinyl carbene **1.66**. In addition, the formation of the ruthenium vinyl carbene **1.66** was also supported by DFT calculations.³² After the formation of the ruthenium vinyl carbene **1.66**, [2+2] cycloaddition, cycloreversion, and a second ruthenium vinyl carbene formation delivers intermediate **1.67**. Finally, coupling of both carbenes results in the release of 1,3-diene **1.65**.



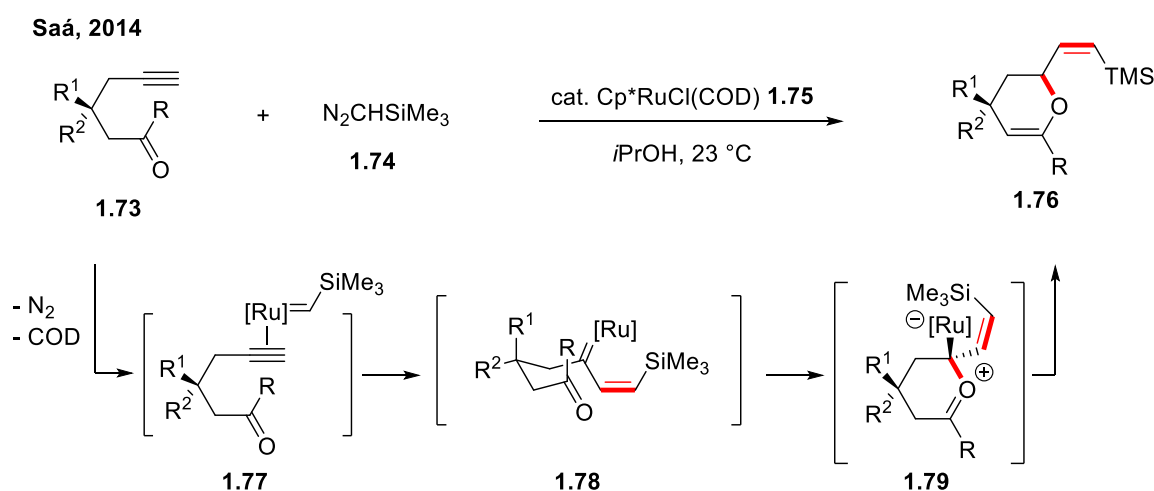
Scheme 1-14: Double addition of diazocompounds to alkynes.

Itoh and Yamamoto studied ruthenium catalyzed annulation reactions.³³ They reported the first regioselective ruthenium catalyzed [2+2+2] cycloaddition of unsymmetrical 1,6-diynes **1.68** with terminal alkynes **1.69** (Scheme 1-15).³⁴ The reaction selectively provides benzene derivatives, **1.71** and **1.72**, with high preference for the *meta*-isomers **1.71** (88:12–98:2 *meta:ortho*).



Scheme 1-15: Regioselective [2+2+2] cycloaddition catalyzed by a $Cp^*Ru(II)$ complex.

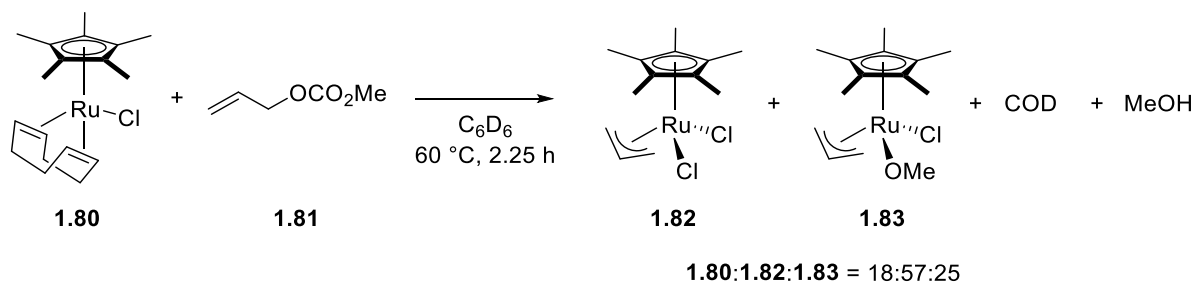
The ruthenium vinyl carbene intermediate was utilized for various catalytic transformations.³⁵ For example, the Saá group reported the synthesis of vinyl dihydropyrans using a catalytic ruthenium carbene (Scheme 1-16).³⁶ The reaction is initiated by the formation of the ruthenium vinyl carbene from $\text{Cp}^*\text{RuCl}(\text{COD})$, followed by coordination of the alkynal or alkynone substrate **1.73**. The resulting intermediate **1.77** undergoes [2+2] cycloaddition and cycloreversion, forming the alkenyl carbene **1.78**. The intramolecular nucleophilic attack of the carbonyl group on the electrophilic carbene produces zwitterionic intermediate **1.79**. The following deprotonation/protonation step gives the desired dihydropyran **1.76**.



Scheme 1-16: A ruthenium vinyl carbene catalyzed synthesis of vinyl dihydropyrans.

The other known reactivity of $\text{Cp}^*\text{Ru}(\text{II})$ complexes is C–O bond insertion. Yamamoto and coworkers showed experimental evidence of C–O bond insertion by $\text{Cp}^*\text{Ru}(\text{II})$. They performed NMR studies for investigating the mechanistic details of a one-pot double allylation/cycloisomerization of 1,3-dicarbonyl compounds (Scheme 1-17).³⁷ $\text{Cp}^*\text{Ru}(\text{COD})\text{Cl}$ **1.80** was exposed to allyl methyl carbonate **1.81** in deuterated benzene. After about 2 h, the reaction mixture contained COD, methanol and two π -allyl complexes, ruthenium dichloride complex **1.82** and ruthenium methoxo complex **1.83**. The formation of π -allyl complexes **1.82** and **1.83** indicates the oxidative addition of ruthenium complex **1.80** into the C–O bond.

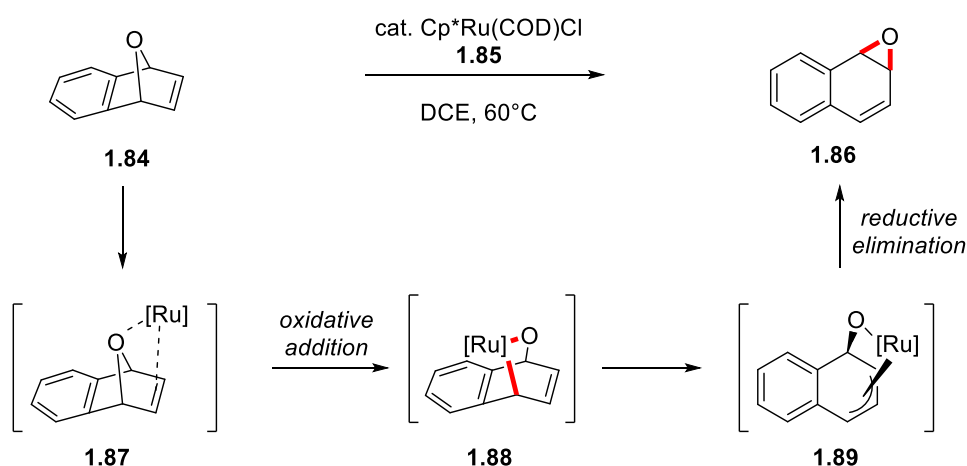
Yamamoto, 2004



Scheme 1-17: NMR studies on C–O insertion of Cp*Ru(II) complex.

The Tam group has developed novel transformations with bicyclic alkenes.³⁸ Among their discoveries, they found conditions for the isomerization of oxa-benzonorbornadiene **1.84** to 1,2-naphthalene oxide **1.86**, which suggests a C–O bond inserted key intermediate (Scheme 1-18). In this reaction, the oxidative addition of ruthenium into a C–O bond results in ruthenacycle **1.88**, followed by π -allyl ruthenium complexation. Subsequent reductive elimination gives 1,2-naphthalene oxide **1.86**.

Tam, 2006



Scheme 1-18: Ruthenium catalyzed isomerization of oxa-benzonorbornadiene **1.84**.

Besides the reactivities introduced in this section, CpRu and Cp*Ru also exhibit rich chemistry in vinylidene, allenylidene intermediate,³⁹ and redox reactions.^{27a}

1.2 Precedents of Chiral Cyclopentadienyl Ligands and Complexes

1.2.1 General properties of the cyclopentadienyl ligand

Cyclopentadienyl (Cp) is a polyenyl ligand, and mainly forms a stable bond between metal and Cp by a pentahapto(η^5) bonding mode.⁴⁰ This bond tends to be tighter than the bond between an arene ligand and a metal because of the additional electrostatic attraction between the partial negative charge of the Cp ligand and the partial positive charge of the metal.⁴¹ The strong η^5 bonding of the Cp ligand and its inert characteristics toward nucleophiles and electrophiles make it a representative spectator ligand.

Most cyclopentadienyl complexes can be classified as four types of complexes (Figure 1-2). The first class contains metal complexes with three cyclopentadienyl ligands, Cp_3M (**1.90**). This type of cyclopentadienyl complexes is usually found with lanthanide or actinide metals.⁴²

The metallocenes, Cp_2M , constitute the second class of cyclopentadienyl complexes. Because of their structure, they are also called sandwich complexes. The metallocenes play an important role in the history of organometallic chemistry (**1.91**). The most famous example of Cp_2M is ferrocene (Cp_2Fe). In 1951, Kealy and Pauson first reported Cp_2Fe , in which they proposed monohapto (η^1) bondings of the Cp ligands.⁴³ Miller, Tebboth, and Tremaine discovered ferrocene independently. Even though they submitted their manuscript about a month earlier than Kealy and Pauson, it was only published in 1952.⁴⁴ In the same year, the structure of ferrocene was re-assigned by two independent groups. Wilkinson and Woodward suggested the correct structure,⁴⁵ which was supported by X-ray-crystallographic data from Fischer.⁴⁶ Cp_2Fe can undergo Friedel-Craft acylation reactions similar to benzene.⁴⁷

Bent metallocenes, Cp_2ML_x ($x = 1-3$), carry two Cp ligands that are not parallel to each other (**1.92**). The number of additional ligands L ranges from 1 to 3. The major application of bent metallocenes is olefin polymerization. Conditions developed by Kaminsky and coworkers use Cp_2ZrCl_2 and trialkyl aluminum and are the current standard procedure for homogeneous Ziegler-Natta catalysis, .⁴⁸

Half-sandwich complexes, CpML_x ($x = 1-4$) contain a single Cp ligand with additional ligands, and have been investigated extensively (**1.93**). They have piano-stool structure, picturing Cp as the seat and the additional ligands as the legs of a stool. When the “legs” are labile ligands, the complexes are prone to generating coordinatively unsaturated intermediates, opening a manifold of possible applications in catalysis.^{27a}

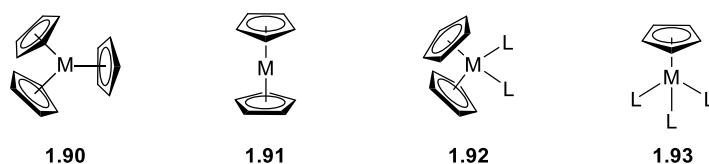


Figure 1-2: Four types of cyclopentadienyl complexes.

1.2.2 Early stage of development of chiral cyclopentadienyl ligands

Assessing optically pure compounds is one of the major challenges in organic synthesis, because optical purity plays a crucial role in biological activity. This results in high demand for optically pure compounds for pharmaceutical applications.⁴⁹ For this reason, the development of enantioselective catalysis has a priority in the synthetic organic community. To this end, chiral cyclopentadienyl metal complexes have been investigated for the development of enantioselective transformations. There are three approaches to create a chiral environment on cyclopentadienyl metal complexes (Figure 1-3).⁵⁰ The first way is applying a chiral bidentate ligand, such as a diol,⁵¹ diamine,⁵² or diphosphine⁵³ (**1.94**) in combination with the Cp ligand. An advantage of the approach is that known bidentate ligands from chiral ligand libraries can be utilized. However, the drawback of the method is that only a single free coordination side is left on the metal. Hence, cyclopentadienyl metal complex with a chiral bidentate ligand cannot be utilized for transformations that require two or more coordination sites. The second approach is using a ligand tethered to the Cp moiety, such as a phosphine⁵⁴ or a sulfoxide⁵⁵ (**1.95**). This type of complex has two vacant coordination sites, and these ligands were successfully applied for enantioselective allylic substitution. However, most transformations of interest require need three vacant coordination sites on the metal, rendering this approach unsuitable as well. In addition, the coordinating additional ligands change the electronic properties of the metal center and the steric bulk of the additional ligand can have an adverse effect on the reactivity of the metal complexes. The third method is introducing chirality on the cyclopentadienyl ring without an additional ligand, Cp^x, (**1.96**). As the Cp^x ligands do not require additional ligands, there are three available coordination sites on the active species. For this reason, Cp^xM complexes can be applied for a large variety of transformations.⁵⁶

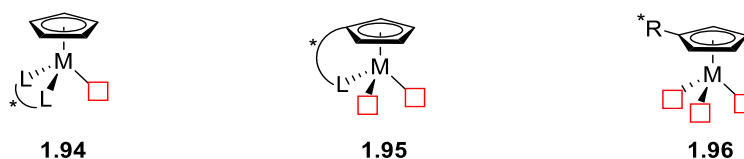
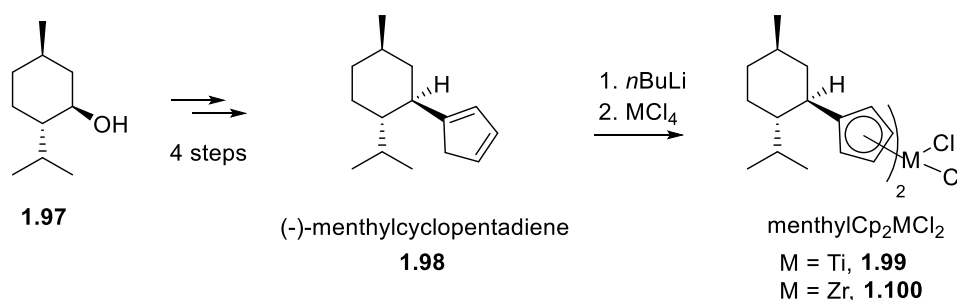


Figure 1-3: Three types of chiral cyclopentadienyl complexes with an increasing number of available coordination sites.

Kagan and coworkers reported early examples of chiral cyclopentadienyl ligands and complexes with group 4 metals, such as Ti and Zr. They synthesized menthylcyclopentadiene **1.98** from (-)-menthol (**1.97**).⁵⁷ This monosubstituted chiral cyclopentadienyl ligand was deprotonated with *n*-BuLi, and subsequent metalation with TiCl₄ or ZrCl₄ resulted in metallocene complexes **1.99** and **1.100** (Scheme 1-19a). They demonstrated the application of menthylCpMCl₂ complexes **1.99** in asymmetric hydrogenation, obtaining *sec*-butylbenzene **1.102** in 57.5:42.5 er (Scheme 1-19).

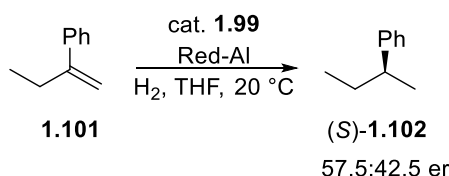
Kagan, 1978

a) Synthesis of menthylCp₂TiCl₂



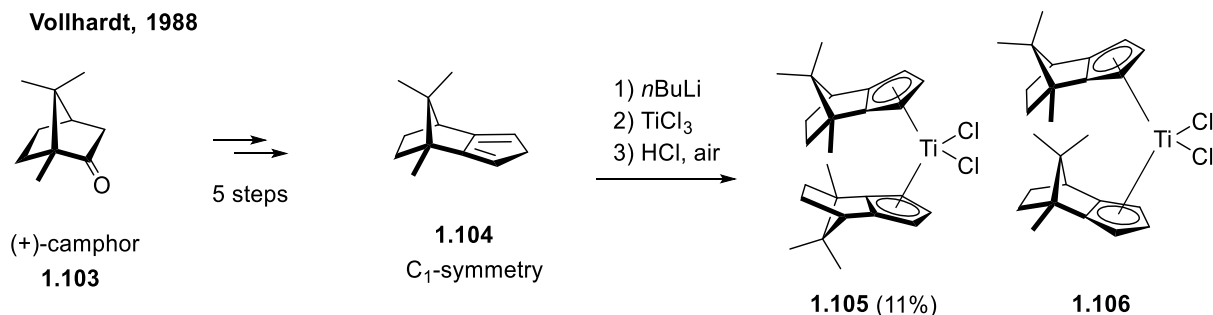
Kagan, 1979

b) Asymmetric hydrogenation



Scheme 1-19: Synthesis of methylCp₂MCl₂ and its application in asymmetric hydrogenation.

For the next generation of chiral cyclopentadienyl ligands, annulated Cp derivatives (Cp^x) were employed. Vollhardt synthesized C₁-symmetric chiral cyclopentadiene **1.104** from (+)-camphor in 1988. Metalation of the ligand resulted in titanocenes **1.105** and **1.106**. The titanium complexes showed catalytic activity for asymmetric hydrogenation, even though the enantioselectivity was low (Scheme 1-20).⁵⁸ In Vollhardt's case, the complexation resulted in a diastereomeric mixture of titanocene **1.105** and **1.106** in 95:5 dr, causing difficulties in the purification process. Recrystallization finally gave pure **1.105** in 11% yield.

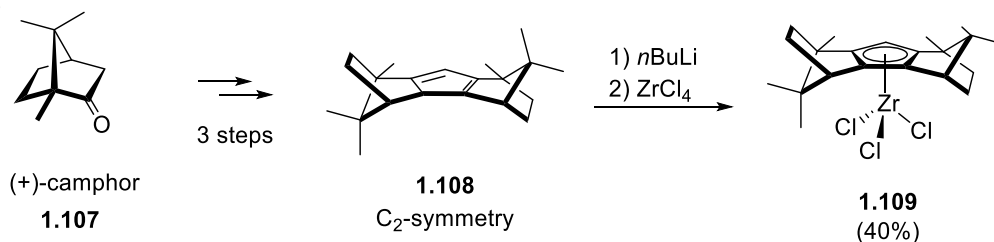


Scheme 1-20: Synthesis of C₁-symmetric chiral cyclopentadienyl ligand

In 1990, Erker developed C₂-symmetric (+)-camphor derived chiral cyclopentadienyl ligand **1.108**, (Scheme 1-21). Zirconium trichloride **1.109** was prepared in 40% yield, much improved compared the complexation step of Vollhardt's C₁-symmetric ligand. Because of the C₂-symmetry the same zirconium complex is generated regardless of the approaching face of the metal precursor to the chiral ligand **1.108**, preventing the formation of a diastereomeric mixture. Zirconium trichloride **1.109** catalyzed the enantioselective electrophilic aromatic substitution of 1-naphthol **1.110** (Scheme 1-21). Reaction with ethyl pyruvate **1.111** resulted in the tertiary alcohol **1.112** in 56% yield with high enantioselectivity(92:8 er). This example shows that Cp^x ligands can achieve high enantioinduction.

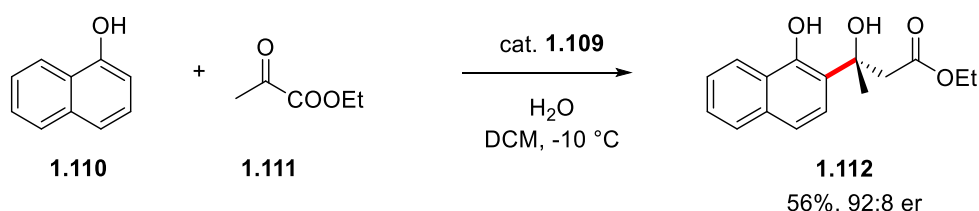
a) Synthesis of a chiral cyclopentadienyl ligand from (+)-camphor

Erker, 1990



b) Enantioselective electrophilic aromatic substitution

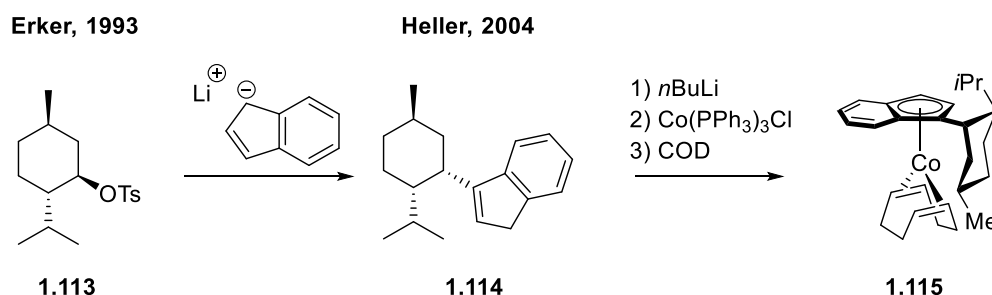
Erker, 1990



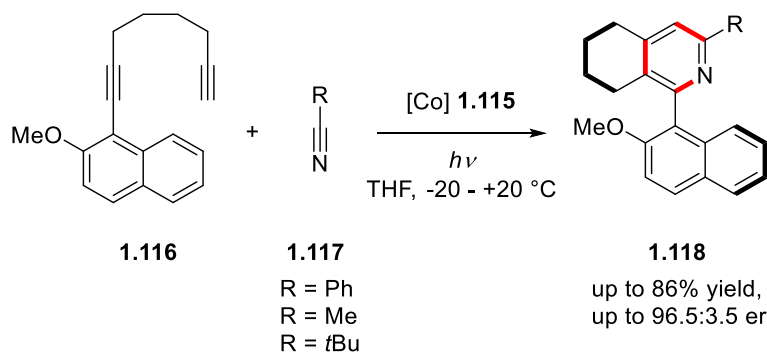
Scheme 1-21: Synthesis of C₂-symmetric chiral cyclopentadienyl ligand **1.108** and its application in electrophilic aromatic substitution.

After Heller's work in 2004, the field plateaued. He applied Erker's menthylindenyl ligand⁵⁹ on cobalt, and developed its application in an enantioselective [2+2+2] cyclization⁶⁰ (Scheme 1-22). Nucleophilic substitution of lithium indenylide on tosylated menthol **1.113** gave menthyl indenyl ligand **1.114**. The chiral indenyl cobalt complex **1.115** was prepared by a sequence of deprotonation of **1.114**, transmetalation to $\text{Co}(\text{PPh}_3)_3\text{Cl}$, and substitution of COD. The resulting cobalt complex **1.115** successfully catalyzed the reaction and produced the desired tetrahydroisoquinolines **1.118** in good to very good yields (up to 86%) and high enantioselectivities (up to 96.5:3.5 er).

a) Synthesis of chiral indenyl ligand **1.114** and cobalt complex **1.115**



b) Enantioselective [2+2+2] cyclization

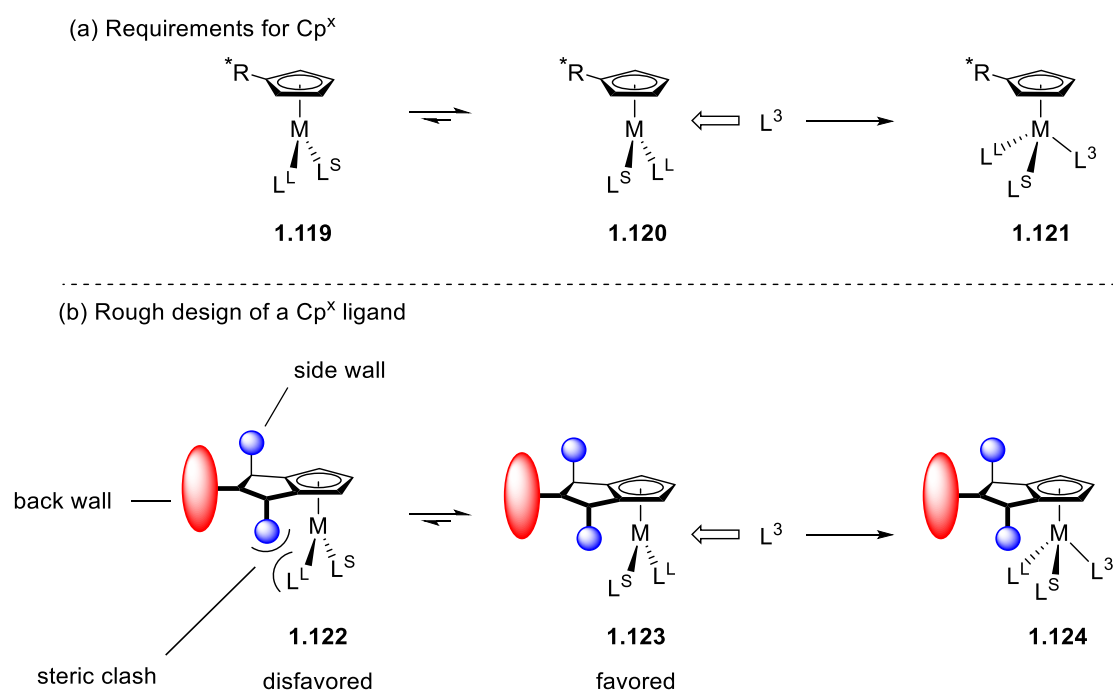


Scheme 1-22: Synthesis of chiral indenyl cobalt complex **1.115** and its application in an enantioselective [2+2+2] cyclization.

The ligands introduced above were synthesized from the chiral pool, which expedites the access to chiral cyclopentadienyl ligands. However, the shortcoming of this approach is that it is difficult to modify and fine-tune toward a desired transformation. For this reason, research on more easily modifiable chiral Cp^x ligands became inevitable.

1.2.3 The advancement of chiral cyclopentadienyl ligand development

Our group has reported a novel class of Cp^x ligands in 2012.⁶¹ The ligands were designed based on the hypothesis that there are two requirements for enantioinduction by Cp^x ligands. The first condition is that the equilibrium between two tricoordinated conformations should be far on one side (**1.119** and **1.120** in Scheme 1-23a), which is a prerequisite for a facial selectivity. The second condition is that the third ligand (L^3) needs to approach the metal center from the same face, as L^3 approaches from the right side of the metal center of **1.120** in Scheme 1-23a. Piano-stool complex **1.121** fulfills both requirements and exhibits a single absolute stereochemistry. With the prerequisites in mind, a rough design of a Cp^x ligand was proposed (Scheme 1-23b). The steric clash between the side wall (blue spheres in Scheme 1-23b) and the large ligand (L^1) shifts the equilibrium to the tricoordinated complex **1.123**. In addition, the back wall (red ellipse in Scheme 1-23b) blocks the approach of L^3 from the left side of the metal center. As a result, a single enantiomer of metal complex **1.124** is obtained. In addition, the hypothesis envisions the fine tuning of a Cp^x by modifying the side wall or the back wall.



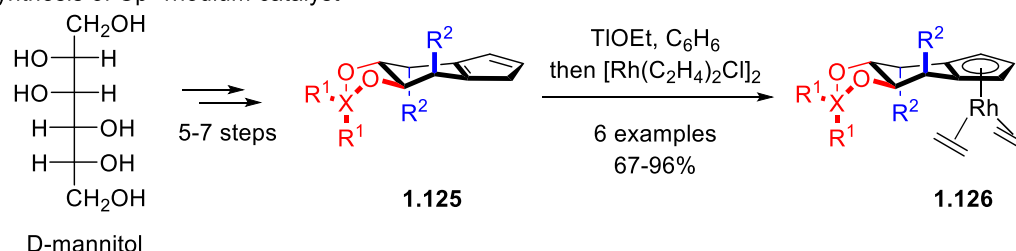
Scheme 1-23: Requirements for Cp^x and a rough design of a Cp^x ligand

Our group's cyclohexane-fused Cp^x ligand fulfill the two conditions mentioned above. The fused 1,3-dioxolane ring and R^2 groups work as back wall and side walls, respectively (Scheme 1-24a). Moreover, the ligand **1.125** has a modifiable back wall, and is C_2 -symmetric, thus preventing the

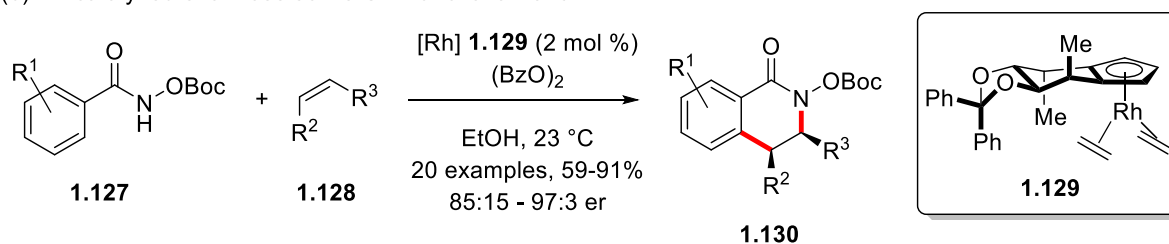
formation of a problematic diastereomeric mixture during complexation to the metal. Cp^x ligand **1.125** was synthesized from D-mannitol *via* 5-7 step-synthesis. Deprotonation of the ligand **1.125** forms the corresponding thallium cyclopentadienide, followed by transmetalation with [Rh(C₂H₄)Cl]₂. The resulting Cp^xRh(I) complex **1.126**, was applied in the enantioselective C–H functionalization of hydroxamic acid derivatives **1.127**. The reactions were performed under mild reaction conditions and gave the products **1.130** in moderate to excellent yields of 59-91% yield and high enantioselectivities (85:15–97:3 er) (Scheme 1-24b).

Cramer, 2012

(a) Synthesis of Cp^x rhodium catalyst

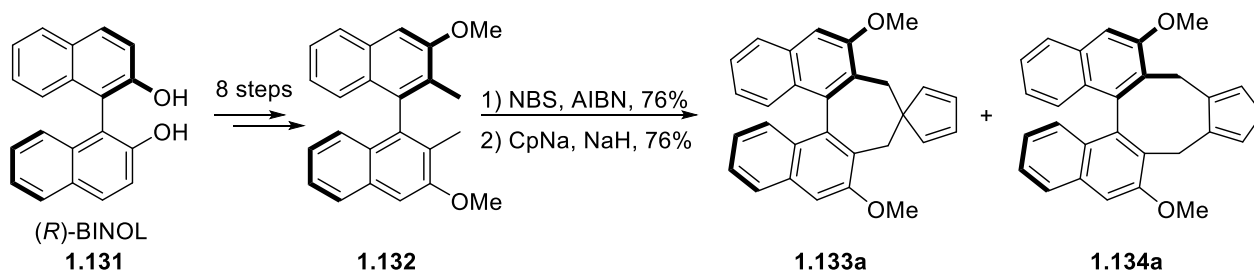


(b) Rh catalyzed enantioselective C–H functionalization

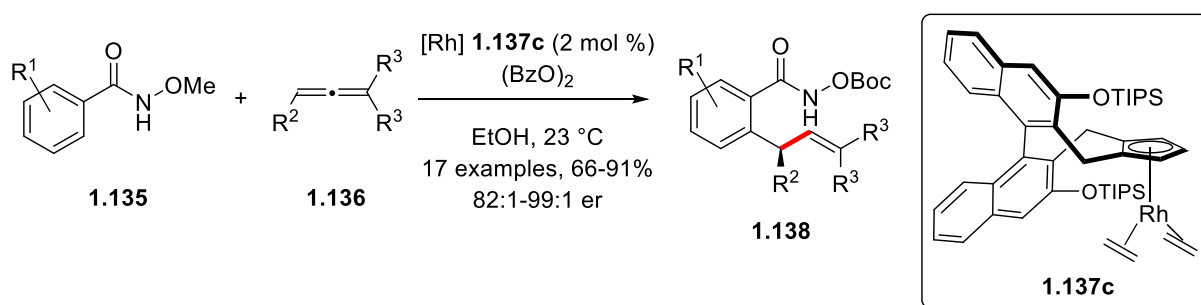


Scheme 1-24: Synthesis of Cp^x rhodium catalyst **1.126** and its application in enantioselective C–H functionalization.

In 2012, our group reported a second generation of C₂-symmetric Cp^x ligands **1.134** and their application in enantioselective Rh(III)-catalyzed C–H allylations of benzamides (Scheme 1-25).⁶² The synthesis of the Cp^x ligand **1.134a** starts from (*R*)-BINOL through intermediate **1.132**, which has been used for the synthesis of Maruoka's chiral quaternary ammonium bromide.⁶³ From the intermediate **1.132**, benzylic bromination and subsequent nucleophilic substitution of sodium cyclopentadienide deliver the desired C₂-symmetric biaryl atrop-chiral cyclopentadienyl ligand (Scheme 1-25a). The corresponding Rh(I) complex **1.137c** successfully catalyzed enantioselective C–H allylations of benzamides under mild conditions (Scheme 1-25b). The allylated benzamides **1.138** were obtained in moderate to excellent yields of 66–91% and as well as high enantioselectivities of 82:18 to 99:1 er.

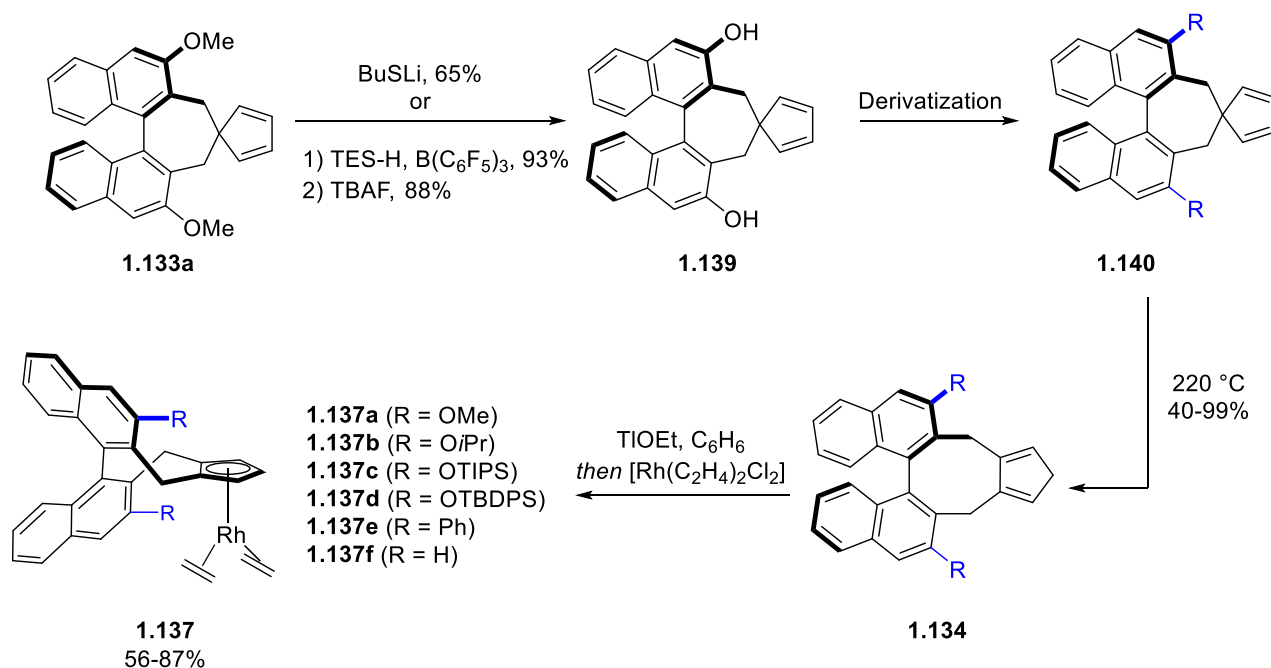
Cramer, 2013a) Synthesis of a binaphthyl-derived Cp^x ligand

b) Enantioselective Rh(III)-catalyzed C-H allylations of benzamides



Scheme 1-25: Synthesis of the binaphthyl derived Cp^x ligands and application in the enantioselective Rh(III)-catalyzed C–H allylation of benzamides

Like the cyclohexane-fused first generation, the second generation binaphthyl-derived Cp^x ligands can also be modified. However, their distinctive the modifiability of the side walls for fine-tuning of a corresponding complexes, while leaving the biaryl back wall unchanged (Scheme 1-26). The demethylation of spiro-isomer **1.133a** can be performed with BuSLi, or in a two-step process consisting of demethylation/silyl protection and silyl deprotection. The two-step demethylation process gave the binaphthol **1.139** in a better yield of 82% overall. Binaphthol **1.139** can be derivatized by etherification or installation of a triflate followed by cross-coupling. Thermal isomerization transforms spiro compound **1.140** to Cp^x ligand **1.141**, which is followed by rhodation *via* a thallium cyclopentadienide intermediate. Screening of different side walls demonstrates their strong influence on enantioselectivity of C–H allylations of benzamide (Scheme 1-25b). The enantiomeric ratio varied from 67.5:32.5 to 90:10 depending on the side walls of Cp^xRh(I) complex **1.137**. Methanol as a solvent in combination with a bulky triisopropylsilyloxy substituent gave the best result of 90:10 er. Only moderate enantioselectivity (67.5:32.5 er), was obtained with hydrogen in the 3 and 3' position of the biaryl group (**1.137c** and **1.137f**).

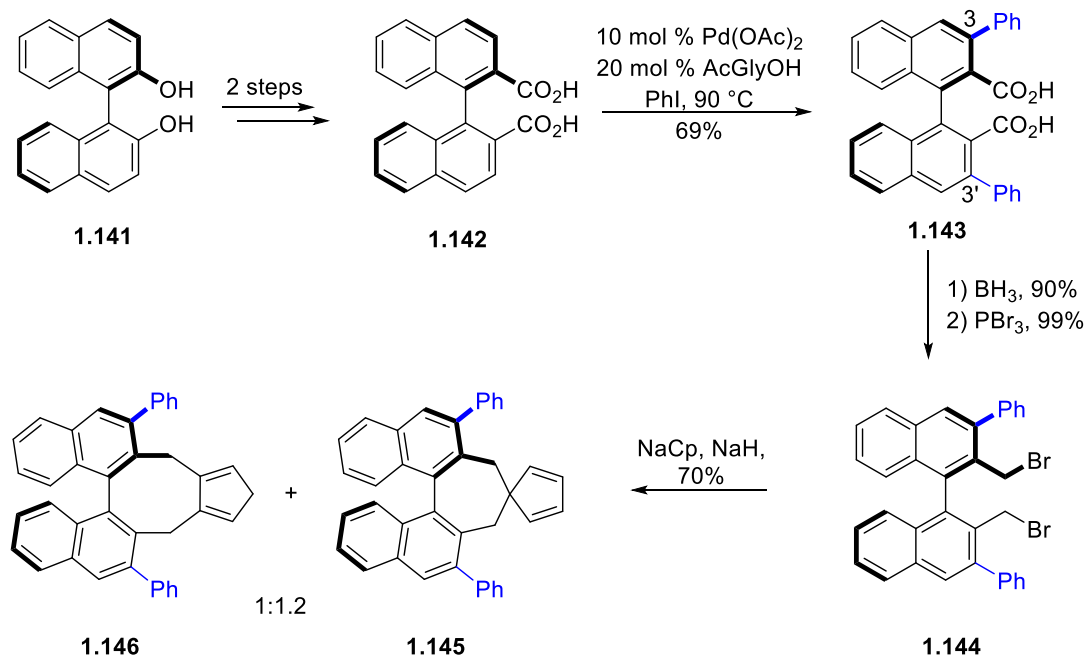


Scheme 1-26: Derivatization of the binaphthyl-derived Cp^x ligands and complexation with a rhodium precursor.

The binaphthyl-derived Cp^x ligands are the most successful Cp^x scaffold thus far. Other transition metals have been applied to that ligand class. For instance, $\text{Cp}^x\text{Ir(III)}$ was synthesized and utilized for the enantioselective synthesis of fused cyclopropanes by enyne cycloisomerization.⁶⁴ $\text{Cp}^x\text{Ru(II)}$ catalyzed enantioselective Yne-enone cyclization and [2+2] cycloaddition were also investigated.⁶⁵ Recently, Cp^x ligands were successfully employed for the first time on a 3d-metal, cobalt. Cp^xCo complexes were applied in the enantioselective C–H functionalization of *N*-chlorobenzamides.⁶⁶ In addition, Hou and coworkers applied binaphthyl-derived Cp^x ligands on rare-earth metals such as scandium, ytterbium, gadolinium, samarium, and lanthanum.⁶⁷

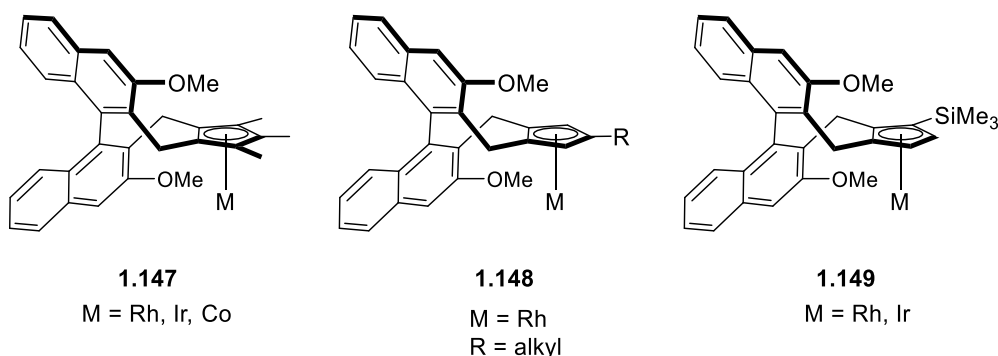
The lengthy synthetic route of the binaphthyl derived Cp^x ligands was improved in 2017 (Scheme 1-27),^{65a} shortening the synthesis of the ligand carrying with phenyl substituents in position 3 and 3' positions. The improved synthesis proceeds by Pd-catalyzed *ortho*-functionalization using the di-carboxylic acid as a directing group. Later on, follow-up investigations extended the method to other and *ortho*-functionalization of di-carboxylic acid **1.143**, broadening scope of derivatization in position 3- and 3'- silyl group and halogens.⁶⁸

Cramer, 2017



Scheme 1-27: Refined synthesis of binaphthyl derived Cp^x ligand with phenyl substituents.

Furthermore, substituents on the Cp ring were installed, leading to penta- and tri-substituted Cp^x metal complexes (Scheme 1-28). Penta-substituted Cp^x **1.147** is a chiral congener of Cp*. The penta-substituted Cp^x metal complexes are obtained by β -carbon elimination of ligand precursors.⁶⁹ The tri-alkyl substituted Cp^xRh complex **1.148** was successfully synthesized and applied in the catalytic C–H functionalization of phosphinic amides by kinetic resolutions.⁷⁰ A mild complexation method gives access to tri-substituted Cp^x metal complexes with a silyl group on the Cp ring **1.149**.⁷¹

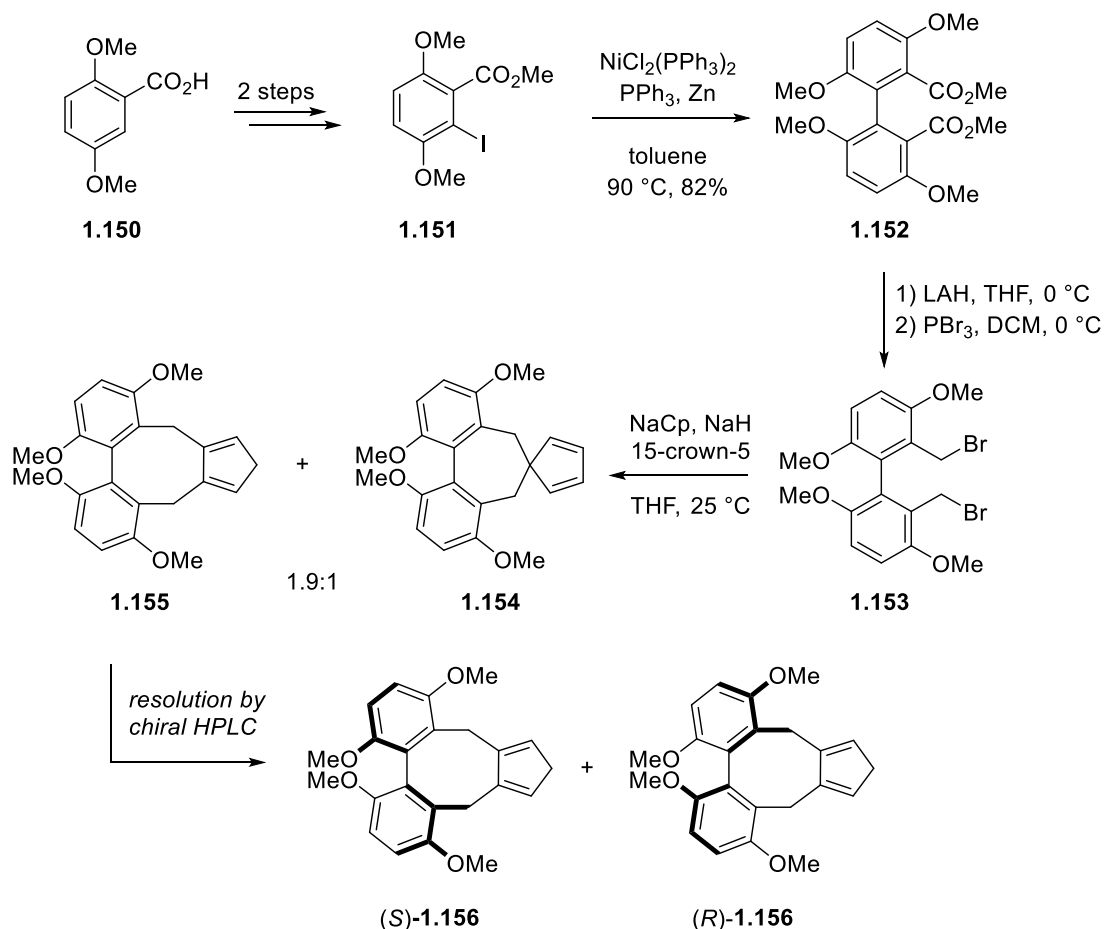


Scheme 1-28: Penta- and tri-substituted binaphthyl derived Cp^x metal complexes.

In order to streamline ligand synthesis, our group recently reported Cp^x ligands containing a biphenyl scaffold as a source of axial chirality (Scheme 1-29).⁶⁸ The synthesis starts from the commercially

available carboxylic acid **1.150**. *ortho*-Functionalization with the carboxylic acid as a directing group and ester group installation gives aryl iodide **1.151**. Ni-catalyzed Ullmann-type coupling delivers biphenyl **1.152**, followed by reduction and conversion of the benzyl alcohol to the corresponding bromide. Nucleophilic substitution of sodium cyclopentadienide towards the resulting di-benzyl bromide **1.153** gives a racemic mixture of both biphenyl derived Cp^x **1.155** and spiro-isomer **1.154**. Enantio-pure **1.156** are obtained by preparatory chiral HPLC.

Cramer, 2019



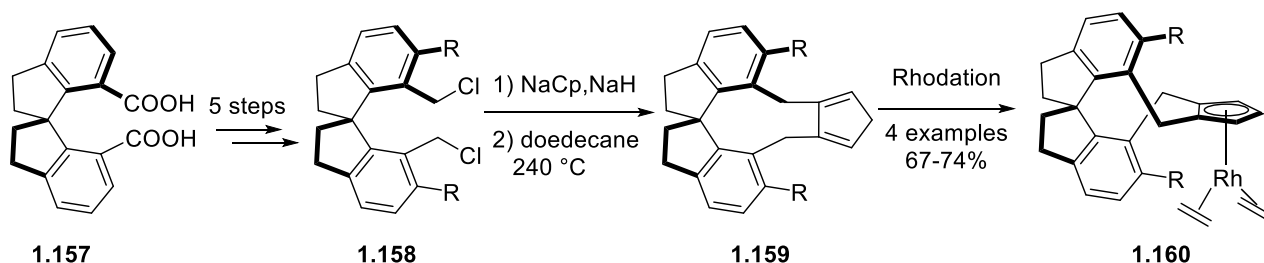
Scheme 1-29: Synthesis of a biphenyl derived Cp^x ligand.

The You group introduced a novel class of Cp^x ligands in 2016.⁷² The structures of those Cp^x ligands are inspired by pioneering work of Zhou and coworkers on 1,1'-spirobiindane-derived phosphines.⁷³ The synthesis starts from the known dicarboxylic acid **1.157** (Scheme 1-30). The synthesis of dialkyl chloride **1.158** proceeds *via ortho*-functionalization. Di-alkylation and thermal rearrangement from the spiro-isomer gives 1,1'-spirobiindane-derived Cp^x ligand **1.159**. The rhodation of the ligand is performed *via* deprotonation using thallium ethoxide as for the previous cases,⁶¹ smoothly giving the

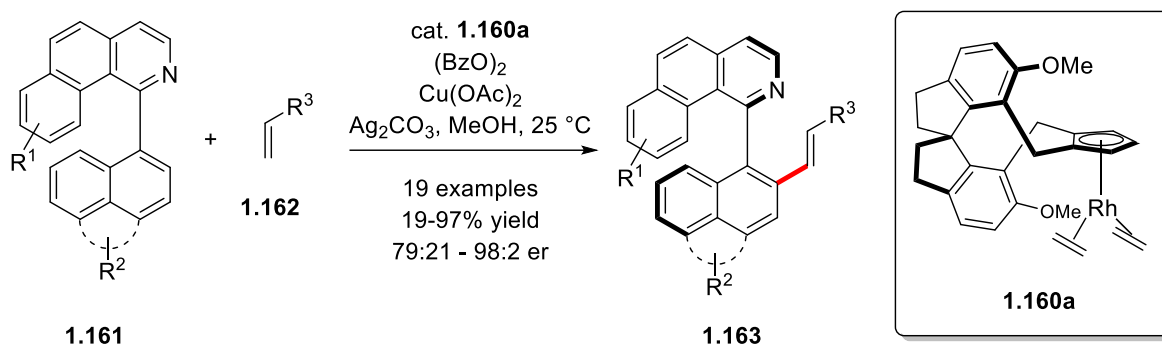
corresponding $\text{Cp}^*\text{Rh(I)}$ complexes **1.160**. These were utilized in the enantioselective C–H functionalization of biaryl compounds with up to 98:2 er.

You, 2016

a) Synthesis of spirobiindane-derived Cp^*Rh complexes



b) Enantioselective C–H functionalization

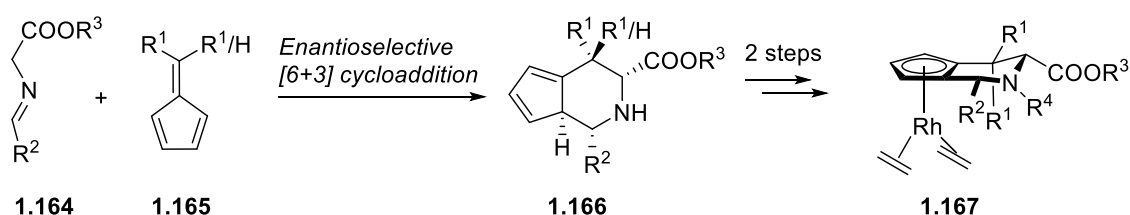


Scheme 1-30: Synthesis and application of spirobiindane-derived Cp^*Rh complexes.

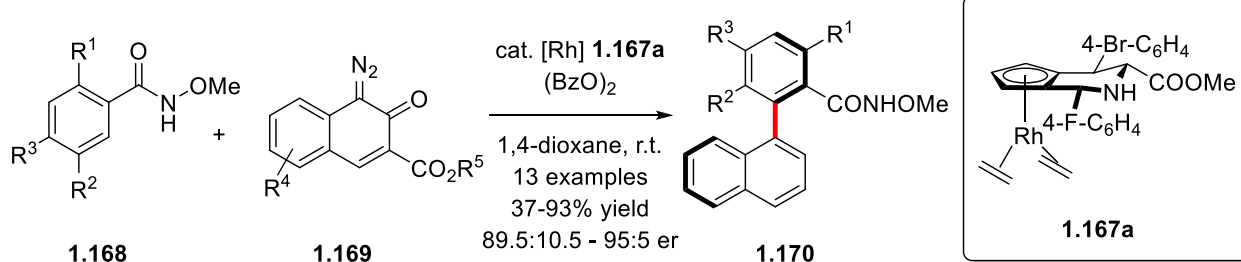
In 2017, the Waldmann group reported piperidine fused cyclopentadienes,⁷⁴ using an enantioselective [6+3] cycloaddition of imino ester with fulvene as a key step of the synthesis⁷⁵ (Scheme 1-31a). The ligand consists of four modifiable part, and is obtained in three steps from commercially available compounds. However, the lack of C_2 -symmetry requires a difficult purification of a diastereomeric mixture of rhodium complexes, using an alumina and silica column under inert atmosphere at -40°C . Despite that major drawback, the Waldmann group successfully demonstrated the potency of the new ligand class in enantioselective catalysis (Scheme 1-31b). Using rhodium catalyst **1.167a**, enantioselective C–H functionalization for the coupling of hydroxamates **1.168** and diazonaphthoquinones **1.169** towards axially chiral biaryl compounds **1.170** proceeded in up to 93% yield and up to 95:5 er.

Waldmann, 2017

a) Synthesis of Waldmann's Cp^x by [6+3] cycloaddition



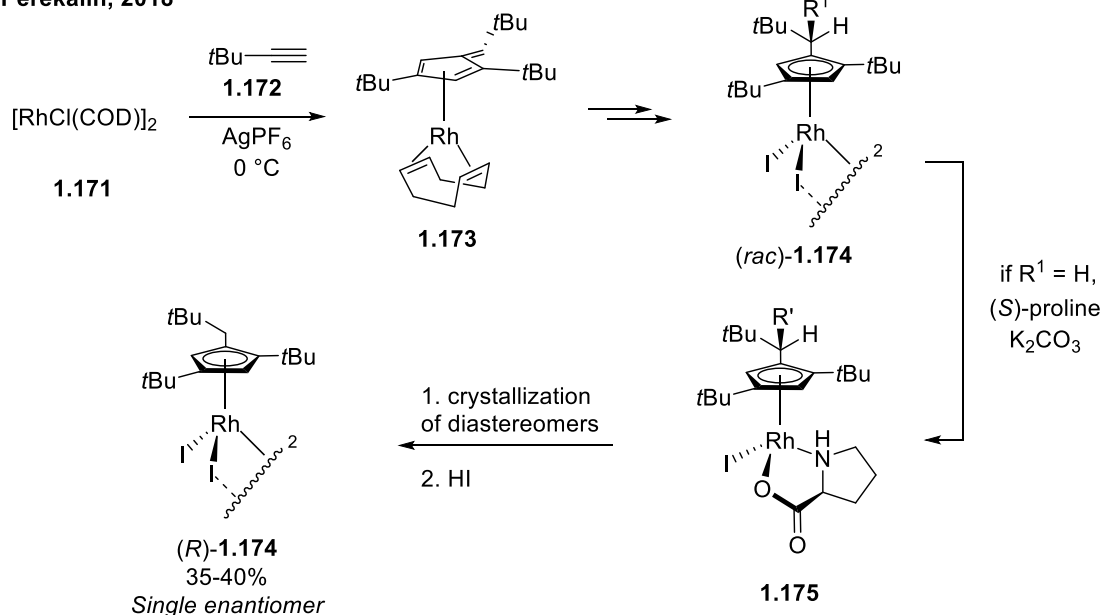
b) C-H functionalization of hydroxamates



Scheme 1-31: Synthesis of piperidine fused cyclopentadienes and their application in C-H functionalization.

The Perekalin group investigated Cp^x ligands with planar chirality, allowing facile access to $\text{Cp}^x\text{Rh(III)}$ complexes **1.174** (Scheme 1-32).⁷⁶ They reported a three-step racemic synthesis of $\text{Cp}^x\text{Rh(III)}$ complexes using a [2+2+1] cyclotrimerization of terminal alkynes. The enantiomers were separated by salt formation with (*S*)-proline and crystallization. The enantiomerically pure $\text{Cp}^x\text{Rh(III)}$ complex (*R*)-**1.174** was employed for the C-H functionalization of aryl hydroxamates in yields up to 97% and enantioselectivities of up to 88:12–97.5:2.5 er.

Perekalin, 2018

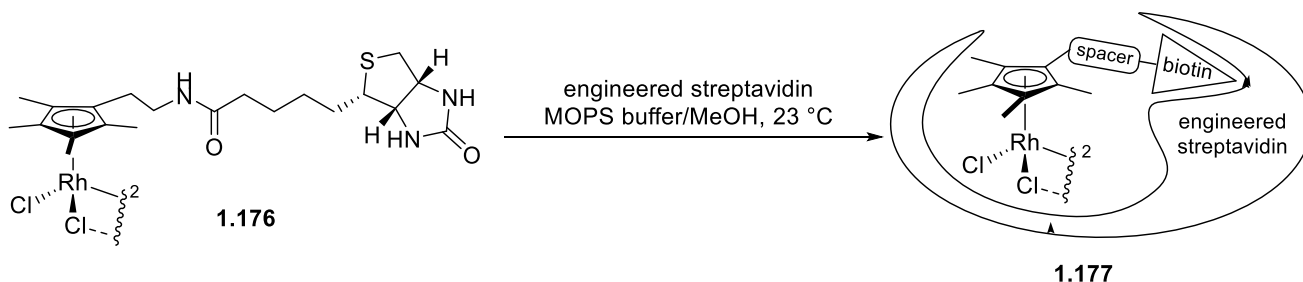


Scheme 1-32: Synthesis of planar chiral cyclopentadienyl ligands and the corresponding Rh(III) complexes.

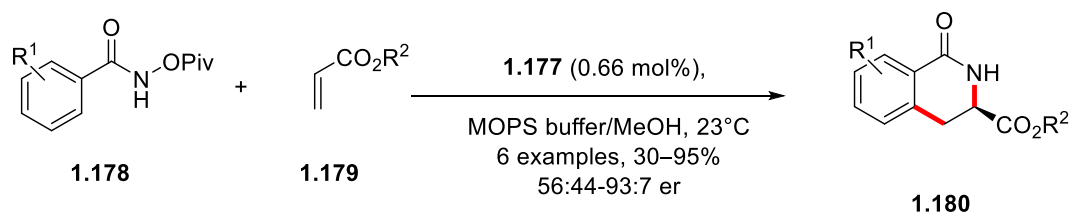
In 2012, Ward and Rovis developed a profoundly different method for creating a chiral environment around Cp^{*}Rh(III) complexes and applied them in catalysis (Scheme 1-33).⁷⁷ They created an artificial metalloenzyme containing an active metal species for a catalysis. Biotin was used as a linker for connecting Cp^{*}Rh(III) to enzyme. For their initial trial, the experiments were conducted using wild-type streptavidin, which gave only traces of the desired dihydroisoquinolones **1.180**. Site-directed mutagenesis introduced carboxylates close to the Rh(III) center. Installation of a carboxylate in position 121 boosted the catalytic activity of the metalloenzyme. The authors proposed that the carboxylate group facilitates C–H activation by concerted metalation-deprotonation (CMD). In addition, they also tuned the enantioselectivity by installing an aromatic amino acid in position 112. The optimized streptavidin and Cp^{*}Rh(III) complex with linker **1.176** forms metalloenzyme **1.177**, which promoted the C–H functionalization of hydroxamates in up to 93:7 er.

Ward and Rovis, 2012

a) Synthesis of metalloenzyme **1.177**



b) Enantioselective C–H functionalization



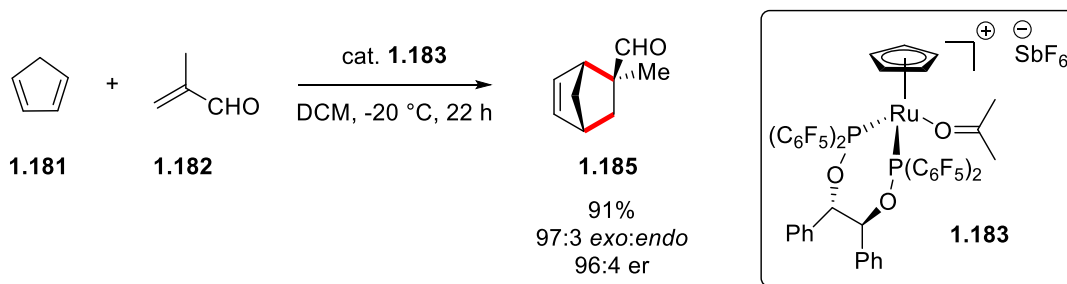
Scheme 1-33: Synthesis of metalloenzyme and its application on enantioselective C–H functionalization.

1.2.4 Precedents of chiral cyclopentadienyl ruthenium complexes

Several approaches for chiral cyclopentadienyl metal complexes described in Section 1.2.2 have been implemented for ruthenium, for instance the combination with chiral bi-dentate ligands, tethered mono-dentate ligands or Cp^x ligands. This section will introduce representative examples of these types of chiral ruthenium complexes and their application in asymmetric synthesis.

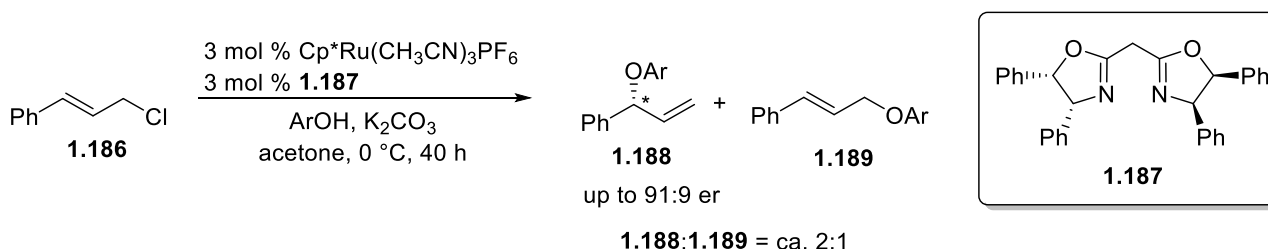
Kündig and co-workers introduced a chiral environment on CpRu complexes by installing a chiral bidentate ligand (**1.94** in Figure 1-3).⁷⁸ They applied a previously developed chiral bidentate ligand, biphop-F, on a CpRu complex.^{22a} The chiral ruthenium complex **1.183** works as a Lewis acid by coordinating to the carbonyl group of enals for catalyzing the enantioselective Diels-Alder reaction of enals with cyclopentadienes, giving the products in high diastereoselectivities of up to 97:3 dr and enantioselectivities of up to 96:4.

Kündig, 1999



Scheme 1-34: Application of a chiral ruthenium complex with a chiral bidentate ligand.

Bruneau and co-workers reported the first example of enantioselective allylic etherification using $\text{Cp}^*\text{Ru}(\text{II})$ complex with chiral bisoxazoline ligands **1.187** (Scheme 1-35).⁷⁹ They applied bisoxazoline ligands, which is thoroughly investigated chiral bidentate ligands,⁸⁰ to a $\text{Cp}^*\text{Ru}(\text{II})$ complex. This catalytic system delivered the substituted allyl aryl ether with a preference to branched one. In addition, it showed high enantioselectivity of **1.188** up to 91:9 *er*.

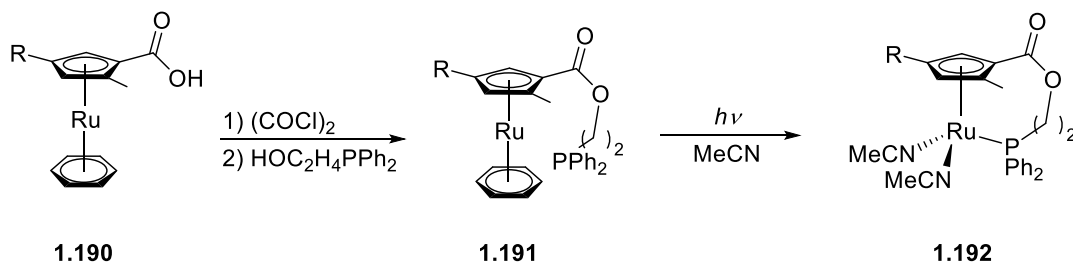


Scheme 1-35: Enantioselective allylic etherification with chiral $\text{Ru}(\text{II})$ bisoxazoline complexes.

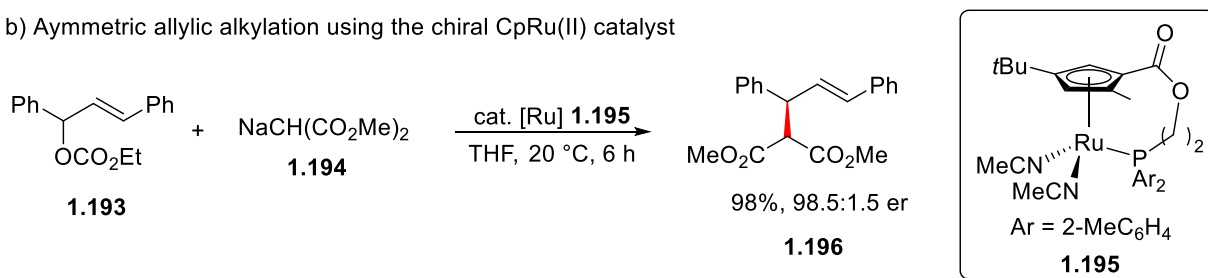
Another class of chiral $\text{CpRu}(\text{II})$ complexes uses a ligand with point chirality tethered to a cyclopentadiene ring (**1.95** in Figure 1-3). Takahashi's planar chiral $\text{CpRu}(\text{II})$ complex was reported in 2000, and one year later, the group demonstrated its application in an asymmetric allylic alkylation (Scheme 1-36).⁵⁴ Acyl chloride formation was followed by nucleophilic acyl substitution. The resulting ester was submitted to UV light with acetonitrile as a solvent for substitution on the arene ligand, giving planar chiral CpRu complex **1.192** with two vacant coordination sites. Even though the scope of the reaction was limited, it proceeded in excellent yields of **1.196** up to 98%, and enantiomeric ratios up to 98.5:1.5.

Takahashi, 2000, 2001

a) Synthesis of chiral CpRu(II) using a tethered ligand



b) Asymmetric allylic alkylation using the chiral CpRu(II) catalyst

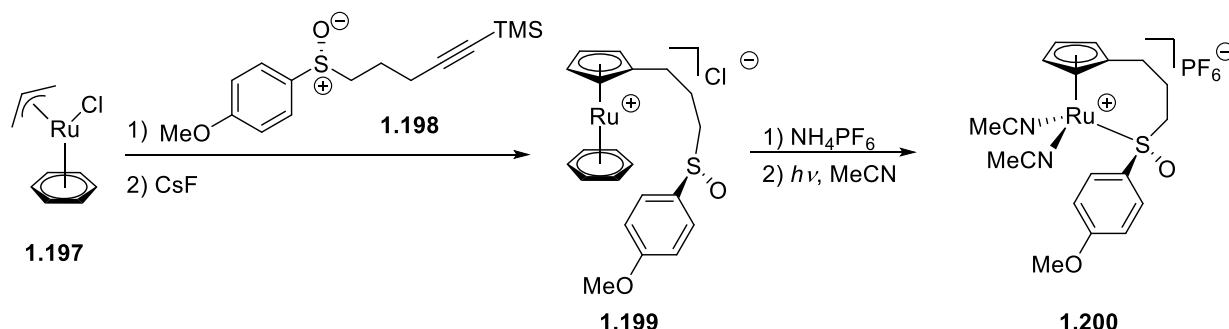


Scheme 1-36: Synthesis of chiral CpRu(II) complexes carrying a tethered ligand and their application in asymmetric allylic alkylation.

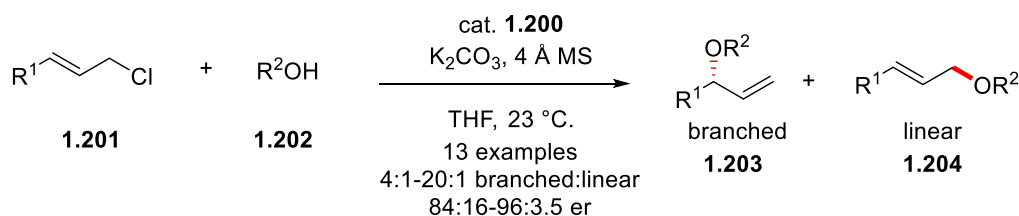
A similar example employs a tethered ligand with point chirality instead of planar chirality (**1.95** in Figure 1-3). The Trost group employed the point chirality of a sulfoxide tethered to a cyclopentadienyl group (Scheme 1-37).⁵⁵ [3+2] cycloaddition between [(η³-allyl)RuCl(C₆H₆)] **1.197** and unsymmetrical alkyne **1.198** constructed the cyclopentadienyl ligand. Subsequent de-silylation, counter anion exchange and arene ligand substitution under UV light resulted in the chiral CpRu(II) complex **1.200**. The branched-selective asymmetric allylic substitution was catalyzed by the chiral CpRu(II) complex **1.200**, proceeding with high enantioselectivities (up to 96.5:3.5 er) on a broad scope of substrates.

Trost, 2013

a) Synthesis of chiral CpRu(II) **1.200** using a tethered sulfoxide ligand



b) Asymmetric allylic substitution using chiral CpRu(II) catalyst **1.200**

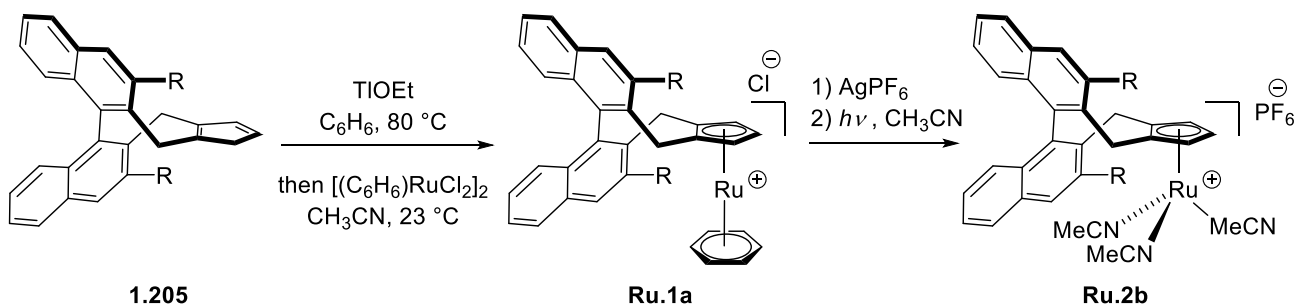


Scheme 1-37: Synthesis of chiral CpRu(II) **1.200** using a tethered sulfoxide and its application in asymmetric allylic substitution.

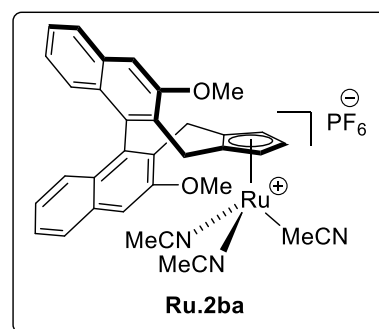
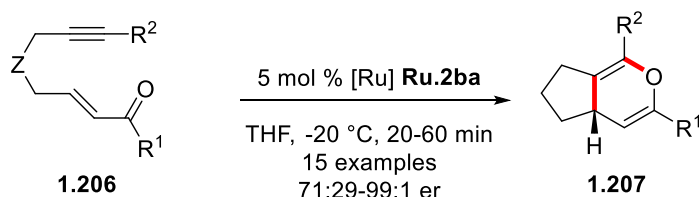
Our group applied binaphthyl-derived Cp^x ligands to ruthenium for the first time in 2015 (**1.96** in Figure 1-3),^{65c} establishing a ruthenation method for Cp^x ligands (Scheme 1-38a). Deprotonation of binaphthyl-derived Cp^x ligands **1.205** by thallium ethoxide and subsequent complexation with [(C₆H₆)RuCl₂]₂ delivers Cp^xRu(arene) complexes **Ru.1a**. A subsequent counteranion exchange with silver hexafluorophosphate and light-mediated removal of the benzene ligand gives the active Cp^xRu(II) complexes **Ru.2b**. These active Cp^xRu(II) complexes successfully catalyze an enantioselective yne-enone cyclization, providing 4*H*-pyrans **1.207** with high enantiomeric ratios up to 99:1 (Scheme 1-38b). Later, the binaphthyl-derived Cp^xRu(II) complexes were adapted for enantioselective [2+2] cycloadditions of internal alkynes and norbornadienes.^{65a, b}

Cramer, 2015

a) Synthesis of binaphthyl-derived Cp^xRu(II) complexes **Ru.2b**



b) Enantioselective yne-enone cyclization using Cp^xRu(II) **Ru.2ba**

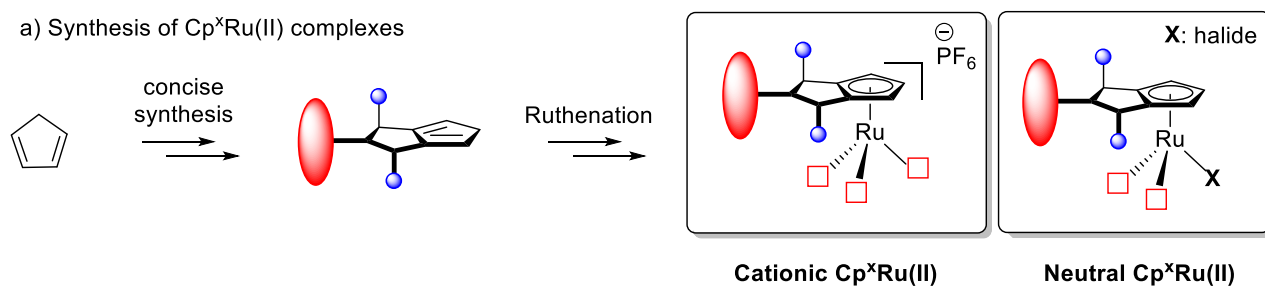


Scheme 1-38: Synthesis of binaphthyl-derived Cp^xRu(II) **Ru.2b** and its application in enantioselective yne-enone cyclization.

1.3 Aims of the thesis

The versatile reactivity of ruthenium, the least expensive platinum group metal, has been actively investigated since the 1980s.⁴ As new reactivities were discovered, the desire for enantioselective transformations in ruthenium catalysis emerged. In this context, the power of Cp^x ligands for realizing enantioselective transformations has been demonstrated successfully.⁵⁶ However, the development of concise syntheses of chiral Cp ligands and their exploitation for enantioselective transition-metal catalyzed reactions remains in its early stages. The first goal of this thesis was to develop streamlined synthetic routes to new Cp^x ligands and their corresponding cationic and neutral Cp^xRu(II) complexes (Figure 1-4a). The second goal was the exploitation of their potential in asymmetric catalysis (Figure 1-4b). Three different enantioselective transformations will be discussed, showcasing the versatile reactivity of Cp^xRu(II) complexes and their high capability for enantio-induction.

a) Synthesis of $\text{Cp}^*\text{Ru(II)}$ complexes



b) Applications of $\text{Cp}^*\text{Ru(II)}$ on enantioselective syntheses

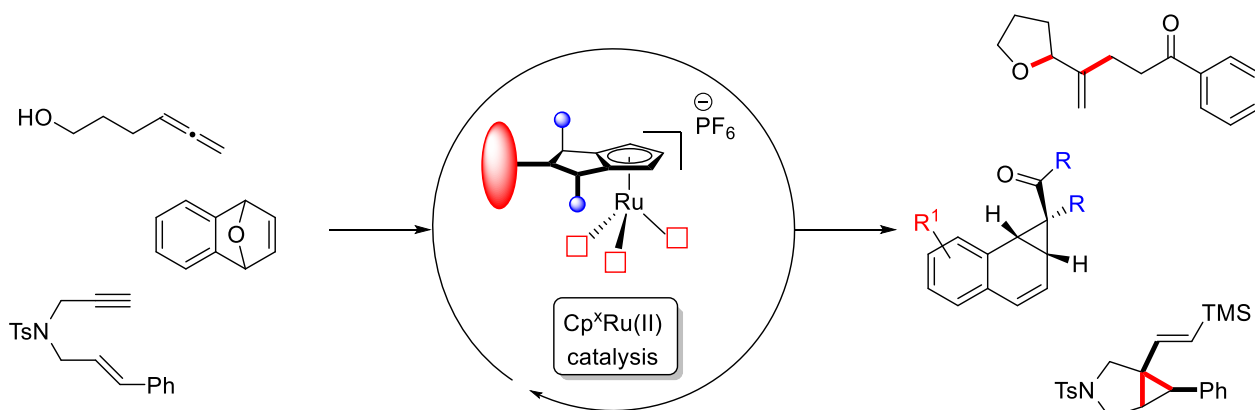


Figure 1-4: Synthesis of $\text{Cp}^*\text{Ru(II)}$ complexes and its applications on enantioselective syntheses.

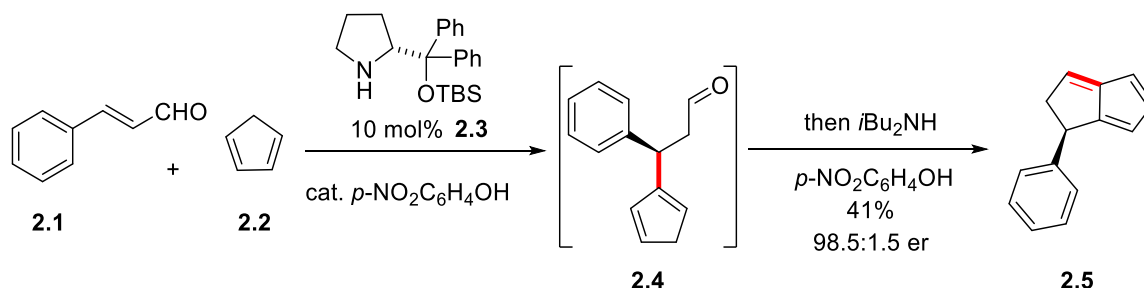
Chapter 2 Synthesis of Chiral Cp^x Ligands and Cp^xRu (II) Complexes

2.1 Cyclopentane Fused Cp^x Ligands

2.1.1 Ligand Synthesis and Complexation

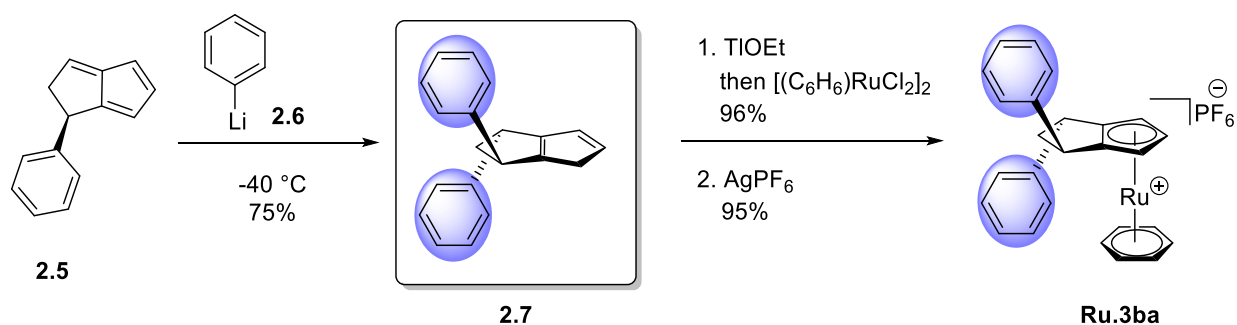
The first class of Cp^x ligands, cyclohexane-fused Cp^x, is accessible by a concise synthetic route. In spite of that, there is a drawback of the cyclohexane-fused Cp^x. As the side walls are difficult to modify, optimizing a reaction for high enantioselectivity is tricky. The C₂-symmetric atropchiral binaphthyl-derived Cp^x ligands has proved its synthetic utility in a variety of asymmetric reactions.^{62, 64-66} However, the lengthy synthesis of the atropchiral binaphthyl-derived ligands gave rise to the desire for a novel chiral Cp^x, combining the advantages of the first two generations: modifiable side walls and concise synthetic access.

The synthesis of the cyclopentane-fused Cp^x ligands was inspired by the enantioselective ene-reaction of cyclopentadiene.⁸¹ The organocatalyzed ene-type reaction of cinnamaldehyde **2.1** and cyclopentadiene **2.2** followed by condensation gives the chiral cyclopentane-fused fulvene **2.5** with excellent enantioselectivity (98.5:1.5 er) (Scheme 2-1).



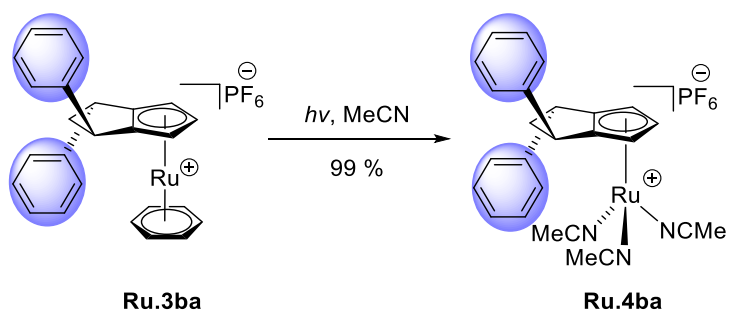
Scheme 2-1: Synthesis of chiral cyclopentane-fused fulvenes.

A subsequent diastereoselective addition of an aryl lithium **2.6** gives cyclopentane-fused chiral cyclopentadiene **2.7**. The metalation of the cyclopentane-fused chiral cyclopentadiene was performed by an established procedure for CpRu complexes.^{65c} Metalation with thallium ethoxide generated the corresponding C₂-symmetric chiral cyclopentadienide and subsequent transmetalation with ruthenium resulted in a 96% yield of Cp^xRu(C₆H₆)Cl **Ru.3aa**. Anion exchange with silver hexafluorophosphate brought Cp^xRu(C₆H₆)PF₆ **Ru.3ba**, and precipitation of silver chloride (Scheme 2-2).



Scheme 2-2: Synthesis of cyclopentane fused Cp^x ligand and complexation of the ligand.

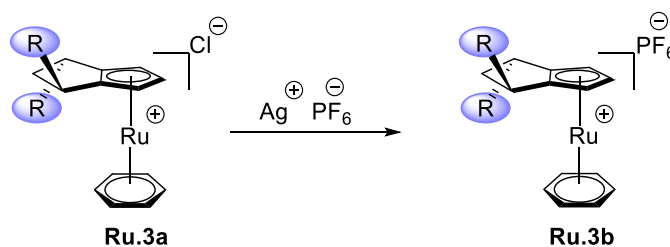
As the benzene ruthenium complex **Ru.3ba** is inert, the benzene ligand was then removed from the complex. UV-facilitated ligand exchange to acetonitrile accompanied by removal of benzene ligand was performed^{65c, 82} to introduce labile ligands. The acetonitrile ligands readily dissociate to generate the catalytically active coordinatively unsaturated species. After the photoreaction, all volatile compounds were evaporated under high vacuum. Due to the high affinity of the desired ruthenium complex **Ru.4ba** to acetonitrile, freeze-drying was performed to removing any residual solvent. This photoreaction produced the desired trisacetonitrile complex **Ru.4ba** in a near-quantitative yield of 99% yield (Scheme 2-3).



Scheme 2-3: UV light facilitated removal of an arene ligand.

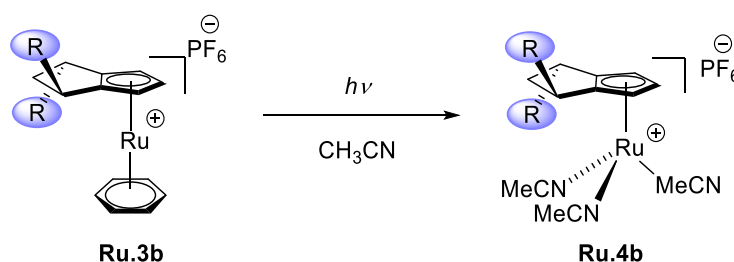
2.1.2 Aryl Group Derivatives

With a synthetic route to the cyclopentane-fused Cp^x ligands in hand, a ligand library carrying different side walls was generated. The established method for anion exchange gave the corresponding $\text{Cp}^x\text{Ru}(\text{C}_6\text{H}_6)\text{PF}_6$ complexes (**Ru.3b**) (Scheme 2-4). The complexes carrying *ortho*- and *para*-substituted aryl groups were obtained in good to excellent yields of 77–96% (Table 2-1, **Ru.3b**). The complex with substituents in both of *meta*-positions was acquired in a moderate yield of 53% (Table 2-1, **Ru.3bg**). However, the complexes carrying 1-naphthyl or 2-naphthyl substituents formed an insoluble sticky solid during the anion exchange step and could not be isolated (Table 2-1, **Ru.3bh** and **Ru.3bi**).



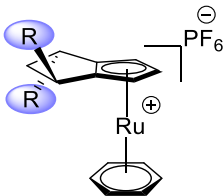
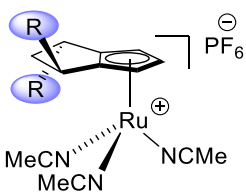
Scheme 2-4: Anion exchange and active complex formation of a library of cyclopentane-fused third generation Cp^xRu complexes.

The active complex preparation by removal of an arene ligand worked smoothly (Scheme 2-5). Regardless of substituents positions on aryl rings, all the cases resulted in high yield, 90% to quantitative conversion. (Table 2-1, **Ru.4b**).



Scheme 2-5: UV light-facilitated removal of the benzene ligand for catalyst library.

Table 2-1: Anion exchange and active ruthenium catalyst synthesis by a removal of an arene ligand

	R = 2-Me-C ₆ H ₄ (83%)	R = 2-Me-C ₆ H ₄ (95%)
	Ru.3bb	Ru.4bb
	R = 2-MeO-C ₆ H ₄ (77%)	R = 2-MeO-C ₆ H ₄ (90%)
	Ru.3bc	Ru.4bc
	R = 4-MeO-C ₆ H ₄ (79%)	R = 4-MeO-C ₆ H ₄ (100%)
	Ru.3bd	Ru.4bd
	R = 4- <i>i</i> Pr-C ₆ H ₄ (92%) ^a	R = 4- <i>i</i> Pr-C ₆ H ₄ (97%) ^a
	Ru.3be	Ru.4be
	R = 4-Ph-C ₆ H ₄ (96%)	R = 4-Ph-C ₆ H ₄ (96%)
	Ru.3bf	Ru.4bf
	R = 3,5-Me ₂ -C ₆ H ₃ (53%) ^b	R = 3,5-Me ₂ -C ₆ H ₃ (100%) ^b
	Ru.3bg	Ru.4bg
	R = 1-naphthyl (0%)	
	Ru.3bh	
	R = 2-naphthyl (0%)	
	Ru.3bi	

Conditions for counter anion exchange: 1.2 equiv. of silver hexafluorophosphate, 0.2 M in DCM, 15 min.; Conditions for removal of arene ligand: UV light, 15 °C, 0.02 M in CH₃CN; [a] Data from Dr. Shou-Guo Wang; [b] Data from Dr. David Kossler, and the Cp^x ligand of **Ru.3bg** has the opposite absolute stereochemistry.

The crystal structures of **Ru.3ba** and **Ru.3bc** were revealed by X-ray diffraction spectroscopy. As expected, one of the phenyl group is placed above the plane of the cyclopentane ring, the other phenyl group is positioned below the cyclopentane ring and shields one side of the ruthenium center (Figure 2-1). The distance between ruthenium and the *meta*-carbon atom of the aryl group ($d_{\text{Ru1-C17}}$) is 4.94 Å. The dihedral angle between cyclohexane ring and aryl group ($\theta_{\text{C5-C6-C15-C16}}$) is 37.3°.

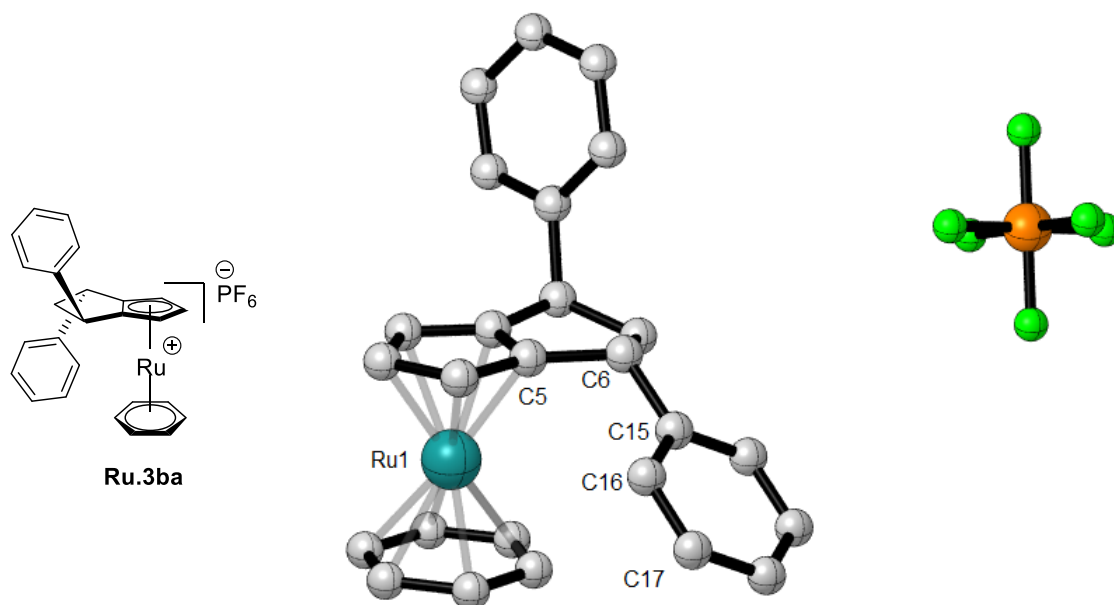


Figure 2-1: X-ray crystal structure of **Ru.3ba**.
For clarity, hydrogen atoms are omitted.

Introduction of 2-methoxy substituents in the aryl group on the Cp^x ligand causes slight structural changes on the ruthenium complex **Ru.3bc** (Figure 2-2). The distance between ruthenium and the *meta*-carbon atom ($d_{\text{Ru1-C11}}$) is increased to 5.42 Å. The change originates from a rotation of the aryl group along the carbon-carbon bond (C1-C9). As a result, the dihedral angle ($\theta_{\text{C8-C1-C9-C10}}$) increases from 37.3 to 64.8 ° compared to phenyl-substituted **Ru.3ba**.

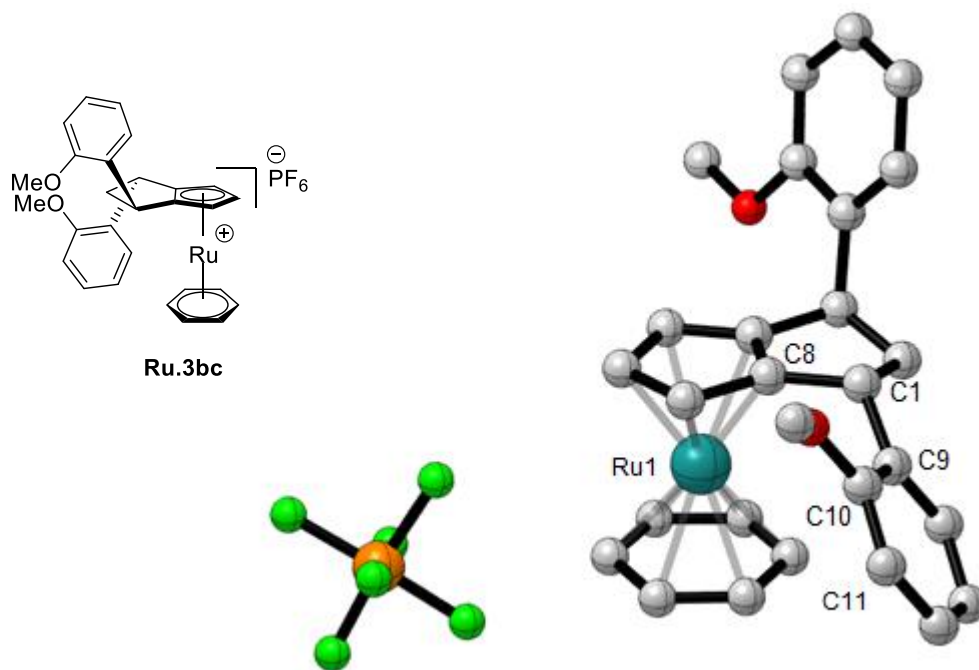
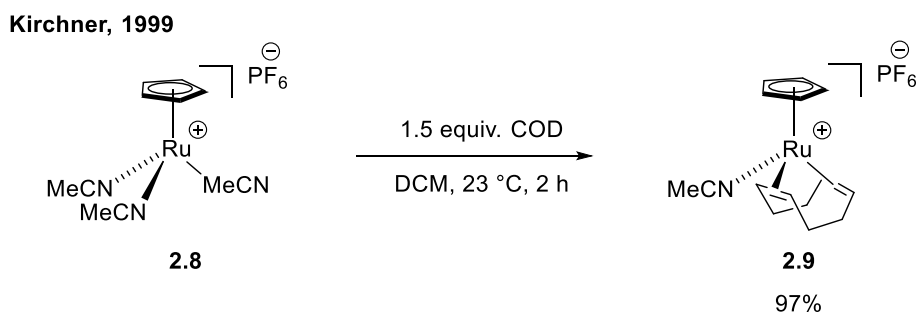


Figure 2-2: X-ray crystal structure of **Ru.3bc**.
For clarity, hydrogen atoms are omitted

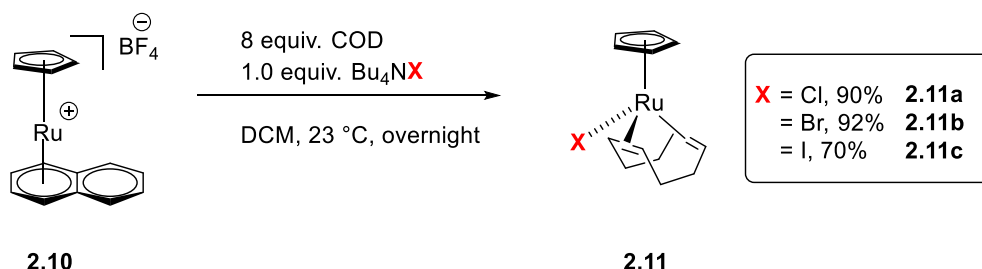
2.1.3 Synthesis of Neutral Complexes

Kirchner and coworkers reported the synthesis of $\text{CpRu}(\text{COD})(\text{CH}_3\text{CN})$ complex **2.9** by ligand exchange of $\text{CpRu}(\text{CH}_3\text{CN})_3\text{PF}_6$ **2.8** (Scheme 2-6).⁸³ In an analogous manner, a solution of $\text{CpRu}(\text{CH}_3\text{CN})_3\text{PF}_6$ in dichloromethane was stirred with an excess amount of cyclooctadiene (COD) at room temperature, smoothly delivering $\text{CpRu}(\text{COD})(\text{CH}_3\text{CN})$ in 97% yield.



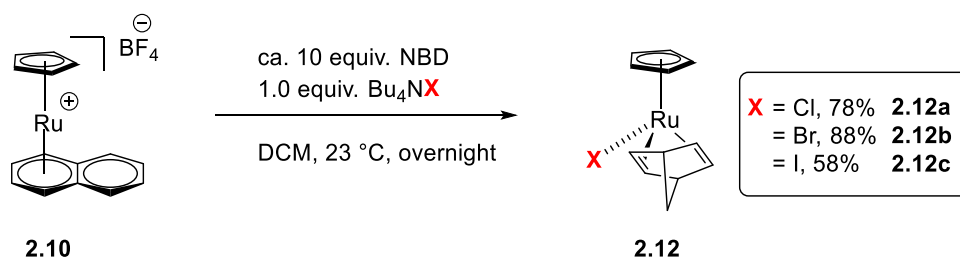
Scheme 2-6: $\text{CpRu}(\text{COD})(\text{CH}_3\text{CN})$ complex synthesis by ligand exchange from $\text{CpRu}(\text{CH}_3\text{CN})_3\text{PF}_6$.

Using similar conditions, Kudinov accessed neutral CpRuL_2X complexes (L = mono- and di-phosphine, dienyl, carbonyl) by substitution of the naphthalene ligand on cationic $\text{CpRu}(\text{C}_{10}\text{H}_8)^+$ complex **2.10** by a halide and cyclooctadiene under mild conditions.⁸⁴



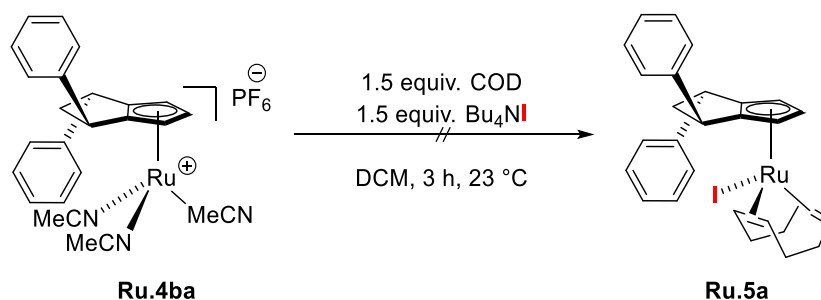
Scheme 2-7: $\text{CpRu}(\text{COD})\text{X}$ synthesis by substitution on a $\text{CpRu}(\text{C}_{10}\text{H}_8)\text{BF}_4$ complex

The analogous norbornadiene complexes **2.12** were obtained in moderate to very good yields by reaction of **2.10** under the same reaction conditions from (Scheme 2-8). Reaction with chloride or bromide gave better yields than iodide for both diene ligands.



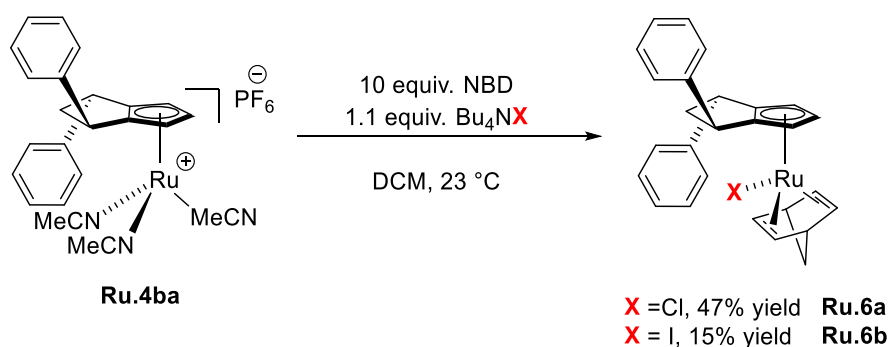
Scheme 2-8: $\text{CpRu}(\text{NBD})\text{X}$ **2.12** synthesis by substitution in a $\text{CpRu}(\text{C}_{10}\text{H}_8)\text{BF}_4$ complex **2.10**.

Reaction of $\text{Cp}^*\text{Ru}(\text{CH}_3\text{CN})_3\text{PF}_6$ **Ru.4ba** with cyclooctadiene and tributylammonium iodide did not give the desired product **Ru.5a** (Scheme 2-9). After the reaction, major compounds in the crude mixture was free COD and tetrabutylammonium iodide. Decomposition occurred instead of ligand substitution.



Scheme 2-9: Neutral Cp^xRu(COD)I **Ru.5a** synthesis by substitution in Cp^xRu(CH₃CN)₃PF₆ **Ru.4ba**.

In contrast to the reaction with 1,5-cyclooctadiene, ligand substitution to norbornadiene delivered the desired neutral Cp^xRu(NBD)X complexes **Ru.6a** and **Ru.6b** (Scheme 2-10), which were, to our surprise, stable on silica. After purification by silica column chromatography, Cp^xRu(NBD)X complexes **Ru.6a** and **Ru.6b** were isolated in 47 and 15% yield, respectively.



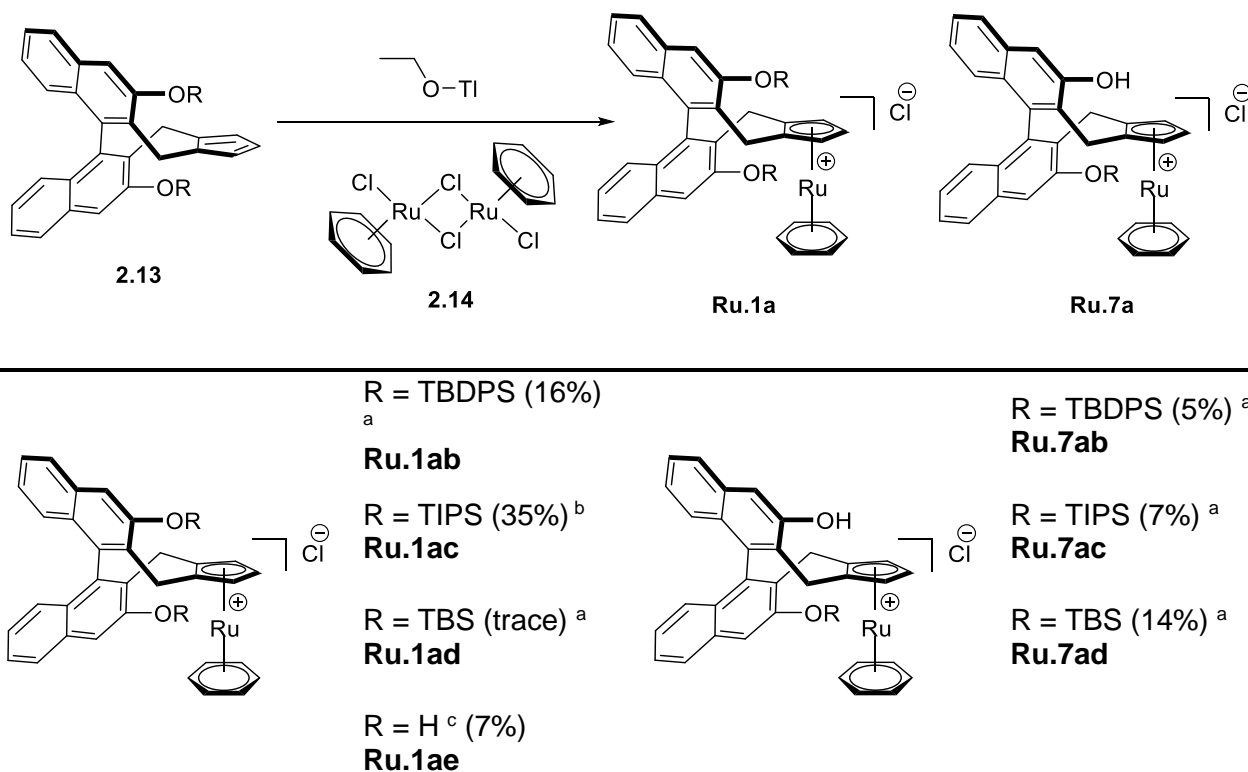
Scheme 2-10: Neutral Cp^xRu(NBD)X (**Ru.6a** and **Ru.6b**) synthesis by substitution in Cp^xRu(CH₃CN)₃PF₆ **Ru.4ba**.

2.2 Synthesis of Atropchiral Binaphthyl-Derived Cp^x Ligands

The synthesis of binaphthyl-derived Cp^xRu(II) complexes has been previously established in our group.^{65c} By following the known procedure, ruthenium complexes with different side wall were accessed (Table 2-2). Thallium ethoxide deprotonates the respective Cp^x ligand **2.13** and forms a thallium cyclopentadienide (TlCp^x), followed by complexation with [Ru(C₆H₆)Cl₂]₂ **2.14**. The desired

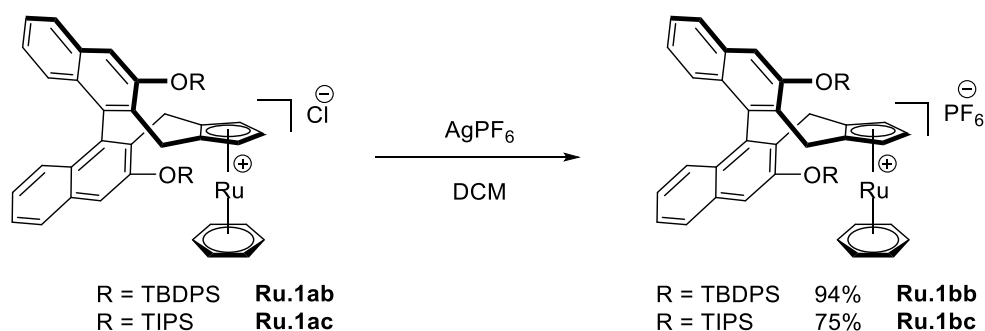
Cp^xRu(C₆H₆)Cl complexes **Ru.1a** were obtained in 7–35% yield. The corresponding mono-silylated products **Ru.7a** were observed as side products in 5–14% yield.

Table 2-2: Complexation of second generation Cp^x ligands.



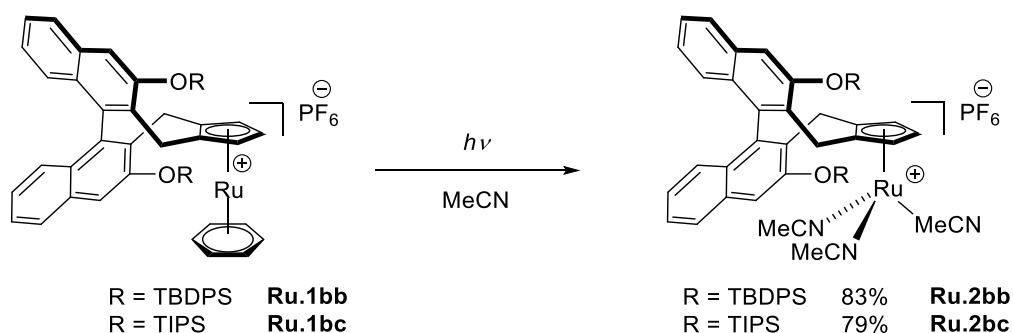
Conditions: [a] Cp^x ligand and 1.1 equiv. of thallium ethoxide were stirred at 80 °C for 3 hr, then mixed and stirred with [Ru(C₆H₆)Cl₂]₂ at room temperature; [b] Cp^x ligand and 1.1 equiv. of thallium ethoxide were stirred at room temperature for 13 hr; [c] Stirred with a Cp^x ligand and 3.0 equiv. of thallium ethoxide at room temperature for 13 hr.

Counteranion exchange on the [Cp^xRu(C₆H₆)]Cl complexes **Ru.1ab** and **Ru.1ac** with silver hexafluorophosphate, gave the corresponding hexafluorophosphate complexes [Cp^xRu(C₆H₆)]PF₆ **Ru.1bb** and **Ru.1bc** (Scheme 2-11).



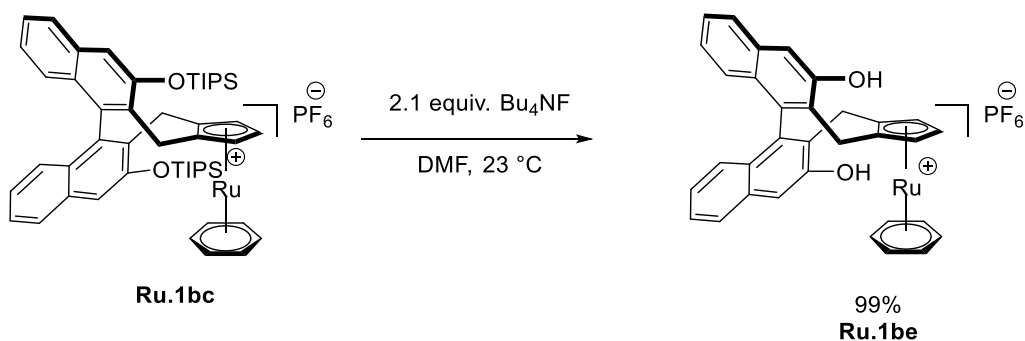
Scheme 2-11: Counteranion exchange on binaphthyl-derived Cp^*Ru complexes.

As the cases of previously reported binaphthyl-derived $\text{Cp}^*\text{Ru}(\text{C}_6\text{H}_6)\text{PF}_6$ complexes **Ru.1b**^{65c} and cyclopentane-fused $\text{Cp}^*\text{Ru}(\text{C}_6\text{H}_6)\text{PF}_6$ complexes **Ru.3b**, $\text{Cp}^*\text{Ru}(\text{CH}_3\text{CN})_3\text{PF}_6$ **Ru.2bb** and **Ru.2bc** were synthesized in good yield, 79–83% (Scheme 2-12).



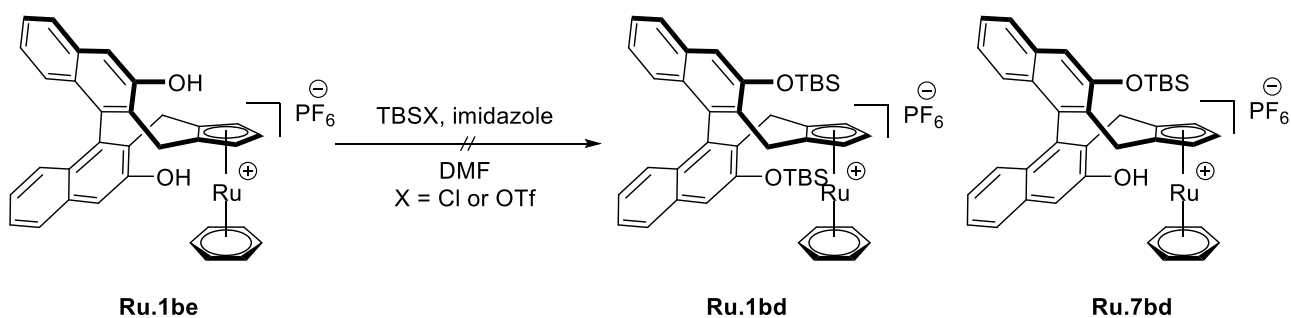
Scheme 2-12: UV-light facilitated removal of benzene ligands from binaphthyl-derived Cp^*Ru complexes.

In order to improve the efficiency of the synthetic route towards $[\text{Cp}^*\text{Ru}(\text{C}_6\text{H}_6)]\text{PF}_6$, late-stage modification of the ruthenium complexes was investigated. Previously, the Cp^* ligand had to be derivatized before complexation with ruthenium. We envisioned a derivatization of the sidewall of the Cp^* ligand on $[\text{Cp}^*\text{Ru}(\text{C}_6\text{H}_6)]\text{PF}_6$. Initial fluoride-mediated TIPS-deprotection of the OH group of **Ru.1bc** by fluoride smoothly gave **Ru.1be** in a near-quantitative yield (Scheme 2-13).



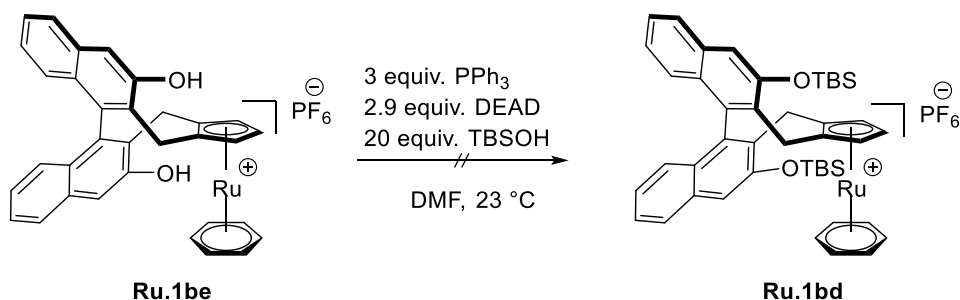
Scheme 2-13: De-silylation of **Ru.1bc**

The desilylated complex **Ru.1be** was submitted to various silyl protecting conditions (Scheme 2-14). However, starting material **Ru.1be** was recovered, or decomposition happened with traces of di-silylated product **Ru.1bd** and mono-silylated product **Ru.7bd**.



Scheme 2-14: Silyl protection on **Ru.1be**.

As an alternative, Mitsunobu type conditions for silyl protection were also evaluated on **Ru.1be**. However, the starting material **Ru.1be** was recovered with no trace of desired product (Scheme 2-15). Overall all, the trials for streamlining the synthetic route by late-stage modification of sidewall on $[\text{Cp}^*\text{Ru}(\text{C}_6\text{H}_6)]\text{PF}_6$ were not successful.



Scheme 2-15: Silyl protection using Mitsunobu type condition.

Chapter 3 Enantioselective Ruthenium(II)- Catalyzed Synthesis of Benzonorcaradienes

3.1 Introduction

Tricyclic sesquiterpenes comprise a large chemical family, which is continuously expanding as a result of their frequent occurrence in various terrestrial and marine natural products.⁸⁵ Among them, chemicals containing benzonorcaradiene and benzonorcarenene moieties possess biological activities and applications in broad areas, such as antibiotics,⁸⁶ neuropathic pain disorder,⁸⁷ osteoarthritis,⁸⁸ immune disorder,⁸⁹ and breast cancer.⁹⁰

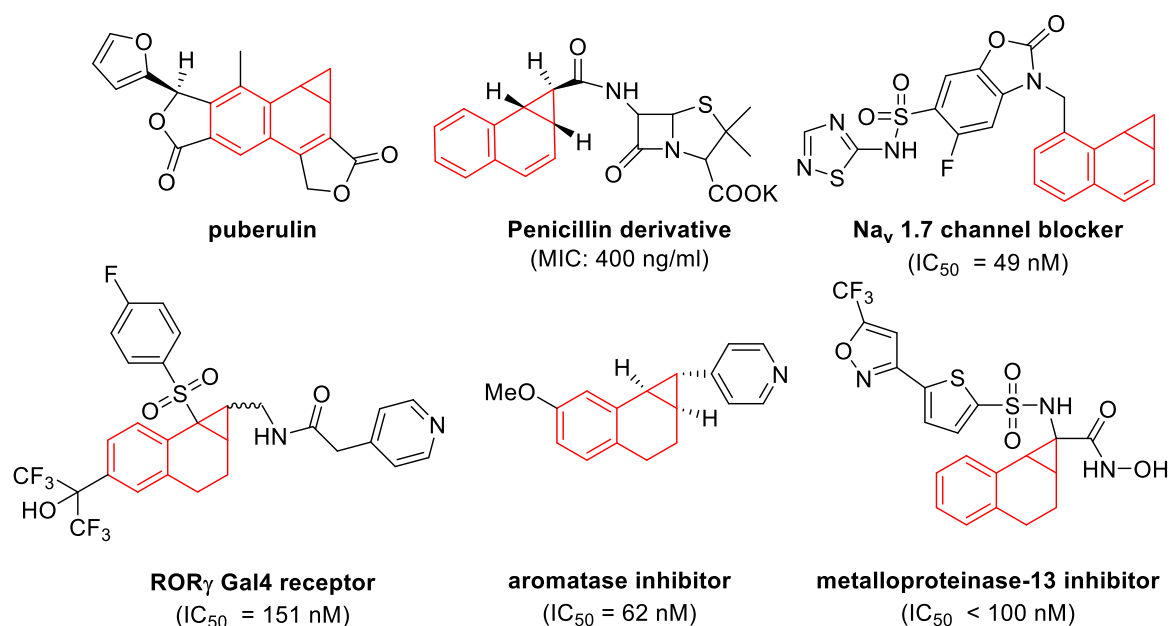
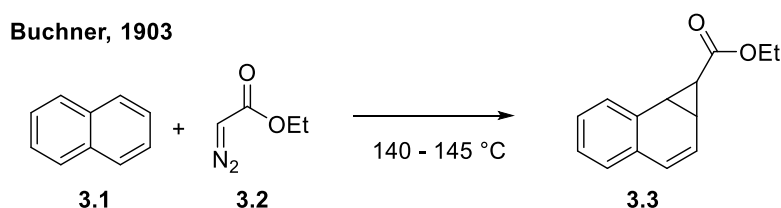


Figure 3-1: Benzonorcaradiene and benzonorcarenene moieties in a natural product and pharmaceutical compounds

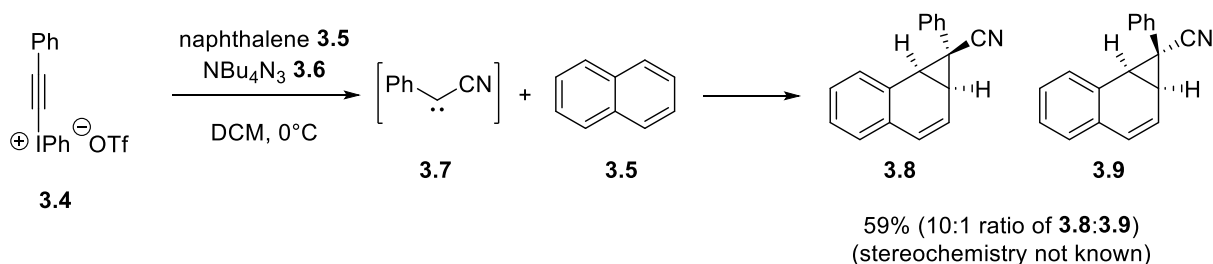
Despite their high potential for pharmaceutical applications, the synthesis of benzonorcaradienes still leaves much room for improvement as it is highly reliant on the cyclopropanation of naphthalenes using carbenes or carbenoids.⁹¹ The first example was reported by Buchner in 1903 (Scheme 3-1).



Scheme 3-1: First reported example of benzonorcaradiene synthesis using a carbene

A recent example used a hypervalent iodonium alkynyl triflate **3.4** and an azide **3.6**, which forms phenylcyanocarbene **3.7** *in situ*, for the cyclopropanation of naphthalene (Scheme 3-2).

Croatt, 2017

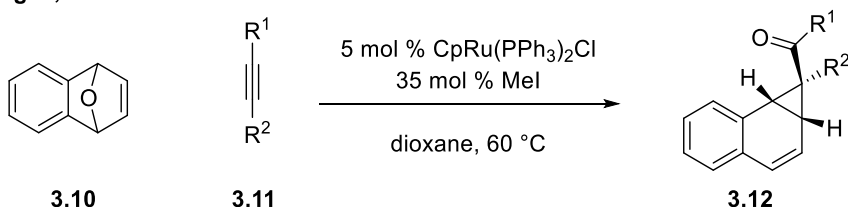


Scheme 3-2: Recent example of benzonorcaradiene synthesis using a carbene

Other isolated examples for accessing benzonorcaradiene have been reported,^{92,93} such as gold-catalyzed transformations.⁹⁴

In 2011, Tenaglia and coworkers reported a ruthenium-catalyzed synthesis of benzonorcaradienes that does not involve carbenoids.⁹⁵ The transformation is a coupling of oxa-benzonorbornadienes **3.10** and alkynes **3.11**, yielding a benzonorcaradiene **3.12** in a single step.

Tenaglia, 2011



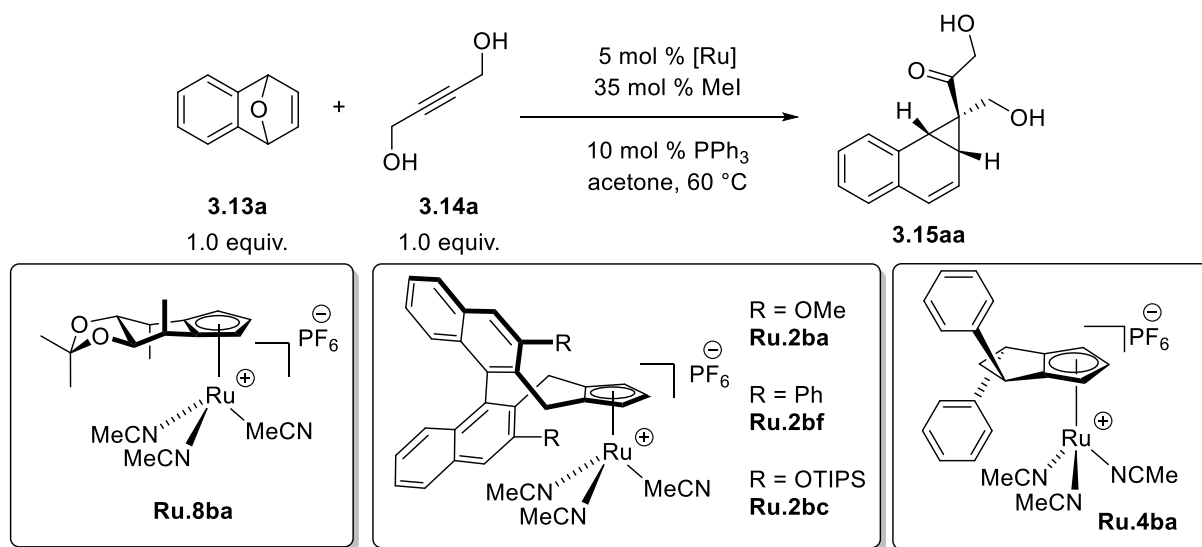
Scheme 3-3: Ruthenium catalyzed coupling of oxa-benzonorbornadienes and alkynes

The enantioselective synthesis of benzonorcaradiene remains an underdeveloped field, despite its high potential for utilization in pharmaceutical applications. To the best of our knowledge, few enantioselective syntheses of norcaradienes or cycloheptatrienes by cyclopropanation of arenes have been reported.⁹⁶ Among them, only a single report studied an intermolecular transformation.⁹⁷ In addition, two reports describe the enantioselective synthesis of benzonorcaradienes.⁹⁸ Only one of them is an intermolecular transformation, which proceeds via rhodium catalyzed asymmetric ring-opening/cyclopropanation.^{98b}

3.2 Optimization Studies for Asymmetric Benzonorcaradiene Synthesis

For initial optimization of the reaction conditions, oxa-benzonorbornadiene **3.13a** and di-propargylic alcohol **3.14a** (Table 3-1) were employed as a model system. The cyclohexane-fused Cp^x complex **Ru.8ba** gave the desired product in moderate yield 27% with moderate enantioselectivity (82.5:17.5 er) (Entry 1). Binaphthyl-derived Cp^x ruthenium complex **Ru.2ba** showed a similar reactivity, but the enantioselectivity decreased substantially to 69.5:30.5 er (Entry 2). Binaphthyl-derived Cp^xRu(II) complexes **Ru.2bf** and **Ru.2bc** with bulkier sidewalls did not improve enantioselectivity (Entry 3 and 4). Significant improvement on enantioselectivity and reactivity was observed upon the adoption of cyclopentane-fused Cp^x complex **Ru.4ba** (Entry 5), resulting in good enantioselectivity (85.5:14.5 er). This result was used as a starting point for further optimization studies.

Table 3-1: Ligand screening.

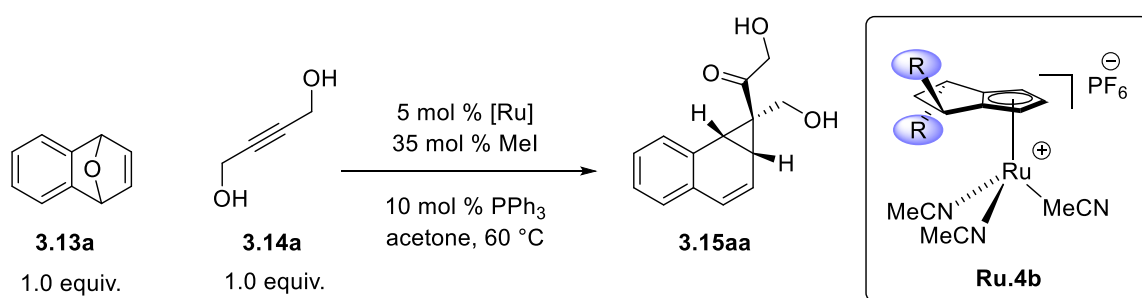


Entry	Ru	Conversion [%]	Yield [%]	er
1	Ru.8ba	72	27	82.5:17.5
2	Ru.2ba	60	30	69.5:30.5
3	Ru.2bf	100	31	70:30
4	Ru.2bc	100	38	60:40
5	Ru.4ba	100	59	85.5:14.5

Conditions: 28 μmol of **3.13a**, 28 μmol of **3.14a**, 1.4 μmol of **[Ru]**, 9.7 μmol of **MeI**, 2.8 μmol of **PPh₃**, 0.125 M in solvent, 18 h; Yields and conversions of oxa-benzonorbornadiene **3.13a** were determined by ¹H NMR with CH₂Br₂ as internal standard; A single diastereomer was observed; enantiomeric ratio was determined by HPLC with a chiral stationary phase.

As a next step, different aryl substituents on the cyclopentane-fused Cp^x ligand were evaluated. In general, only a minor influence on both yield and enantioselectivity was observed (Table 3-2), with yields in a narrow range of (53–63%) and an almost unchanged enantioselectivity for 2- or 4-alkyl aryl (Entry 2 and 3). However, changing to a 2-methoxy substituted aryl group resulted in a slight decrease in enantioselectivity, 82:18 er (Entry 4), while a 4-methoxy aryl substituent gave similar results to phenyl and 2-tolyl (Entry 5). Biphenyl substituents and 3,5-dimethyl aryl substituents caused a slight decrease in enantioselectivity to ca. 81:19 er (Entry 6 and 7).

Table 3-2: Ligand substituent screening.



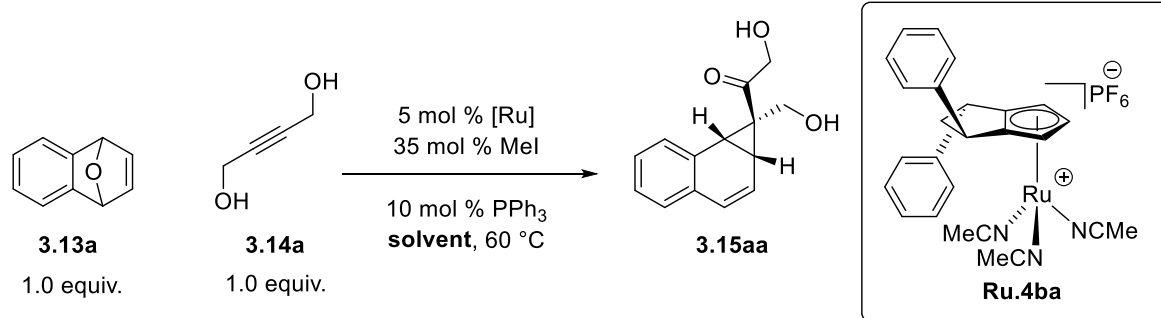
Entry	Substituent (R)	Conversion [%]	Yield [%]	er
1	C ₆ H ₄	100	59	85.5:14.5
2	2-Me-C ₆ H ₄	100	63	85.5:14.5
3	4- <i>i</i> Pr-C ₆ H ₄	100	62	84.5:15.5
4	2-MeO-C ₆ H ₄	100	57	82:18
5	4-MeO-C ₆ H ₄	100	63	86.5:13.5
6	biphenyl	100	65	81:19
7	3,5-Me ₂ -C ₆ H ₃ ^a	100	53	19.5:80.5

Conditions: 28 μmol of **3.13a**, 28 μmol of **3.14a**, 1.4 μmol of [Ru], 9.7 μmol of MeI, 2.8 μmol of PPh₃, 0.125 M in solvent, 18 h; Yields and conversions of oxa-benzonorbornadiene **3.13a** were determined by ¹H NMR with CH₂Br₂ as internal standard; A single diastereomer was observed; enantiomeric ratio was determined by HPLC with a chiral stationary phase. [a] Opposite absolute stereochemistry of the catalyst.

Subsequently, solvent screening was conducted, evaluating with aromatic, chlorinated, polar aprotic, and polar protic solvents (Table 3-3). Acetone gave the best balance between yield and enantioselectivity (59% yield, 85.5:14.5 er) (Entry 1). 2-Butanone, which has similar properties to acetone but with a higher boiling point, resulted in virtually the same results (57%, 84:16 er) (Entry 2). Benzene, representative for aromatic solvents, had an adverse effect on both yield and enantioselectivity (Entry 3). Dioxane, which was used for the racemic version of the reaction, and tetrahydrofuran resulted in a loss of enantioselectivity (Entry 4 and 5). As examples of chlorinated solvents, dichloromethane and dichloroethane were also evaluated (Entry 6 and 7).

Dichloromethane gave a similar result to acetone (62% yield, 85:15 er), while dichloroethane led to a slight loss in both of yield and enantioselectivity (55%, 82.5:17.5 er). Polar aprotic solvents that can coordinate to ruthenium induced similar or improved enantioselectivity, but accompanied by a considerable decrease in yield to ca. 15% (Entry 8 and 9). Alcoholic solvents increased enantioselectivity to ca. 85:15 er, but had an adverse effect on the yield (27–40% yield) (Entry 10–12)

Table 3-3: Solvent screening.



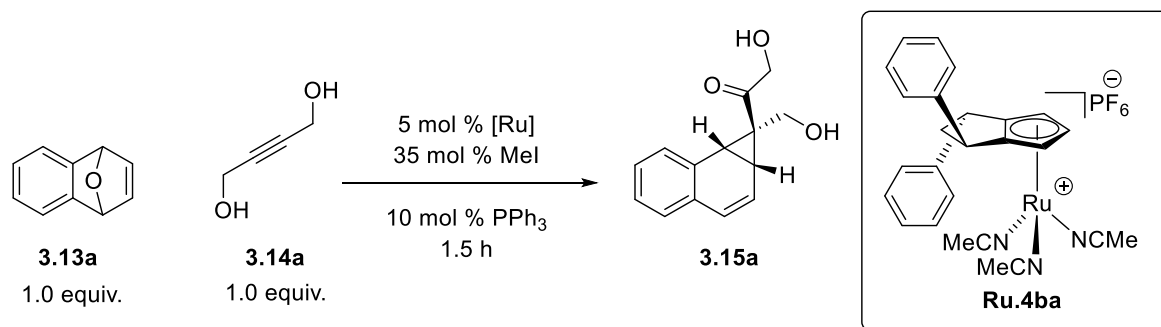
Entry	Solvent	Conversion [%]	Yield [%]	er
1	acetone	100	59	85.5:14.5
2	2-butanone	100	57	84:16
3	benzene	95	47	81.5:18.5
4	dioxane	100	63	79:21
5	THF	100	55	80:20
6	DCM	100	62	85:15
7	DCE	100	55	82.5:17.5
8	DMF	68	14	89.5:10.5
9	acetonitrile	78	16	83:17
10	<i>t</i> BuOH	77	27	82:18
11	<i>i</i> PrOH	92	40	87.5:12.5
12	EtOH	97	36	88.5:11.5

Conditions: 28 μmol of **3.13a**, 28 μmol of **3.14a**, 1.4 μmol of **Ru.4ba**, 9.7 μmol of MeI, 2.8 μmol of PPh₃, 0.125 M in solvent, 18 h; Yields and conversions of oxa-benzonorbomadiene **3.13a** were determined by ¹H NMR with CH₂Br₂ as internal standard; A single diastereomer was observed; enantiomeric ratio was determined by HPLC with a chiral stationary phase.

Temperature screening showed that the reaction temperature affected both enantioselectivity and yield of the reaction (Table 3-4). With acetone as solvent, 60 °C was the optimal temperature in

terms of yield. However, a higher enantioselectivity was obtained with higher reaction temperatures. (Entry 1–3). In order to run the reaction at higher temperatures, 2-butanone and 3-pentanone, congeners of acetone with higher boiling points, were used. For 2-butanone, 80 °C was the best reaction temperature, resulting in a slightly improved enantiomeric ratio (89.5:10.5) and yield (61%) compared to the reaction in acetone at 60 °C (Entry 4–6). The reactions were also conducted in 3-pentanone. Temperatures above 80 °C had a detrimental effect on yield (Entry 7–9).

Table 3-4: Solvent and temperature screening.

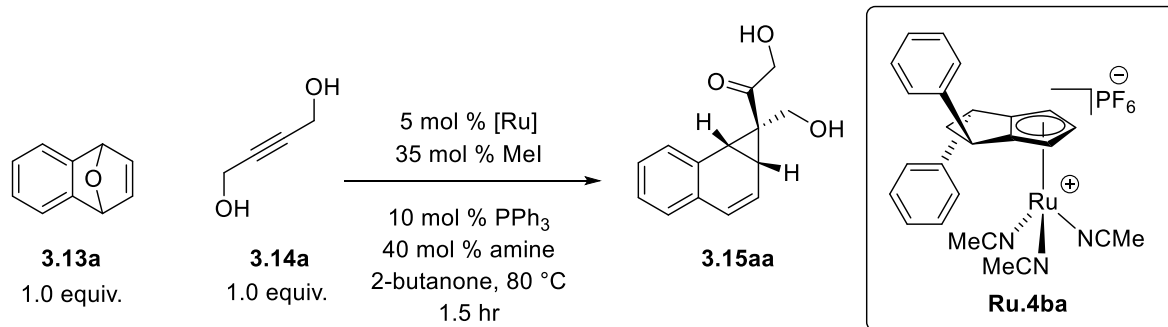


Entry	Temperature	Solvent	Conversion [%]	Yield [%]	er
1	40	acetone	96	42	73.5:26.5
2	60		100	59	85.5:14.5
3	80		57	27	90:10
4	60	2-butanone	100	57	84:16
5	80		100	61	89.5:10.5
6	100		100	59	89.5:10.5
7	80	3-pentanone	100	63	87.5:12.5
8	100		100	59	91.5:8.5
9	120		100	37	90.5:9.5

Conditions: 28 μmol of **3.13a**, 28 μmol of **3.14a**, 1.4 μmol of **Ru.4ba**, 9.7 μmol of MeI, 2.8 μmol of PPh₃, 0.125 M in solvent; Yields and conversions of oxa-benzonorbornadiene **3.13a** were determined by ¹H NMR with CH₂Br₂ as internal standard; A single diastereomer was observed; enantiomeric ratio was determined by HPLC with a chiral stationary phase.

The effect of amine bases were evaluated (Table 3-5). DMAP and pyridine improved enantioselectivity up to 97.5:2.5 er, but decreasing the yield (Entry 2 and 3). DBU only made marginal change in terms of yield without effect on enantioselectivity (Entry 4).

Table 3-5: Screening of amine base.

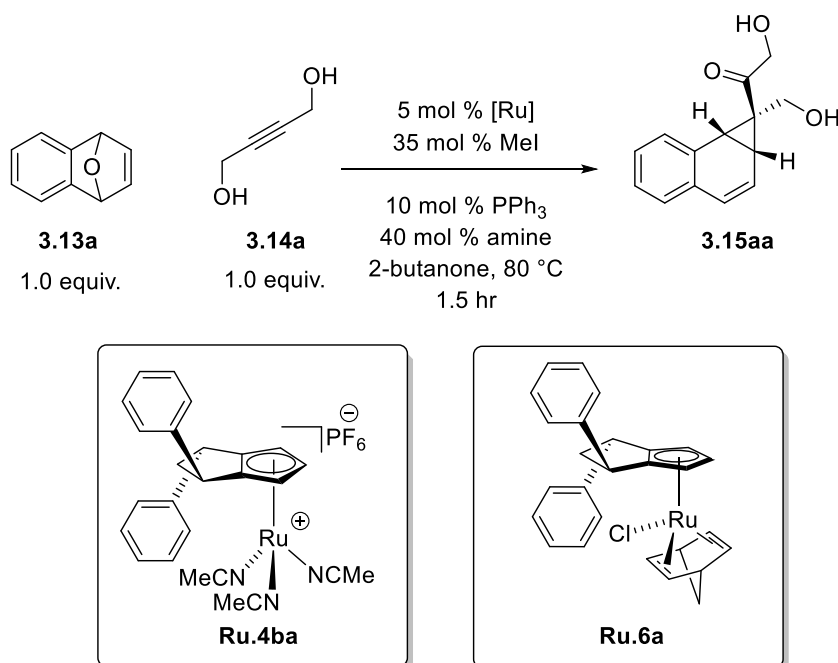


Entry	Amine	Conversion [%]	Yield [%]	er
1	none	100	61	89.5:10.5
2	DMAP	45	12	95:5
3	Pyridine	76	36	97.5:2.5
4	DBU	100	58	89.5:10.5

Conditions: 28 μmol of **3.13a**, 28 μmol of **3.14a**, 1.4 μmol of **Ru.4ba**, 9.7 μmol of MeI, 2.8 μmol of PPh₃, 11 μmol of amine, 0.125 M in solvent; Yields and conversions of oxa-benzonornbornadiene **3.13a** were determined by ¹H NMR with CH₂Br₂ as internal standard; A single diastereomer was observed; enantiomeric ratio was determined by HPLC with a chiral stationary phase.

Because pyridine and 4-dimethylaminopyridine boosted enantioselectivity, further screening with pyridine derivatives was conducted (Table 3-6). All evaluated pyridine derivatives substantially increased enantioselectivity to ca. 97:3 er. Compared with the addition of pyridine, *o*-substituted pyridines improved the yield to about 50% with nearly the same enantioselectivity (up to 97.5:2.5 er (Entry 3–5). In contrast, 2-substituted or 4-substituted pyridine derivatives decreased the yield, even though the enantioselectivity was constantly high (Entry 6 and 7). Neutral ruthenium complex **Ru.6a** was also evaluated (Entry 8). It gave virtually the same enantioselectivity (96.5:3.5 er), as the cationic complex **Ru.4ba**, but did not give any improvement in yield.

Table 3-6: Screening of pyridine derivatives.

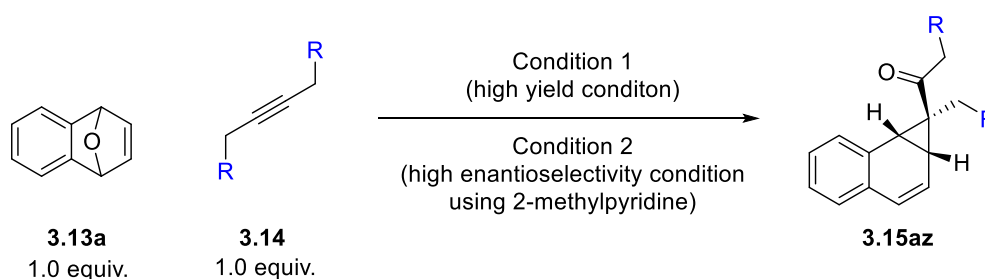


Entry	Ru cat.	Amine	Conversion [%]	Yield [%]	er
1	Ru.4ba	none	100	61	89.5:10.5
2	Ru.4ba	pyridine	76	36	97.5:2.5
3	Ru.4ba	2,6-lutidine	100	50	97:3
4	Ru.4ba	2-methylpyridine	97	47	97.5:2.5
5	Ru.4ba	2-isopropylpyridine	95	48	96.5:3.5
6	Ru.4ba	3-methylpyridine	66	29	96.5:3.5
7	Ru.4ba	4-methylpyridine	55	22	96.5:3.5
8	Ru.6a^a	2-methylpyridine	89	33	96.5:3.5

Conditions: 28 μmol of **3.13a**, 28 μmol of **3.14a**, 1.4 μmol of [Ru], 9.7 μmol of MeI, 2.8 μmol of PPh₃, 11 μmol of a pyridine derivative, 0.125 M in solvent; Yields and conversions of oxa-benzonorbornadiene **3.13a** were determined by ¹H NMR with CH₂Br₂ as internal standard; A single diastereomer was observed; enantiomeric ratio was determined by HPLC with a chiral stationary phase.; [a] Without addition of iodomethane.

The influence of 2-methylpyridine as an additive was checked on other alkynes. Two sets of reaction conditions were evaluated (Table 3-7). The first one, without additive, gave the best yield for di-propargyl alcohol **3.14a**, while the conditions employing 2-methylpyridine gave the highest enantioselectivity in that case. In contrast to the reaction with di-propargyl alcohol **3.14a**, the additive did not increase selectivity for the reaction of alkynes such as dimethyl ether **3.14b** or dicarbonate **3.14c** (Entry 3–6). In both cases, the addition of 2-methylpyridine resulted in a slight loss in yield with virtually the same enantioselectivity. Those results lead to the conclusion that pyridine derivatives increase the enantioselectivity only for di-propargyl alcohol substrate **3.14a**.

Table 3-7: The effect of a pyridine derivative on other alkynes.

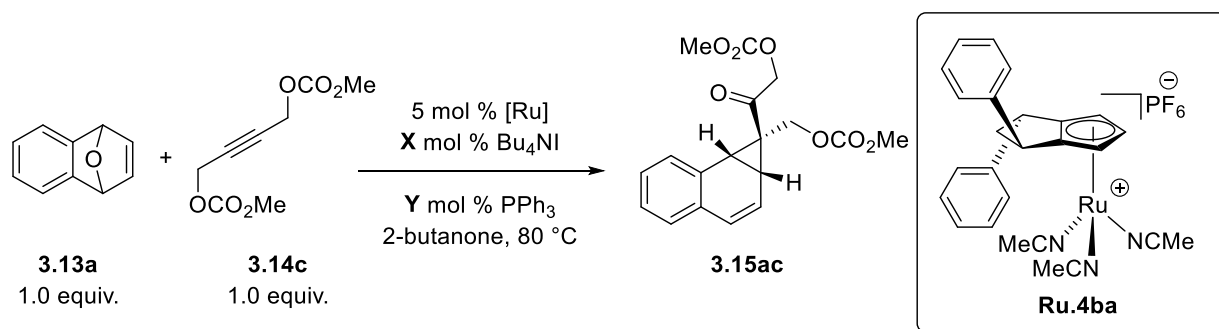


Entry	R	Condition	Conversion [%]	Yield [%]	er
1	OH	Condition 1	100	71	85.5:14.5
2	OH	Condition 2	97	47	97.5:2.5
3	OMe	Condition 1	100	63	76.5:23.5
4	OMe	Condition 2	98	59	77.5:22.5
5	OCO ₂ Me	Condition 1	100	57	93.5:6.5
6	OCO ₂ Me	Condition 2	100	49	94:6

Conditions 1: 28 μ mol of **3.13a**, 28 μ mol of **14**, 1.4 μ mol of **Ru.4ba**, 9.7 μ mol of Bu₄NI, 1.4 μ mol of PPh₃, 0.125 M in solvent; Conditions 2.: 28 μ mol of **3.13a**, 28 μ mol of **3.14**, 1.4 μ mol of **Ru.4ba**, 9.7 μ mol of MeI, 2.8 μ mol of PPh₃, 11 μ mol of 2-methylpyridine, 0.125 M in solvent; Yields and conversions of oxa-benzonornbornadiene **3.13a** were determined by ¹H NMR with CH₂Br₂ as internal standard; A single diastereomer was observed; enantiomeric ratio was determined by HPLC with a chiral stationary phase.

With those results in hand, the optimization for the reaction was performed again with butyne dicarbonate **3.14c**. Each component of the previous reaction conditions was re-evaluated to confirm its effect (Table 3-8). At first, the effects of triphenyl phosphine and tetrabutylammonium iodide were investigated. In contract to the case with di-propargyl alcohol **3.13a**, the omission of triphenylphosphine showed very little effect on enantioselectivity, (94:6 er, Entry 1 and 2) A decreased loading of tetrabutylammonium iodide was also evaluated, having virtually no effect on both yield and enantioselectivity (57% yield with 95:5 er, Entry 3 and 4).

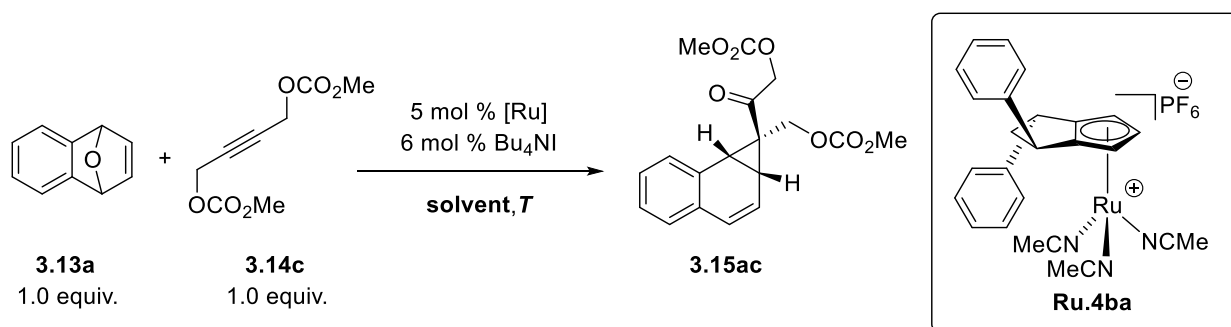
Table 3-8: Effect of triphenylphosphine and tetrabutylammonium iodide.



Entry	PPh ₃	Bu ₄ NI	Conversion [%]	Yield [%]	er
1	5 mol %	35 mol %	100	57	93.5:6.5
2	None	35 mol %	100	53	94:6
3	None	10 mol %	100	56	95:5
4	None	6 mol %	100	57	95:5

Conditions: 42 μmol of **3.13a**, 42 μmol of **3.14c**, 2.1 μmol of **Ru.4ba**, 6–35 mol % of Bu₄NI, 2.1 μmol of PPh₃ or not, 0.125 M in solvent; Yields and conversions of oxa-benzonorbornadiene **3.13a** were determined by ¹H NMR with CH₂Br₂ as internal standard; A single diastereomer was observed; enantiomeric ratio was determined by HPLC with a chiral stationary phase.

The choice of solvent was also re-evaluated (Table 3-9). Polar coordinating solvents such as acetonitrile lowered the reaction rate and brought about a poor yield (10%) with moderate enantioselectivity, 87.5:12.5 er (Entry 1). Dioxane and acetone improved both yield and enantioselectivity, 58% yield with 93:7 er (Entry 2 and 3). 2-Butanone, which has similar properties to acetone, slightly improved enantioselectivity (95:5 er) with 57% yield (Entry 4). The reaction temperature screening was performed without triphenylphosphine and a lower loading of tetrabutylammonium iodide at 6 mol%, (Entry 5–8). This screening showed that 100 °C is the optimal temperature for the reaction (Entry 7), giving the product in the highest yield, 71%, along with a high enantioselectivity (95:5 er). Notably, enantioselectivity was not affected by the reaction temperature.

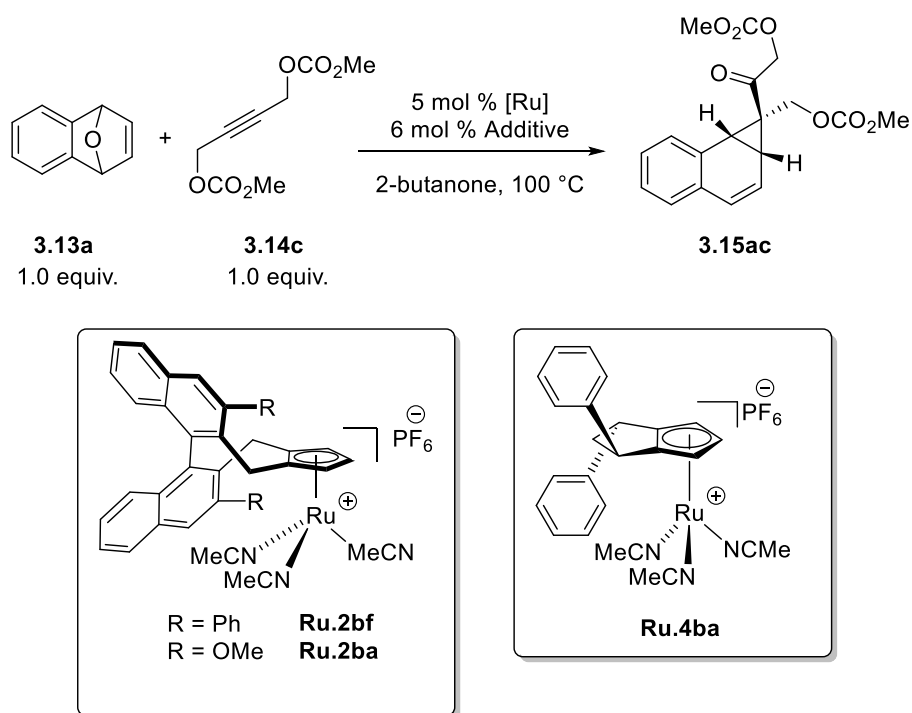
Table 3-9: Temperature and solvent screening without PPh₃.

Entry	Solvent	Temperature	Conversion [%]	Yield [%]	er
1	acetonitrile	60	55	10	87.5:12.5
2	dioxane	60	100	58	93:7
3	acetone	60	100	53	93:7
4	2-butanone	60	100	57	95:5
5	2-butanone	40	100	19	95:5
6	2-butanone	80	100	66	95:5
7	2-butanone	100	100	71	95:5
8	2-butanone	120	100	61	95:5

Conditions: 42 μmol **3.13a**, 42 μmol of **3.14c**, 2.1 μmol **Ru.4ba**, 2.5 μmol Bu_4NI , 0.125 M in solvent, 30 min.; Isolated yields, conversions determined by ^1H NMR with CH_2Br_2 as internal standard; A single diastereomer was observed; enantiomeric ratio was determined by HPLC with a chiral stationary phase.

The effect of the halide counterion and ligand were then reinvestigated (Table 3-10). Binaphthyl-derived Cp^x ruthenium complexes **Ru.2bf** and **Ru.2ba**,^{65c} which have been successfully utilized for other ruthenium catalyzed asymmetric reactions, gave the product in poor yield of 9–23% and low enantioselectivity (Entry 1 and 2). Cyclopentane-fused Cp^x ruthenium complex **Ru.4ba** induced a significantly higher yield, 71%, with excellent enantioselectivity (95:5 er) (Entry 3). Other halides, bromide and chloride, had detrimental effects on the reaction in terms of reactivity and enantioselectivity (Entry 4 and 5). Conducting the reaction without a halide additive resulted in a substantially decreased yield and enantioselectivity (31% yield and 69.5:30.5 er). (Entry 6), showing the importance of a coordinating halide on the ruthenium complex. Starting materials **3.13a** and **3.14c** were recovered from the control reaction without ruthenium and halide additive.

Table 3-10: Ligand and halide additive screening.



Entry	Ru cat.	Additive	Conversion [%]	Yield [%]	er
1	Ru.2bf	Bu ₄ NI	100	9	67:33
2	Ru.2ba	Bu ₄ NI	100	23	70.5:29.5
3	Ru.4ba	Bu ₄ NI	100	71	95:5
4	Ru.4ba	Bu ₄ NBr	100	47	94:6
5	Ru.4ba	Bu ₄ NCl	64	17	87.5:12.5
6	Ru.4ba	none	100	31	69.5:30.5
8	none	none	7		

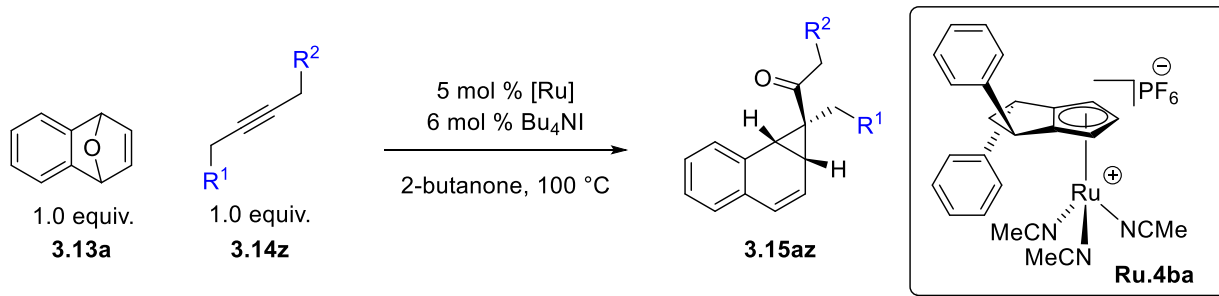
Conditions: 42 μmol **3.13a**, 42 μmol of **3.14c**, 2.1 μmol [Ru], 2.5 μmol Additive, 0.125 M in 2-butanone, 30 min.; Isolated yields, conversions determined by ^1H NMR with CH_2Br_2 as internal standard; A single diastereomer was observed; enantiomeric ratio was determined by HPLC with a chiral stationary phase.

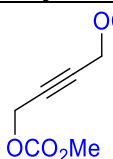
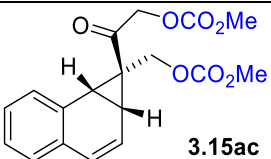
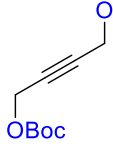
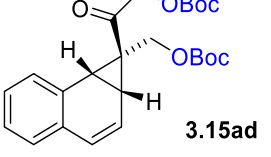
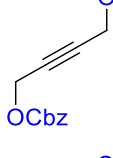
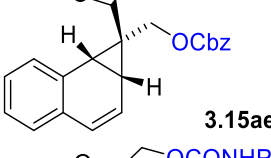
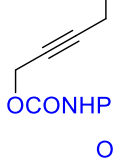
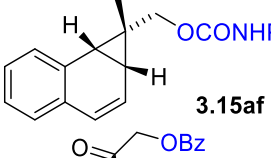
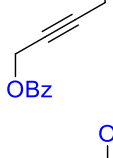
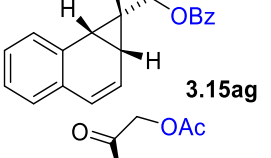
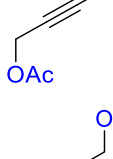
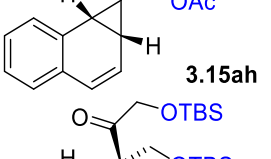
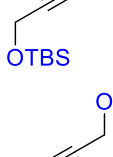
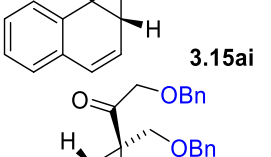
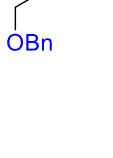
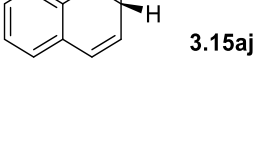
3.3 Reaction Scope

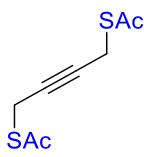
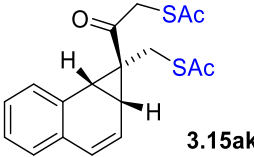
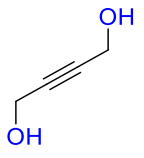
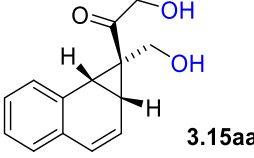
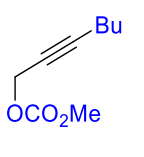
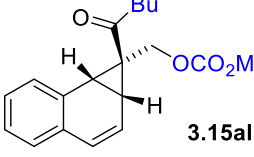
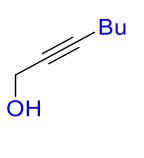
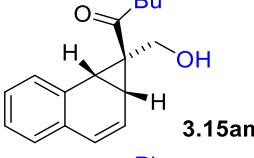
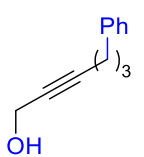
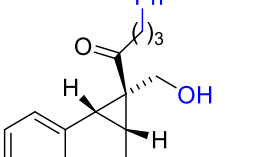
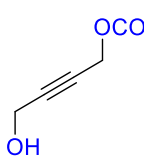
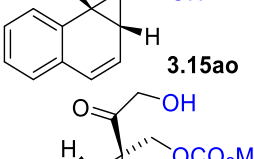
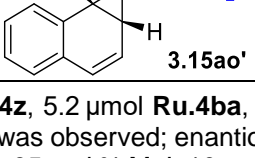
The scope of the reaction was investigated, firstly by examining different alkyne groups (Table 3-11). Internal alkynes with propargylic carbonates delivered the desired *exo*-benzonorcaradiene **3.15** well, with yields ranging from 65–76% as well as high enantioselectivities (ca. 95:5 er) (Table 3-11, Entry 1–3). Alkyne **3.14f** with carbamoyl moieties also worked well, and brought about a good yield of **3.15af** (63%) with high enantioselectivity, 93:7 er (Table 3-11, Entry 4). Alkynes with propargylic benzoate **3.14g** and acetate substituents **3.14h** were transformed to the corresponding

benzonorcaradienes (**3.15ag** and **3.15ah**) in good yields and high enantioselectivities (Table 3-11, Entry 5 and 6). The influence of coordinating groups on the substrates was probed with alkynes bearing *tert*-butyldimethylsilyl ether **3.14i** or benzyl ether moieties **3.14j** (Table 3-11, Entry 7 and 8). They both gave the corresponding product with decreased enantioselectivities of 74:26 er and 75:25 er, respectively. Compared to the case of propargylic benzoate **3.14g** (Table 3-11, Entry 5), the case of benzyl ether substrate **3.14j** exhibits the impact of coordinating substituents on enantioselectivity. A noticeable result came from employing thioester-containing alkyne **3.14k**, which was transformed to the respective product with a high enantioselectivity of 97.5: 2.5 er (Table 3-11, Entry 9). An alkyne substrate with free hydroxyl groups **3.14a** was tolerated, and delivered the corresponding benzonorcaradiene in 63% yield and 85:15 er (Table 3-11, Entry 10). As described in the previous chapter, enantioselectivity for this substrate could be increased to 97.5:2.5 er by using 2-methylpyridine as an additive (Table 3-6, Entry 4). Unsymmetrical alkynes that contain only a single propargylic oxygen induced lower yields than the cases with symmetrical ones (Table 3-11, Entry 11–14). The main cause of the decrease in yield was a competing [2+2]-cycloaddition process, which produced cyclobutene byproducts.^{65a, b} Even though yield of the desired benzonorcaradiens was low, only a single regioisomer was observed. Inter-ligand interaction by hydrogen bonding between ruthenium halide and a hydroxyl group of propargyl alcohol⁹⁹ or interaction between lone pair of a halide and π^* orbital of a carbonyl group¹⁰⁰ set the orientation of a coordinating alkyne. Presumably, it induces high regioselectivity on these unsymmetrical alkynes. The enantiomeric ratio of the desired benzonorcaradiene **3.15al**, **3.15am** and **3.15an** was excellent, 94:6 to 97:3 er. The alkyne possessing one free hydroxyl group and one methyl carbonate gave a 2.9:1 mixture of regioisomers **3.15ao** and **3.15ao'** in 60% combined yield (Table 3-11, Entry 14).

Table 3-11: Variation of alkyne.



Entry	alkyne	benzonorcaradiene	Yield [%]	er
1	 3.14c	 3.15ac	76	95:5
2	 3.14d	 3.15ad	71	93.5:6.5
3	 3.14e	 3.15ae	65	94:6
4	 3.14f	 3.15af	63	93:7
5	 3.14g	 3.15ag	61	95:5
6	 3.14h	 3.15ah	63	95.5:4.5
7	 3.14i	 3.15ai	48	74:26
8	 3.14j	 3.15aj	63	75:25

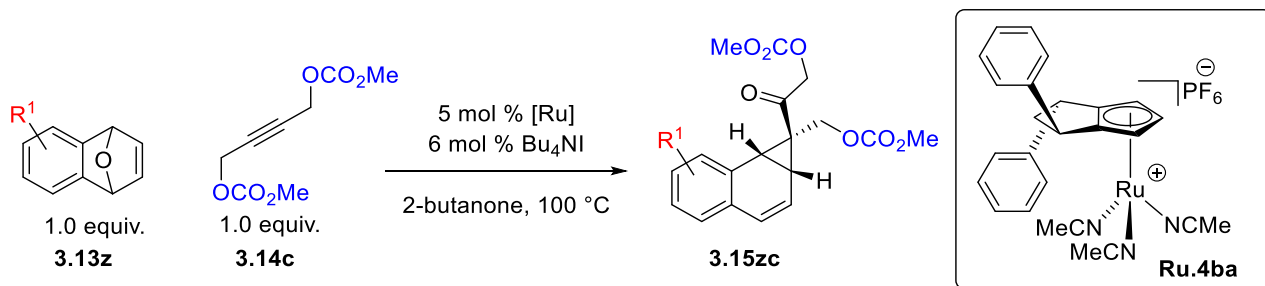
9		3.14k		3.15ak	51	97.5:2.5
10		3.14a		3.15aa	64 (47) ^a	85:15 (97.5:2.5) ^a
11		3.14l		3.15al	26	97:3
12		3.14m		3.15am	39	94:6
13		3.14n		3.15an	34	95:5
14		3.14o		3.15ao	60 (3.15ao:3.15ao' = 2.9:1)	86:14 (3.15ao)
				3.15ao'		91.5:8.5 (3.15ao')

Conditions: 104 μ mol **3.13a**, 104 μ mol of **14z**, 5.2 μ mol **Ru.4ba**, 6.2 μ mol Bu₄NI, 0.125 M in 2-butanone, 30 min.; Isolated yields; A single diastereomer was observed; enantiomeric ratio was determined by HPLC with a chiral stationary phase.; [a] 5 mol % **Ru.4ba**, 35 mol % MeI, 10 mol % PPh₃, 40 mol % 2-methylpyridine, 0.125 M at 80 °C for 90 min.

Next, the scope of oxa-benzonorbornadienes was explored (Table 3-12). An oxa-benzonorbornadiene bearing electron-donating methoxy groups **3.13b** was converted to the desired benzonorcaradiene **3.15bc** in 65% yield and 92:8 er (Entry 1). Analogously, 5,8-dimethoxy oxa-benzonorbornadiene **3.13c**, an isomer of **3.13b**, gave the corresponding benzonorcaradiene **3.15cc** in 62% yield and 88:12 er (Entry 2). In this case, a slight decrease of enantioselectivity was observed. Presumably, the methoxy group proximal to the newly generated stereogenic centers slightly impedes the enantiodetermining step. A slight decrease in yield was attributed to the relatively lower stability of the benzonorcaradiene products **3.15bc** and **3.15cc** compared to the parent product **3.15ac**. 6,7-Dimethyl-substituted oxa-benzonorbornadiene **3.13d** smoothly delivered the

corresponding benzonorcaradiene **3.15dc** in 81% yield and 92.5:7.5 er (Entry 3). An oxa-benzonorbornadiene containing electron withdrawing groups, 6,7-dibromo substituted oxa-benzonorbornadiene, gave product **3.15ec** in a moderate yield of 48% (Entry 4), but with high enantioselectivity (96:4 er).

Table 3-12: Variation of oxa-benzonorbonadiene.



Entry	oxa-norbornadiene	benzonorcaradiene	Yield [%]	er
1	 3.13b	 3.15bc	65	92:8
2	 3.13c	 3.15cc	62	88:12
3	 3.13d	 3.15dc	81	92.5:7.5
4	 3.13e	 3.15ec	48	96:4

Conditions: 104 µmol **3.13z**, 104 µmol of **3.14c**, 5.2 µmol **Ru.4ba**, 6.2 µmol Bu₄NI, 0.125 M in 2-butanone, 30 min.; Isolated yields; A single diastereomer was observed; enantiomeric ratio was determined by HPLC with a chiral stationary phase.

A crystal of benzonorcaradiene **3.15aa** was obtained by slow evaporation of a solution of **3.15aa** in dichloromethane. The absolute stereochemistry of benzonorcaradiene of **3.15aa** was determined by X-ray crystallography (Figure 3-2).¹⁰¹

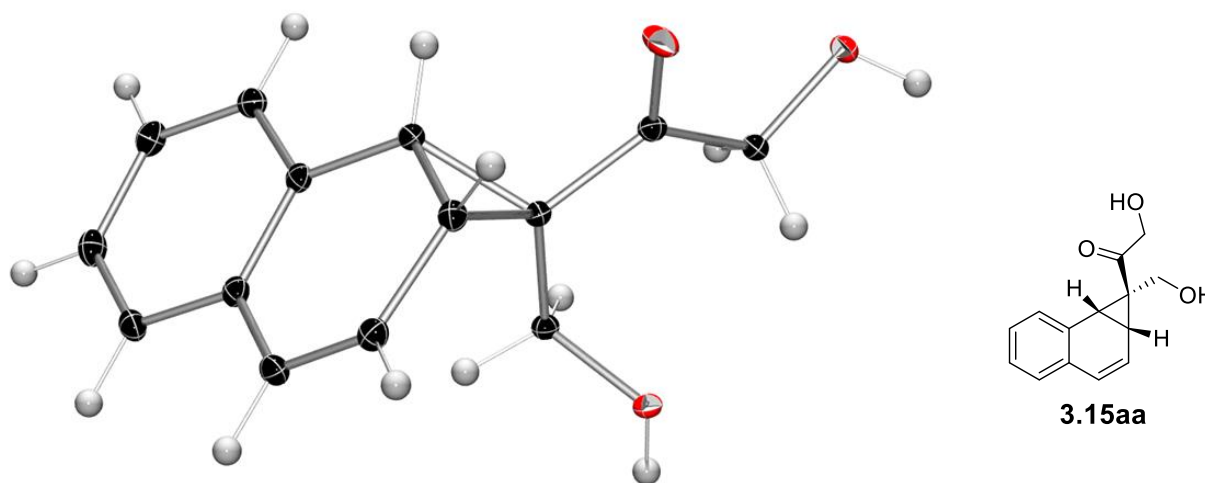
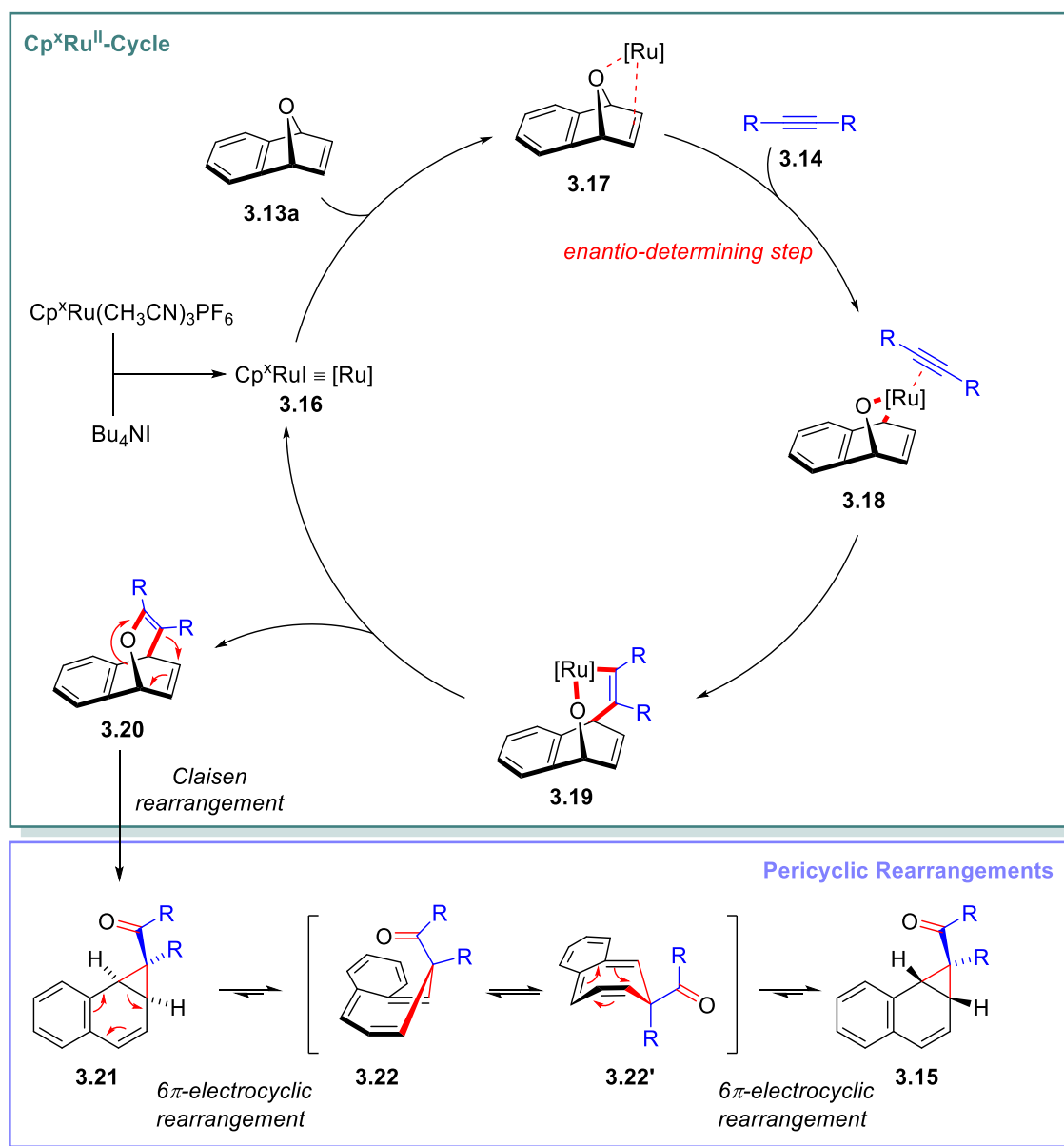


Figure 3-2: Crystal structure of **3.15aa**.

3.4 Reaction Mechanism Study

The reaction mechanism can be grouped into two parts: a ruthenium-based catalytic cycle followed by a series of pericyclic reactions (Scheme 3-4).⁹⁵ The cationic ruthenium species, $\text{Cp}^*\text{Ru}(\text{CH}_3\text{CN})_3\text{PF}_6$, and tetrabutylammonium iodide produce a neutral ruthenium iodide complex. Coordination of oxa-benzonorcaradiene **3.13a** and the resulting neutral ruthenium iodide form intermediate **3.17**. Oxidative addition of the ruthenium iodide into a C–O bond of intermediate **3.17** and subsequent coordination of an alkyne results in the formation of ruthenacycle **3.18**. Particularly, the oxidative addition into a C–O bond¹⁰² is the enantio-determining step of the reaction: the stereochemistry is determined by which C–O bond reacts. Migratory insertion of intermediate **3.18** into the coordinated alkyne brings about ruthenacycle **3.19**, followed by reductive elimination regenerating ruthenium iodide **3.16** ($[\text{Ru}]$) and releasing allylvinyl ether **3.20**. The allylvinyl ether **3.20** forms an *endo*-product **3.21** through a Claisen rearrangement. Thermal conditions allow the *endo*-product **3.21** to isomerize into benzo cycloheptatriene **3.22** via 6π -electrocyclic ring opening. Ring-flip of benzo cycloheptatriene **3.22** results in a benzo cycloheptatriene **3.22'**, which is followed by a

6 π -electrocyclic ring closing. As a result, the thermodynamically more stable *exo*-product **3.15** is generated.

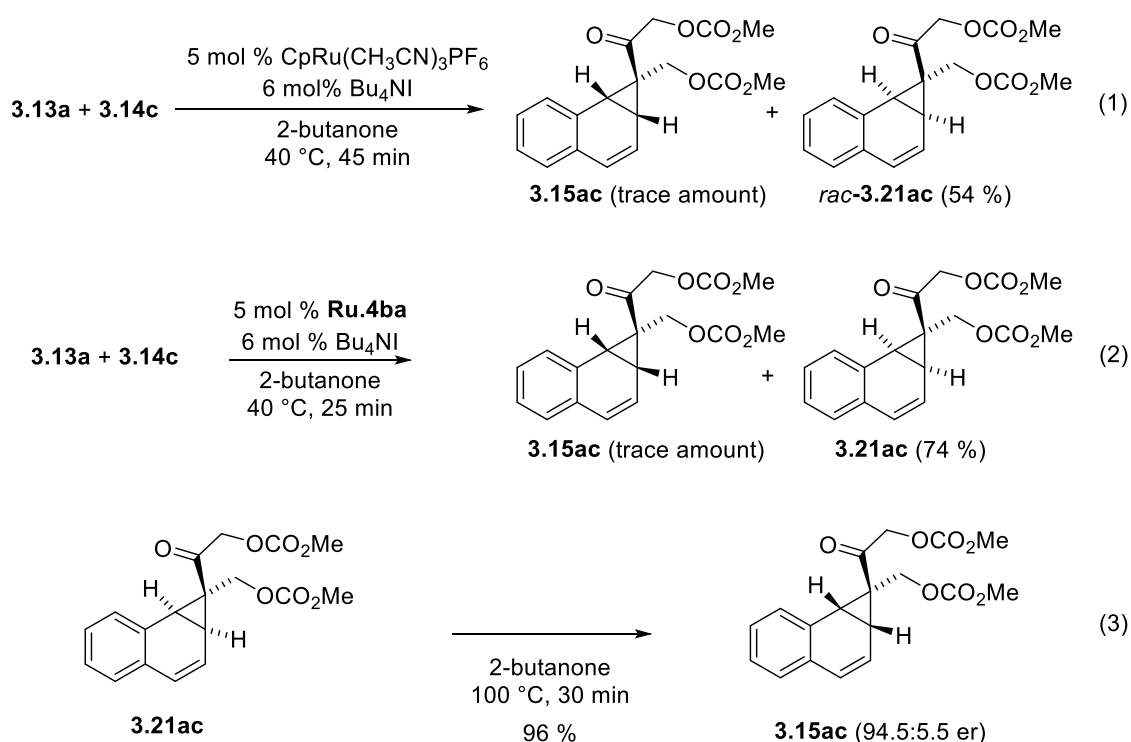


Scheme 3-4: Proposed reaction mechanism of the Cp^xRu(II)-catalyzed coupling of oxa-benzonorbornadienes and alkynes..

3.4.1 Control Experiments

Experimental evidence to support the proposed reaction mechanism was obtained from a series of experiments. Reactions at a lower temperature of 40 °C were conducted using CpRu(CH₃CN)₃PF₆ and cyclopentane-fused chiral Cp^xRu(II) complex **Ru.4ba**, respectively. At this lower reaction temperature, the achiral catalyst delivered 54% yield of *endo*-product **3.21ac** with trace amounts of

exo-product **3.15ac** (Scheme 3-5, equation 1). Analogous results were obtained with chiral catalyst **Ru.4ba**, which gave *endo*-product **3.21ac** in 74% yield with trace amounts of *exo*-product **3.15ac** (Scheme 3-5, equation 2). Under the standard reaction conditions without ruthenium catalyst, the isolated *endo*-product **3.21ac** isomerized to *exo*-product **3.15ac** in a near-quantitative yield of 96% (Scheme 3-5, equation 3). This corroborates the hypothesis that the *endo*-to-*exo* isomerization is a thermal process that does not require the ruthenium catalyst. In addition, the enantiomeric ratio of the *exo*-product **3.15ac** obtained from the control experiment was 94.5:5.5, which is virtually same as that obtained from the standard reaction conditions. This observation indicates that the enantio-determining step of the reaction occurs prior to the formation of *endo*-product **3.21ac**, and *endo*-to-*exo* isomerization is a stereospecific process.



Scheme 3-5: Mechanistic experiments.

3.4.2 Computational Studies

The experimental results were corroborated by DFT calculations. For the optimization of geometries of all species, the B3LYP¹⁰³ functional was used with the Pople basis set¹⁰⁴ 6-31G. The same method and basis set were applied to thermal analysis and zero-point energy correction for computing Gibbs free energy, and a scale factor for vibrational analysis was applied.¹⁰⁵ All transition states only have a single imaginary vibrational mode, and none of the intermediates have an imaginary vibrational frequency.

In order to further confirm the Claisen-electrocyclic pathway,¹⁰⁶ computational studies were conducted using GAMESS¹⁰⁷. The results of computational studies are summarized in an energy profile diagram (Figure 3-3). This profile fits well with the experimental results and explains. The activation energy of the Claisen rearrangement (allyl vinyl ether **3.20ac** to *endo*-isomer **3.21ac**) is 15.8 kcal/mol, which means that allyl vinyl ether **3.20ac** has a half-life of only 11 ms at 40 °C, explaining the failure to experimentally observe allyl vinyl ether **3.20ac**. In addition, a decrease of Gibbs free energy from allyl vinyl ether **3.20ac** to *endo*-product **3.21ac** to -9.7 kcal/mol conveys that this Claisen rearrangement is a spontaneous process. **TS1** has a boat-like geometry due to structural constraints of allyl vinyl ether **3.20ac**. In addition, the computational results account for the high preference of *exo*-benzonorcaradiene **3.15ac** over *endo*-benzonorcaradiene **3.21ac**. The *endo*-to-*exo* isomerization is an energetically downhill process. The energies of *endo*-benzonorcaradiene **3.21ac** and *exo*-benzonorcaradiene **3.15ac** are -9.7 kcal/mol and -13.1 kcal/mol, respectively. The energy gap between *endo*-isomer **3.21ac** and *exo*-isomer **3.15ac** of 3.4 kcal/mol translates to a molar ratio of >98:1 at 100 °C if the system reaches an equilibrium state. Hence, only *exo*-isomer **3.15ac** was observed after thermal isomerization of the isolated *endo*-product **3.21ac**. Furthermore, even though the *endo*-to-*exo* isomerization is an energetically favorable process, it has a high activation energy of 27.8 kcal/mol, which is 12 kcal/mol higher than that of the Claisen rearrangement step. This high activation energy made it feasible to isolate *endo*-product **3.21ac**. The other experimental observation that the computational study accounts for the reason why the two cycloheptatrienes **3.22ac** and **3.22ac'** were not observed. They both have a 14-20 kcal/mol higher energy than benzonorcaradienes **3.21ac** and **3.15ac**, indicating that the equilibrium between benzonorcaradienes (**3.21ac**, **3.15ac**) and cycloheptatrienes (**3.22ac**, **3.22ac'**) will lean significantly to the benzonorcaradienes. In addition, the conversion from cycloheptatrienes **3.22ac** and **3.22ac'** to benzonorcaradienes **3.21ac** and **3.15ac** has almost no barrier, enabling a rapid transition to the benzonorcaradienes. Overall, the computational results corroborate the experimental results and the proposed mechanism.

An alternative reaction pathway was ruled out based on the computational results. This proposed pathway consists of a ring-contraction of dihydrofuran **3.23ac** as an intermediate, producing *endo*-benzonorcaradiene **3.21ac**.^{95, 108} However, the transformation from dihydrofuran **3.23ac** to *exo*-benzonorcaradiene **3.15ac** is energetically uphill in terms of Gibbs free energy. In other words, if there is a chemical equilibrium between dihydrofuran **3.23ac** and *exo*-benzonorcaradiene **3.15ac**, dihydrofuran **3.23ac** should be the major product because of its lower Gibbs free energy. As the major product was *exo*-benzonorcaradiene **3.15ac** and no dihydrofurane was observed in the reaction mixture, this pathway was discarded.

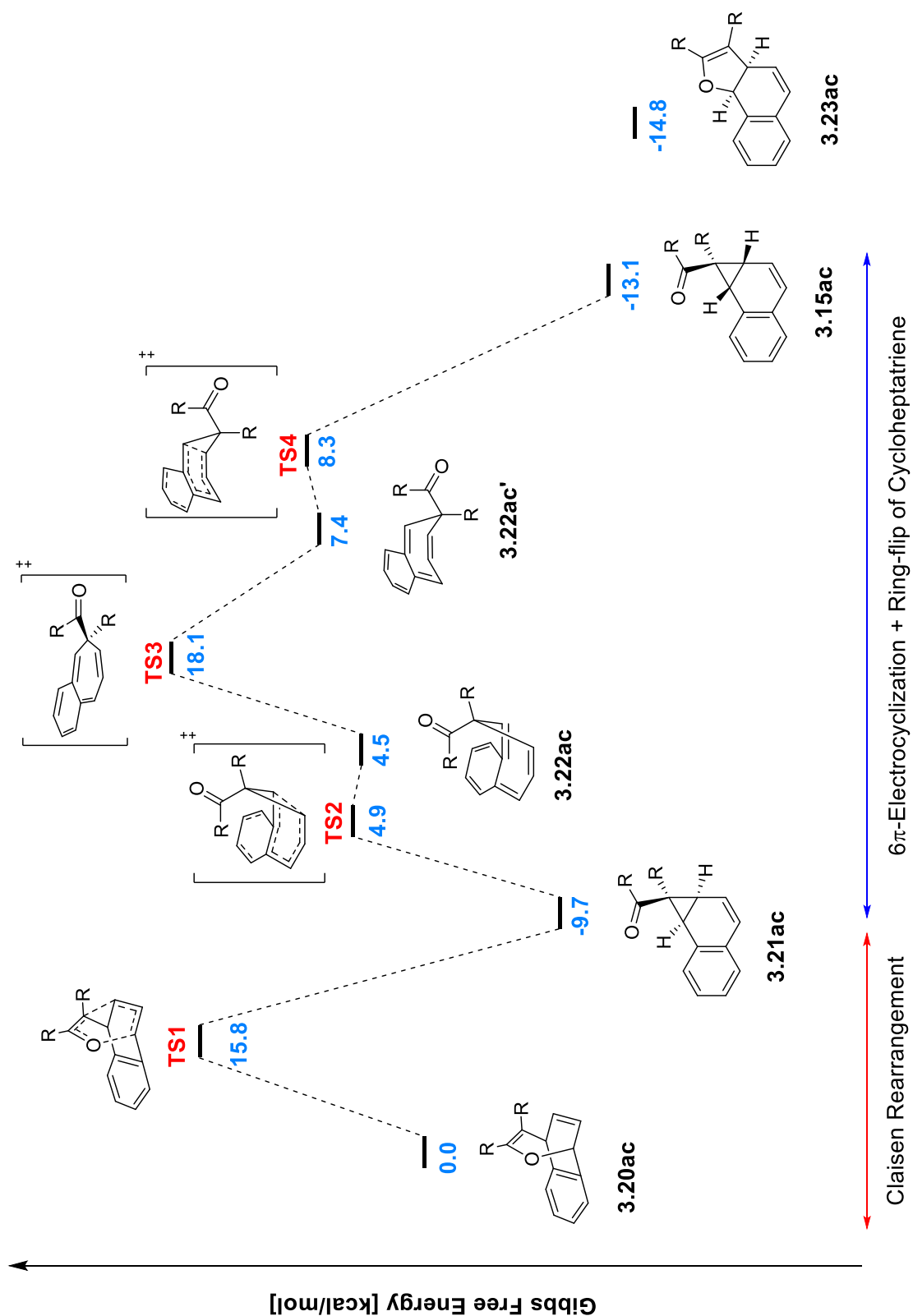


Figure 3-3: Energy profile of Claisen-electrocyclic pathway.
(R = CH₂OCO₂Me)

Chapter 4 Enantioselective Ruthenium(II)- Catalyzed Alkylative Cycloetherification

4.1 Introduction

Oxygen-containing heterocycles are one of the major structural motifs in natural products and pharmaceutical compounds. Among them, furan, pyrrole and spiroketal moieties are associated with intriguing biological activities, such as cytotoxic activity on leukemia and breast cancer cells,¹⁰⁹ antitumor activity,¹¹⁰ inhibition of monoamine oxidase (MAO)¹¹¹ and reverse transcriptase of HIV-1, and anti-telomerase activity.¹¹² Because of their high potency in pharmaceutical applications, there is a strong demand for concise, enantioselective synthetic approaches towards these oxa-cycles.

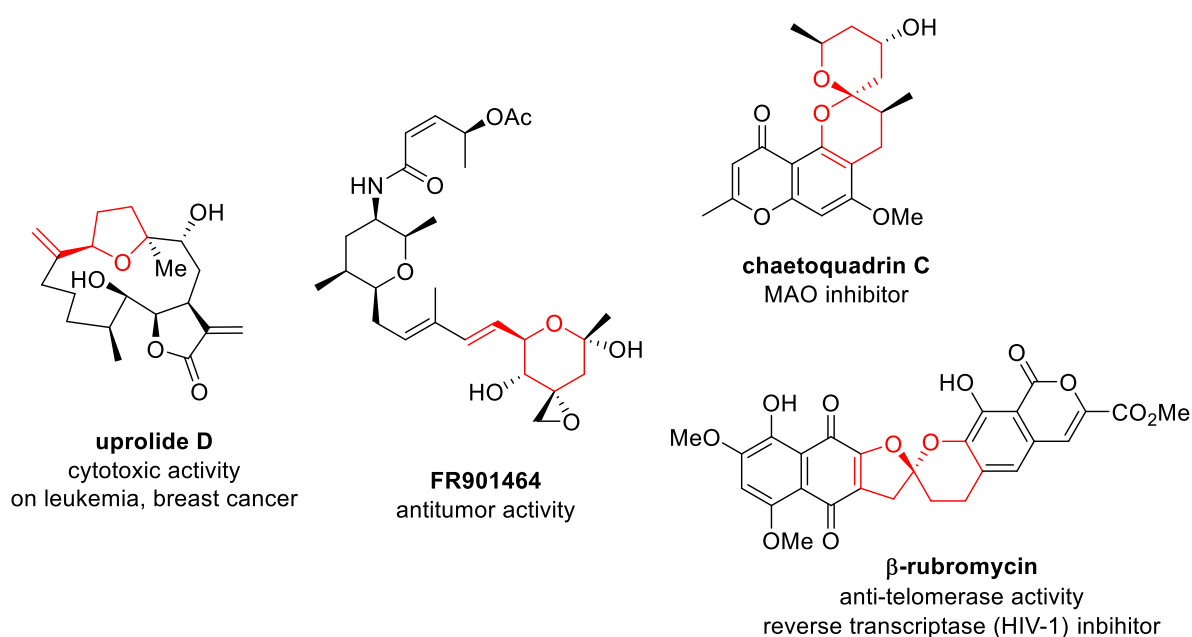
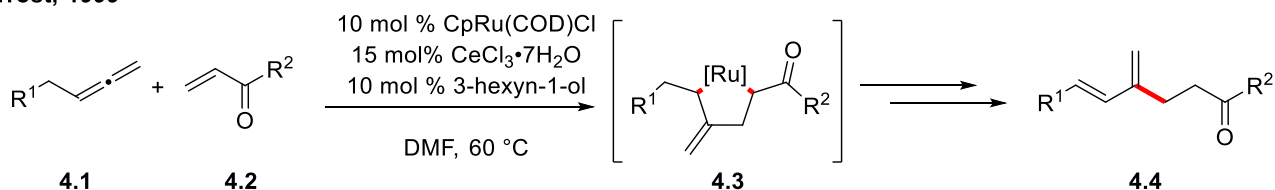


Figure 4-1: Biologically active compounds containing furan, pyran, and spiroketal motifs.

The Trost group has explored ruthenium-catalyzed transformations and proposed the possibility of an alkylative cycloetherification.^{27a, b} They reported a ruthenium catalyzed ene type reaction, and proposed the formation of an allylruthenium intermediate **4.3**, which, in turn, forms an 1,3-diene (Scheme 4-1).³⁰

Trost, 1999

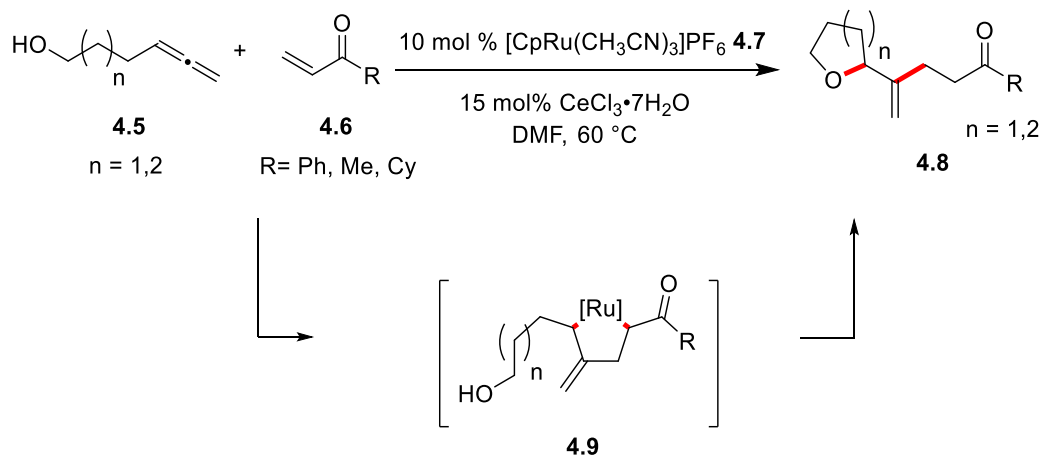


Scheme 4-1: Ruthenium catalyzed ene-type reaction towards 1,3-dienes.

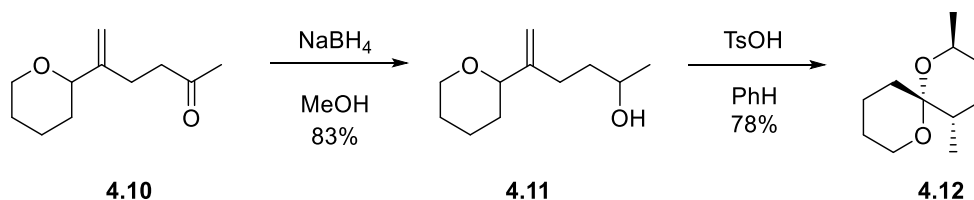
As an extension of their previous research, they developed a ruthenium-catalyzed cycloetherification of allenols (Scheme 4-2a).¹¹³ They postulated the formation of a π -allylruthenium complex, followed by intramolecular nucleophilic addition. This transformation gives an atom-economic approach to cyclic ethers and gives experimental support for the involvement of allylruthenium intermediate **4.9**. The resulting cyclic ethers **4.10** were utilized as precursors for spiroketals **4.12** (Scheme 4-2b).

Trost, 1999

a) Alkylative cycloetherification



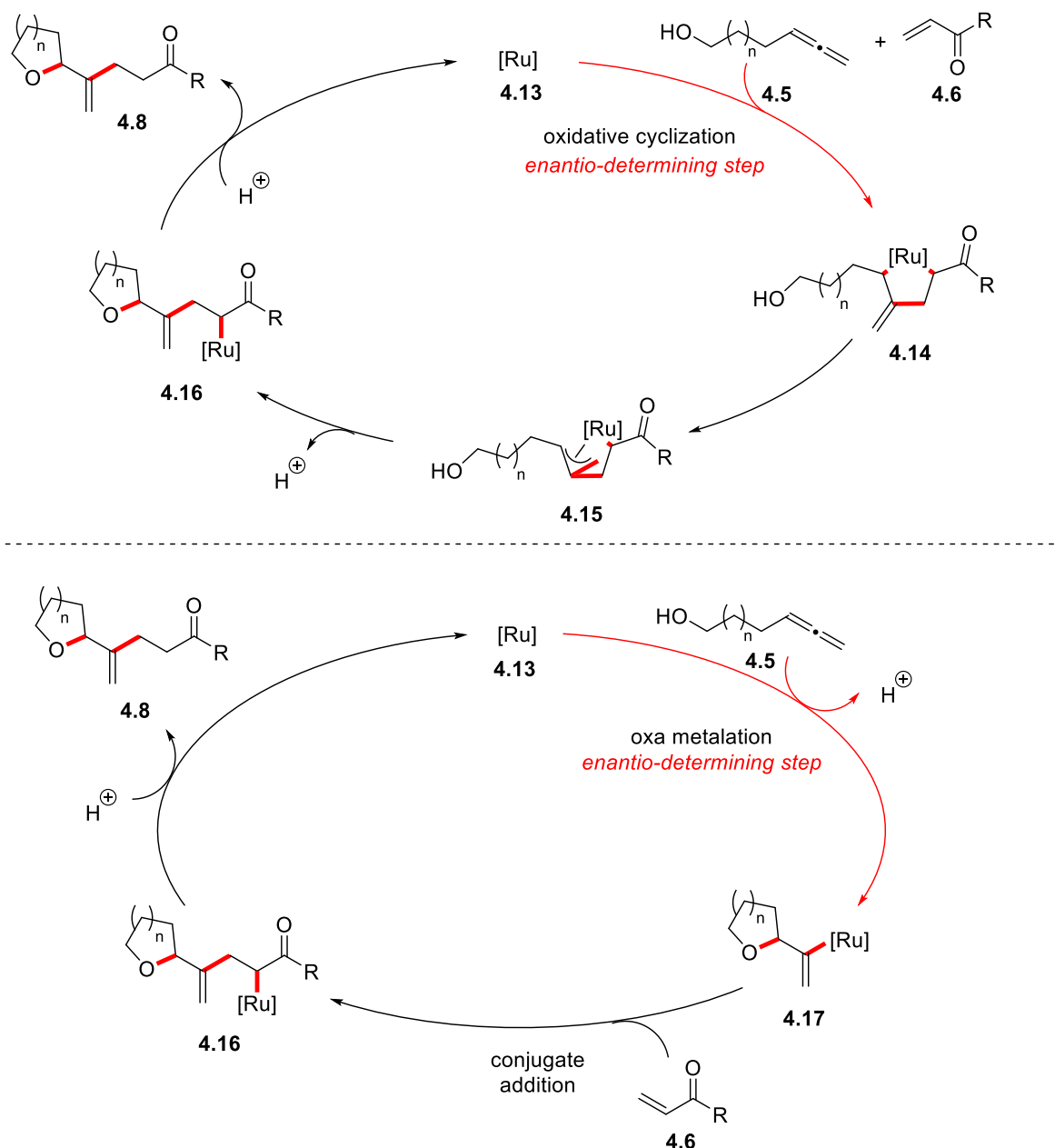
b) Spiroketal formation using the resulting cyclic ether



Scheme 4-2: Ruthenium catalyzed cycloetherification.

The authors proposed two different mechanisms. The first mechanism is initiated by oxidative cyclization of allenol **4.5** and Michael acceptor **4.6**, which constitutes the enantio-determining step

(Scheme 4-3). The resulting σ -allylruthenium intermediate **4.14** (Scheme 4-3) forms a π -allylruthenium complex (**4.15**). An intramolecular nucleophilic attack of the hydroxyl group produces ruthenium enolate (**4.16**, Scheme 4-3). Protonation of intermediate **4.16** releases the desired cyclic ether **4.8** and regenerates the active ruthenium species. The second possible pathway is a ruthenium catalyzed intramolecular addition of the allene, forming intermediate **4.17**. Conjugate addition of alkenyl ruthenium intermediate **4.17** delivers ruthenium enolate **4.16** in the enantio-determining step of this reaction pathway. Protonation gives the desired cyclic ether **4.8**.

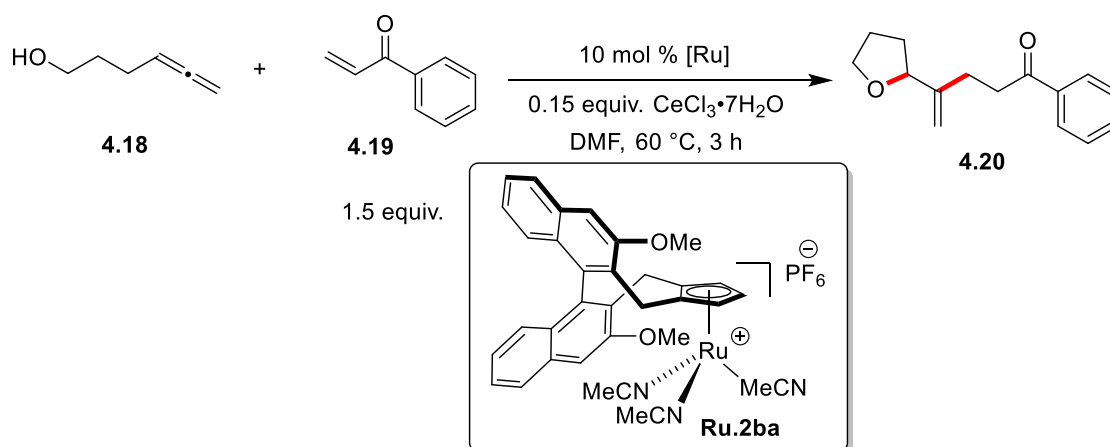


Scheme 4-3: Two proposed mechanisms of ruthenium catalyzed cycloetherification.

4.2 Optimization Studies for Enantioselective Ruthenium(II)-Catalyzed Alkylative Cycloetherification

Allenol **4.18** and phenylvinyl ketone **4.19** were chosen as a model system for optimization of the enantioselective ruthenium(II)-catalyzed alkylative cycloetherification (Table 4-1). Achiral cationic CpRu(II) complex **4.21** gave the desired tetrahydrofuran **4.20** in 62% yield (Entry 1). The reactivity of Cp^{*}Ru(II) complex **4.22** was much lower than that of CpRu(II) complex **4.21**, giving **4.20** in only 21% yield (Entry 2). The reaction with binaphthyl-derived Cp^{*}Ru(II) complex **Ru.2ba** gave a similar reactivity, (22% yield) with an enantiomeric ratio of 70:30 (Entry 3), demonstrating the feasibility of rendering the transformation enantioselective.

Table 4-1: Proof of concept for enantioselective ruthenium(II)-catalyzed alkylative cycloetherification.



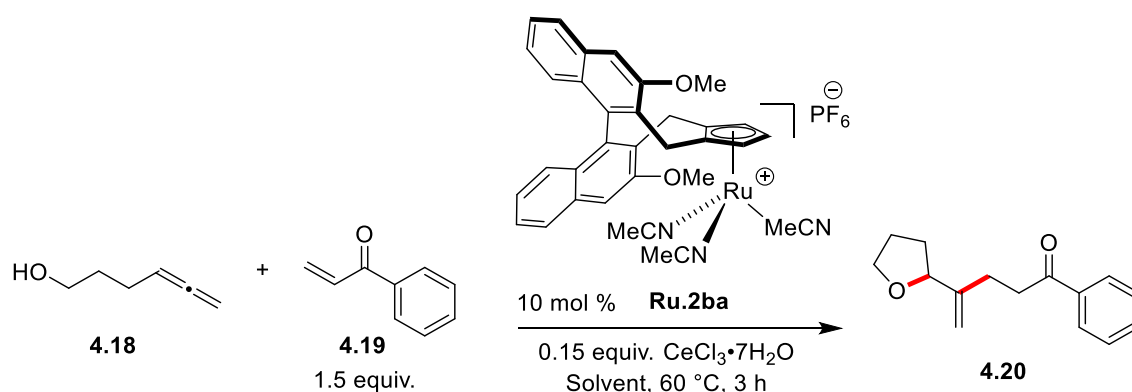
Entry	Ru	Conversion [%]	Yield [%]	er
1	CpRu(CH ₃ CN)PF ₆ 4.21	100	62	-
2	Cp [*] Ru(CH ₃ CN)PF ₆ 4.22	100	21	-
3	Ru.2ba	100	22	70:30

Conditions: 30 μmol **4.18**, 45 μmol of **4.19**, 3.0 μmol **Ru.2ba**, 4.6 μmol CeCl₃·7H₂O, 0.25 M in solvent, 2 h; Yields and conversions of allenol **4.18** determined by ¹H NMR with an internal standard; enantiomeric ratio was determined by HPLC with a chiral stationary phase.

As a next step, different solvents were evaluated (Table 4-2). Among the ethereal solvents, THF and cyclopentyl methyl ether brought about ca. 40% yield with low enantioselectivity (up to 63:37 er,

Entry 1 and 2). Compared to other ethereal solvents, 1,4-dioxane improved the yield to 66%, but with no improvement in enantioselectivity (Entry 3). The reaction in 2-butanone gave similar results (62% yield and 62:38 er, Entry 4). 1,2-Dichloroethane as an example for chlorinated solvents gave only a marginal change in enantioselectivity, 60:40 er (Entry 5). A polar aprotic solvents dimethylformamide (DMF) was beneficial for increasing the enantioselectivity to ca. 70:30 er. However, the yield of **4.20** decreased to 22% (Entry 6). Dimethylacetamide (DMA) had a similar effect on both of yield and enantioselectivity (Entry 7). Even though the yield was poor, the polar aprotic solvents dimethyl sulfoxide, acetonitrile, and dimethylpropyleneurea (DMPU) slightly improved enantioselectivity to 76:24 er (Entry 8–10). The use of an alcoholic solvent, isopropyl alcohol, resulted in poor yield and enantioselectivity (Entry 11).

Table 4-2: Solvent screening.

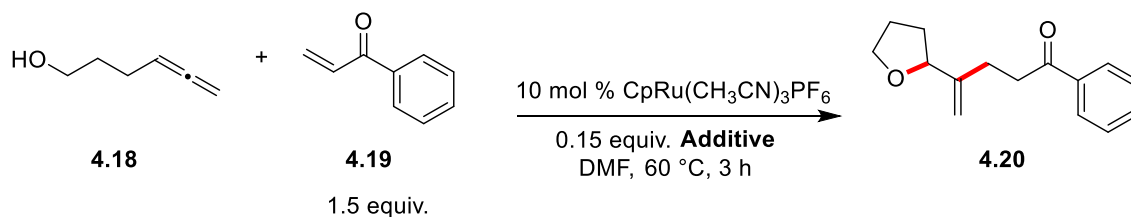


Entry	Solvent	Conversion [%]	Yield [%]	er
1	THF	100	41	63:37
2	cyclopentyl methyl ether	100	37	58:42
3	1,4-dioxane	100	66	61:39
4	2-butanone	100	62	62:38
5	1,2-dichloroethane	100	46	60:40
6	DMF	100	22	70:30
7	DMA	100	21	69:31
8	DMSO	64	5	75:25
9	acetonitrile	100	24	76:24
10	DMPU	100	26	64:36
11	isopropyl alcohol	100	21	58.5:41.5

Conditions: 13 μmol **4.18**, 20 μmol of **4.19**, 1.3 μmol **Ru.2ba**, 2.0 μmol $\text{CeCl}_3 \cdot 7\text{H}_2\text{O}$, 0.25 M in solvent, 3 h; Yields and conversions of allenol **4.18** determined by ^1H NMR with an internal standard; enantiomeric ratio was determined by HPLC with a chiral stationary phase.

A control experiment was performed without the addition of any Lewis acid, causing a drastic drop in yield compared to the reaction with cerium (III) chloride hydrate. (Table 4-3).

Table 4-3: The effect of Lewis acid with achiral CpRu complex.

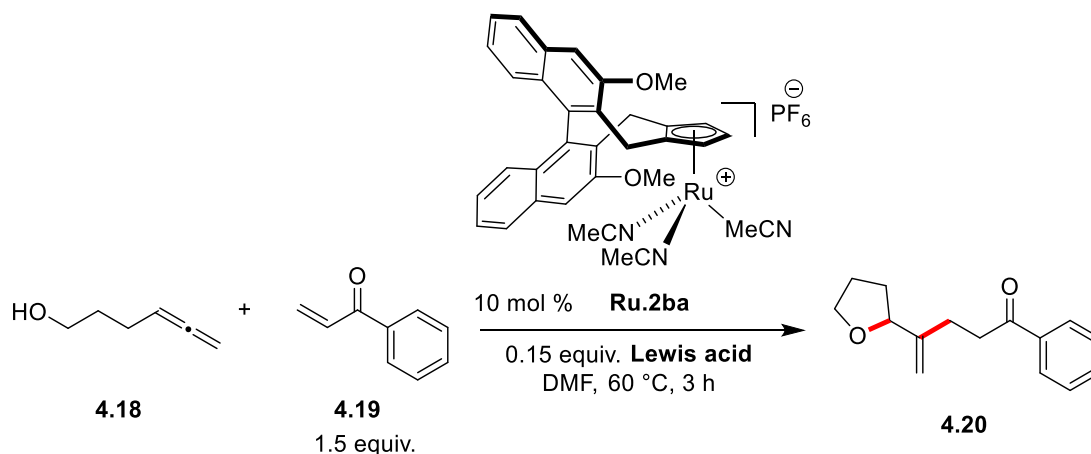


Entry	Lewis acid	Conversion [%]	Yield [%]
1	none	100	20
2	$\text{CeCl}_3 \cdot 7\text{H}_2\text{O}$	100	62

Conditions: 21 μmol **4.18**, 32 μmol of **4.19**, 2.1 μmol $\text{CpRu}(\text{CH}_3\text{CN})_3\text{PF}_6$, 3.2 μmol $\text{CeCl}_3 \cdot 7\text{H}_2\text{O}$, 0.25 M in DMF, 2 h; Yields and conversions of allenol **4.18** determined by ^1H NMR with an internal standard; enantiomeric ratio was determined by HPLC with a chiral stationary phase.

However, an opposing effect was observed on the $\text{Cp}^x\text{Ru}(\text{II})$ system (Table 4-4). Adding cerium (III) chloride hydrate had an adverse effect on both yield and enantioselectivity, (22% yield and 70:30 er, Entry 2). Tin(IV) chloride gave slightly better results, but still worse than the reaction without Lewis acid (Entry 3). Stronger Lewis acids also gave no improvement (Entry 3–6).

Table 4-4: Lewis acid screening with $\text{Cp}^x\text{Ru}(\text{II})$.

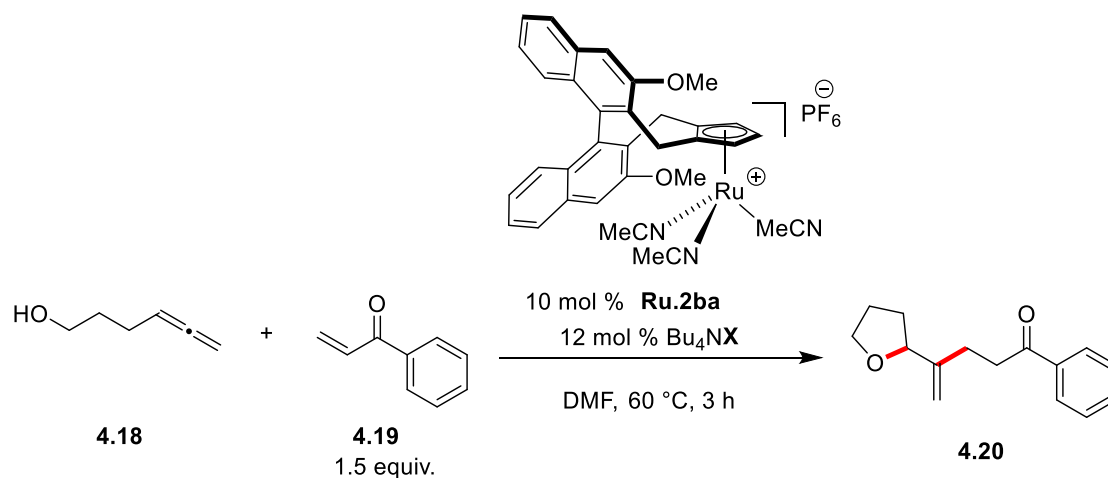


Entry	Lewis Acid	Conversion [%]	Yield [%]	er
1	none	100	37	82:18
2	CeCl ₃ ·7H ₂ O	100	22	70:30
3	SnCl ₄ ·5H ₂ O	100	35	73:27
4	TiCl ₄	100	30	72:28
5	B(C ₆ F ₅) ₃	100	29	79.5:29.5
6	BF ₃ ·OEt ₂	100	36	81.5:18.5

Conditions: 13 μ mol **4.18**, 20 μ mol of **4.19**, 1.3 μ mol **Ru.2ba**, 2.0 μ mol Lewis acid, 0.25 M in solvent, 3 h; Yields and conversions of allenol **4.18** determined by ¹H NMR with an internal standard; enantiomeric ratio was determined by HPLC with a chiral stationary phase.

The effect of halide additives, which lead to the formation of a neutral ruthenium complex, was also evaluated (Table 4-5). A fluoride additive shut down reactivity (Entry 2), while chloride, bromide and iodide caused slight drop yield, accompanied by a notable decrease in enantioselectivity (Entry 3–5).

Table 4-5: Halide additive screening.

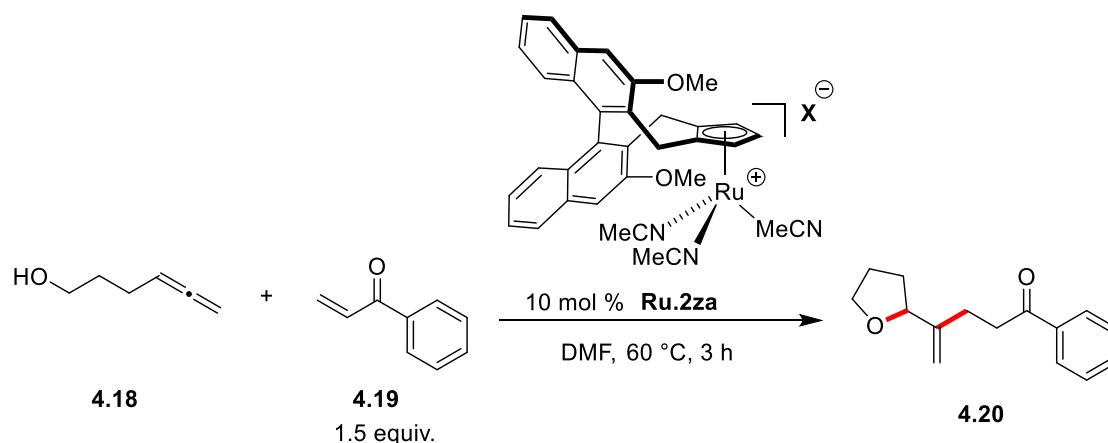


Entry	Bu ₄ NX	Conversion [%]	Yield [%]	er
1	none	100	37	82:18
2	Bu ₄ NF	57	0	-
3	Bu ₄ NCl	100	36	71:29
4	Bu ₄ NBr	100	33	72:28
5	Bu ₄ NI	100	31	67:33

Conditions: 13 μ mol **4.18**, 20 μ mol of **4.19**, 1.3 μ mol **Ru.2ba**, 1.5 μ mol tetrabutylammonium halide, 0.25 M in solvent, 3 h; Yields and conversions of allenol **4.18** determined by ¹H NMR with an internal standard; enantiomeric ratio was determined by HPLC with a chiral stationary phase.

The effect of the counteranion of the ruthenium complex was conducted, revealing a substantial impact on both reactivity and enantioselectivity (Table 4-6). A triflate anion, which is a stronger σ -donor, caused a decrease in yield and enantioselectivity (Entry 1). Similar results were obtained using bistriflimide (NTf_2^-) (Entry 2). Tetrafluoroborate (BF_4^-), as weakly coordination anion,¹¹⁴ brought about significantly worse results than hexafluorophosphate (PF_6^-) and hexafluoroantimonate (SbF_6^-). Among these three anions, hexafluorophosphate gave the best yield of 37% and enantioselectivity (82:18 er). The bad results obtained by using tetrafluoroborate can be explained by its low stability, as it can release fluoride, which inhibits the catalytic cycle (Entry 3–5). Tetrakis[3,5-bis(trifluoromethyl)phenyl]borate (BArF_{24}^-), which is known as a more weakly coordinating anion than hexafluorophosphate, had a detrimental effect on reactivity (8% yield and 64% conversion) and enantioselectivity (67:33 er, Entry 6).¹¹⁵

Table 4-6: Counter anion screening.

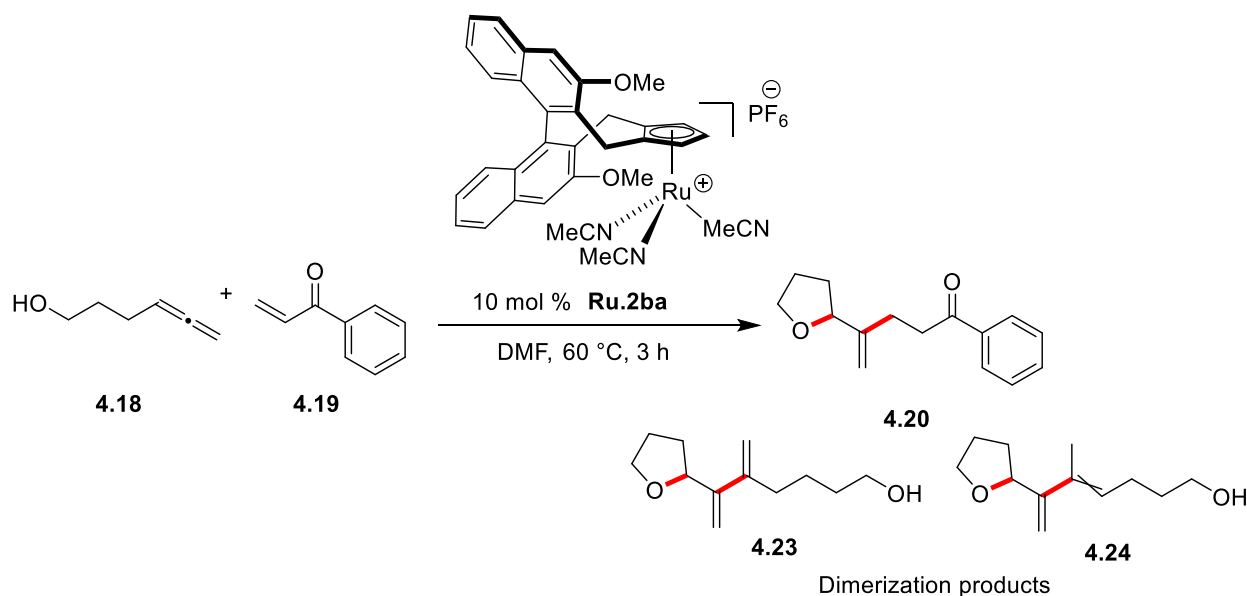


Entry	Counter anion	Conversion [%]	Yield [%]	er
1	OTf^-	92	26	69.5:30.5
2	NTf_2^-	95	23	69:31
3	BF_4^-	81	15	69.5:30.5
4	PF_6^-	100	37	82:18
5	SbF_6^-	96	30	72.5:27.5
6	BArF_{24}^-	64	8	67:33

Conditions: 13 μmol **4.18**, 20 μmol of **4.19**, 1.3 μmol **Ru.2za**, 0.25 M in solvent, 3 h; Yields and conversions of allenol **4.18** determined by ^1H NMR with an internal standard; enantiomeric ratio was determined by HPLC with a chiral stationary phase.

To explain the low efficiency, high conversion and low yield, side products were investigated. Dimerization of allenol **4.18** was revealed as one of the side reaction pathways, forming 1, 3-diene **4.23** and **4.24**. The stoichiometry of the reaction was modulated to reduce dimerization (Table 4-7). When phenyl vinyl ketone **4.19** was used as a limiting reagent with 1.5 equiv. of allenol **4.18**, the yield of the desired tetrahydrofuran derivative decreased to 26%, and it formed 0.18 equiv. of dimerized products (Entry 1). When equal amounts of allenol **4.18** and phenyl vinyl ketone **4.19** were used, it decreased amount of dimerization product to 0.11 equiv, but also decreasing the yield of the desired product **4.20** to 19% (Entry 2). Compared to the standard conditions (Entry 3), a higher amount of phenyl vinyl ketone (4 equiv) almost shut down the dimerization of allenol **4.18**. However, it also caused a slight drop in yield and enantioselectivity, implying that other side reaction pathways exist in the system (Entry 4).

Table 4-7: Effect of different stoichiometry.

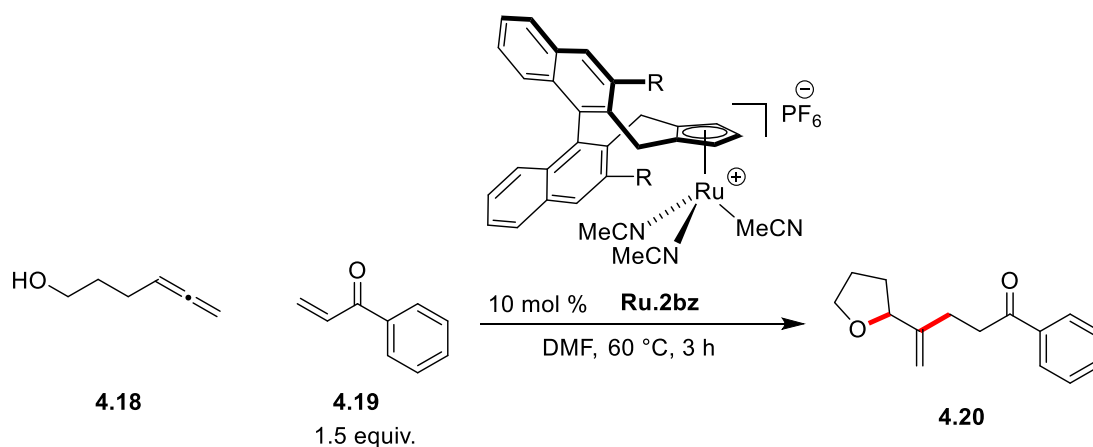


Entry	allenol [equiv.]	phenyl vinyl ketone [equiv.]	Conversion [%]	Yield [%]	er	dimerization
1	1.5	1	86 ^a	26 ^a	80:20	0.18 equiv.
2	1	1	94	19	81:19	0.11 equiv.
3	1	1.5	100	37	82:18	0.07 equiv.
4	1	4	100 ^b	33	78:22	trace

Conditions: Used **4.18** and **4.19** mention above, 10 mol % of **Ru.2ba**, 0.25 M in solvent, 3 h; Yields and conversions of allenol **4.18** determined by ¹H NMR with an internal standard; enantiomeric ratio was determined by HPLC with a chiral stationary phase.; [a] With respect to phenyl vinyl ketone; [b] 2.7 equiv. of phenyl vinyl ketone were consumed.

As a next step, binaphthyl-derived Cp^x ligands with different side walls were investigated (Table 4-8). A phenyl substituent, which has been used for yne-enone cyclization^{65c} and [2+2] cycloaddition,^{65a} lowered both reactivity and enantioselectivity (Entry 2). A high enantiomeric ratio of 90:10 was observed from the reaction with a triisopropoxy substituent. The reactivity with an OTIPS side wall (**Ru.2bc**) was similar to that with a methoxy side wall **Ru.2ba** (Entry 3). However, an even bulkier silyloxy group, *tert*-butyldiphenylsilyloxy, was detrimental on both yield and enantioselectivity (Entry 4).

Table 4-8: Ligand substrate screening



Entry	Ligand substituent (R)	Conversion [%]	Yield [%]	er
1	-OMe (Ru.2ba)	100	37	82:18
2	-Ph (Ru.2bf)	66	16 (24)	79.5:20.5
3	-OTIPS (Ru.2bc)	100	35	90:10
4	-OTBDPS (Ru.2bb)	67	11 (16)	80:20

Conditions: 13 μmol **4.18**, 20 μmol of **4.19**, 1.3 μmol **Ru.2bz**, 0.25 M in solvent, 3 h; Yields and conversions of allenol **4.18** determined by ^1H NMR with an internal standard; enantiomeric ratio was determined by HPLC with a chiral stationary phase. The numbers in parentheses are yield based on recovered starting material.

4.3 Outlook for Enantioselective Ruthenium (II)-Catalyzed Alkylative Cycloetherification

The reaction conditions for the enantioselective Ruthenium (II)-Catalyzed alkylative cycloetherification require further optimization. Exploring other silyl ether moieties like *tert*-butyldimethylsilyl ether or triethylsilyl ether as side walls could further improve enantioselectivity. In addition, different alkoxy groups such as isopropoxy or *tert*-butoxy have not been investigated yet and could potentially also enhance enantioselectivity.

The other important issue is the poor efficiency of the reaction. A detailed analysis of side reaction pathways is necessary, as the known dimerization of allenol **4.23** does not explain the high consumption of the other reaction partner, phenyl vinyl ketone **4.19**. In addition, a slow addition of allenol **4.18** could be helpful for inhibiting the dimerization process.

After optimization of the reaction, different ring sizes should be evaluated. As the Trost group only employed the reaction for the synthesis of 5- and 6-membered rings, an extension of the scope to medium-size rings would greatly add to the synthetic potential of the transformation.

Chapter 5 Preliminary Results for Developing Enantioselective Ru(II)-catalyzed [2+1] Cycloaddition of Ruthenium Vinyl Carbenes

5.1 Introduction

Fused heterocyclic compounds such as cyclopropane-fused pyrrolidines and epoxypyrrolidines are a frequently occurring structural motif in bioactive molecules and natural products. Molecules containing a cyclopropane-fused pyrrolidine moiety are known to exhibit antidepressant effects¹¹⁶ and antibiotic activities.¹¹⁷ Epoxypyrrolidines or 6-oxa-3-azabicyclo[3.1.0]hexanes, have been discovered e.g. in epolactaene, which has neuritogenic activity,¹¹⁸ and hirsutellon C¹¹⁹ (Figure 5-1).

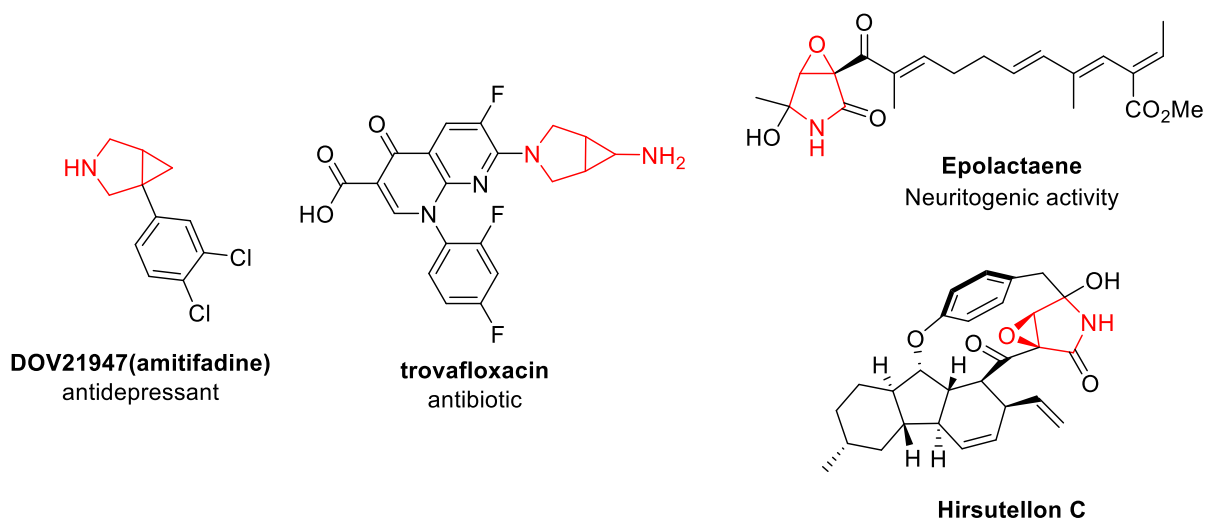
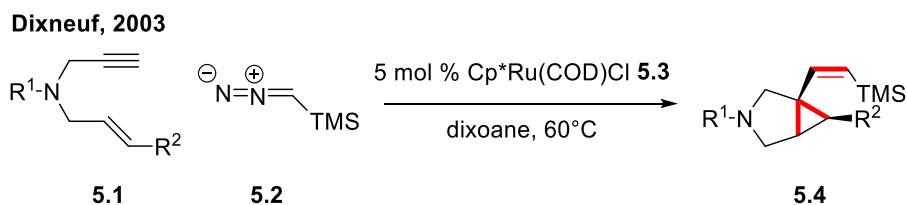


Figure 5-1: Biologically active compounds containing bicyclo[3.1.0]hexane and epoxypyrrolidine motifs.

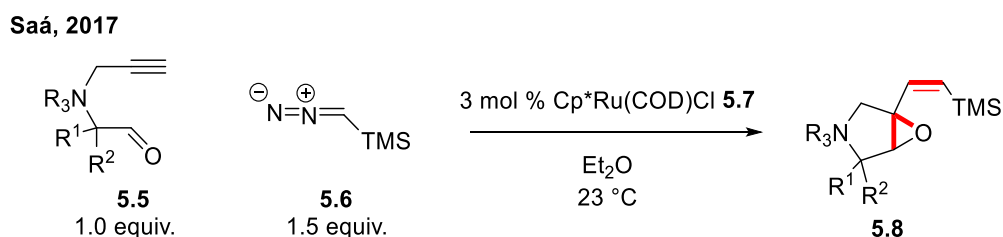
Dérien and Dixneuf reported a [2+1] cycloaddition of a catalytically generated ruthenium vinyl carbene with 1, 6-enyne substrates **5.1** (Scheme 5-1). This reaction produces alkenylbicyclo[3.1.0]hexanes **5.4** and is initiated by the *in situ* generation of the ruthenium vinyl carbene from a Cp^{*}Ru precursor and (trimethylsilyl)diazomethane.^{32, 120}



Scheme 5-1: [2+1] Cycloaddition of catalytically generated ruthenium vinyl carbenes and enynes.

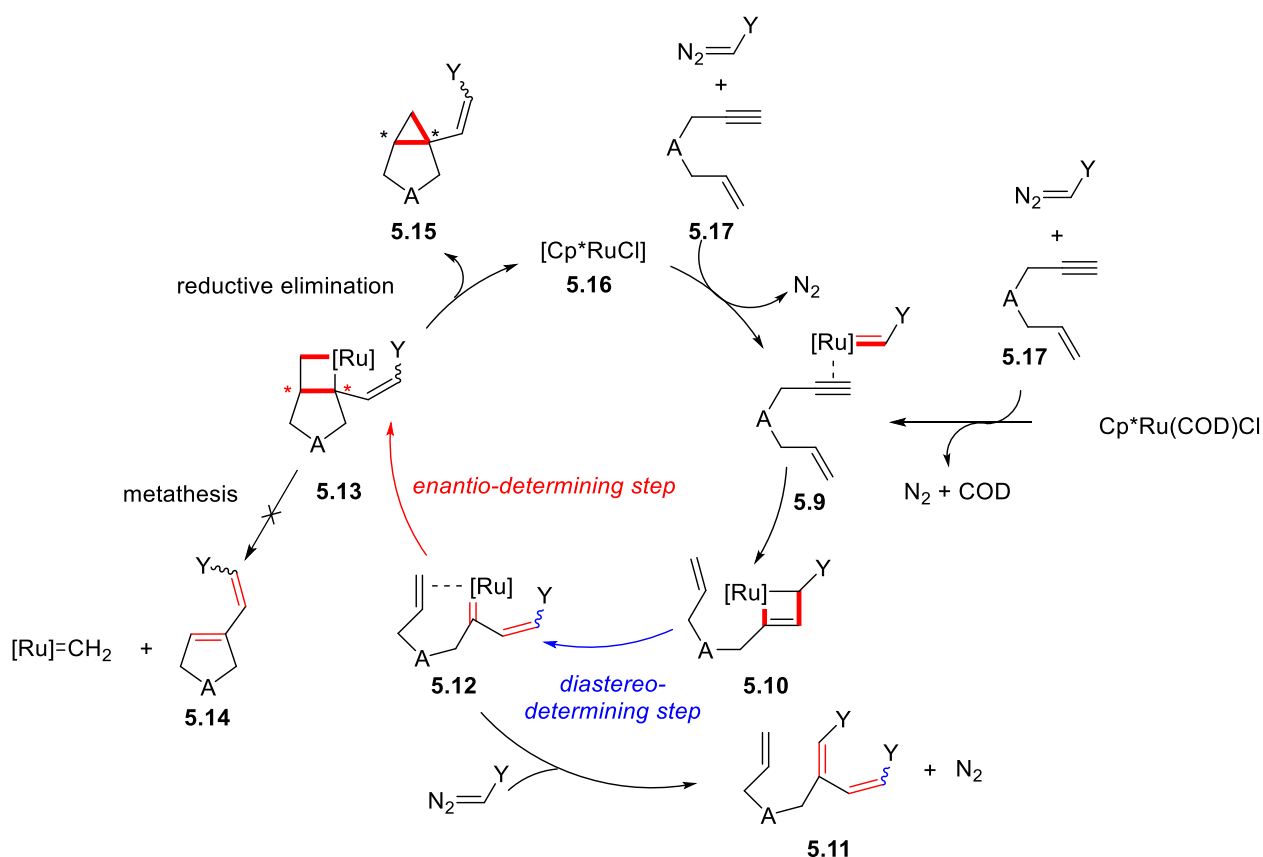
A similar transformation was reported by Saá and coworkers in 2017, using 1,5-alkynal **5.5** as a substrate to form epoxypyrrolidines **5.8** (Scheme 5-2).¹²¹ Similar to the reaction of Dérien and

Dixneuf, the reaction with (trimethylsilyl)diazomethane selectively gave the *Z*-isomer of the alkenyl moiety of the desired epoxypyrrolidine **5.8**, (>95:5 *Z*:*E*).¹²¹



Scheme 5-2: [2+1] Cycloaddition of catalytic Ruthenium vinyl carbenes on an alkynal substrate.

The proposed mechanism of Dérien and Dixneuf commences with the formation of a ruthenium vinyl carbene, which is followed by coordination to the alkyne moiety of enyne substrate **5.17** (Scheme 5-3).³² [2+2] Cycloaddition of the resulting intermediate (**5.9**) produces ruthenacyclobutene intermediate **5.10**. Cycloreversion of **5.10** gives ruthenium carbene **5.12**, followed by a second [2+2] cycloaddition to ruthenacyclobutane **5.13**, followed by reductive elimination and release of the desired alkenylbicyclo[3.1.0]hexane **5.15**. The cycloreversion step from intermediate **5.10** determines the diastereoselectivity, while the second [2+2] cycloaddition is the enantio-determining step. The reaction mechanism is similar to ene-yne metathesis. However, in contrast to the Grubbs catalysts, the Cp*Ru complex does not undergo a cycloreversion of ruthenacyclobutane intermediate **5.13** to form 1, 3-diene **5.14**.



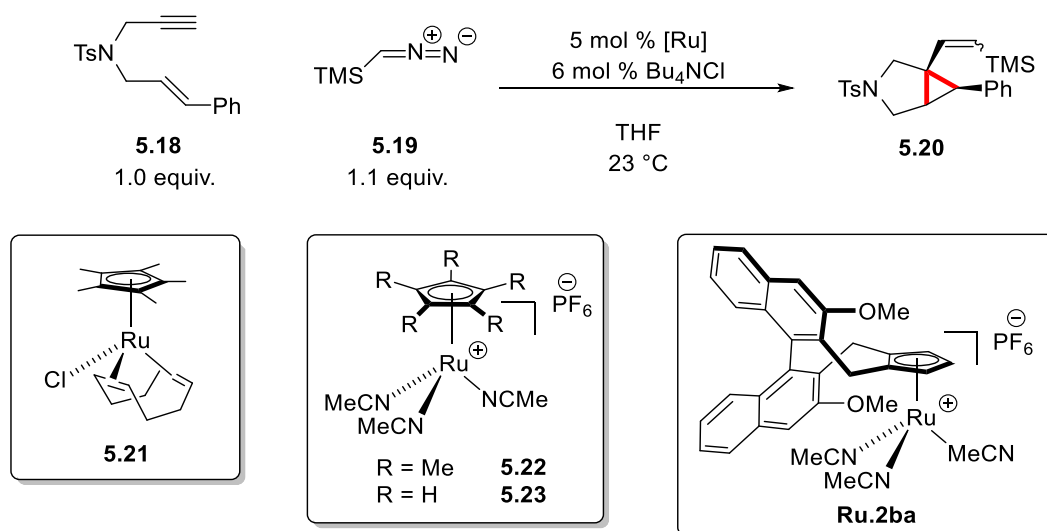
Scheme 5-3: Proposed mechanism of the [2+1] cycloaddition of catalytically generated ruthenium vinyl carbenes.

5.2 Optimization Studies for the Enantioselective [2+1] Cycloaddition of Catalytic Ruthenium Vinyl Carbenes

To prove the concept that Cp^*Ru complexes are competent catalysts for the [2+1] cycloaddition, the reaction was conducted with enyne substrate **5.18** and trimethylsilyldiazomethane **5.19** (Table 5-1). Initially, the reaction conditions for racemic synthesis were reproduced, forming the *Z*-isomer of the desired bicyclo[3.1.0]hexane **5.20** exclusively in 94% yield (Entry 1).³² Cationic Cp^*Ru complex **5.22** with tetrabutylammonium chloride also gave *Z*-isomer **5.20** in 85% yield (Entry 2), while the corresponding CpRu complex resulted in lower reactivity (37% yield, 50% conversion, Entry 3). In this case, the desired product was obtained as a mixture of *E*- and *Z*-isomer, with the *E*-isomer as

the major product (6.7:1). The enantioenriched bicyclo[3.1.0]hexane **5.20** was obtained in 41% yield with 81% conversion, by using binaphthyl-derived Cp^{*}Ru complex **Ru.2ba** (Table 5-1Entry 4). The diastereoselectivity was in between that of Cp^{*}Ru(II) **5.22** and CpRu(II) **5.23**, with a 2.0:1 *E/Z* ratio. The enantioselectivity of both of isomers was similar, giving 70.5:29.5 er and 70:30 er for the *E*- and *Z*-isomer, respectively.

Table 5-1: Proof of concept for the enantioselective Ru(II)-catalyzed [2+1] cycloaddition of ruthenium vinyl carbenes.



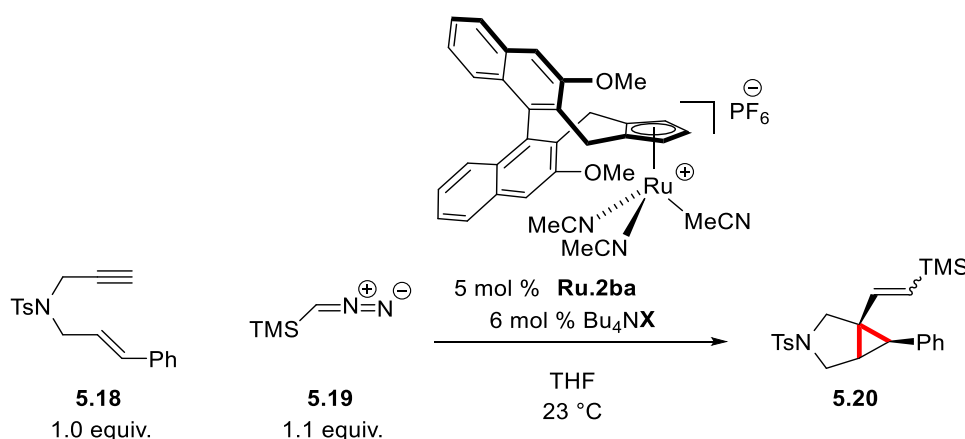
Entry	Ru	Conversion [%]	Yield [%] ^b	<i>E:Z</i>	er (<i>E</i> -isomer)	er (<i>Z</i> -isomer)
1	Cp [*] Ru(COD)Cl 5.21	100	94	<i>Z</i> -isomer	-	-
2	Cp [*] Ru(CH ₃ CN)PF ₆ 5.22	100	85	<i>Z</i> -isomer	-	-
3	CpRu(CH ₃ CN)PF ₆ 5.23	50	37 (74)	6.7:1	-	-
4	Ru.2ba	81	41 (51)	2.0:1	70.5:29.5	70:30

Conditions: 28 μmol **5.18**, 30 μmol of **5.19**, 1.4 μmol [Ru], 1.7 μmol Bu₄NCl, 0.30 M in THF, 18 h; Yields and conversions of enyne **5.18** determined by ¹H NMR with an internal standard.; Enantiomeric ratio was determined by HPLC with a chiral stationary phase.; [a] Without tetrabutylammonium chloride.; [b] Yields based on recovered starting material in parentheses.

The halide additive was investigated next and shown to have a significant impact on reactivity (Table 5-2). The omission of a halide additive caused a significant decrease in reactivity, giving only trace amounts of the desired product **5.20** (Entry 1). In addition, an impact on diastereoselectivity was observed. Comparing chloride with iodide, the *E*-isomer is less favored, and the reaction with iodide gave the *Z*-isomer as a major product (Entry 2–4). In terms of enantioselectivity, bulkier halides

showed an adverse influence, with an enantiomeric ratio of ca. 70:30 for both diastereomers using a chloride additive (Entry 2), and significantly lower enantioselectivities for the reactions with bromide and iodide (Entry 3 and 4).

Table 5-2: Evaluation of halide additives.

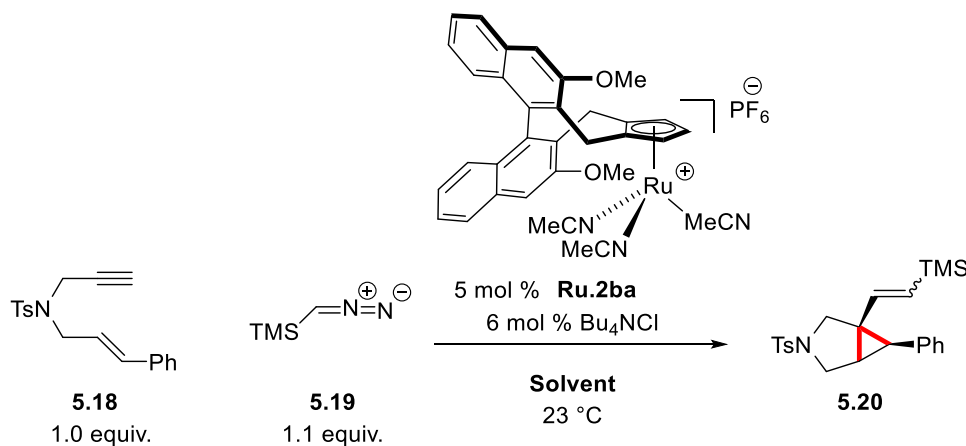


Entry	Bu ₄ NX	Conversion [%]	Yield [%]	<i>E</i> : <i>Z</i>	er (<i>E</i> -isomer)	er (<i>Z</i> -isomer)
1	none	31	trace	-	-	-
2	Bu ₄ NCl	81	41	1.6:1	70.5:29.5	70:30
3	Bu ₄ NBr	80	45	1.2:1	69:31	66:34
4	Bu ₄ NI	48	14	0.8:1	56.5:43.5	62.5:37.5

Conditions: 28 μmol **5.18**, 30 μmol of **5.19**, 1.4 μmol **Ru.2ba**, 1.7 μmol tetrabutylammonium halide, 0.30 M in THF, 18 h; Yields and conversions of enyne **5.18** determined by ¹H NMR with an internal standard.; Enantiomeric ratio was determined by HPLC with a chiral stationary phase.

The reaction was conducted in different solvents, showing an impact on yield, diastereoselectivity, and enantioselectivity (Table 5-3). All reactions gave the *E*-isomer as the major product, with selectivities between 1.2:1 and 2.5:1. In most of cases, the *E*-isomer was obtained in a higher enantioselectivity than the *Z*-isomer. Aromatic solvents were beneficial in terms of yield (65–72%) yield, as well as – moderately – enantioselectivity (Entry 1–3). Etheral solvents gave slightly decrease in both conversion and yield (Entry 4–6). Dichloromethane gave moderate reactivity in terms of yield based on recovered starting material, while notably giving a slightly higher enantioselectivity of 67:33 er for the *Z*-isomer, (62.5:37.5 er for *E*) (Entry 7). The use of 2-butanone substantially decreased reactivity to 11% yield and 57% conversion (Entry 8). In this case, the highest enantioselectivity for *Z*-isomer was obtained with 77.5:22.5 er. The coordinating solvents dimethylformamide and acetonitrile, induced poor yield (20–26%) without improvement on enantioselectivity (Entry 9 and 10)

Table 5-3: Solvent screening



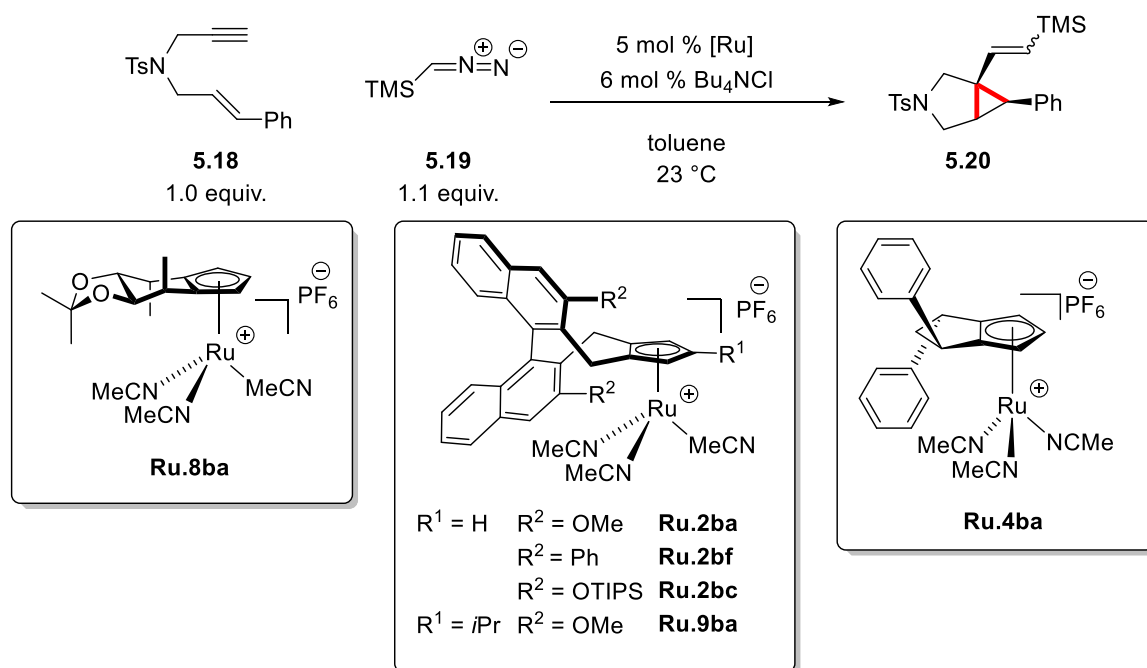
Entry	Solvent	Conversion [%]	Yield [%] ^a	<i>E</i> : <i>Z</i>	er (<i>E</i> -isomer)	er (<i>Z</i> -isomer)
1	trifluorotoluene	100	66	2.4:1	68:32	ca.67.5:32.5
2	toluene	100	72	1.6:1	72.5:27.5	63.5:36.5
3	benzene	100	65	1.7:1	68:32	65:35
4	diethyl ether	82	51 (62)	1.7:1	70:30	67:33
5	dioxane	75	48 (64)	1.2:1	75:25	59:41
6	THF	81	41 (51)	2.0:1	70.5:29.5	70:30
7	DCM	59	38 (64)	1.9:1	62.5:37.5	67:33
8	2-butanone	57	11 (19)	1.6:1	65:35	77.5:22.5
9	DMF	69	26 (38)	2.3:1	70:30	66:34
10	acetonitrile	51	20 (39)	2.5:1	67.5:32.5	ca. 65:35

Conditions: 25 μmol **5.18**, 27 μmol of **5.19**, 1.2 μmol **Ru.2ba**, 1.4 μmol Bu_4NCl , 0.30 M in solvent, 18 h; Yields and conversions of enyne **5.18** determined by ^1H NMR with an internal standard.; Enantiomeric ratio was determined by HPLC with a chiral stationary phase. [a] Yields based on recovered starting material in parentheses.

As a next step, the effect of different chiral Cp ligands was evaluated (Table 5-4). Cyclohexane-fused Cp^x ruthenium complex **Ru.8ba** gave diminished reactivity (25% yield and 60% conversion, Entry 1) and similar or slightly better enantioselectivity compared to binaphthyl-derived Cp^x ruthenium complex **Ru.2ba**. Interestingly, it gave the other enantiomer of the *E*-isomer as a major product **5.20** (Entry 1 and 2). Binaphthyl-derived Cp^x ligands with bulkier OTIPS sidewalls caused a decrease in yield and conversion compared to methoxy sidewall complex **Ru.2ba**, with virtually the same enantioselectivity for the *E*-isomer. A phenyl side wall **Ru.2bf** resulted in slight loss in the enantioselectivity of the *Z*-isomer (60:40 er). OTIPS side wall complex **Ru.2bc** reversed enantioselectivity for the *Z*-isomer (44.5:55.5 er) (Entry 3 and 4). An interesting outcome was

observed for tri-substituted Cp^xRu complex **Ru.9ba**. The diastereoselectivity was inversed, with *E*-isomer as the minor diastereomer. Even though the reactivity was poor (35% conversion and 13% yield), the *E*-isomer was obtained in a good enantiomeric ratio of 87:13. However, the *Z*-isomer was obtained virtually as a racemate (Entry 5). Poor reactivity was observed for the reaction with cyclopentane-fused third generation Cp^x ruthenium complex **Ru.4ba**, with virtually no enantioselectivity induced for both diastereomers (Entry 6).

Table 5-4: Screening of different ruthenium complexes with enyne substrate **5.18**



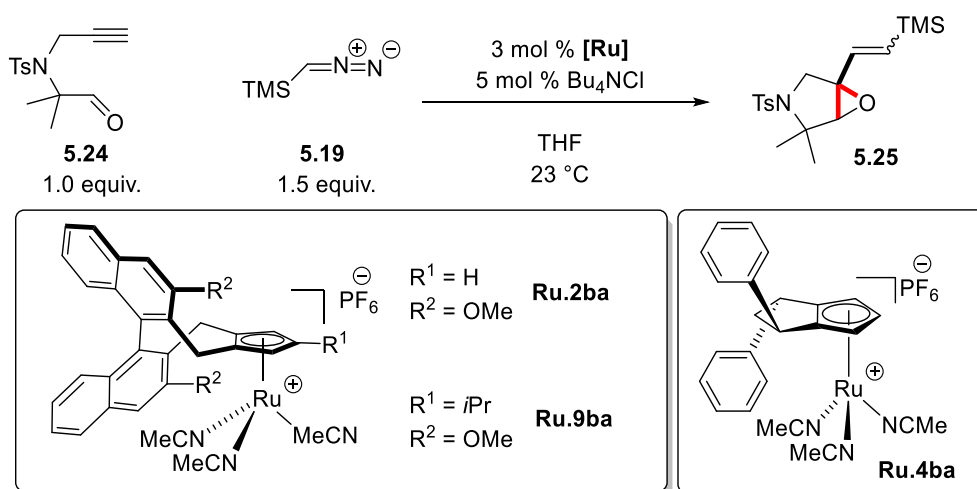
Entry	Ru	Conversion [%]	Yield [%]	<i>E:Z</i>	er (<i>E</i> -isomer)	er (<i>Z</i> -isomer)
1	Ru.8ba	60	25	2.0:1	25:75	76:24
2	Ru.2ba	100	72	1.6:1	72.5:27.5	63.5:36.5
3	Ru.2bf	86	49	2.6:1	73.5:26.5	60:40
4	Ru.2bc	37	12	1:2.3	70:30	ca. 44.5:55.5
5	Ru.9ba	35	13	1:1.8	ca. 87:13	59.5:40.5
6	Ru.4ba	30	6	2.3:1	50:50	54:46

Conditions: 25 μmol **5.18**, 27 μmol of **5.19**, 1.2 μmol [Ru], 1.4 μmol Bu₄NCl, 0.30 M in toluene, 18 h; Yields and conversions of enyne **5.18** determined by ¹H NMR with an internal standard.; Enantiomeric ratio was determined by HPLC with a chiral stationary phase.

Alkynal substrate **5.24** was also evaluated under similar reaction conditions to the racemic synthesis, obtaining similar trends for the different ligands¹²¹ (Table 5-5). The neutral Cp^{*}Ru(II) complex (Cp^{*}Ru(COD)Cl) delivered exclusively the *Z*-isomer of the desired epoxypyrrolidine **5.25** in 95% yield

(Entry 1). Cationic Cp*Ru(II) complex (Cp*Ru(CH₃CN)₃PF₆) with an additional halide additive worked well, yielding 87% of the *Z*-isomer (Entry 2). As in the case of enyne substrate **5.18**, CpRu(II) complex (CpRu(CH₃CN)₃PF₆) brought lower reactivity (54% conversion and 40% yield) with the *E*-isomer as the major product (Entry 3). Binaphthyl-derived Cp^xRu(II) **Ru.2ba** gave enantio-enriched epoxypyrrolidine **5.25**, (74:26 er for *E*-isomer) in 17% yield with 33% conversion, which makes the yield based on recovered starting material was 51% similar to enyne substrate **5.18**. (Entry 4). The diastereoselectivity was 2.1:1 dr with the *E*-isomer as the major product (Entry 4). Tri-substituted Cp^xRu(II) complex **Ru.9ba** again induced an inversion of diastereoselectivity (1:1.4 dr), (Entry 5). Low enantioselectivity and reactivity were obtained with cyclopentane-fused third generation Cp^x ruthenium **Ru.4ba** (Entry 6).

Table 5-5: Screening of different ruthenium complexes with alkynal substrate **5.24**



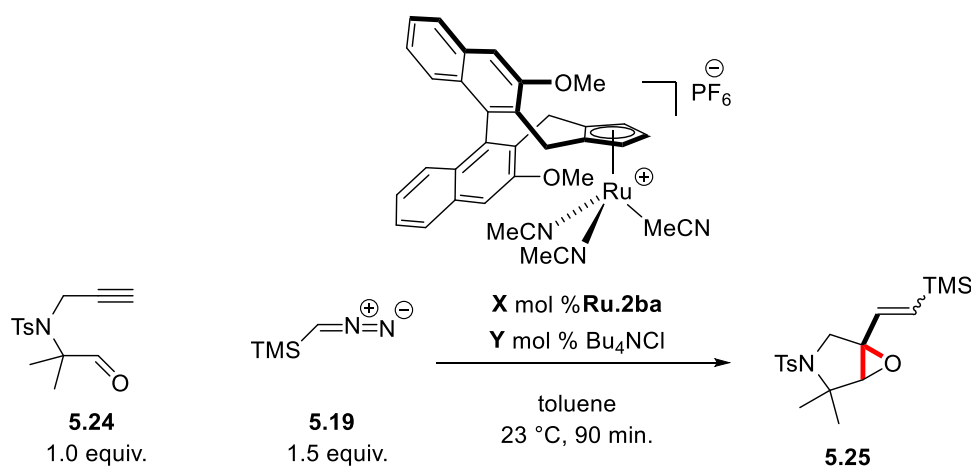
Entry	Ru	Conversion [%]	Yield [%] ^a	<i>E</i> : <i>Z</i>	er (<i>E</i> -isomer)	er (<i>Z</i> -isomer)
1	Cp*Ru(COD)Cl	100	95	<i>Z</i> -isomer	-	-
2	Cp*Ru(CH ₃ CN)PF ₆	100	87	<i>Z</i> -isomer	-	-
3	CpRu(CH ₃ CN)PF ₆	54	40 (78)	6.0:1	-	-
4	Ru.2ba	33	17 (51)	2.1:1	74:26	70.5:29.5
5	Ru.9ba	22	5 (24)	1:1.4	-	-
6	Ru.4ba	25	8 (33)	1.8:1	54:46	67.5:32.5

Conditions: 25 μmol **5.24**, 38 μmol of **5.19**, 0.75 μmol [Ru], 1.3 μmol Bu₄NCl, 0.14 M in THF, 90 min; Yields and conversions of alkynal **5.24** determined by ¹H NMR with an internal standard.; Enantiomeric ratio was determined by HPLC with a chiral stationary phase. [a] Yields based on recovered starting material in parentheses

The low conversion and poor yield of the reaction appoint to a low catalyst turnover. In order to verify this assumption, the reactions were conducted with a prolonged reaction time or a higher catalyst loading (Table 5-6). The reaction with a longer reaction time brought about nearly the same results

as the previous conditions (Entry 2), indicating that turnover of the ruthenium catalyst stops after ca.30% conversion. A lower concentration of the substrates had a negligible effect (Entry 3). Increasing the catalyst loading to 5 mol % improved the yield to 49% and the conversion to 61%, which is equal to ca. twelve catalyst turnovers, only a marginal change compared to the previous conditions (Entry 4). This indicates that ca. 8 to 10 mol % catalyst would be necessary to drive the reaction to completion.

Table 5-6: The effect of solvent and catalyst loading

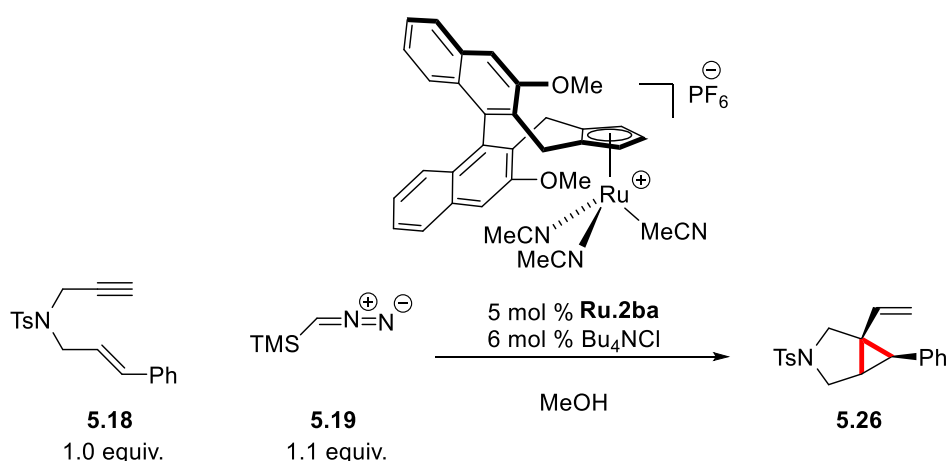


Entry	Cat.	Bu_4NCl	Conc.	Conv. [%]	Yield [%] ^a	<i>E</i> : <i>Z</i>	er (<i>E</i> -isomer)	er (<i>Z</i> -isomer)
1	3 mol %	5 mol %	0.14 M	32	24 (73)	1.7:1	77:23	66:34
2	3 mol %	5 mol %	0.14 M, 19 h	29	23 (82)	1.9:1	78:22	65.5:34.5
3	3 mol %	5 mol %	0.08 M	32	26 (80)	1.7:1	79:21	64.5:35.5
4	5 mol %	8 mol %	0.08 M	61	49 (80)	1.7:1	80:20	64.5:35.5

Conditions: 25 μmol **5.24**, 38 μmol of **5.19**, 0.75 μmol **Ru.2ba**, 1.3 μmol Bu_4NCl , 0.14 M in toluene, 90 min; Yields and conversions of alkyne **5.24** determined by ^1H NMR with an internal standard.; Enantiomeric ratio was determined by HPLC with a chiral stationary phase. [a] Yields based on recovered starting material in parentheses

Changing the reaction solvent to methanol gave an interesting result, as terminal alkene **5.26** was obtained instead of alkenylsilane **5.19** (Table 5-7).¹²¹ The reaction with neutral Cp*Ru(II) complex **5.21** produced this terminal alkene **5.26** in 61% yield (Entry 1). However, binaphthyl-derived Cp*Ru(II) complex **Ru.2ba** only delivered a trace amount **5.26** (Entry 2 and 3). Using tetrahydrofuran as a co-solvent slightly improved the yield to 9% with 62.5:37.5 er.

Table 5-7: Terminal alkene formation in methanol



Entry	Ru	Solvent	Temp. [°C]	Conversion [%]	Yield [%]	er
1	Cp*Ru(COD)Cl ^a 5.21	MeOH	25	85	61	-
2	Ru.2ba	MeOH	25	33	trace	-
3	Ru.2ba	MeOH	50	34	2	-
4	Ru.2ba	MeOH/THF (50/50, v/v')	25	29	trace	-
5	Ru.2ba	MeOH/THF (50/50, v/v')	50	41	9	62.5:37.5

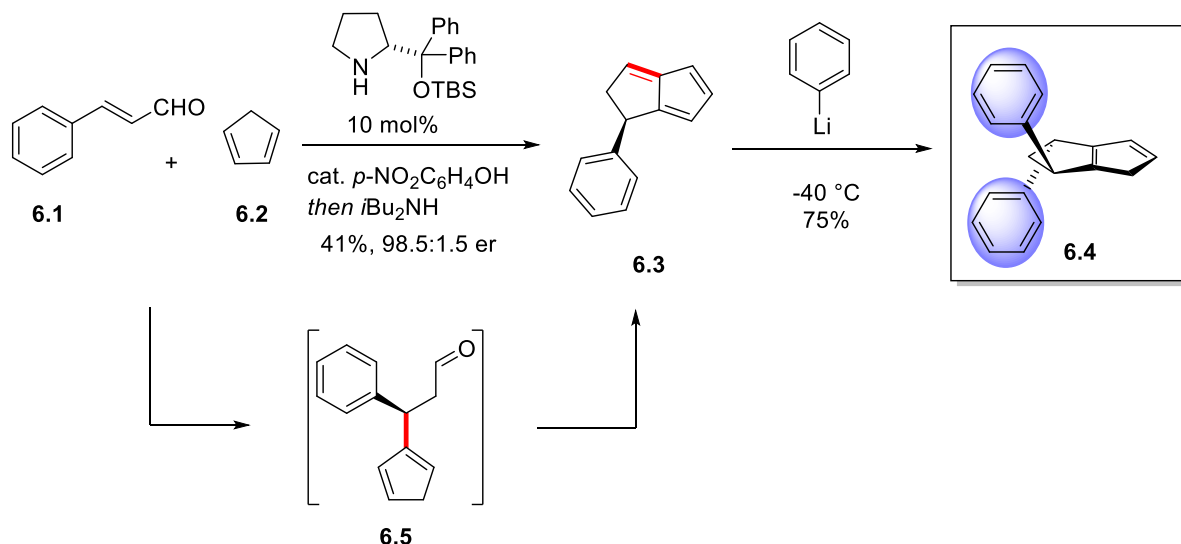
Conditions: 25 μmol **5.18**, 28 μmol of **5.19**, 1.3 μmol **Ru.2ba**, 1.5 μmol Bu_4NCl , 0.30 M in MeOH, 18 h; Yields and conversions of alkyne **5.18** determined by ^1H NMR with an internal standard.; Enantiomeric ratio was determined by HPLC with a chiral stationary phase. [a] Without Bu_4NCl .

5.3 Outlook for Enantioselective [2+1] Cycloaddition of Catalytically Generated Ruthenium Vinyl Carbenes

In order to increase the enantioselectivity of the transformation, more ruthenium complexes with different sidewalls should be evaluated. In particular, the effect of bulkier alkoxy sidewalls such as isopropoxy (*i*PrO-) and *tert*-butoxy (*t*BuO-) needs to be explored. In addition, the low diastereoselectivity needs to be addressed, possibly by employing a penta-substituted chiral congener of Cp*, as the reaction showed a high preference for the *Z*-isomer with achiral Cp*Ru(II) complexes. A chiral penta-substituted Cp*-like ligand is available in our group,⁶⁹ but has not yet been applied to ruthenium catalysis. Synthesis of the corresponding Ru(II) complexes will not only be valuable for this particular transformation, but also extend and complement the available ligand library and open potential for new reactivities.

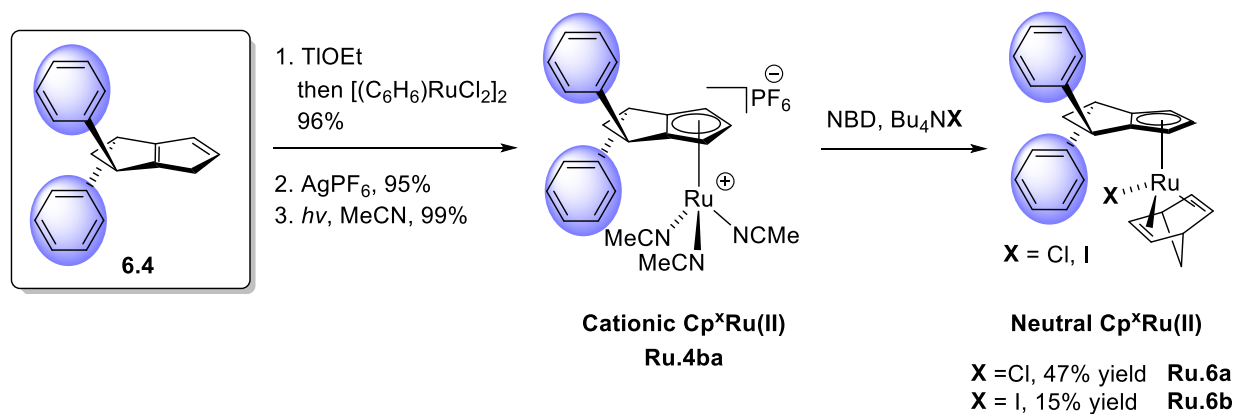
Chapter 6 Summary

This thesis describes the synthesis of a novel class of Cp^x ligands and the application of the corresponding $\text{Cp}^x\text{Ru(II)}$ complexes in enantioselective catalysis. The novel Cp^x ligands consist of a C_2 -symmetric cyclopentane-fused bicyclic skeleton with a modifiable aryl group, and can be accessed in high enantiopurity (98.5:1.5 er) by a convenient two-step synthesis (Scheme 6-1).



Scheme 6-1: Two step-synthesis of cyclopentane-fused Cp^x ligands.

A synthesis of cationic $\text{Cp}^x\text{Ru(II)}$ complexes and the corresponding neutral complexes was developed (Scheme 6-2). The cationic $\text{Cp}^x\text{Ru(II)}$ complexes were accessed by complexation with TiCp^x and $[\text{Ru}(\text{C}_6\text{H}_6)\text{Cl}_2]_2$, and subsequent benzene removal under UV light. The neutral complexes were also obtained from the corresponding cationic complex by ligand substitution. They can be employed as chiral congeners of $\text{CpRu}(\text{CH}_3\text{CN})_3\text{PF}_6$ and $\text{CpRu}(\text{NBD})\text{X}$, respectively.



Scheme 6-2: Cationic and neutral $\text{Cp}^x\text{Ru(II)}$ complexes.

Modification of the aryl moiety gave access to cyclopentane-fused Cp^x ligands with different sidewalls (Figure 6-1). The resulting ligand library can be used for tuning the chiral environment of the corresponding ruthenium complexes.

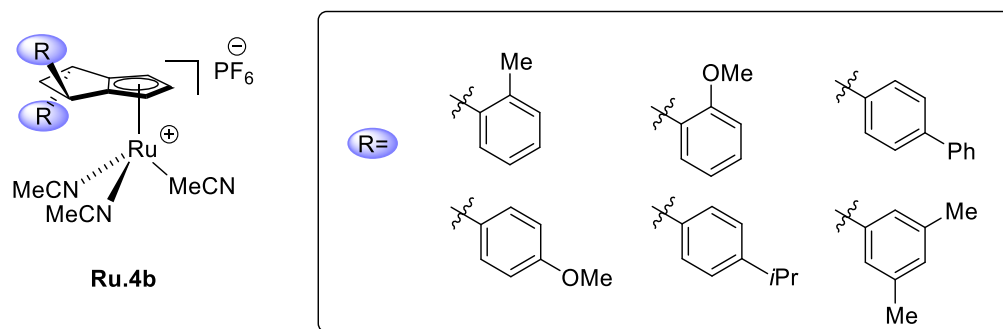
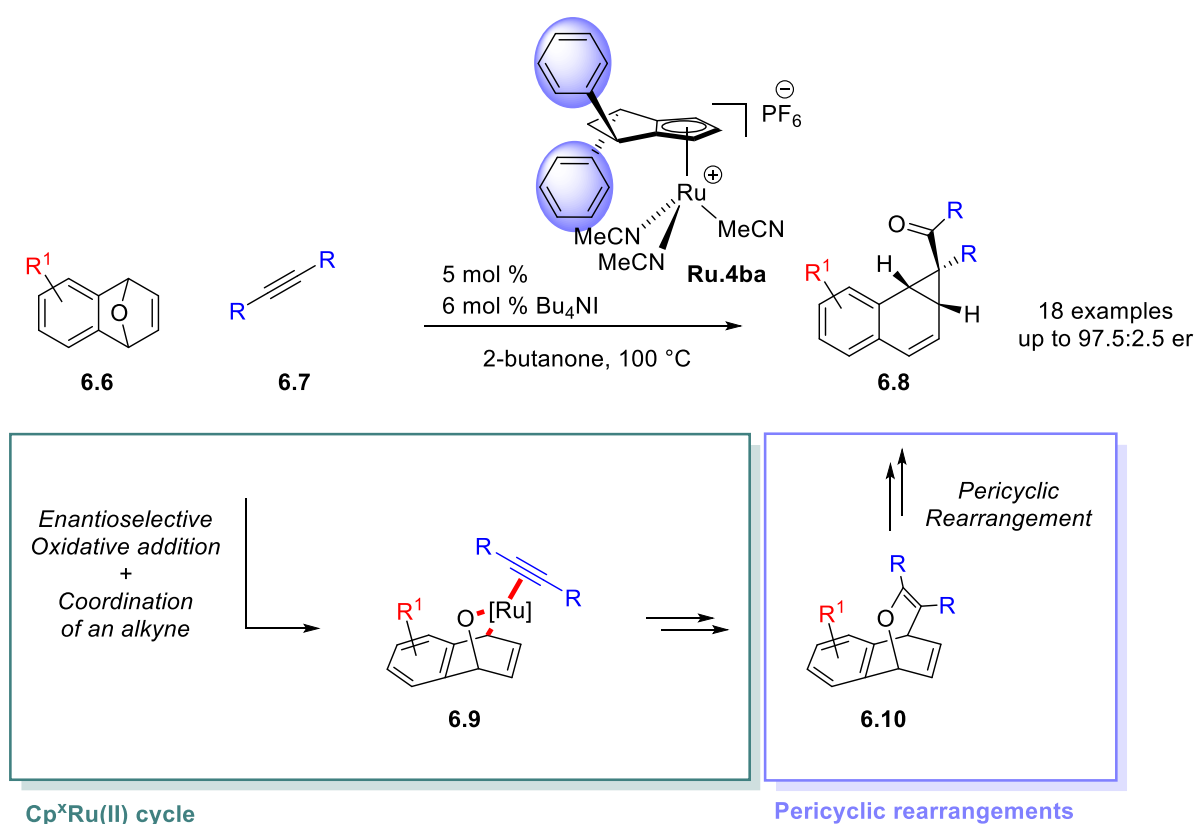


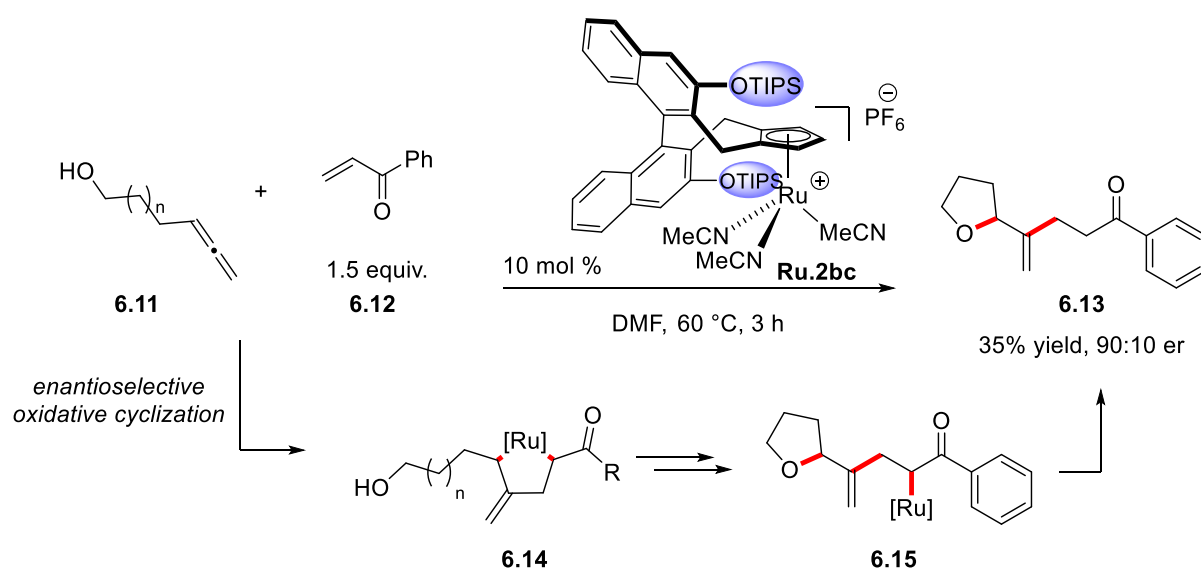
Figure 6-1: Cyclopentane-fused Cp^xRu(II) complexes with various sidewalls.

The potential of the novel cyclopentane-fused Cp^xRu(II) complexes for enantioselective catalysis was demonstrated in the diastereoselective and enantioselective synthesis of benzonorcaradienes by coupling of oxa-benzonorbornadienes and internal alkynes (Scheme 6-3). In this transformation, the cyclopentane-fused Cp^x ligands performed significantly better in reactivity and enantioselectivity than binaphthyl-derived Cp^x ligands, the most commonly employed chiral Cp ligands. The product of this transformation, a highly functionalized tricyclic sesquiterpene, has diverse biological activities. The reaction performed well for various substrates, and 18 examples were obtained in very good yields and with very good enantioselectivities up to 97.5:2.5 er. Mechanistic studies were conducted by control experiments as well as computational studies, showing that the reaction mechanism consists of two parts: a ruthenium-catalyzed cycle and a series of pericyclic reactions.



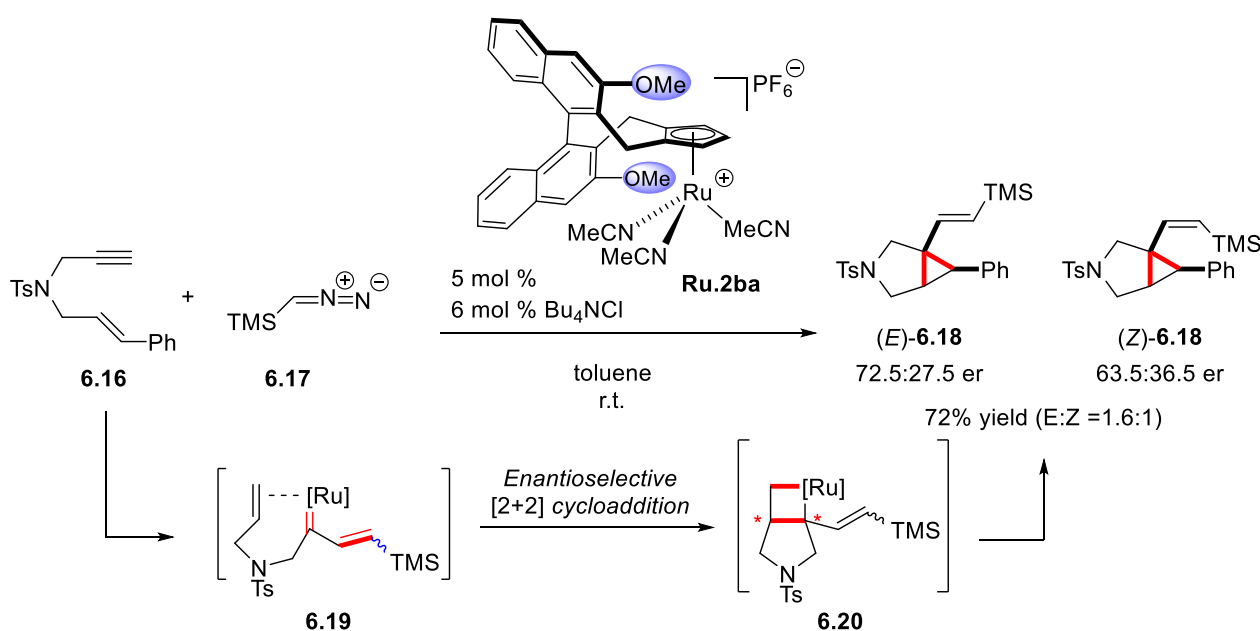
Scheme 6-3: Enantioselective benzonorcaradiene synthesis

The binaphthyl-derived Cp^xRu complexes showed promising results on the enantioselective alkylative cycloetherification of an allenol **6.11** and a Michael acceptor **6.12** (Scheme 6-4). The transformation is atom economic, forming C–O and C–C bonds in a single step. The resulting cyclic ethers can be useful precursors for spiroketals. The reaction condition optimization revealed that steric bulk of the substituents on Cp^x ligands has a significant impact on reactivity and enantioselectivity. The transformation showcases the potential of the binaphthyl-derived Cp^xRu complexes for enantioselective catalysis, giving promising results with a high enantioselectivity (90:10 er).



Scheme 6-4: Enantioselective Cp^xRu(II) catalyzed alkylative cycloetherification.

Preliminary results were also obtained for a [2+1] cycloaddition of enynes. Binaphthyl-derived $\text{Cp}^*\text{Ru}(\text{II})$ catalysts provided enantio-enriched alkenylbicyclo[3.1.0]hexanes in good yields and with up to 72.5:27.5 er for the *E*-isomer. The reaction mechanism is similar to olefin metathesis, but the cyclopentadienyl ruthenacyclopentane intermediate undergoes reductive elimination instead of cycloreversion, forming a fused cyclopropane. The substitution patterns on the Cp^* ligands affected the diastereoselectivity of alkenyl moiety. These initial results encourage us for further studies on the structures of Cp^* ligands, which can be key for inducing high diastereoselectivity and enantioselectivity.



Scheme 6-5: Enantioselective $\text{Cp}^*\text{Ru}(\text{II})$ catalyzed [2+1] cycloaddition of ruthenium vinyl carbenes

In conclusion, we report a novel class of Cp^* ligands and the corresponding $\text{Ru}(\text{II})$ complexes. Modification of the cyclopentane-fused $\text{Cp}^*\text{Ru}(\text{II})$ catalysts was conducted by changing the side wall aryl substituents and by accessing the respective neutral ruthenium halide complexes. With the novel Cp^*Ru catalysts, a catalytic enantioselective synthesis of benzonorcaradienes by coupling of oxabenzonorbornadienes and internal alkynes was established (up to 97.5:2.5 er). The application potential of binaphthyl-derived Cp^*Ru complexes for atom-economic transformations, and their capability for enantio-induction was shown on an alkylative cycloetherification (up to 90:10 er) and a [2+1] cycloaddition of enynes (up to 89:11 er).

Chapter 7 Outlook

Building chiral ligand libraries is important for the discovery of new reactivities and the realization of envisioned catalytic enantioselective approaches. In particular, a novel class of ligand opens up new possibilities for improving the efficiency of reactions or developing complementary synthetic methods. The ruthenium complexes of binaphthyl-derived (**7.2**) and cyclopentane-fused (**7.3**) Cp^x ligands have been applied as catalysts for enantioselective reactions. There is still a plethora of potential applications of these ligands in ruthenium catalysis. Furthermore, the potential of other Cp^x classes like cyclohexane-fused Cp^x (**7.1**) and biphenyl-derived Cp^x (**7.4**), has not yet been explored in $\text{Cp}^x\text{Ru(II)}$ catalysis. These new combinations of Cp^x ligands with ruthenium will give new opportunities for enantioselective catalysis (Figure 7-1). In addition, modifying the sidewalls modulates the reactivity and enantioselectivity of $\text{Cp}^x\text{Ru(II)}$ complexes, which was shown to be key for enhancing the enantioselectivity of an enantioselective ruthenium-catalyzed alkylative cycloetherification.

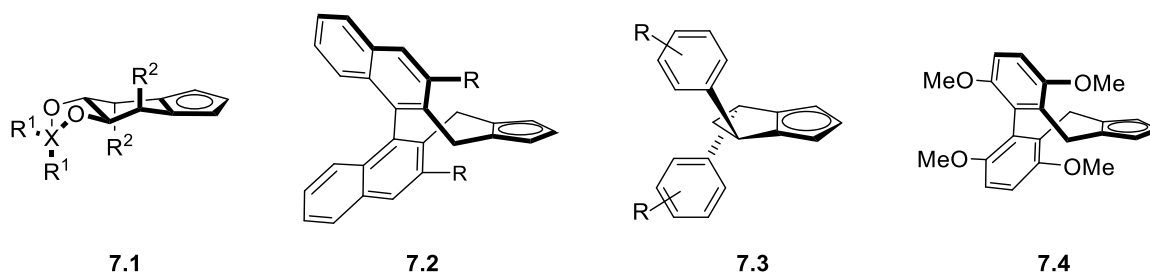


Figure 7-1: Four different classes of Cp^x ligands.

In addition to the ligand backbone, substitution patterns on the Cp ring constitute an interesting topic for research (Figure 7-2). Establishing a ruthenation method for TMS-substituted Cp^x complexes **7.6** and a penta-substituted Cp^x complexes **7.7** is desirable, which will broaden the library of available complexes. The substitution pattern on the Cp ring provides an additional handle for catalyst tuning, which can improve the enantio- and diastereoselectivity of the enantioselective [2+1] cycloaddition of ruthenium vinyl carbenes.

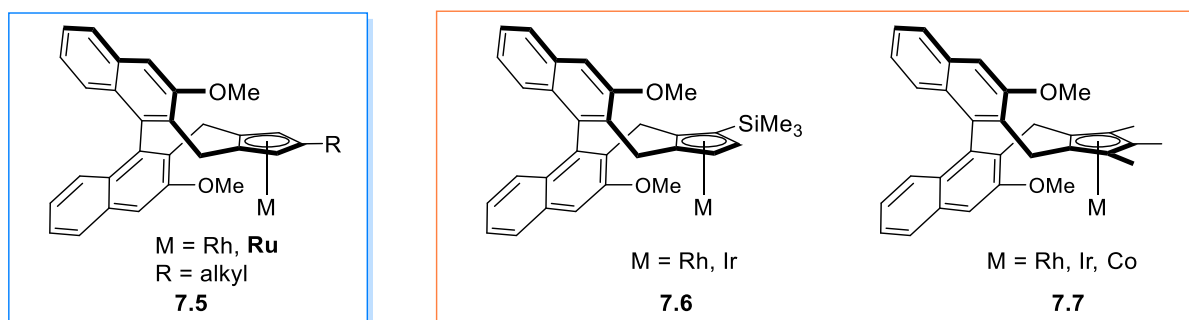


Figure 7-2: Various substitution patterns on the Cp ring.

Chapter 8 Experimental Part

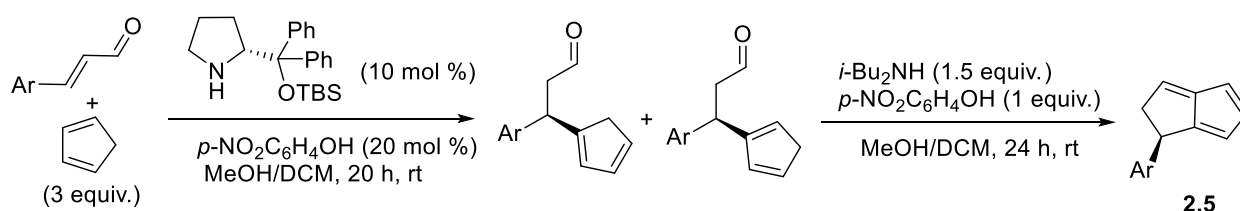
8.1 General Methods

All reactions were carried out under an atmosphere of nitrogen in oven-dried glassware with magnetic stirring, unless otherwise indicated. THF, Et₂O and dichloromethane were purified by a Innovative Technology Solvent Delivery System. DMF was dried over 4A molecular sieves. Chemicals were used as obtained from the suppliers unless stated otherwise. Flash chromatography was performed with Silicycle silica gel 60 (0.040-0.063 μm grade) or phosphate buffered silica (pH=7). Analytical thin-layer chromatography was performed with commercially available 0.25 mm silica gel coated on a glass plate (Merck, TLC Silicagel 60 F₂₅₄). Compounds were either visualized under UV-light at 254 nm or stained the plates with an aqueous potassium permanganate solution. Proton nuclear magnetic resonance (¹H NMR) data were acquired at 400 MHz on a Bruker AV400 spectrometer or at 600 MHz on a Bruker AV600 spectrometer. Chemical shifts (δ) are reported in parts per million (ppm) relative to residual chloroform (s, 7.26 ppm) or residual dichloromethane (s, 5.32 ppm). 1D NOE experiments were performed with a Bruker AV600. Proton decoupled Carbon-13 nuclear magnetic resonance (¹³C NMR) data were acquired at 100 MHz on a Bruker AV400 or at 151 MHz on a Bruker AV600 spectrometer. Chemical shifts are reported in ppm relative to residual chloroform (77.16 ppm) or residual dichloromethane (53.84 ppm). Splitting patterns are designated as s, singlet; d, doublet; t, triplet; q, quartet; sept, septet; m, multiplet. All NMR data were recorded at 298 K unless stated otherwise. Infrared (IR) data were recorded on a Bruker Alpha FT-IR Spectrometer. Absorbance frequencies are reported in reciprocal centimeters (cm⁻¹). HRMS measurements were performed on an Agilent LC-MS TOF. High resolution mass are given in *m/z*. Enantiomeric excesses were measured on an Agilent HPLC. Optical rotations were measured on a Polartronic M polarimeter using a 0.5 cm cell with a Na 589 nm filter. X-ray analysis was performed by Dr. R. Scopelliti and Dr. F. F. Tirani at the EPF Lausanne.

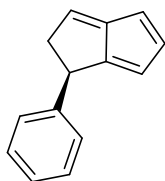
8.2 Synthesis of Chiral Cp^x Ligands and Cp^xRu (II) Complexes

Procedures for Preparation of Chiral Bicycle[3.3.0]octatrienes (2.5).

The synthesis of chiral bicycle[3.3.0]octatrienes were accomplished based on the reported procedures.^{81, 122}



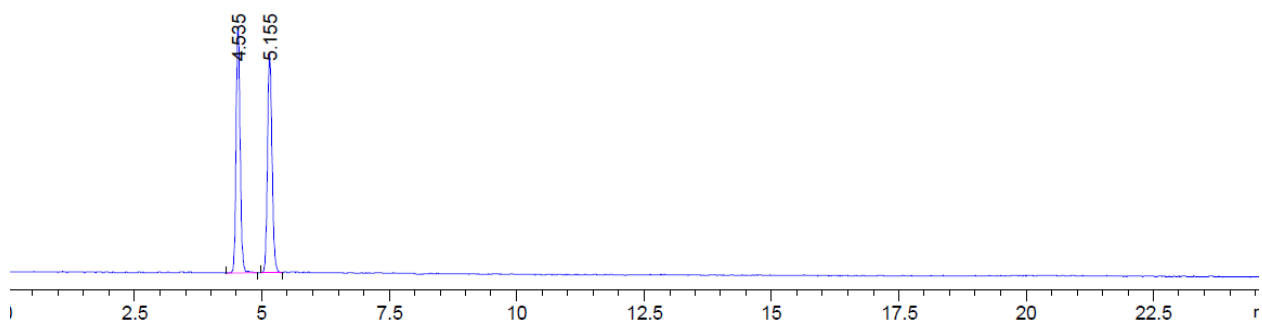
To a solution of (*R*)-2-(((*tert*-butyldimethylsilyl)oxy)diphenylmethyl)pyrrolidine (10 mol %, 334 mg, 0.908 mmol) and *p*-nitrophenol (20 mol %, 253 mg, 1.82 mmol) in MeOH/DCM (9.1 mL/9.1 mL) was added α,β -unsaturated aldehyde (9.08 mmol) at room temperature under N₂. The mixture was stirred for 1 min before the addition of cyclopentadiene (2.29 mL, 3 equiv., 27.2 mmol). After stirring the reaction mixture for 20 h at room temperature, excess cyclopentadiene was azeotropically removed with toluene from the reaction mixture. To the solution of crude mixture in MeOH/DCM (3 mL/3 mL) were added *p*-nitrophenol (1.26 mg, 1 equiv., 9.08 mmol) and diisobutylamine (2.38 mL, 1.5 equiv., 13.6 mmol) at room temperature. The obtained solution was stirred for 24 h under N₂. The resulting mixture was quenched with pH 7.0 phosphate buffer. The organic layer was extracted with EtOAc (3 \times 40 mL), the combined organic layer was washed with brine, dried over Na₂SO₄ and filtrated. After the solvent was removed under reduced pressure, the residue was purified by silica gel column chromatography (*n*-pentane to *n*-pentane/EtOAc = 100/1/1 to *n*-pentane/EtOAc/DCM = 50/1/1) to afford the product **2.5**.



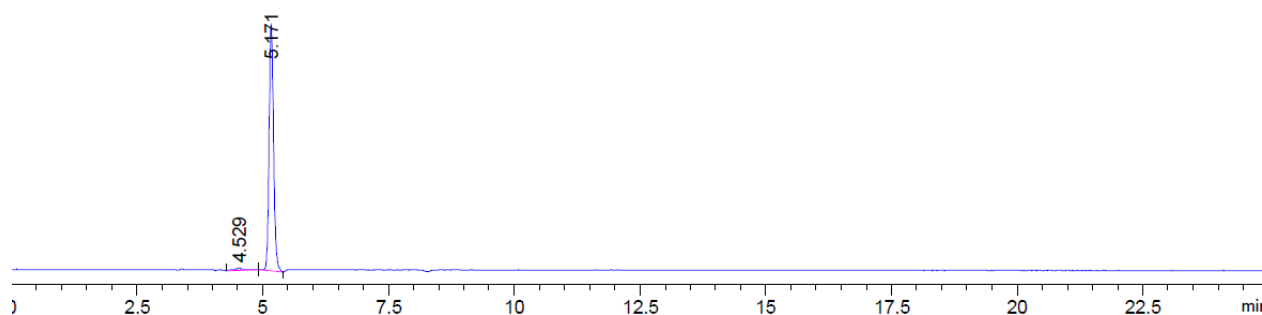
(*R*)-1-Phenyl-1,2-dihydropentalene (2.5)

Orange solid, 669 mg, 41% yield (Over two steps); 98.5:1.5 *er*. [α]_D²⁰ -60.2 (*c* 0.44, CH₂Cl₂); Analytical data: ¹H NMR (400 MHz, Benzene-*d*₆) δ 7.14 – 7.07 (m, 3H), 7.07 – 7.02 (m, 1H), 6.86 (dd, *J* = 5.2, 1.8 Hz, 1H), 6.37 – 6.19 (m, 2H), 5.91 (q, *J* = 2.0 Hz, 1H), 3.93 (dt, *J* = 6.8, 2.3 Hz, 1H),

3.15 (ddd, $J = 19.9, 6.6, 2.8$ Hz, 1H), 2.66 (dt, $J = 19.9, 2.5$ Hz, 1H). ^{13}C NMR (101 MHz, C_6D_6) δ 154.28, 153.86, 145.01, 142.58, 140.29, 128.82, 127.62, 126.53, 117.09, 112.82, 51.75, 42.56. The enantiomeric excess was determined by Daicel Chiralpak IB (25 cm), Hexanes/IPA = 99/1, 1.0 mL/min $^{-1}$, $\lambda = 254$ nm, t_{R} (major) = 5.17 min, t_{R} (minor) = 4.53 min. After crystallization in pentane and ether, **2.5** was obtained with >99.5:0.5 *er*.

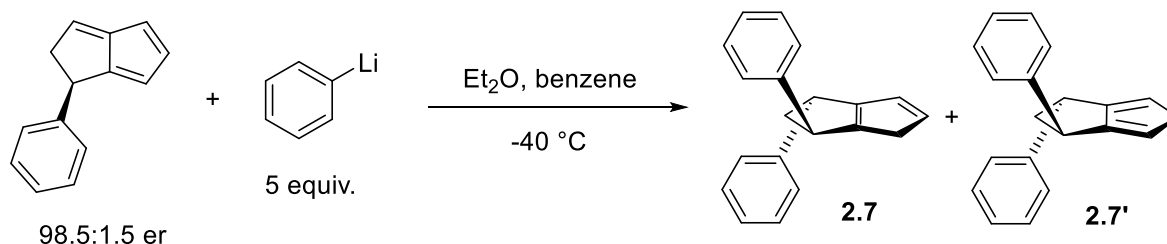


Peak #	RetTime [min]	Type	Width [min]	Area [mAU*s]	Height [mAU]	Area %
1	4.535	BB	0.0857	228.60638	41.85774	50.0582
2	5.155	BB	0.0936	228.07510	37.17632	49.9418

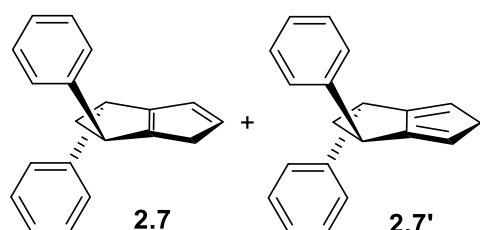


Peak #	RetTime [min]	Type	Width [min]	Area [mAU*s]	Height [mAU]	Area %
1	4.529	BB	0.1537	10.22106	9.19750e-1	1.6916
2	5.171	BB	0.0957	594.00787	96.71053	98.3084

General Procedures for Preparation of Chiral Ligands (2.7).

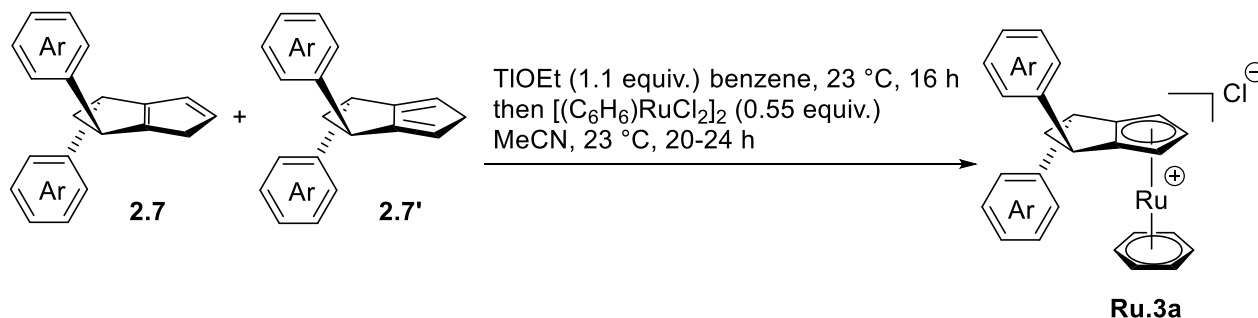


The freshly prepared Ph-Li solution (5 equiv., 6.7 mmol in 6.7 mL Et₂O) in Et₂O was added slowly to a solution of corresponding *(R)*-1-Phenyl-1,2-dihydropentalene (1.34 mmol) in anhydrous Et₂O (11 mL) and benzene (4.4 mL) at -40 °C. The reaction was stirred at -40 °C, and allowed to warm up slowly. After the reaction was complete (monitored by TLC), at the time, the temperature became -18 °C. Then, the reaction mixture was stirred at 0 °C and quenched with water. The organic layer was extracted with ether (3×30 mL). The combined organic layer was dried over Na₂SO₄ and filtered. After the solvent was removed under reduced pressure, the residue was purified through silica gel (PE to PE/Et₂O 100/1) giving the desired product as a mixture of Cp^x compounds.



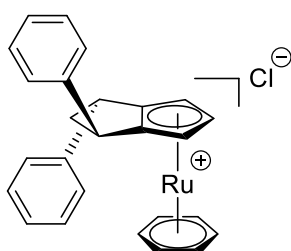
Pale yellow gum, 267 mg, 6.8:1 ratio of double bond isomers, 75% yield. Analytical data for major isomer **2.7**: ¹H NMR (400 MHz, Chloroform-*d*) δ 7.30 (m, 5H), 7.24 – 7.13 (m, 5H), 6.47 (d, *J* = 5.4 Hz, 1H), 6.38 (dt, *J* = 5.3, 1.8 Hz, 1H), 4.28 – 4.15 (m, 2H), 2.96 – 2.78 (m, 2H), 2.75 (ddd, *J* = 7.6, 5.7, 2.0 Hz, 2H). ¹³C NMR (101 MHz, CDCl₃) δ 153.22, 152.84, 146.44, 145.62, 136.77, 129.27, 128.64, 128.52, 127.74, 127.45, 127.31, 126.26, 51.36, 47.81, 46.42, 36.90. HRMS (ESI) calcd for C₂₀H₁₉⁺: [M+H]⁺: 259.1481, Found: 259.1486.

General Procedures for the Syntheses of [Cp^xRu(C₆H₆)]Cl Complexes (Ru.3a)

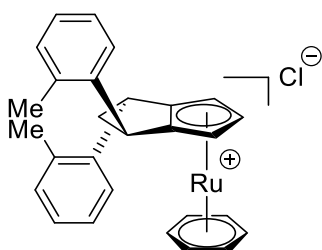


In a dry Schlenk tube, the mixture of ligand isomers **2.7** and **2.7'** (400 mg, 1.548 mmol) were dissolved in degassed benzene (8 mL) under N₂. TIOEt (425 mg, 1.1 equiv., 1.703 mmol) dissolved

in benzene (2 mL) was injected to Schlenk tube. The obtained mixture was stirred under N₂ at room temperature and protected from light for 16 h. The obtained brown TiCp-suspension was added to a suspension of [(C₆H₆)RuCl₂]₂ (426 mg, 0.55 equiv., 0.852 mmol) in 45 ml degassed acetonitrile. The mixture was stirred under N₂ at room temperature in the dark for 24 h. The brown mixture was filtered through a short pad of celite and washed with DCM. After the solvent was removed under reduced pressure, the residue was purified by acidic alumina column chromatography (DCM to DCM/MeOH = 30/1) to afford the product **Ru.3a**.



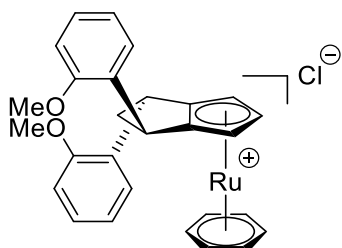
Brown foam, 700 mg, 96% yield. $[\alpha]_D^{20}$ -32.2 (c 0.44, CH₂Cl₂); Analytical data **Ru.3aa**, ¹H NMR (400 MHz, Chloroform-*d*) δ 7.42 (t, *J* = 7.5 Hz, 2H), 7.30 (dd, *J* = 14.7, 7.6 Hz, 4H), 7.24 (s, 1H), 7.19 (t, *J* = 7.2 Hz, 1H), 7.10 (d, *J* = 7.5 Hz, 2H), 6.05 (s, 6H), 5.59 (s, 1H), 5.43 (s, 1H), 5.40 (s, 1H), 4.40 (d, *J* = 7.9 Hz, 1H), 4.18 (dd, *J* = 10.5, 6.9 Hz, 1H), 3.03 (td, *J* = 12.0, 8.1 Hz, 1H), 2.76 (dd, *J* = 12.8, 7.0 Hz, 1H). ¹³C NMR (101 MHz, Chloroform-*d*) δ 141.81, 140.31, 128.97, 127.53, 127.25, 126.83, 126.37, 113.29, 111.84, 87.38, 84.33, 74.40, 43.49, 42.38, 39.75. IR (ATR): ν (cm⁻¹) = 3018, 1495, 1443, 833, 760, 737, 557; HRMS (ESI) calcd for [C₂₆H₂₃Ru]⁺: 407.0838, Found: 407.0846.



The reaction was carried out in 0.35 mmol scale.

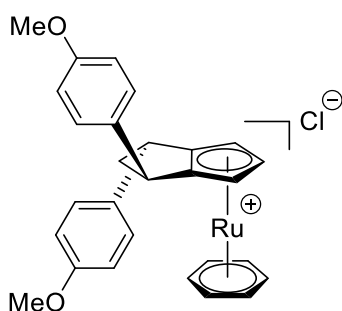
Brown foam, 138 mg, 79% yield. $[\alpha]_D^{20}$ -5.7 (c 0.27, CH₂Cl₂); Analytical data **Ru.3ab**, ¹H NMR (400 MHz, Chloroform-*d*) δ 7.41 (d, *J* = 7.7 Hz, 1H), 7.32 (d, *J* = 7.0 Hz, 1H), 7.25 – 7.17 (m, 3H), 7.14 (t, *J* = 7.3 Hz, 1H), 7.07 (t, *J* = 7.4 Hz, 1H), 6.62 (d, *J* = 7.6 Hz, 1H), 6.26 (s, 6H), 5.66 (s, 1H), 5.48 (s, 1H), 5.14 (s, 1H), 4.48 (d, *J* = 7.5 Hz, 1H), 4.08 (dd, *J* = 10.8, 6.4 Hz, 1H), 3.11 (td, *J* = 11.7, 7.6 Hz, 1H), 2.46 (s, 3H), 2.44 – 2.36 (m, 1H), 2.32 (s, 3H). ¹³C NMR (101 MHz, Chloroform-*d*) δ 139.48, 136.80, 136.74, 136.25, 131.44, 131.20, 127.73, 127.31, 126.20, 126.16, 124.90, 124.78, 115.90, 111.23, 88.08, 84.46, 42.25, 39.82, 37.51, 20.47, 19.68. IR (ATR): ν (cm⁻¹) = 3052, 3017, 2912, 2851,

1487, 1439, 1380, 1053, L 1027, 926, 830, 749. 725; **HRMS** (ESI) calcd for $[\text{C}_{28}\text{H}_{27}\text{Ru}]^+$: 465.1151, Found: 465.1151.



The reaction was carried out in 0.46 mmol scale.

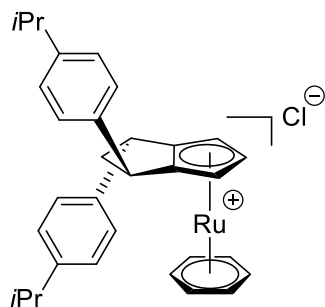
Pale brown foam, 180 mg, 73% yield. $[\alpha]_{\text{D}}^{20}$ -7.3 (*c* 0.33, CH_2Cl_2); Analytical data **Ru.3ac**, **^1H NMR** (400 MHz, CHCl_3 -*d*) δ 7.31 (td, *J* = 6.3, 5.8, 3.0 Hz, 2H), 7.21 (ddd, *J* = 8.6, 5.9, 3.2 Hz, 1H), 7.03 (td, *J* = 7.5, 1.1 Hz, 1H), 6.93 (dd, *J* = 8.5, 1.1 Hz, 1H), 6.88 – 6.82 (m, 3H), 6.02 (s, 6H), 5.55 (s, 1H), 5.34 (d, *J* = 1.7 Hz, 1H), 5.26 – 5.22 (m, 1H), 4.34 (d, *J* = 7.9 Hz, 1H), 4.19 (dd, *J* = 10.9, 6.6 Hz, 1H), 3.87 (s, 3H), 3.85 (s, 3H), 2.99 (ddd, *J* = 12.9, 10.9, 8.1 Hz, 1H), 2.55 (dd, *J* = 13.0, 6.9 Hz, 1H). **^{13}C NMR** (101 MHz, CHCl_3 -*d*) δ 157.71, 156.73, 129.46, 128.83, 128.57, 128.47, 126.30, 125.14, 120.51, 120.35, 115.28, 111.57, 110.72, 110.58, 87.05, 84.08, 74.92, 55.56, 55.45, 39.98, 36.79, 35.76. **IR** (ATR): $\nu(\text{cm}^{-1})$ = 2964, 2835, 1597, 1490, 1456, 1437, 1242, 1106, 1025, 925, 753, 720; **HRMS** (ESI) calcd for $[\text{C}_{28}\text{H}_{27}\text{RuO}_2]^+$: 497.1049, Found: 497.1053.



The reaction was carried out in 0.35 mmol scale.

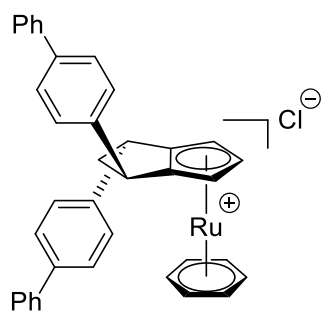
Pale brown foam, 163 mg, 88% yield. $[\alpha]_{\text{D}}^{20}$ -23.6 (*c* 0.31, CH_2Cl_2); Analytical data **Ru.3ad**, **^1H NMR** (400 MHz, CHCl_3 -*d*) δ 7.22 (d, *J* = 8.4 Hz, 2H), 7.04 (d, *J* = 8.6 Hz, 2H), 6.97 (d, *J* = 8.4 Hz, 2H), 6.82 (d, *J* = 8.4 Hz, 2H), 6.08 (s, 6H), 5.63 (s, 1H), 5.49 (s, 1H), 5.41 (s, 1H), 4.30 (d, *J* = 7.7 Hz, 1H), 4.14 (dd, *J* = 10.4, 6.9 Hz, 1H), 3.85 (s, 3H), 3.77 (s, 3H), 2.92 (ddd, *J* = 12.6, 10.5, 7.8 Hz, 1H), 2.76 (dd, *J* = 12.7, 7.0 Hz, 1H). **^{13}C NMR** (101 MHz, CHCl_3 -*d*) δ 158.55, 133.92, 132.34, 127.78, 127.42, 114.17, 114.10, 113.68, 111.96, 87.13, 84.04, 74.61, 74.27, 55.42, 55.33, 43.87,

41.50, 38.95. **IR** (ATR): $\nu(\text{cm}^{-1}) = 2988, 2912, 1608, 1509, 1439, 1243, 1178, 1027, 826, 743$; **HRMS** (ESI) calcd for $[\text{C}_{28}\text{H}_{27}\text{RuO}_2]^+$: 497.1049, Found:



The reaction was carried out in 0.876 mmol scale.

Pale brown foam, 459 mg, 94% yield. $[\alpha]_{\text{D}}^{20} -35.3$ (c 0.15, CH_2Cl_2); Analytical data **Ru.3ae**, **¹H NMR** (400 MHz, Chloroform-d) δ 7.27 (d, $J = 9.6$ Hz, 2H), 7.20 (d, $J = 8.1$ Hz, 2H), 7.12 (d, $J = 8.0$ Hz, 2H), 7.01 (d, $J = 8.0$ Hz, 2H), 6.05 (s, 6H), 5.43 (d, $J = 2.1$ Hz, 1H), 5.40 (d, $J = 2.1$ Hz, 1H), 4.27 (d, $J = 7.8$ Hz, 1H), 4.15 (dd, $J = 10.5, 6.9$ Hz, 1H), 3.01 – 2.88 (m, 2H), 2.84 (p, $J = 6.9$ Hz, 1H), 2.76 (dd, $J = 12.7, 7.0$ Hz, 1H), 1.26 (d, $J = 6.9$ Hz, 6H), 1.19 (d, $J = 7.0$ Hz, 6H). **¹³C NMR** (101 MHz, Chloroform-d) δ 148.24, 147.87, 139.06, 137.74, 126.96, 126.84, 126.71, 126.31, 113.64, 112.05, 87.29, 84.42, 77.37, 74.81, 74.44, 43.60, 42.08, 39.45, 33.75, 33.71, 24.11, 24.01. **IR** (ATR): $\nu(\text{cm}^{-1}) = 2957, 2868, 1511, 1438, 1415, 1382, 1055, 1017, 857, 825$; **HRMS** (ESI) calcd for $[\text{C}_{32}\text{H}_{35}\text{Ru}]^+$: 521.1777, Found: 521.1780.

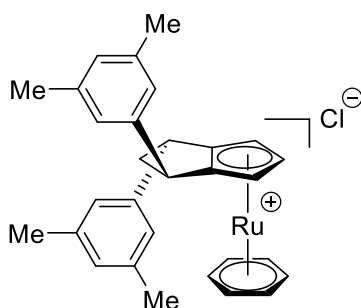


The reaction was carried out in 0.21 mmol scale.

Brown foam, 105 mg, 81% yield. $[\alpha]_{\text{D}}^{20} -37.2$ (c 1.0, CHCl_3); Analytical data **Ru.3af**, **¹H NMR** (400 MHz, CDCl_3) δ 7.68 (d, $J = 7.9$ Hz, 2H), 7.63 (d, $J = 7.7$ Hz, 2H), 7.56 - 7.29 (m, 12H), 7.21 (d, $J = 8.0$ Hz, 2H), 6.11 (s, 6H), 5.62 (s, 1H), 5.51 (s, 1H), 5.47 (s, 1H), 4.50 (d, $J = 7.7$ Hz, 1H), 4.25 (dd, $J = 10.4, 7.0$ Hz, 1H), 3.16 - 3.00 (m, 1H), 2.85 (dd, $J = 12.8, 7.0$ Hz, 1H). **¹³C NMR** (100 MHz, CDCl_3) δ 140.87, 140.50, 140.24, 140.23, 140.01, 139.30, 129.07, 128.91, 127.80, 127.65, 127.50, 127.46,

127.39, 127.08, 127.04, 127.01, 113.22, 111.87, 87.66, 84.58, 75.33, 74.68, 43.80, 42.21, 39.69. **IR** (ATR): $\nu(\text{cm}^{-1}) = 3381, 3056, 3030, 2930, 1599, 1487, 1440, 1407, 925, 831, 765, 742, 698, 499$; **HRMS** (ESI) calcd for $[\text{C}_{38}\text{H}_{31}\text{Ru}]^+$: 589.1464, Found: 589.1468.

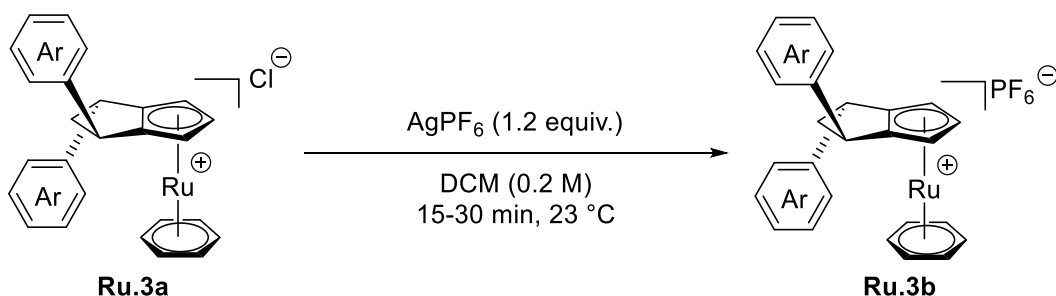
497.1049.



The reaction was carried out in 0.55 mmol scale.

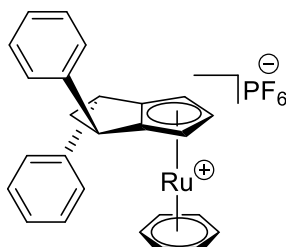
Brown foam, 83.1 mg, 54% yield. $[\alpha]_{\text{D}}^{20} -4.0$ (c 0.25, CH_2Cl_2); Analytical data **Ru.3ag**, **^1H NMR** (400 MHz, CDCl_3) $\delta = 6.95$ (s, 1H), 6.89 (s, 2H), 6.83 (s, 1H), 6.67 (s, 2H), 5.97 (s, 6H), 5.61 (s, 1H), 5.44 (s, 1H), 5.38 (s, 1H), 4.25 (d, $J=7.4$, 1H), 4.11 (dd, $J=10.3, 6.9$, 1H), 3.00 – 2.86 (m, 1H), 2.72 (dd, $J=12.6, 7.1$, 1H), 2.37 (s, 6H), 2.23 (s, 6H). **^{13}C NMR** (101 MHz, CDCl_3) δ 141.73, 140.21, 138.48, 138.37, 128.95, 128.86, 124.56, 124.15, 113.35, 111.89, 87.81, 85.20, 77.37, 75.42, 74.69, 43.90, 42.44, 39.67, 21.70, 21.42. **IR** (ATR): $\nu(\text{cm}^{-1}) = 3033, 2917, 2863, 1601, 1438, 1376, 1036, 925, 846, 724$; **HRMS** (ESI) calcd for $[\text{C}_{30}\text{H}_{31}\text{Ru}]^+$: 493.1464, Found: 493.1468.

General Procedures for Counteranion Exchange of Chiral $[\text{Cp}^*\text{Ru}(\text{C}_6\text{H}_5)]\text{Cl}$ Complexes (**Ru.3a**)

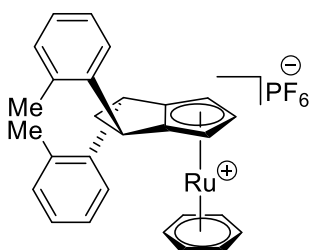


To a solution of obtained complex **Ru.3a** (1 equiv.) in dry DCM at room temperature was added a solution of AgPF_6 (1.20 equiv.) in dry DCM under N_2 . The mixture was stirred for 15-30 min at room temperature in the dark. AgCl was removed by filtration over paper and all volatiles removed under

reduced pressure. The residue was purified by acidic alumina column chromatography (DCM to DCM/MeOH = 30/1) to afford the product **Ru.3b**.

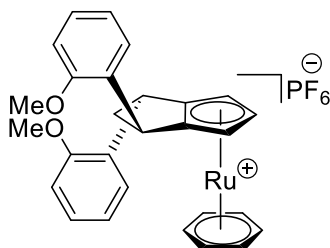


Brown foam, 109 mg, 97% yield; Analytical data **Ru.3ba**, $[\alpha]_{\text{D}}^{20}$ -26.3 (c 1.0, CH₂Cl₂); Mp = 196.7-197.5 °C; Analytical data **Ru.3ba**: **¹H NMR** (400 MHz, CD₂Cl₂) δ 7.46 (t, J = 7.5 Hz, 2H), 7.37 (d, J = 7.6 Hz, 1H), 7.35 - 7.28 (m, 4H), 7.27 - 7.22 (m, 1H), 7.15 - 7.10 (m, 2H), 5.83 (s, 6H), 5.38 (d, J = 1.4 Hz, 2H), 5.31 - 5.30 (t, J = 1.1 Hz, 1H), 4.25 (dd, J = 10.5, 7.1 Hz, 1H), 4.17 (d, J = 8.0 Hz, 1H), 2.95 (ddd, J = 12.9, 10.5, 8.0 Hz, 1H), 2.80 (dd, J = 12.9, 7.1 Hz, 1H). **¹³C NMR** (100 MHz, CD₂Cl₂) δ 142.12, 140.64, 129.30, 129.27, 127.85, 127.62, 127.03, 126.57, 114.07, 112.36, 86.98, 83.65, 74.66, 74.64, 43.63, 42.65, 40.02. **¹⁹F NMR** (376 MHz, CD₂Cl₂) δ -72.73 (d, J = 711.3 Hz). **³¹P NMR** (162 MHz, CD₂Cl₂) δ -144.37 (hept, J = 711.2 Hz). **IR** (ATR): ν_{max} (cm⁻¹) = 3671, 3096, 3061, 3029, 2967, 2945, 1602, 1497, 1444, 835, 761, 704, 557, 489, 470, 407, 385; **HRMS** (ESI) calcd for [C₂₆H₂₃Ru]⁺: 407.0838, Found: 407.0818.

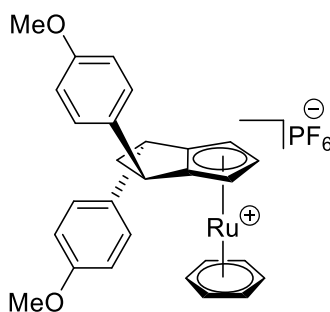


Brown foam, 50.5 mg, 83% yield; Analytical data **Ru.3bb**, $[\alpha]_{\text{D}}^{20}$ +12.8 (c 1.0, CHCl₃); Analytical data **Ru.3bb**: **¹H NMR** (400 MHz, CDCl₃) 7.39 (d, J = 7.7 Hz, 1H), 7.32 (ddd, J = 8.0, 5.5, 3.2 Hz, 1H), 7.23 - 7.19 (m, 2H), 7.17 (dd, J = 7.5, 1.6 Hz, 1H), 7.12 (td, J = 7.4, 1.4 Hz, 1H), 7.06 (td, J = 7.5, 1.6 Hz, 1H), 6.62 (dd, J = 7.6, 1.4 Hz, 1H), 6.04 (s, 6H), 5.42 (t, J = 2.4 Hz, 1H), 5.28 (d, J = 2.3 Hz, 1H), 5.11 (d, J = 2.3 Hz, 1H), 4.34 (d, J = 7.7 Hz, 1H), 4.06 (dd, J = 10.9, 6.4 Hz, 1H), 3.06 (ddd, J = 12.5, 10.9, 7.9 Hz, 1H), 2.42 (s, 3H), 2.40 - 2.35 (m, 1H), 2.31 (s, 3H). **¹³C NMR** (100 MHz, CDCl₃) δ 139.67, 136.73, 136.63, 136.37, 131.36, 131.17, 127.67, 127.23, 126.27, 126.11, 124.85, 124.76,

115.85, 111.30, 86.95, 82.99, 74.30, 73.40, 41.95, 39.28, 37.51, 19.77, 19.62. **¹⁹F NMR** (376 MHz, CDCl₃) δ -72.20 (d, *J* = 713.0 Hz). **³¹P NMR** (162 MHz, CDCl₃) δ -146.46 (hept, *J* = 711.2 Hz). **IR** (ATR): *v*_{max} (cm⁻¹) = 3102, 3018, 2951, 1490, 1443, 914, 837, 756, 731, 558, 453, 399; **HRMS** (ESI) calcd for [C₂₈H₂₇Ru]⁺: 465.1151, Found: 465.1151.

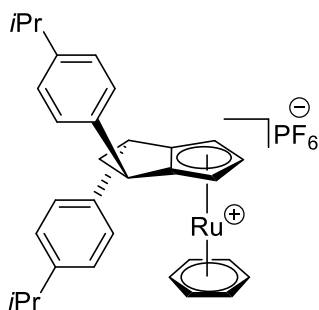


White foam, 70.6 mg, 77% yield; Analytical data **Ru.3bc**, [*α*]_D²⁰ -4.60 (c 1.0, CH₂Cl₂); Mp = 140.3-141.0 °C; Analytical data **Ru.3bc**: **¹H NMR** (400 MHz, CDCl₃) δ 7.37 - 7.31 (m, 2H), 7.26 - 7.19 (m, 1H), 7.05 (t, *J* = 7.0 Hz, 1H), 6.97 (d, *J* = 8.5 Hz, 1H), 6.91 - 6.82 (m, 3H), 5.86 (s, 6H), 5.35 - 5.26 (m, 3H), 4.34 (d, *J* = 7.9 Hz, 1H), 4.24 (dd, *J* = 10.8, 6.7 Hz, 1H), 3.89 (d, *J* = 2.4 Hz, 6H), 3.00 (ddd, *J* = 13.0, 10.8, 8.2 Hz, 1H), 2.61 (dd, *J* = 12.9, 6.8 Hz, 1H). **¹³C NMR** (100 MHz, CDCl₃) 157.79, 156.91, 129.60, 128.90, 128.62, 128.57, 126.29, 125.11, 120.53, 120.35, 115.41, 112.07, 110.82, 110.71, 86.34, 82.80, 75.02, 74.32, 55.52, 55.35, 39.69, 36.75, 35.97. **¹⁹F NMR** (376 MHz, CDCl₃) δ -72.68 (d, *J* = 713.0 Hz). **³¹P NMR** (162 MHz, CDCl₃) δ -142.10 (hept, *J* = 712.8 Hz). **IR** (ATR): *v*_{max} (cm⁻¹) 3097, 2941, 2840, 1599, 1586, 1462, 1289, 1246, 1109, 1053, 1027, 912, 836, 755, 729, 648, 557, 488, 475, 461, 404, 382; **HRMS** (ESI) calcd for [C₂₈H₂₇RuO₂]⁺: 497.1049, Found: 497.1052.

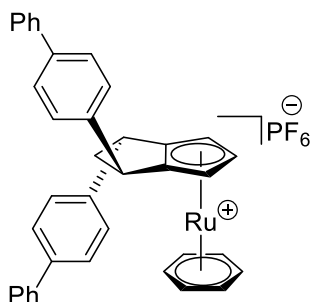


Brown foam, 23.0 mg, 79% yield; Analytical data **Ru.3bd**, [*α*]_D²⁰ -8.50 (c 1.0, CH₂Cl₂); Analytical data **Ru.3bd**: **¹H NMR** (400 MHz, CD₂Cl₂) δ 7.18 (d, *J* = 8.3 Hz, 2H), 7.01 (d, *J* = 8.6 Hz, 2H), 6.96 (d, *J* = 8.7 Hz, 2H), 6.81 (d, *J* = 8.8 Hz, 2H), 5.82 (s, 6H), 5.34 (t, *J* = 2.4 Hz, 1H), 5.30 - 5.29 (m, 1H),

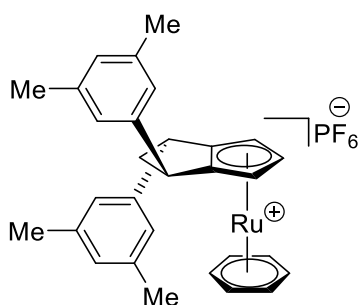
5.28 (dd, $J = 2.3, 0.7$ Hz, 1H), 4.15 (dd, $J = 10.5, 7.1$ Hz, 1H), 4.08 (d, $J = 7.8$ Hz, 1H), 3.81 (s, 3H), 3.73 (s, 3H), 2.83 (ddd, $J = 12.8, 10.5, 7.8$ Hz, 1H), 2.73 (dd, $J = 12.8, 7.1$ Hz, 1H). **^{13}C NMR** (100 MHz, CD_2Cl_2) δ 158.80, 133.73, 132.28, 127.65, 127.23, 114.26, 114.18, 114.10, 112.30, 86.55, 83.16, 74.15, 74.11, 55.32, 55.26, 43.61, 41.55, 38.93. **^{19}F NMR** (376 MHz, CD_2Cl_2) δ -72.76 (d, $J = 711.0$ Hz). **^{31}P NMR** (162 MHz, CD_2Cl_2) δ -144.37 (hept, $J = 711.3$ Hz). **IR** (ATR): ν_{max} (cm^{-1}) = 3101, 2958, 2930, 2840, 1610, 1582, 1511, 1461, 1443, 1304, 1248, 1180, 1115, 1030, 956, 836, 767, 734, 709, 556, 412; **HRMS** (ESI) calcd for $[\text{C}_{28}\text{H}_{27}\text{O}_2\text{Ru}]^+$: 497.1049, Found: 497.1058.



White foam, 38 mg, 93% yield; Analytical data **Ru.3be**, $[\alpha]_{\text{D}}^{20}$ -33.3 (c 0.42, CH_2Cl_2); Analytical data **Ru.3be**: **^1H NMR** (400 MHz, Chloroform- d) δ 7.30 (d, $J = 8.0$ Hz, 2H), 7.20 (d, $J = 8.0$ Hz, 2H), 7.12 (d, $J = 7.9$ Hz, 2H), 7.02 (d, $J = 8.1$ Hz, 2H), 5.85 (s, 6H), 5.41 (d, $J = 2.4$ Hz, 1H), 5.39 (d, $J = 2.4$ Hz, 1H), 4.16 (dd, $J = 10.4, 7.3$ Hz, 2H), 2.99 – 2.87 (m, 2H), 2.87 – 2.81 (m, 1H), 2.77 (dt, $J = 12.8, 6.1$ Hz, 1H), 1.27 (d, $J = 6.9$ Hz, 6H), 1.20 (s, 6H). **^{13}C NMR** (101 MHz, Chloroform- d) δ 148.18, 147.77, 139.33, 137.88, 126.97, 126.89, 126.73, 126.29, 113.66, 112.37, 86.67, 83.50, 74.39, 74.27, 43.45, 41.77, 39.43, 33.78, 33.73, 24.15, 24.12, 24.05. **^{19}F NMR** (376 MHz, Chloroform- d) δ -72.28 (d, $J = 713.1$ Hz). **^{31}P NMR** (162 MHz, Chloroform- d) δ -144.22 (hept, $J = 713.1$ Hz). **IR** (ATR): ν_{max} (cm^{-1}) = 2959, 2929, 2870, 1512, 1443, 1055, 1018, 833, 557; **HRMS** (ESI) calcd for $[\text{C}_{32}\text{H}_{35}\text{Ru}]^+$: 521.1777, Found: 521.1782.

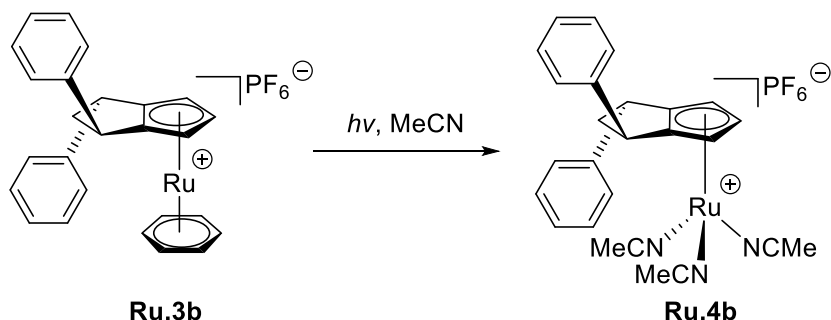


Brown foam, 45.0 mg, 96% yield; Analytical data **Ru.3bf**, $[\alpha]_D^{20}$ -38.6 (c 1.0, CHCl₃); Analytical data **Ru.3bf**: **¹H NMR** (400 MHz, CDCl₃) δ 7.67 (d, J = 8.0 Hz, 2H), 7.63 (d, J = 7.4 Hz, 2H), 7.54 - 7.29 (m, 12H), 7.16 (d, J = 8.1 Hz, 2H), 5.85 (s, 6H), 5.39 (d, J = 5.0 Hz, 1H), 5.33 (s, 1H), 4.26 (d, J = 7.8 Hz, 2H), 4.19 (dd, J = 10.5, 7.2 Hz, 1H), 2.96 (ddd, J = 12.9, 10.6, 8.0 Hz, 1H), 2.80 (dd, J = 12.9, 7.1 Hz, 1H). **¹³C NMR** (100 MHz, CDCl₃) δ 141.04, 140.42, 140.09, 140.04, 140.02, 139.35, 129.06, 128.96, 127.73, 127.58, 127.53, 127.40, 127.33, 127.05, 127.01, 126.92, 113.09, 111.88, 86.76, 83.57, 74.49, 74.38, 43.60, 41.78, 39.53. **¹⁹F NMR** (376 MHz, CHCl₃) δ -72.02 (d, J = 713.2 Hz). **³¹P NMR** (162 MHz, CHCl₃) δ -144.17 (hept, J = 712.8 Hz). **IR** (ATR): ν_{\max} (cm⁻¹) = 3097, 3056, 3030, 2961, 2927, 2855, 1519, 1488, 1443, 1407, 1261, 1217, 1007, 914, 835, 764, 699, 557, 499; **HRMS** (ESI) calcd for [C₃₈H₃₁Ru]⁺: 589.1464, Found: 589.1457.

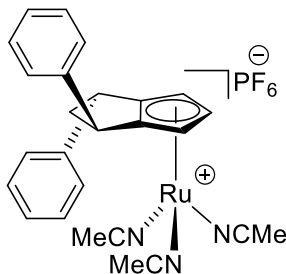


Brown foam, 27.1 mg, 54% yield; Analytical data **Ru.3bg**, $[\alpha]_D^{20}$ -19.0 (c = 1.45, CHCl₃); Analytical data **Ru.3bg**: **¹H NMR** (400 MHz, CDCl₃) δ (ppm) = 6.97 (s, 1H), 6.88 (s, 2H), 6.85 (s, 1H), 6.68 (s, 2H), 5.87 (s, 6H), 5.45 (t, J = 2.3 Hz, 1H), 5.42 (s, 1H), 5.36 (s, 1H), 4.18 - 4.11 (m, 1H), 4.11 - 4.06 (m, 1H), 2.94 - 2.82 (m, 1H), 2.81 - 2.71 (m, 1H), 2.38 (s, 6H), 2.25 (s, 6H); **¹³C NMR** (101 MHz, CDCl₃) δ (ppm) = 141.8, 140.3, 138.7, 138.6, 129.1, 129.0, 124.6, 124.1, 113.5, 112.3, 86.8, 83.8, 74.7, 43.6, 42.2, 39.7, 21.7, 21.5; **¹⁹F NMR** (376 MHz, CDCl₃) δ (ppm) = -72.4 (d, J = 712.7 Hz); **³¹P NMR** (162 MHz, CDCl₃) δ (ppm) = -144.3 (hept, J = 712.7 Hz); **IR** (ATR): ν_{\max} (cm⁻¹) = 3095, 2920, 1676, 1603, 1443, 837, 558; **HRMS** (ESI) calcd for [C₃₀H₃₁Ru]⁺: 493.1464, Found: 493.1465.

Procedures for the Synthesis of the Active Complex (Ru.4b)

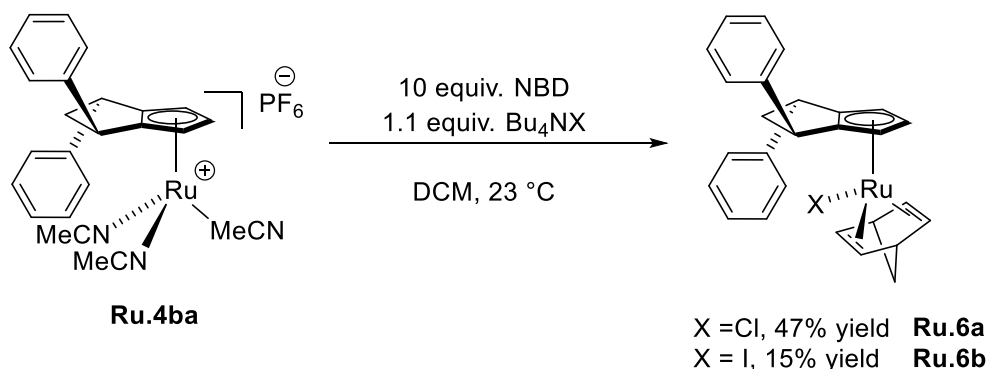


A solution of complex **Ru.3b** (0.029 mmol, 1 equiv.) in degassed acetonitrile (0.02 M) transferred to a photochemical reactor (ACE glass, PenRay ® low-pressure mercury lamp, 5.5 Watts, 254 nm wavelength). The system was closed and irradiated for 24 h under nitrogen purging. The reaction mixture turned to yellow from colorless solution. The resulting solution was concentrated under reduced pressure. In order to remove residual volatiles, freeze-dry using liquid N₂ and high vacuum was used. After removing volatiles, it produced corresponding trisacetonitrile **Ru.4b** as a brown foam.

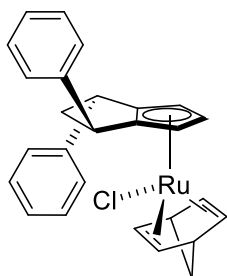


Brown foam, 17.8 mg, 100% yield; Analytical data **Ru.4ba**, $[\alpha]_{\text{D}}^{20}$ -25.9 (*c* 0.8, CH₃CN);: **¹H NMR** (600 MHz, CD₃CN) δ 7.47 - 7.43 (m, 2H), 7.37 (t, *J* = 7.7 Hz, 2H), 7.32 - 7.28 (m, 2H), 7.25 (d, *J* = 7.4 Hz, 1H), 7.22 (d, *J* = 8.0 Hz, 3H), 4.36 (t, *J* = 2.2 Hz, 1H), 4.14 (d, *J* = 2.3 Hz, 1H), 3.97 (dd, *J* = 10.9, 6.7 Hz, 1H), 3.87 - 3.84 (m, 2H), 2.93 (ddd, *J* = 12.3, 10.9, 8.1 Hz, 1H), 2.53 (dd, *J* = 12.3, 6.6 Hz, 1H). **¹³C NMR** (151 MHz, CD₃CN) δ 144.10, 141.64, 129.54, 129.08, 128.64, 128.00, 127.51, 127.48, 102.73, 95.35, 78.50, 61.76, 55.17, 44.22, 42.20, 40.82. **¹⁹F NMR** (376 MHz, CD₃CN) δ -72.87 (d, *J* = 706.4 Hz). **³¹P NMR** (243 MHz, CD₃CN) δ -143.18 (hept, *J* = 707.1 Hz). **IR** (ATR): ν_{max} (cm⁻¹) = 3088, 3057, 3028, 2936, 1652, 1601, 1496, 1449, 1031, 836, 763, 703, 558; **HRMS** (ESI) calcd for [C₂₀H₁₇Ru]⁺: 359.0368, Found: 359.0360.

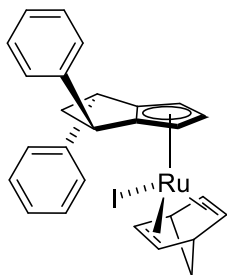
Procedures for the Synthesis of Neutral Cp^xRuX Complexes (Ru.6a and Ru.6b).



A solution of **Ru.4ba** (1 equiv.) and tetrabutylammonium chloride (1.1 equiv.) was dissolved in DCM. Then, freshly distilled norbornadiene (10 equiv.) was added into the reaction mixture. Stirred the reaction mixture for 15 h, then, all volatiles were removed under reduced pressure. The crude mixture was purified by silica column chromatography (DCM to *n*-pentane/EA = 3/1 (v/v')).

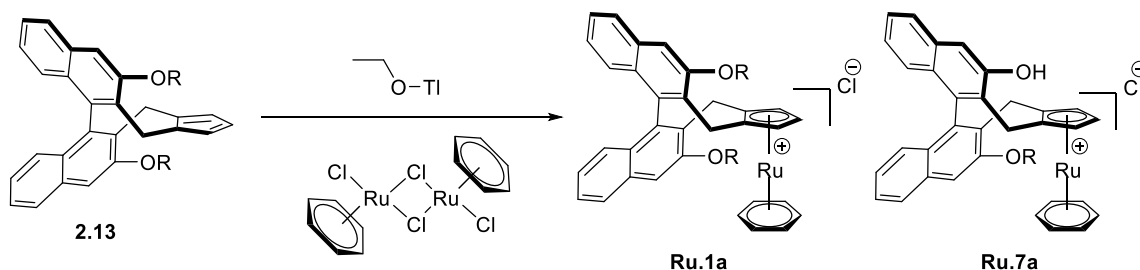


Brown foam, 2.64 mg, 47% yield; Analytical data **Ru.6a**, $[\alpha]_D^{20} +103.3$ ($c = 0.1$, CH₂Cl₂);: **¹H NMR** (400 MHz, CD₂Cl₂) δ (ppm) 7.36 - 7.27 (m, 4H), 7.23 (dd, $J = 11.2, 6.4$ Hz, 4H), 7.18 (d, $J = 7.7$ Hz, 2H), 5.04 (s, 1H), 4.70 (d, $J = 2.9$ Hz, 2H), 4.54 - 4.45 (m, 1H), 4.22 (d, $J = 6.3$ Hz, 2H), 4.13 (d, $J = 2.6$ Hz, 1H), 4.07 (d, $J = 8.1$ Hz, 1H), 3.58 (s, 1H), 3.56 - 3.52 (m, 1H), 3.35 (s, 1H), 2.75 (td, $J = 11.4, 8.2$ Hz, 1H), 2.29 (dd, $J = 12.4, 6.7$ Hz, 1H), 1.22 (d, $J = 8.0$ Hz, 1H), 1.14 (d, $J = 8.7$ Hz, 1H). **¹³C NMR** (151 MHz, CD₂Cl₂) δ (ppm) = 143.25, 140.23, 128.90, 128.63, 127.92, 127.61, 127.17, 126.78, 122.37, 111.17, 90.17, 76.16, 73.21, 71.25, 65.30, 62.73, 50.69, 50.32, 49.43, 48.54, 42.60, 42.07, 1.16. **IR** (ATR): ν_{\max} (cm⁻¹) = 3060, 3024, 3001, 2927, 2849, 1601, 1495, 1450, 1415, 1304, 1184, 1079, 1031, 870, 799, 766, 734, 701, 484; **HRMS** (ESI) calcd for [C₂₇H₂₅Ru]⁺, [M-Cl]⁺, exact mass: 451.0994, found 451.1005.

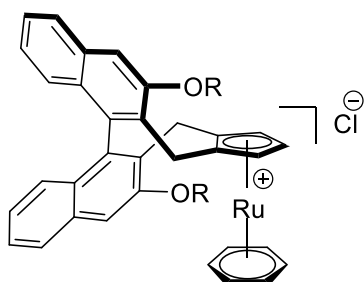


Yellow solid, 0.7 mg, 16% yield; Analytical data **Ru.6b**, ^1H NMR (400 MHz, CD_2Cl_2) δ 7.36 – 7.27 (m, 4H), 7.22 (td, J = 8.9, 8.0, 6.6 Hz, 4H), 7.14 – 7.10 (m, 2H), 5.10 (dd, J = 2.2, 1.1 Hz, 1H), 5.01 (t, J = 2.7 Hz, 1H), 4.64 (d, J = 8.0 Hz, 1H), 4.58 (t, J = 4.0 Hz, 1H), 4.38 (t, J = 4.3 Hz, 1H), 4.33 (t, J = 4.0 Hz, 1H), 4.24 – 4.20 (m, 1H), 4.19 (dd, J = 2.8, 1.2 Hz, 1H), 3.41 (s, 1H), 3.26 (s, 1H), 3.13 (t, J = 4.2 Hz, 1H), 2.67 – 2.53 (m, 1H), 2.28 (dd, J = 12.4, 6.6 Hz, 1H), 1.12 – 1.01 (m, 1H), 1.01 – 0.93 (m, 1H). IR (ATR): $\tilde{\nu}$ (cm^{-1}) = 3083, 3056, 3024, 2958, 2920, 1733, 1600, 1581, 1494, 1450, 1303, 1261, 1182, 1077, 1030, 953, 909, 865, 799, 762, 736, 700, 651, 552, 488, 468, 453, 427, 416.

General Procedure for the Synthesis of Chiral Cp^*Ru Complexes



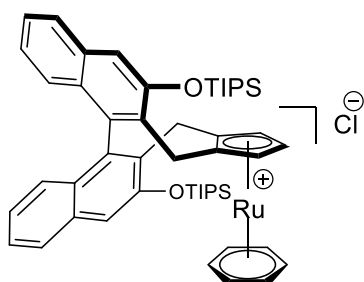
The Cp^* ligand **2.13** (mixture of isomers, 106 μmol , 1.00 eq.) was dissolved in benzene (1.00 mL, degassed by pump-freeze-thaw, 3 cycles). Then, thallium ethoxide (117 μmol , 1.10 eq.) was added as a solution in degassed benzene (0.50 mL) under nitrogen atmosphere under the absence of light at room temperature. The mixture was stirred the mixture at room temperature for 12 h or it was heated to 80 $^\circ\text{C}$ for shortening the reaction time for deprotonation of Cp ligands. After cooling back to room temperature the resulting brown solution was added dropwise to a suspension of $[\text{Ru}(\text{C}_6\text{H}_6)\text{Cl}_2]_2$ (63.0 μmol , 0.60 eq.) in 8.00 mL degassed acetonitrile. The resulting mixture was stirred for 18 h protected from light. TiCl_4 was removed by filtration over Kimtech paper and all volatiles were removed under reduced pressure. The residue was dissolved in 1.00 mL MeOH and filtered again over a pipette filled with paper, washed with MeOH (3 x 1 mL) to remove insoluble impurities and ruthenocene (Cp^*_2Ru) byproducts. The filtrate was evaporated to dryness and purified by column chromatography on acidic alumina (changing the gradient from pure DCM to DCM/MeOH = 50/1 (v/v')) to yield sandwich complex with chloride counter anion **Ru.1a** as brown solid.



R = TBDPS

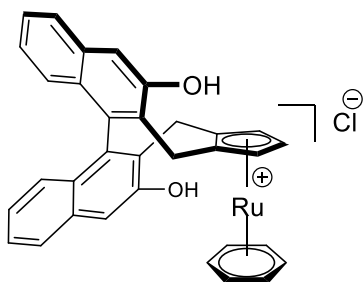
Following the general procedure using 60 mg (0.070 mmol) of corresponding Cp^x ligand. Stirred the Cp^x ligand with thallium ethoxide at 80 °C for 3 h for the deprotonation.

Pale yellow solid, 12 mg, 16% yield; Analytical data **Ru.1ab**: ¹H NMR (400 MHz, CDCl₃) δ 7.86 – 7.78 (m, 2H), 7.75 – 7.68 (m, 2H), 7.63 (ddd, *J* = 8.1, 2.7, 1.3 Hz, 4H), 7.59 – 7.49 (m, 4H), 7.48 – 7.41 (m, 4H), 7.36 (dtd, *J* = 11.6, 7.5, 5.3 Hz, 7H), 7.20 (ddd, *J* = 14.8, 7.7, 1.3 Hz, 2H), 7.13 (ddd, *J* = 8.2, 6.8, 1.2 Hz, 1H), 6.98 (ddd, *J* = 8.3, 6.5, 1.5 Hz, 1H), 6.92 (s, 1H), 6.88 (d, *J* = 8.4 Hz, 1H), 6.51 – 6.44 (m, 1H), 6.07 (s, 6H), 5.72 (s, 1H), 5.44 (s, 1H), 5.20 (s, 1H), 4.15 (d, *J* = 13.9 Hz, 1H), 4.04 (d, *J* = 15.0 Hz, 1H), 3.13 (d, *J* = 13.9 Hz, 1H), 2.88 (d, *J* = 15.1 Hz, 1H), 1.25 (s, 9H), 1.17 (s, 9H).



Following the general procedure using 72.9 mg (0.106 mmol) of corresponding Cp^x ligand. Stirred the Cp^x ligand with thallium ethoxide at room temperature for 12 h for the deprotonation.

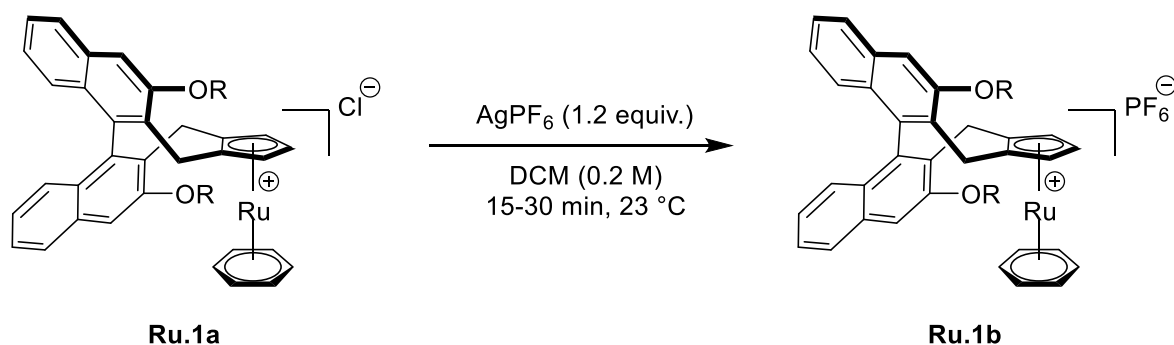
Yellow solid, 34 mg, 35% yield; Analytical data **Ru.1ac**: ¹H NMR (400 MHz, CDCl₃) 7.84 (d, *J* = 8.2 Hz, 1H), 7.71 (d, *J* = 8.2 Hz, 1H), 7.56 (s, 1H), 7.48 (ddd, *J* = 8.1, 6.8, 1.2 Hz, 1H), 7.36 (ddd, *J* = 8.1, 6.8, 1.2 Hz, 1H), 7.27 (s, 1H), 7.18 (ddd, *J* = 8.3, 6.9, 1.2 Hz, 1H), 7.08 – 6.96 (m, 2H), 6.73 (d, *J* = 8.5 Hz, 1H), 6.03 (s, 6H), 5.75 (s, 1H), 5.44 (s, 1H), 5.12 (s, 1H), 3.93 (dd, *J* = 14.4, 10.8 Hz, 2H), 3.02 (d, *J* = 13.9 Hz, 1H), 2.91 (d, *J* = 14.9 Hz, 1H), 1.43 (h, *J* = 7.4 Hz, 6H), 1.23 (d, *J* = 7.5 Hz, 9H), 1.19 – 1.11 (m, 27H).



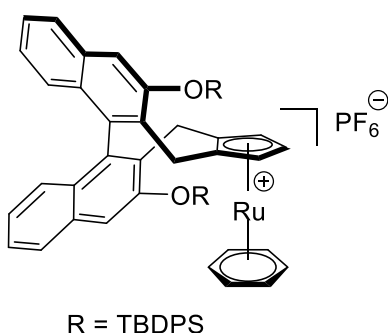
Following the general procedure using 14.6 mg (0.039 mmol) of corresponding Cp^x ligand. Stirred the Cp^x ligand with thallium ethoxide at room temperature for 12 h for the deprotonation.

White solid, 1.5 mg, 7% yield; Analytical data **Ru.1ae**: ¹H NMR (400 MHz, CD₃OD) δ 7.81 (d, *J* = 8.3 Hz, 1H), 7.68 (s, 1H), 7.51 (s, 1H), 7.43 – 7.36 (m, 1H), 7.36 – 7.29 (m, 1H), 7.26 (s, 1H), 7.10 – 6.98 (m, 2H), 6.88 (dd, *J* = 17.3, 8.4 Hz, 2H), 6.01 (s, 6H), 5.49 (s, 1H), 5.34 (d, *J* = 2.4 Hz, 1H), 5.19 (t, *J* = 2.4 Hz, 1H), 4.05 (d, *J* = 15.3 Hz, 1H), 3.90 (d, *J* = 13.7 Hz, 1H), 3.02 (d, *J* = 13.7 Hz, 1H), 2.83 (d, *J* = 15.3 Hz, 1H).

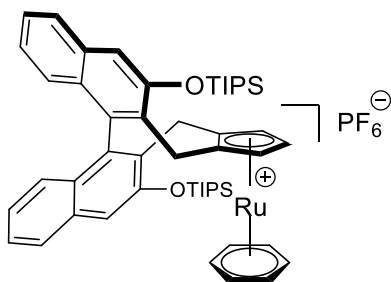
General Procedure for Counteranion Exchange of Chiral $[\text{Cp}^*\text{Ru}(\text{C}_6\text{H}_6)]\text{Cl}$ Complexes (**Ru.1a**)



To a solution of obtained $[\text{Cp}^*\text{Ru}(\text{C}_6\text{H}_6)]\text{Cl}$ complex **Ru.1a** (1 equiv.) in dry DCM at room temperature was added a solution of AgPF_6 (1.20 equiv.) in dry DCM under N_2 . The mixture was stirred for 15-30 min at room temperature in the dark. AgCl was removed by filtration over paper and all volatiles removed under reduced pressure. The residue was purified by acidic alumina column chromatography (DCM to DCM/MeOH = 30/1) to afford the product **4**.

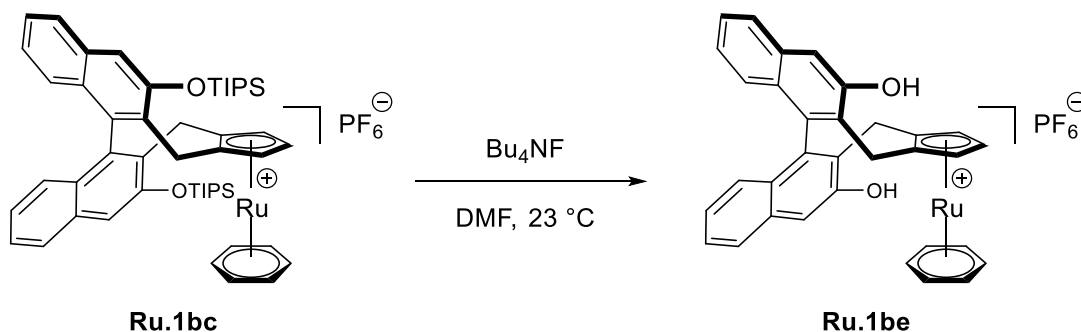


Brown solid 7.3 mg, 94% yield; Analytical data **Ru.1bb**: $^1\text{H NMR}$ (400 MHz, CDCl_3) δ 7.84 – 7.75 (m, 2H), 7.72 (dd, J = 8.1, 1.4 Hz, 2H), 7.64 (td, J = 8.3, 1.4 Hz, 4H), 7.59 – 7.54 (m, 2H), 7.54 – 7.50 (m, 2H), 7.48 – 7.42 (m, 4H), 7.42 – 7.32 (m, 8H), 7.21 (ddd, J = 8.2, 6.6, 1.2 Hz, 1H), 7.14 (ddd, J = 8.2, 6.8, 1.3 Hz, 1H), 6.99 (ddd, J = 8.3, 6.6, 1.5 Hz, 1H), 6.94 (s, 1H), 6.90 (dd, J = 8.4, 1.1 Hz, 1H), 6.49 (dd, J = 8.5, 1.1 Hz, 1H), 5.94 (s, 6H), 5.38 (d, J = 2.4 Hz, 1H), 5.37 – 5.33 (m, 1H), 5.19 (t, J = 1.7 Hz, 1H), 4.13 (d, J = 14.0 Hz, 1H), 4.04 (d, J = 15.1 Hz, 1H), 3.10 (d, J = 14.0 Hz, 1H), 2.88 (d, J = 15.1 Hz, 1H), 1.26 (s, 9H), 1.18 (s, 9H). $^{31}\text{P NMR}$ (162 MHz, CDCl_3) δ -129.73, -135.56, -139.96, -144.36, -148.76, -153.16, -157.56.

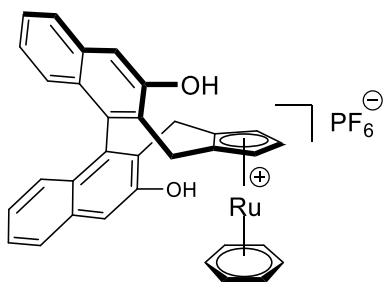


Yellow solid, 15 mg, 75% yield; Analytical data **Ru.1bc**: $^1\text{H NMR}$ (400 MHz, CDCl_3) δ 7.84 (d, J = 8.2 Hz, 1H), 7.71 (d, J = 8.2 Hz, 1H), 7.57 (s, 1H), 7.49 (ddd, J = 8.1, 6.8, 1.1 Hz, 1H), 7.36 (ddd, J = 8.1, 6.7, 1.1 Hz, 1H), 7.28 (s, 1H), 7.19 (ddd, J = 8.2, 6.8, 1.2 Hz, 1H), 7.09 – 6.98 (m, 2H), 6.74 (d, J = 8.5 Hz, 1H), 5.91 (s, 6H), 5.43 (s, 1H), 5.34 (t, J = 2.5 Hz, 1H), 5.14 (s, 1H), 3.95 (dd, J = 14.5, 7.5 Hz, 2H), 3.01 (d, J = 13.9 Hz, 1H), 2.92 (d, J = 14.9 Hz, 1H), 1.44 (h, J = 7.5 Hz, 6H), 1.24 (d, J = 7.5 Hz, 9H), 1.20 – 1.10 (m, 27H). $^{31}\text{P NMR}$ (162 MHz, CDCl_3) δ -131.21, -135.60, -140.01, -144.40, -144.42, -148.81, -153.20, -157.60.

Procedures for the Deprotection of Silyloxy group on $[\text{Cp}^*\text{Ru}(\text{C}_6\text{H}_6)]\text{PF}_6$ Complexes (**Ru.1bc**)

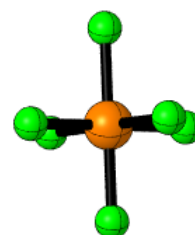
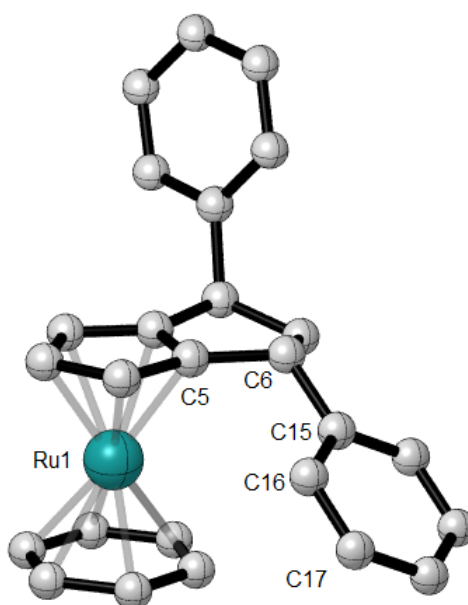
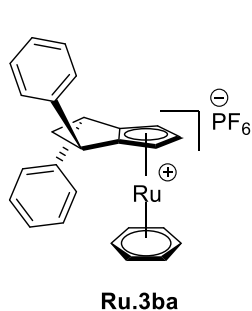


The ruthenium complex **Ru.1bc** (4.02 mg, 3.97 μmol , 1.0 equiv.) was suspended in DMF. To the mixture was added tetrabutylammonium fluoride (8.34 μl , 8.34 μmol , 2.1 equiv.) as a 1.00 M solution in THF. Stirred the reaction mixture at room temperature for 20 h, then, the reaction mixture was concentrated under reduced pressure. The crude product was filtered through Kimtech paper using chloroform. The filtered solid contained the desired **Ru.1be** and excess amount of Bu_4NF was dissolved in the filtrate. The filtered solid can be dissolved in methanol, which was purified by acidic alumina column chromatography (DCM to DCM/MeOH = 10/1 (v/v')).

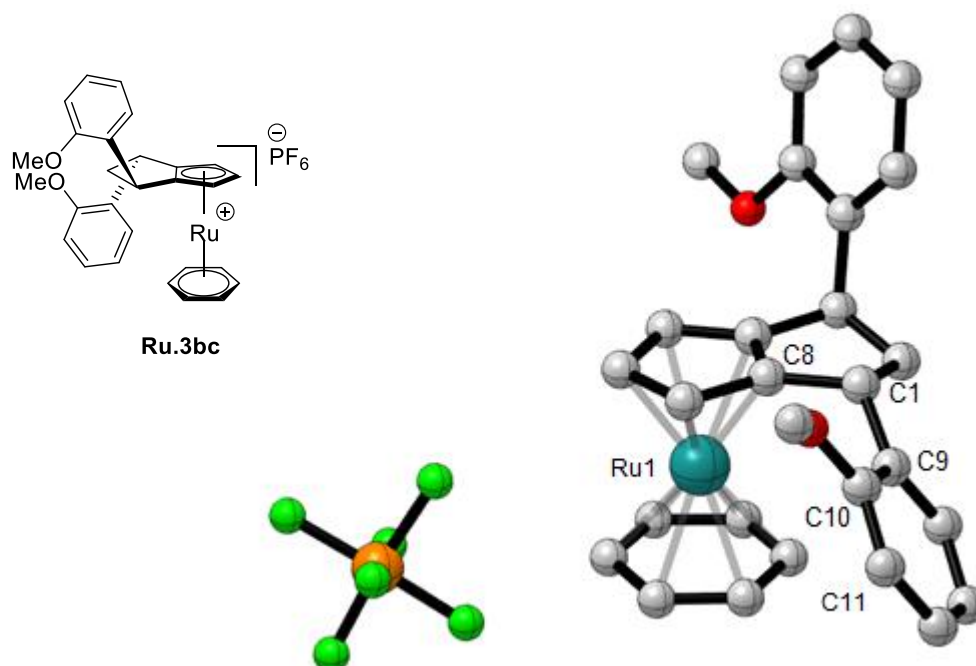


white solid, 2.7 mg, 99% yield; Analytical data **Ru.1be**: $^1\text{H NMR}$ (400 MHz, CD_3OD) δ 7.79 (d, J = 8.2 Hz, 1H), 7.68 (d, J = 8.2 Hz, 1H), 7.50 (s, 1H), 7.38 (ddd, J = 8.1, 6.8, 1.2 Hz, 1H), 7.31 (ddd, J = 8.2, 6.8, 1.3 Hz, 1H), 7.25 (s, 1H), 7.02 (dddd, J = 15.1, 8.2, 6.8, 1.3 Hz, 2H), 6.93 – 6.82 (m, 2H), 6.01 (s, 6H), 5.51 – 5.45 (m, 1H), 5.37 – 5.30 (m, 1H), 5.18 (t, J = 2.4 Hz, 1H), 4.05 (d, J = 15.2 Hz, 1H), 3.90 (d, J = 13.8 Hz, 1H), 3.02 (d, J = 13.7 Hz, 1H), 2.82 (d, J = 15.3 Hz, 1H).

X-ray structures of Ru.3ba



X-ray structures of Ru.3bc



Crystallographic data: CCDC 1816539 for **Ru.3ba**, 1816540 for **Ru.3bc** contain the supplementary crystallographic data for this paper. These data can be obtained free of charge from The Cambridge Crystallographic Data Centre via www.ccdc.cam.ac.uk/data_request/cif.

8.3 Enantioselective Ruthenium(II)-Catalyzed Synthesis of Benzonorcaradienes

Preparation of phosphate buffered silica (pH = 7)

To 100 g of silica (Silicycle silica gel 60) was added 1 L of disodium hydrogen phosphate (aq, 0.2 M). The pH of the mixture was adjusted to 7 by adding phosphoric acid. The mixture was filtered and the resulting silica was dried in the oven.

Preparation of chiral Cp^xRu complexes

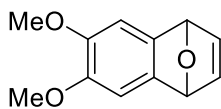
Cyclopentane-derived Cp^xRu(II)(CH₃CN)₃PF₆ complexes **Ru.2b** were prepared by following the procedures mentioned in Chapter 8.2, and binaphthyl-derived Cp^xRu(II) complexes **Ru.2ba** and **Ru.2bf**^{65a, 65c} were prepared according to the reported procedures.

Preparation of oxa-benzonorbornadienes and alkynes

But-2-yne-1,4-diol was purified by flash column chromatography and hept-2-yn-1-ol was distilled with a Hickman condenser prior to use.

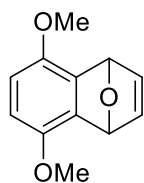
The following compounds were prepared according to the published procedures.

6,7-Dimethoxy-1,4-dihydro-1,4-epoxynaphthalene (**3.13b**),¹²³ 5,8-dimethoxy-1,4-dihydro-1,4-epoxynaphthalene (**3.13c**),¹²⁴ 6,7-dimethyl-1,4-dihydro-1,4-epoxynaphthalene (**3.13d**),¹²⁵ 6,7-dibromo-1,4-dihydro-1,4-epoxynaphthalene (**3.13e**),¹²⁶ but-2-yne-1,4-diyl dimethyl bis(carbonate) (**3.14c**),¹²⁷ but-2-yne-1,4-diyl di-tert-butyl bis(carbonate) (**3.14d**),¹²⁵ dibenzyl but-2-yne-1,4-diyl bis(carbonate) (**3.14e**),¹²⁵ but-2-yne-1,4-diyl bis(phenylcarbamate) (**3.14f**),¹²⁸ but-2-yne-1,4-diyl dibenzoate (**3.14g**),¹²⁹ but-2-yne-1,4-diyl diacetate (**3.14h**),¹³⁰ 2,2,3,3,10,10,11,11-octamethyl-4,9-dioxa-3,10-disiladodec-6-yne (**3.14i**),¹³¹ 1,4-bis(benzyloxy)but-2-yne (**3.14j**),¹²⁵ hept-2-yn-1-yl methyl carbonate (**3.14l**),¹³² 6-phenylhex-2-yn-1-ol (**3.14n**),¹³³ 4-hydroxybut-2-yn-1-yl methyl carbonate (**3.14o**).¹³⁴



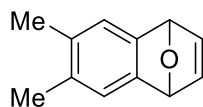
6,7-dimethoxy-1,4-dihydro-1,4-epoxynaphthalene (**3.13b**)

White solid, 430 mg, 62% yield; Analytical data: ¹H NMR (400 MHz, CDCl₃) δ 7.05 (s, 2H), 6.97 (s, 2H), 5.68 (s, 2H), 3.85 (s, 6H). ¹³C NMR (101 MHz, CDCl₃) δ 145.96, 143.47, 141.85, 106.89, 82.71, 56.60. IR (ATR): $\tilde{\nu}$ (cm⁻¹) = 3086, 3008, 2962, 2944, 2916, 2836, 1599, 1485, 1467, 1455, 1412, 1325, 1285, 1206, 1190, 1180, 1062, 966, 871, 856, 787, 735, 694, 638; HRMS (APPI/LTQ-Orbitrap) calcd for C₁₂H₁₂O₃⁺ [M]⁺: 204.0781, Found: 204.0780.



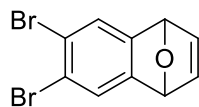
5,8-dimethoxy-1,4-dihydro-1,4-epoxynaphthalene (3.13c)

White solid, 681 mg, 72% yield; Analytical data: **¹H NMR** (400 MHz, CDCl₃) δ 7.07 (s, 2H), 6.54 (s, 2H), 5.93 (s, 2H), 3.79 (s, 6H). **¹³C NMR** (101 MHz, CDCl₃) δ 148.00, 143.02, 137.57, 111.75, 80.45, 56.49. **IR** (ATR): $\tilde{\nu}$ (cm⁻¹) = 3016, 2999, 2942, 2906, 2835, 1615, 1493, 1462, 1278, 1253, 1076, 1002, 868, 835, 722, 711; **HRMS** (APPI/LTQ-Orbitrap) calcd for C₁₂H₁₂O₃⁺ [M]⁺: 204.0781, Found: 204.0783.



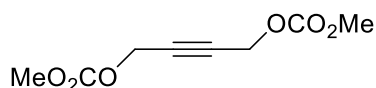
6,7-dimethyl-1,4-dihydro-1,4-epoxynaphthalene (3.13d)

White solid, 243 mg, 79% yield; Analytical data: **¹H NMR** (400 MHz, CDCl₃) δ 7.06 (s, 2H), 7.00 (s, 2H), 5.66 (s, 2H), 2.20 (s, 6H). **¹³C NMR** (101 MHz, CDCl₃) δ 146.75, 143.24, 132.67, 122.27, 82.34, 19.91. **IR** (ATR): $\tilde{\nu}$ (cm⁻¹) = 3081, 3014, 1572, 1430, 1348, 1315, 1279, 1229, 1195, 1159, 1082, 993, 892, 868, 846, 815, 753, 698, 645, 578; **HRMS** (APPI/LTQ-Orbitrap) calcd for C₁₂H₁₃O⁺ [M+H]⁺: 173.0961, Found: 173.0963.



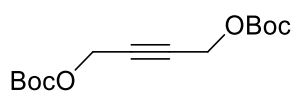
6,7-dibromo-1,4-dihydro-1,4-epoxynaphthalene (3.13e)

White solid, 1.01 g, 66% yield; Analytical data: **¹H NMR** (400 MHz, CDCl₃) δ 7.48 (s, 2H), 7.00 (s, 2H), 5.67 (s, 2H). **¹³C NMR** (101 MHz, CDCl₃) δ 150.34, 142.82, 125.61, 120.79, 81.93. **IR** (ATR): $\tilde{\nu}$ (cm⁻¹) = 3081, 3014, 1572, 1431, 1279, 1082, 994, 868, 846, 698, 645, 578; **HRMS** (APPI/LTQ-Orbitrap) calcd for C₁₀H₆OBr₂⁺ [M]⁺: 299.8780, Found: 299.8779.



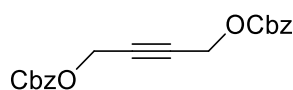
but-2-yne-1,4-diyl dimethyl bis(carbonate) (3.14c)

White solid, 703 mg, 86% yield; Analytical data: **¹H NMR** (400 MHz, CDCl₃) δ 4.77 (s, 4H), 3.81 (s, 6H). **¹³C NMR** (101 MHz, CDCl₃) δ 155.22, 81.01, 55.45, 55.31. **IR** (ATR): $\tilde{\nu}$ (cm⁻¹) = 3009, 2961, 1751, 1445, 1376, 1252, 1156, 949, 902, 790; **HRMS** (ESI/QTOF) calcd for C₈H₁₀O₆Na⁺ [M+Na]⁺: 225.0370, Found: 225.0369.



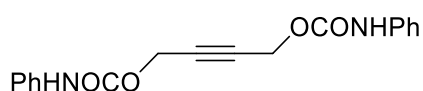
but-2-yne-1,4-diyl di-tert-butyl bis(carbonate) (3.14d)

Colorless oil, 1.09 g, 95% yield; Analytical data: **¹H NMR** (400 MHz, CDCl₃) 4.70 (s, 4H), 1.49 (s, 18H). **¹³C NMR** (101 MHz, CDCl₃) δ 152.85, 83.17, 81.03, 54.59, 27.84. **IR** (ATR): $\tilde{\nu}$ (cm⁻¹) = 2981, 2938, 1745, 1479, 1457, 1436, 1370, 1271, 1251, 1148, 1086, 931, 856, 791; **HRMS** (APCI/QTOF) calcd for C₁₄H₂₂O₆Na⁺ [M+Na]⁺: 309.1309, Found: 309.1300.



dibenzyl but-2-yne-1,4-diyl bis(carbonate) (3.14e)

White solid, 0.69 g, 48% yield; Analytical data: **¹H NMR** (400 MHz, CDCl₃) δ 7.38 (ddd, *J* = 3.5, 2.4, 1.3 Hz, 7H), 7.36 – 7.33 (m, 3H), 5.19 (s, 4H), 4.78 (s, 4H). **¹³C NMR** (101 MHz, CDCl₃) δ 154.60, 134.97, 128.79, 128.75, 128.50, 81.09, 70.25, 55.54. **IR** (ATR): $\tilde{\nu}$ (cm⁻¹) = 3066, 3034, 2956, 1748, 1455, 1390, 1366, 1233, 1157, 938, 787, 754, 697; **HRMS** (ESI/QTOF) calcd for C₂₀H₁₈O₆Na⁺ [M+Na]⁺: 377.0996, Found: 377.0993.



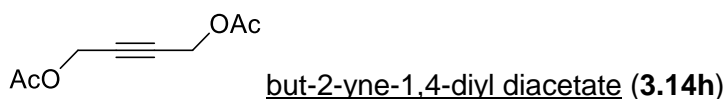
but-2-yne-1,4-diyl bis(phenylcarbamate) (3.14f)

White solid, 593 mg, 83% yield; Analytical data: **¹H NMR** (400 MHz, CDCl₃) δ 7.38 (d, *J* = 8.0 Hz, 4H), 7.31 (dd, *J* = 8.6, 7.2 Hz, 4H), 7.09 (tt, *J* = 7.1, 1.3 Hz, 2H), 6.66 (s, 2H), 4.84 (s, 4H). **¹³C NMR**

(101 MHz, CDCl₃) δ 152.63, 137.53, 129.25, 123.96, 118.90, 81.25, 53.01. **IR** (ATR): $\tilde{\nu}$ (cm⁻¹) 3331, 3053, 1702, 1604, 1542, 1502, 1447, 1316, 1301, 1233, 1060, 742, 691; **HRMS** (ESI/QTOF) calcd for C₁₈H₁₆N₂O₄Na⁺ [M+Na]⁺: 347.1002, Found: 347.1005.



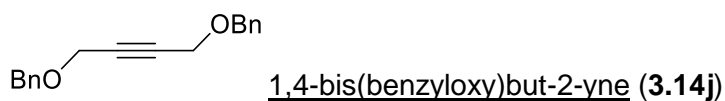
White solid, 763 mg, 89% yield; Analytical data: **¹H NMR** (400 MHz, CDCl₃) δ 8.08 (d, *J* = 7.4 Hz, 4H), 7.58 (t, *J* = 7.5 Hz, 2H), 7.45 (t, *J* = 7.5 Hz, 4H), 5.00 (s, 4H). **¹³C NMR** (101 MHz, CDCl₃) δ 165.93, 133.45, 129.94, 129.51, 128.55, 81.11, 52.75. **IR** (ATR): $\tilde{\nu}$ (cm⁻¹) = 3064, 2944, 1721, 1601, 1452, 1371, 1315, 1260, 1177, 1156, 1093, 1069, 1026, 956, 708, 687; **HRMS** (ESI/QTOF) calcd for C₁₈H₁₄O₄Na⁺ [M+Na]⁺: 317.0784, Found: 317.0784.



Colorless oil, 470 mg, 91% yield; Analytical data: **¹H NMR** (400 MHz, CDCl₃) δ 4.71 (s, 4H), 2.10 (s, 6H). **¹³C NMR** (101 MHz, CDCl₃) δ 170.09, 80.84, 52.10, 20.68. **IR** (ATR): $\tilde{\nu}$ (cm⁻¹) = 2947, 1742, 1434, 1378, 1361, 1215, 1155, 1025, 966, 917, 831; **HRMS** (EXI/QTOF) calcd for C₈H₁₀O₄Na⁺ [M+Na]⁺: 193.0471, Found: 193.0472.



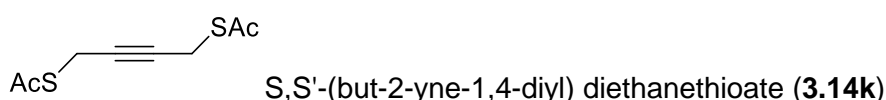
Colorless oil, 522 mg, 95% yield; Analytical data: **¹H NMR** (400 MHz, CDCl₃) δ 4.34 (s, 4H), 0.91 (s, 18H), 0.12 (s, 12H). **¹³C NMR** (101 MHz, CDCl₃) δ 83.49, 51.95, 25.98, 18.45, -5.00. **IR** (ATR): $\tilde{\nu}$ (cm⁻¹) = 2955, 2930, 2887, 2858, 1472, 1463, 1363, 1254, 1135, 1095, 1069, 1005, 833, 815, 776; **HRMS** (APPI/LTQ-Orbitrap) calcd for C₁₀H₃₄O₂Si₂⁺ [M]⁺: 314.2092, Found: 314.2092.



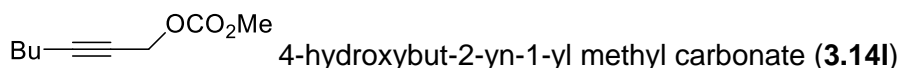
Colorless oil, 600 mg, 84% yield; Analytical data: **¹H NMR** (400 MHz, CDCl₃) 7.40 – 7.27 (m, 10H), 4.62 (s, 4H), 4.25 (s, 4H). **¹³C NMR** (101 MHz, CDCl₃) δ 137.49, 128.57, 128.18, 128.00, 82.64, 71.75, 57.56. **IR** (ATR): $\tilde{\nu}$ (cm⁻¹) = 3029, 2942, 2854, 1496, 1454, 1386, 1348, 1260, 1207, 1138, 1118, 1068, 1027, 939, 905, 736, 696, 605; **HRMS** (APPI/LTQ-Orbitrap) calcd for C₁₈H₁₈O₂⁺ [M]⁺: 266.1301, Found: 266.1302.

Preparation of S,S'-(but-2-yne-1,4-diyl) diethanethioate (3.14k)

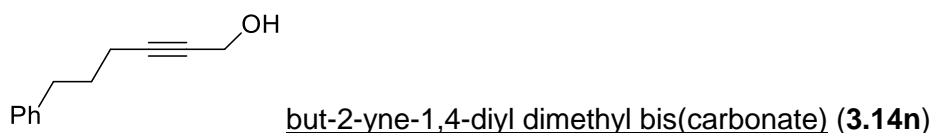
1,4-Dibromobut-2-yne (0.223 ml, 2.12 mmol) was added to 3 mL of DMF and cooled to 0 °C. Potassium thioacetate (0.534 g, 4.67 mmol) in 3 ml of DMF was added within 30 min. The ice bath was subsequently removed and the reaction mixture was stirred for 1 h at room temperature. The reaction mixture was added to 60 mL of 1 N HCl. Next, the aqueous layer was extracted with Et₂O (2 × 15 ml). The combined organic layers were washed with 1 N HCl (aq) (2 × 25 ml) and dried over MgSO₄. After the solvent was removed under reduced pressure, the residue was purified by silica gel column chromatography (*n*-pentane/ethyl acetate = 10/1) to afford the product **2i** (515 mg, 91% yield).



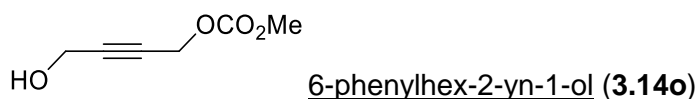
Pale yellow solid, 515 mg, 91% yield; Mp = 42-43 °C; Analytical data: **¹H NMR** (400 MHz, CDCl₃) δ 3.64 (s, 4H), 2.35 (s, 6H). **¹³C NMR** (101 MHz, CDCl₃) δ 194.06, 77.54, 30.26, 18.08. **IR** (ATR): $\tilde{\nu}$ (cm⁻¹) = 2962.09, 2918.61, 1688.04, 1398.93, 1353.16, 1241.64, 1128.33, 1101.60, 1003.66, 954.14, 708.66, 619.32, 528.56; **HRMS** (APPI/LTQ-Orbitrap) calcd for C₈H₁₀O₂S₂Na⁺ [M+Na]⁺: 225.0014, Found: 225.0017.



Colorless oil, 244 mg, 54% yield; Analytical data: **¹H NMR** (400 MHz, CDCl₃) δ 4.72 (t, *J* = 2.2 Hz, 2H), 3.81 (s, 3H), 2.22 (tt, *J* = 7.1, 2.2 Hz, 2H), 1.59 – 1.45 (m, 2H), 1.45 – 1.31 (m, 2H), 0.90 (t, *J* = 7.2 Hz, 3H). **¹³C NMR** (101 MHz, CDCl₃) 155.46, 88.67, 73.44, 56.42, 55.13, 30.51, 22.03, 18.56, 13.69. **IR** (ATR): $\tilde{\nu}$ (cm⁻¹) = 2958, 2935, 2873, 2235, 1750, 1444, 1375, 1251, 1150, 945, 901, 791; **HRMS** (APPI/LTQ-Orbitrap) calcd for C₁₀H₆OBr₂⁺ [M+H]⁺: 171.1016, Found: 171.1009.

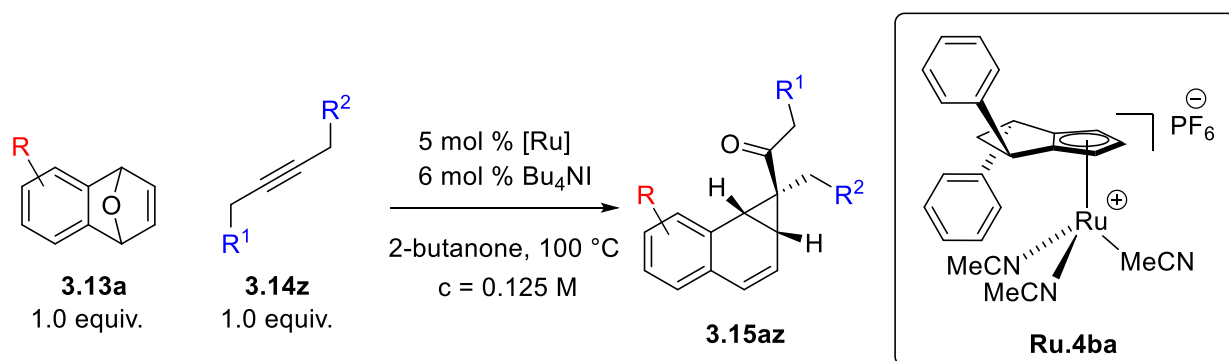


Colorless oil, 3.03 g, 87% yield; Analytical data: **¹H NMR** (400 MHz, CDCl₃) δ 7.33 – 7.26 (m, 2H), 7.23 – 7.15 (m, 3H), 4.27 (t, *J* = 2.1 Hz, 2H), 2.76 – 2.68 (m, 2H), 2.24 (tt, *J* = 7.0, 2.2 Hz, 2H), 1.84 (p, *J* = 7.2 Hz, 2H), 1.50 (s, 1H). **¹³C NMR** (101 MHz, CDCl₃) δ 141.62, 128.62, 128.46, 126.02, 86.16, 78.97, 51.49, 34.91, 30.21, 18.30. **IR** (ATR): $\tilde{\nu}$ (cm⁻¹) = 3330, 3026, 2936, 2861, 2289, 2224, 1603, 1496, 1454, 1430, 1133, 1009, 745, 699; **HRMS** (APPI/LTQ-Orbitrap) calcd for C₁₂H₁₄O⁺ [M]⁺: 174.1039, Found: 174.1037.



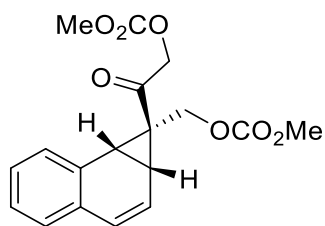
Colorless oil, 293 mg, 68% yield; Analytical data: **¹H NMR** (400 MHz, CDCl₃) 4.78 (t, *J* = 1.8 Hz, 1H), 4.31 (t, *J* = 1.8 Hz, 1H), 3.82 (s, 1H), 1.65 (s, 1H). **¹³C NMR** (101 MHz, CDCl₃) δ 155.40, 85.98, 79.16, 55.75, 55.32, 51.01. **IR** (ATR): $\tilde{\nu}$ (cm⁻¹) = 3405, 2960, 2863, 1746, 1445, 1376, 1253, 1138, 1017, 942, 902, 789; **HRMS** (APPI/LTQ-Orbitrap) calcd for C₆H₈O₄⁺ [M]⁺: 144.0417, Found: 144.0414.

General Procedures for the Ruthenium(II)-Catalyzed Enantioselective Synthesis of Benzonorcaradiene by Coupling of Oxa-benzonorbornadienes and Internal Alkynes



Ru.4ba (5.00 mol %, 5.20 μ mol, 3.26 mg) and tetrabutylammonium iodide (6.00 mol %, 6.24 μ mol, 2.30 mg) were dissolved in freshly distilled 2-butanone (0.45 ml) in a microwave tube under an N₂ atmosphere. A solution of an oxa-benzonorbornadiene **3.13a** (0.104 mmol, 15.0 mg, 1.00 equiv.) and an alkyne **3.14z** (0.104 mmol, 1.00 equiv.) in 2-butanone (0.38 ml) was added in one portion. The reaction mixture was heated to 100 °C and stirred at that temperature. After completion of the reaction (TLC control), the reaction mixture was cooled to room temperature. The solvent was removed under reduced pressure. The reaction mixture was purified by silica gel column chromatography (*n*-pentane/ethyl acetate) to afford the desired benzonorcaradiene **3.15az**.

For the compounds (**3.15bc** and **3.15cc**), phosphate buffered silica (pH=7) was used because of instability of the compounds on silica gel.

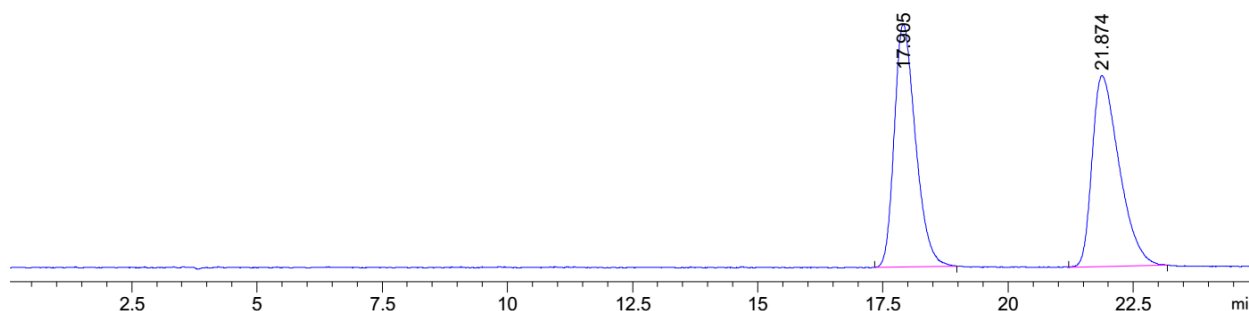


2-((1S,1aR,7bR)-1-(((methoxycarbonyl)oxy)methyl)-1a,7b-dihydro-1H-cyclopropa[a]naphthalen-1-yl)-2-oxoethyl methyl carbonate (3.15ac)

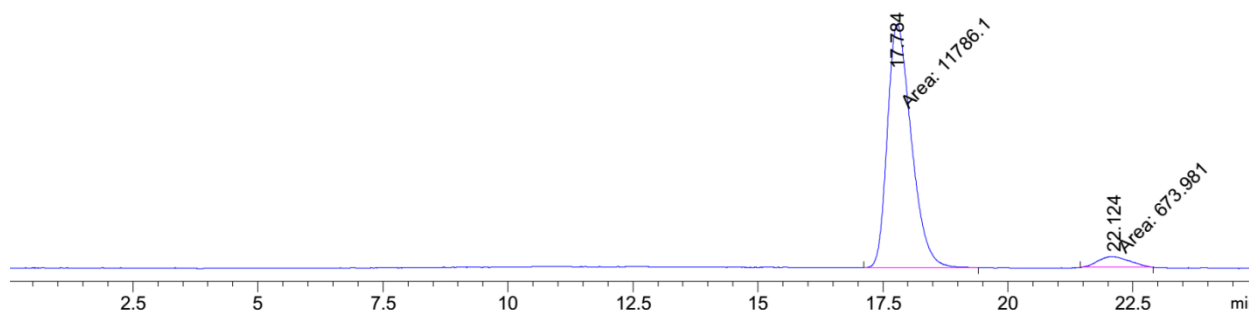
Off-white solid, 25.5 mg, 76% yield, 95:5 *er*. $[\alpha]_D^{20}$ -94.7 ($c = 1.0$, CH_2Cl_2);

Mp = 96-97 °C; Analytical data: **^1H NMR** (400 MHz, CDCl_3) δ 7.39 (dd, J

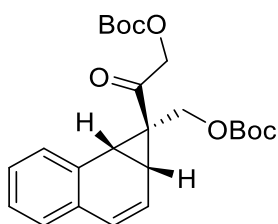
= 6.9, 1.9 Hz, 1H), 7.32 – 7.23 (m, 2H), 7.20 (m, 1H), 6.68 (d, $J = 9.6$ Hz, 1H), 6.19 (dd, $J = 9.5, 5.2$ Hz, 1H), 5.15 (s, 2H), 4.05 (d, $J = 13.2$ Hz, 1H), 3.85 (s, 3H), 3.82 (d, $J = 13.2$ Hz, 1H), 3.65 (s, 3H), 3.42 (d, $J = 8.7$ Hz, 1H), 3.02 (dd, $J = 8.7, 5.2$ Hz, 1H). **^{13}C NMR** (101 MHz, CDCl_3) δ 203.07, 155.55, 155.21, 132.43, 130.30, 130.11, 129.32, 128.42, 128.26, 127.98, 122.63, 70.02, 61.63, 55.45, 54.99, 38.52, 36.05, 24.26. **IR** (ATR): $\tilde{\nu}$ (cm^{-1}) = 3024, 2958, 2857, 1751, 1704, 1488, 1444, 1421, 1378, 1265, 1191, 1166, 1108, 1066, 997, 964, 917, 842, 789; **HRMS** (ESI) calcd for $\text{C}_{18}\text{H}_{18}\text{O}_7\text{Na}^+$ $[\text{M}+\text{Na}]^+$: 369.0945, Found: 369.0945. The enantiomeric excess was determined by Daicel Chiralpak ID (25 cm), Hexane/IPA = 80/20, 1.0 mL/min, $\lambda = 254$ nm, t_R (major) = 17.9 min, t_R (minor) = 21.9 min.



Peak #	RetTime [min]	Type	Width [min]	Area [mAU*s]	Height [mAU]	Area %
1	17.905	BB	0.4411	4408.57129	149.02773	49.9908
2	21.874	BB	0.5404	4410.19629	117.35560	50.0092



Peak #	RetTime [min]	Type	Width [min]	Area [mAU*s]	Height [mAU]	Area %
1	17.784	MM	0.5564	1.17861e4	353.07254	94.5909
2	22.124	MM	0.7225	673.98114	15.54729	5.4091

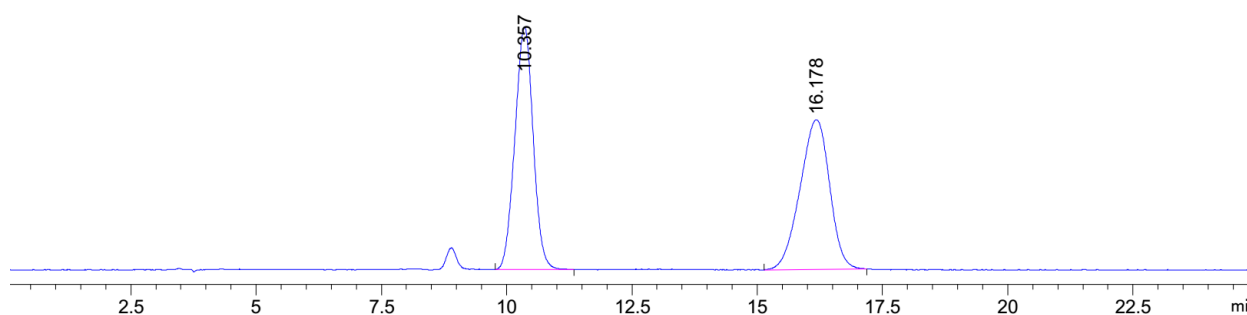


2-(((1S,1aR,7bR)-1-(((tert-butoxycarbonyl)oxy)methyl)-1a,7b-dihydro-1H-cyclopropa[a]naphthalen-1-yl)-2-oxoethyl tert-butyl carbonate (3.15ad)

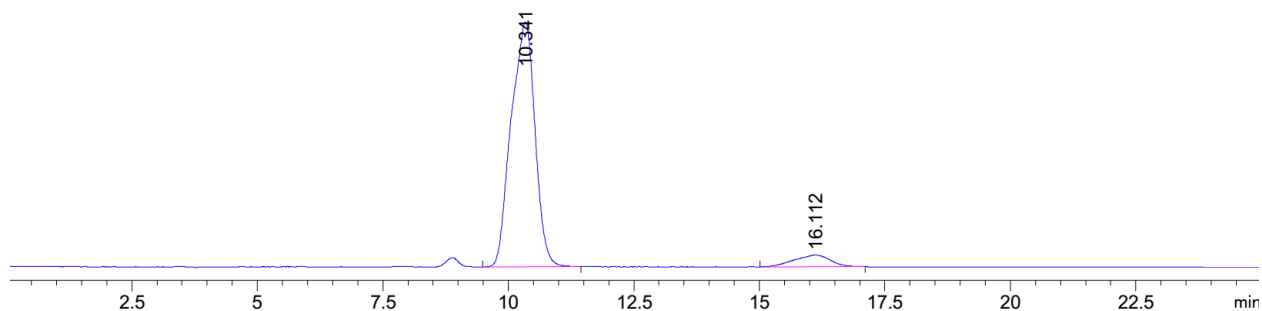
White solid, 32.0 mg, 71% yield, 93.5:6.5 *er*. $[\alpha]_{\text{D}}^{20}$ -85.4 ($c = 1.0$, CH_2Cl_2);

Mp = 112-113 °C; Analytical data: **¹H NMR** (400 MHz, CDCl_3) δ 7.43 – 7.36

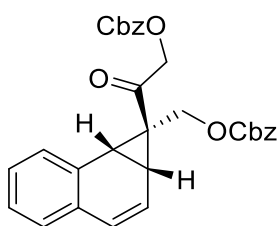
(m, 1H), 7.26 – 7.23 (m, 2H), 7.23 – 7.18 (m, 1H), 6.67 (d, $J = 9.6$ Hz, 1H), 6.18 (dd, $J = 9.6, 5.2$ Hz, 1H), 5.11 (s, 2H), 3.99 (d, $J = 13.2$ Hz, 1H), 3.77 (d, $J = 13.3$ Hz, 1H), 3.39 (d, $J = 8.7$ Hz, 1H), 2.99 (dd, $J = 8.7, 5.2$ Hz, 1H), 1.52 (s, 9H), 1.36 (s, 9H). **¹³C NMR** (101 MHz, CDCl_3) δ 203.63, 153.16, 153.02, 132.49, 130.30, 130.01, 129.64, 128.33, 128.19, 127.82, 122.73, 83.02, 82.54, 69.42, 60.40, 38.26, 36.03, 27.86, 27.78, 24.35. **IR** (ATR): $\tilde{\nu}$ (cm^{-1}) = 2981, 2935, 1742, 1705, 1477, 1456, 1422, 1394, 1369, 1280, 1248, 1157, 1133, 1105, 1092, 1061, 1037, 980, 948, 913, 861, 791, 778, 732; **HRMS** (ESI) calcd for $\text{C}_{24}\text{H}_{30}\text{O}_7\text{Na}^+$ $[\text{M}+\text{Na}]^+$: 453.1884, Found: 453.1884. The enantiomeric excess was determined by Daicel Chiralpak IC (25 cm), Hexane/IPA = 80/20, 1.0 mL/min, $\lambda = 254$ nm, t_{R} (major) = 10.3 min, t_{R} (minor) = 16.1 min.



Peak #	RetTime [min]	Type	Width [min]	Area [mAU*s]	Height [mAU]	Area %
1	10.357	BB	0.3961	2886.00635	113.72443	50.0178
2	16.178	BB	0.6034	2883.94678	70.18487	49.9822



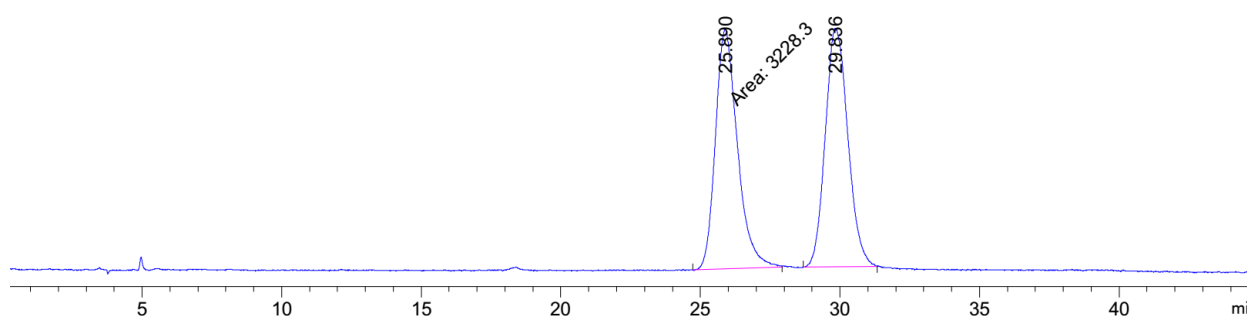
Peak #	RetTime [min]	Type	Width [min]	Area [mAU*s]	Height [mAU]	Area %
1	10.341	BB	0.4669	1.00922e4	305.88452	93.2309
2	16.112	BB	0.6141	732.75281	14.53579	6.7691



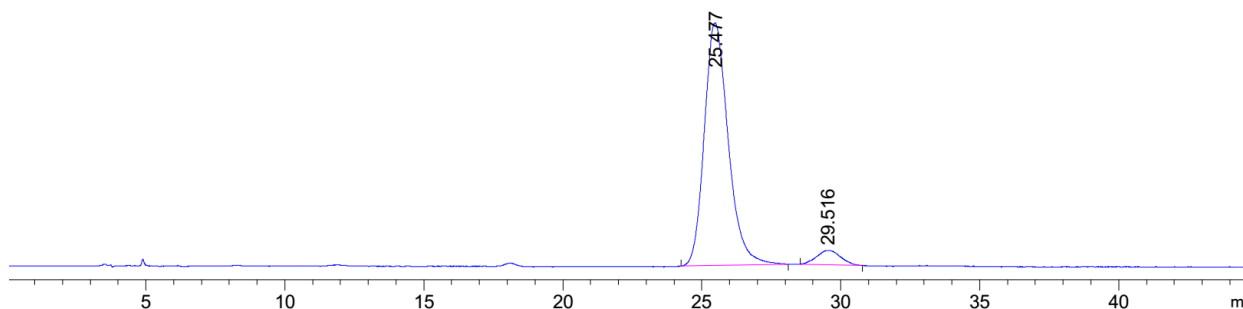
benzyl (2-((1S,1aR,7bR)-1-(((benzyloxy)carbonyl)oxy)methyl)-1a,7b-dihydro-1H-cyclopropa[a]naphthalen-1-yl)-2-oxoethyl) carbonate (3.15ae)

Yellow oil, 33.5 mg, 65% yield, 94:6 *er.* $[\alpha]_D^{20}$ -69.3 (*c* = 1.0, CH₂Cl₂);

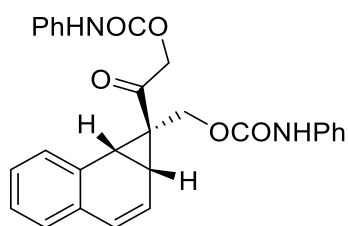
Analytical data: **¹H NMR** (400 MHz, CDCl₃) δ 7.35 – 7.21 (m, 8H), 7.22 – 7.17 (m, 2H), 7.17 – 7.07 (m, 3H), 6.55 (d, *J* = 9.6 Hz, 1H), 6.05 (dd, *J* = 9.6, 5.2 Hz, 1H), 5.13 (s, 2H), 5.05 (s, 2H), 4.90 (s, 2H), 3.96 (d, *J* = 13.1 Hz, 1H), 3.77 (d, *J* = 13.1 Hz, 1H), 3.32 (d, *J* = 8.7 Hz, 1H), 2.92 (dd, *J* = 8.7, 5.2 Hz, 1H). **¹³C NMR** (101 MHz, CDCl₃) δ 202.91, 154.92, 154.57, 135.11, 135.05, 132.43, 130.30, 130.14, 129.36, 128.72, 128.72, 128.69, 128.41, 128.37, 128.35, 128.25, 127.95, 122.60, 70.29, 70.09, 69.86, 61.70, 38.49, 36.12, 24.38. **IR** (ATR): $\tilde{\nu}$ (cm⁻¹) = 3065, 3034, 2952, 1748, 1703, 1455, 1424, 1383, 1263, 1236, 1192, 1165, 1107, 1063, 952, 910, 842, 780, 737, 697; **HRMS** (ESI) calcd for C₃₀H₂₆O₇Na⁺ [*M*+Na]⁺: 521.1571, Found: 521.1565. The enantiomeric excess was determined by Daicel Chiralpak IC (25 cm), Hexane/IPA = 80/20, 1.0 mL/min, λ = 254 nm, *t_R* (major) = 25.5 min, *t_R* (minor) = 29.5 min.



Peak #	RetTime [min]	Type	Width [min]	Area [mAU*s]	Height [mAU]	Area %
1	25.890	MM	0.9138	3228.29712	58.88136	49.5036
2	29.836	BB	0.7360	3293.04346	58.56320	50.4964



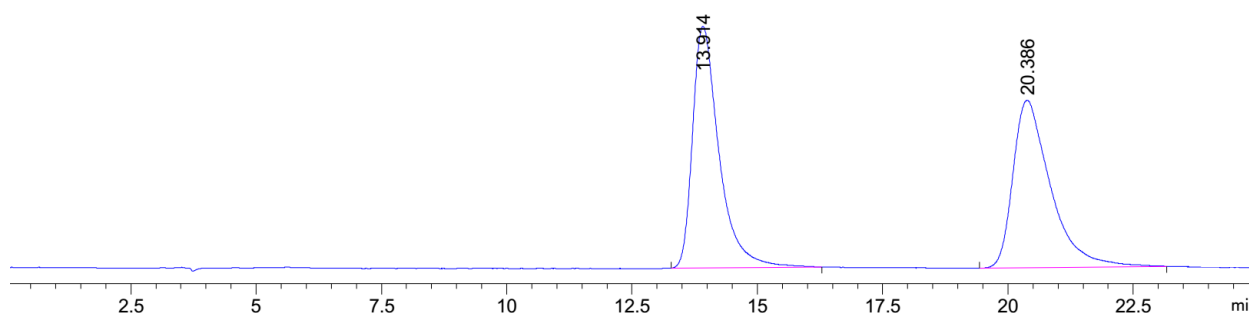
Peak #	RetTime [min]	Type	Width [min]	Area [mAU*s]	Height [mAU]	Area %
1	25.477	BB	0.8522	9669.59277	161.57611	94.4050
2	29.516	BB	0.7005	573.07703	9.68280	5.5950



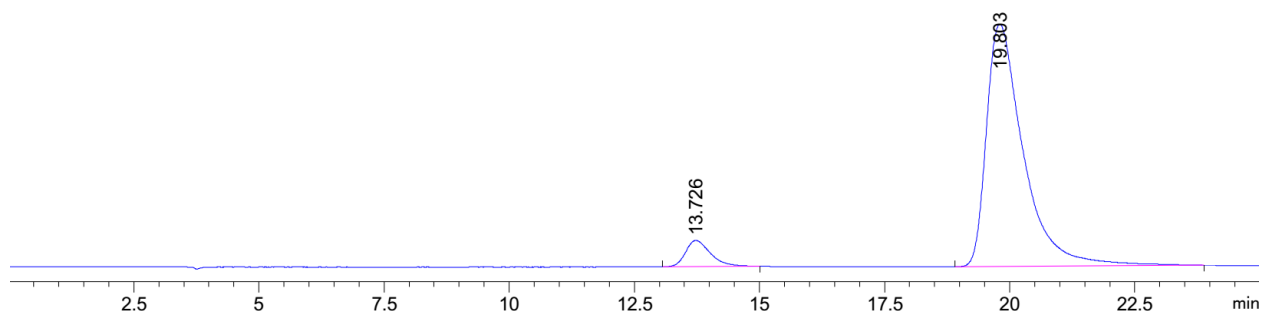
2-oxo-2-((1S,1aR,7bR)-1-(((phenylcarbamoyl)oxy)methyl)-1a,7b-dihydro-1H-cyclopropa[a]naphthalen-1-yl)ethyl phenylcarbamate (3.15af)

Yellow solid, 30.8 mg, 63% yield, 7:93 *er.* [α]_D²⁰ -65.2 (*c* = 1.0, CH₂Cl₂), Mp = 103-104 °C; Analytical data: ¹H NMR (400 MHz, CDCl₃) δ 7.35 (t, *J* = 9.6 Hz, 3H), 7.26 (s, 3H), 7.24 – 7.13 (m, 5H), 7.10 – 6.98 (m, 3H), 6.72 (s, 1H), 6.65 (d, *J* = 9.6 Hz, 1H), 6.12 (dd, *J* = 9.6, 5.2 Hz, 1H), 5.37 – 5.13 (m, 2H), 4.06 (d, *J* = 13.2 Hz, 1H), 3.90 (d, *J* = 13.3 Hz, 1H), 3.39 (d, *J* = 8.7 Hz, 1H), 3.00 (dd, *J* = 8.8, 5.2 Hz, 1H). ¹³C NMR (151 MHz, CDCl₃) δ 205.02, 152.91, 137.62, 137.54, 132.45, 130.16, 130.14, 129.47, 129.17, 129.14, 128.35, 128.33, 127.97, 123.92, 123.68, 122.54, 118.94, 118.66, 77.37, 76.95, 68.05, 58.83, 38.53, 35.89, 24.59. IR (ATR): $\tilde{\nu}$ (cm⁻¹) = 3317, 3057, 3043, 2936, 2252, 1698, 1600, 1529, 1501, 1444, 1376, 1314, 1214, 1191, 1165, 1117, 1102, 1083, 1058, 1027, 978, 908, 849, 788, 754, 730, 692, 649, 506; HRMS (ESI) calcd for C₂₈H₂₄N₂O₅Na⁺ [M+Na]⁺: 491.1577, Found: 491.1583. The enantiomeric excess was determined by Daicel Chiralpak

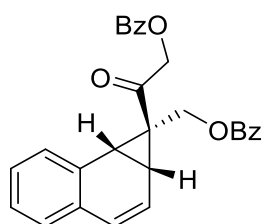
IF (25 cm), Hexane/IPA = 80/20, 1.0 mL/min, λ = 254 nm, t_R (major) = 19.8 min, t_R (minor) = 13.7 min.



Peak #	RetTime [min]	Type	Width [min]	Area [mAU*s]	Height [mAU]	Area %
1	13.914	BB	0.5518	4348.52881	118.05169	50.4772
2	20.386	BB	0.7405	4266.31689	81.79529	49.5228



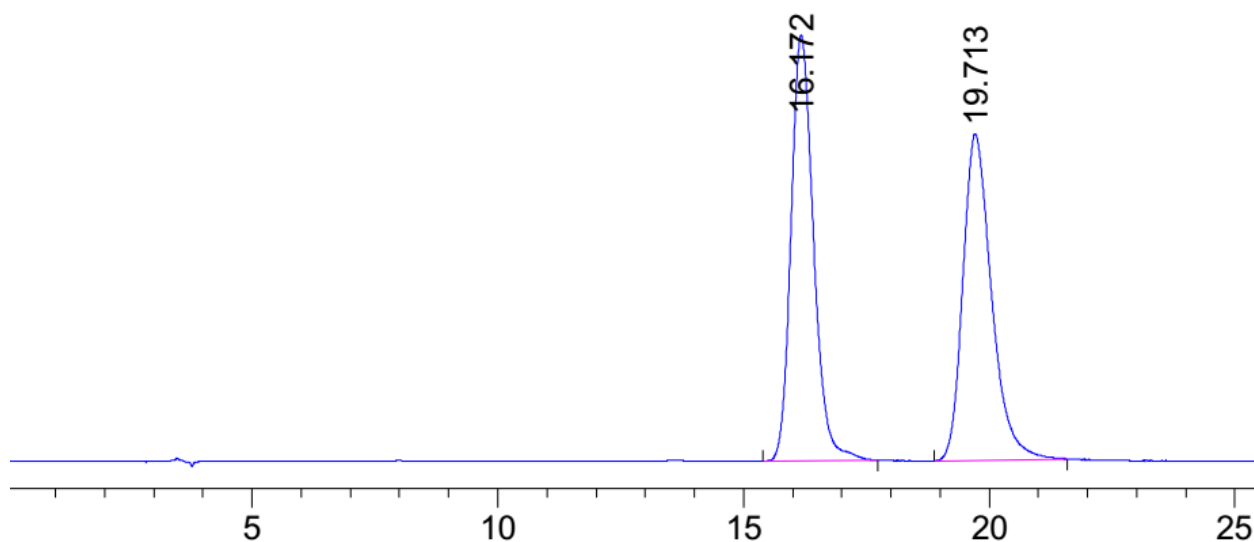
Peak #	RetTime [min]	Type	Width [min]	Area [mAU*s]	Height [mAU]	Area %
1	13.726	BB	0.5046	732.69067	21.02078	6.8124
2	19.803	BB	0.7564	1.00225e4	194.12154	93.1876



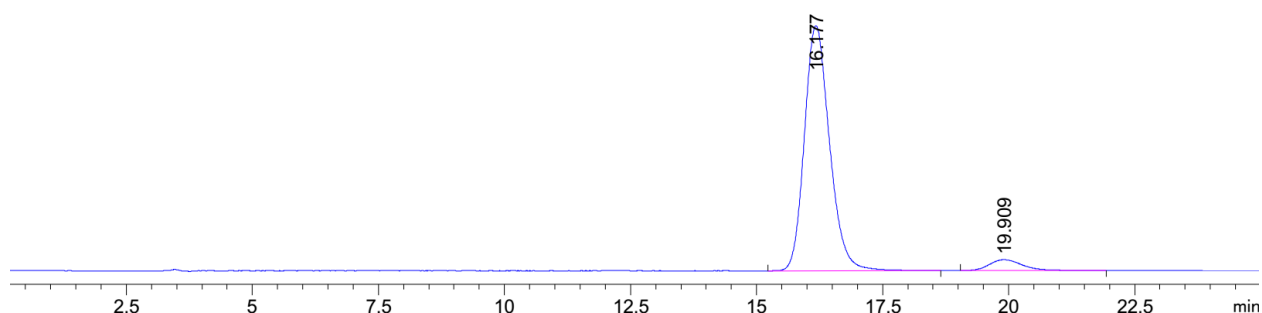
((1S,1aR,7bR)-1-(2-(benzyloxy)acetyl)-1a,7b-dihydro-1H-cyclopropa[a]naphthalen-1-yl)methyl benzoate (3.15ag)

Off-white solid, 28.0 mg, 61% yield, 5:95 *er*. $[\alpha]_D^{20}$ -38.5 (c = 1.0, CH_2Cl_2), Mp = 150 °C; Analytical data: ^1H NMR (400 MHz, CDCl_3) δ 8.17 (d, J = 7.8 Hz, 2H), 7.98 (d, J = 7.7 Hz, 2H), 7.62 (dd, J = 9.7, 7.2 Hz, 2H), 7.56 – 7.42 (m, 5H), 7.36 – 7.21 (m, 3H), 6.74 (d, J = 9.6 Hz, 1H), 6.26 (dd, J = 9.6, 5.2 Hz, 1H), 5.63 – 5.41 (m, 2H), 4.40 – 4.16 (m,

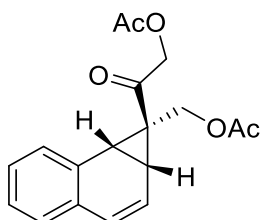
2H), 3.56 (d, $J = 8.7$ Hz, 1H), 3.17 (dd, $J = 8.7, 5.2$ Hz, 1H). **^{13}C NMR** (101 MHz, CDCl_3) δ 203.60, 166.24, 166.08, 133.48, 133.33, 132.48, 130.25, 130.18, 130.06, 129.72, 129.70, 129.60, 129.51, 128.59, 128.41, 128.30, 127.92, 122.68, 68.01, 58.87, 38.43, 36.07, 24.58. **IR** (ATR): $\tilde{\nu}$ (cm^{-1}) = 3063, 3035, 2936, 1719, 1704, 1601, 1451, 1418, 1375, 1315, 1271, 1192, 1177, 1108, 1064, 1026, 968, 791, 778, 708, 687; **HRMS** (ESI) calcd for $\text{C}_{28}\text{H}_{22}\text{O}_5\text{Na}^+$ $[\text{M}+\text{Na}]^+$: 461.1359, Found: 461.1365. The enantiomeric excess was determined by Daicel Chiralpak IC (25 cm), Hexane/IPA = 80/20, 1.0 mL/min, $\lambda = 254$ nm, t_R (major) = 16.2 min, t_R (minor) = 19.9 min.



Peak #	RetTime [min]	Type	Width [min]	Area [mAU*s]	Height [mAU]	Area %
1	16.172	BB	0.4893	3781.79053	118.83089	50.5939
2	19.713	BB	0.6268	3693.00366	91.13680	49.4061



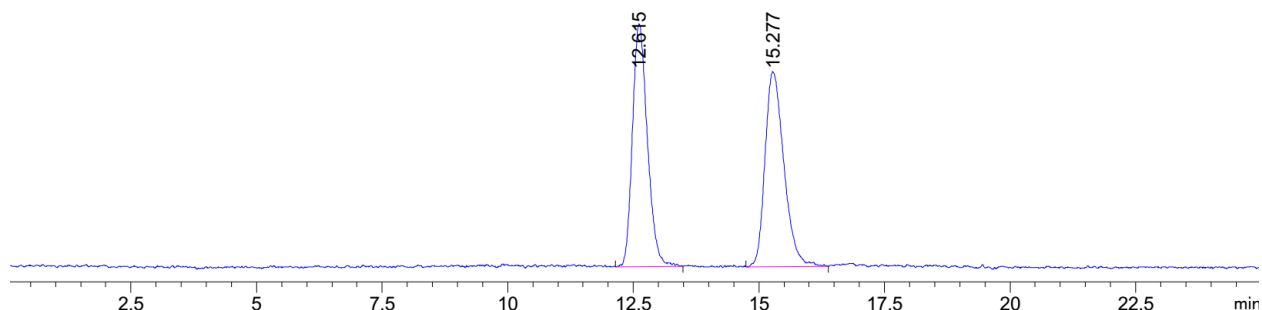
Peak #	RetTime [min]	Type	Width [min]	Area [mAU*s]	Height [mAU]	Area %
1	16.177	BB	0.5288	1.26864e4	365.58609	94.3974
2	19.909	BB	0.7033	752.94751	16.28921	5.6026



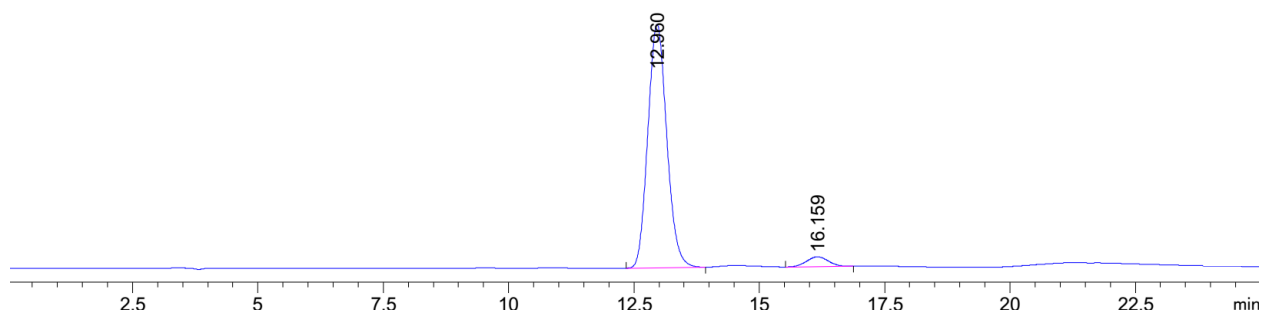
((1S,1aR,7bR)-1-(2-acetoxyacetyl)-1a,7b-dihydro-1H-cyclopropa[a]naphthalen-1-yl)methyl acetate (3.15ah)

Yellow oil, 19.3 mg, 63% yield, 95.5:4.5 *er.* $[\alpha]_D^{20}$ -97.5 ($c = 1.0$, CH_2Cl_2);

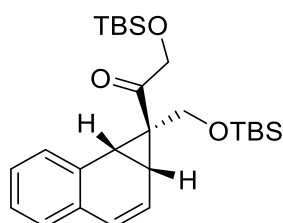
Analytical data: $^1\text{H NMR}$ (400 MHz, CDCl_3) δ 7.37 (dd, $J = 6.4, 2.4$ Hz, 1H), 7.26 (m, 2H), 7.19 (dd, $J = 7.0, 2.1$ Hz, 1H), 6.67 (d, $J = 9.6$ Hz, 1H), 6.16 (dd, $J = 9.6, 5.2$ Hz, 1H), 5.12 (d, $J = 3.6$ Hz, 2H), 3.96 (d, $J = 13.5$ Hz, 1H), 3.82 (d, $J = 13.6$ Hz, 1H), 3.38 (d, $J = 8.7$ Hz, 1H), 3.00 (dd, $J = 8.7, 5.2$ Hz, 1H), 2.21 (s, 3H), 1.88 (s, 3H). $^{13}\text{C NMR}$ (101 MHz, CDCl_3) δ 203.66, 170.50, 170.41, 132.43, 130.16, 130.11, 129.65, 128.28, 127.89, 122.58, 67.42, 58.17, 38.23, 35.89, 24.33, 20.67, 20.65. **IR** (ATR): $\tilde{\nu}$ (cm^{-1}) = 3035, 3024, 2936, 1745, 1702, 1488, 1421, 1374, 1229, 1188, 1166, 1092, 1055, 1030, 966, 840, 794, 780, 601, 494; **HRMS** (ESI) calcd for $\text{C}_{18}\text{H}_{18}\text{O}_5\text{Na}^+$ $[\text{M}+\text{Na}]^+$: 337.1046, Found: 337.1053. The enantiomeric excess was determined by Daicel Chiralpak ID (25 cm), Hexane/IPA = 80/20, 1.0 mL/min, $\lambda = 254$ nm, t_R (major) = 13.0 min, t_R (minor) = 16.2 min.



Peak #	RetTime [min]	Type	Width [min]	Area [mAU*s]	Height [mAU]	Area %
1	12.615	BB	0.3172	3346.28931	161.83864	49.5821
2	15.277	BB	0.4012	3402.70337	130.09207	50.4179

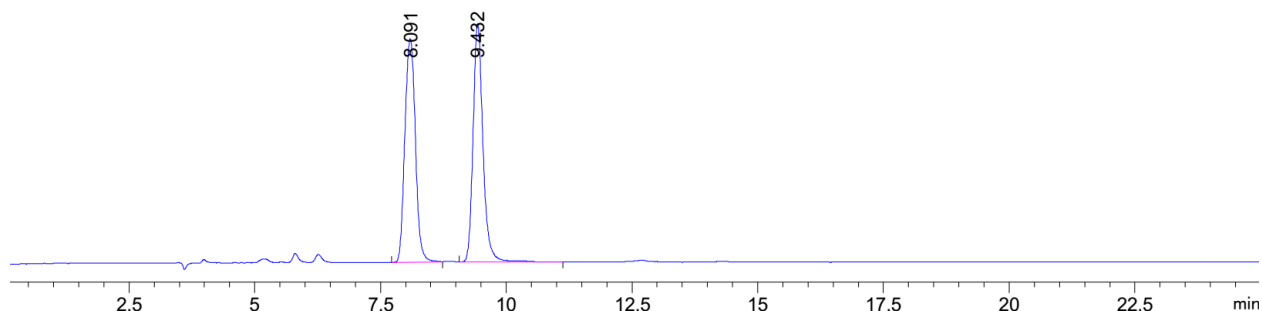


Peak #	RetTime [min]	Type	Width [min]	Area [mAU*s]	Height [mAU]	Area %
1	12.960	BB	0.4100	6476.92383	246.90945	95.6517
2	16.159	BB	0.4630	294.44159	9.84381	4.3483

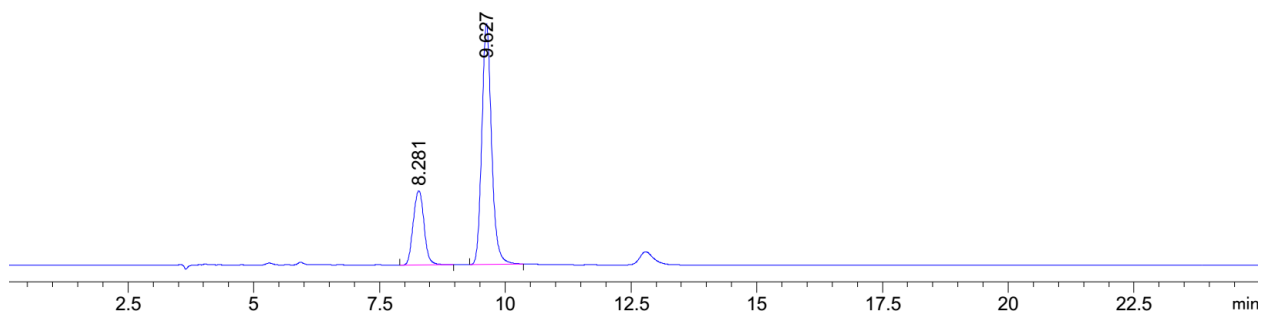


2-((tert-butyldimethylsilyl)oxy)-1-((1S,1aR,7bR)-1-(((tert-butyldimethylsilyl)oxy)methyl)-1a,7b-dihydro-1H-cyclopropa[a]naphthalen-1-yl)ethan-1-one (3.15ai)

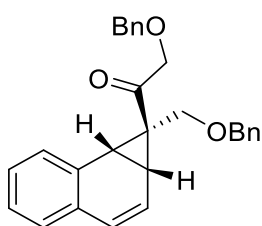
Colorless oil, 23.0 mg, 48% yield, 26:74 *er.* $[\alpha]_D^{20}$ -41.5 ($c = 1.0$, CH_2Cl_2); Analytical data **^1H NMR** (400 MHz, CDCl_3) δ 7.32 (d, $J = 2.8$ Hz, 1H), 7.24 – 7.19 (m, 2H), 7.17 – 7.13 (m, 1H), 6.57 (d, $J = 9.6$ Hz, 1H), 6.12 (dd, $J = 9.6, 5.2$ Hz, 1H), 5.02 – 4.87 (m, 2H), 3.36 (d, $J = 12.1$ Hz, 1H), 3.27 (d, $J = 12.8$ Hz, 1H), 3.23 (d, $J = 8.5$ Hz, 1H), 2.78 (dd, $J = 8.6, 5.2$ Hz, 1H), 0.94 (s, 9H), 0.77 (s, 9H), 0.12 (s, 3H), 0.12 (s, 3H), -0.22 (s, 3H), -0.33 (s, 3H). **^{13}C NMR** (101 MHz, CDCl_3) δ 210.00, 132.74, 130.83, 130.40, 128.93, 128.05, 127.65, 127.25, 123.87, 69.04, 56.10, 36.73, 34.59, 26.25, 26.03, 25.88, 18.73, 18.12, -5.17, -5.22, -5.85, -5.94. **IR** (ATR): $\tilde{\nu}$ (cm^{-1}) = 2952, 2928, 2885, 2856, 1702, 1471, 1463, 1389, 1361, 1253, 1150, 1121, 1079, 1052, 1023, 1006, 973, 835, 775, 745; **HRMS** (ESI) calcd for $\text{C}_{26}\text{H}_{42}\text{O}_3\text{Si}_2\text{Na}^+$ $[\text{M}+\text{Na}]^+$: 481.2565, Found: 481.2581. The enantiomeric excess was determined by Daicel Chiralpak IF (25 cm), Hexane/IPA = 99.5/0.5, 1.0 mL/min, $\lambda = 254$ nm, t_R (major) = 9.6 min, t_R (minor) = 8.3 min.



Peak #	RetTime [min]	Type	Width [min]	Area [mAU*s]	Height [mAU]	Area %
1	8.091	BB	0.2360	1463.81738	100.45472	49.9431
2	9.432	BB	0.2077	1467.15088	107.18236	50.0569



Peak #	RetTime [min]	Type	Width [min]	Area [mAU*s]	Height [mAU]	Area %
1	8.281	BV	0.2412	1088.55225	72.49139	25.5972
2	9.627	BB	0.2092	3164.07275	234.80605	74.4028

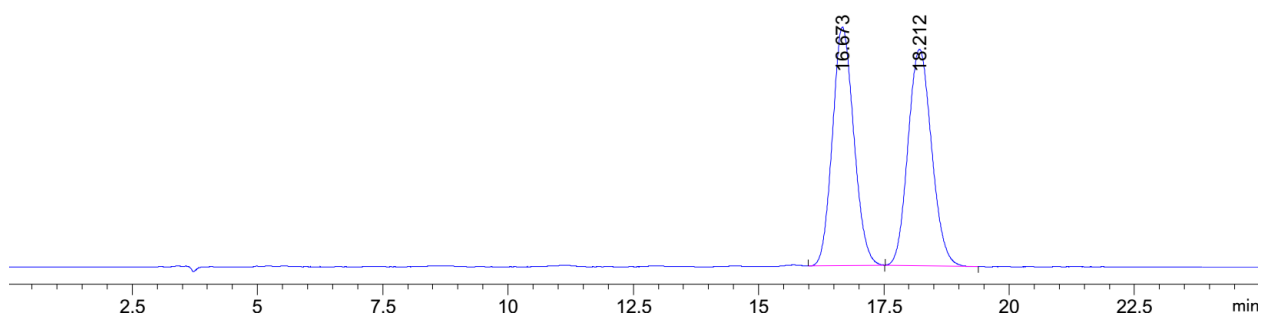


2-(benzyloxy)-1-((1S,1aR,7bR)-1-((benzyloxy)methyl)-1a,7b-

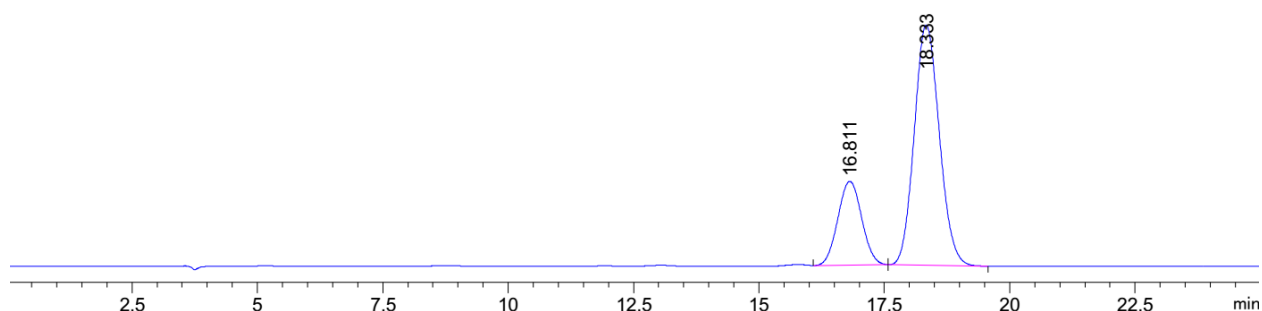
dihydro-1H-cyclopropa[a]naphthalen-1-yl)ethan-1-one (3.15aj)

Pale yellow oil, 25.0 mg, 63% yield, 25:75 *er*. $[\alpha]_D^{20}$ -56.3 ($c = 1.0$, CH_2Cl_2);

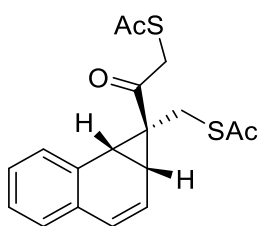
Analytical data: **^1H NMR** (400 MHz, CDCl_3) δ 7.43 – 7.31 (m, 6H), 7.26 (s, 5H), 7.16 – 7.11 (m, 1H), 7.05 – 6.97 (m, 2H), 6.53 (d, $J = 9.5$ Hz, 1H), 6.15 (dd, $J = 9.6, 5.2$ Hz, 1H), 4.72 (d, $J = 2.6$ Hz, 2H), 4.64 (d, $J = 2.1$ Hz, 2H), 4.11 (q, $J = 11.8$ Hz, 2H), 3.32 (d, $J = 8.6$ Hz, 1H), 3.19 (d, $J = 11.6$ Hz, 1H), 3.08 (d, $J = 11.7$ Hz, 1H), 2.91 (dd, $J = 8.6, 5.2$ Hz, 1H). **^{13}C NMR** (101 MHz, CDCl_3) 208.44, 137.74, 137.68, 132.74, 130.63, 130.24, 129.00, 128.56, 128.40, 128.18, 128.06, 127.97, 127.82, 127.74, 127.37, 123.73, 74.15, 73.46, 73.40, 63.04, 37.41, 35.03, 25.21. **IR** (ATR): $\tilde{\nu}$ (cm^{-1}) = 3062, 3030, 2924, 2856, 1697, 1495, 1488, 1454, 1362, 1270, 1187, 1164, 1121, 1099, 1075, 1058, 1028, 976, 950, 836, 780, 738, 698; **HRMS** (ESI) calcd for $\text{C}_{28}\text{H}_{26}\text{O}_3\text{Na}^+$ $[\text{M}+\text{Na}]^+$: 433.1774, Found: 433.1778. The enantiomeric excess was determined by Daicel Chiralpak IG (25 cm), Hexane/IPA = 80/20, 1.0 mL/min, $\lambda = 254$ nm, t_R (major) = 18.3 min, t_R (minor) = 16.8 min.



Peak #	RetTime [min]	Type	Width [min]	Area [mAU*s]	Height [mAU]	Area %
1	16.673	BB	0.4594	3105.66479	104.90746	49.9072
2	18.212	BB	0.5203	3117.21533	95.13756	50.0928



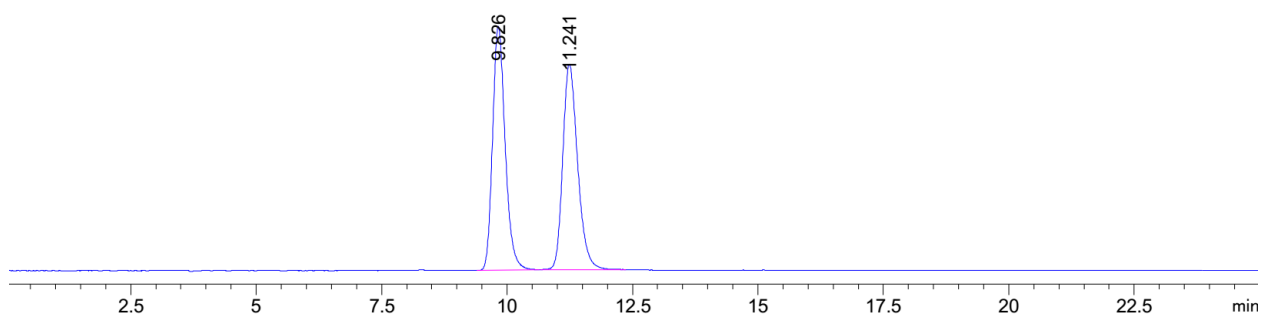
Peak #	RetTime [min]	Type	Width [min]	Area [mAU*s]	Height [mAU]	Area %
1	16.811	BB	0.5178	2069.53662	62.58076	24.8852
2	18.333	BB	0.5378	6246.81152	179.59009	75.1148



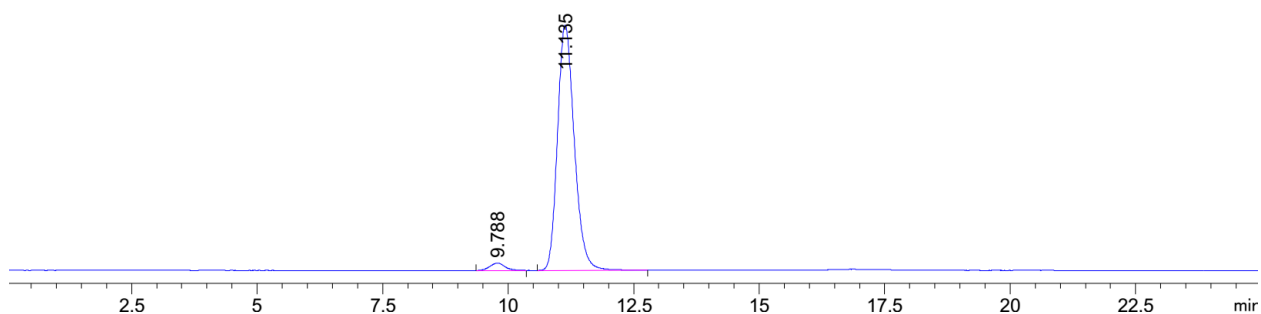
S-(((1*R*,1*aR*,7*bR*)-1-(2-(acetylthio)acetyl)-1*a*,7*b*-dihydro-1*H*-cyclopropa[*a*]naphthalen-1-yl)methyl) ethanethioate (**3.15ak**)

Colorless oil, 18.2 mg, 51% yield, 2.5:97.5 *er*. $[\alpha]_D^{20}$ -175.0 ($c = 1.0$, CH_2Cl_2);

Analytical data: $^1\text{H NMR}$ (400 MHz, CDCl_3) δ 7.43 – 7.35 (m, 1H), 7.32 – 7.26 (m, 2H), 7.23 – 7.19 (m, 1H), 6.68 (d, $J = 9.5$ Hz, 1H), 6.14 (dd, $J = 9.6, 5.2$ Hz, 1H), 4.13 (s, 2H), 3.37 (d, $J = 8.8$ Hz, 1H), 3.03 (d, $J = 14.9$ Hz, 1H), 2.96 (dd, $J = 8.8, 5.3$ Hz, 1H), 2.87 (d, $J = 15.0$ Hz, 1H), 2.39 (s, 3H), 2.22 (s, 3H). $^{13}\text{C NMR}$ (101 MHz, CDCl_3) δ 204.32, 195.28, 194.39, 132.69, 130.71, 130.04, 129.71, 128.36, 128.22, 127.84, 122.99, 39.64, 38.33, 36.91, 30.56, 30.30, 26.85, 24.01. **IR** (ATR): $\tilde{\nu}$ (cm^{-1}) = 3036, 2991, 2965, 2919, 1684, 1488, 1433, 1354, 1304, 1283, 1132, 1099, 1055, 1022, 996, 958, 820, 779, 627; **HRMS** (ESI) calcd for $\text{C}_{18}\text{H}_{18}\text{O}_3\text{S}_2\text{Na}$ $[\text{M}+\text{Na}]^+$: 369.0590, Found: 369.0595. The enantiomeric excess was determined by Daicel Chiralpak IF (25 cm), Hexane/IPA = 80/20, 1.0 mL/min, $\lambda = 254$ nm, t_R (major) = 11.1 min, t_R (minor) = 9.8 min.

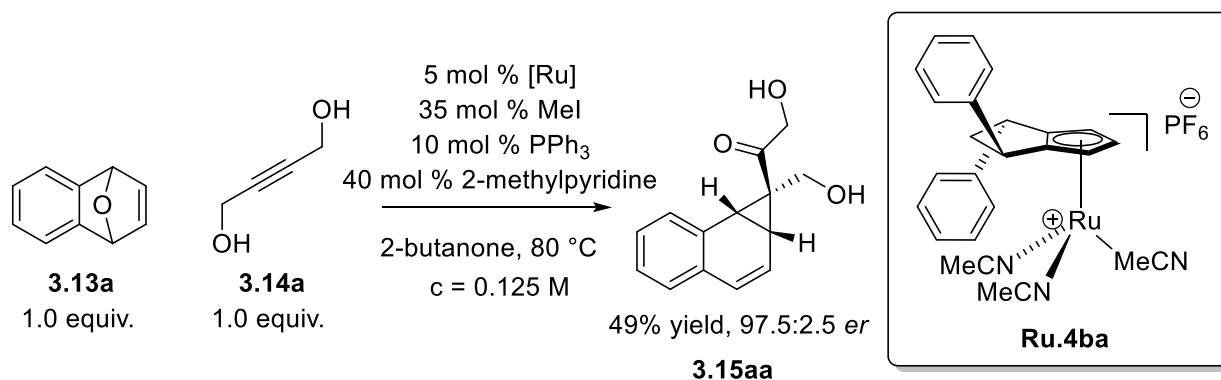


Peak #	RetTime [min]	Type	Width [min]	Area [mAU*s]	Height [mAU]	Area %
1	9.826	BB	0.2673	4441.49072	254.94209	50.1375
2	11.241	BB	0.3159	4417.13428	214.77298	49.8625

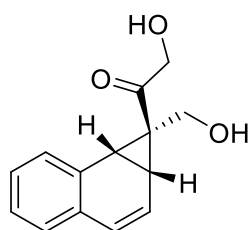


Peak #	RetTime [min]	Type	Width [min]	Area [mAU*s]	Height [mAU]	Area %
1	9.788	BB	0.3196	314.64703	15.19195	2.6278
2	11.135	BB	0.3596	1.16591e4	500.78586	97.3722

Alternative Conditions for 2-hydroxy-1-((1*S*,1*aR*,7*bR*)-1-(hydroxymethyl)-1*a*,7*b*-dihydro-1*H*-cyclopropa[*a*]naphthalen-1-yl)ethan-1-one (3.15aa)

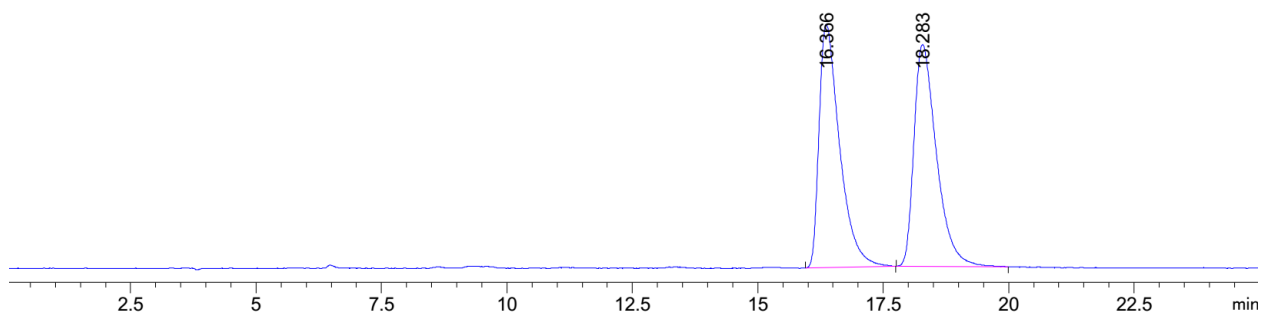


Ru.4ba (5 mol %, 1.39 μ mol, 0.869 mg) and triphenylphosphine (10 mol %, 2.77 μ mol, 0.728 mg) were dissolved in freshly distilled 2-butanone (0.10 ml) in a microwave reaction vial under N₂ atmosphere. Iodomethane (35 mol %, 9.71 μ mol, 1.39 mg) was added followed by addition of a solution of an oxa-benzonorbornadiene **3.13a** (1.00 equiv., 27.7 μ mol, 4 mg), but-2-yne-1,4-diol **3.14a** (1.00 equiv., 27.7 μ mol, 2.39 mg) and 2-methylpyridine (40 mol %, 11.1 μ mol, 1.03 mg) in 2-butanone (0.12 ml). The reaction mixture was heated to 80 °C for 90 min. After completion of the reaction (TLC control), the reaction mixture was cooled to room temperature. The solvent was removed under reduced pressure. The reaction mixture was purified by silica gel column chromatography (*n*-pentane/ethyl acetate) to afford benzonorcaradiene **3.15aa**.

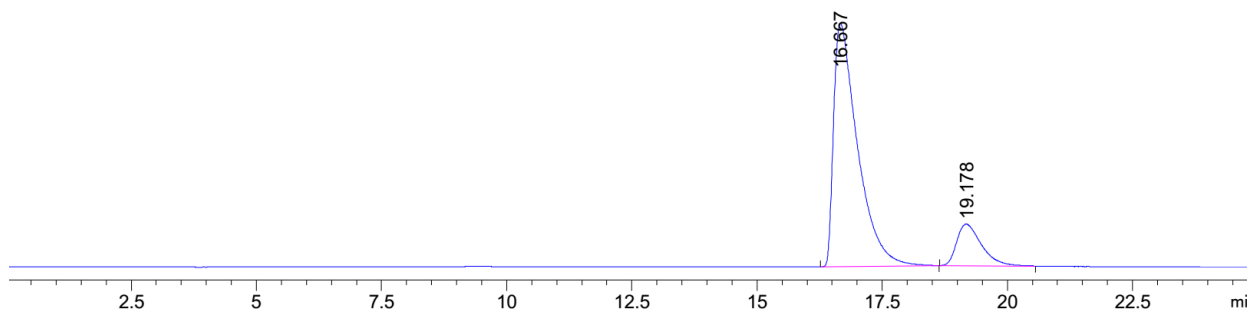


2-hydroxy-1-((1*S*,1*aR*,7*bR*)-1-(hydroxymethyl)-1*a*,7*b*-dihydro-1*H*-cyclopropa[*a*]naphthalen-1-yl)ethan-1-one (**3.15aa**)

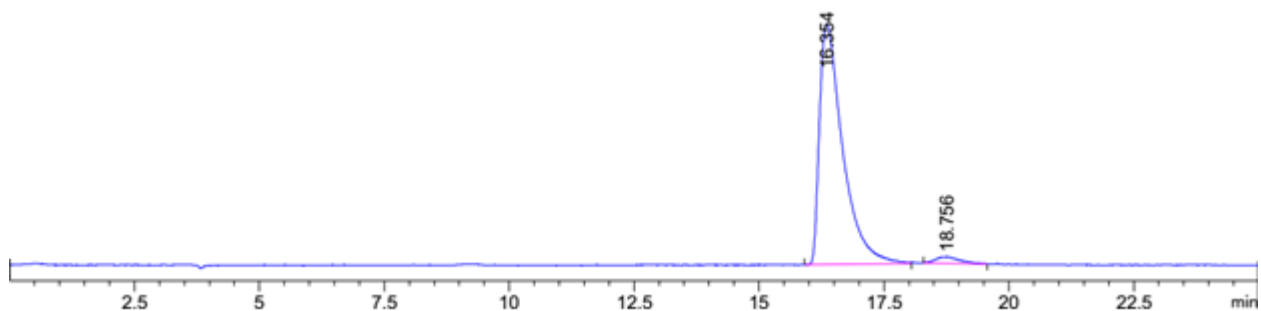
White solid, 15.4 mg, 64% yield, 85:15 *er*. [α]_D²⁰ -106.2 (*c* = 1.0, CH₂Cl₂); Mp = 145-146 °C; Analytical data: **¹H NMR** (400 MHz, CDCl₃) δ 7.46 – 7.35 (m, 1H), 7.31 – 7.27 (m, 2H), 7.24 – 7.20 (m, 1H), 6.69 (d, *J* = 9.6 Hz, 1H), 6.22 (dd, *J* = 9.6, 5.2 Hz, 1H), 4.80 (d, *J* = 4.6 Hz, 2H), 3.48 – 3.31 (m, 4H), 2.96 (dd, *J* = 8.7, 5.2 Hz, 1H), 1.06 (t, *J* = 6.3 Hz, 1H). **¹³C NMR** (101 MHz, CDCl₃) δ 211.90, 132.56, 129.84, 129.81, 129.76, 128.49, 128.07, 127.75, 122.74, 67.48, 55.70, 37.88, 35.69, 27.31. **IR** (ATR): $\tilde{\nu}$ (cm⁻¹) = 3424, 3035, 2894, 1681, 1487, 1366, 1308, 1270, 1187, 1164, 1094, 1056, 1024, 960, 841, 778; **HRMS** (ESI) calcd for C₁₄H₁₄O₃Na⁺ [*M*+Na]⁺: 253.0835, Found: 253.0834. The enantiomeric excess was determined by Daicel Chiralpak ID (25 cm), Hexane/IPA = 80/20, 1.0 mL/min, λ = 254 nm, *t_R* (major) = 16.7 min, *t_R* (minor) = 19.2 min.



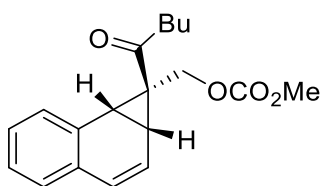
Peak #	RetTime [min]	Type	Width [min]	Area [mAU*s]	Height [mAU]	Area %
1	16.366	BB	0.4282	3891.32446	136.65958	49.9978
2	18.283	BB	0.4663	3891.66895	124.62547	50.0022



Peak #	RetTime [min]	Type	Width [min]	Area [mAU*s]	Height [mAU]	Area %
1	16.667	BB	0.4781	1.39498e4	419.35922	85.0501
2	19.178	BB	0.5076	2452.06348	71.59395	14.9499



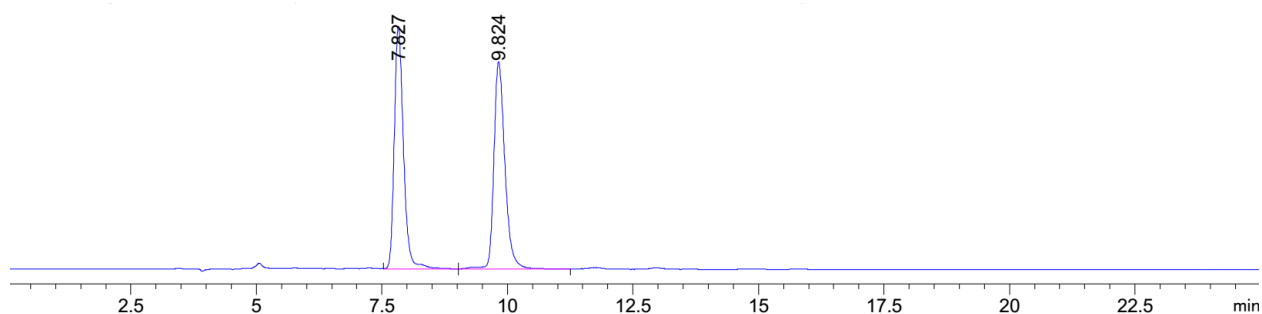
Peak #	RetTime [min]	Type	Width [min]	Area [mAU*s]	Height [mAU]	Area %
1	16.354	BV	0.4710	3478.51978	107.63944	97.3773
2	18.756	BB	0.4034	93.68734	2.80709	2.6227



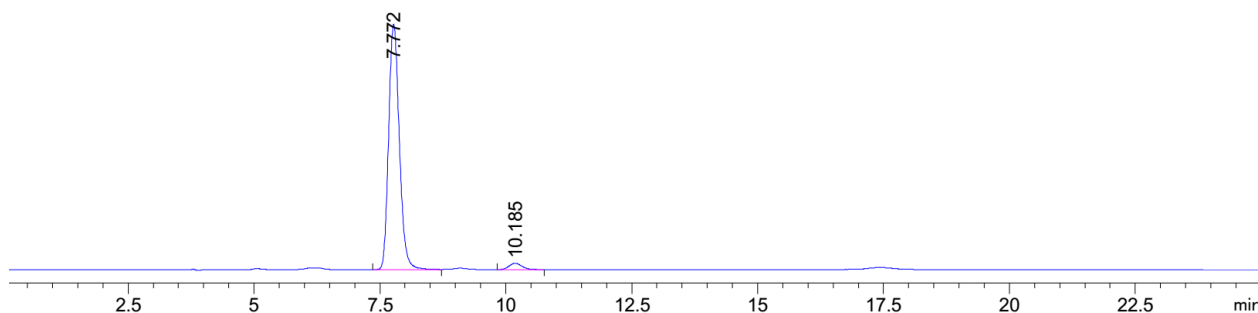
methyl (((1S,1aR,7bR)-1-pentanoyl-1a,7b-dihydro-1H-cyclopropa[a]naphthalen-1-yl)methyl) carbonate (3.15al)

Pale yellow oil, 8.5 mg, 26% yield, 97:3 *er.* $[\alpha]_D^{20}$ -179.4 (*c* = 0.3, CH₂Cl₂);

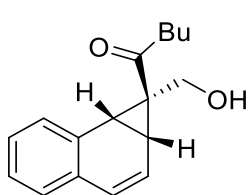
Analytical data: **¹H NMR** (400 MHz, CDCl₃) 7.35 (dd, *J* = 6.6, 2.2 Hz, 1H), 7.27 – 7.18 (m, 2H), 7.20 – 7.16 (m, 1H), 6.63 (d, *J* = 9.6 Hz, 1H), 6.19 (dd, *J* = 9.6, 5.2 Hz, 1H), 4.15 (d, *J* = 12.8 Hz, 1H), 3.86 (d, *J* = 12.7 Hz, 1H), 3.65 (s, 3H), 3.27 (d, *J* = 8.6 Hz, 1H), 2.92 (dd, *J* = 8.6, 5.2 Hz, 1H), 2.76 (t, *J* = 7.3 Hz, 2H), 1.63 (p, *J* = 7.4 Hz, 2H), 1.45 – 1.30 (m, 2H), 0.93 (t, *J* = 7.3 Hz, 3H). **¹³C NMR** (101 MHz, CDCl₃) δ 210.64, 155.54, 132.57, 130.18, 130.16, 129.45, 128.20, 128.17, 127.63, 123.48, 63.03, 54.82, 40.21, 37.68, 34.90, 26.22, 25.15, 22.50, 14.06. **IR** (ATR): $\tilde{\nu}$ (cm⁻¹) 2958, 2932, 2873, 1749, 1686, 1443, 1382, 1265, 1182, 1058, 952, 781; **HRMS** (ESI) calcd for C₁₉H₂₂O₄Na⁺ [M+Na]⁺: 337.1410, Found: 337.1410. The enantiomeric excess was determined by Daicel Chiralpak ID (25 cm), Hexane/IPA = 90/10, 1.0 mL/min, λ = 254 nm, *t_R* (major) = 7.8 min, *t_R* (minor) = 10.2 min.



Peak #	RetTime [min]	Type	Width [min]	Area [mAU*s]	Height [mAU]	Area %
1	7.827	VB	0.1946	2712.95435	212.92879	49.3596
2	9.824	BV	0.2345	2783.35449	181.90279	50.6404



Peak #	RetTime [min]	Type	Width [min]	Area [mAU*s]	Height [mAU]	Area %
1	7.772	BV	0.2303	8013.73535	542.60797	96.9957
2	10.185	BB	0.2700	248.21368	13.79074	3.0043



1-((1S,1aR,7bR)-1-(hydroxymethyl)-1a,7b-dihydro-

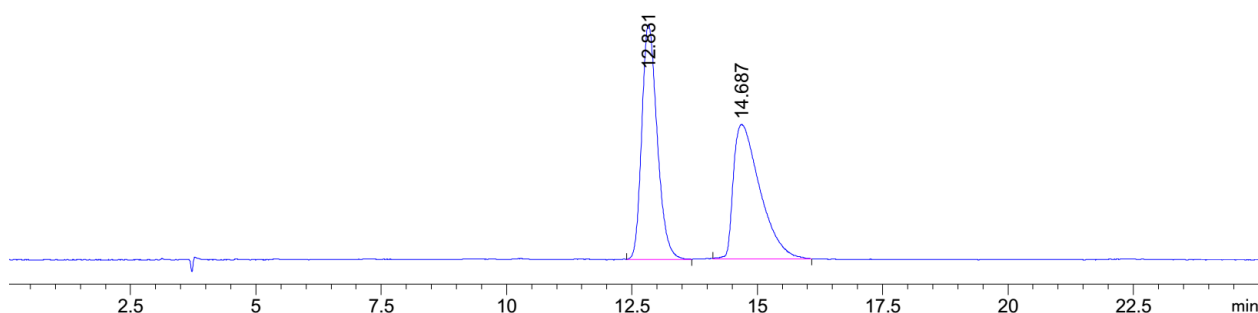
1H-cyclopropa[a]naphthalen-1-yl)pentan-1-one (3.15am)

Yellow oil, 10.5 mg, 39% yield, 94:6 *er.* $[\alpha]_D^{20}$ -122.7 ($c = 1.0$, CH_2Cl_2);

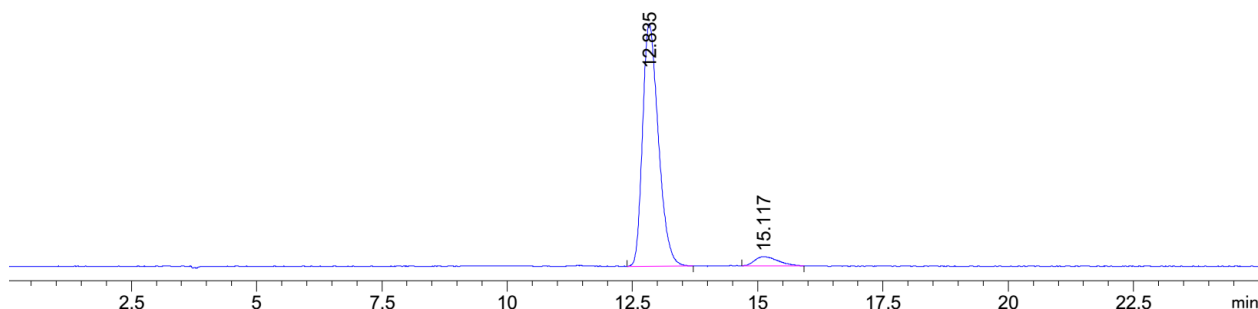
Analytical data: $^1\text{H NMR}$ (400 MHz, CDCl_3) δ 7.39 – 7.34 (m, 1H), 7.28 – 7.23 (m, 2H), 7.21 – 7.16 (m, 1H), 6.63 (d, $J = 9.4$ Hz, 1H), 6.20 (dd, $J = 9.6, 5.2$ Hz, 1H), 3.51 (dd, $J = 13.3, 4.8$ Hz, 1H), 3.40 (dd, $J = 13.2, 5.6$ Hz, 1H), 3.23 (d, $J = 8.6$ Hz, 1H), 2.87 – 2.82 (m, 2H), 2.80 (dd, $J = 8.6, 5.2$ Hz, 1H), 1.65 (p, $J = 7.4$ Hz, 2H), 1.44 – 1.32 (m, 2H), 1.25 (t, $J = 5.2$ Hz, 1H), 0.94 (t, $J = 7.3$ Hz, 3H).

$^{13}\text{C NMR}$ (101 MHz, CDCl_3) δ 212.84, 132.74, 130.64, 129.80, 129.36, 128.36, 128.07, 127.51, 123.62, 57.01, 39.69, 36.43, 34.14, 28.86, 26.32, 22.55, 14.13. **IR** (ATR): $\tilde{\nu}$ (cm^{-1}) = 3458, 3035, 2957, 2932, 2871, 1679, 1488, 1456, 1408, 1379, 1344, 1270, 1162, 1060, 1024, 965, 822, 777;

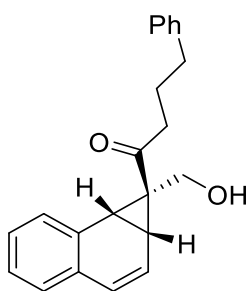
HRMS (ESI) calcd for $\text{C}_{17}\text{H}_{20}\text{O}_2\text{Na}^+$ $[\text{M}+\text{Na}]^+$: 279.1356, Found: 279.1354. The enantiomeric excess was determined by Daicel Chiralpak IG (25 cm), Hexane/IPA = 90/10, 1.0 mL/min, $\lambda = 254$ nm, t_R (major) = 12.8 min, t_R (minor) = 14.7 min.



Peak #	RetTime [min]	Type	Width [min]	Area [mAU*s]	Height [mAU]	Area %
1	12.831	VB	0.3251	9726.29395	455.56976	50.2446
2	14.687	VV	0.4946	9631.58691	260.96353	49.7554



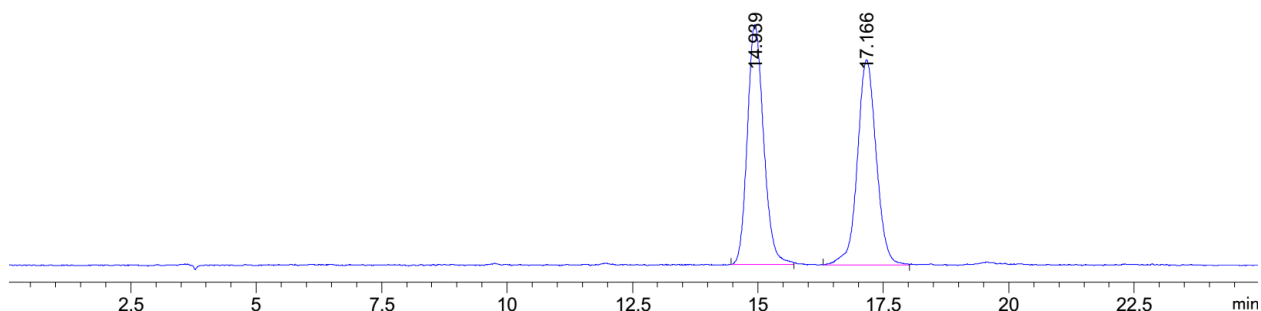
Peak #	RetTime [min]	Type	Width [min]	Area [mAU*s]	Height [mAU]	Area %
1	12.835	BB	0.3396	9057.16992	413.37427	94.7439
2	15.117	BB	0.3816	502.46075	15.60681	5.2561



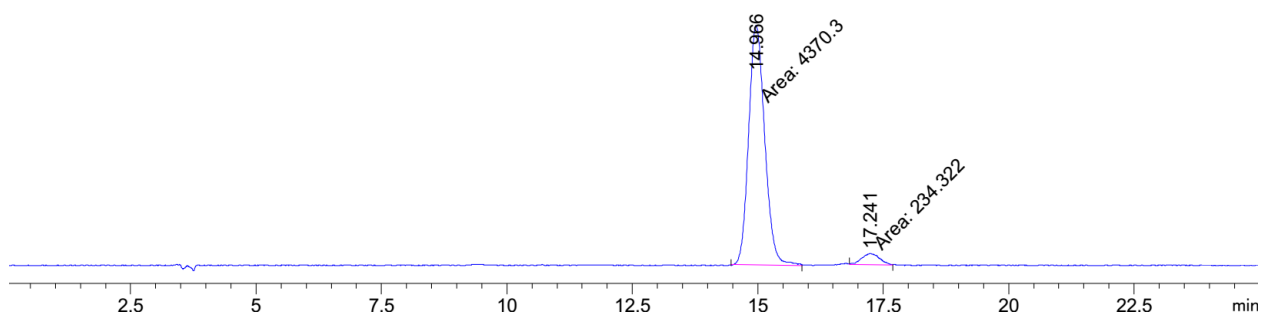
1-((1S,1aR,7bR)-1-(hydroxymethyl)-1a,7b-dihydro-1H-cyclopropa[a]naphthalen-1-yl)-4-phenylbutan-1-one (3.15an)

Pale yellow oil, 11.2 mg, 34% yield, 95:5 *er*. $[\alpha]_D^{20}$ -146.5 ($c = 0.5$, CH_2Cl_2);

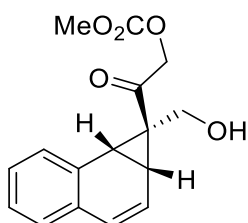
Analytical data: $^1\text{H NMR}$ (400 MHz, CDCl_3) δ 7.39 – 7.33 (m, 1H), 7.33 – 7.24 (m, 4H), 7.23 – 7.16 (m, 4H), 6.63 (d, $J = 9.6$ Hz, 1H), 6.19 (dd, $J = 9.6, 5.2$ Hz, 1H), 3.48 (d, $J = 13.2$ Hz, 1H), 3.37 (d, $J = 13.2$ Hz, 1H), 3.22 (d, $J = 8.5$ Hz, 1H), 2.91 – 2.84 (m, 2H), 2.78 (dd, $J = 8.6, 5.2$ Hz, 1H), 2.68 (dd, $J = 8.4, 6.9$ Hz, 2H), 2.01 (p, $J = 7.4$ Hz, 2H). $^{13}\text{C NMR}$ (101 MHz, CDCl_3) δ 212.44, 141.97, 132.72, 130.58, 129.80, 129.39, 128.66, 128.52, 128.38, 128.09, 127.54, 126.05, 123.57, 56.92, 39.22, 36.56, 35.30, 34.35, 28.90, 25.63. **IR** (ATR): $\tilde{\nu}$ (cm^{-1}) = 3466, 3059, 3025, 2930, 2857, 1677, 1495, 1488, 1454, 1407, 1372, 1270, 1160, 1104, 1071, 1052, 1027, 967, 777, 747, 700; **HRMS** (ESI) calcd for $\text{C}_{22}\text{H}_{22}\text{O}_2\text{Na}^+$ $[\text{M}+\text{Na}]^+$: 341.1512, Found: 341.1509. The enantiomeric excess was determined by Daicel Chiralpak IC (25 cm), Hexane/IPA = 90/10, 1.0 mL/min, $\lambda = 254$ nm, t_R (major) = 14.9 min, t_R (minor) = 17.2 min.



Peak #	RetTime [min]	Type	Width [min]	Area [mAU*s]	Height [mAU]	Area %
1	14.939	BV	0.3447	2881.30591	127.96694	50.2151
2	17.166	BV	0.3948	2856.62280	109.35695	49.7849



Peak #	RetTime [min]	Type	Width [min]	Area [mAU*s]	Height [mAU]	Area %
1	14.966	MM	0.3715	4370.30127	196.05707	94.9112
2	17.241	MM	0.4264	234.32150	9.15981	5.0888

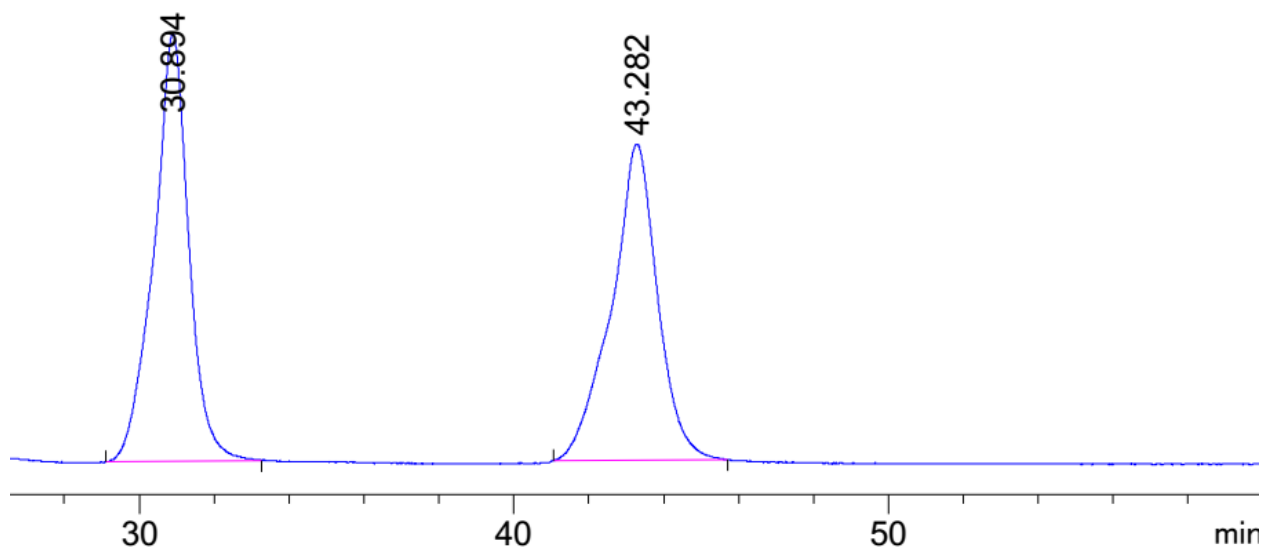


2-((1S,1aR,7bR)-1-(hydroxymethyl)-1a,7b-dihydro-

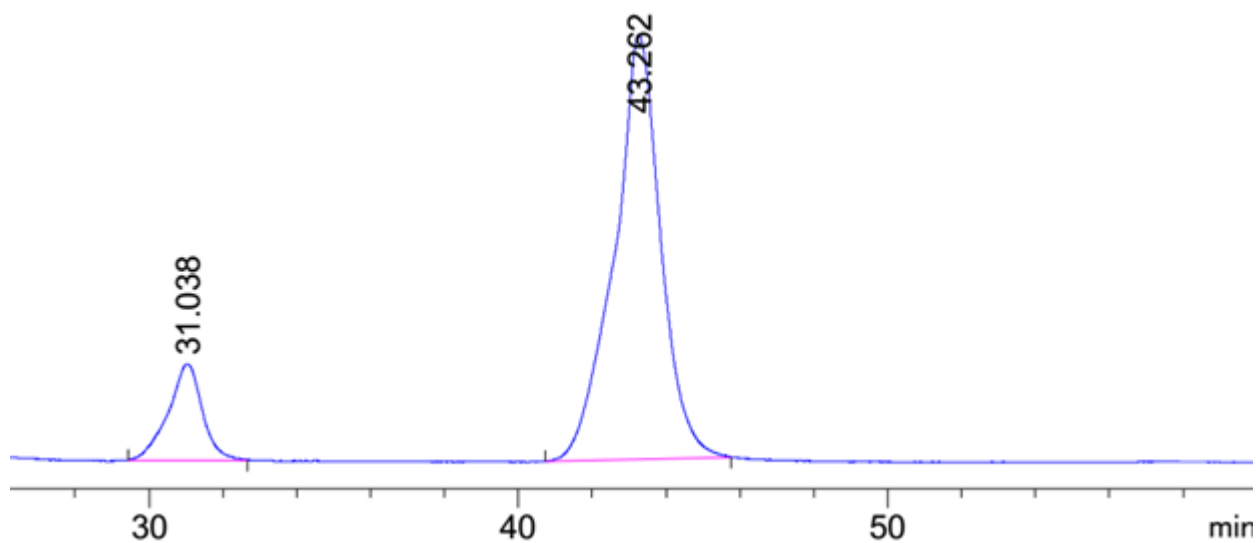
1H-cyclopropa[a]naphthalen-1-yl)-2-oxoethyl methyl carbonate (3.15ao)

Colorless oil, 18.6 mg, 60% combined yield (**3an** and **3an'**), 14:86 *er.* $[\alpha]_D^{20}$ -37.0 (*c* = 0.5, CH₂Cl₂); Analytical data: **¹H NMR** (400 MHz, CDCl₃) δ 7.42 – 7.35 (m, 1H), 7.31 – 7.21 (m, 3H), 7.22 – 7.15 (m, 1H), 6.65 (d, *J* = 9.5 Hz, 1H), 6.19 (dd, *J* = 9.5, 5.2 Hz, 1H), 5.31 (d, *J* = 3.6 Hz, 2H), 3.88 – 3.79 (m, 6H), 3.48 – 3.34 (m, 3H), 3.33 (d, *J* = 8.6 Hz, 1H), 2.90 (dd, *J* = 8.7, 5.2 Hz, 1H), 1.12 (m, 1H). **¹³C NMR** (101 MHz, CDCl₃) δ 204.67, 155.76, 132.81, 130.14, 130.04, 129.94, 128.61, 128.18, 127.84, 123.02, 70.51, 56.06, 55.32, 37.52, 35.37,

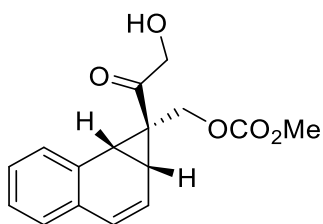
27.64. **IR** (ATR): $\tilde{\nu}$ (cm⁻¹) = 3501, 3022, 2957, 1754, 1697, 1446, 1419, 1377, 1269, 1182, 1164, 1066, 995, 956, 917, 841, 790, 778; **HRMS** (ESI) calcd for C₁₆H₁₆O₅Na⁺ [M+Na]⁺: 311.0890, Found: 311.0896. The enantiomeric excess was determined by Daicel Chiralpak IA (25 cm), Hexane/IPA = 95/5, 1.0 mL/min, λ = 254 nm, t_R (major) = 43.3 min, t_R (minor) = 30.9 min.



Peak #	RetTime [min]	Type	Width [min]	Area [mAU*s]	Height [mAU]	Area %
1	30.894	BB	0.8860	3609.71460	55.55563	50.5176
2	43.282	BB	1.0258	3535.74390	41.09584	49.4824



Peak #	RetTime [min]	Type	Width [min]	Area [mAU*s]	Height [mAU]	Area %
1	31.038	BB	0.8142	1142.64392	17.91417	14.1311
2	43.262	BB	1.1911	6943.40137	79.17642	85.8689

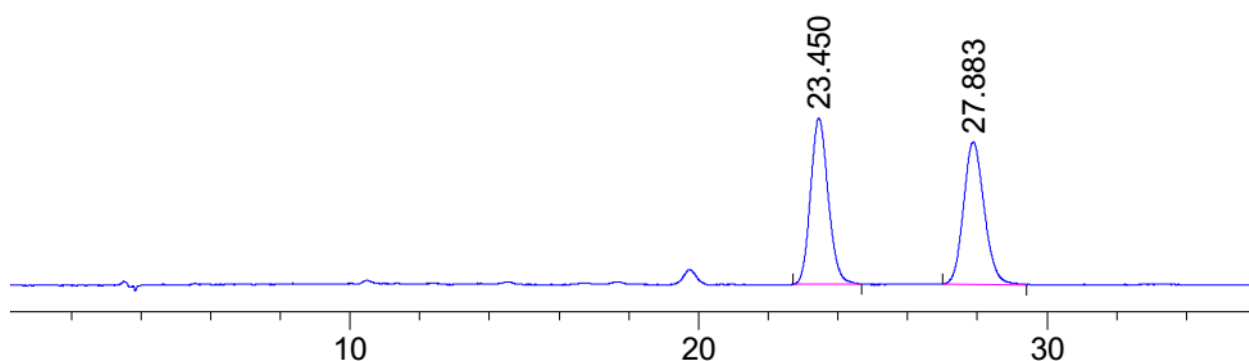


((1S,1aR,7bR)-1-(2-hydroxyacetyl)-1a,7b-dihydro-

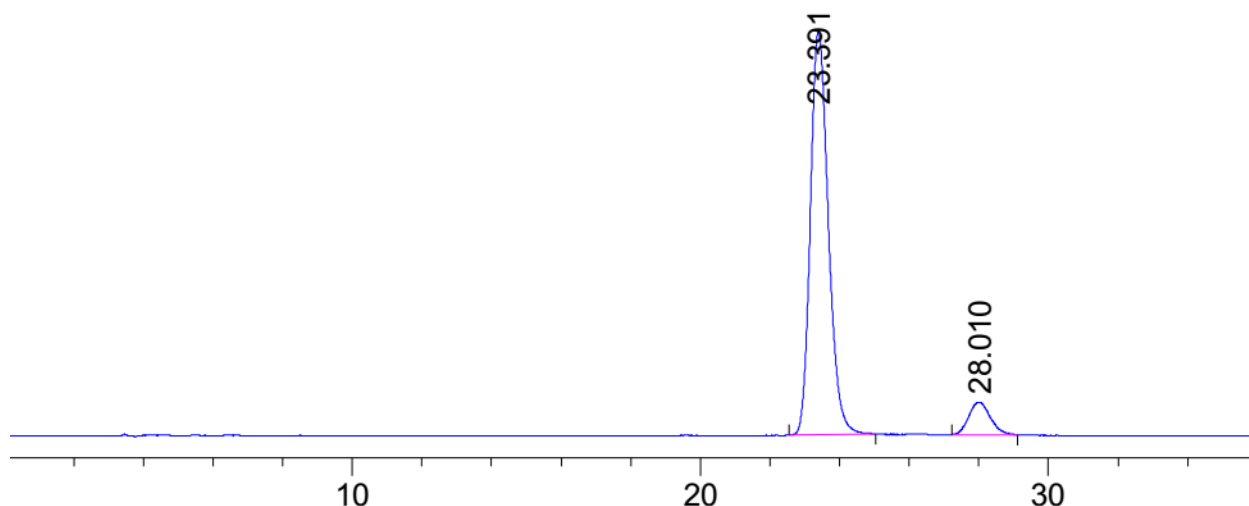
1H-cyclopropa[a]naphthalen-1-yl)methyl methyl carbonate (3.15ao')

Colorless oil, 18.6 mg, 60% combined yield (**3an** and **3an'**), 91.5:8.5 *er*.

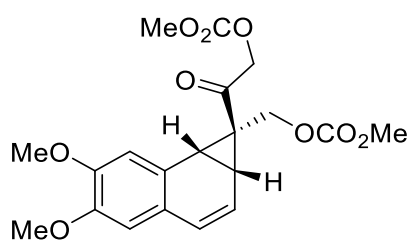
$[\alpha]_D^{20}$ -178.9 ($c = 0.15$, CH_2Cl_2); Analytical data: **^1H NMR** (400 MHz, CDCl_3) δ 7.38 (dd, $J = 6.9, 1.9$ Hz, 1H), 7.34 – 7.24 (m, 2H), 7.25 – 7.19 (m, 1H), 6.69 (d, $J = 9.5$ Hz, 1H), 6.20 (dd, $J = 9.6, 5.2$ Hz, 1H), 4.66 (d, $J = 4.6$ Hz, 2H), 4.04 (d, $J = 13.1$ Hz, 1H), 3.79 (d, $J = 13.1$ Hz, 1H), 3.65 (s, 3H), 3.46 (d, $J = 8.7$ Hz, 1H), 3.31 (t, $J = 4.7$ Hz, 1H), 3.08 (dd, $J = 8.7, 5.2$ Hz, 1H). **^{13}C NMR** (151 MHz, CDCl_3) δ 210.43, 155.28, 132.45, 130.25, 130.18, 129.25, 128.50, 128.35, 128.09, 122.57, 67.42, 61.44, 55.03, 39.08, 36.47, 24.06. **IR** (ATR): $\tilde{\nu}$ (cm^{-1}) = 3472, 3024, 2957, 2857, 1748, 1687, 1443, 1282, 1266, 1197, 1098, 1055, 950, 784; **HRMS** (ESI) calcd for $\text{C}_{16}\text{H}_{16}\text{O}_5\text{Na}^+$ $[\text{M}+\text{Na}]^+$: 311.0890, Found: 311.0895. The enantiomeric excess was determined by Daicel Chiralpak IC (25 cm), Hexane/IPA = 80/20, 1.0 mL/min, $\lambda = 254$ nm, t_R (major) = 23.4 min, t_R (minor) = 28.0 min.



Peak #	RetTime [min]	Type	Width [min]	Area [mAU*s]	Height [mAU]	Area %
1	23.450	BB	0.5329	1431.08960	40.63544	49.8484
2	27.883	BB	0.6223	1439.79211	34.82635	50.1516



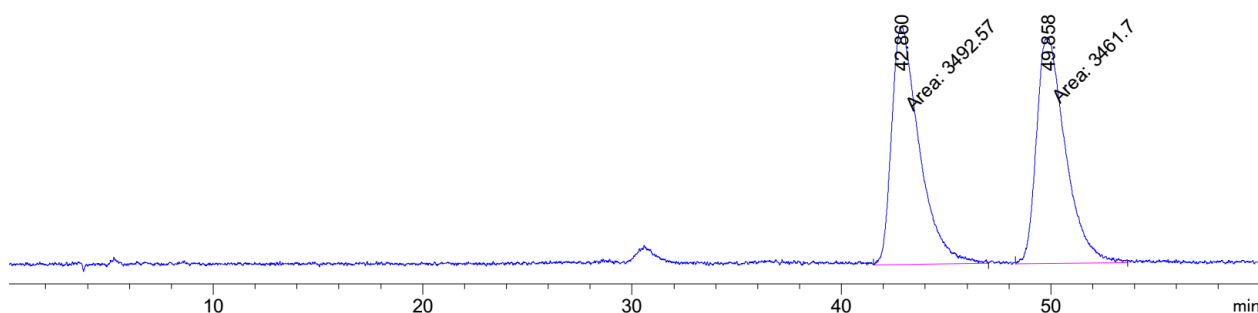
Peak #	RetTime [min]	Type	Width [min]	Area [mAU*s]	Height [mAU]	Area %
1	23.391	BB	0.5410	1.13931e4	318.77936	91.2583
2	28.010	BB	0.5792	1091.34668	25.60997	8.7417



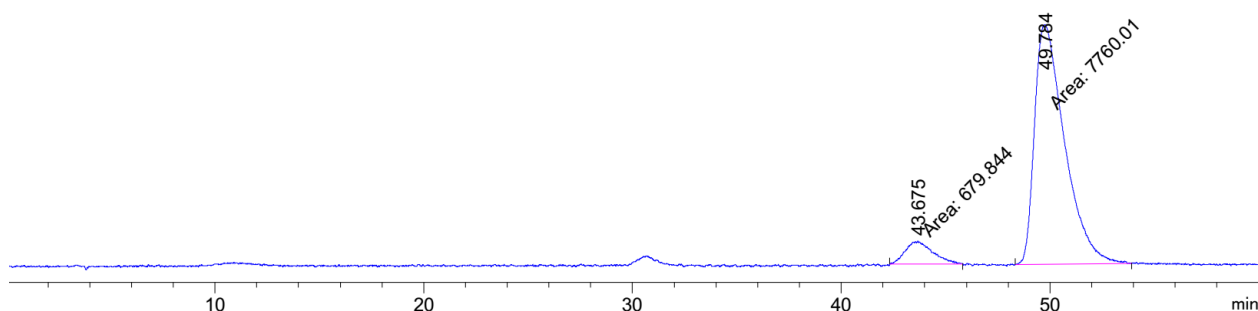
2-((1*S*,1*aR*,7*bR*)-5,6-dimethoxy-1-
(((methoxycarbonyl)oxy)methyl)-1*a*,7*b*-dihydro-1*H*-
cyclopropa[*a*]naphthalen-1-yl)-2-oxoethyl methyl carbonate
(**3.15bc**)

Off-white solid, 25.9 mg, 65% yield, 8:92 *er*. $[\alpha]_D^{20}$ -123.3 (*c* = 0.5, CH₂Cl₂), Mp = 97-101 °C; Analytical data: ¹H NMR (400 MHz, CDCl₃) δ 6.89 (s, 1H), 6.69 (s, 1H), 6.59 (d, *J* = 9.5 Hz, 1H), 6.09 (dd, *J* = 9.5, 5.2 Hz, 1H), 5.22 – 5.10 (m, 2H), 4.00 (d, *J* = 13.1 Hz, 1H), 3.90 (s, 3H), 3.89 (s, 3H), 3.85 (s, 3H), 3.83 (d, *J* = 13.3 Hz, 1H), 3.66 (s, 3H), 3.40 (d, *J* = 8.9 Hz, 1H), 3.02 (dd, *J* = 8.9, 5.2 Hz, 1H). ¹³C NMR (101 MHz, CDCl₃) δ 203.23, 155.63, 155.32, 149.30, 148.79, 129.76, 125.76, 122.32, 120.70, 112.60, 110.66, 70.09, 61.78, 56.21, 56.08, 55.45, 54.99, 39.00, 36.74, 24.07. IR (ATR): $\tilde{\nu}$ (cm⁻¹) = 3004, 2958, 2837, 1751, 1700, 1514, 1445, 1352, 1264,

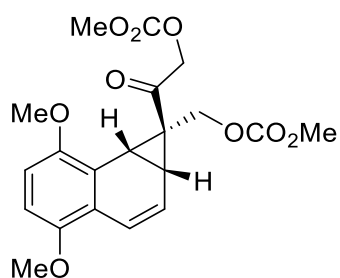
1194, 1171, 1130, 1060, 996, 967, 847, 789; **HRMS** (ESI) calcd for C₂₀H₂₂O₉Na⁺ [M+Na]⁺: 429.1156, Found: 429.1152. The enantiomeric excess was determined by Daicel Chiralpak ID (25 cm), Hexane/IPA = 80/20, 1.0 mL/min, λ = 254 nm, t_R (major) = 49.9 min, t_R (minor) = 42.9 min.



Peak #	RetTime [min]	Type	Width [min]	Area [mAU*s]	Height [mAU]	Area %
1	42.860	MM	1.5299	3492.56934	38.04867	50.2220
2	49.858	MM	1.5958	3461.69580	36.15487	49.7780



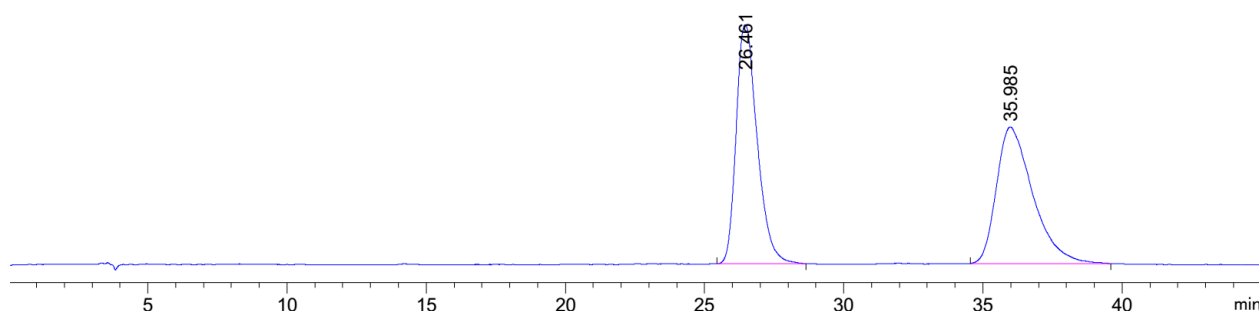
Peak #	RetTime [min]	Type	Width [min]	Area [mAU*s]	Height [mAU]	Area %
1	43.675	MM	1.5203	679.84412	7.45286	8.0552
2	49.784	MM	1.6689	7760.00830	77.49805	91.9448



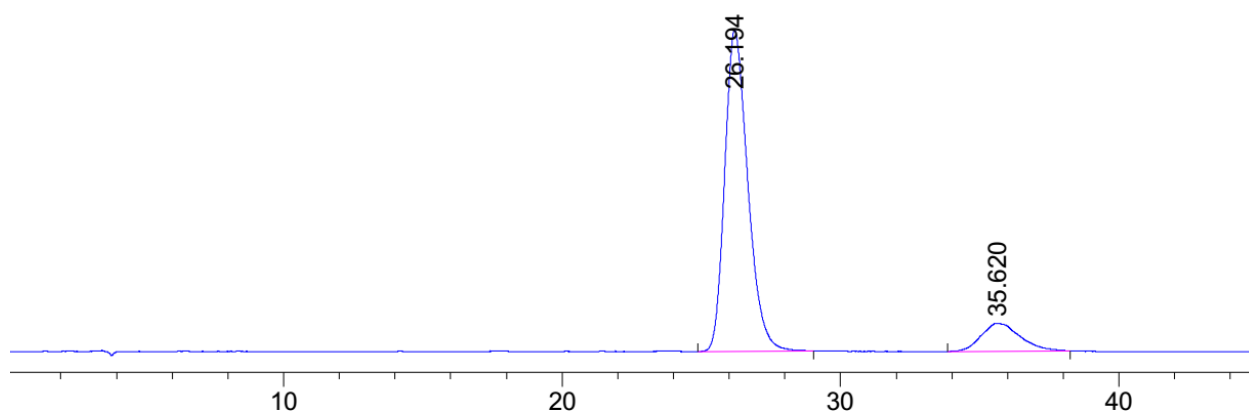
2-(((1S,1aR,7bR)-4,7-dimethoxy-1-(((methoxycarbonyl)oxy)methyl)-1a,7b-dihydro-1H-cyclopropa[a]naphthalen-1-yl)-2-oxoethyl) methyl carbonate (3.15cc)

Brown solid, 24.8 mg, 62% yield, 88:12 *er*. [α]_D²⁰ -90.2 (*c* = 1.0, CH₂Cl₂); Mp = 121-123 °C; Analytical data: ¹H NMR (400 MHz, CDCl₃) δ 7.08 (d,

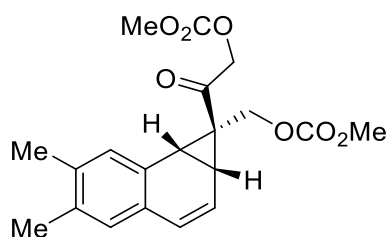
$J = 9.8$ Hz, 1H), 6.73 (s, 2H), 6.19 (ddd, $J = 9.8, 5.2, 0.7$ Hz, 1H), 5.29 – 5.04 (m, 2H), 4.10 (d, $J = 13.1$ Hz, 1H), 3.86 (s, 3H), 3.80 (s, 3H), 3.78 (s, 3H), 3.76 (dd, $J = 13.6, 4.4$ Hz, 1H), 3.67 (s, 3H), 3.59 (d, $J = 8.9$ Hz, 1H), 3.01 (dd, $J = 9.0, 5.2$ Hz, 1H). **^{13}C NMR** (101 MHz, CDCl_3) δ 203.00, 155.54, 155.33, 152.78, 149.89, 123.64, 122.99, 122.33, 119.39, 110.46, 109.97, 69.97, 61.90, 56.28, 56.21, 55.42, 54.96, 35.15, 33.89, 23.10. **IR** (ATR): $\tilde{\nu}$ (cm^{-1}) = 3004, 2957, 2838, 1751, 1704, 1483, 1443, 1421, 1378, 1344, 1261, 1192, 1103, 1086, 963, 910, 843, 791, 731; **HRMS** (ESI) calcd for $\text{C}_{20}\text{H}_{22}\text{O}_9\text{Na}^+$ $[\text{M}+\text{Na}]^+$: 429.1156, Found: 429.1157. The enantiomeric excess was determined by Daicel Chiralpak ID (25 cm), Hexane/IPA = 80/20, 1.0 mL/min, $\lambda = 254$ nm, t_R (major) = 26.2 min, t_R (minor) = 35.6 min.



Peak #	RetTime [min]	Type	Width [min]	Area [mAU*s]	Height [mAU]	Area %
1	26.461	BB	0.7768	2819.69873	53.51037	50.3652
2	35.985	BB	1.1353	2778.80273	30.60352	49.6348

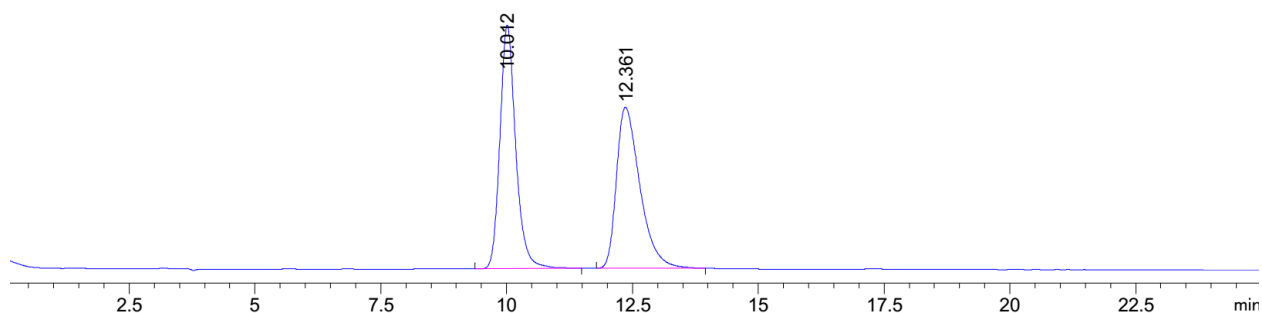


Peak #	RetTime [min]	Type	Width [min]	Area [mAU*s]	Height [mAU]	Area %
1	26.194	BV	0.8901	7161.63281	123.93897	87.2968
2	35.620	BB	1.1431	1042.14478	10.76838	12.7032

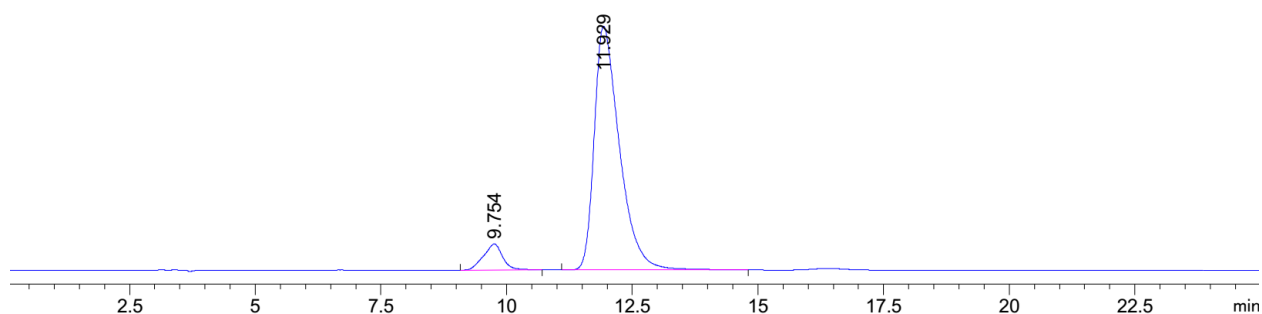


2-((1*S*,1*aR*,7*bR*)-1-(((methoxycarbonyl)oxy)methyl)-5,6-dimethyl-1*a*,7*b*-dihydro-1*H*-cyclopropa[*a*]naphthalen-1-yl)-2-oxoethyl methyl carbonate (3.15dc)

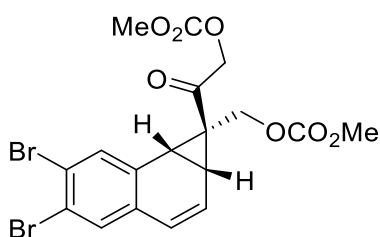
Off-white solid, 35.2 mg, 81% yield, 7.5:92.5 *er*. $[\alpha]_D^{20}$ -109.5 (*c* 1.0, CH₂Cl₂); Mp = 111 °C; Analytical data: **¹H NMR** (400 MHz, CDCl₃) δ 7.15 (s, 1H), 6.96 (s, 1H), 6.60 (d, *J* = 9.5 Hz, 1H), 6.11 (dd, *J* = 9.6, 5.2 Hz, 1H), 5.13 (s, 2H), 4.06 (d, *J* = 13.1 Hz, 1H), 3.85 (s, 3H), 3.76 (d, *J* = 13.1 Hz, 1H), 3.67 (s, 3H), 3.35 (d, *J* = 8.8 Hz, 1H), 3.01 (dd, *J* = 8.8, 5.2 Hz, 1H), 2.25 (s, 3H), 2.24 (s, 3H). **¹³C NMR** (101 MHz, CDCl₃) δ 203.04, 155.57, 155.28, 137.24, 136.41, 131.27, 130.27, 129.91, 129.29, 126.70, 121.57, 70.02, 61.91, 55.42, 54.96, 38.60, 36.02, 24.68, 19.73, 19.58. **IR** (ATR): $\tilde{\nu}$ (cm⁻¹) = 3009, 2957, 2860, 1748, 1701, 1501, 1443, 1421, 1376, 1253, 1190, 1143, 1106, 997, 949, 911, 884, 842, 786, 729, 648, 581, 543, 432; **HRMS** (ESI) calcd for C₂₀H₂₂O₇Na⁺ [M+Na]⁺: 397.1258, Found: 397.1262. The enantiomeric excess was determined by Daicel Chiralpak IF (25 cm), Hexane/IPA = 80/20, 1.0 mL/min, λ = 254 nm, *t*_R (major) = 11.9 min, *t*_R (minor) = 9.7 min.



Peak #	RetTime [min]	Type	Width [min]	Area [mAU*s]	Height [mAU]	Area %
1	10.012	BB	0.3325	4263.61719	195.46851	50.3397
2	12.361	BB	0.5052	4206.06934	129.40663	49.6603

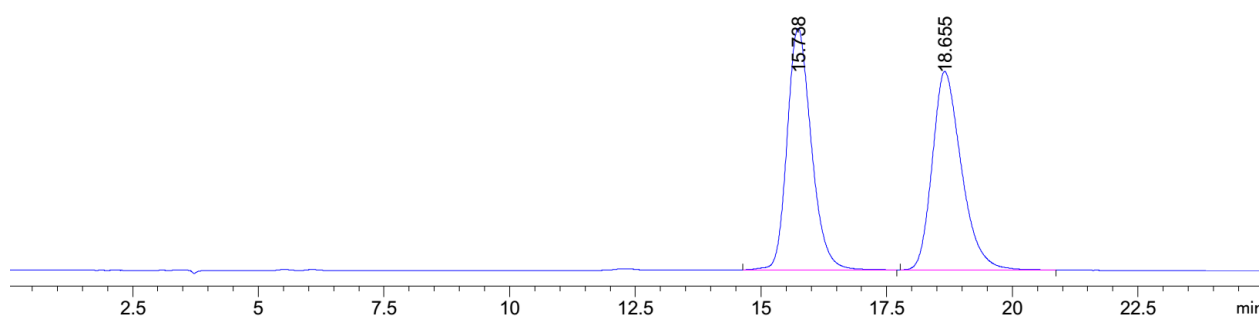


Peak #	RetTime [min]	Type	Width [min]	Area [mAU*s]	Height [mAU]	Area %
1	9.754	BB	0.3786	889.36096	33.62734	7.4910
2	11.929	BB	0.5292	1.09830e4	314.65701	92.5090

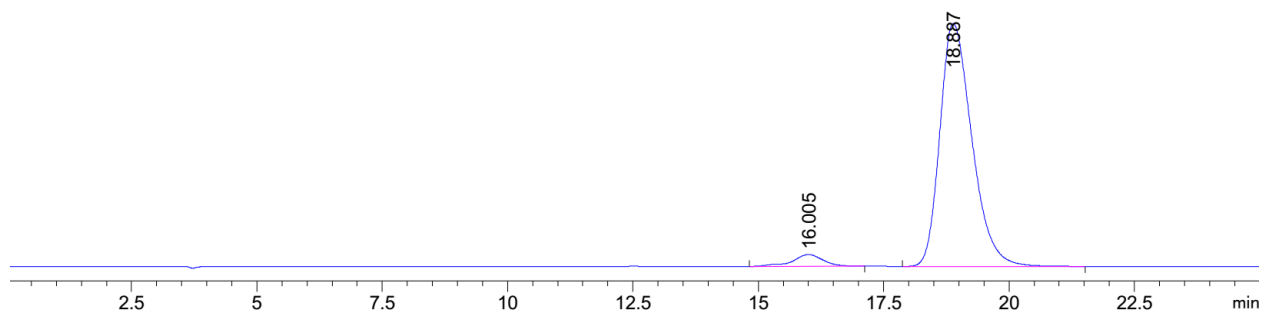


2-((1S,1aR,7bR)-5,6-dibromo-1-(((methoxycarbonyl)oxy)methyl)-1a,7b-dihydro-1H-cyclopropa[a]naphthalen-1-yl)-2-oxoethyl methyl carbonate (3.15ec)

White solid, 24.0 mg, 48% yield, 4:96 *er*. $[\alpha]_D^{20}$ -106.8 ($c = 1.0$, CH_2Cl_2), Mp = 136-137 °C; Analytical data: **^1H NMR** (400 MHz, CDCl_3) δ 7.65 (s, 1H), 7.46 (s, 1H), 6.58 (d, $J = 9.6$ Hz, 1H), 6.27 (dd, $J = 9.6, 5.2$ Hz, 1H), 5.14 (s, 2H), 4.04 (d, $J = 13.4$ Hz, 1H), 3.86 (d, $J = 13.4$ Hz, 1H) 3.85 (s, 3H), 3.68 (s, 3H), 3.29 (d, $J = 8.6$ Hz, 1H), 2.99 (dd, $J = 8.7, 5.3$ Hz, 1H). **^{13}C NMR** (101 MHz, CDCl_3) δ 202.34, 155.54, 155.16, 134.98, 132.97, 132.64, 130.02, 128.17, 124.65, 124.10, 123.98, 70.00, 61.24, 55.52, 55.20, 36.67, 35.30, 24.55. **IR** (ATR): $\tilde{\nu}$ (cm^{-1}) = 2957, 2855, 2258, 1747, 1703, 1583, 1466, 1442, 1419, 1372, 1242, 1186, 1159, 1112, 1065, 997, 959, 907, 856, 836, 809, 787, 768, 727, 664, 649, 588, 524; **HRMS** (ESI) calcd for $\text{C}_{18}\text{H}_{16}\text{Br}_2\text{O}_7\text{Na}^+$ $[\text{M}+\text{Na}]^+$: 524.9155, Found: 524.9172. The enantiomeric excess was determined by Daicel Chiralpak IG (25 cm), Hexane/IPA = 80/20, 1.0 mL/min, $\lambda = 254$ nm, t_R (major) = 18.9 min, t_R (minor) = 16.0 min.

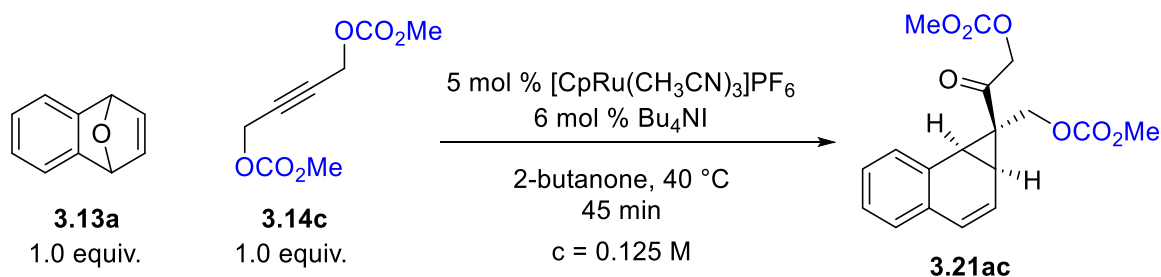


Peak #	RetTime [min]	Type	Width [min]	Area [mAU*s]	Height [mAU]	Area %
1	15.738	BB	0.5164	5301.86621	158.44095	50.2908
2	18.655	BB	0.6017	5240.55078	130.16704	49.7092

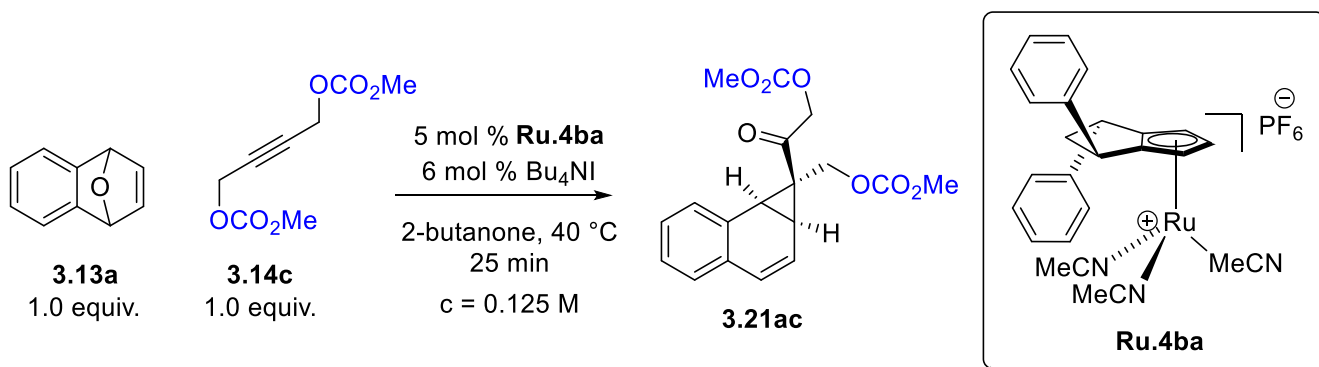


Peak #	RetTime [min]	Type	Width [min]	Area [mAU*s]	Height [mAU]	Area %
1	16.005	BB	0.5982	686.46088	16.13927	4.4370
2	18.887	BB	0.6824	1.47849e4	332.74652	95.5630

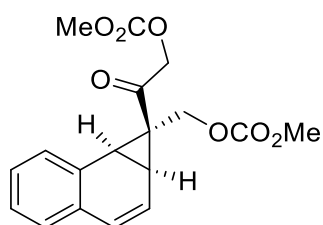
Preparation of *endo*-benzonorcaradiene (**3.21ac**)



$[\text{CpRu}(\text{CH}_3\text{CN})_3]\text{PF}_6$ (5.00 mol %, 10.4 μmol , 4.52 mg) and tetrabutylammonium iodide (6 mol %, 12.4 μmol , 4.60 mg) were dissolved in freshly distilled 2-butanone (0.55 ml) in a microwave reaction vial under N_2 atmosphere. The solution of an oxa-benzonorbornadiene (0.208 mmol, 30 mg, 1.0 equiv.) and but-2-yne-1,4-diyl dimethyl dicarbonate (0.208 mmol, 42.1 mg, 1.0 equiv.) in 2-butanone (1.1 ml) was added into the microwave reaction vial. The reaction mixture was stirred at 40 °C for 45 min. The reaction mixture was cooled to room temperature. The solvent was removed under reduced pressure. The reaction mixture was purified by column chromatography with phosphate buffered silica gel (pH = 7) (*n*-pentane/ethyl acetate = 5/1 (v/v')) to afford the *endo*-product (*rac*-**3.21ac**) (39 mg, 54% yield).



Ru.4ba (5 mol %, 10.4 μmol , 6.52 mg) and tetrabutylammonium iodide (6 mol %, 12.0 μmol , 4.60 mg) were dissolved with freshly distilled 2-butanone (0.55 ml) in a microwave reaction vial under N_2 atmosphere. The solution of an oxa-benzonorbornadiene (208 μmol , 30.0 mg, 1.0 equiv.) and but-2-yne-1,4-diyl dimethyl dicarbonate (208 μmol , 42.1 mg, 1.00 equiv.) in 2-butanone (1.10 ml) was added in one portion. The reaction mixture was stirred at 40 °C for 25 min, then to room temperature. The solvent was removed under reduced pressure. The reaction mixture was purified by column chromatography on phosphate buffered silica gel ($\text{pH} = 7$) (n -pentane/ethyl acetate = 5/1 (v/v')) to afford the *endo*-product (**3.21ac**) (53 mg, 74% yield).

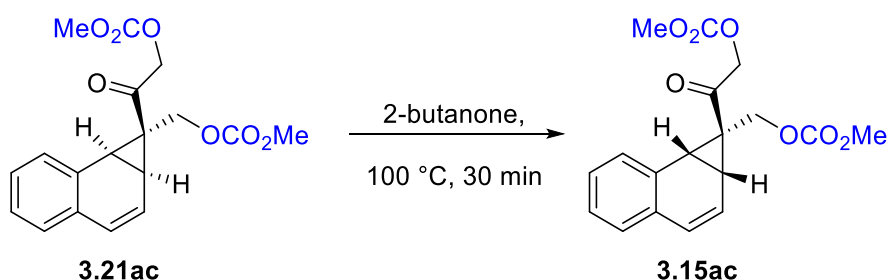


rac-2-((1*S*,1*aS*,7*bS*)-1-(((methoxycarbonyl)oxy)methyl)-1*a*,7*b*-dihydro-1*H*-cyclopropa[*a*]naphthalen-1-yl)-2-oxoethyl methyl carbonate (**3.21ac**)

Colorless oil, 39 mg, 54% yield; Analytical data: ^1H NMR (600 MHz, CD_2Cl_2) δ 7.44 – 7.39 (m, 1H), 7.28 (td, $J = 7.5, 1.5 \text{ Hz}$, 1H), 7.24 (td, $J = 7.5, 1.4 \text{ Hz}$, 1H), 7.11 (dd, $J = 7.5, 1.4 \text{ Hz}$, 1H), 6.48 (d, $J = 9.6 \text{ Hz}$, 1H), 6.11 (dd, $J = 9.7, 5.1 \text{ Hz}$, 1H), 4.56 (d, $J = 17.2 \text{ Hz}$, 1H), 4.48 (d, $J = 11.9 \text{ Hz}$, 1H), 4.32 (d, $J = 12.0 \text{ Hz}$, 1H), 4.29 (d, $J = 17.2 \text{ Hz}$, 1H), 3.79 (s, 3H), 3.69 (s, 3H), 2.97 (d, $J = 8.3 \text{ Hz}$, 1H), 2.55 (dd, $J = 8.3, 5.1 \text{ Hz}$, 1H). ^{13}C NMR (151 MHz, CD_2Cl_2) δ 196.75, 155.65, 155.08, 131.50, 129.98, 129.46, 128.35, 128.06, 127.81, 127.43, 122.15, 72.60, 69.66, 55.41, 55.36, 31.41, 29.09, 28.84.; IR (ATR): $\tilde{\nu}$ (cm^{-1}) = 3020, 2958, 1746, 1442, 1375, 1252, 1167, 1118, 1064, 951, 780, 741; HRMS (ESI) calcd for $\text{C}_{18}\text{H}_{18}\text{O}_7\text{Na}^+$ [$\text{M}+\text{Na}$] $^+$: 369.0945, Found: 369.0942.

All NMR data for the *endo* product (**3.21ac**) were acquired at 0 °C because the *endo* product is slowly converted to *exo* product at room temperature.

Thermal isomerization from *endo*-benzonorcaradiene (3.21ac**) to *exo*-benzonorcaradiene (**3.15ac**)**

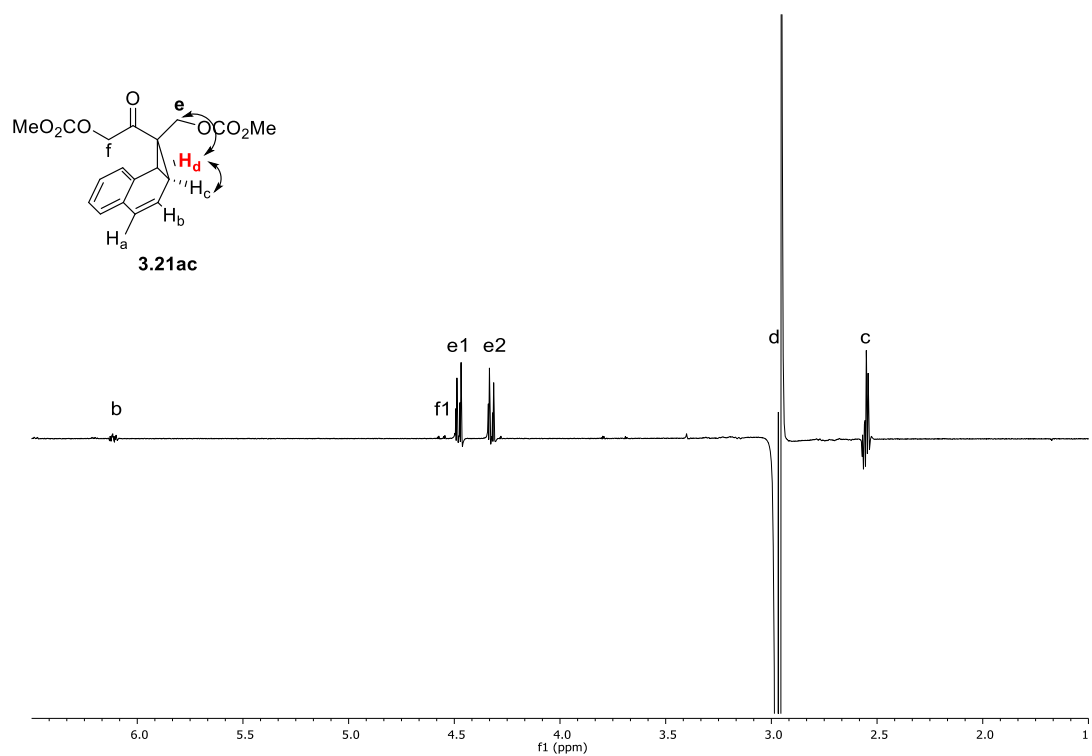
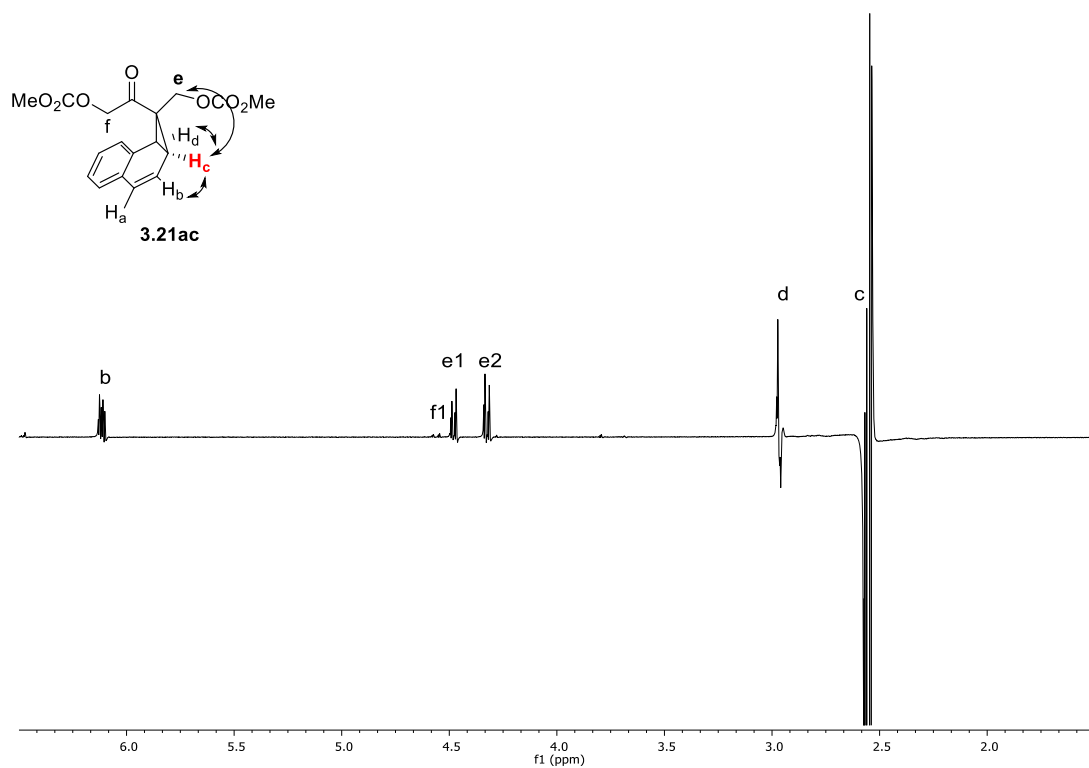


endo-benzonorcaradiene (**3.21ac**) (0.051 mmol, 17.7 mg) was dissolved in freshly distilled 2-butanone (0.56 ml) in a microwave reaction vial under N₂ atmosphere. The reaction mixture was stirred at 100 °C for 30 min. The reaction mixture was cooled to room temperature. The solvent was removed under reduced pressure. The reaction mixture was purified by column chromatography with silica gel (*n*-pentane/ethyl acetate = 5/1 (v/v')) to afford the *exo*-benzonorcaradiene (**3.15ac**) (17.0 mg, 96% yield).

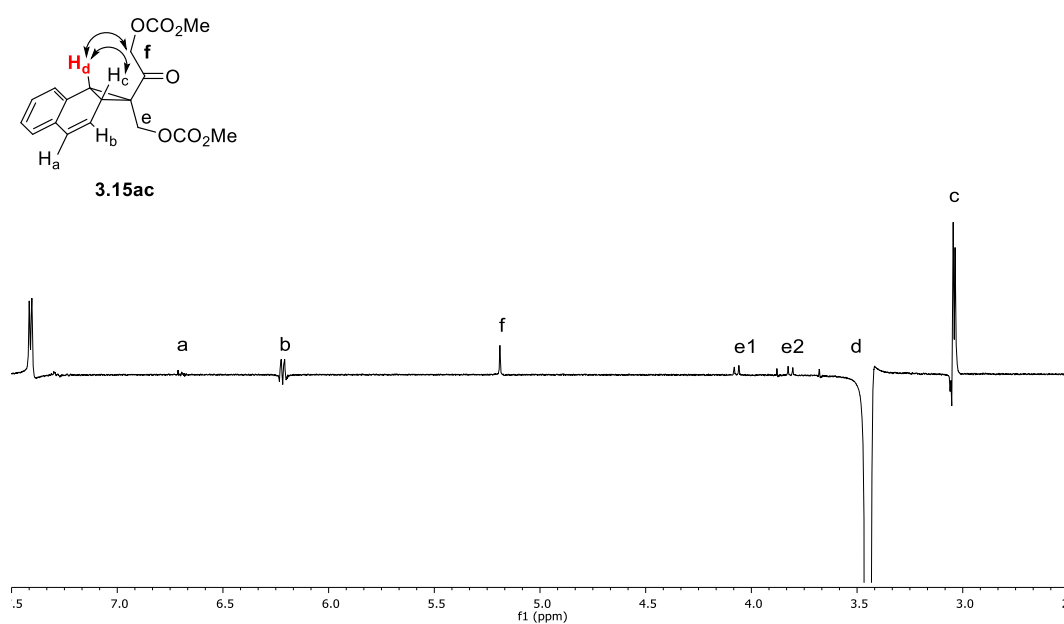
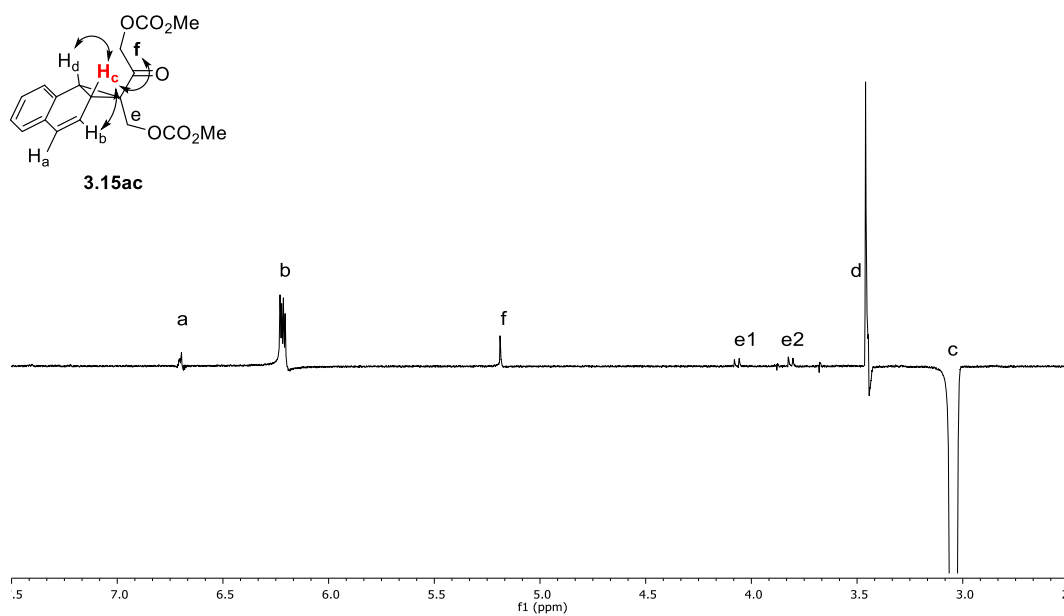
1D NOE experiments on *exo*-benzonorcaradiene (3.15ac**) and *endo*-benzonorcaradiene (**3.21ac**)**

1D NOE experiments were performed with *exo*-benzonorcaradiene (**3.15ac**) and *endo*-benzonorcaradiene (**3.21ac**). Both samples were measured at 0 °C. Deuterated dichloromethane (CD₂Cl₂) and deuterated chloroform (CDCl₃) were used for *endo*-benzonorcaradiene and *exo*-benzonorcaradiene, respectively.

1D NOE results of the *endo* product (3.21ac)

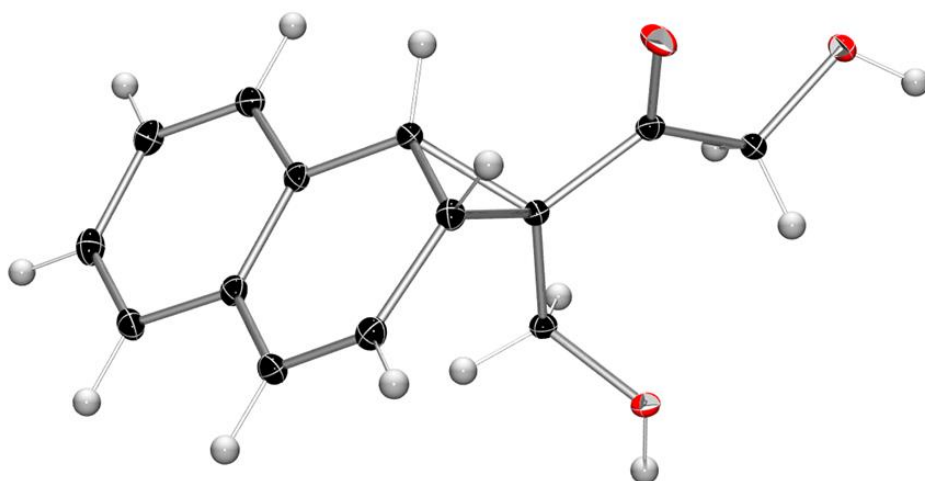


1D NOE results of the exo product (3.15ac)



X-ray Structure of 3.15aa.

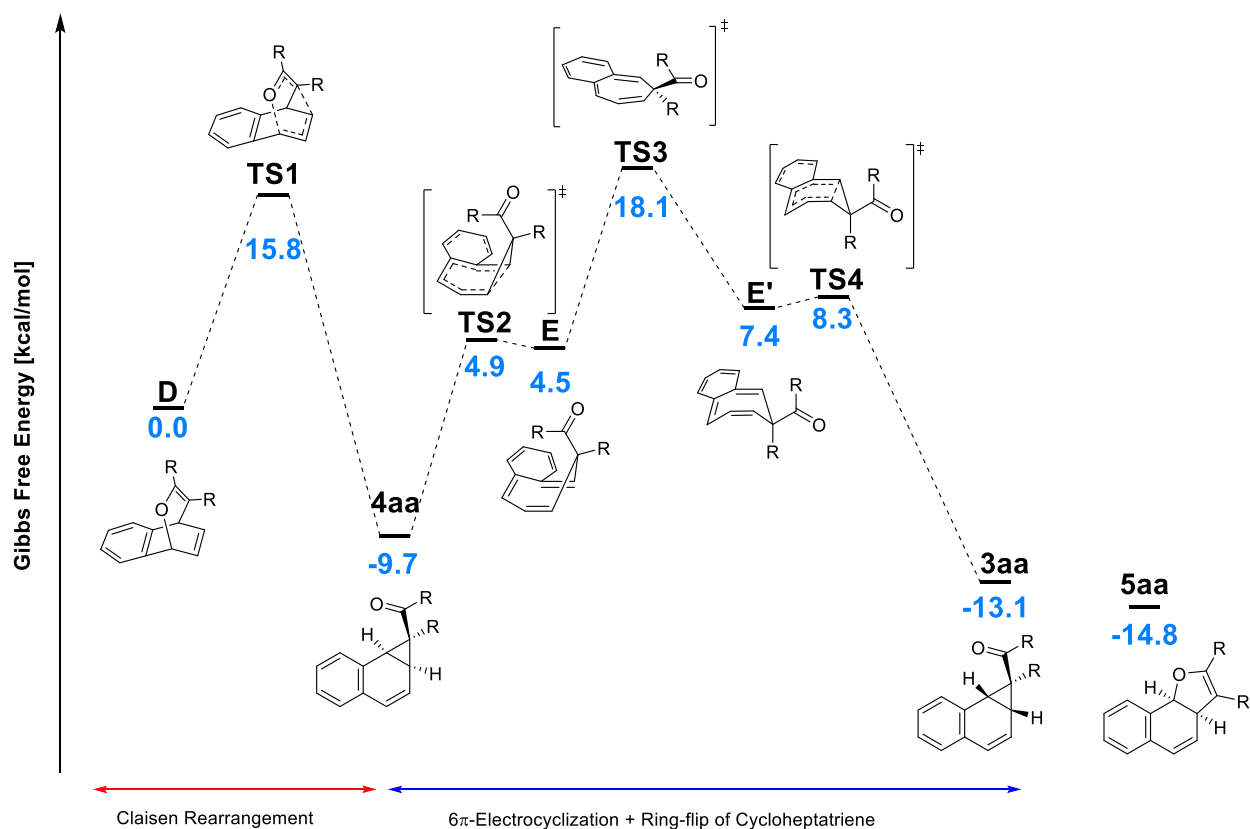
Crystallographic data: CCDC 1947117 contains the supplementary crystallographic data for this paper. These data can be obtained free of charge from The Cambridge Crystallographic Data Centre via www.ccdc.cam.ac.uk/data_request/cif.



Computational Details

GAMESS¹⁰⁷ was used for the quantum chemical calculation. The geometries of all species were optimized with B3LYP¹⁰³/6-31G(d,p)¹⁰⁴. The same method and basis sets are used for computing Gibbs free energy considering thermal and zero-point energy contribution, and scale factor for vibrational frequencies are adapted.¹⁰⁵ All of transition states have only one imaginary vibrational mode and none of minima has an imaginary vibrational mode.

Energy Profile



Summary of Computed Energies of Relevant Species

	B3LYP/6-31G(d,p) Electronic Energy (hartree)	B3LYP/6-31G(d,p) Gibbs Free Energy Correction (298.15 K, scale factor =1) (kcal/mol)	B3LYP/6-31G(d,p) Gibbs Free Energy Correction (373.15 K, scale factor =0.9627) (kcal/mol)	Total Gibbs Free Energy (373.15 K, scale factor = 0.9627) (kcal/mol)	Relative Gibbs Free Energy (373.15K) (kcal/mol)
3.20	-1222.627860	178.125	156.094	-767053.892	0.0
TS1	-1222.601644	177.246	155.484	-767038.051	15.8
3.21ac	-1222.641955	177.353	155.267	-767063.564	-9.7
TS2	-1222.617120	176.205	154.289	-767048.957	4.9
3.22ac	-1222.617415	176.180	154.046	-767049.386	4.5
TS3	-1222.597438	176.937	155.058	-767035.838	18.1
3.22ac'	-1222.609816	174.734	152.178	-767046.485	7.4
TS4	-1222.609669	175.209	152.985	-767045.586	8.3
3.15ac	-1222.652013	179.743	158.145	-767066.997	-13.1
3.23ac	-1222.653823	179.416	157.622	-767068.656	-14.8

8.4 Enantioselective Ruthenium(II)-Catalyzed Alkylative Cycloetherification

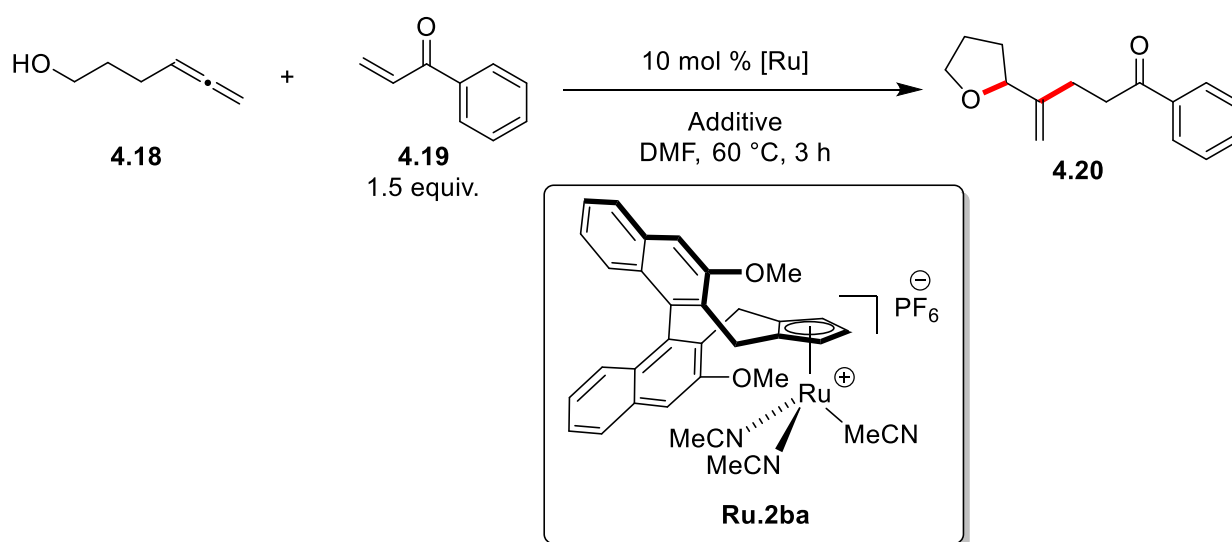
Preparation of hexa-4,5-dien-1-ol (4.18)

Hexa-4,5-dien-1-ol was prepared according to the published procedures.¹³⁵



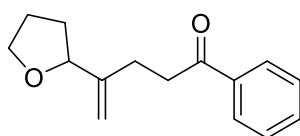
pale yellow oil, 2.10 g, 37% yield; Analytical data: $^1\text{H NMR}$ (400 MHz, CDCl_3) δ 5.13 (p, $J = 6.7$ Hz, 1H), 4.69 (dt, $J = 6.6, 3.3$ Hz, 2H), 3.70 (q, $J = 6.0$ Hz, 2H), 1.27 (br, 1H). $^{13}\text{C NMR}$ (101 MHz, CDCl_3) δ 208.61, 89.54, 75.24, 62.37, 31.96, 24.57. **IR** (ATR): $\tilde{\nu}$ (cm^{-1}) = 3339, 2939, 2867, 1956, 1704, 1438, 1058, 844.

General Procedures for the Ruthenium(II)-Catalyzed Enantioselective Alkylative Cycloetherification



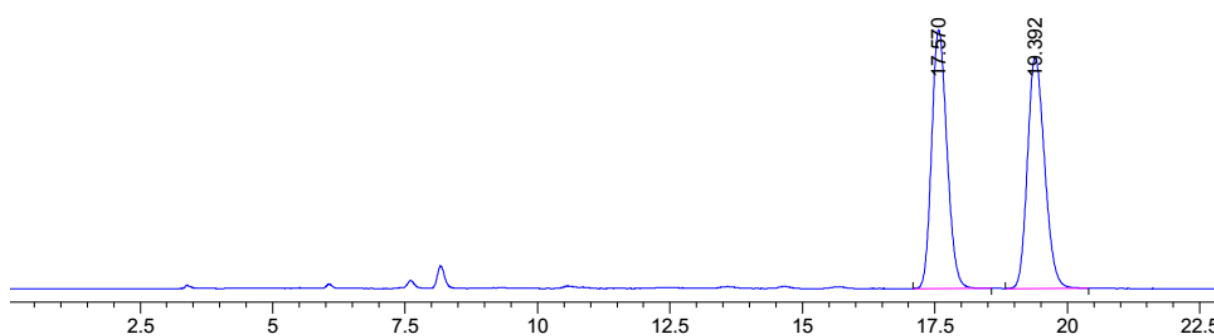
Ru.2ba (10.0 mol %, 1.28 μmol , 0.976 mg), hexa-4,5-dien-1-ol (0.013 mmol, 1.31 mg, 1 equiv.), phenyl vinyl ketone (0.019 mmol, 2.54 mg, 1.5 equiv.) and additive were dissolved in freshly distilled DMF (51 μl , 0.25 M) under an N_2 atmosphere. The reaction vessel was covered by aluminum foil, and the reaction mixture was stirred for 3 h at 60 $^\circ\text{C}$. Then, the reaction mixture was cooled to room

temperature. The reaction mixture was filtered through short silica pad. The reaction mixture was purified by silica gel column chromatography (*n*-pentane/ethyl acetate = 4/1 (v/v')) to afford the desired cyclic ether **4.20**.

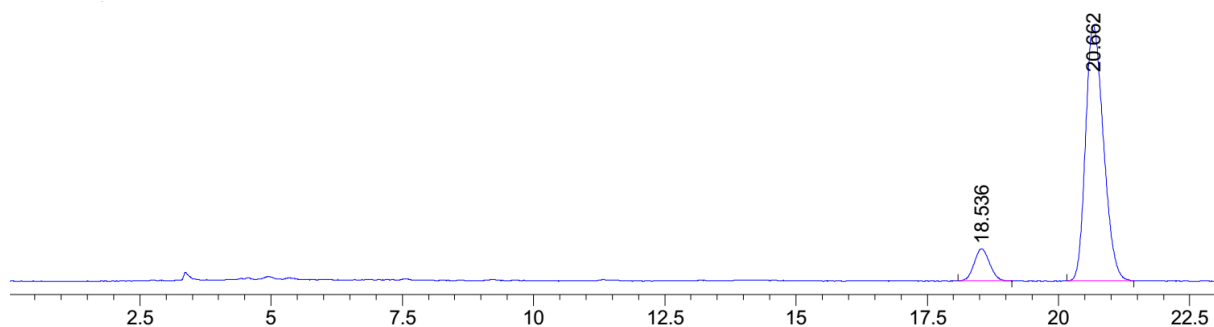


1-phenyl-4-(tetrahydrofuran-2-yl)pent-4-en-1-one (4.20)

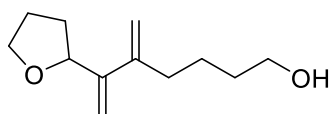
Colorless oil, Analytical data: **¹H NMR** (400 MHz, CDCl₃) δ 8.02 – 7.93 (m, 2H), 7.61 – 7.52 (m, 1H), 7.51 – 7.42 (m, 2H), 5.13 – 5.07 (m, 1H), 4.87 – 4.82 (m, 1H), 4.35 (t, *J* = 7.3 Hz, 1H), 3.94 (dt, *J* = 8.2, 6.7 Hz, 1H), 3.82 (td, *J* = 7.8, 6.3 Hz, 1H), 3.29 – 3.11 (m, 2H), 2.61 – 2.37 (m, 2H), 2.18 – 2.02 (m, 1H), 1.99 – 1.87 (m, 2H), 1.79 – 1.66 (m, 1H). **¹³C NMR** (101 MHz, CDCl₃) δ 199.85, 149.25, 137.08, 133.17, 128.75, 128.20, 109.25, 81.98, 68.57, 37.44, 31.37, 26.19, 26.02. **IR** (ATR): $\tilde{\nu}$ (cm⁻¹) = 2950, 2868, 1686, 1649, 1597, 1448, 1320, 1280, 1204, 1057, 981, 900, 746, 691; **HRMS** (APCI/QTOF) *m/z*: [M + Na]⁺ Calcd for C₁₅H₁₈NaO₂⁺ 253.1199; Found 253.1199. The enantiomeric excess was determined by Daicel Chiralpak ID (25 cm), Hexane/IPA = 95/05, 1.0 mL/min, λ = 254 nm, *t_R* (major) = 20.7 min, *t_R* (minor) = 18.5 min



Peak #	RetTime [min]	Type	Width [min]	Area [mAU*s]	Height [mAU]	Area %
1	17.570	BB	0.3143	3811.32837	189.75511	49.9286
2	19.392	BB	0.3502	3822.22412	170.04115	50.0714



Peak #	RetTime [min]	Type	Width [min]	Area [mAU*s]	Height [mAU]	Area %
1	18.537	BB	0.3208	747.82477	36.52925	9.7398
2	20.664	BB	0.3686	6930.18750	292.31909	90.2602



5-methylene-6-(tetrahydrofuran-2-yl)hept-6-en-1-ol (4.23)

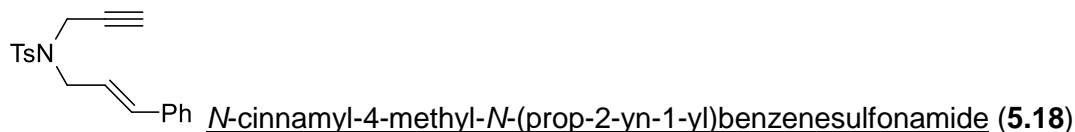
Colorless oil; Analytical data: ^1H NMR (400 MHz, CDCl_3) δ 5.27 (d, J = 1.5 Hz, 1H), 5.13 (s, 1H), 4.99 (d, J = 1.3 Hz, 1H), 4.96 (t, J = 1.3 Hz, 1H), 4.68 – 4.63 (m, 1H), 3.98 (t, J = 6.4 Hz, 1H), 3.86 – 3.81 (m, 1H), 3.65 (t, J = 6.0 Hz, 2H), 2.30 – 2.25 (m, 2H), 2.17 – 2.12 (m, 1H), 1.92 – 1.86 (m, 2H), 1.73 – 1.60 (m, 1H), 1.60 – 1.48 (m, 4H).

8.5 Enantioselective Ru(II)-catalyzed [2+1] Cycloaddition of Ruthenium Vinyl Carbene

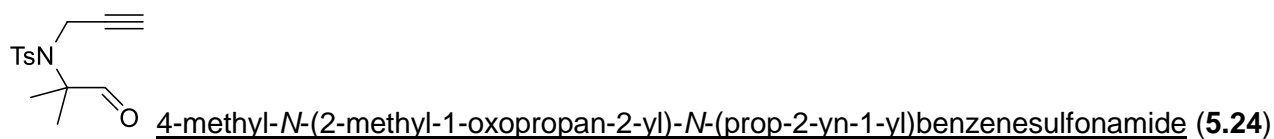
Preparation of Substrates

The following compounds were prepared according to the published procedures.

N-cinnamyl-4-methyl-*N*-(prop-2-yn-1-yl)benzenesulfonamide (**5.18**),¹³⁶ 4-methyl-*N*-(2-methyl-1-oxopropan-2-yl)-*N*-(prop-2-yn-1-yl)benzenesulfonamide (**5.24**).¹²¹

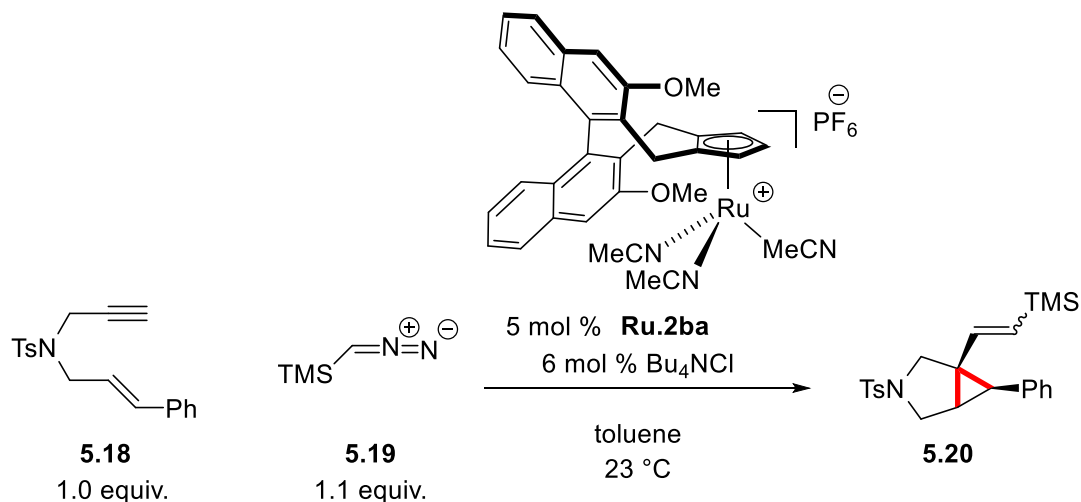


White solid, 357 mg, 75% yield; Analytical data: **¹H NMR** (400 MHz, CDCl₃) δ 7.77 (d, *J* = 8.4 Hz, 2H), 7.41 – 7.18 (m, 7H), 6.57 (dt, *J* = 15.8, 1.4 Hz, 1H), 6.08 (dt, *J* = 15.8, 6.9 Hz, 1H), 4.13 (d, *J* = 2.5 Hz, 2H), 4.00 (dd, *J* = 6.9, 1.3 Hz, 2H), 2.44 (s, 3H), 2.05 (t, *J* = 2.4 Hz, 1H). **¹³C NMR** (101 MHz, CDCl₃) δ 143.74, 136.22, 136.17, 135.04, 129.65, 128.74, 128.20, 127.92, 126.67, 123.02, 76.73, 73.96, 48.71, 36.02, 21.70. **IR** (ATR): $\tilde{\nu}$ (cm⁻¹) = 3288, 3027, 2921, 2858, 1597, 1495, 1447, 1345, 1158, 1094, 968, 897, 814, 754, 735, 692, 658, 568, 542.

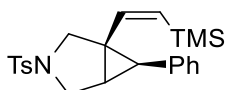


White solid, 1.34 g, 70% yield; Analytical data: **¹H NMR** (400 MHz, CDCl₃) δ 9.65 (s, 1H), 7.81 (d, *J* = 8.4 Hz, 2H), 7.37 – 7.28 (m, 2H), 4.11 (d, *J* = 2.5 Hz, 2H), 2.44 (s, 3H), 2.19 (t, *J* = 2.5 Hz, 1H), 1.49 (s, 6H). **¹³C NMR** (101 MHz, CDCl₃) δ 198.42, 144.28, 136.90, 129.79, 128.26, 79.40, 73.55, 67.34, 34.53, 21.91, 21.70. **IR** (ATR): $\tilde{\nu}$ (cm⁻¹) = 3279, 2988, 2817, 1736, 1597, 1327, 1305, 1167, 1150, 1083, 1050, 881, 814, 730, 663, 583, 544.

General Procedure for the Ruthenium(II)-Catalyzed Enantioselective Ru(II)-catalyzed [2+1] Cycloaddition of Ruthenium Vinyl Carbene for Bicycle[3.1.0]hexanes (5.20)

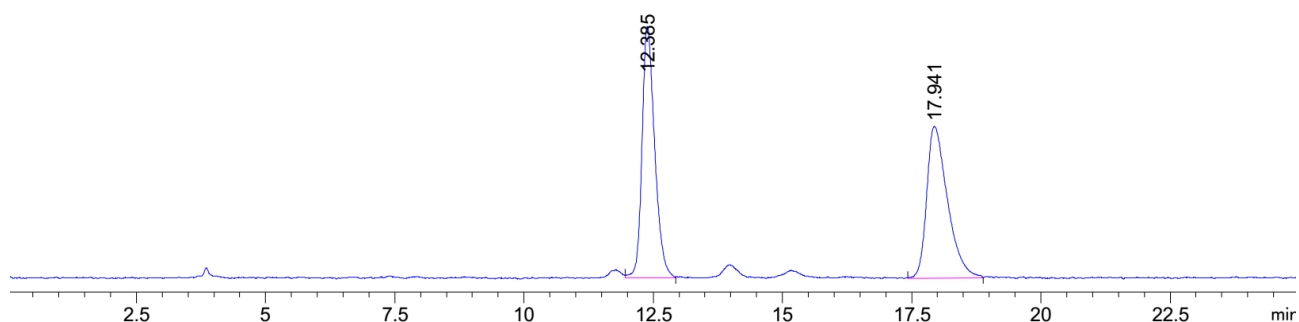


N-cinnamyl-4-methyl-*N*-(prop-2-yn-1-yl)benzenesulfonamide **5.18** (0.024 mmol, 7.75 mg, 1.0 equiv.), **Ru.2ba** (5.00 mol %, 1.19 μmol , 0.907 mg) and tetrabutylammonium chloride (6.00 mol %, 1.43 μmol , 0.397 mg) were dissolved in toluene (80.0 μl , 0.3 M) in a test tube under N_2 atmosphere. A solution of TMS-diazomethane in ether (2 M, 0.026 mmol, 13.1 μl , 1.1 equiv.) was added to the reaction mixture. The reaction mixture was stirred at room temperature for 18 h. The reaction mixture was filtered through silica pad. The filtrate was concentrated under reduced pressure. The crude product was purified by silica gel column chromatography (*n*-pentane/ethyl acetate = 15/1 (v/v)), which delivered the bicyclo[3.1.0]hexane (**5.20**).

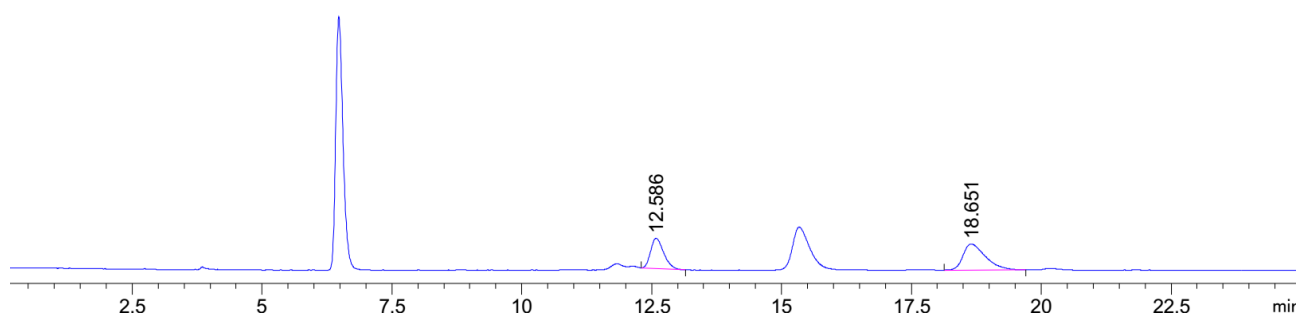


cis-6-phenyl-3-tosyl-1-((*Z*)-2-(trimethylsilyl)vinyl)-3-azabicyclo[3.1.0]hexane ((*Z*)-**5.20**)

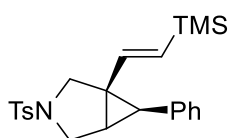
Pale yellow oil, Analytical data: $^1\text{H NMR}$ (400 MHz, CDCl_3) δ 7.73 (d, J = 8.3 Hz, 2H), 7.39 – 7.33 (m, 2H), 7.22 (dd, J = 8.1, 6.5 Hz, 2H), 7.18 – 7.11 (m, 1H), 6.93 (dd, J = 8.3, 1.3 Hz, 2H), 6.00 (d, J = 15.1 Hz, 1H), 5.65 (d, J = 15.2 Hz, 1H), 3.80 (d, J = 9.4 Hz, 1H), 3.73 (d, J = 9.4 Hz, 1H), 3.36 (dd, J = 9.4, 3.9 Hz, 1H), 3.15 (d, J = 9.4 Hz, 1H), 2.46 (s, 3H), 2.17 (d, J = 4.2 Hz, 1H), 1.91 (t, J = 4.0 Hz, 1H), -0.09 (s, 9H). The enantiomeric excess of was determined by Daicel Chiralpak IB (25 cm), Hexane/IPA = 98/02, 1.0 mL/min, λ = 254 nm, t_R (major) = 18.7 min, t_R (minor) = 12.6 min



Peak #	RetTime [min]	Type	Width [min]	Area [mAU*s]	Height [mAU]	Area %
1	12.385	VV	0.2525	2466.82324	144.95869	50.0666
2	17.941	VV	0.3892	2460.25830	87.71539	49.9334



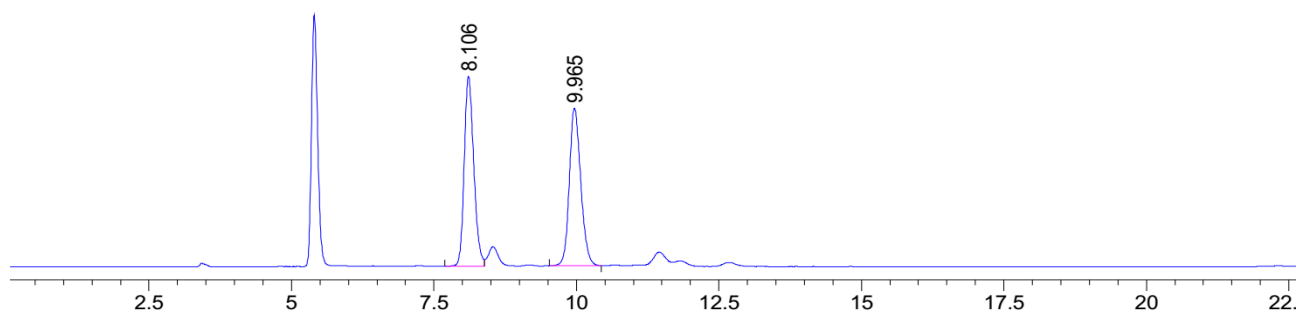
#	[min]		[min]	[mAU*s]	[mAU]	%
1	12.586	BB	0.2663	1487.83936	84.96594	40.3606
2	18.651	BB	0.4362	2198.52515	73.25211	59.6394



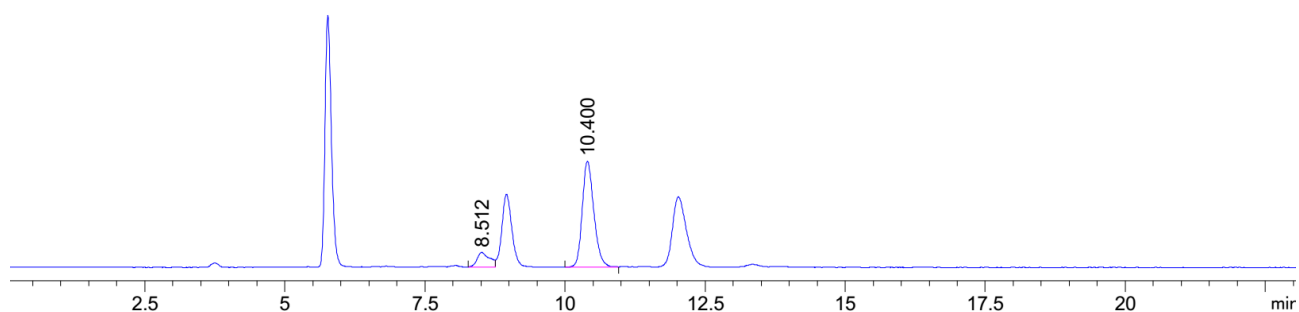
cis-6-phenyl-3-tosyl-1-((E)-2-(trimethylsilyl)vinyl)-3-azabicyclo[3.1.0]hexane ((E)-5.20)

Pale yellow oil, Analytical data: $^1\text{H NMR}$ (400 MHz, CDCl_3) δ 7.75 (d, J = 8.3 Hz, 2H), 7.42 – 7.32 (m, 2H), 7.24 (d, J = 7.6 Hz, 2H), 7.20 – 7.14 (m, 1H), 7.11 – 7.04 (m, 2H), 5.54 (d, J = 19.2 Hz, 1H), 5.44 (d, J = 19.2 Hz, 1H), 3.74 (dd, J = 9.2, 2.8 Hz, 2H), 3.32 (d, J = 9.3 Hz, 1H), 3.24 (dd, J = 9.2,

3.9 Hz, 1H), 2.49 (d, $J = 4.6$ Hz, 1H), 2.45 (s, 3H), 2.08 (t, $J = 4.2$ Hz, 1H), -0.14 (s, 9H). **^{13}C NMR** (101 MHz, CDCl_3) δ 143.74, 142.50, 136.45, 133.63, 130.17, 129.88, 129.09, 128.19, 127.77, 126.51, 51.69, 50.20, 38.20, 32.10, 28.79, 21.71, -1.30. **IR** (ATR): $\tilde{\nu}(\text{cm}^{-1}) = 3062, 3031, 2953, 2855, 1601, 1347, 1247, 1162, 1101, 1027, 1007, 987, 910, 864, 836, 815, 797, 729, 708, 698, 665, 621, 586, 549$; **HRMS** (ESI/QTOF) m/z : $[\text{M} + \text{Na}]^+$ Calcd for $\text{C}_{23}\text{H}_{29}\text{NO}_2\text{SSiNa}^+$ 434.1581; Found 434.1585. The enantiomeric excess of was determined by Daicel Chiralpak IB (25 cm), Hexane/IPA = 95/05, 1.0 mL/min, $\lambda = 254$ nm, t_R (major) = 10.4 min, t_R (minor) = 8.5 min

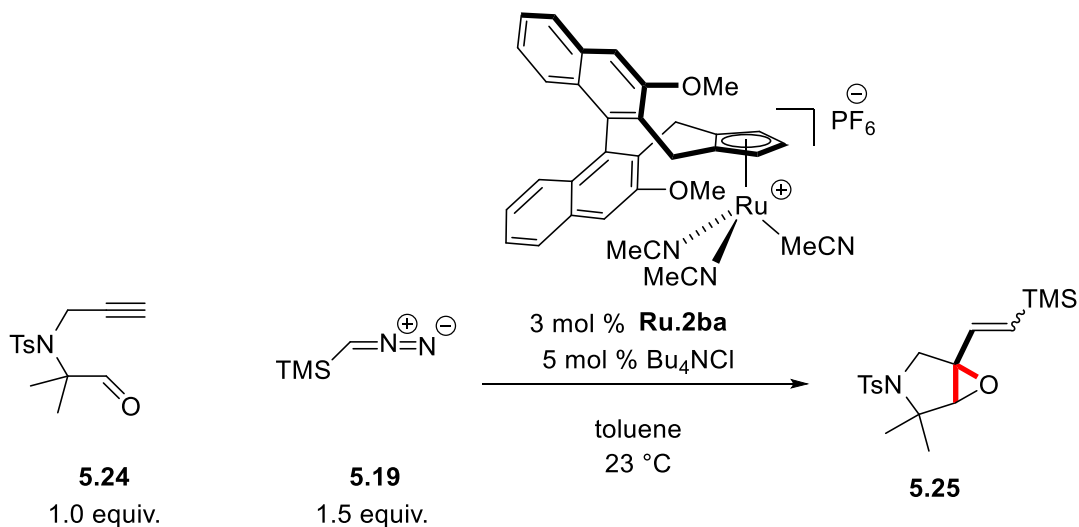


Peak #	RetTime [min]	Type	Width [min]	Area [mAU*s]	Height [mAU]	Area %
1	8.106	BV	0.1773	4350.51318	375.16248	49.8650
2	9.965	BB	0.2155	4374.07324	312.09882	50.1350

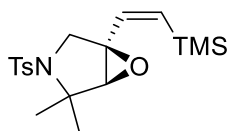


Peak #	RetTime [min]	Type	Width [min]	Area [mAU*s]	Height [mAU]	Area %
1	8.512	BV	0.2125	438.31512	28.32762	12.8429
2	10.400	BB	0.2219	2974.57837	206.65404	87.1571

General Procedure for the Ruthenium(II)-Catalyzed Enantioselective Ru(II)-catalyzed [2+1] Cycloaddition of Ruthenium Vinyl Carbene for Epoxypyrrolidenes (5.25)



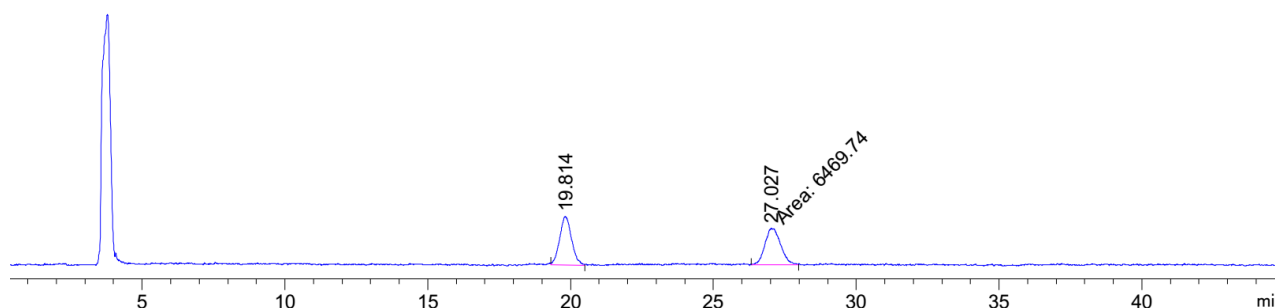
4-methyl-*N*-(2-methyl-1-oxopropan-2-yl)-*N*-(prop-2-yn-1-yl)benzenesulfonamide **5.24** (0.025 mmol, 6.98 mg, 1.0 equiv.), **Ru.2ba** (3.00 mol %, 0.750 μmol, 0.571 mg) and tetrabutylammonium chloride (5.00 mol %, 1.25 μmol, 0.347 mg) were dissolved in toluene (179 μl, 0.3 M) in a test tube under N₂ atmosphere. A solution of TMS-diazomethane in ether (2 M, 0.038 mmol, 19.0 μl, 1.5 equiv.) was added to the reaction mixture. The reaction mixture was stirred at room temperature for 1.5 h. The reaction mixture was filtered through silica pad. The filtrate was concentrated under reduced pressure. The crude product was purified by silica gel column chromatography (*n*-pentane/ethyl acetate = 15/1 (v/v')), which delivered the epoxypyrrolidine **5.25**.



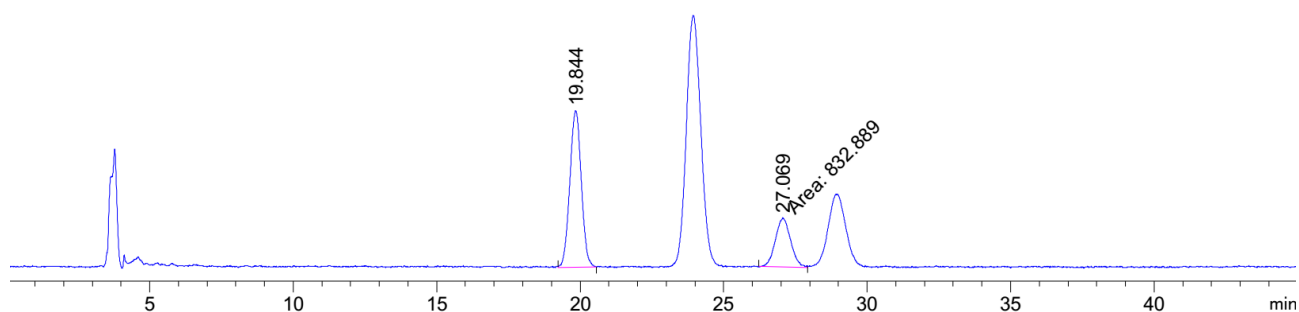
(1*R*,5*S*)-4,4-dimethyl-3-tosyl-1-((*Z*)-2-(trimethylsilyl)vinyl)-6-oxa-3-azabicyclo[3.1.0]hexane ((*Z*)-**5.25**)

Colorless oil, Analytical data: : ¹H NMR (400 MHz, CDCl₃) δ 7.69 (d, *J* = 8.1 Hz, 2H), 7.25 (d, *J* = 4.2 Hz, 2H), 6.41 (d, *J* = 14.9 Hz, 1H), 5.82 (d, *J* = 14.9 Hz, 1H), 4.92 (s, 1H), 3.66 (d, *J* = 11.6 Hz, 1H), 3.58 (d, *J* = 11.6 Hz, 1H), 3.04 (s, 1H), 2.40 (s, 3H), 1.47 (s, 3H), 0.09 (s, 9H). The enantiomeric

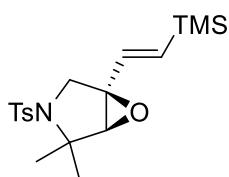
excess of was determined by Daicel Chiralpak IC (25 cm), Hexane/IPA = 95/05, 1.0 mL/min, λ = 254 nm, t_R (major) = 19.8 min, t_R (minor) = 27.0 min



Peak #	RetTime [min]	Type	Width [min]	Area [mAU*s]	Height [mAU]	Area %
1	19.814	VV	0.3645	6513.07861	224.46626	50.1669
2	27.027	MM	0.6363	6469.74219	169.46347	49.8331



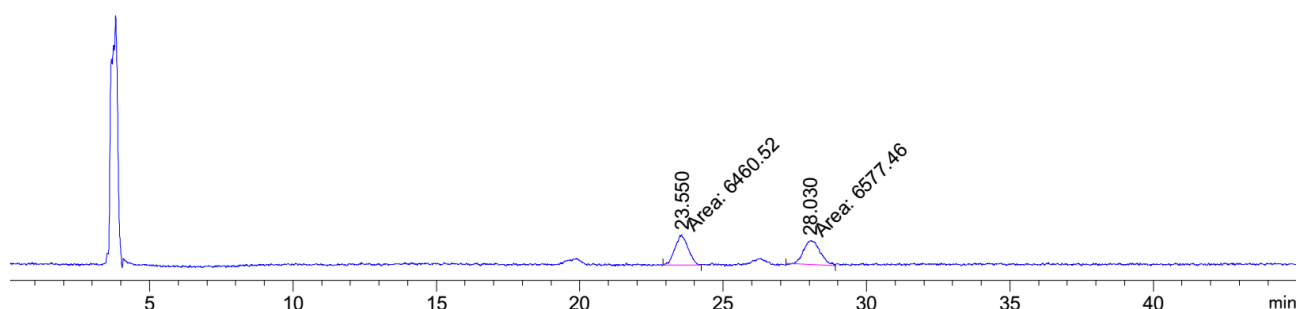
Peak #	RetTime [min]	Type	Width [min]	Area [mAU*s]	Height [mAU]	Area %
1	19.844	VB	0.4269	1990.71924	71.92060	70.5027
2	27.069	MM	0.6172	832.88910	22.49172	29.4973



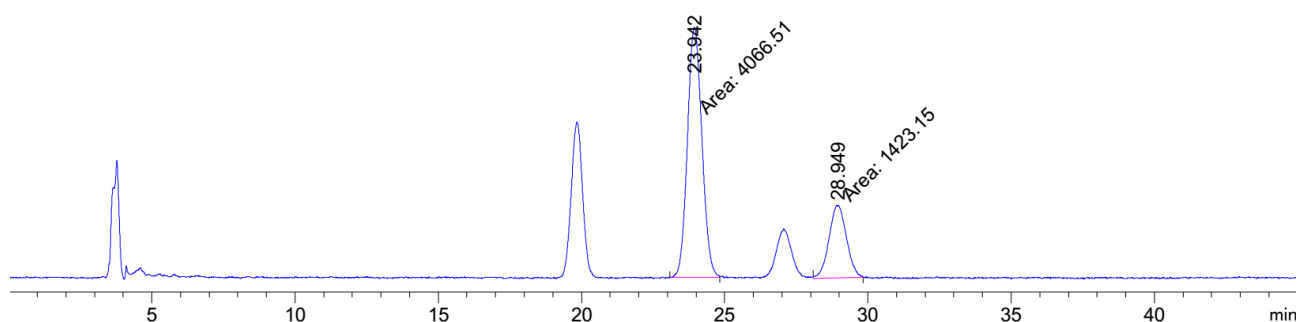
E:Z = 4.4:1

(1*R*,5*S*)-4,4-dimethyl-3-tosyl-1-((*E*)-2-(trimethylsilyl)vinyl)-6-oxa-3-azabicyclo[3.1.0]hexane ((*E*)-**5.25**)

Colorless oil, Analytical data: ¹H NMR (400 MHz, CDCl₃) δ 7.71 (d, J = 8.3 Hz, 2H), 7.26 (d, J = 8.0 Hz, 4H), 6.11 (d, J = 19.2 Hz, 1H), 5.88 (d, J = 19.2 Hz, 1H), 3.85 (d, J = 11.4 Hz, 1H), 3.59 (d, J = 11.3 Hz, 1H), 3.25 (s, 1H), 2.40 (s, 3H), 1.51 (s, 3H), 1.47 (s, 3H), 0.08 (s, 9H). The enantiomeric excess of was determined by Daicel Chiralpak IC (25 cm), Hexane/IPA = 95/05, 1.0 mL/min, λ = 254 nm, t_R (major) = 23.9 min, t_R (minor) = 28.9 min

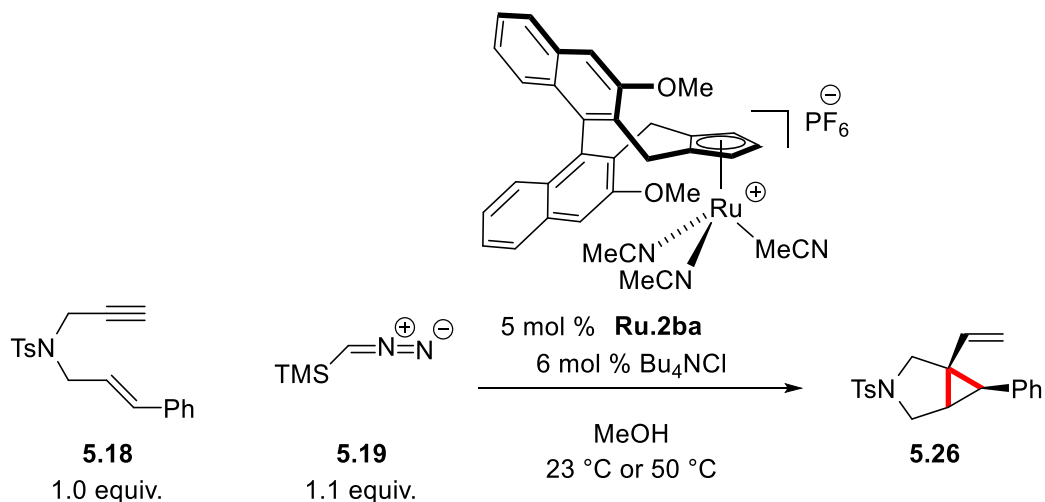


Peak #	RetTime [min]	Type	Width [min]	Area [mAU*s]	Height [mAU]	Area %
1	23.543	BB	0.4617	2588.43359	79.53472	49.7382
2	28.059	VV	0.5143	2615.68433	66.59066	50.2618



Peak #	RetTime [min]	Type	Width [min]	Area [mAU*s]	Height [mAU]	Area %
1	23.942	MM	0.5869	4066.51025	115.48965	74.0758
2	28.949	MM	0.7094	1423.15259	33.43679	25.9242

General Procedure for the Ruthenium(II)-Catalyzed Enantioselective Ru(II)-catalyzed [2+1] Cycloaddition of Ruthenium Vinyl Carbene for Terminal Alkenyl Bicyclo[3.1.0]hexanes (5.26)



N-cinnamyl-4-methyl-*N*-(prop-2-yn-1-yl)benzenesulfonamide **5.18** (0.025 mmol, 8.13 mg, 1.0 equiv.), **Ru.2ba** (5.00 mol %, 1.25 μmol, 0.951 mg) and tetrabutylammonium chloride (6.00 mol %, 1.50 μmol, 0.417 mg) were dissolved in methanol (83.2 μl, 0.3 M) or methanol/THF mixture (50/50 mixture (v/v'), 0.3 M) in a test tube under N₂ atmosphere. A solution of TMS-diazomethane in ether (2 M, 0.027 mmol, 13.7 μl, 1.1 equiv.) was added to the reaction mixture. The reaction mixture was stirred at room temperature or 50 °C for 18 h. The reaction mixture was filtered through silica pad. The filtrate was concentrated under reduced pressure. The crude product was purified by silica gel column chromatography (*n*-pentane/ethyl acetate = 10/1 (v/v')), which delivered the epoxypyrrolidine **5.26**.



Colorless oil, Analytical data: ¹H NMR (400 MHz, CDCl₃) 7.74 (d, *J* = 8.3 Hz, 1H), 7.36 (d, *J* = 8.0 Hz, 1H), 7.26 (s, 0H), 7.21 – 7.16 (m, 1H), 7.12 – 7.06 (m, 1H), 5.31 (dd, *J* = 17.9, 10.5 Hz, 1H), 4.94 (d, *J* = 0.9 Hz, 1H), 4.91 (dd, *J* = 5.5, 1.1 Hz, 0H), 3.75 (dd, *J* = 9.2, 4.8 Hz, 1H), 3.31 (d, *J* = 9.3 Hz, 1H), 3.24 (dd, *J* = 9.2, 3.9 Hz, 1H), 2.48 (d, *J* = 4.8 Hz, 1H), 2.45 (s, 2H), 2.06 (t, *J* = 4.3 Hz, 1H).

Curriculum Vitae

Sung Hwan PARK

Born September 13th, 1988 in Seoul, Republic of Korea

Education

2015.11 - Present	PhD in Organic Chemistry École polytechnique fédérale de Lausanne, Advisor: Prof. Nicolai Cramer
2009.9 - 2011.8	Master of Science in Chemistry Seoul National University, Advisor: Prof. Chulbom Lee
2006.3 - 2009.8	Bachelor of Science in Chemistry Seoul National University, summa cum laude
2004.3 - 2006.2	Gyeonggi Science High School

Fellowships and Awards

2009	Best Senior Paper Award, Outstanding Undergraduate Research, Seoul National University
2009	Dean's List, College of Natural Sciences, Seoul National University
2009	Scholarship for Undergraduate Students (Spring Semester), Kwanak Corporation
2008	National Scholarship for Science and Engineering (Fall Semester), Korea Student Aid Foundation
2007 - 2008	Merit-based Scholarship, Seoul National University
2006 - 2007	National Scholarship for Science and Engineering, Korea Student Aid Foundation
2006	Merit-based Scholarship (Spring Semester), Seoul National University
2005	Silver Prizes, Korean Chemistry Olympiad for High School Students, The Korean Chemical Society
2004	Gold Prizes, Korean Chemistry Olympiad for High School Students, The Korean Chemical Society

Research Experiences

2015.11 - Present	Graduate Research, École polytechnique fédérale de Lausanne Advisor: Prof. Nicolai Cramer Thesis: Catalytic Enantioselective Transformations with Chiral Cyclopentadienyl Ruthenium(II) Complexes
-------------------	--

2014.10 – 2015.9	Research Institute for Basic Sciences (Seoul National University) Job position: Researcher Advisor: Prof. Chulbom Lee Project: Quantum Calculation for an Allylic Sulfinic Acid Rearrangement (Retro-Ene reaction)
2011.9 - 2014.8	Korea Institute of Industrial Technology Job position: Researcher Advisor: Ph. D. Hyun Aee Chun Project: Development of Low-CTE (coefficient of thermal expansion) Epoxy Composite
2009.9 - 2011.8	Graduate Research, Seoul National University Advisor: Prof. Chulbom Lee Thesis: Ruthenium-Catalyzed Three-Component Coupling via Hydrative Conjugate Addition of Alkynes to Alkenes: One-Pot Synthesis of 1,4-Dicarbonyl Compounds

Publication

Sung Hwan Park, Shou-Guo Wang, Nicolai Cramer* "Enantioselective Ruthenium(II)-Catalyzed Access to Benzonorcaradienes by Coupling of Oxabenzonorbornadienes and Alkynes" *ACS Catal.* **2019**, 9, 10226-10231.

Shou-Guo Wang, Sung Hwan Park, Nicolai Cramer* "A Readily Accessible Class of Chiral Cp Ligands and their Application in Ru^{II}-Catalyzed Enantioselective Syntheses of Dihydrobenzoindoles." *Angew. Chem. Int. Ed.* **2018**, 57, 5459-5462.

Yiyun Chen, Sung Hwan Park, Chung Whan Lee and Chulbom Lee* "Ruthenium-Catalyzed Three-Component Coupling via Hydrative Conjugate Addition of Alkynes to Alkenes: One-Pot Synthesis of 1,4-Dicarbonyl Compounds" *Chem.-Asian J.* **2011**, 6, 2000-2004.

Patents

Granted Patent

Domestic Patent

Hyun Aee Chun, Sang Yong Tak, Su Jin Park, Yun Ju Kim, Sung Hwan Park, "Epoxy Compound Having Alkoxyisilyl Group, Preparing Method Thereof, Composition comprising the Same and Cured Product and Use Thereof" Korea Patent 10-1252063, filed August 24, 2012, Issued April 2, 2013.

Hyun Aee Chun, Sang Yong Tak, Su Jin Park, Yun Ju Kim, Sung Hwan Park, Sook Yeon Park "Isocyanurate Epoxy Compound Having Alkoxyisilyl Group, Preparing method thereof, Composition comprising the Same

and Crude Product and Use Thereof" Korea Patent 10-1456025, filed November 1, 2012. Issued October 23, 2014.

Hyun Aee Chun, Su Jin Park, Sook Yeon Park, Yun Ju Kim, Sang Yong Tak, Sung Hwan Park, Kyung Nam Kang" Composition and Cured Product Comprising Epoxy Compound Having Alkoxysilyl Group and Inorganic Particle, Use Thereof and Preparing Method of Epoxy Compound Having Alkoxysilyl Group" Korea Patent 10-1520764, filed February 1, 2013. , Issued May 11, 2015.

Hyun Aee Chun, Yun Ju Kim, Sang Yong Tak, Su Jin Park, Sung Hwan Park "Novolac-based Epoxy Compound, Preparing Method Thereof, Composition, Cured Product thereof, And Use Thereof" Korea Patent 10-1863111, filed July 4, 2013. Issued May 25, 2018.

Hyun Aee Chun, Yun Ju Kim, Su Jin Park, Sang Yong Tak, Sung Hwan Park, Kyung Nam Kang, Sook Yeon Park "Epoxy Compound Having Alkoxysilyl Group, Preparing Method Thereof, Composition Comprising the Same and Cured Product and Use Thereof" Korea Patent 10-1596880, filed September 17, 2013, Issued February 17, 2016.

Hyun Aee Chun, Sung Hwan Park, Yun Ju Kim, Su Jin Park, Sook Yeon Park, Sang Yong Tak "Epoxy Compound Having Alkoxysilyl Group, Preparing Method Thereof, Composition Comprising the Same and Cured Product and Use Thereof" Korea Patent 10-1655857, filed February 25, 2014, Issued September 2, 2016.

Hyun Aee Chun, Su Jin Park, Sang Yong Tak, Yun Ju Kim, Sook Yeon Park, Sung Hwan Park "Epoxy Compound Having Alkoxysilyl Group, Composition, Cured Product Thereof, Use Thereof And Preparing Method of Epoxy Compound Having Alkoxysilyl Group" Korea Patent 10-1898526, filed April 2, 2013, Issued September 7, 2018.

Hyun Aee Chun, Sung Hwan Park, Yun Ju Kim, Su Jin Park, Sook Yeon Park, Sang Yong Tak "Alkoxysilyl Compound Having at Least Two Alkoxysilyl Groups, Composition, Cured Product Thereof, Use Thereof and Preparing Method of Alkoxysilyl Compound Having at Least Two Alkoxysilyl Groups" Korea Patent 10-1644531, filed June 10, 2014, Issued July 27, 2016.

Hyun Aee Chun, Yun Ju Kim, Su Jin Park, Sook Yeon Park, Sung Hwan Park, Sang Yong Tak "Epoxy Compound Having Alkoxysilyl Group, Composition, Cured Product Thereof, Use Thereof And Preparing Method Of Epoxy Compound Having Alkoxysilyl Group" Korea Patent 10-1992845, filed March 14, 2013, Issued June 19, 2019.

International Patent

Hyun Aee Chun, Sang Yong Tak, Su Jin Park, Yun Ju Kim, Sung Hwan Park, "Epoxy Compound Having Alkoxysilyl Group, Method for Preparing Same, Composition and Cured Material Comprising Same, and Usage Thereof" PCT/KR2012/006832, filed August 27, 2012, EU 2767535, JP 5852243.

Hyun Aee Chun, Sang Yong Tak, Su Jin Park, Yun Ju Kim, Sung Hwan Park, Sook Yeon Park, "Isocyanurate Epoxy Compound Having Alkoxysilyl Group, Method of Preparing Same, Composition Including Same, Cured Product of the Composition, and Use of the Composition" PCT/KR2012/009130, filed November 1, 2012. EU 2774929, US 9534075.

Hyun Aee Chun, Yun Ju Kim, Su Jin Park, Sook Yeon Park, Sung Hwan Park, Sang Yong Tak, "Epoxy Compound Having Alkoxy Silyl Group, Composition Comprising Same, Cured Product, Use Thereof and Method for Preparing Epoxy Compound Having Alkoxy Silyl Group" PCT/KR2013/002062, filed March 14, 2013, US 9902803.

Hyun Aee Chun, Yun Ju Kim, Sang Yong Tak, Su Jin Park, Sung Hwan Park, "Novolac-based Epoxy Compound, Production Method for Same, Composition and Cured Article Comprising Same, and Use for Same" PCT/KR2013/006005, filed July 5, 2013, EU 2871182, US 9670309.

Hyun Aee Chun, Yun Ju Kim, Su Jin Park, Sang Yong Tak, Sung Hwan Park, Kyung Nam Kang, Sook Yeon Park "Epoxy Compound Having Alkoxysilyl Group, Method for Preparing Same, Composition Comprising Same, Cured Product Made Therefrom, and Use Thereof" PCT/KR2013/008439, filed September 17, 2013, EU 2933257, US 9725590, JP 6173464.

Hyun Aee Chun, Sung Hwan Park, Yun Ju Kim, Su Jin Park, Sook Yeon Park, Sang Yong Tak "Epoxy Compound Having Alkoxysilyl Group, Method for Manufacturing Same, Composition and Cured Product Including Same, and Use Thereof" PCT/KR2014/001528, filed February 25, 2014, JP 6153631.

Pending Patent

International Patent

Hyun Aee Chun, Su Jin Park, Sook Yeon Park, Yun Ju Kim, Sang Yong Tak, Sung Hwan Park, Kyung Nam Kang, "Composition and Cured Article Comprising Inorganic Particles and Epoxy Compound Having Alkoxysilyl Group, Use for Same, and Production Method for Epoxy Compound Having Alkoxysilyl Group" PCT/KR2013/001211, filed February 15, 2013. Patent Pending.

Hyun Aee Chun, Su Jin Park, Sang Yong Tak, Yun Ju Kim, Sook Yeon Park, Sung Hwan Park "Epoxy Compound Having Alkoxysilyl Group, Composition and Hardened Material Comprising Same, Use For Same, and Production Method for Epoxy Compound Having Alkoxysilyl Group" PCT/KR2013/002730, filed April 2, 2013. Patent Pending.

Others

2009	Certificate of the KCS-approved Bachelor's Degree in Chemistry and Related Fields, The Korean Chemical Society
------	--

Chapter 9 Appendix

9.2 Optimized Geometry

Allyl vinyl ether (**3.20ac**)

C	6.0	-2.4901476069	-1.9961422854	-0.1453761804
C	6.0	-1.3704001544	-2.6934888220	0.5890125912
C	6.0	-2.0952425638	-1.2219641996	-1.2475777115
C	6.0	-0.6023791816	-1.2103007028	-1.5332841531
C	6.0	-0.4103378433	-3.3502035736	-0.3736771147
C	6.0	-0.0280437174	-2.6152005580	-1.4219443797
C	6.0	-3.8326909857	-2.0685777359	0.2192224194
C	6.0	-4.7901837767	-1.3680023619	-0.5214339159
C	6.0	-4.3957454076	-0.5869073794	-1.6082842804
C	6.0	-3.0463714142	-0.5063040964	-1.9699970635
O	8.0	-0.6339167090	-1.7195757179	1.4184496122
C	6.0	0.1057781324	-0.3623917517	-0.4622445793
C	6.0	0.0320964987	-0.6684399836	0.8524644715
C	6.0	0.7229106964	0.1117622013	1.9424838383
C	6.0	0.9547186186	0.7634372998	-0.9604423207
O	8.0	2.1461985865	-0.1745108238	1.8760025799
C	6.0	2.9763323257	0.3519630313	2.7926205739
O	8.0	4.1663014766	0.1557973981	2.7783714746
O	8.0	2.3197392401	1.1100265004	3.6994768361
C	6.0	3.1621785053	1.7006851765	4.7049472135
O	8.0	0.0864900116	1.6856077189	-1.6885086737
C	6.0	0.6163044501	2.7472062107	-2.3149512420
O	8.0	-0.0460931684	3.5196958961	-2.9640265563
O	8.0	1.9527619921	2.8374060279	-2.1237016505
C	6.0	2.5753991907	3.9600765579	-2.7714150147
H	1.0	-1.7537664961	-3.3908690104	1.3354776142
H	1.0	-0.4118799395	-0.7717045798	-2.5152411452
H	1.0	-0.0090257205	-4.3350014224	-0.1561575534
H	1.0	0.7226470559	-2.9511370672	-2.1323400789
H	1.0	-4.1325840062	-2.6704059504	1.0738955966
H	1.0	-5.8395213096	-1.4305041972	-0.2480668038
H	1.0	-5.1391103570	-0.0392375749	-2.1807844321
H	1.0	-2.7385812662	0.1127684587	-2.8082830071
H	1.0	0.3261564224	-0.2033275373	2.9087514338
H	1.0	0.5664295686	1.1876689851	1.8336385153
H	1.0	1.7185204415	0.3954542959	-1.6553713464
H	1.0	1.4729967122	1.3014679552	-0.1668305570
H	1.0	2.4906080348	2.2643444855	5.3527312094
H	1.0	3.6829296639	0.9251336542	5.2709872460
H	1.0	3.8992399444	2.3633112768	4.2453647508
H	1.0	3.6390789134	3.8711579164	-2.5503051124
H	1.0	2.4010481816	3.9254999731	-3.8492838155
H	1.0	2.1777842671	4.8983490848	-2.3771181726

Transition state 1 (TS1)

C	6.0	-2.5773601175	-2.2756809836	-0.2569420986
C	6.0	-1.4458941877	-2.8894822252	0.4469068337
C	6.0	-2.2714977302	-1.2891752436	-1.2108527938
C	6.0	-0.8192099671	-0.9560438215	-1.4167668439
C	6.0	-0.2153036676	-3.0556144406	-0.2213437126
C	6.0	0.1143788740	-2.1031618937	-1.1577504186
C	6.0	-3.9073515662	-2.6234343919	-0.0074318326
C	6.0	-4.9343439662	-2.0004074378	-0.7193851804
C	6.0	-4.6303903775	-1.0246501134	-1.6696680147
C	6.0	-3.2993255130	-0.6688518215	-1.9149760248
O	8.0	-1.0791652024	-1.2396170437	1.5280286213
C	6.0	-0.0878381744	-0.1453070157	-0.3375638179
C	6.0	-0.2389497595	-0.4019601157	1.0261027943
C	6.0	0.6574880261	0.2757750785	2.0565511068
C	6.0	0.9179863360	0.8296467809	-0.8661747329
O	8.0	2.0365950389	-0.1202876588	1.8222997506
C	6.0	3.0103132401	0.3195586340	2.6379388934
O	8.0	4.1683521458	0.0156816572	2.4876837420
O	8.0	2.5341586891	1.1259152092	3.6117905029
C	6.0	3.5373016540	1.6300573375	4.5115949861
O	8.0	0.1728010855	1.8297613146	-1.6331229652
C	6.0	0.8248040349	2.8188370569	-2.2610643255
O	8.0	0.2609109855	3.6496503393	-2.9311490621
O	8.0	2.1602394108	2.7668014133	-2.0481907045
C	6.0	2.9088094546	3.8090460440	-2.6970112927
H	1.0	-1.6798740718	-3.5364043767	1.2869740874
H	1.0	-0.6643458770	-0.4826930745	-2.3871887504
H	1.0	0.5222674250	-3.7595692520	0.1497563892
H	1.0	1.0887097336	-2.0898183914	-1.6353008381
H	1.0	-4.1363586752	-3.3798045108	0.7388610737
H	1.0	-5.9683371031	-2.2721431540	-0.5282425723
H	1.0	-5.4285365099	-0.5340837589	-2.2194191198
H	1.0	-3.0652505558	0.0997372110	-2.6469156158
H	1.0	0.3383919222	-0.0559608870	3.0455132933
H	1.0	0.5795395981	1.3668151730	2.0070798844
H	1.0	1.6461510953	0.3646572896	-1.5399389164
H	1.0	1.4822285088	1.3264057905	-0.0786314433
H	1.0	3.0001040093	2.2513963844	5.2280417329
H	1.0	4.0441087831	0.8059060599	5.0186928893
H	1.0	4.2764784735	2.2213694310	3.9662879519
H	1.0	3.9516084346	3.6213513375	-2.4409686652
H	1.0	2.7643558109	3.7680087527	-3.7792254326
H	1.0	2.5933486550	4.7899709397	-2.3337763591

endo-benzonorcaradiene (**3.21ac**)

C	6.0	1.4328447747	0.5671342591	-0.5763684977
C	6.0	0.1880999339	-0.0795701207	-0.1037534554
C	6.0	2.6154482229	-0.0727052540	-0.5864916041
C	6.0	2.7548350748	-1.4805580884	-0.2159325187
C	6.0	1.6167645908	-2.2226085857	0.1846034721
C	6.0	0.2945417694	-1.5518405727	0.3276755466
C	6.0	0.0157857281	-0.4628129890	1.3516668863
C	6.0	-1.3820924191	-0.3715474931	1.9575596747
C	6.0	1.0274916078	-0.0078061749	2.3965149941
O	8.0	-2.3455956414	-0.7976856620	0.9785316904
O	8.0	1.2753060591	1.1659200110	2.5681327541
C	6.0	1.6301676253	-1.0917720817	3.2904891742
O	8.0	2.2335798967	-0.5416246808	4.4567985800
C	6.0	-3.6060377034	-0.9279399694	1.4361174142
O	8.0	-4.3734998055	-1.3106826030	0.4077985121
C	6.0	-5.7631313558	-1.4904646525	0.7348211552
C	6.0	3.9922677001	-2.1371643556	-0.3201608116
C	6.0	1.7412705829	-3.5968342699	0.4154900440
C	6.0	4.1094609782	-3.4986901665	-0.0524896462
C	6.0	3.4222989688	0.0906833795	4.3647342579
O	8.0	3.9001813459	0.6955394748	5.2897637245
O	8.0	3.9996492261	-0.0875909269	3.1588465115
C	6.0	5.2613937348	0.5798917424	2.9977725050
C	6.0	2.9779690098	-4.2346838879	0.3079284107
O	8.0	-3.9702168135	-0.7349568876	2.5739501876
H	1.0	1.3605637229	1.5919667451	-0.9296846995
H	1.0	-0.7289331364	0.2200063465	-0.6047894394
H	1.0	3.5094529952	0.4418916185	-0.9299296562
H	1.0	-0.5640725630	-2.1814513052	0.1108889537
H	1.0	-1.5958941286	0.6623931079	2.2497040700
H	1.0	-1.4775396092	-0.9998985059	2.8503930580
H	1.0	2.3345015688	-1.6935889417	2.7097455780
H	1.0	0.8377650012	-1.7551407094	3.6530120224
H	1.0	-6.1984317698	-0.5537063289	1.0907586223
H	1.0	-5.8817425178	-2.2559079323	1.5055717779
H	1.0	-6.2386636300	-1.8053604402	-0.1936681310
H	1.0	4.8653097510	-1.5670684889	-0.6289085744
H	1.0	0.8599836412	-4.1688519762	0.6961769574
H	1.0	5.0760819660	-3.9870462996	-0.1351762562
H	1.0	5.6089410672	0.3074096299	2.0013302095
H	1.0	5.9709257710	0.2474127003	3.7588636281
H	1.0	5.1311563721	1.6618008841	3.0769694326
H	1.0	3.0574920677	-5.2992242410	0.5078512149

Transition state 2 (TS2)

C	6.0	1.3417312015	0.3999490711	-0.7802151475
C	6.0	0.1554071036	0.1106031653	-0.1256286348
C	6.0	2.5562861929	-0.2656588929	-0.6066274476
C	6.0	2.6997611296	-1.6053519167	-0.1824809573
C	6.0	1.5597708682	-2.4377410637	0.1506665304
C	6.0	0.3230343075	-1.9327163384	0.5742626968
C	6.0	0.1114255245	-0.5938542090	1.1887767573
C	6.0	-1.2509115931	-0.4484353404	1.8907729855
C	6.0	1.1282787807	-0.0966606541	2.2504490355
O	8.0	-2.2799890309	-0.8988493573	0.9916715242
O	8.0	1.3146249689	1.0859656151	2.4246085840
C	6.0	1.7800027779	-1.1460382636	3.1558485199
O	8.0	2.1527335498	-0.5784969255	4.4086573725
C	6.0	-3.5304191601	-0.8476016474	1.4935776591
O	8.0	-4.3684827811	-1.2818059784	0.5440343446
C	6.0	-5.7549397293	-1.2847673201	0.9289206830
C	6.0	3.9737782587	-2.2475291079	-0.3296769528
C	6.0	1.7197726972	-3.8614836552	0.0559214139
C	6.0	4.1019238731	-3.6107189081	-0.2945226114
C	6.0	3.2518641805	0.1990191991	4.5031880422
O	8.0	3.5029321058	0.8307837197	5.4971684784
O	8.0	4.0254264759	0.1281633921	3.4006169060
C	6.0	5.1902367393	0.9685570356	3.4391483968
C	6.0	2.9499393601	-4.4322429049	-0.1335258793
O	8.0	-3.8312492634	-0.4757208219	2.6050276353
H	1.0	1.3084186969	1.1859396668	-1.5328594253
H	1.0	-0.7897448977	0.4585209456	-0.5321026816
H	1.0	3.4439733976	0.1947850592	-1.0353122682
H	1.0	-0.5454829302	-2.5832731797	0.5147673433
H	1.0	-1.4190605721	0.6005115310	2.1499045479
H	1.0	-1.2914953463	-1.0426772056	2.8098527760
H	1.0	2.6360701996	-1.5887681398	2.6398991252
H	1.0	1.0729646797	-1.9469400511	3.3902901056
H	1.0	-6.0878565765	-0.2732953569	1.1740468565
H	1.0	-5.9125770914	-1.9322914825	1.7947267078
H	1.0	-6.2938603283	-1.6656446399	0.0618764331
H	1.0	4.8413261964	-1.6211418131	-0.5209913733
H	1.0	0.8439724085	-4.4854789196	0.2149574703
H	1.0	5.0770074683	-4.0710885153	-0.4246516840
H	1.0	5.7277460511	0.7670707268	2.5123247113
H	1.0	5.8095261780	0.7265826161	4.3057981596
H	1.0	4.8964808928	2.0196837875	3.4901576990
H	1.0	3.0523553585	-5.5133179190	-0.1488547407

Cycloheptatriene (3.22ac)

C	6.0	1.3355792268	0.4169626056	-0.7501957560
C	6.0	0.1764099649	0.1987951657	-0.0574329768
C	6.0	2.5481561676	-0.2937854964	-0.6030298665
C	6.0	2.6862665701	-1.6260963123	-0.1999838323
C	6.0	1.5519112418	-2.4685412572	0.1742660414
C	6.0	0.3534631132	-1.9870497882	0.6734731866
C	6.0	0.1343977374	-0.6069431849	1.2083535043
C	6.0	-1.2268593151	-0.4668993004	1.9176858072
C	6.0	1.1472928879	-0.1134400797	2.2864966332
O	8.0	-2.2555769953	-0.9082090182	1.0128577816
O	8.0	1.3316862766	1.0679595424	2.4699365584
C	6.0	1.8011824258	-1.1659301247	3.1874536337
O	8.0	2.1774281620	-0.6012224982	4.4405248485
C	6.0	-3.5074033514	-0.8461552690	1.5091158223
O	8.0	-4.3459134320	-1.2699207169	0.5549758610
C	6.0	-5.7337775224	-1.2586764957	0.9337523378
C	6.0	3.9625331980	-2.2727823822	-0.3783141111
C	6.0	1.7160390323	-3.8991778835	0.0474271792
C	6.0	4.0895583926	-3.6312645913	-0.3637042075
C	6.0	3.2747926760	0.1786906331	4.5333539420
O	8.0	3.5276276808	0.8089808956	5.5278157155
O	8.0	4.0461695261	0.1112606813	3.4287722783
C	6.0	5.2095643417	0.9535564452	3.4663684070
C	6.0	2.9364277838	-4.4608089152	-0.1839869937
O	8.0	-3.8102653601	-0.4740089856	2.6201669966
H	1.0	1.3184535219	1.1916736311	-1.5153445353
H	1.0	-0.7548822403	0.6368043990	-0.4051843060
H	1.0	3.4379145895	0.1666200243	-1.0285616262
H	1.0	-0.4950912217	-2.6659110818	0.7053976445
H	1.0	-1.3957839835	0.5787900370	2.1887530496
H	1.0	-1.2673207101	-1.0710951058	2.8301942358
H	1.0	2.6562244965	-1.6070909965	2.6681372059
H	1.0	1.0959186299	-1.9680192928	3.4222487703
H	1.0	-6.0579930297	-0.2435307279	1.1758003410
H	1.0	-5.9021739660	-1.9027865941	1.8002221922
H	1.0	-6.2729189086	-1.6360002051	0.0651666846
H	1.0	4.8254506846	-1.6435641615	-0.5807581623
H	1.0	0.8449660230	-4.5257491860	0.2210123492
H	1.0	5.0602446571	-4.0912460131	-0.5242039502
H	1.0	5.7489950676	0.7501415444	2.5411540503
H	1.0	5.8277745122	0.7155858417	4.3347093236
H	1.0	4.9137476248	2.0043279149	3.5132167156
H	1.0	3.0421058236	-5.5410486971	-0.2214067735

Transition state 3 (TS3)

C	6.0	-4.0987172561	-0.7144984077	0.4534754179
C	6.0	-4.2795439148	-1.0751178258	-0.9340990566
C	6.0	-3.2060211806	-1.1775011097	-1.7529587017
C	6.0	-1.8433994549	-0.9386496731	-1.3052665305
C	6.0	-1.6479184516	-0.5577116080	0.1175645537
C	6.0	-2.8599503438	-0.4755521439	0.9407503650
C	6.0	-0.8479740251	-1.0939629905	-2.2324482590
C	6.0	0.5799443936	-0.9523625829	-2.1026867645
C	6.0	1.3472790310	-0.5888133601	-1.0570413360
C	6.0	0.9728361900	-0.1655449285	0.3529916018
C	6.0	-0.4807568256	-0.2784256650	0.7630061403
C	6.0	1.8909395434	-1.0308728330	1.2848817103
C	6.0	1.4447825593	1.3027926625	0.5271265517
O	8.0	3.0451120896	-0.7155314932	1.4890907042
C	6.0	1.3377543798	-2.3028222800	1.9277541692
O	8.0	0.6465059899	-3.0929096456	0.9493910044
C	6.0	-0.5395965445	-3.6789282634	1.2097333144
O	8.0	-1.1185245585	-4.3340349620	0.3812915802
O	8.0	-0.9680154793	-3.4516886037	2.4681903805
C	6.0	-2.2611196421	-4.0112415386	2.7670950061
O	8.0	1.2017844029	1.6762039989	1.9008112052
C	6.0	1.7912766675	2.7594928569	2.4338961426
O	8.0	1.6288347396	3.0815655329	3.5848500963
O	8.0	2.5548899670	3.4174149994	1.5362476724
C	6.0	3.2319631091	4.5727881639	2.0625392275
H	1.0	-4.9673858436	-0.6305590220	1.1003059447
H	1.0	-5.2798282141	-1.2663072963	-1.3109023970
H	1.0	-3.3383427019	-1.4568190746	-2.7946772873
H	1.0	-2.7275821392	-0.1948308854	1.9821092720
H	1.0	-1.1763556167	-1.3877313021	-3.2270173032
H	1.0	1.1287304159	-1.1882031567	-3.0132028622
H	1.0	2.4236015785	-0.5755620717	-1.2218572505
H	1.0	-0.6057951700	-0.0117244240	1.8110090789
H	1.0	0.8725286767	1.9560419643	-0.1377077133
H	1.0	2.5083343497	1.3816817303	0.3005934935
H	1.0	0.6767161257	-2.0291159517	2.7543052943
H	1.0	2.1840362607	-2.8744142612	2.3175636282
H	1.0	-2.2661212742	-5.0850404938	2.5697390039
H	1.0	-3.0282794319	-3.5257308910	2.1593995975
H	1.0	-2.4254237209	-3.8115303712	3.8260344568
H	1.0	3.8223625895	4.9658086448	1.2348606837
H	1.0	2.5082524727	5.3155908750	2.4064317211
H	1.0	3.8775043203	4.2888422488	2.8965874741

Cycloheptatriene (3.22ac')

C	6.0	-3.1235638096	-0.5512100160	-2.1739671989
C	6.0	-2.5221742130	0.0085893662	-3.3459823857
C	6.0	-1.1673218148	-0.0197839659	-3.5027841751
C	6.0	-0.2988651262	-0.5856089335	-2.5014159195
C	6.0	-0.8999054365	-0.9785492843	-1.2297345007
C	6.0	-2.3430670642	-1.0498704638	-1.1739712597
C	6.0	1.0057729380	-0.9343098742	-2.8642937548
C	6.0	1.9175448440	-1.6987759179	-2.0993654944
C	6.0	1.9539501231	-1.8399632235	-0.7366813956
C	6.0	1.2318456254	-0.9217686068	0.2115722209
C	6.0	-0.1936257856	-1.2889966914	-0.0799658648
C	6.0	1.6513832733	-1.2180747107	1.6725823546
C	6.0	1.6090789570	0.5565387649	-0.0424301407
O	8.0	2.7893598055	-1.5503509396	1.9298182110
C	6.0	0.6420055519	-1.0199590795	2.8120045051
O	8.0	-0.0914551103	-2.2648725972	2.9087984017
C	6.0	-1.0236438352	-2.4141695609	3.8736284070
O	8.0	-1.6818012606	-3.4177656609	3.9801308265
O	8.0	-1.1075351595	-1.3258575452	4.6625683399
C	6.0	-2.0832445574	-1.4224357046	5.7174475944
O	8.0	0.9009953041	1.3583701345	0.9320504413
C	6.0	0.9802767287	2.7005246624	0.8942338353
O	8.0	0.4273752378	3.4031350477	1.7033759828
O	8.0	1.7390835775	3.1315503468	-0.1342857009
C	6.0	1.8653683629	4.5621253308	-0.2268772166
H	1.0	-4.2054900079	-0.5649404006	-2.0806602217
H	1.0	-3.1542553131	0.4232738808	-4.1259668961
H	1.0	-0.7128977383	0.3447581629	-4.4205400234
H	1.0	-2.7956108112	-1.4445792253	-0.2681558376
H	1.0	1.2728169309	-0.7552880602	-3.9041024226
H	1.0	2.6454328003	-2.2785665820	-2.6658654241
H	1.0	2.5765051370	-2.6092176084	-0.2896004516
H	1.0	-0.7258187939	-1.8311515915	0.6964522890
H	1.0	1.3326903774	0.8647659383	-1.0483721502
H	1.0	2.6879554714	0.6786873425	0.0903290546
H	1.0	-0.0376652437	-0.1896052483	2.6126214954
H	1.0	1.1998201032	-0.8396962996	3.7328194689
H	1.0	-1.8273541265	-2.2387066761	6.3967634320
H	1.0	-3.0772392486	-1.6002378931	5.3012820473
H	1.0	-2.0462886958	-0.4641208222	6.2345856855
H	1.0	2.4923551491	4.7419965169	-1.1000284387
H	1.0	0.8844303351	5.0253654992	-0.3541489808
H	1.0	2.3365768658	4.9620697349	0.6739830593

Transition state 4 (TS4)

C	6.0	-3.0877086326	-0.5129191258	-2.1779148386
C	6.0	-2.4856237093	0.0663931908	-3.3323635191
C	6.0	-1.1266431021	0.0323150117	-3.4881344179
C	6.0	-0.2684649103	-0.5537303211	-2.4981052783
C	6.0	-0.8704653731	-0.9840553026	-1.2496657975
C	6.0	-2.3061460358	-1.0437044918	-1.1887567470
C	6.0	1.0453655837	-0.9124606804	-2.8615773799
C	6.0	1.9164405493	-1.7018944647	-2.1001061060
C	6.0	1.8893077908	-1.8903986751	-0.7290965790
C	6.0	1.2406607069	-0.9388170919	0.2280579369
C	6.0	-0.1518558479	-1.3608512121	-0.1113338687
C	6.0	1.6553046424	-1.2539999401	1.6849453059
C	6.0	1.6171487306	0.5339456155	-0.0283425028
O	8.0	2.7865944686	-1.6131401665	1.9356743801
C	6.0	0.6529385241	-1.0411886764	2.8270981087
O	8.0	-0.1558577885	-2.2411282411	2.8807011593
C	6.0	-1.0824791707	-2.3742918455	3.8533689041
O	8.0	-1.8099200294	-3.3325193429	3.9198078974
O	8.0	-1.0732056978	-1.3274163109	4.6999533333
C	6.0	-2.0350771083	-1.4095762539	5.7688515027
O	8.0	0.9014667475	1.3351970143	0.9409954043
C	6.0	0.9472024875	2.6781895154	0.8843198108
O	8.0	0.3801327426	3.3767553955	1.6872192575
O	8.0	1.6904610504	3.1148761800	-0.1527415161
C	6.0	1.7694159768	4.5472577300	-0.2702719743
H	1.0	-4.1693646901	-0.5202989093	-2.0807265546
H	1.0	-3.1133288208	0.5022577351	-4.1043225638
H	1.0	-0.6693542275	0.4122753923	-4.3982641827
H	1.0	-2.7615768849	-1.4568164140	-0.2925787050
H	1.0	1.3184586884	-0.7304056165	-3.8989844672
H	1.0	2.6571565271	-2.2798712202	-2.6512242987
H	1.0	2.4365614057	-2.7186605989	-0.2890965992
H	1.0	-0.6660768147	-1.9721588806	0.6245494360
H	1.0	1.3479767037	0.8417848390	-1.0358472628
H	1.0	2.6951264803	0.6583483832	0.1115726287
H	1.0	0.0250696322	-0.1658388706	2.6508809202
H	1.0	1.2161351917	-0.9245143851	3.7546244903
H	1.0	-1.8494566162	-2.2966864314	6.3783741536
H	1.0	-3.0490571265	-1.4559517428	5.3652960278
H	1.0	-1.8943089993	-0.5015412374	6.3543154678
H	1.0	2.3954466608	4.7326078804	-1.1429073755
H	1.0	0.7738835618	4.9739130039	-0.4122008766
H	1.0	2.2202464121	4.9793828590	0.6260556355

exo-benzonorcaradiene (3.15ac)

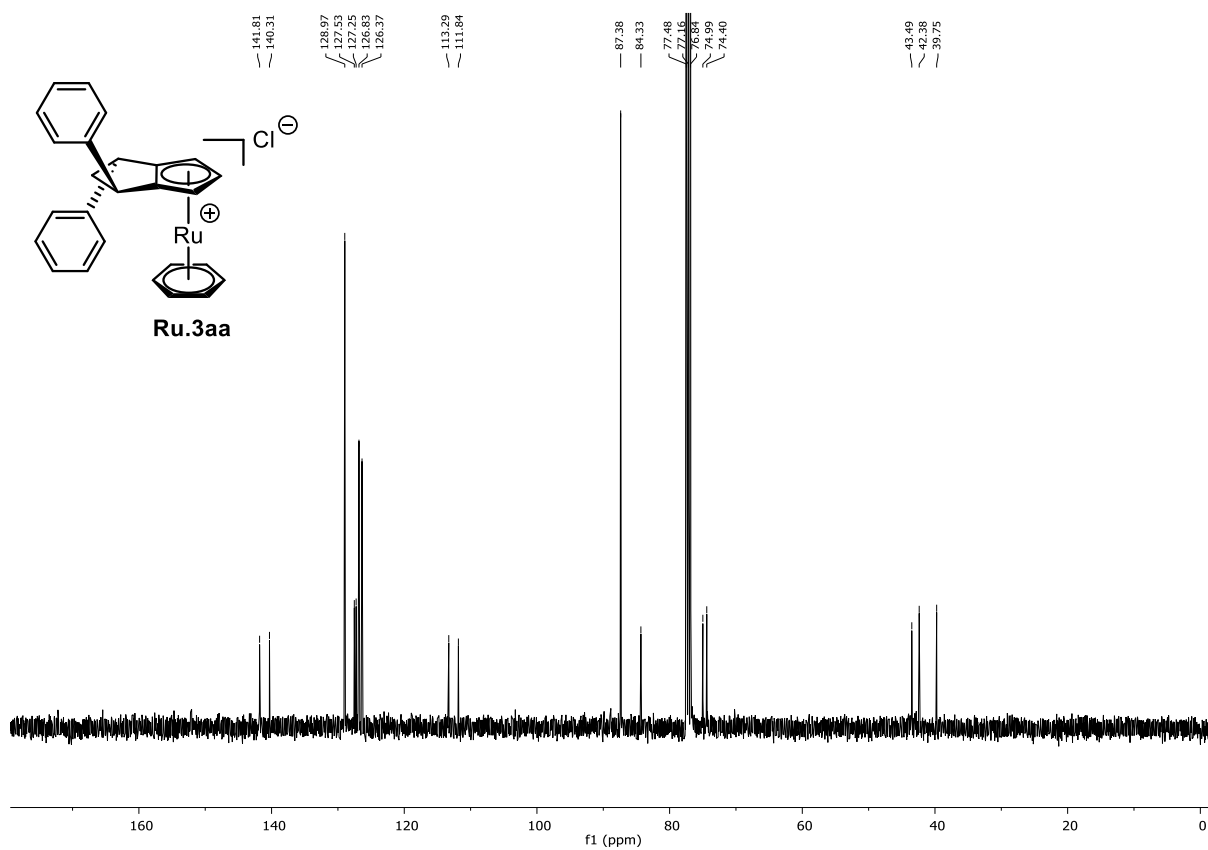
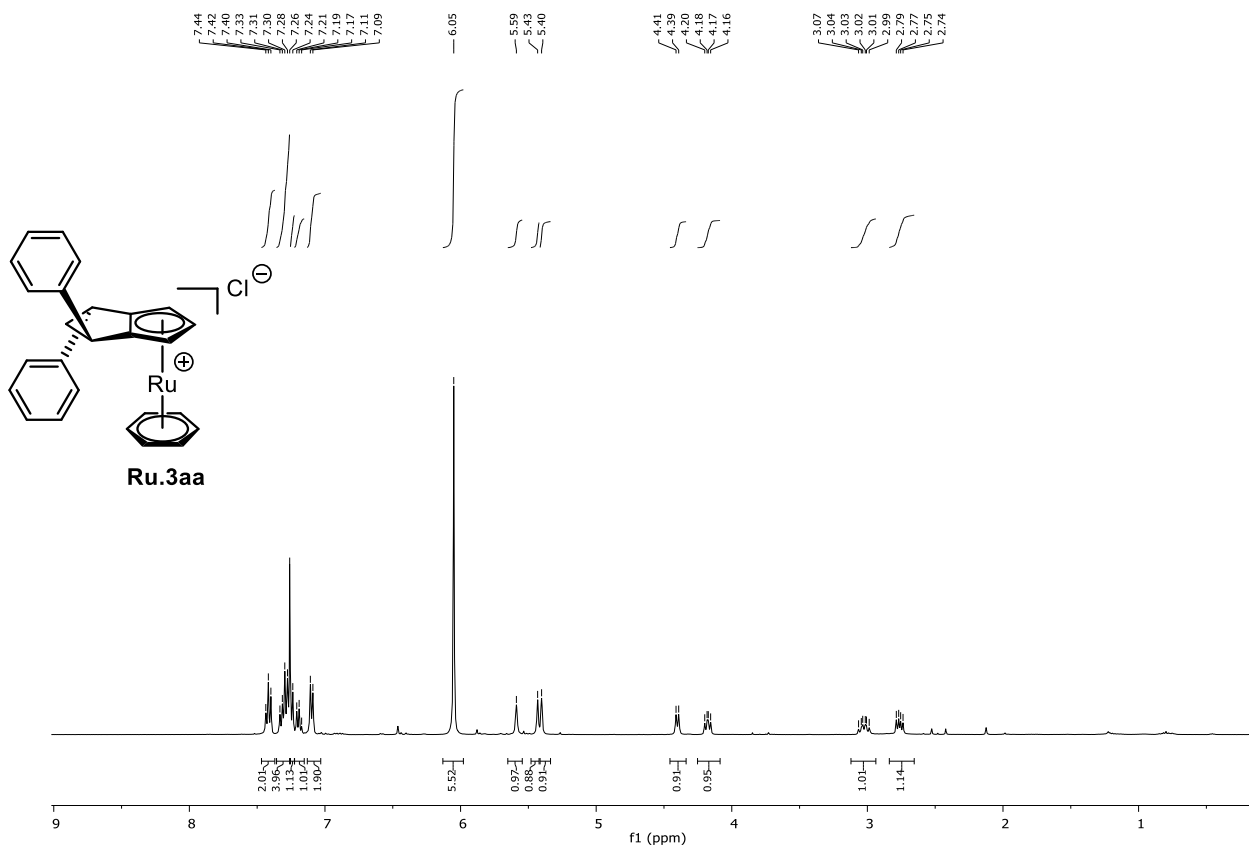
O	8.0	-1.0406798585	-1.1367420300	-0.4113061378
C	6.0	-2.1560886641	-1.2815987027	0.3242724751
O	8.0	1.4693888164	0.4705730901	-3.3306625271
O	8.0	-3.1052475624	-1.9206148408	-0.0701206472
O	8.0	-2.0713608609	-0.6517506993	1.5075336890
C	6.0	1.0107985360	-0.1070549242	-1.0761472195
C	6.0	2.1919570656	-1.1274177043	-1.1310312176
C	6.0	2.3347405486	-2.1740356462	-0.1023449857
C	6.0	2.6751185991	-1.8809556619	1.1686928056
C	6.0	2.9709512693	-0.5192879968	1.6087046312
C	6.0	3.3844691616	-0.2531601293	2.9249772995
C	6.0	3.7283289770	1.0363300363	3.3195138737
C	6.0	3.6745773360	2.0845960578	2.3958013754
C	6.0	3.2641314766	1.8367632603	1.0864630227
C	6.0	2.8911865960	0.5501846671	0.6829706575
C	6.0	2.4636506051	0.2914913724	-0.7172075718
C	6.0	-0.0133009159	-0.2017955265	0.0243552318
C	6.0	0.6253462428	0.3523819701	-2.4523734080
C	6.0	-0.8315347089	0.5822710651	-2.8614186545
C	6.0	-3.2960324901	-0.6164530710	2.2645456225
O	8.0	-1.5471659044	1.3310351087	-1.8647742818
C	6.0	-2.8558352632	1.0901943190	-1.6416817548
O	8.0	-3.4152414693	1.5069875458	-0.6546054577
O	8.0	-3.4182515850	0.3731980547	-2.6248497774
C	6.0	-4.7738259161	-0.0549837929	-2.3698399412
H	1.0	2.4458903791	-1.3988556146	-2.1516433776
H	1.0	2.1816180919	-3.2056611604	-0.4067978491
H	1.0	2.7785982540	-2.6768082315	1.9025191381
H	1.0	3.4404136153	-1.0735028727	3.6364687435
H	1.0	4.0443312704	1.2250101500	4.3414550937
H	1.0	3.9479851314	3.0919750126	2.6959090960
H	1.0	3.2207428181	2.6508333025	0.3671828393
H	1.0	2.8966497109	0.9404566790	-1.4740573553
H	1.0	0.4313930058	-0.5758276106	0.9450601330
H	1.0	-0.4738654852	0.7658419133	0.2240821160
H	1.0	-0.8194643553	1.1330461278	-3.8047052667
H	1.0	-1.3041879207	-0.3911292424	-3.0167103040
H	1.0	-3.0319745907	-0.1664878601	3.2214412085
H	1.0	-4.0305330563	0.0004610348	1.7418645129
H	1.0	-3.6887688529	-1.6254843928	2.4047590640
H	1.0	-5.0950595538	-0.5472077489	-3.2874647828
H	1.0	-4.7803489275	-0.7551091540	-1.5326405997
H	1.0	-5.4062335662	0.8072718457	-2.1504115118

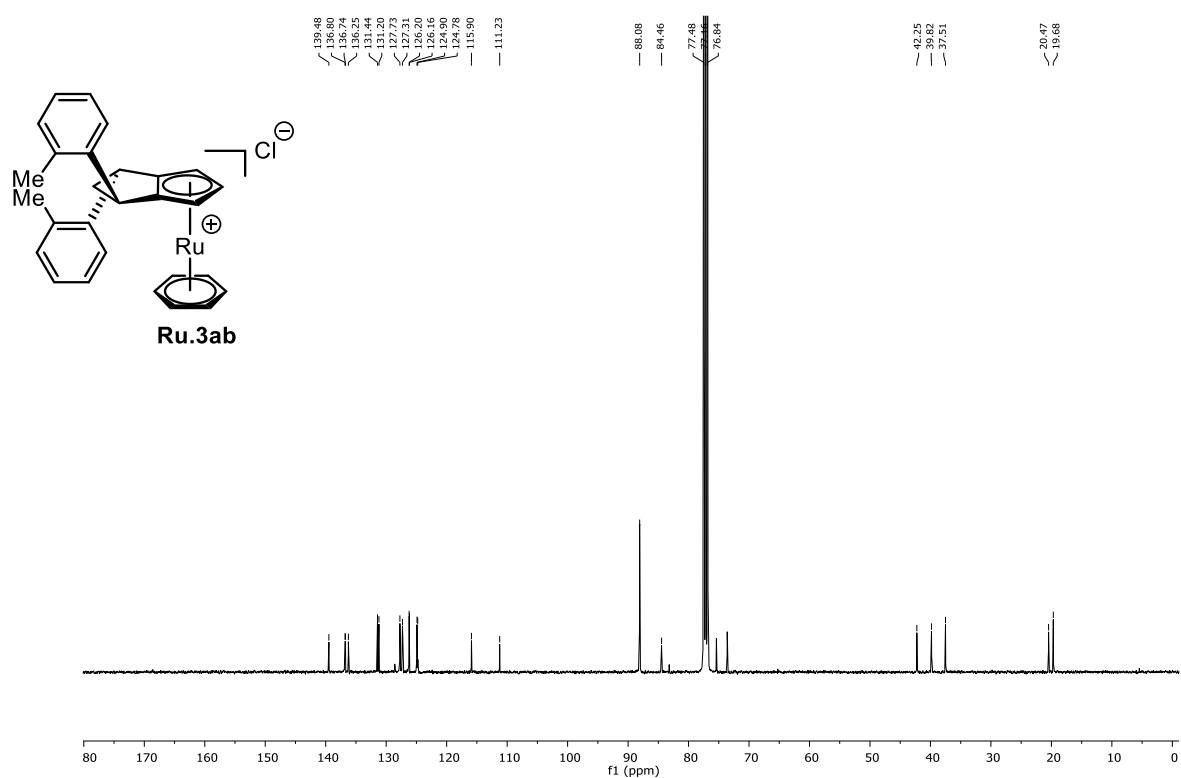
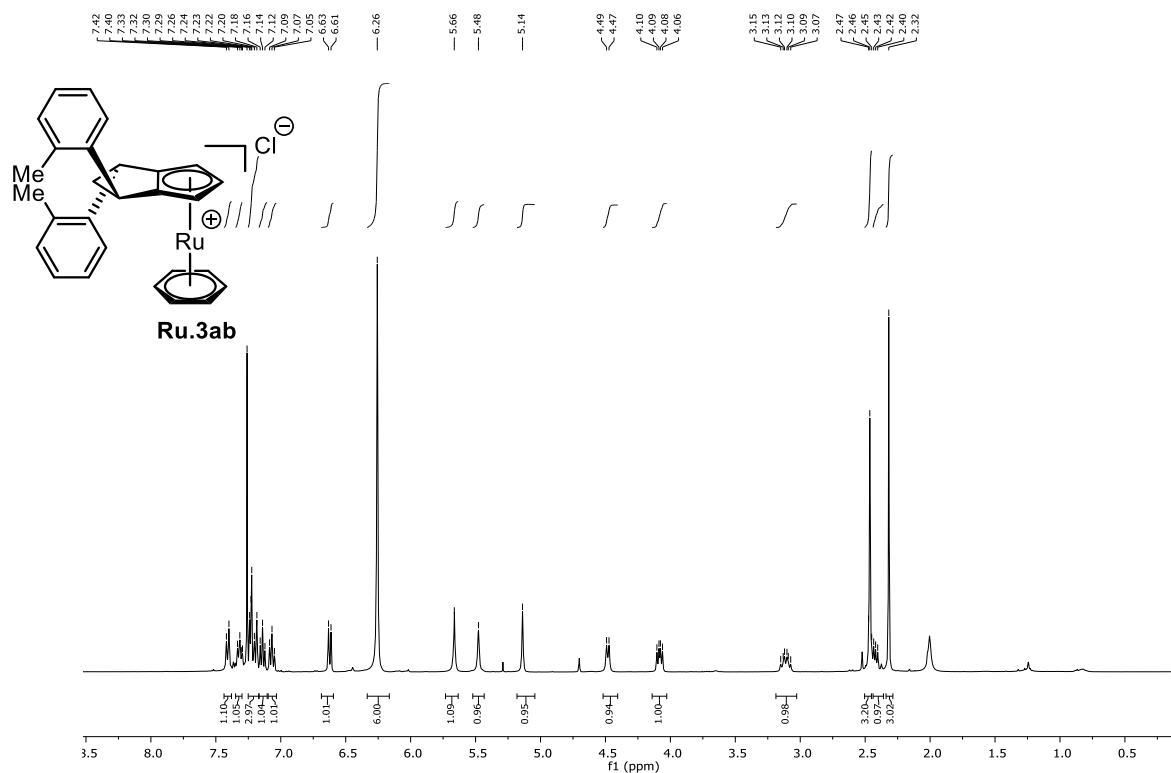
Dihydrofuran (3.23ac)

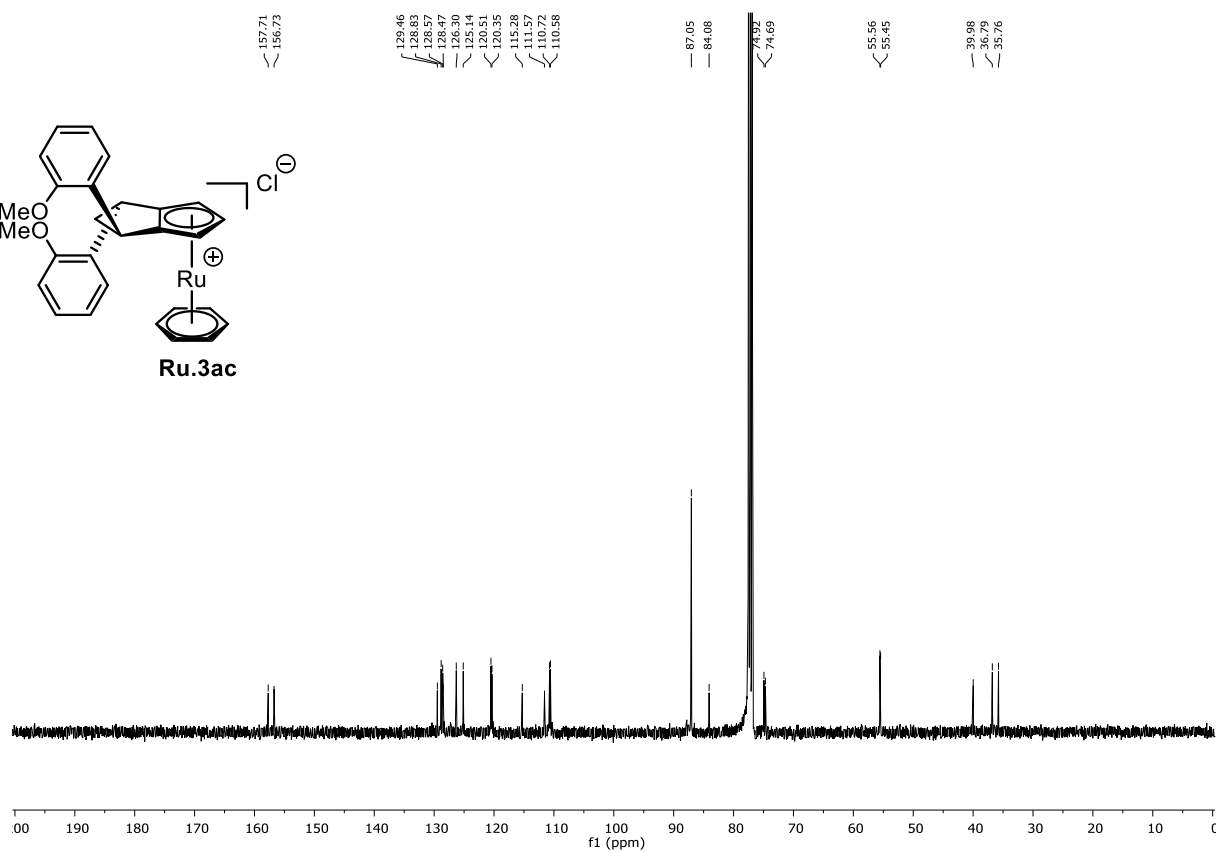
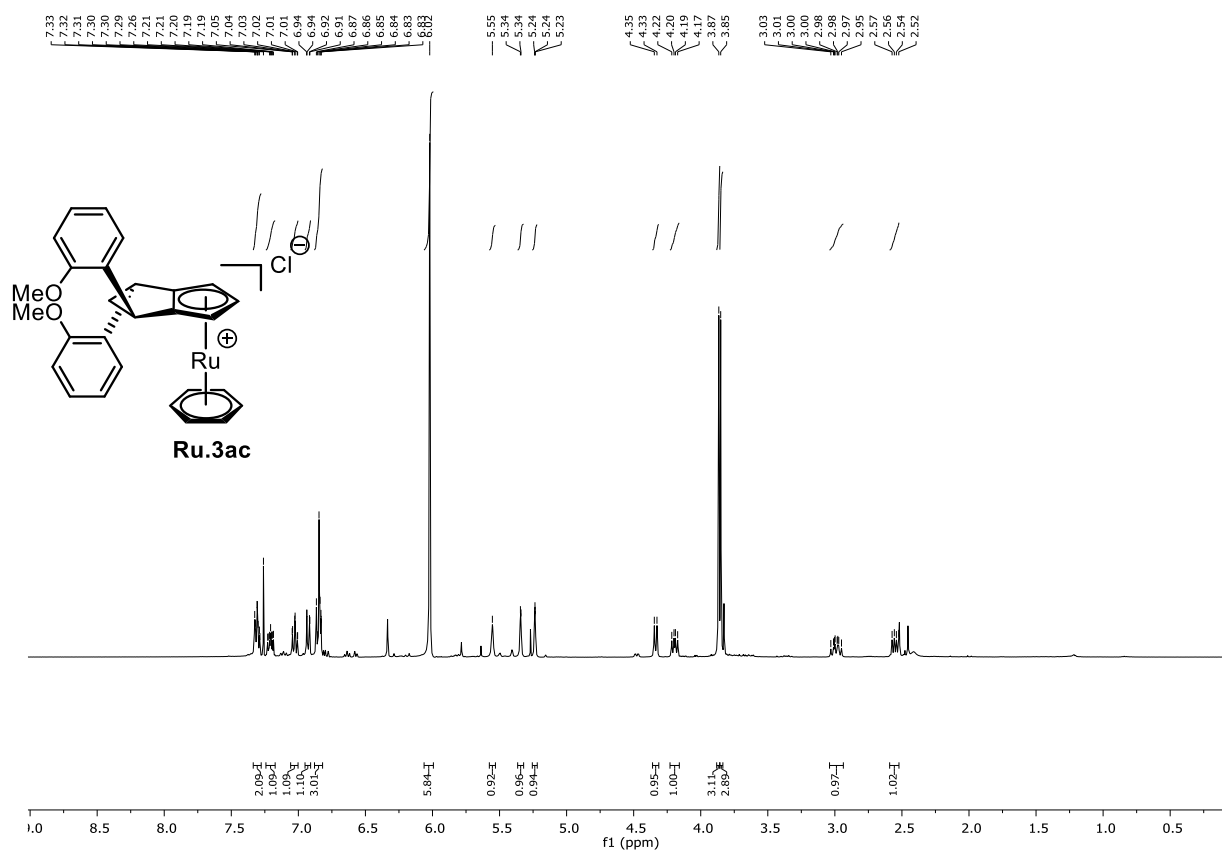
C	6.0	1.0083860707	1.2660477169	4.6255888748
C	6.0	-0.2339028120	1.5275586947	5.2068383979
C	6.0	-1.3019411209	1.9282166251	4.4071959137
C	6.0	-1.1487777530	2.0745930760	3.0196695597
C	6.0	0.1099441461	1.8197377512	2.4401007441
C	6.0	1.1746799450	1.4172221345	3.2477129323
C	6.0	-2.2768293901	2.4689889544	2.1717547098
C	6.0	-2.1964256844	2.4950127184	0.8351626819
C	6.0	-0.9424109676	2.1310506496	0.0804328422
C	6.0	0.3369741889	2.0406963440	0.9540631935
C	6.0	-0.9597232003	0.7435845984	-0.5760513971
C	6.0	0.2416401846	0.1836537621	-0.3724715883
O	8.0	1.0968734373	0.9151575836	0.4058469318
C	6.0	0.8808767004	-1.0991829446	-0.8210237140
C	6.0	-2.0847468445	0.2377125556	-1.4041919593
O	8.0	0.1761117506	-1.7631009295	-1.8789162985
C	6.0	0.2587834704	-1.3060152181	-3.1499757938
O	8.0	-0.3930852416	-1.7947746457	-4.0385360956
O	8.0	1.1318933019	-0.2931009061	-3.2730838275
C	6.0	1.1615178429	0.3139366007	-4.5809704810
O	8.0	-1.9454108282	0.8180410740	-2.7447173331
C	6.0	-2.8981043675	0.4519792960	-3.6161730902
O	8.0	-3.8758968579	-0.2194458684	-3.3731331329
O	8.0	-2.5797862976	0.9741425091	-4.8153414188
C	6.0	-3.4859983691	0.6183411372	-5.8728749488
H	1.0	1.8456035008	0.9503043764	5.2413613606
H	1.0	-0.3698005390	1.4184685897	6.2790513168
H	1.0	-2.2736929341	2.1227184031	4.8545860465
H	1.0	2.1382403204	1.2128904153	2.7899338304
H	1.0	-3.2088169397	2.7270166057	2.6696971097
H	1.0	-3.0633196138	2.7735149969	0.2412622749
H	1.0	-0.7921447237	2.8837876031	-0.7081011914
H	1.0	0.9812931991	2.9150272449	0.8167385012
H	1.0	1.9157144152	-0.8914354315	-1.1065450441
H	1.0	0.8905807604	-1.8212431494	0.0015400625
H	1.0	-2.0793884699	-0.8480213396	-1.5006969649
H	1.0	-3.0556056655	0.5406830482	-1.0022515797
H	1.0	1.9320118984	1.0826281345	-4.5243007797
H	1.0	1.4128760627	-0.4311940524	-5.3387706076
H	1.0	0.1877214924	0.7539336995	-4.8059237447
H	1.0	-3.1088524612	1.1246553763	-6.7615118511
H	1.0	-3.4918367851	-0.4640632398	-6.0222831634
H	1.0	-4.5001208211	0.9536674499	-5.6420252789

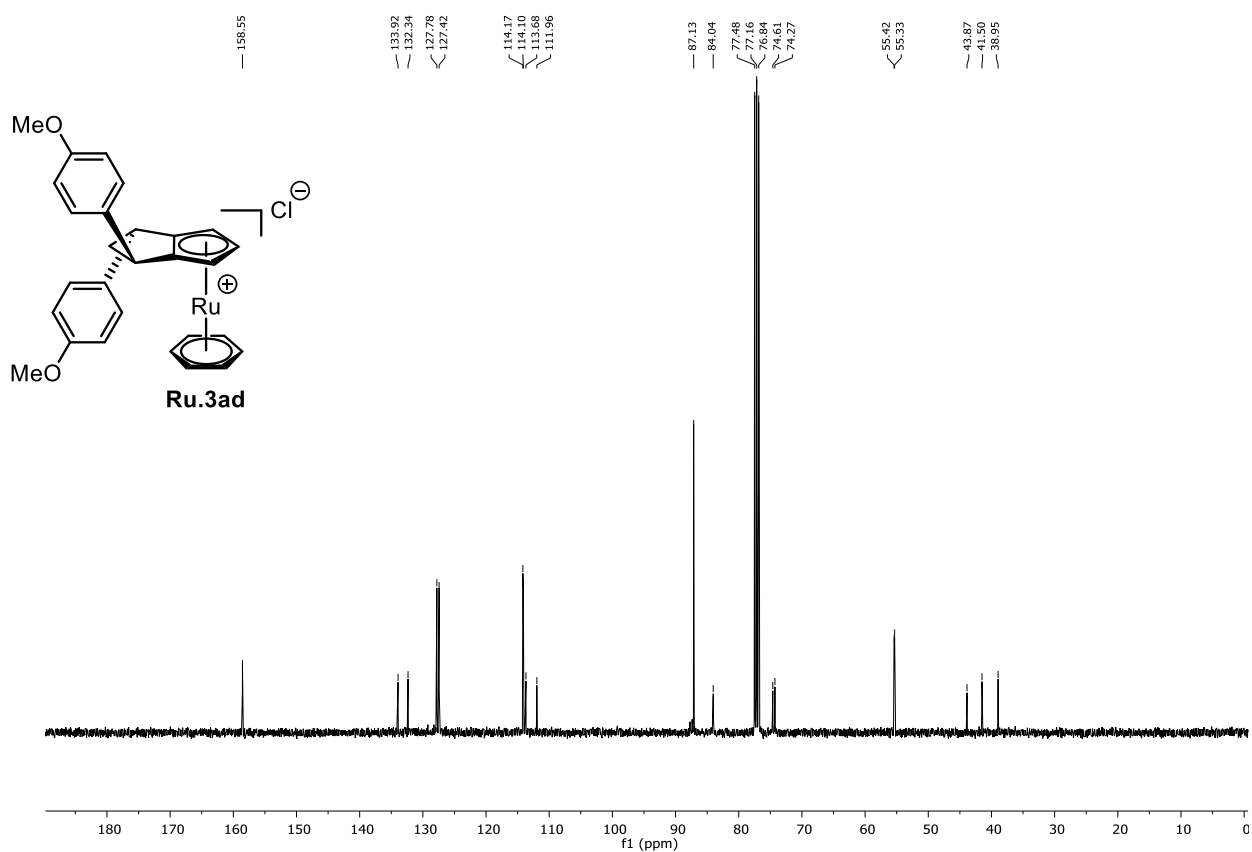
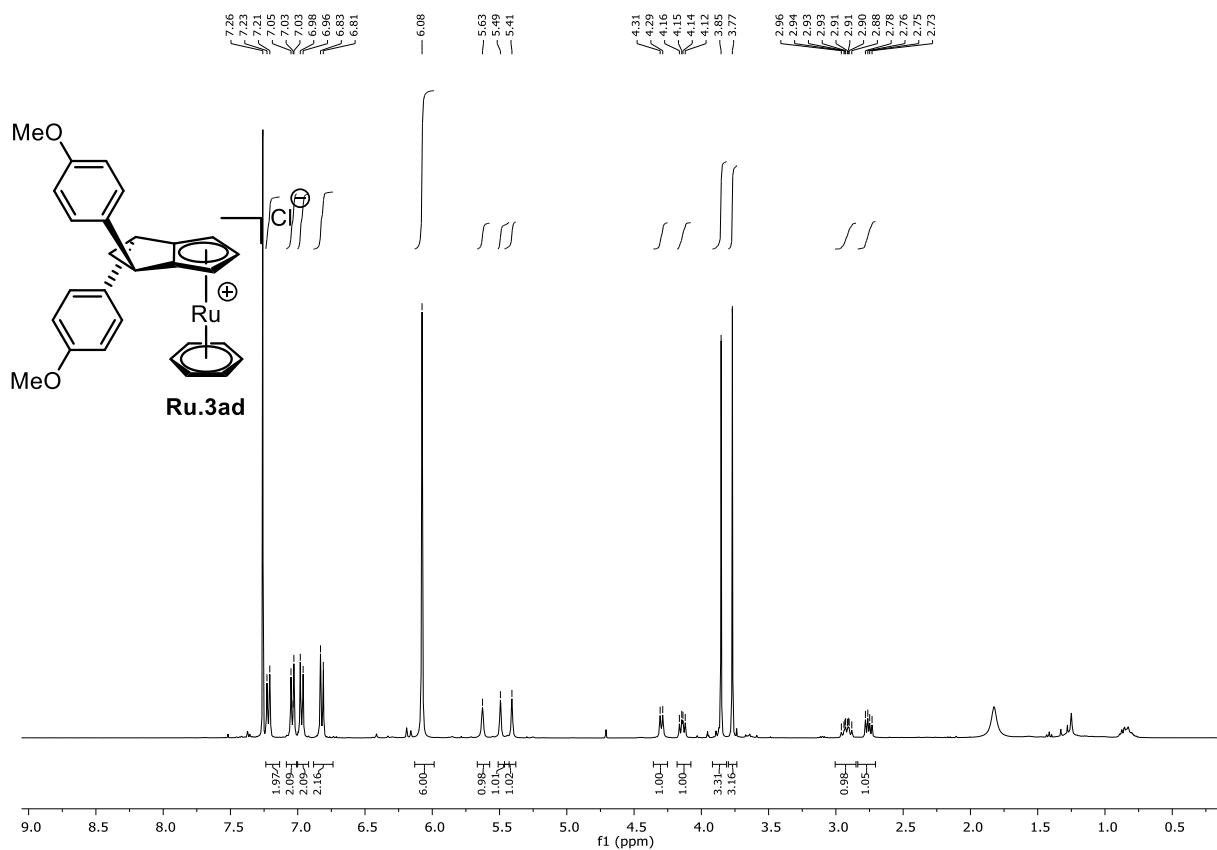
9.3 NMR spectra

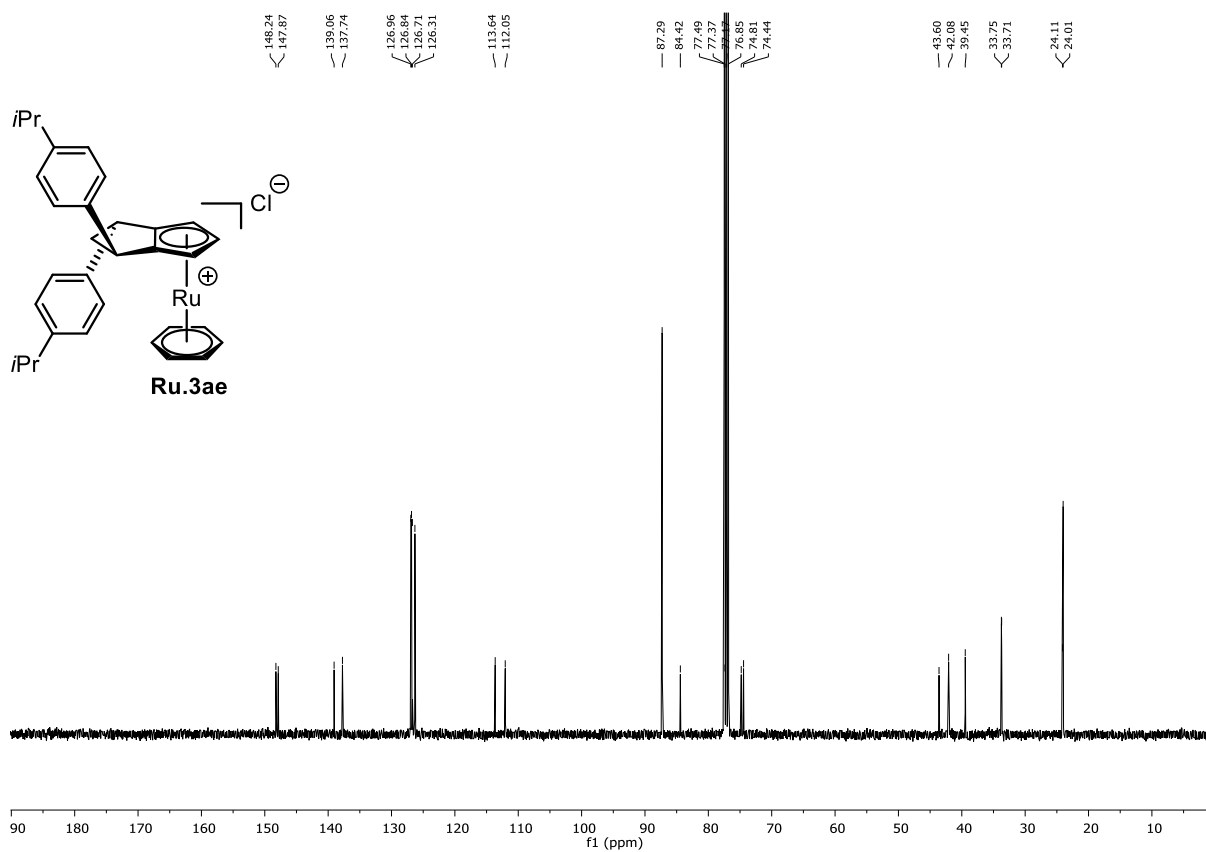
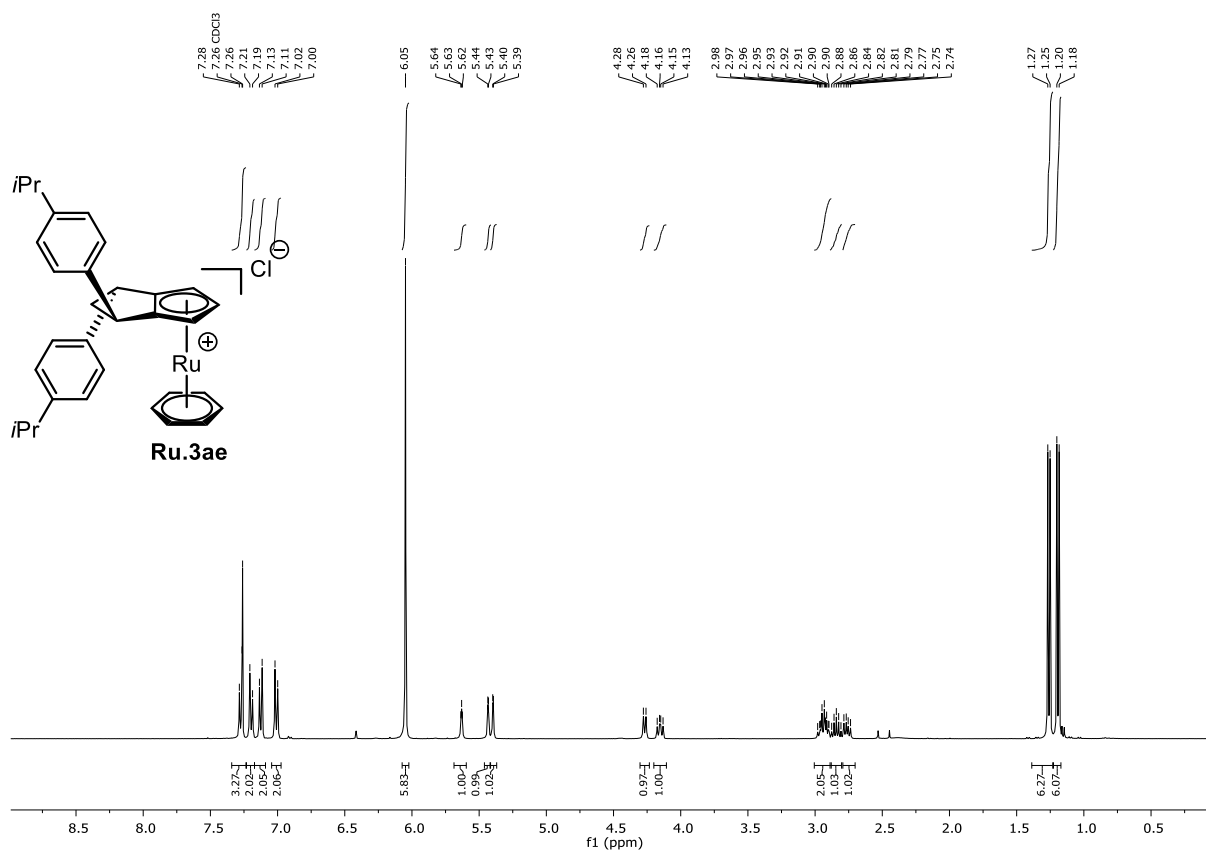
NMR spectra for Chapter 2

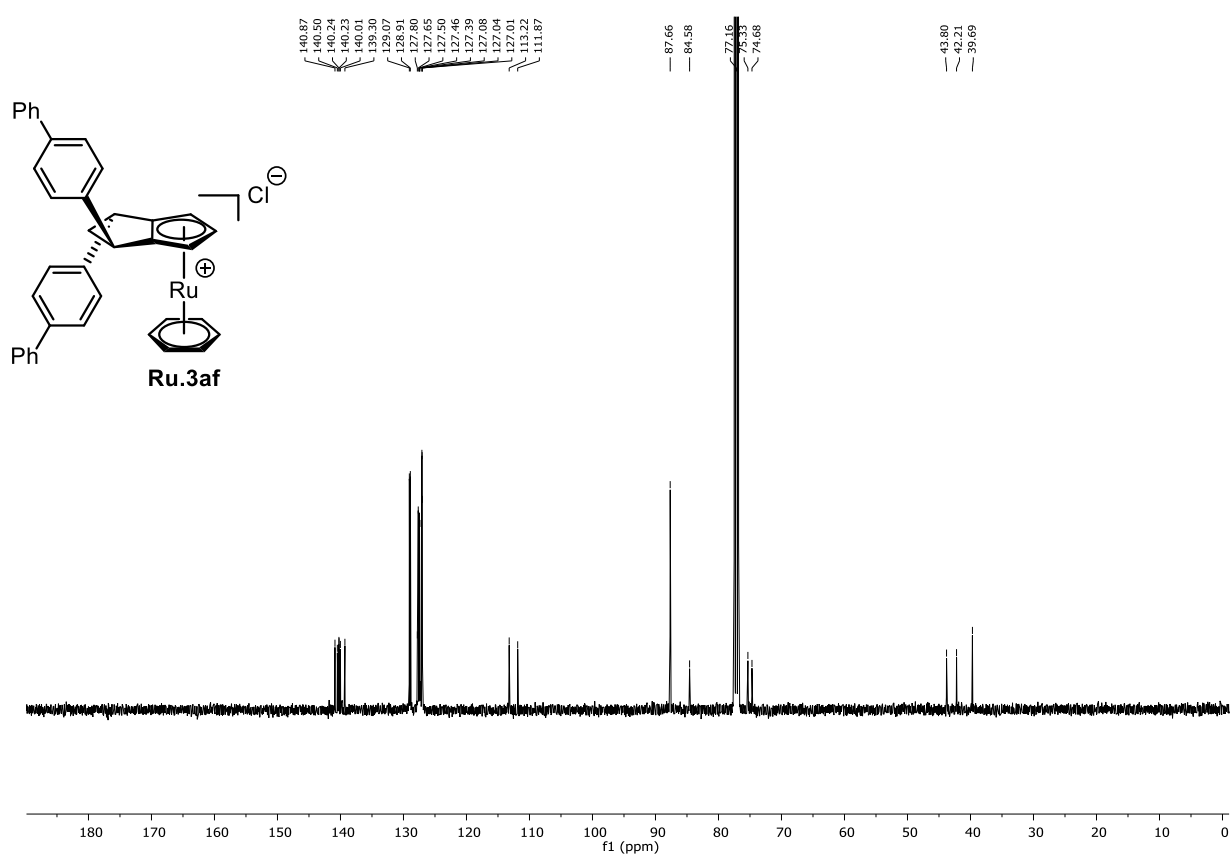
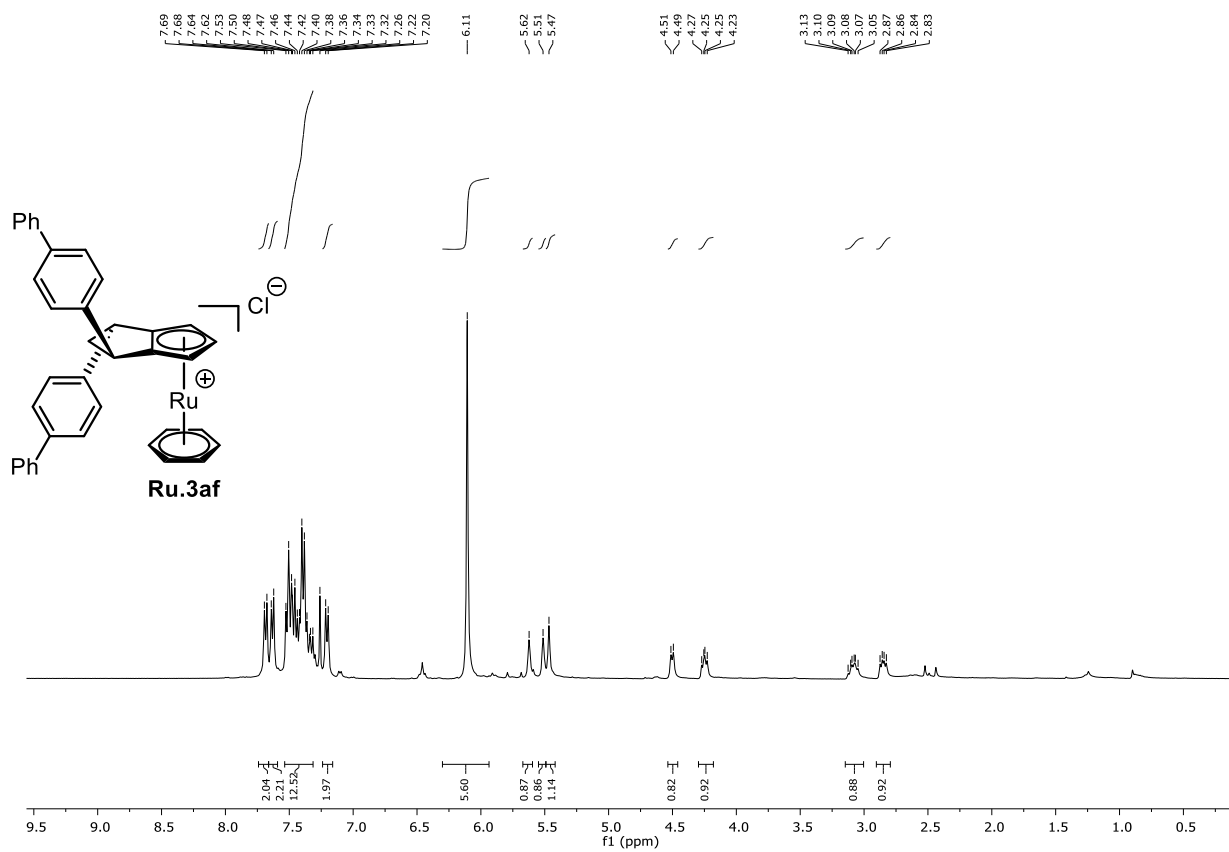


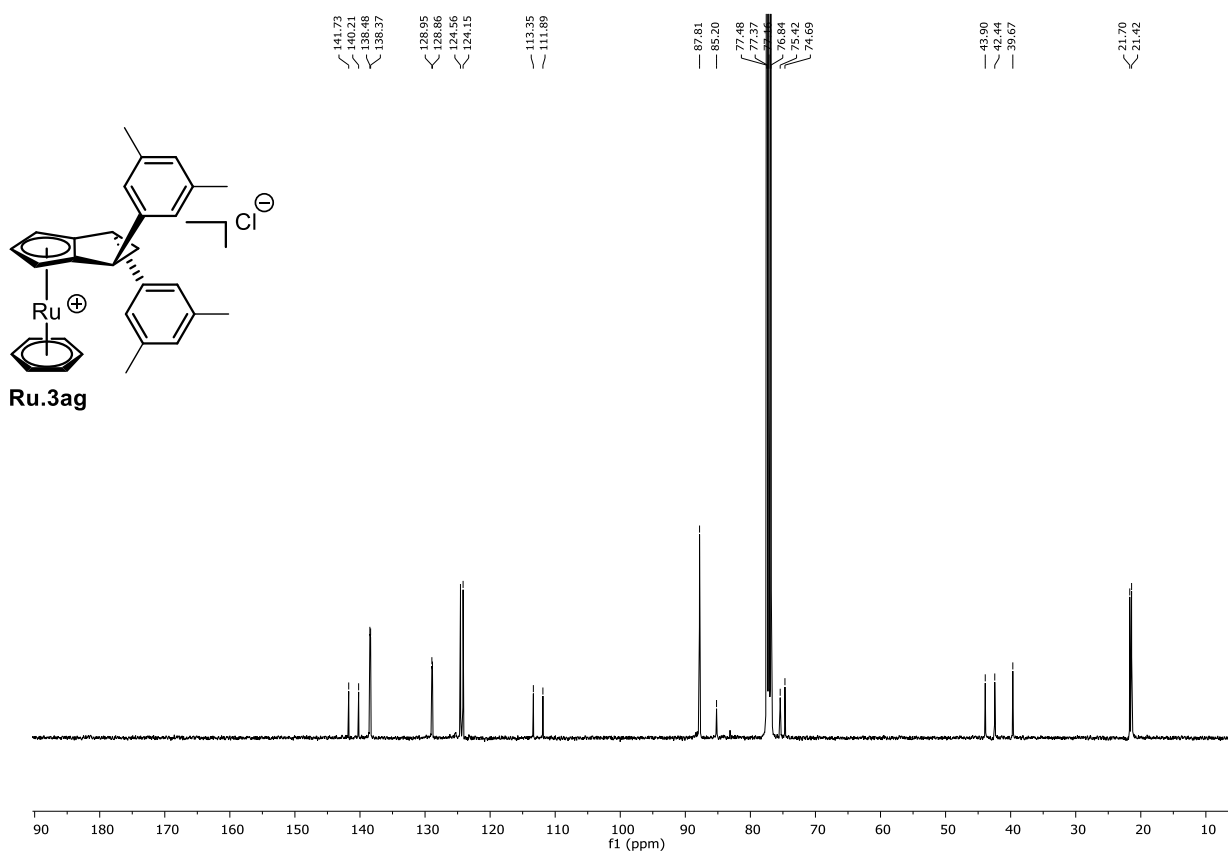
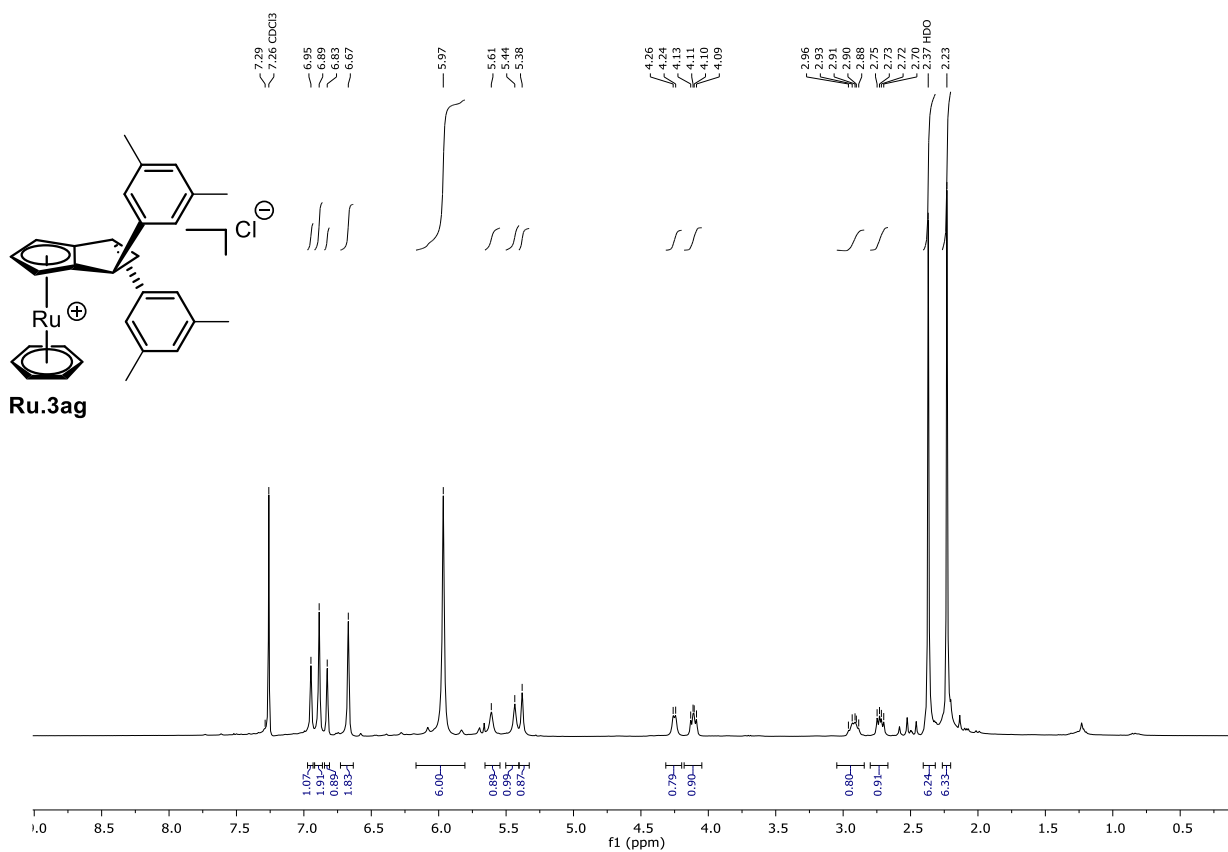


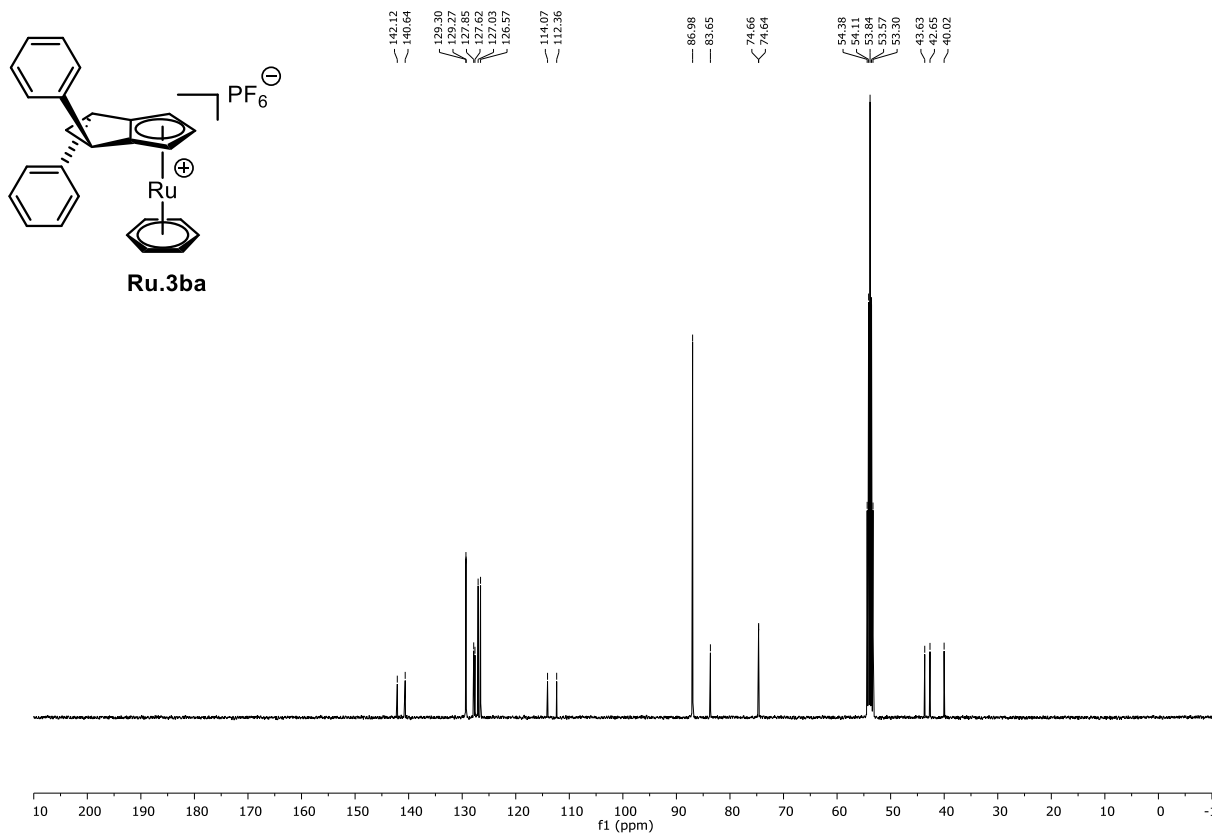
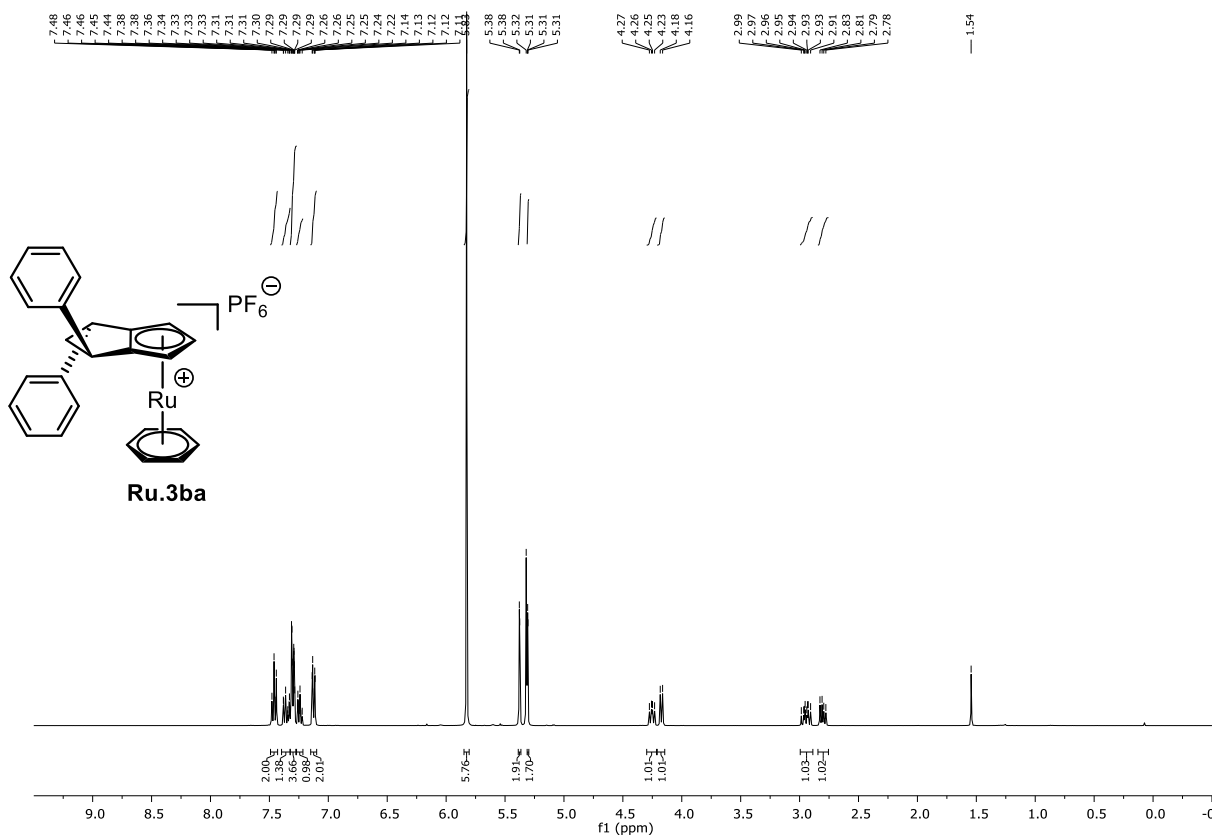


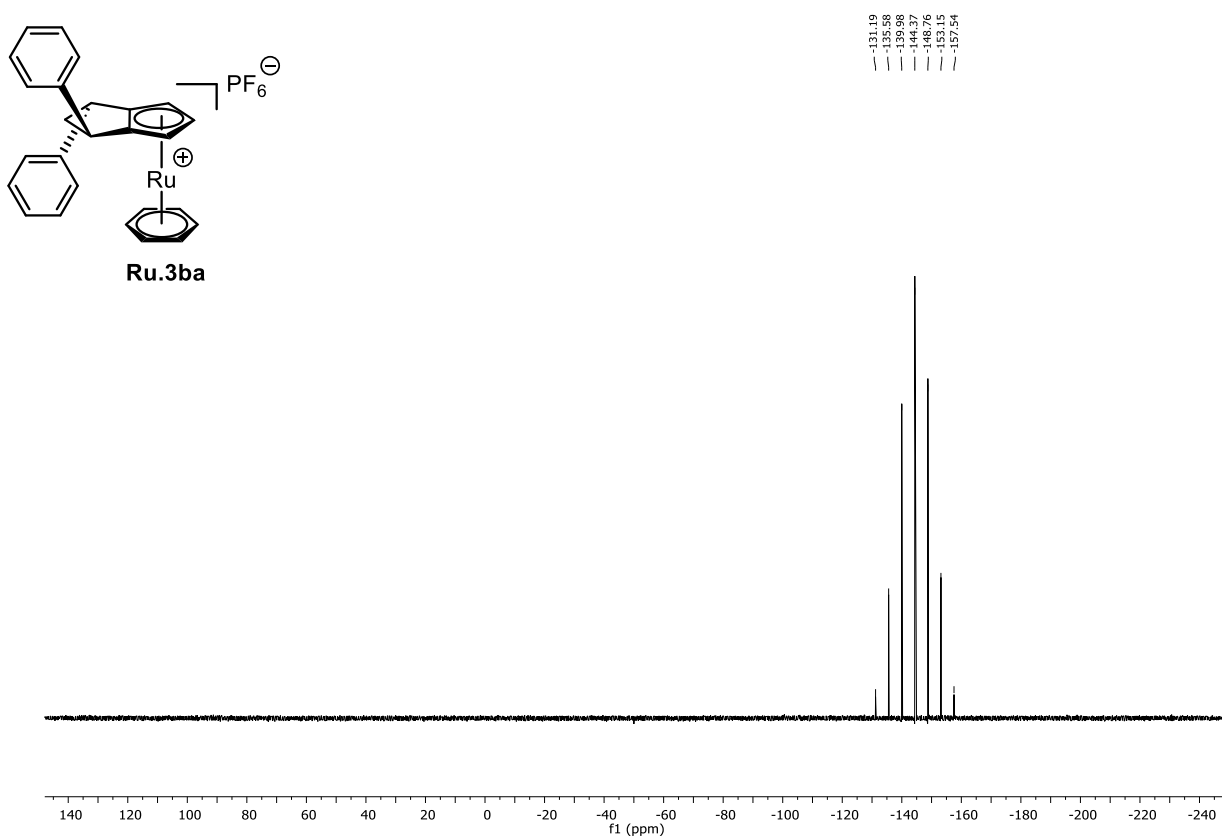
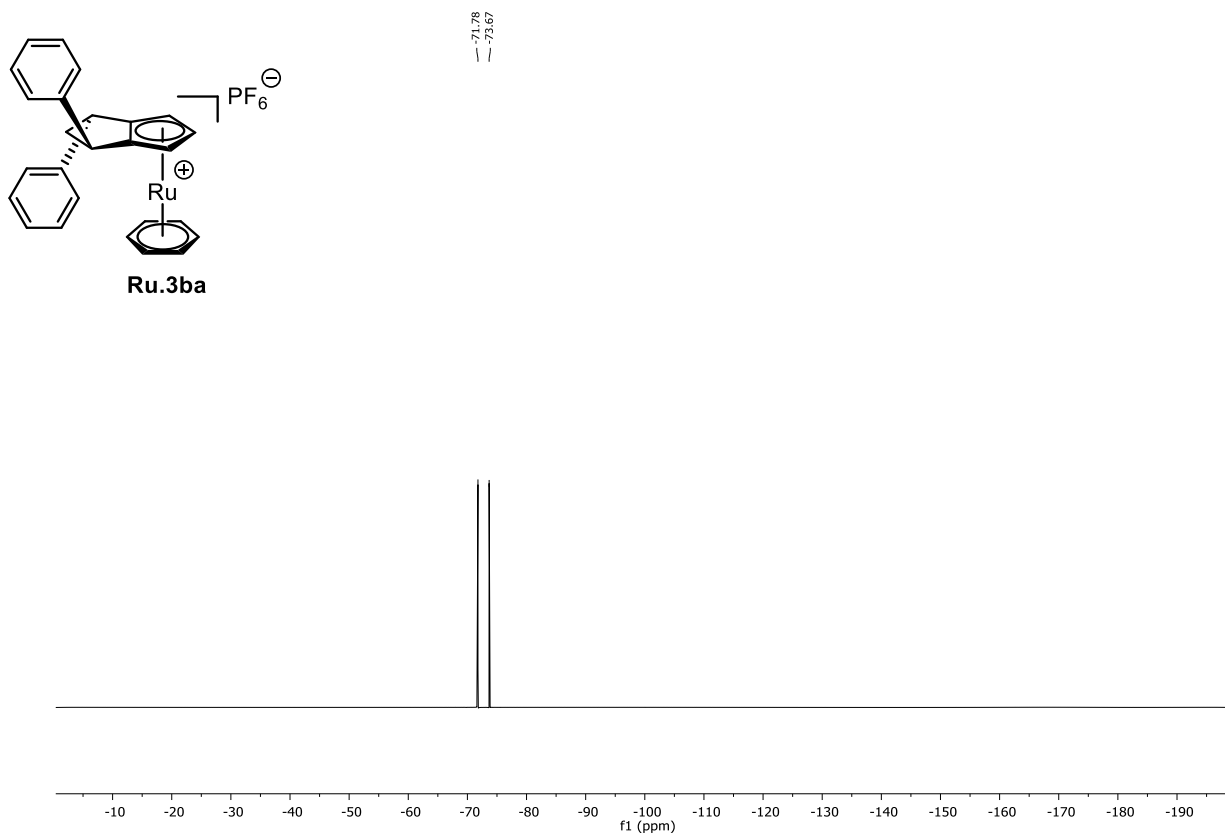


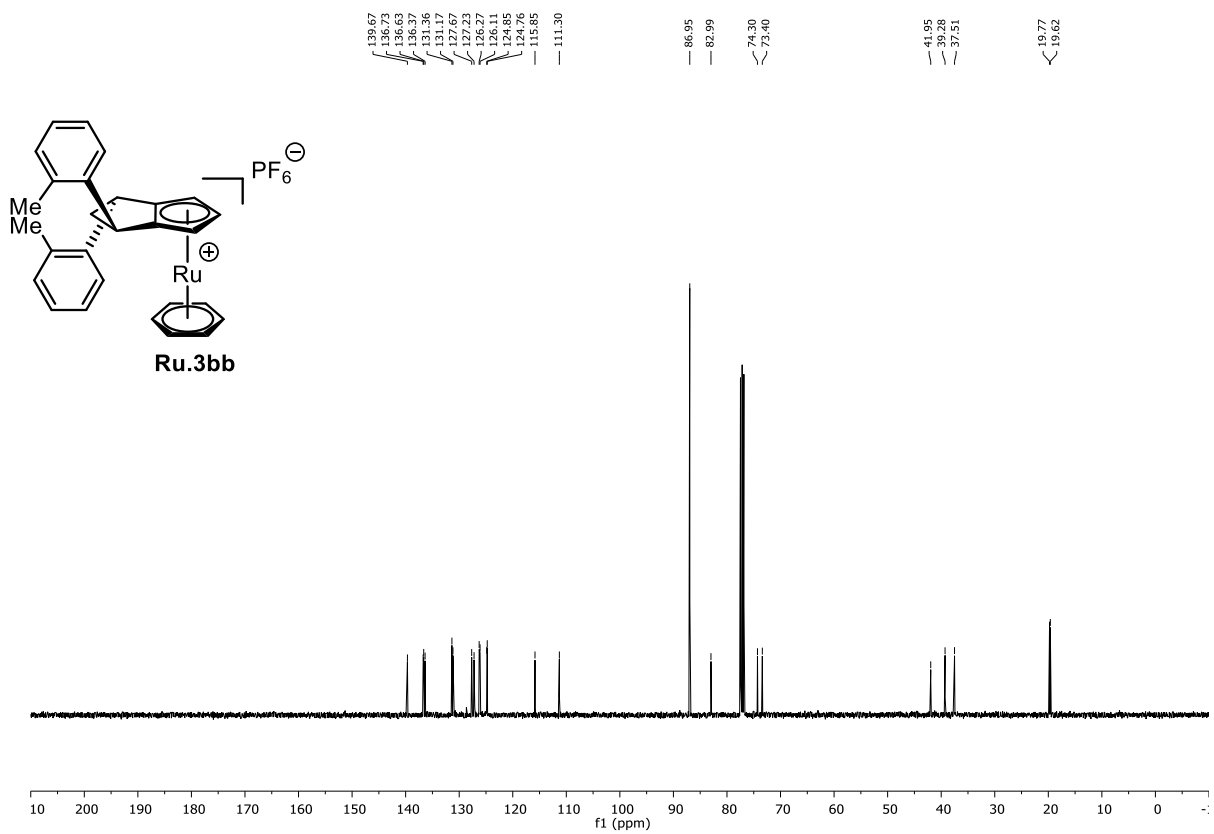
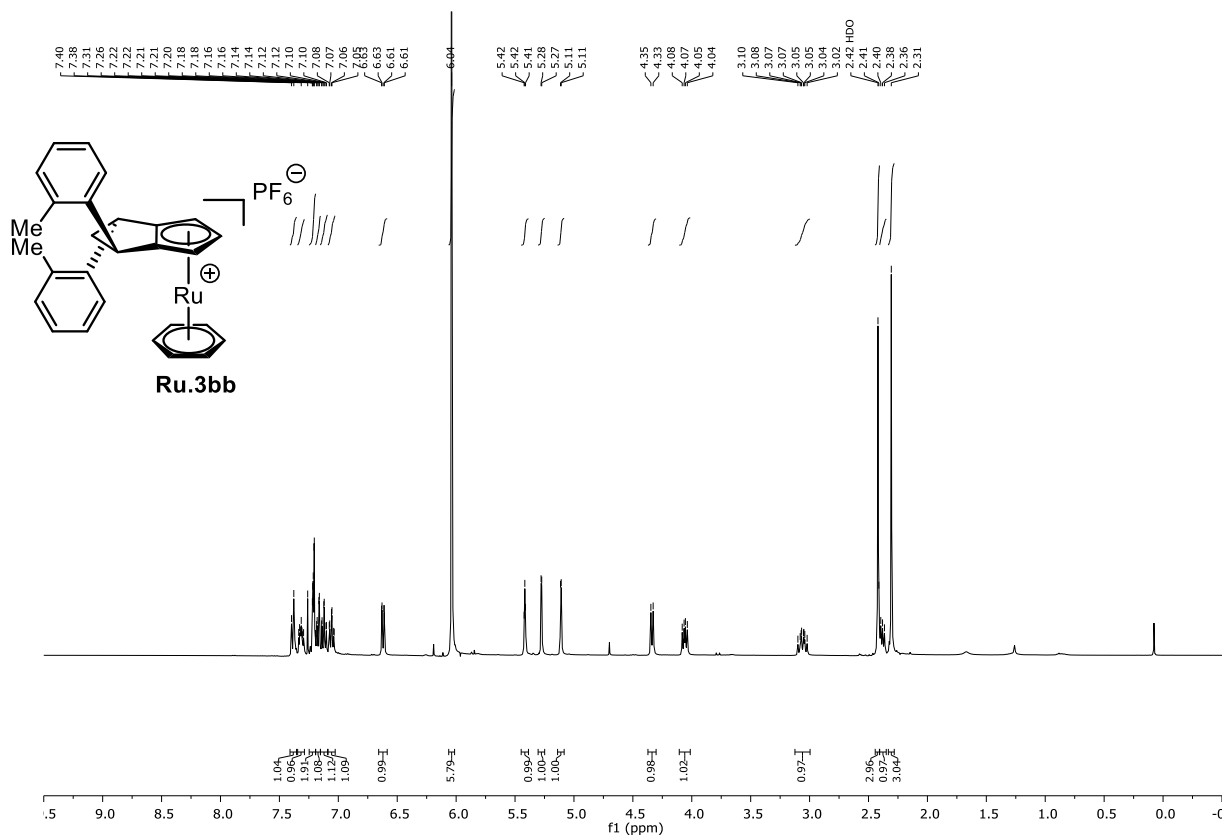


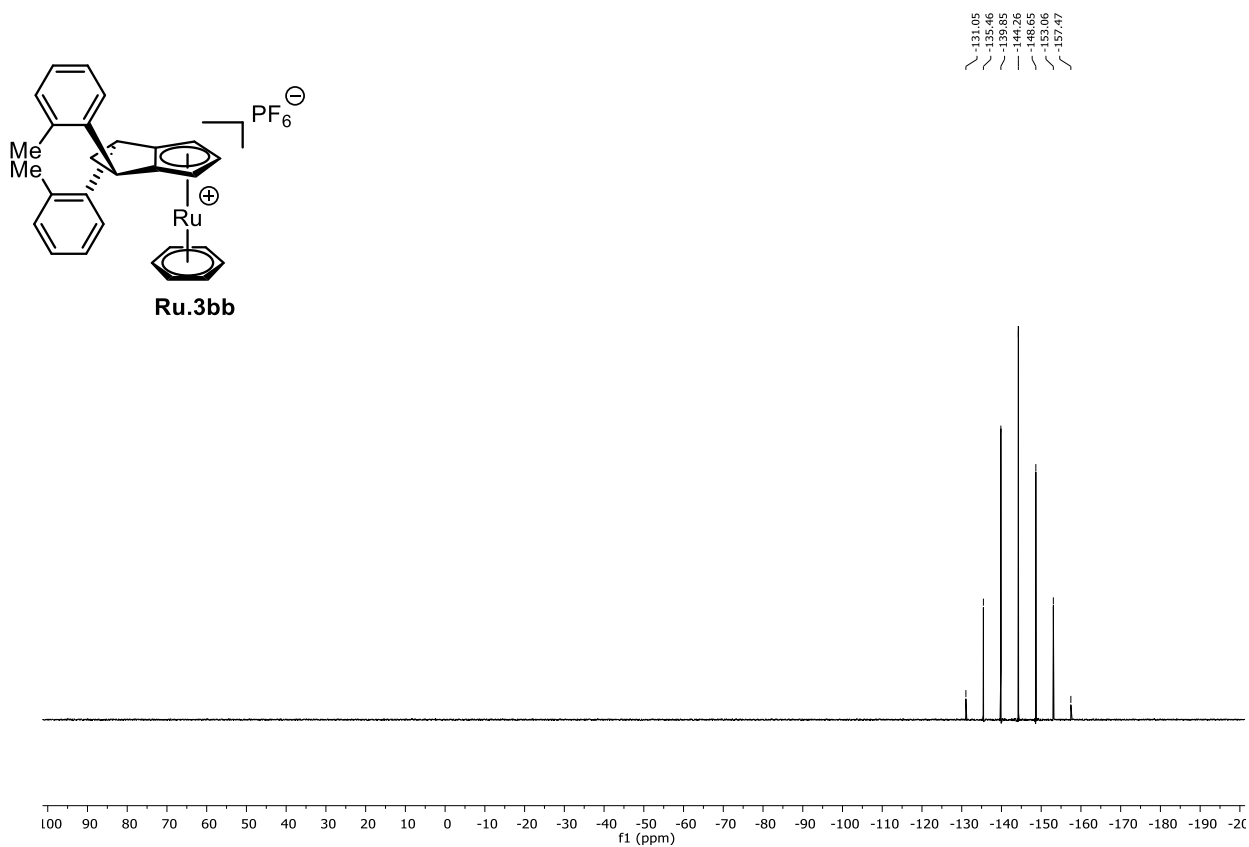
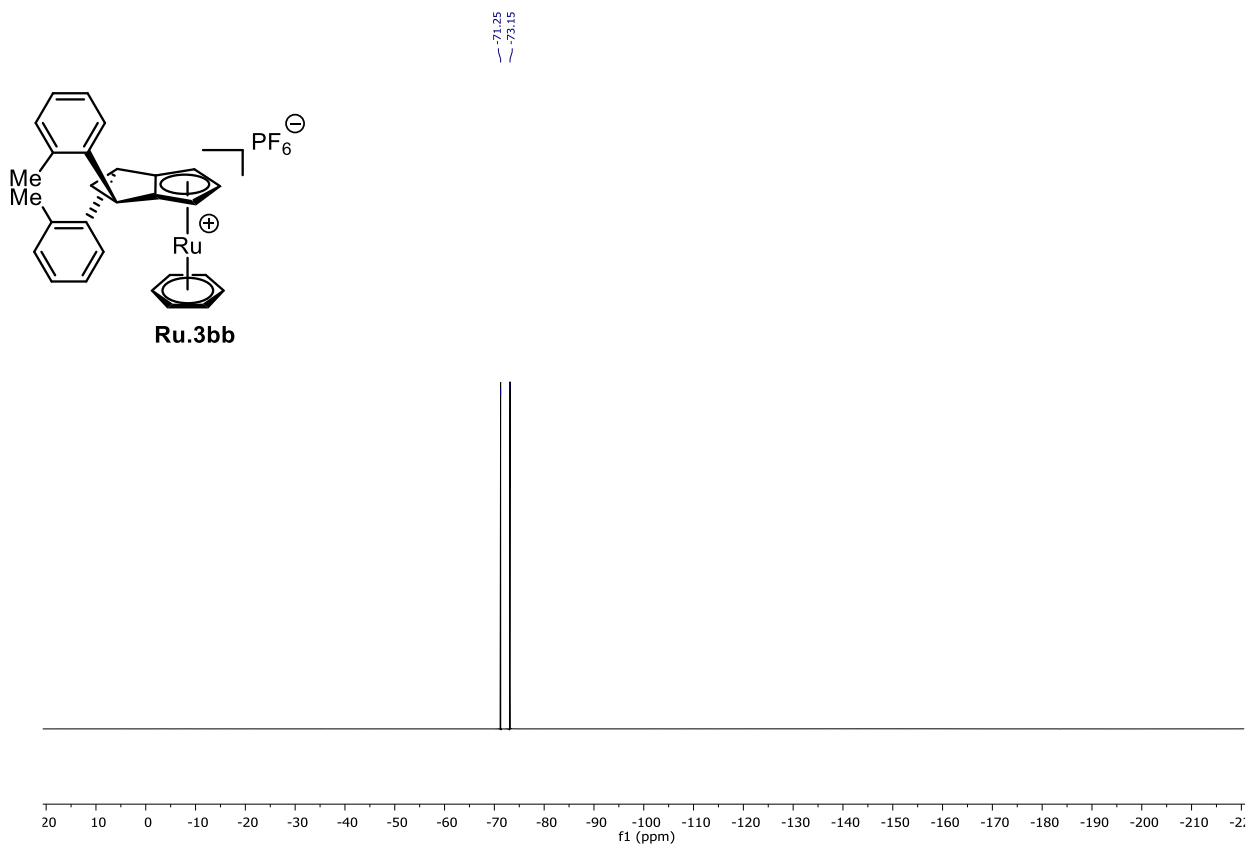


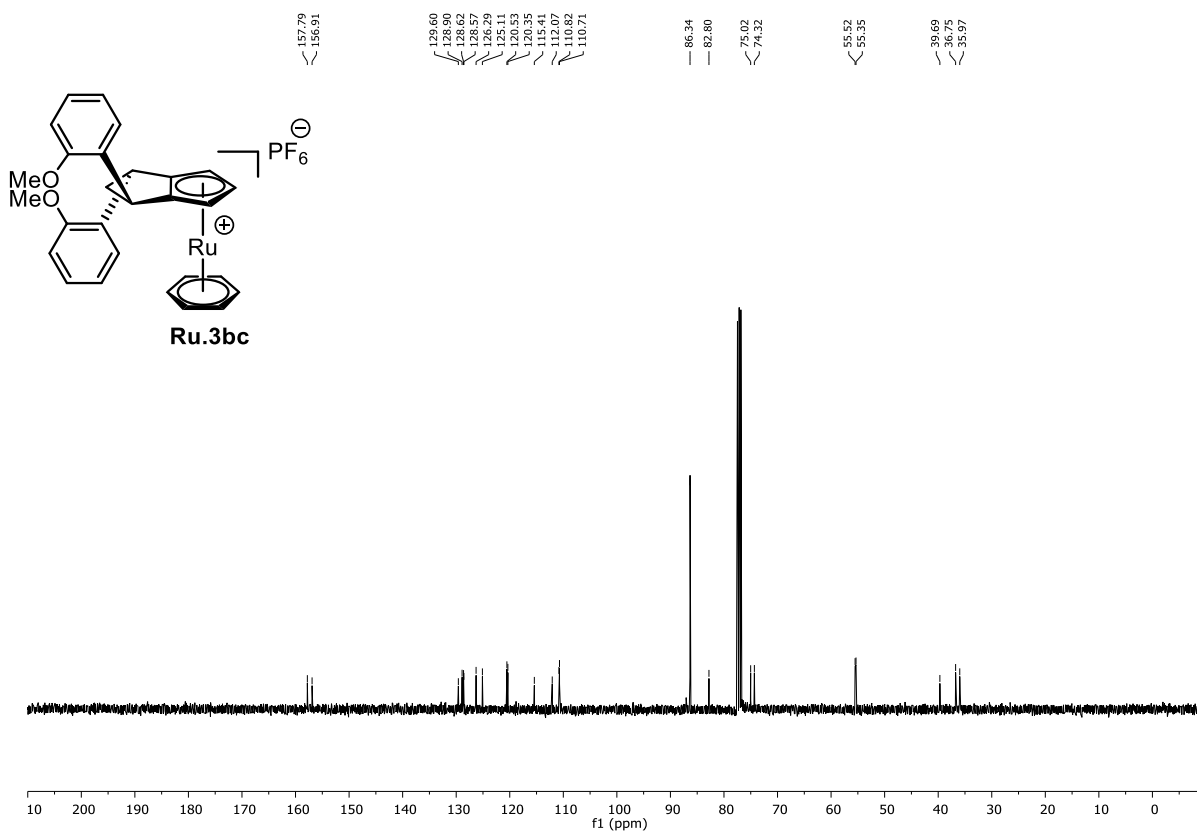
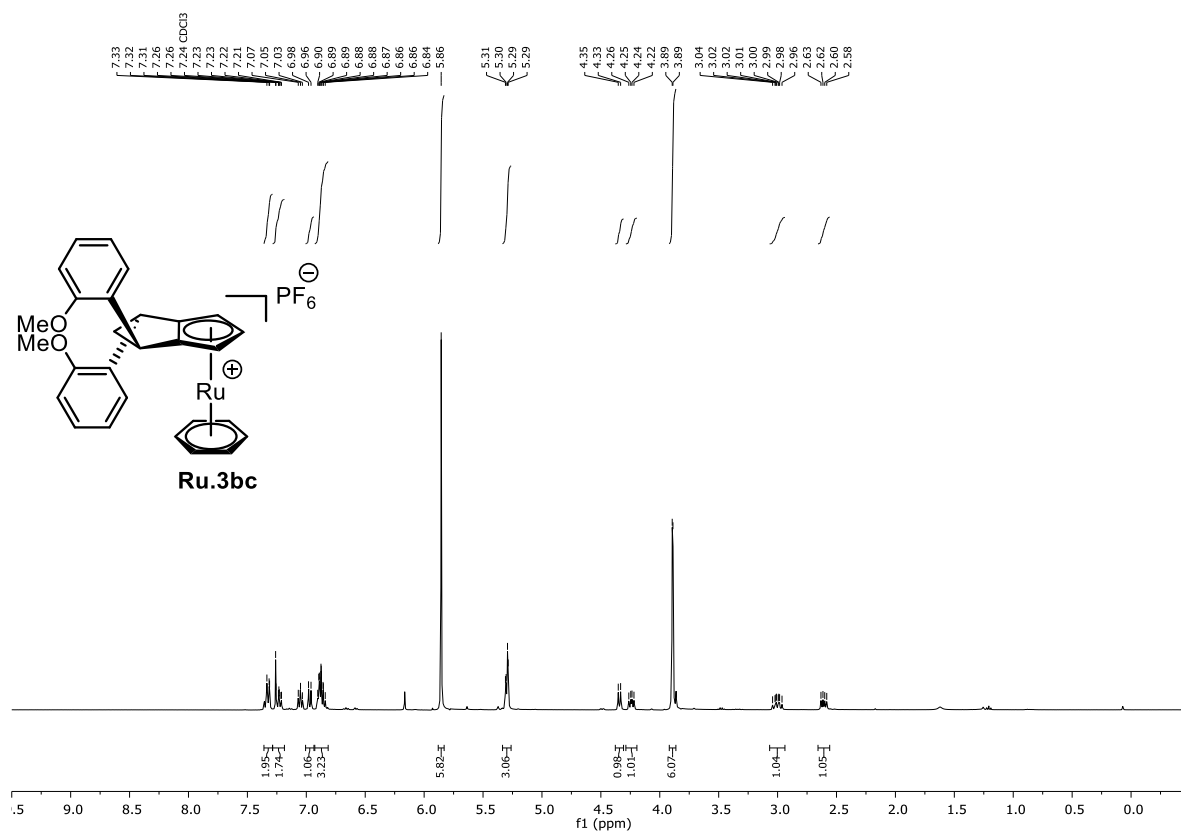


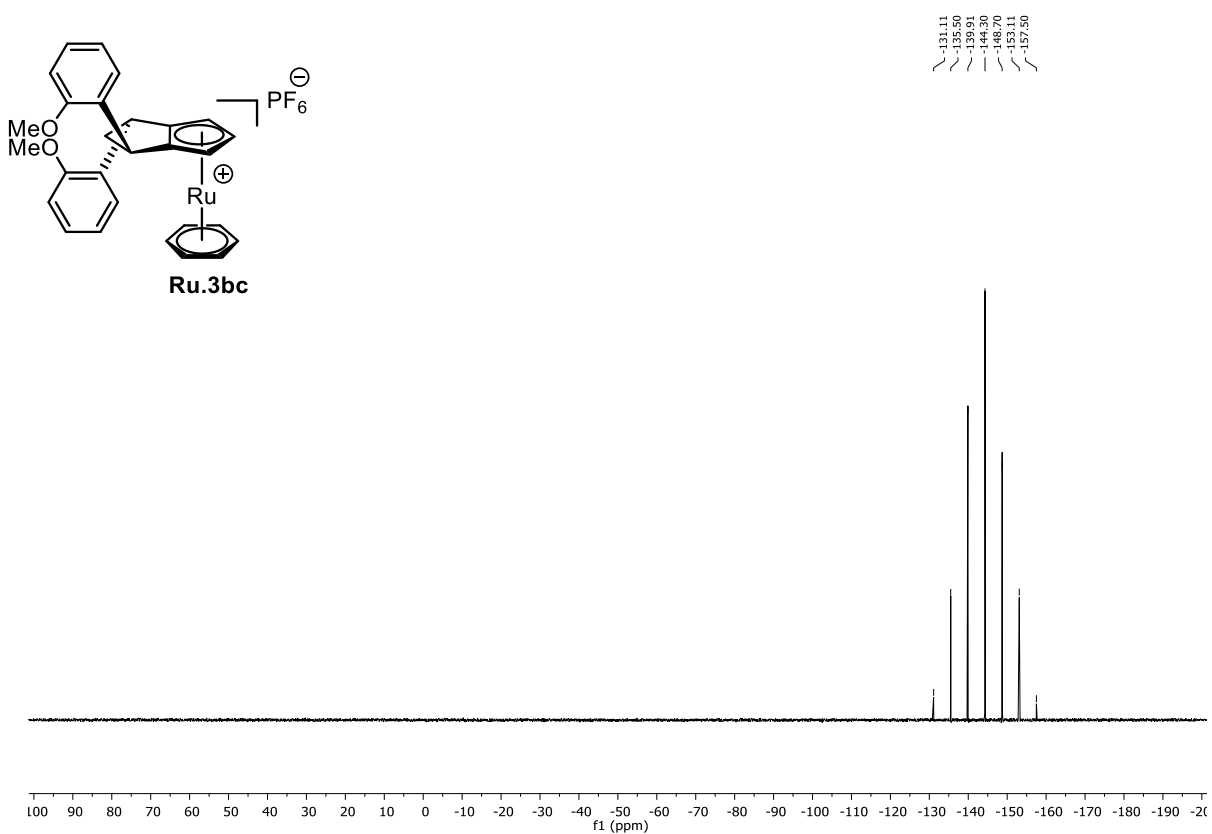
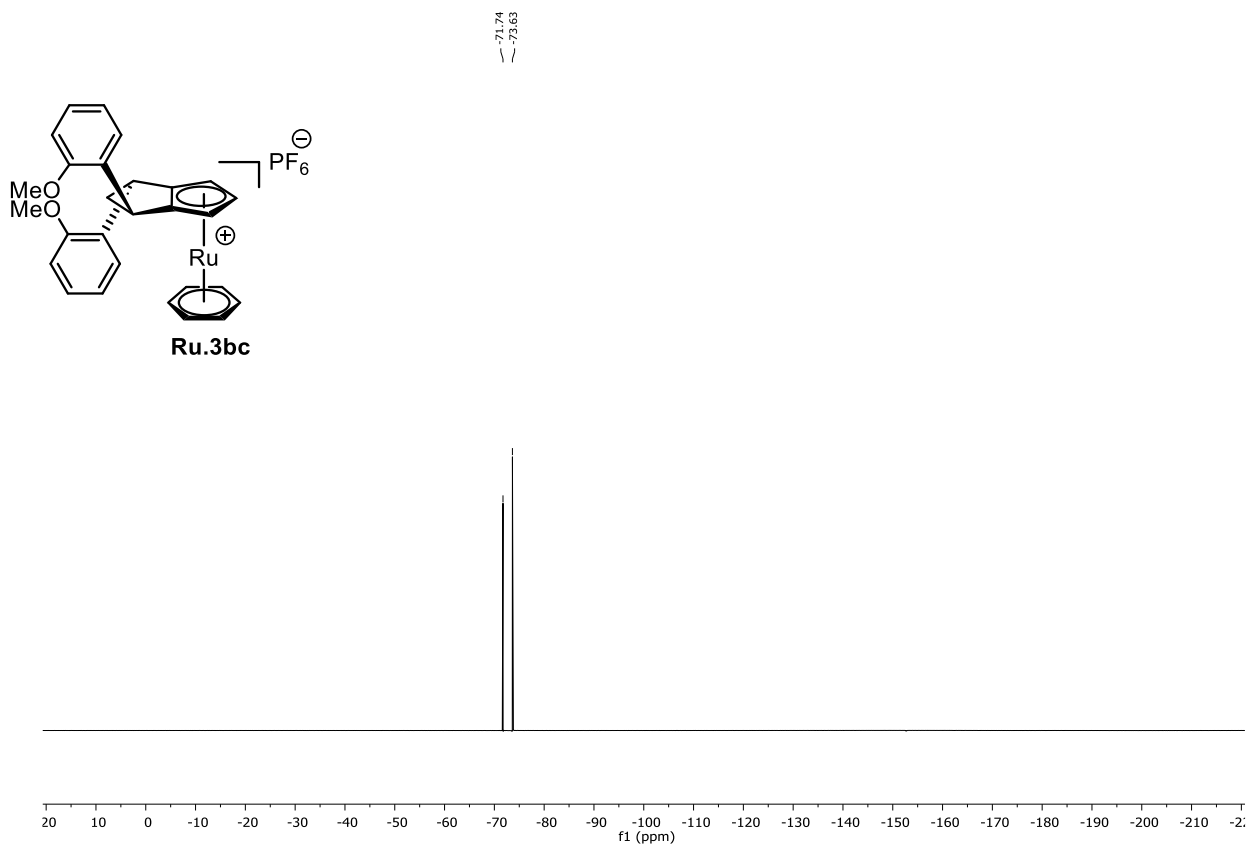


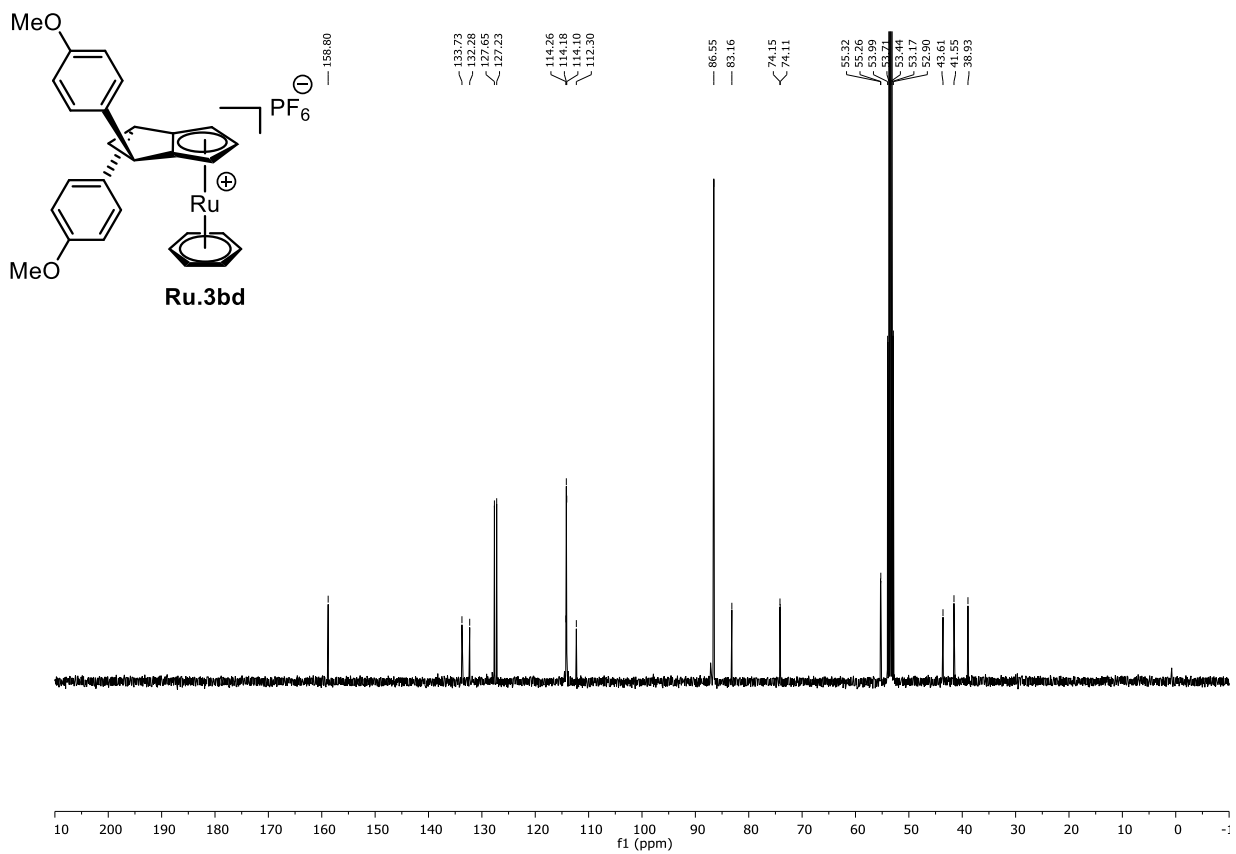
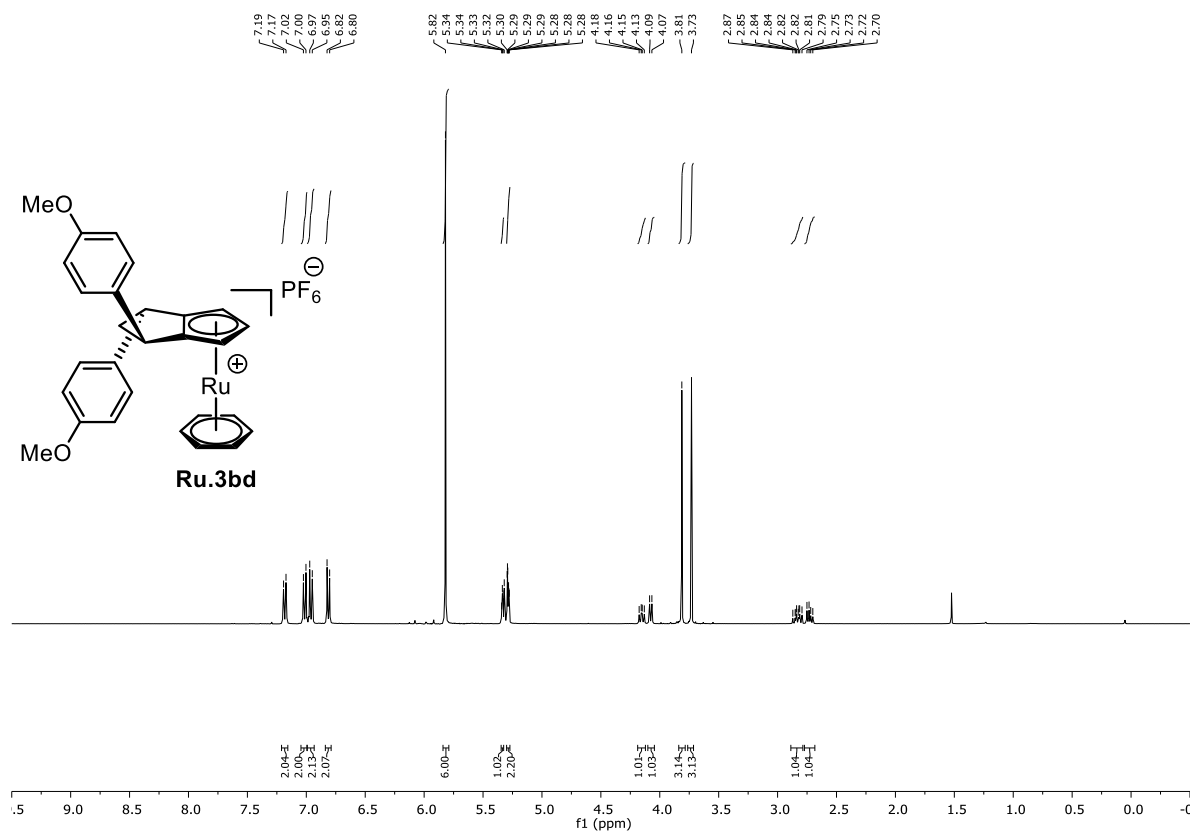


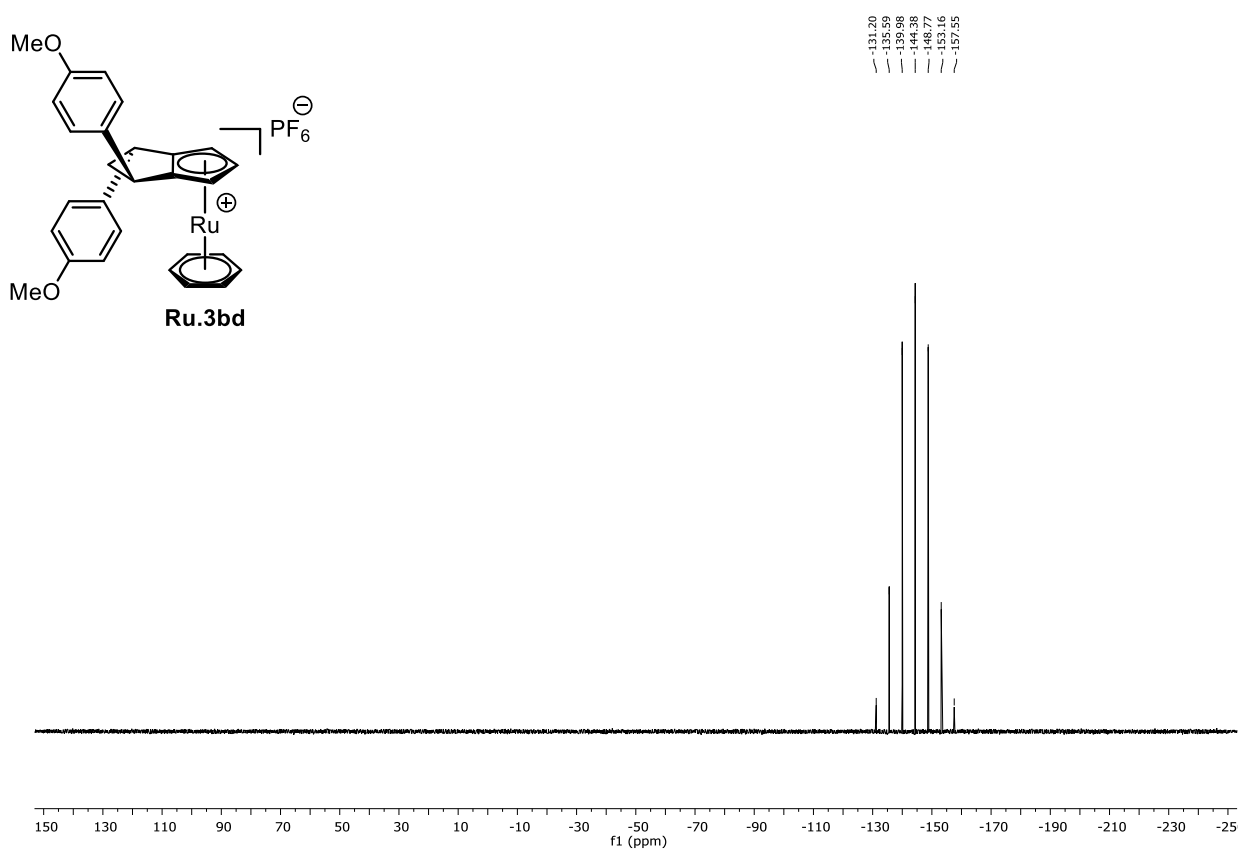
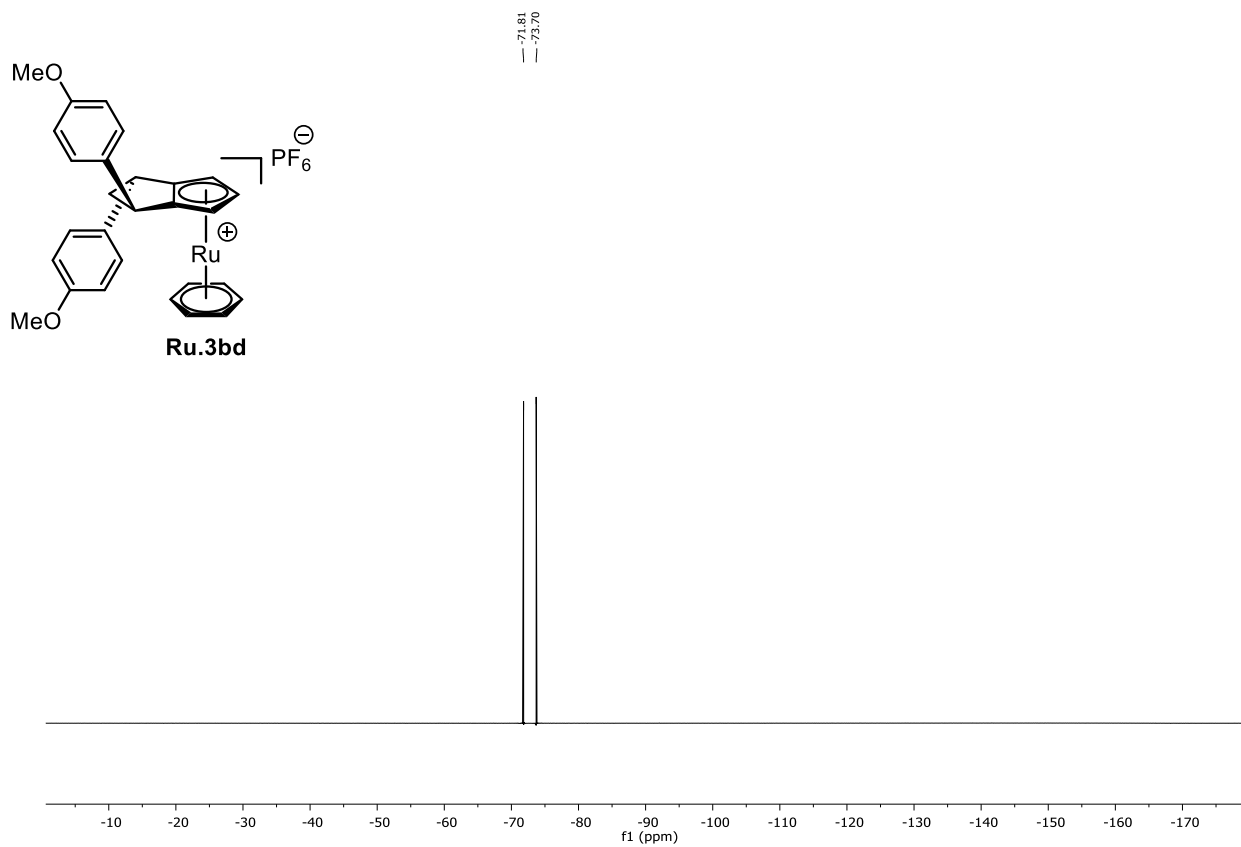


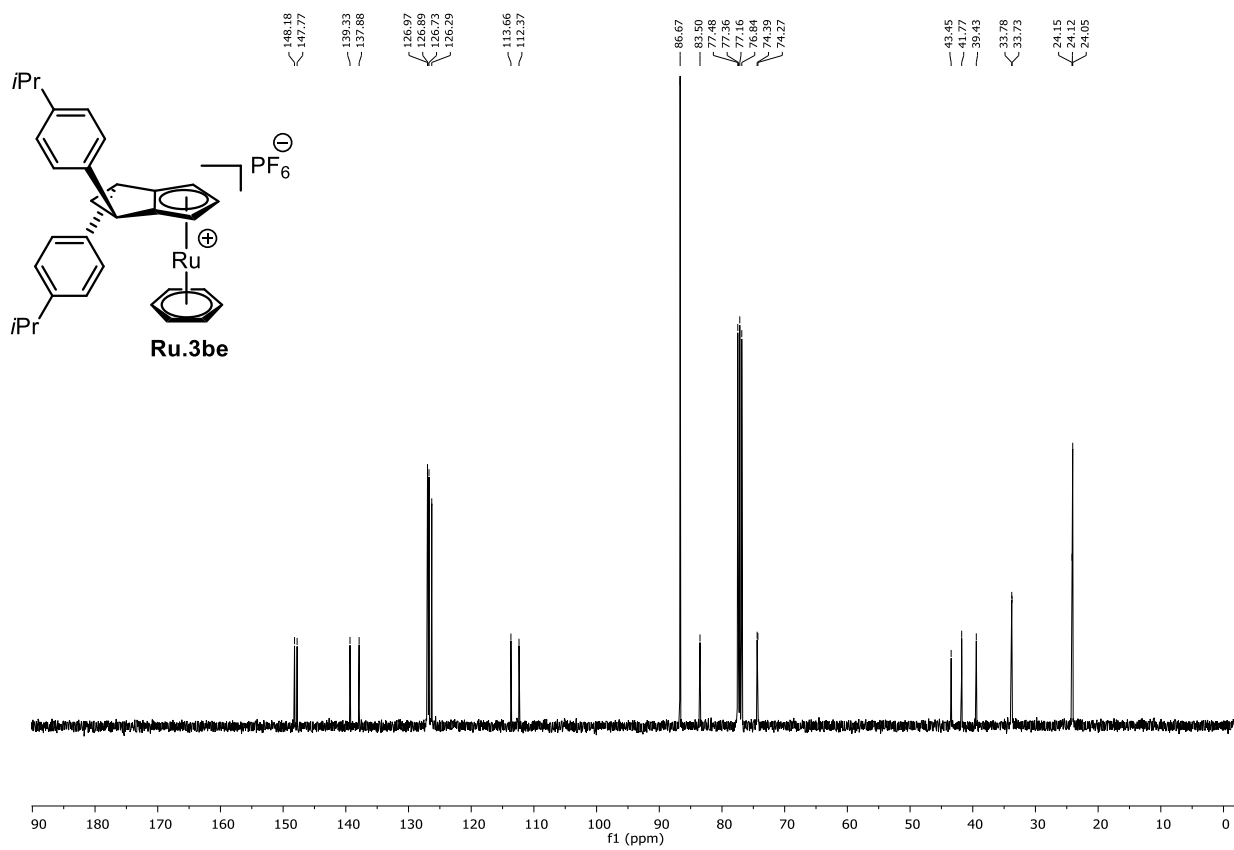
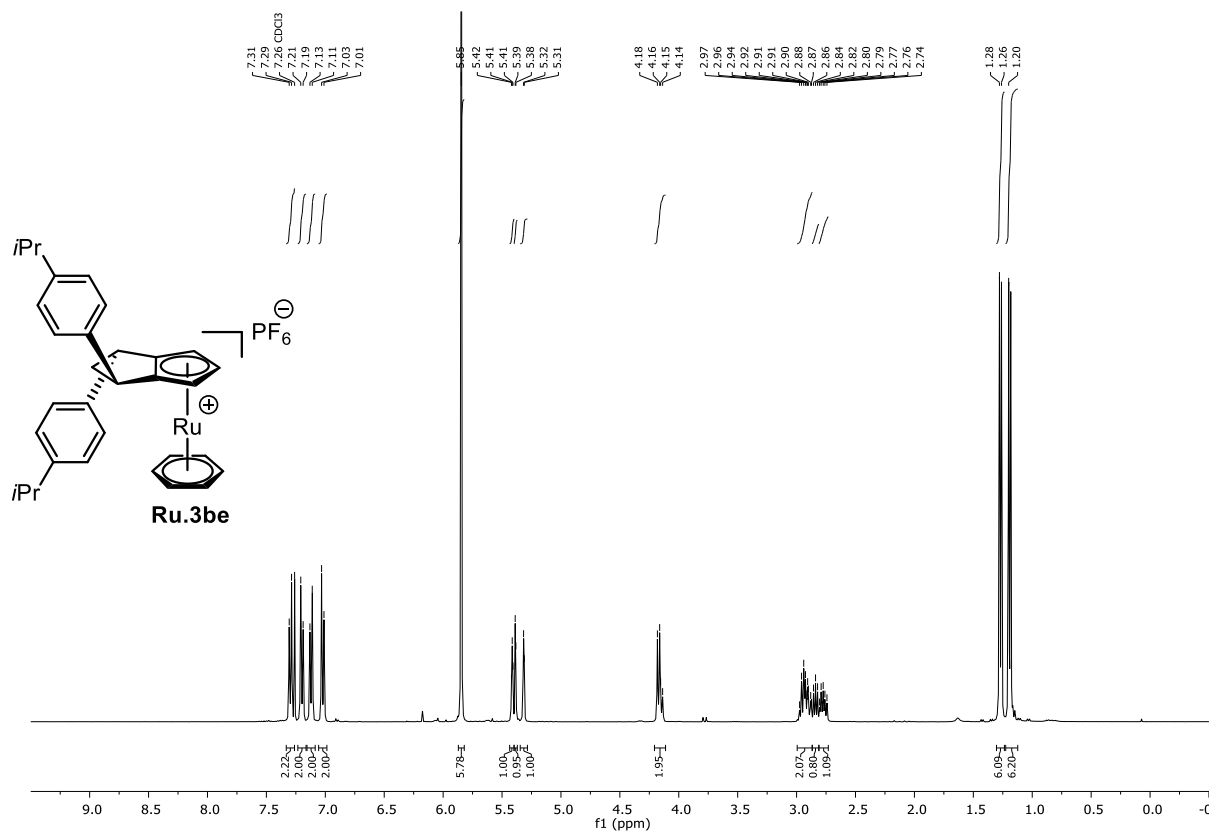


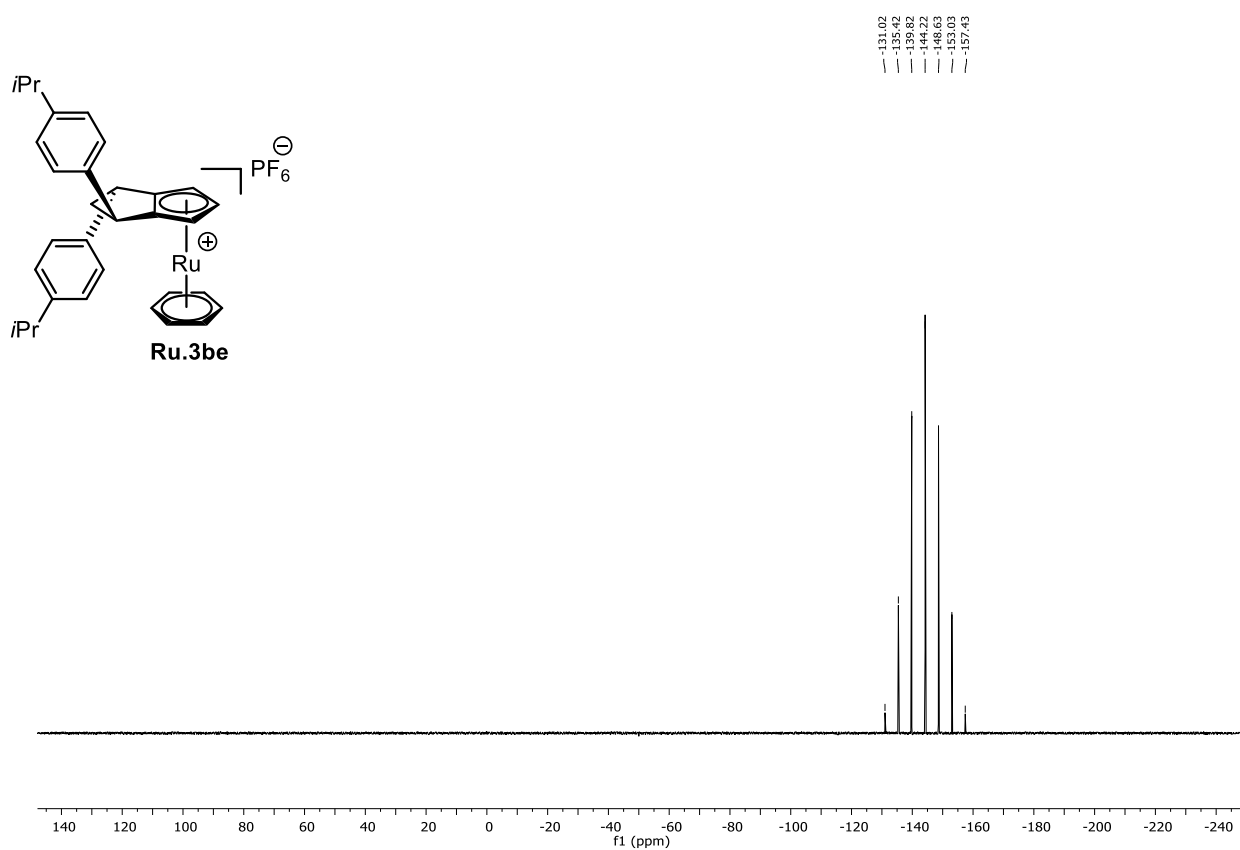
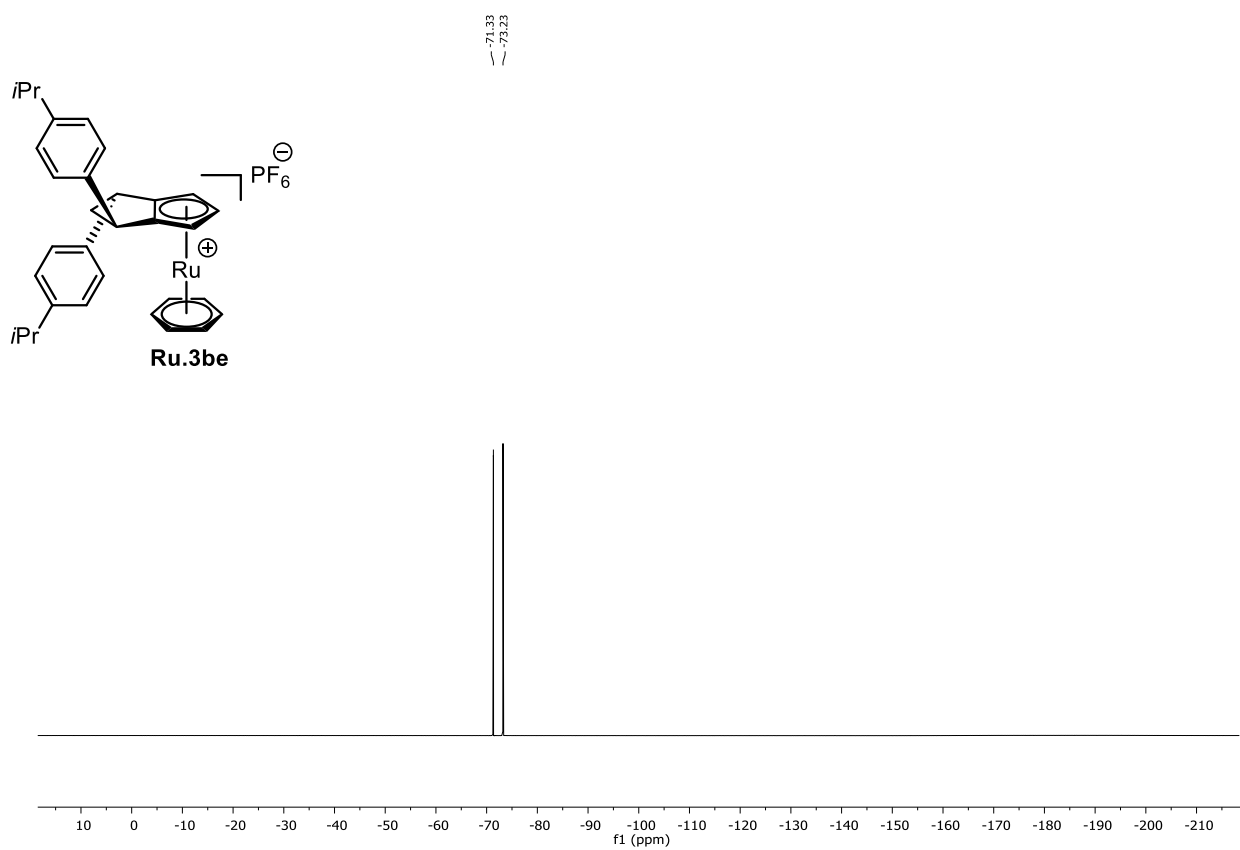


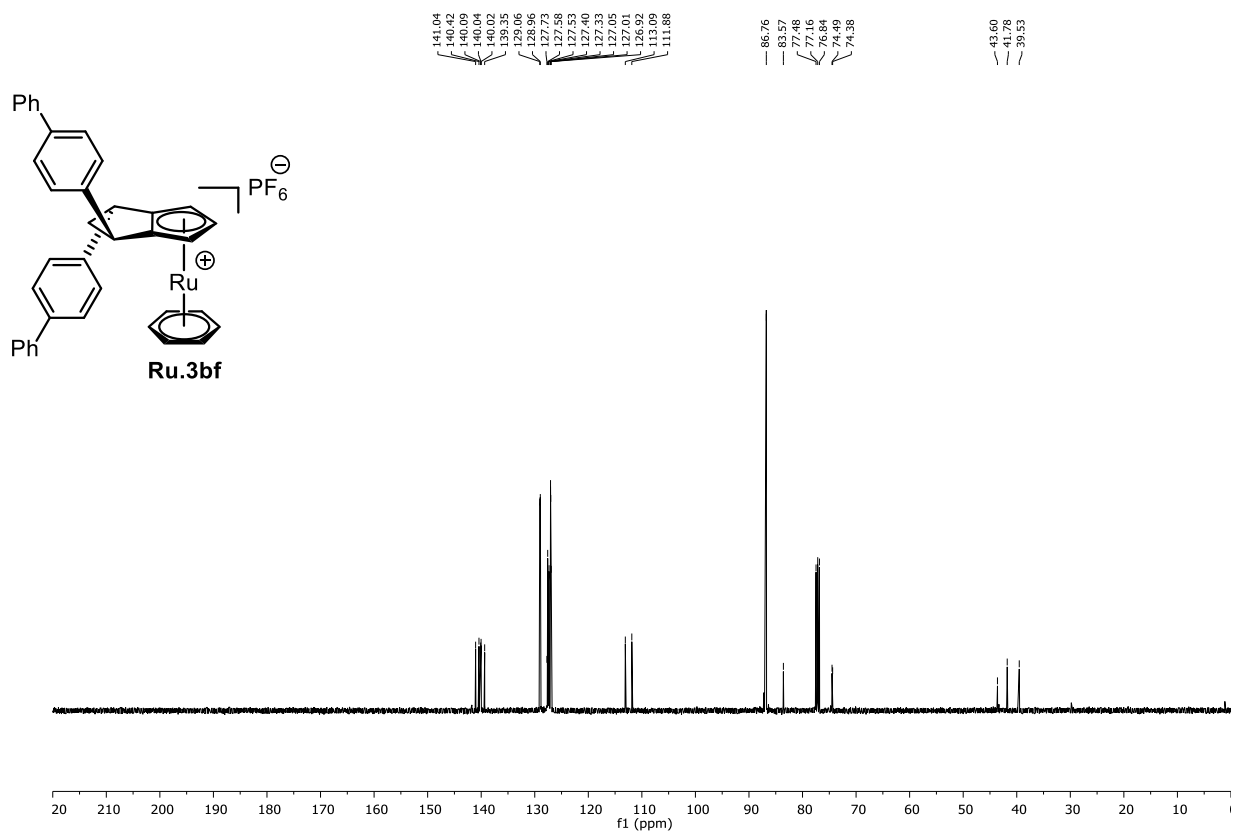
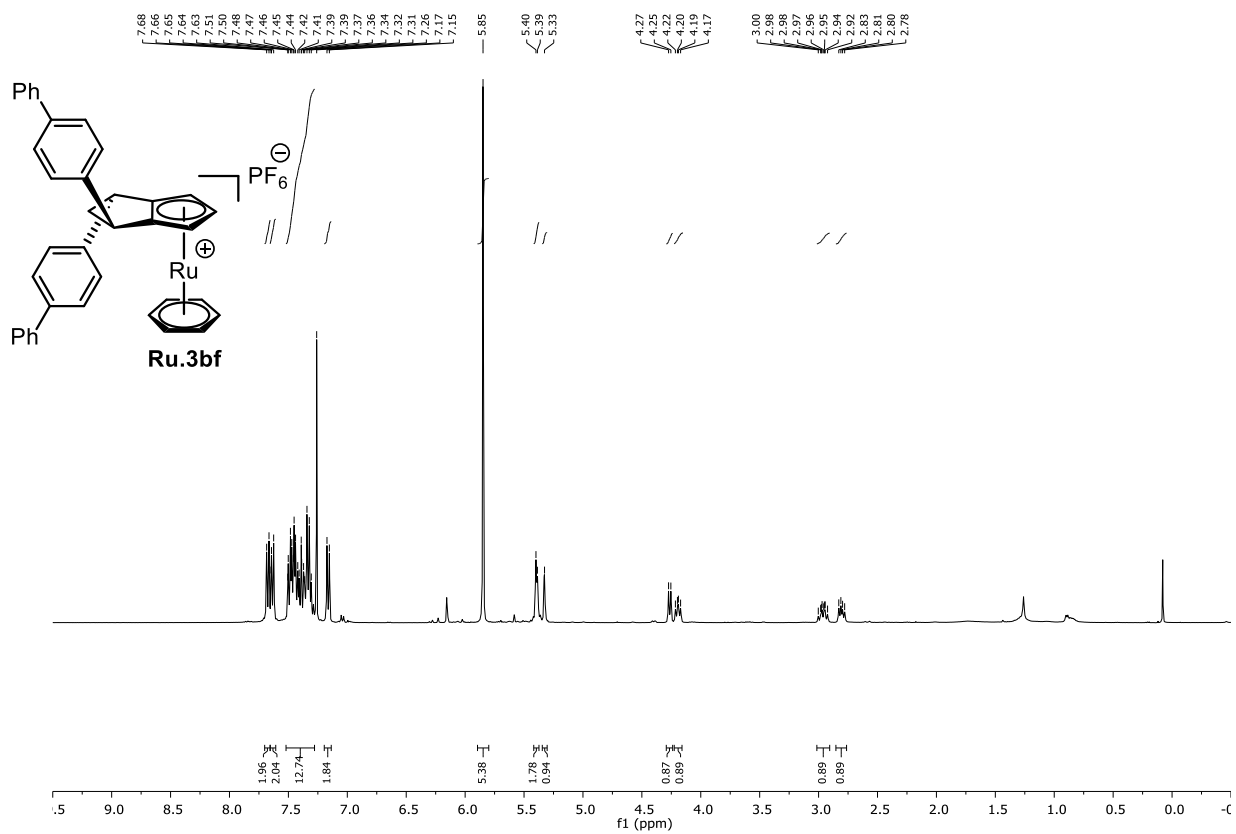


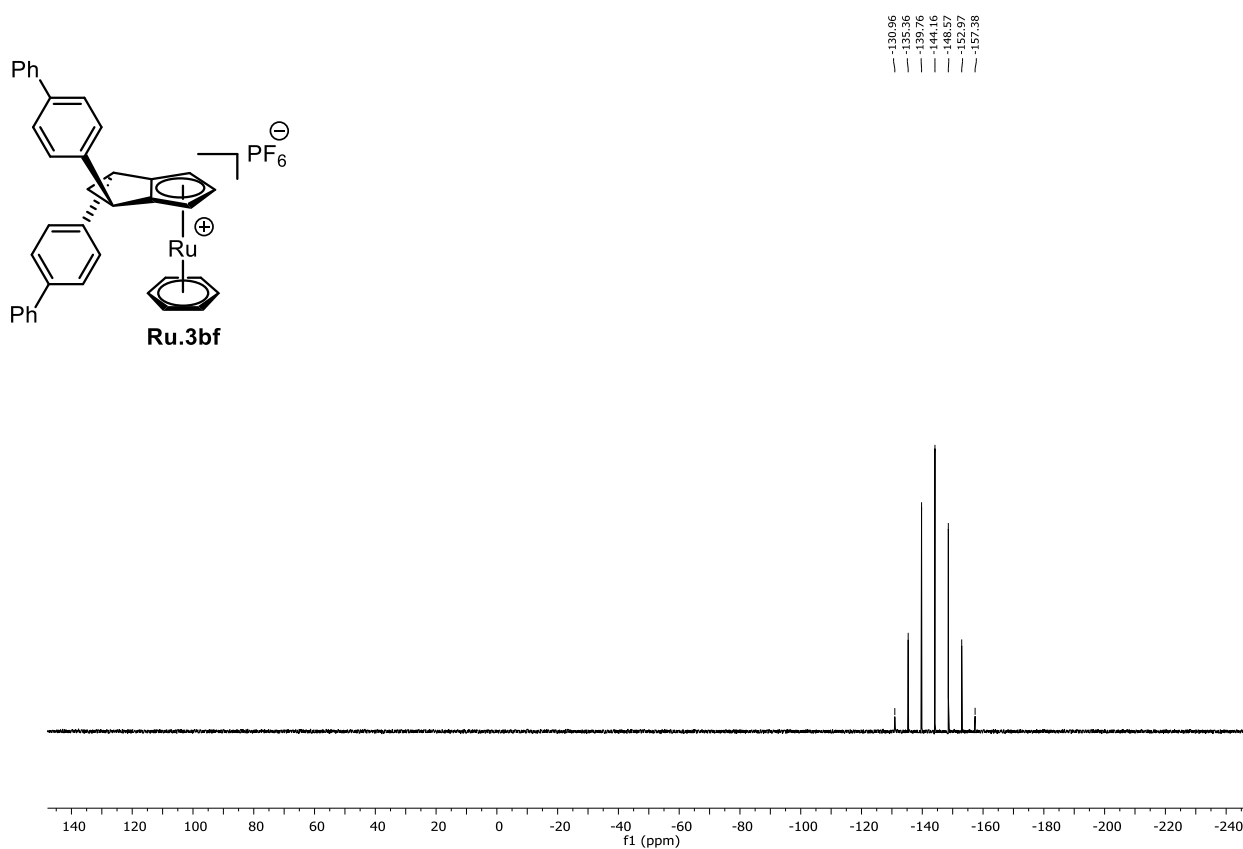
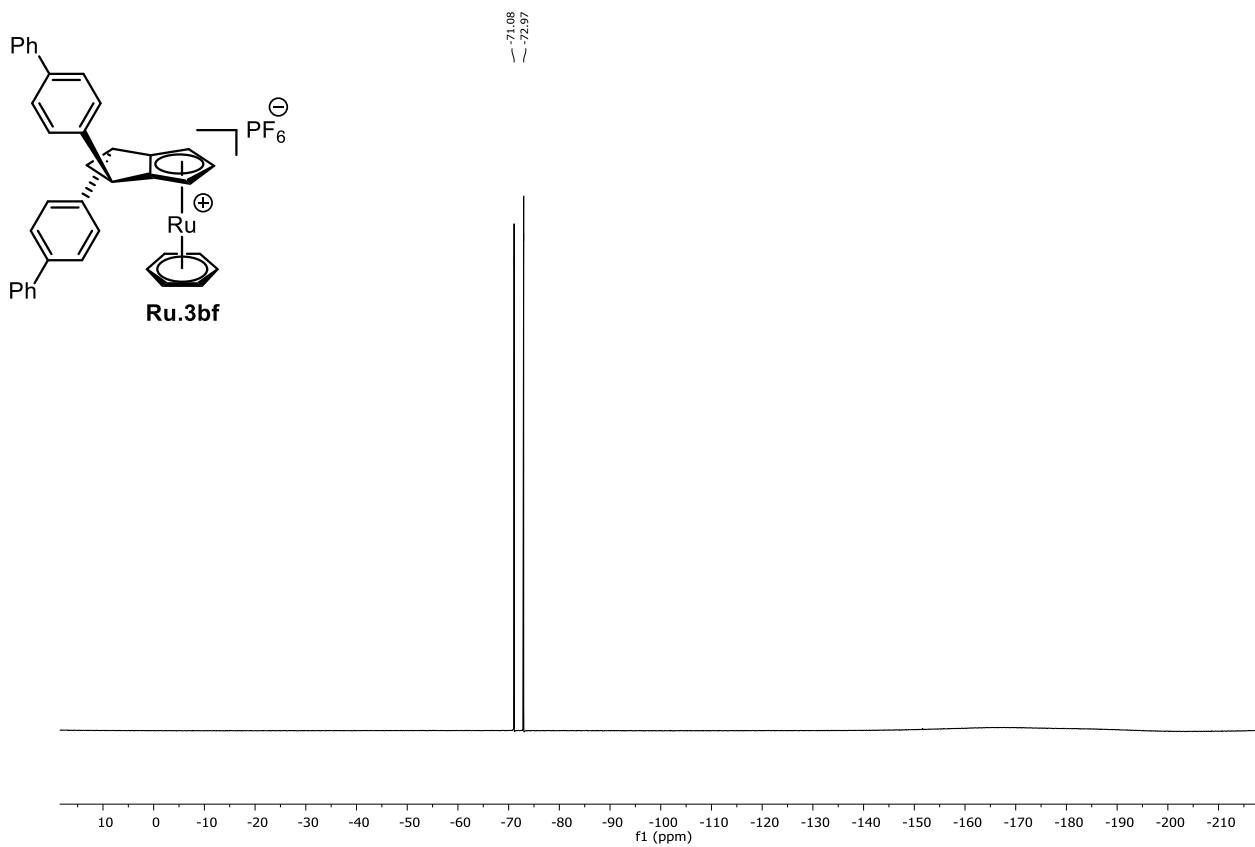


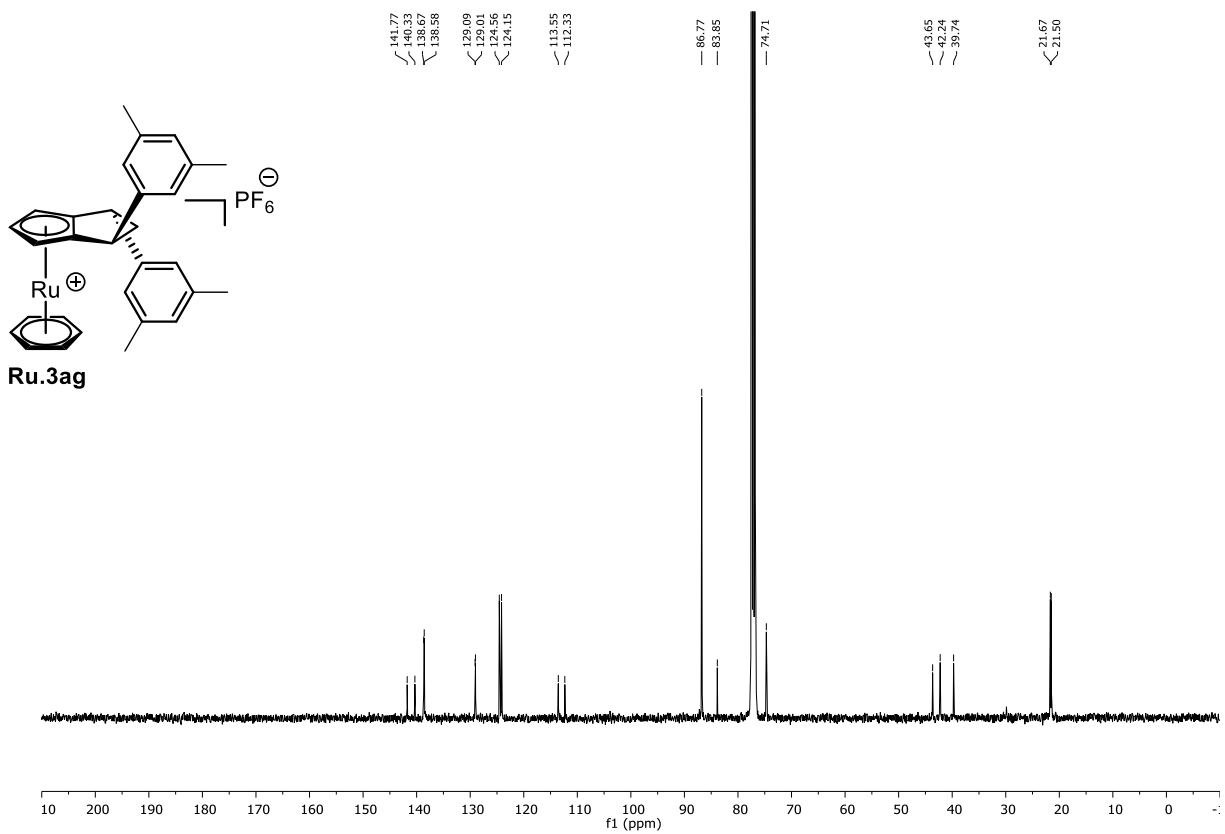
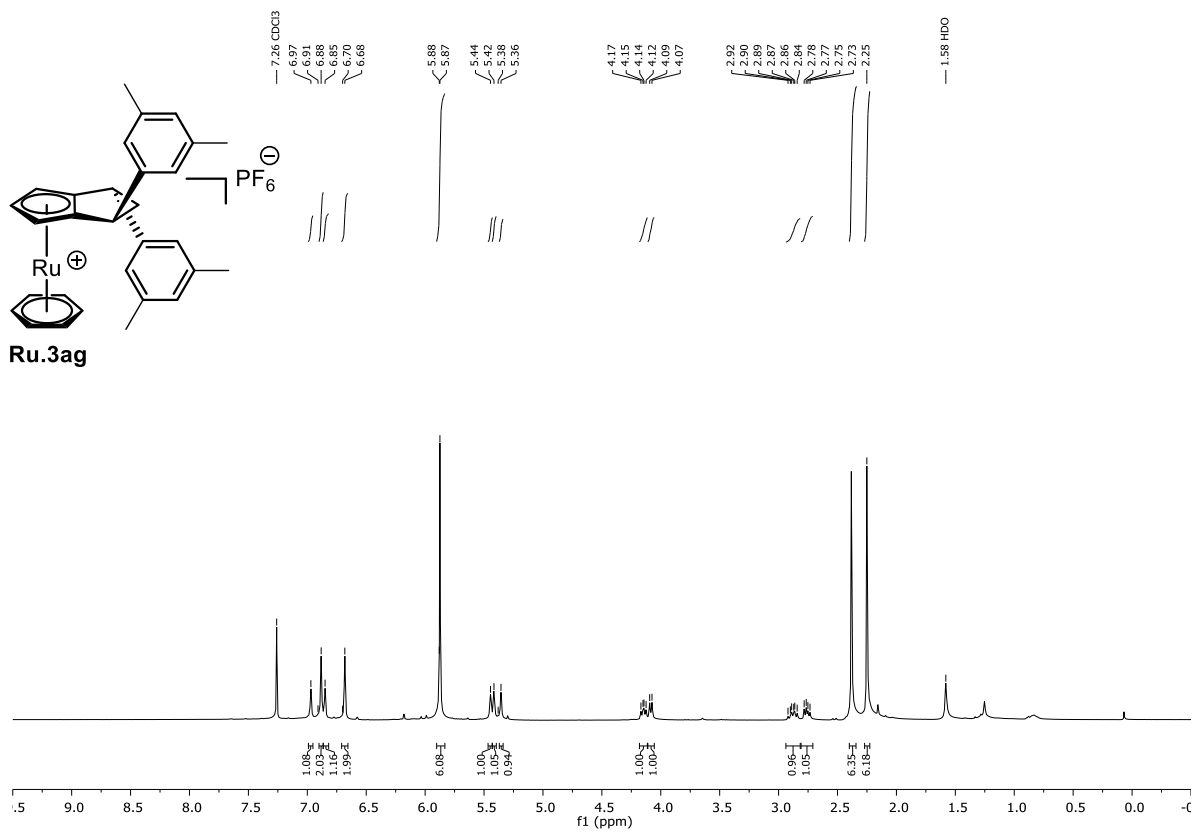


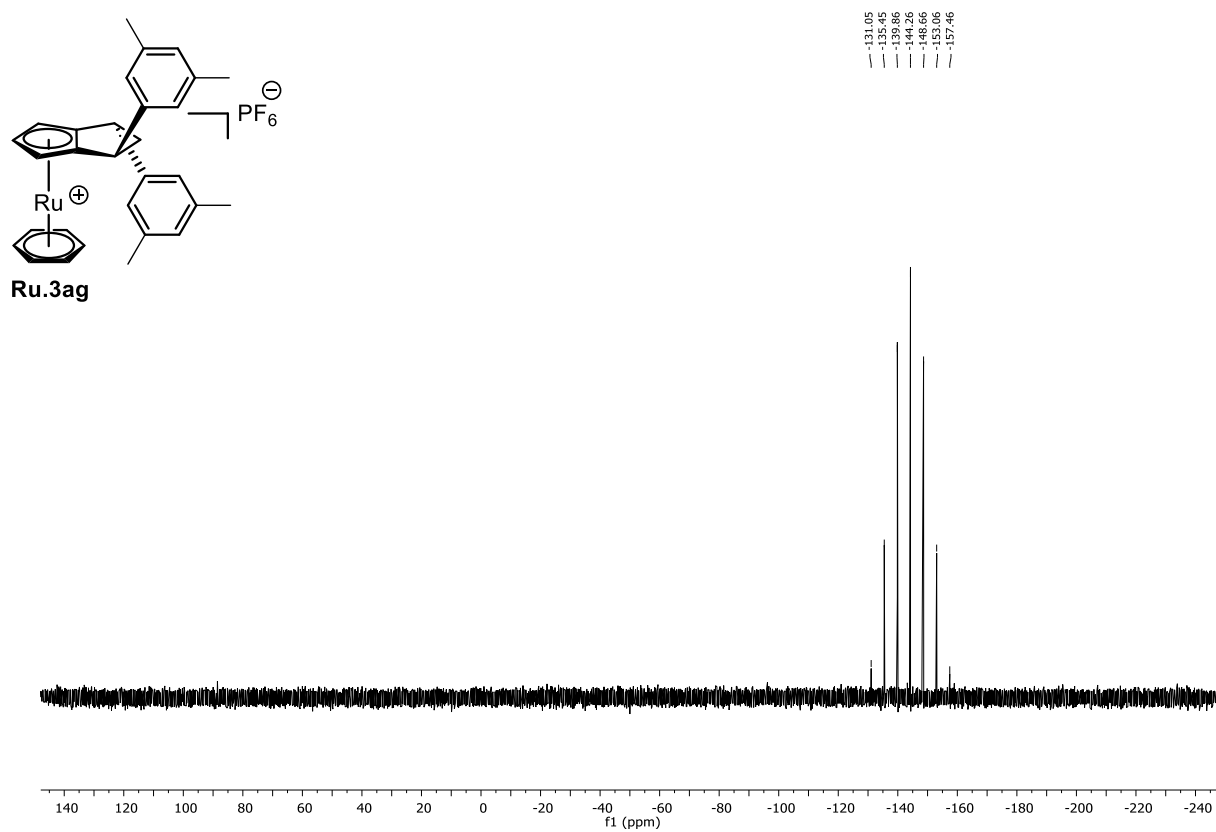
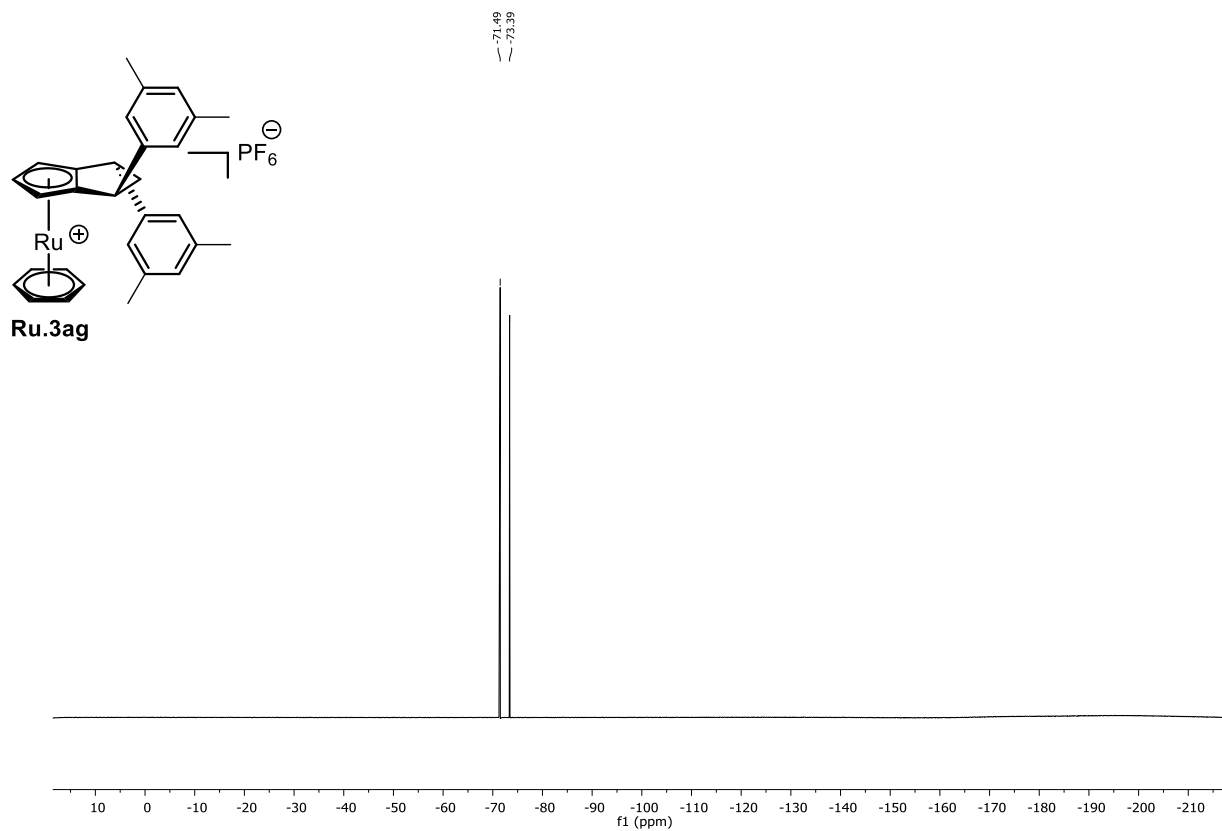


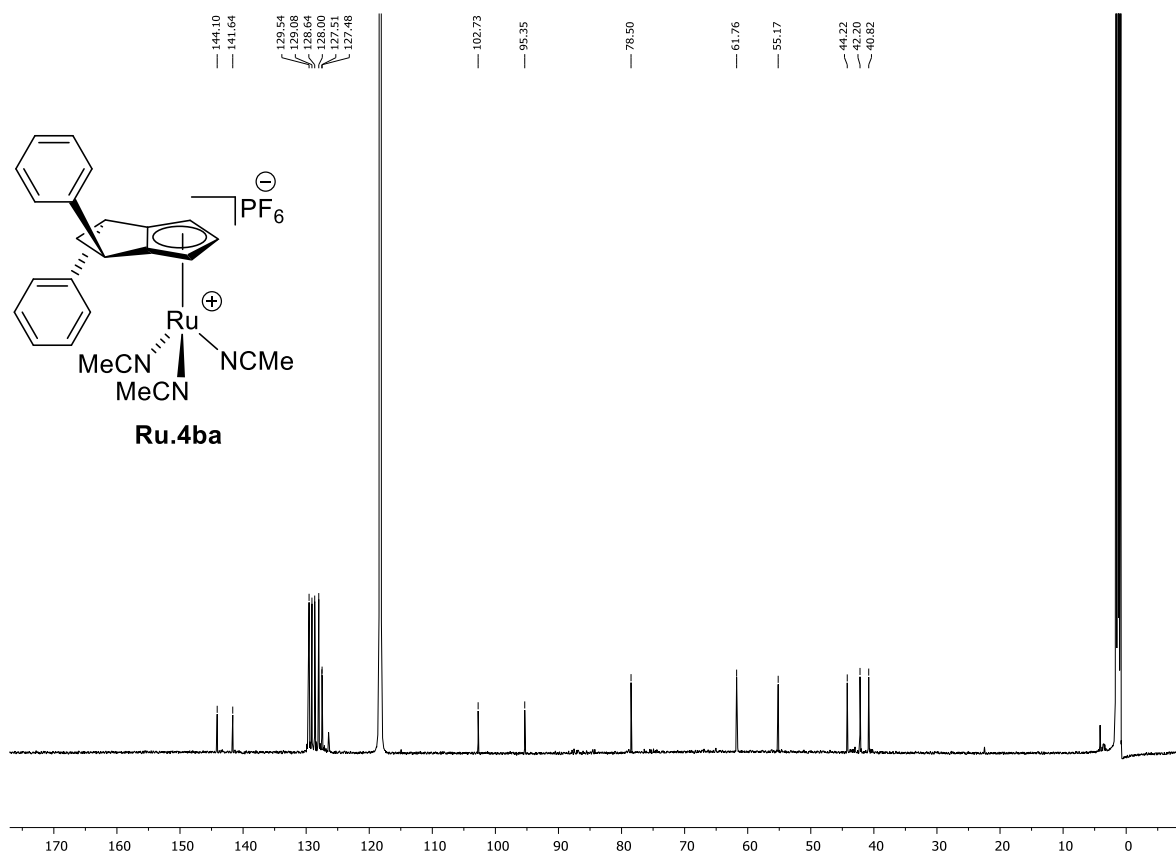
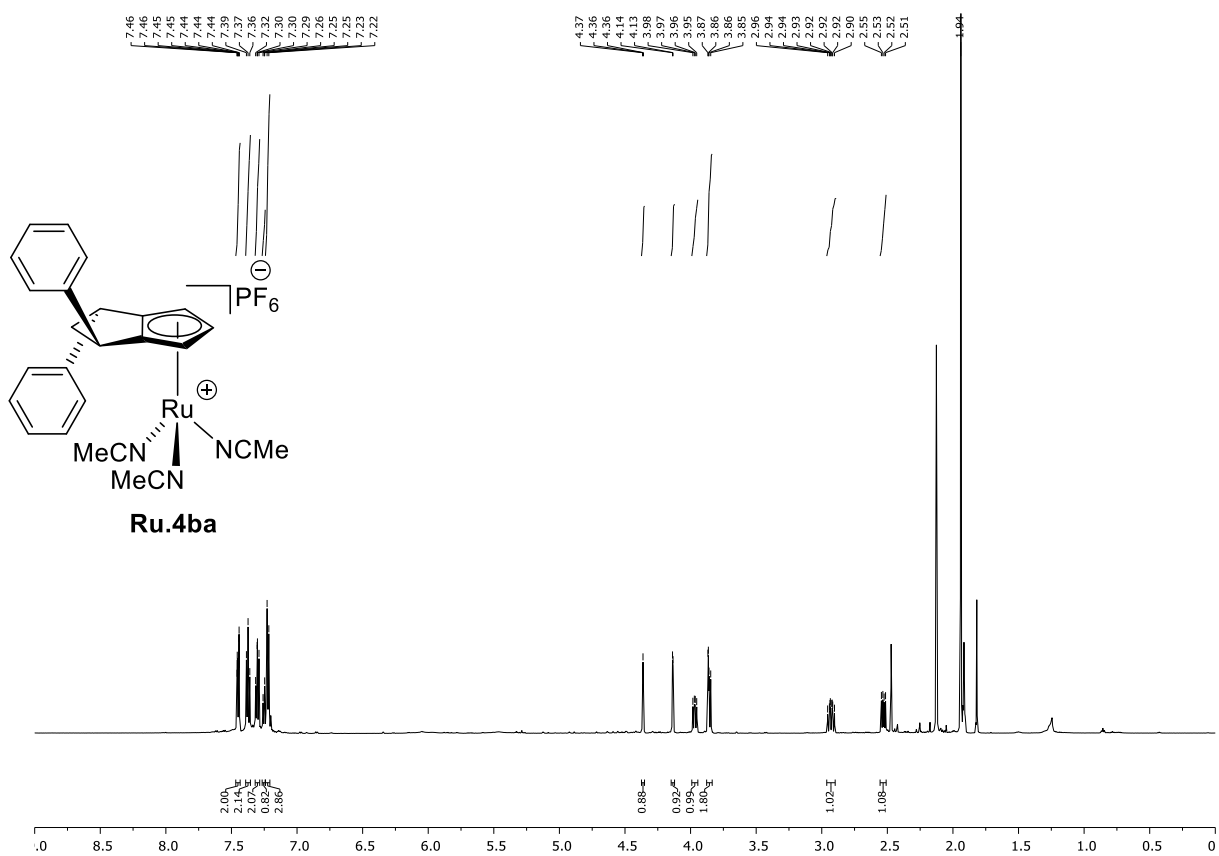


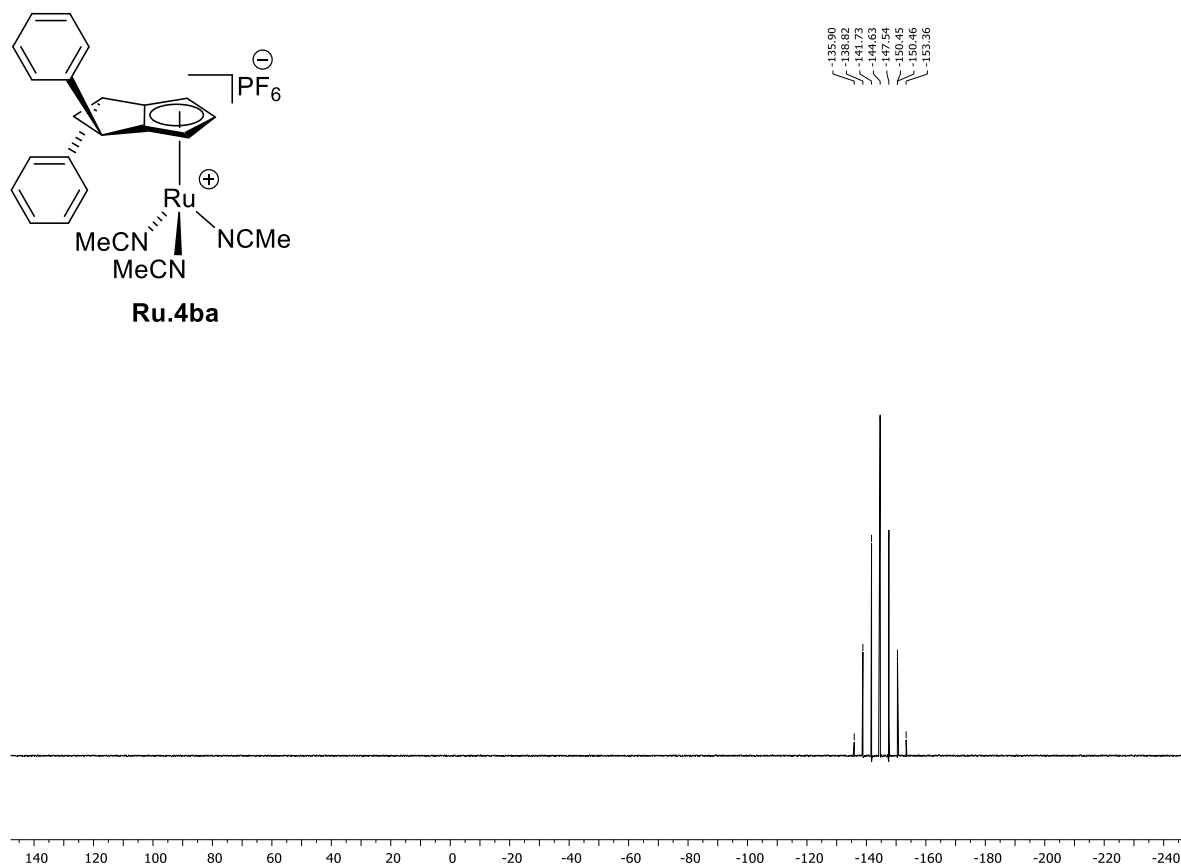
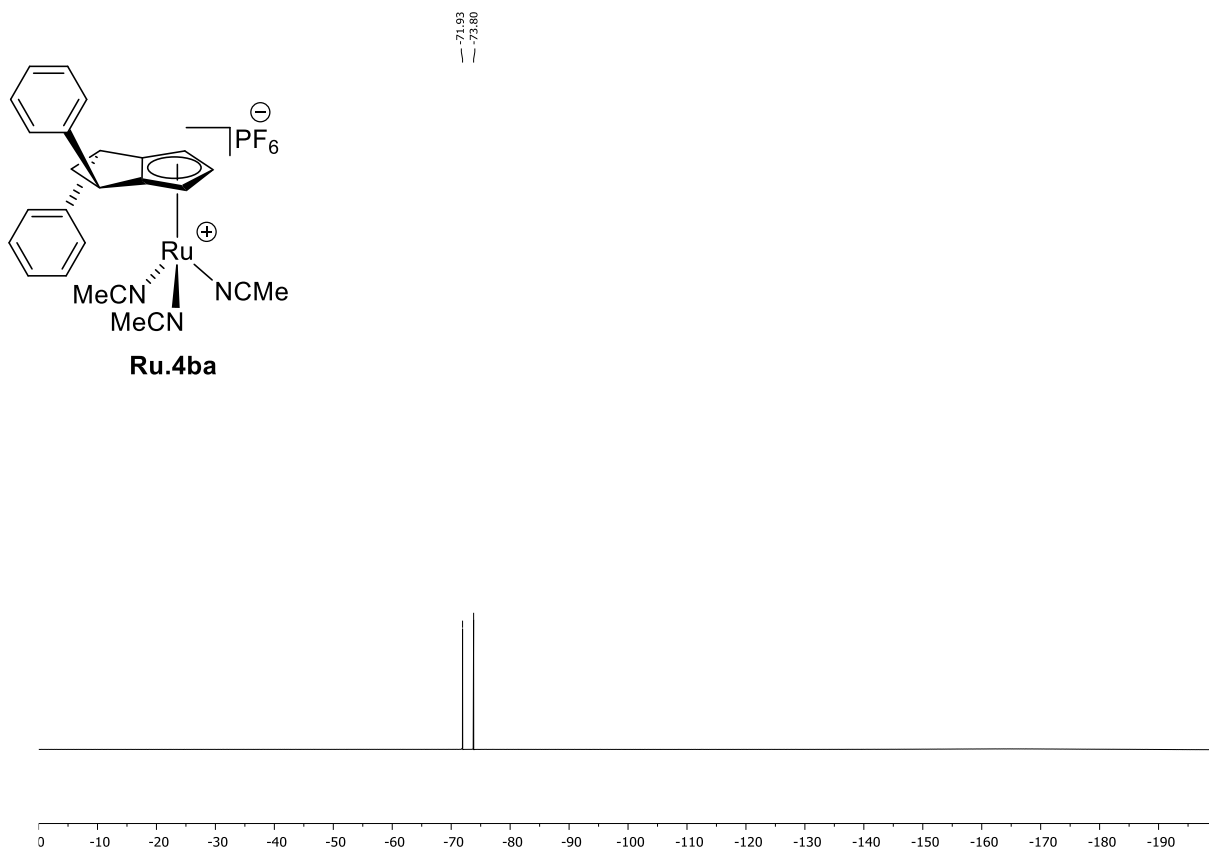


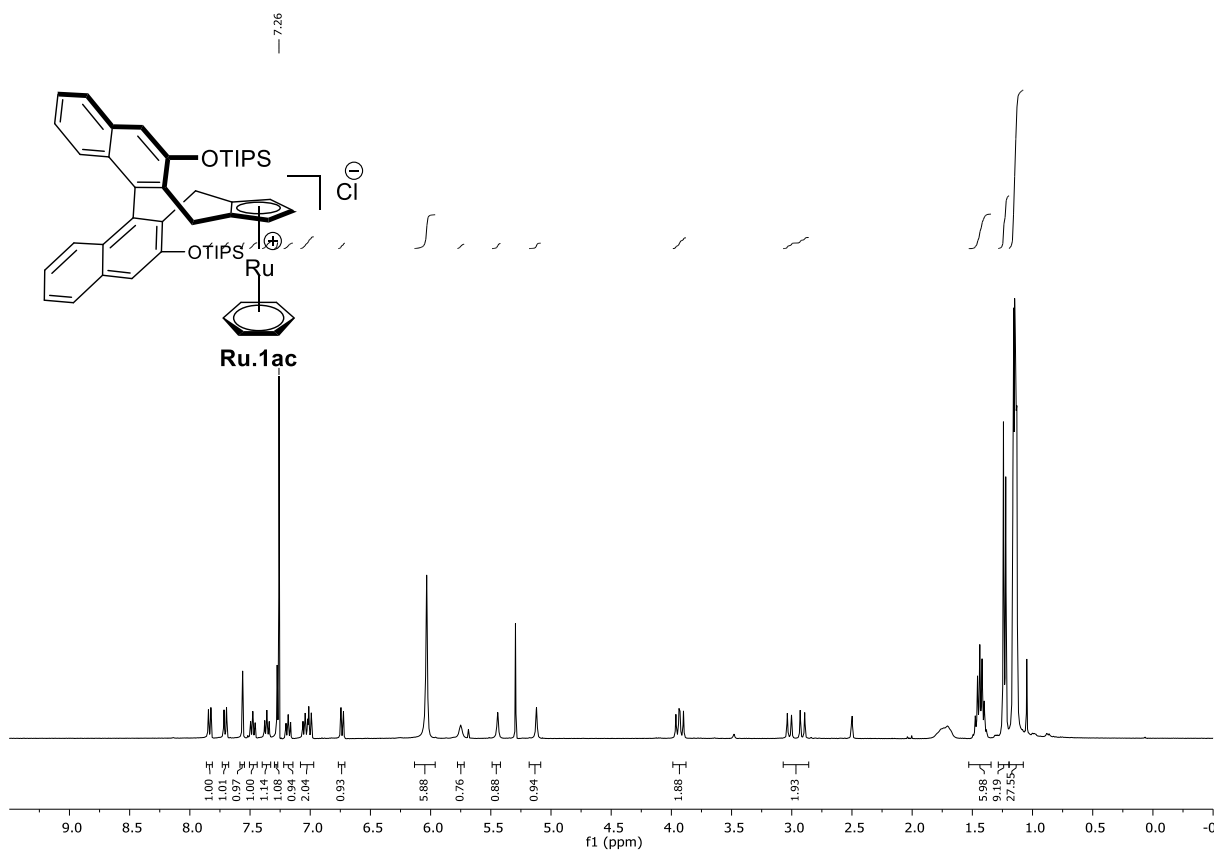
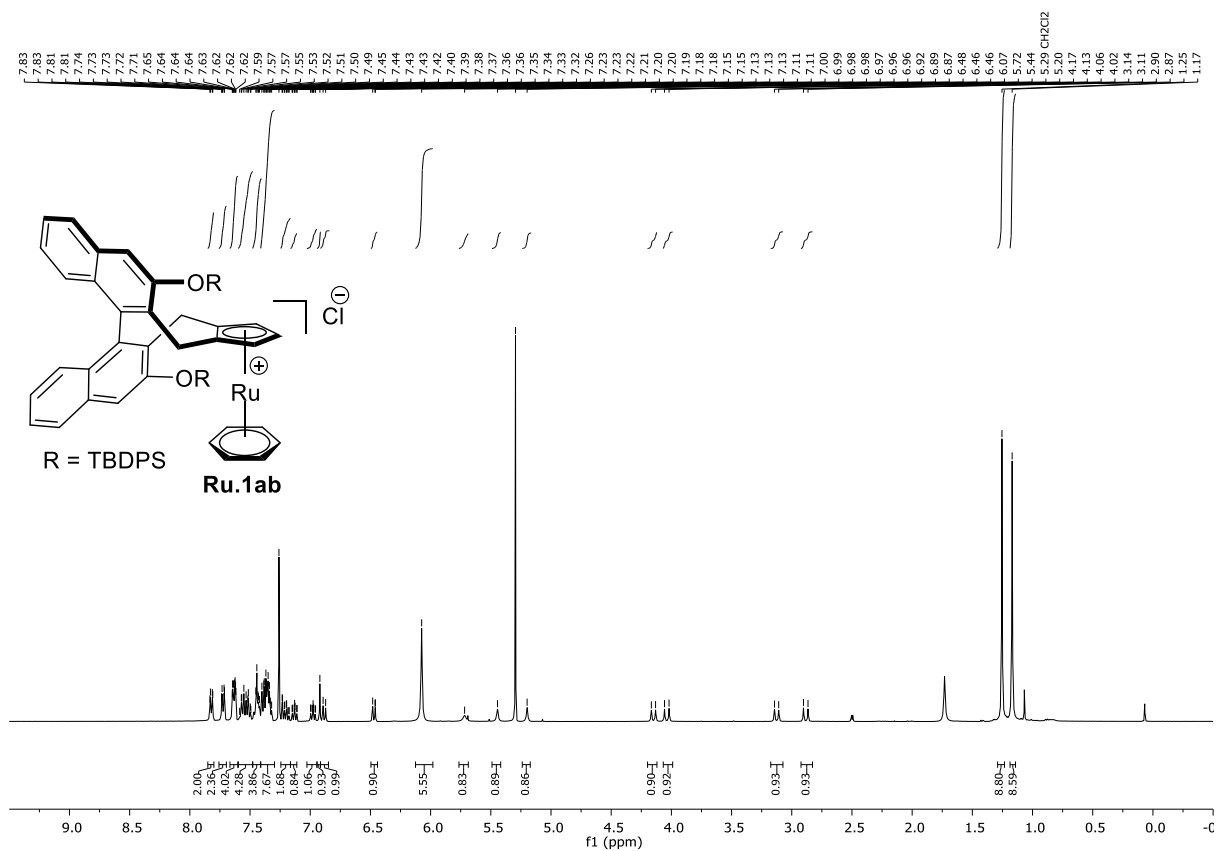


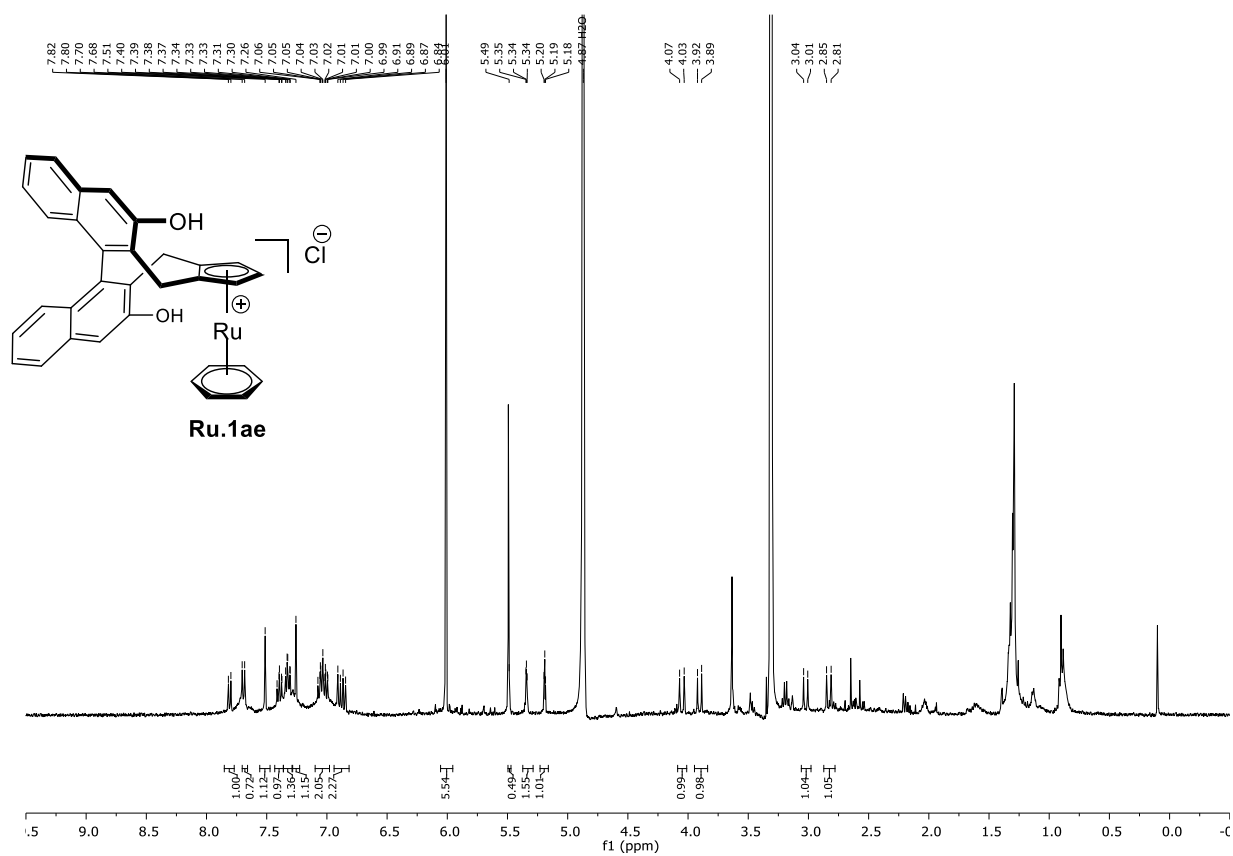


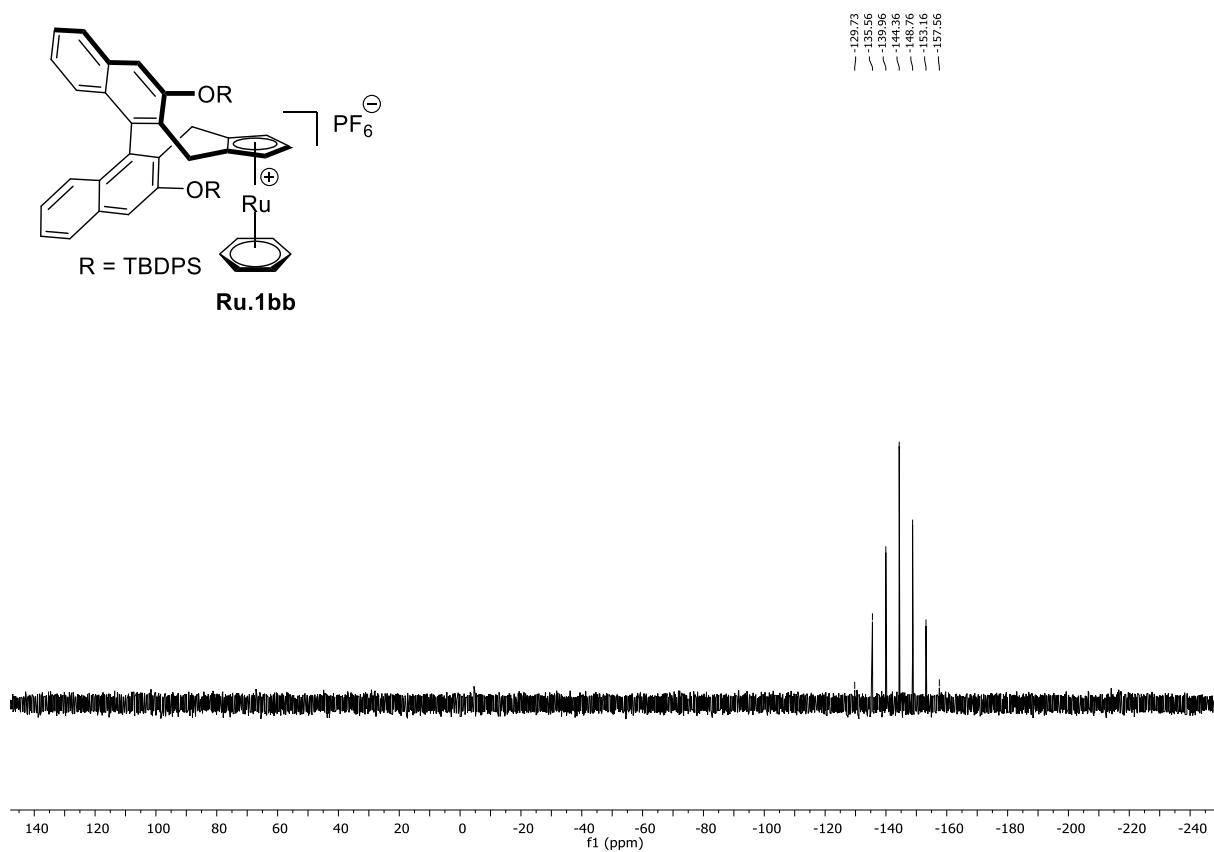
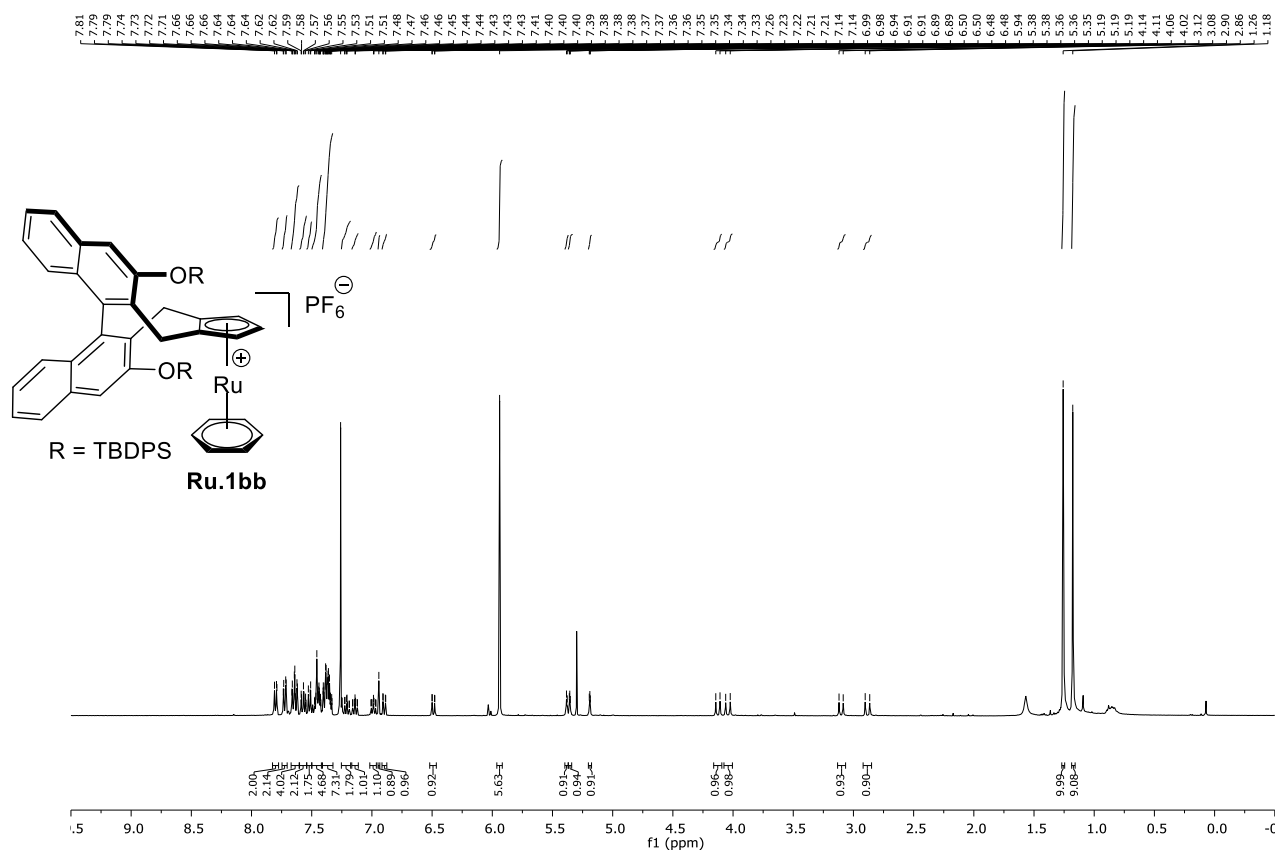


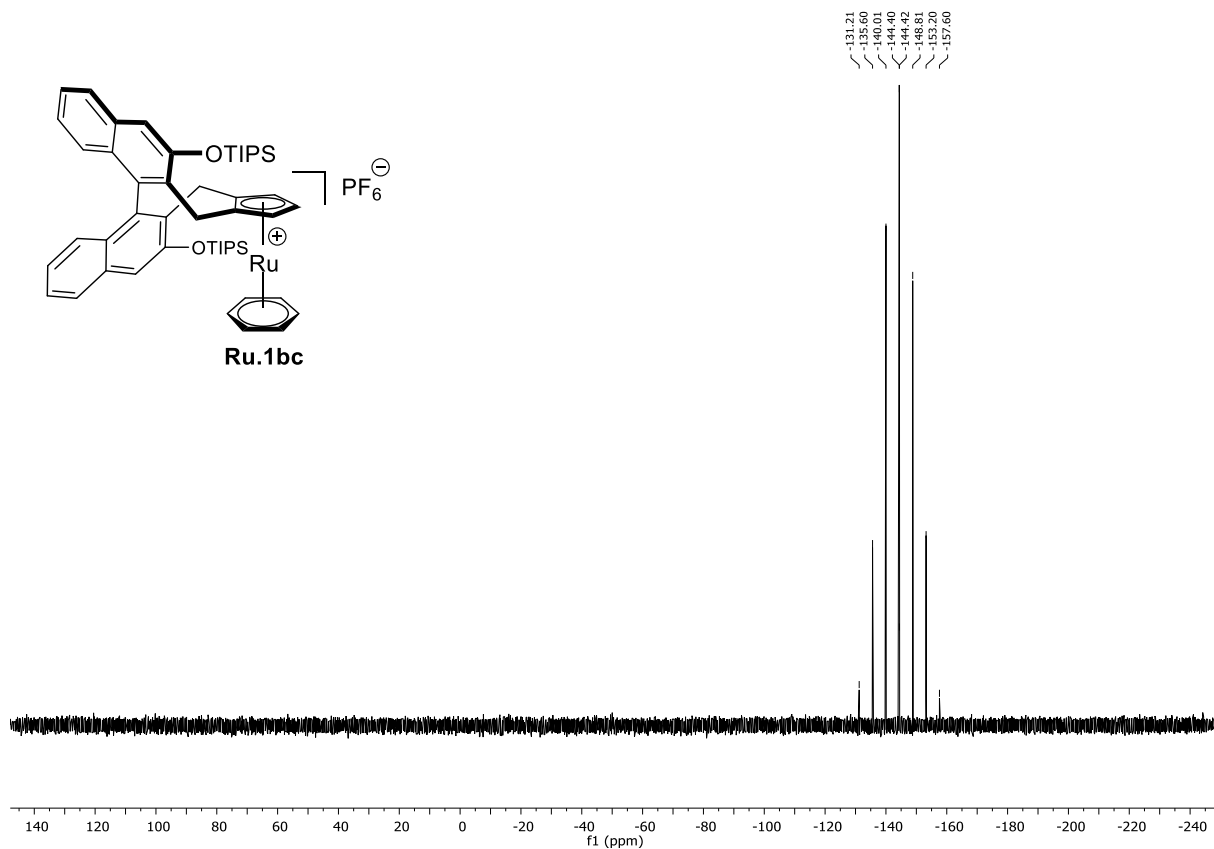
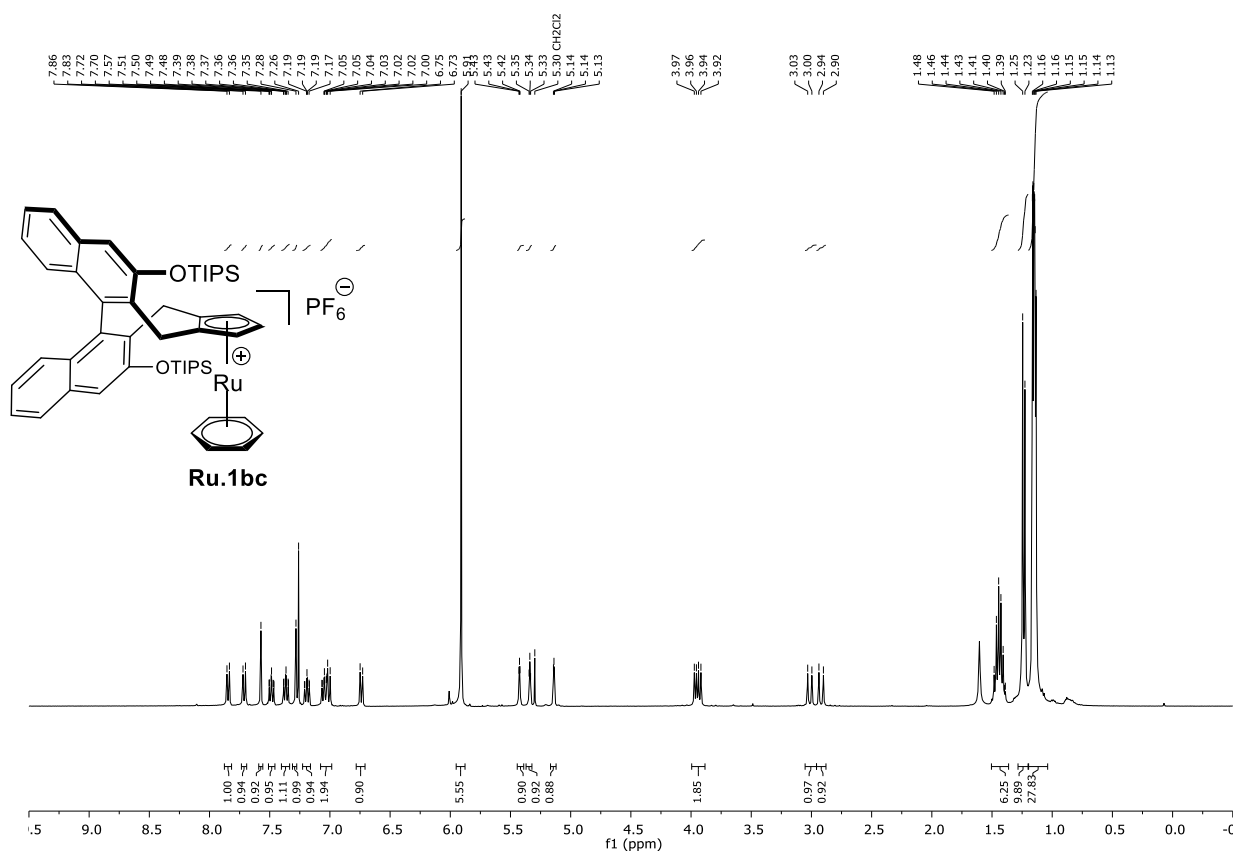


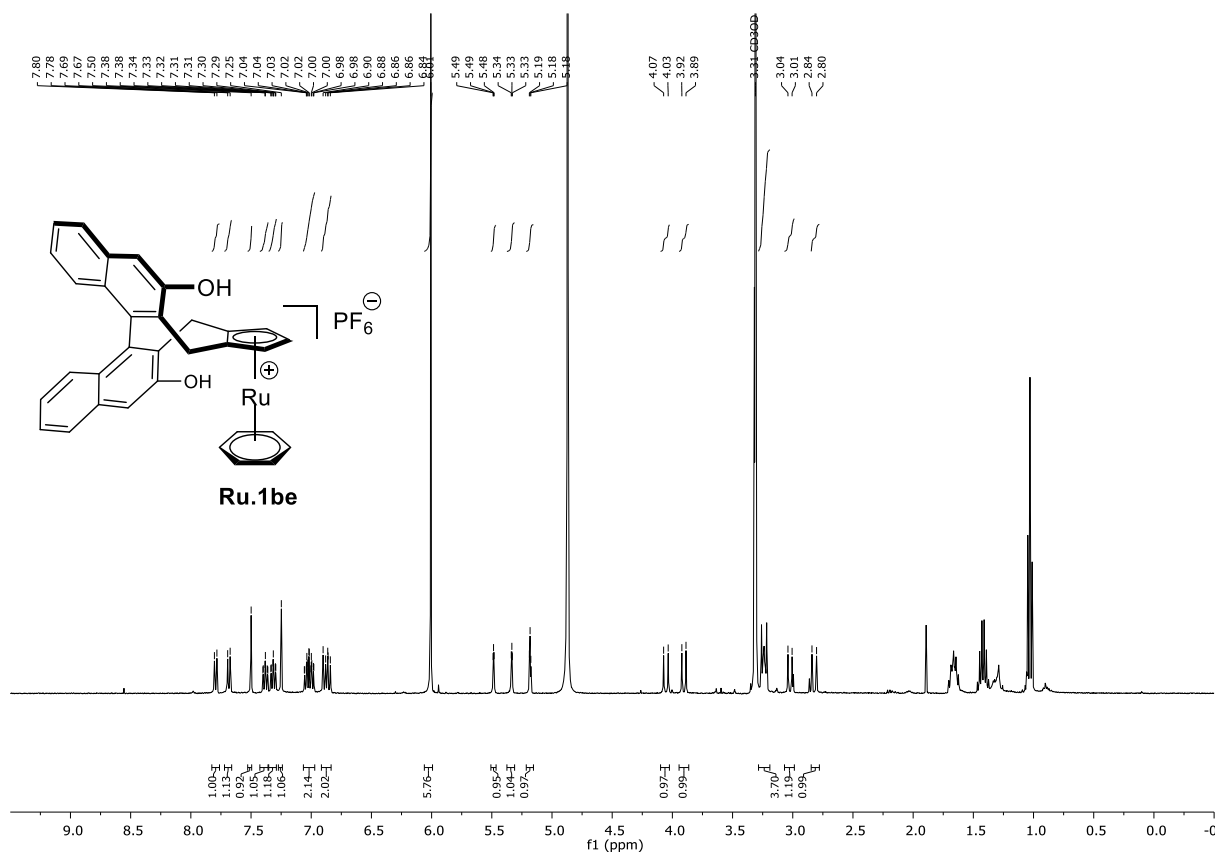


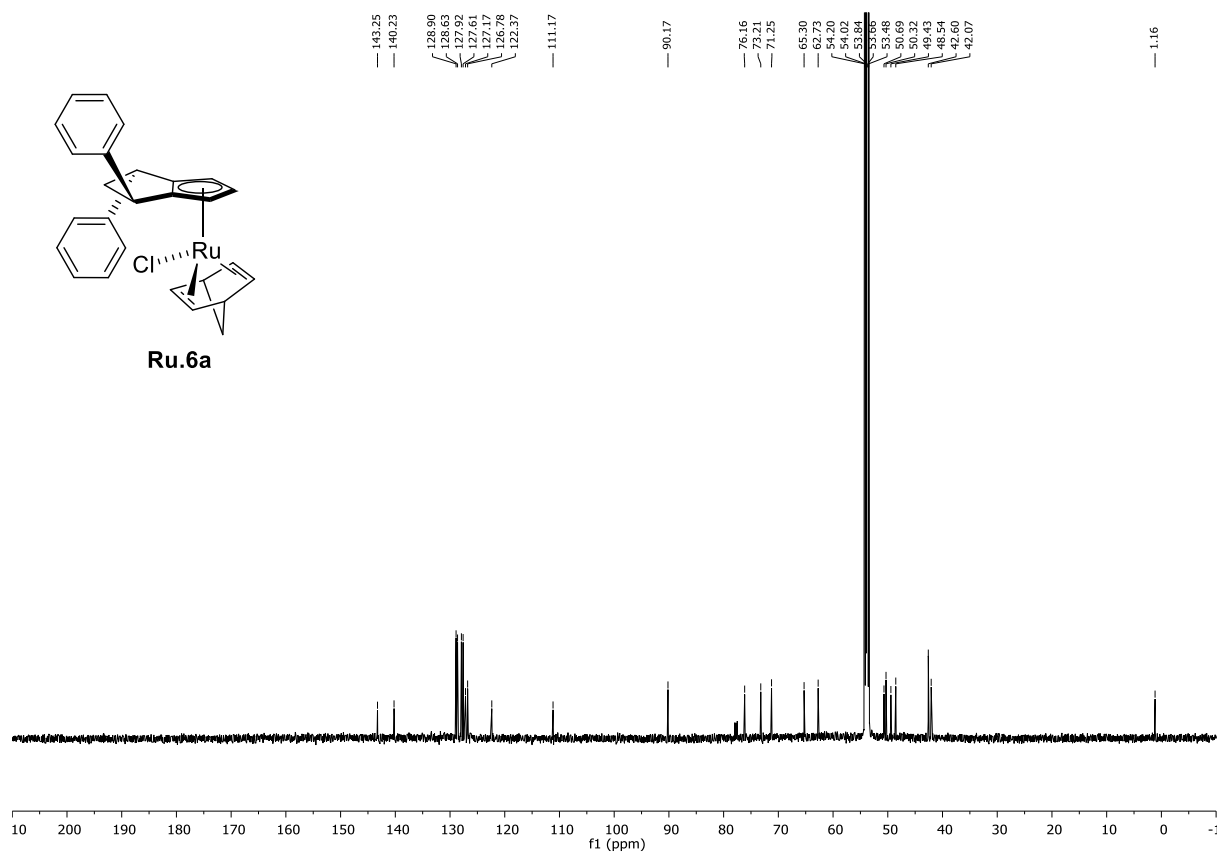
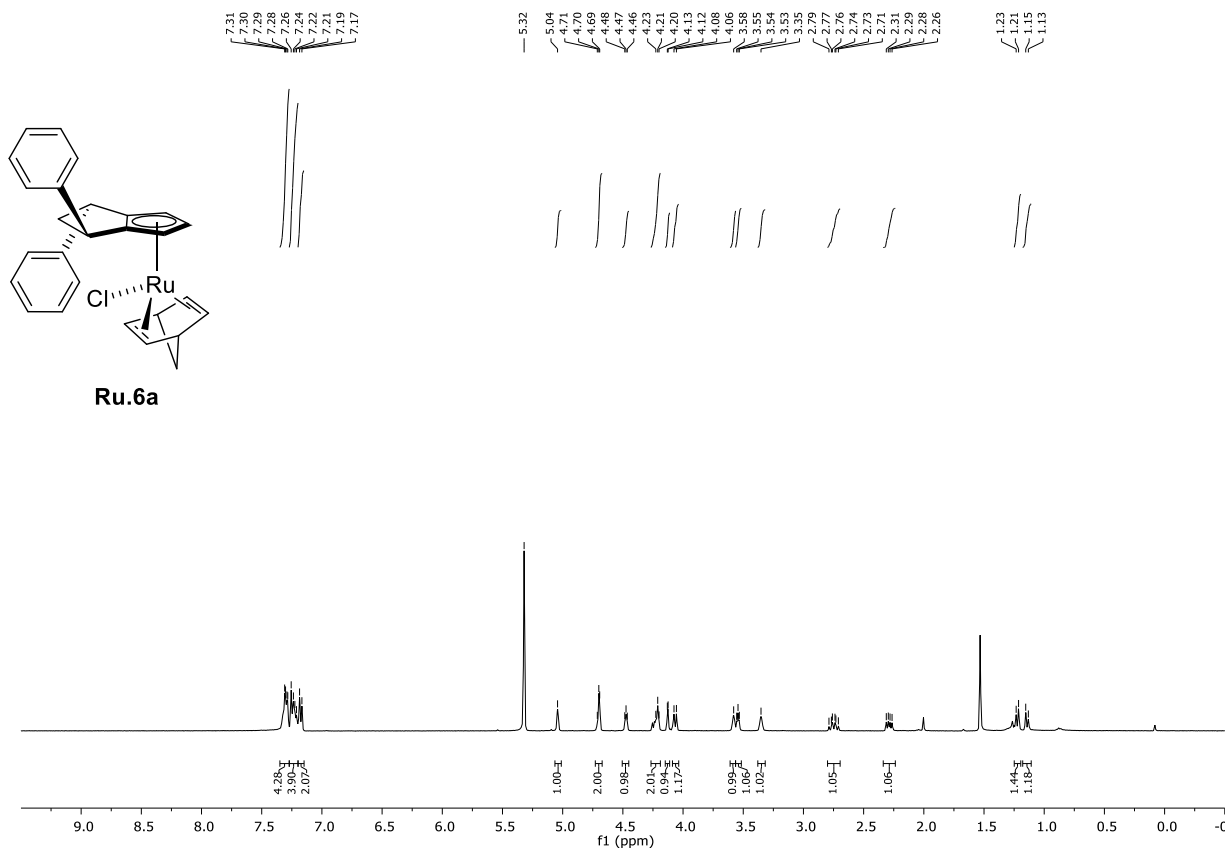


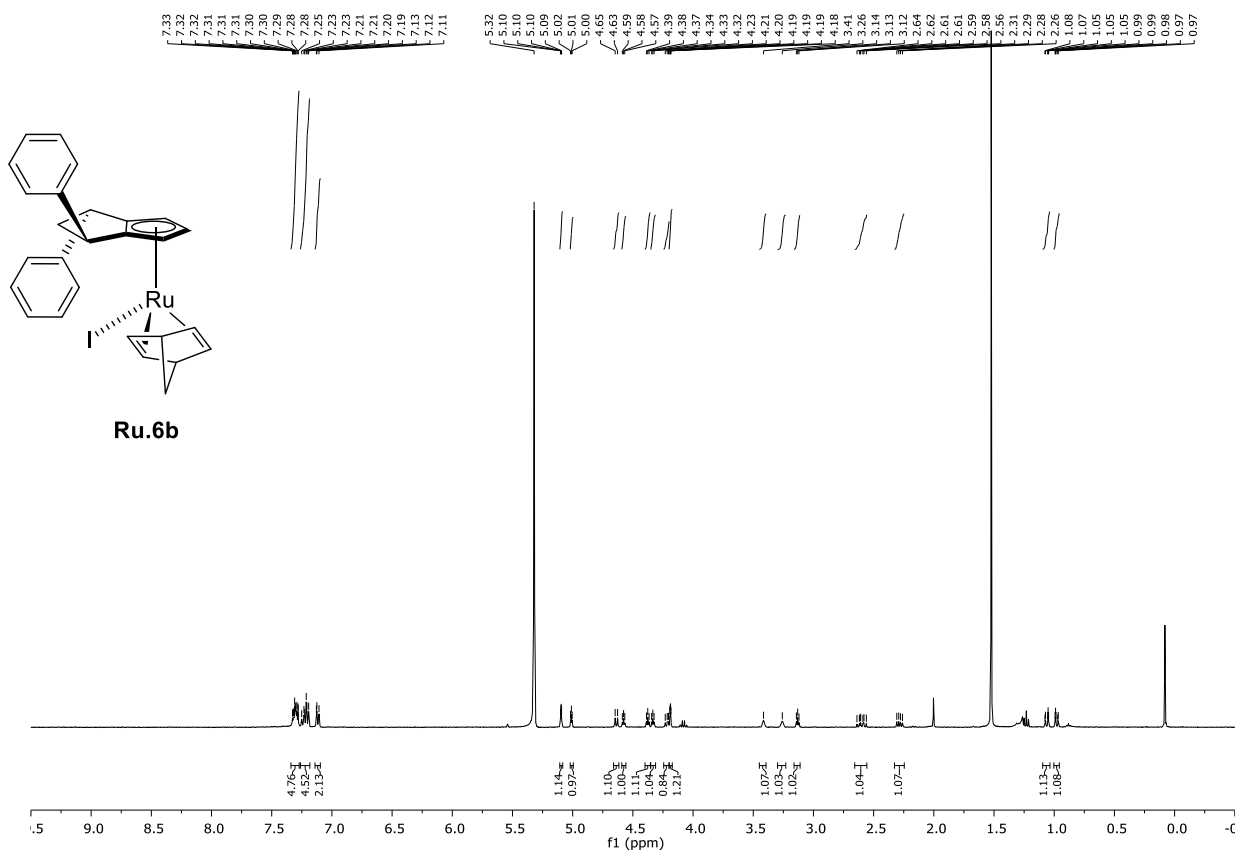




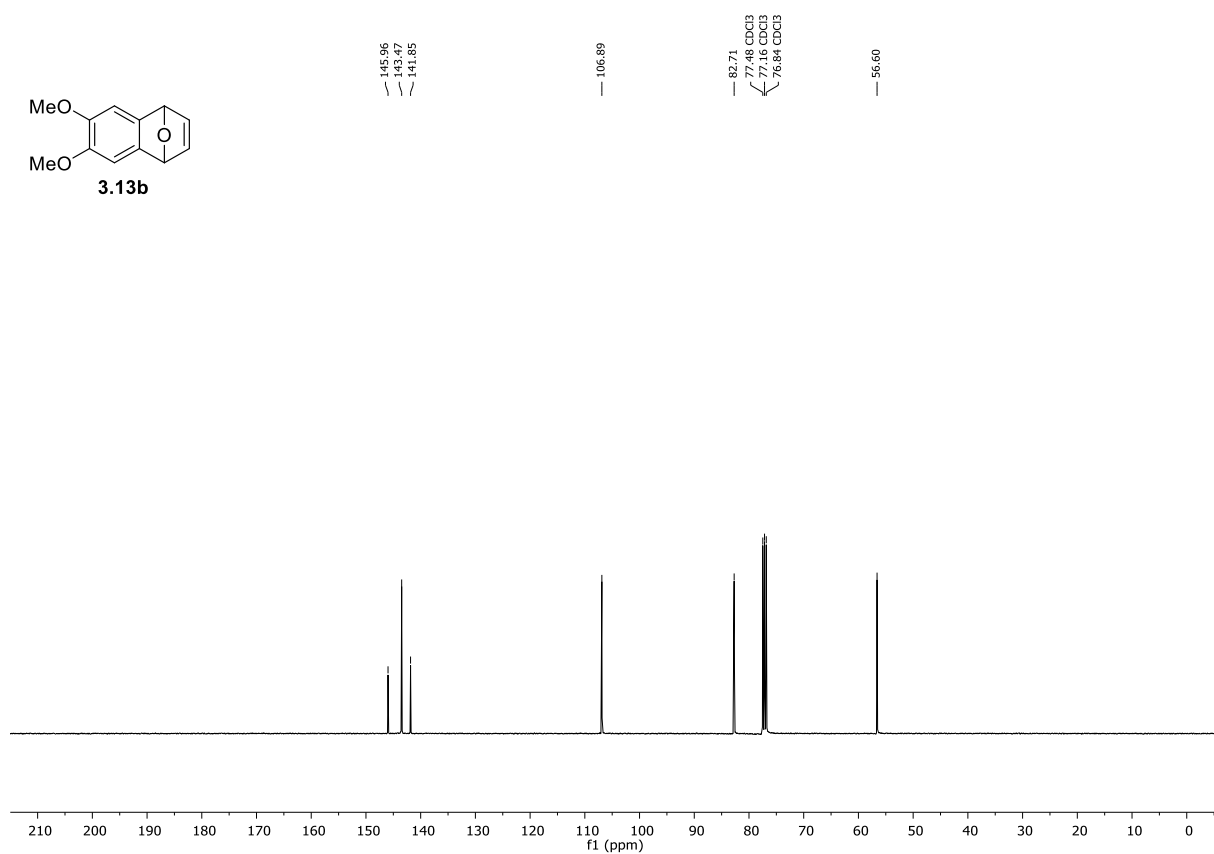
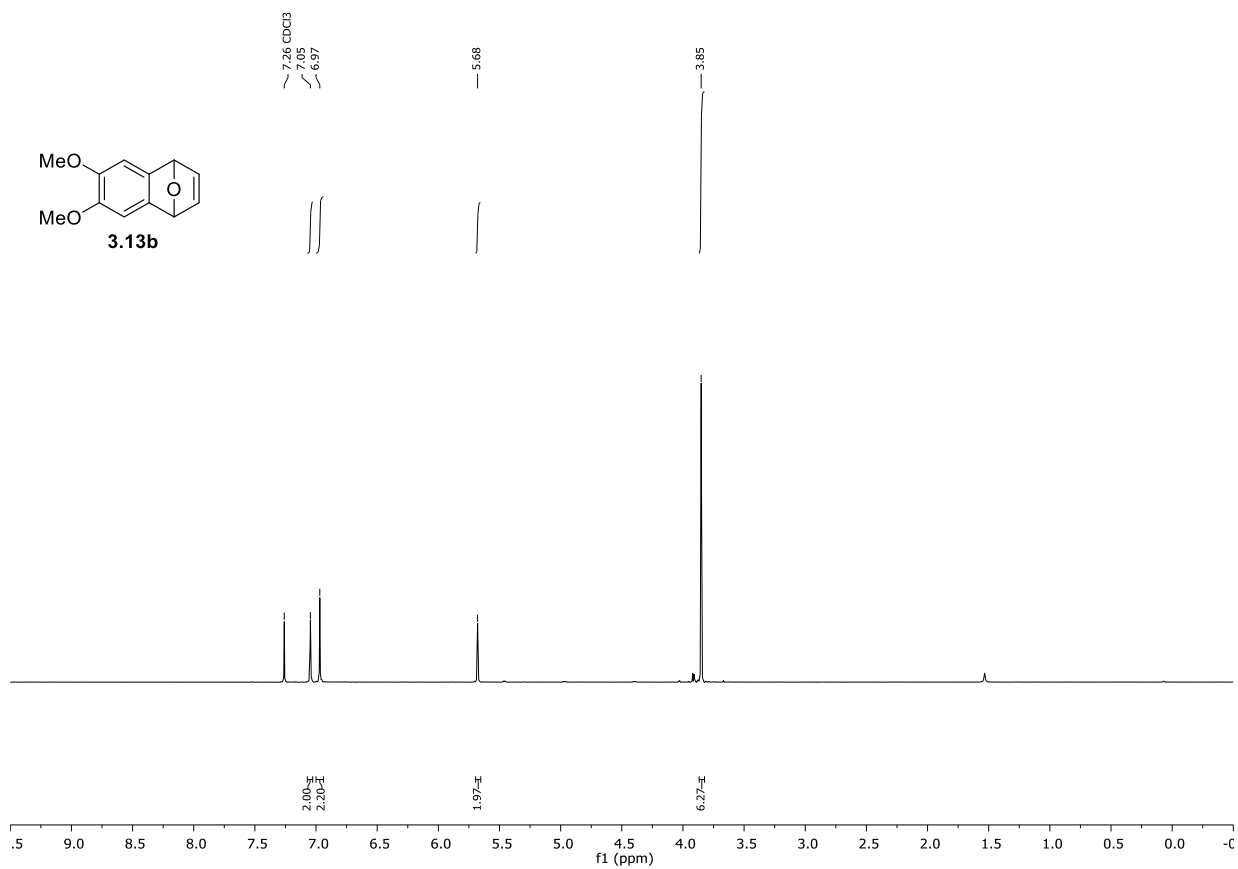


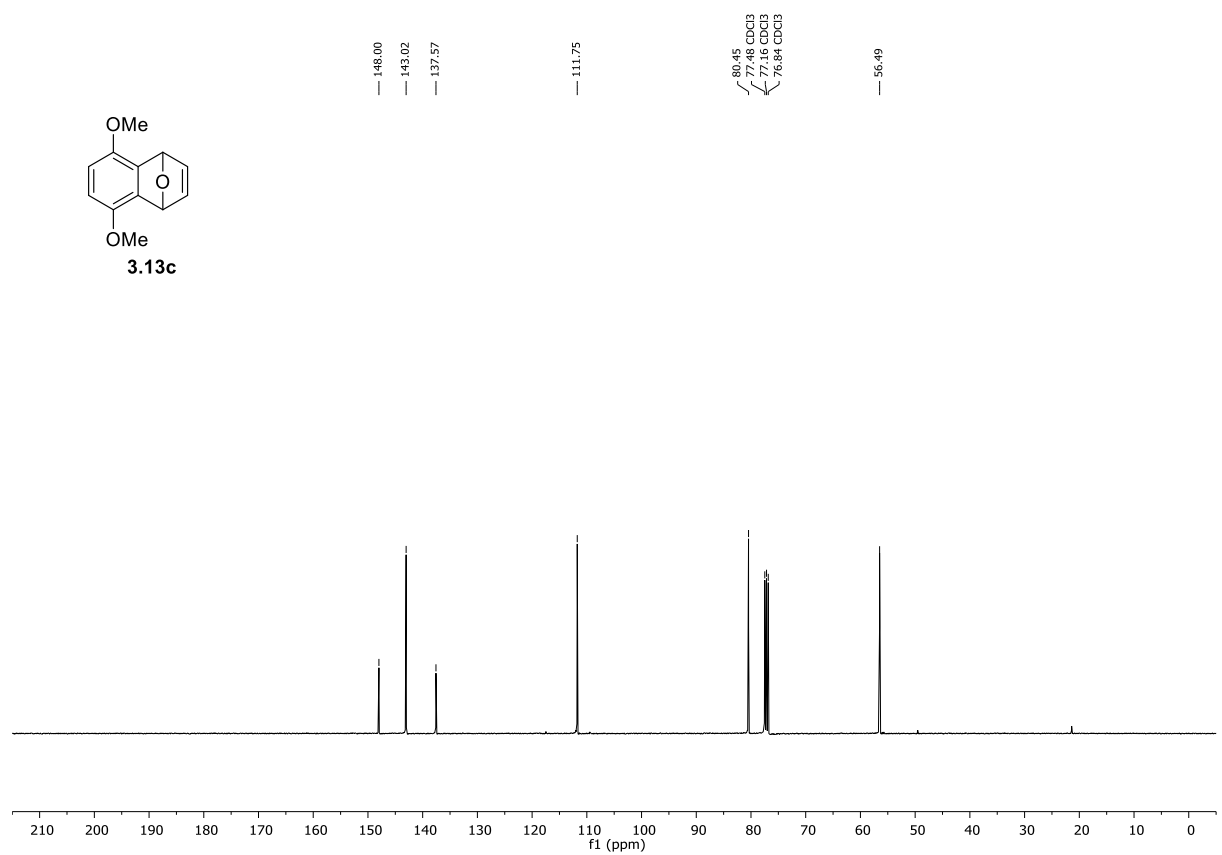
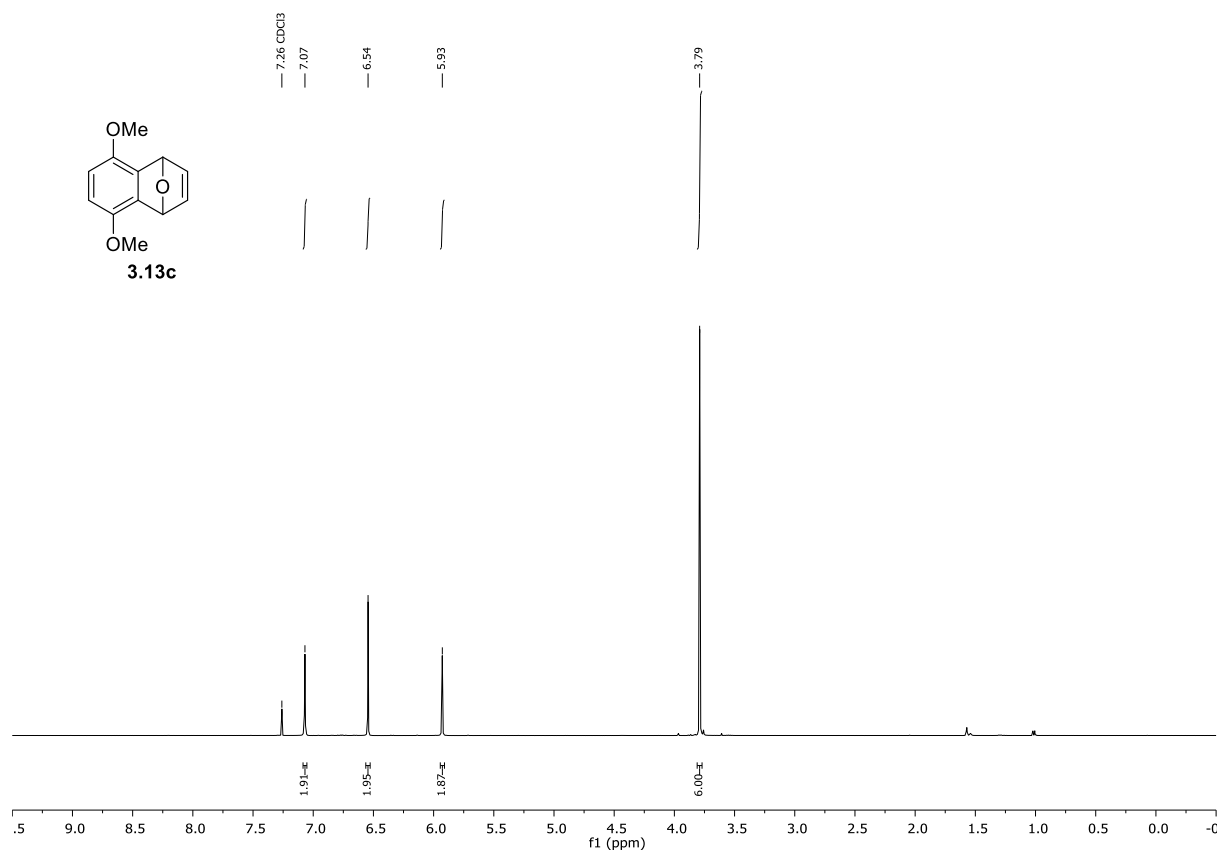


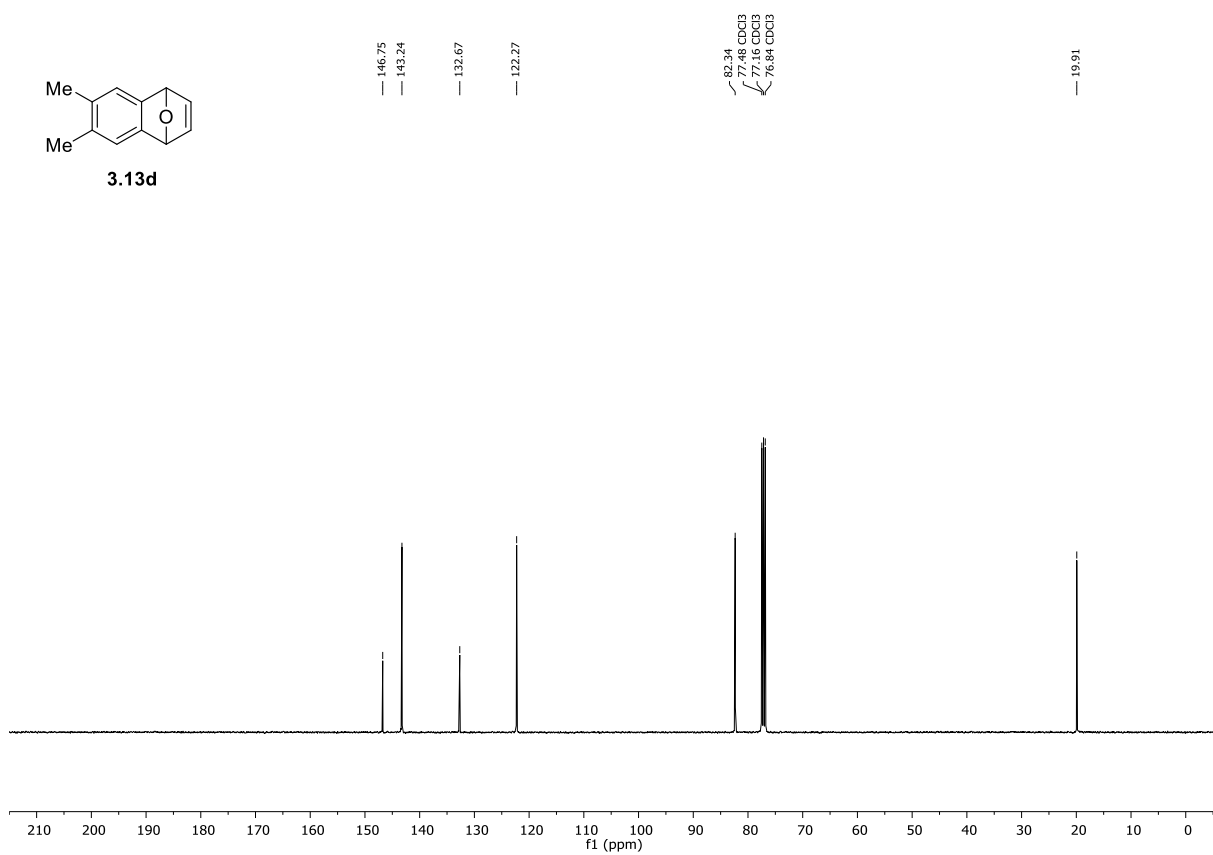
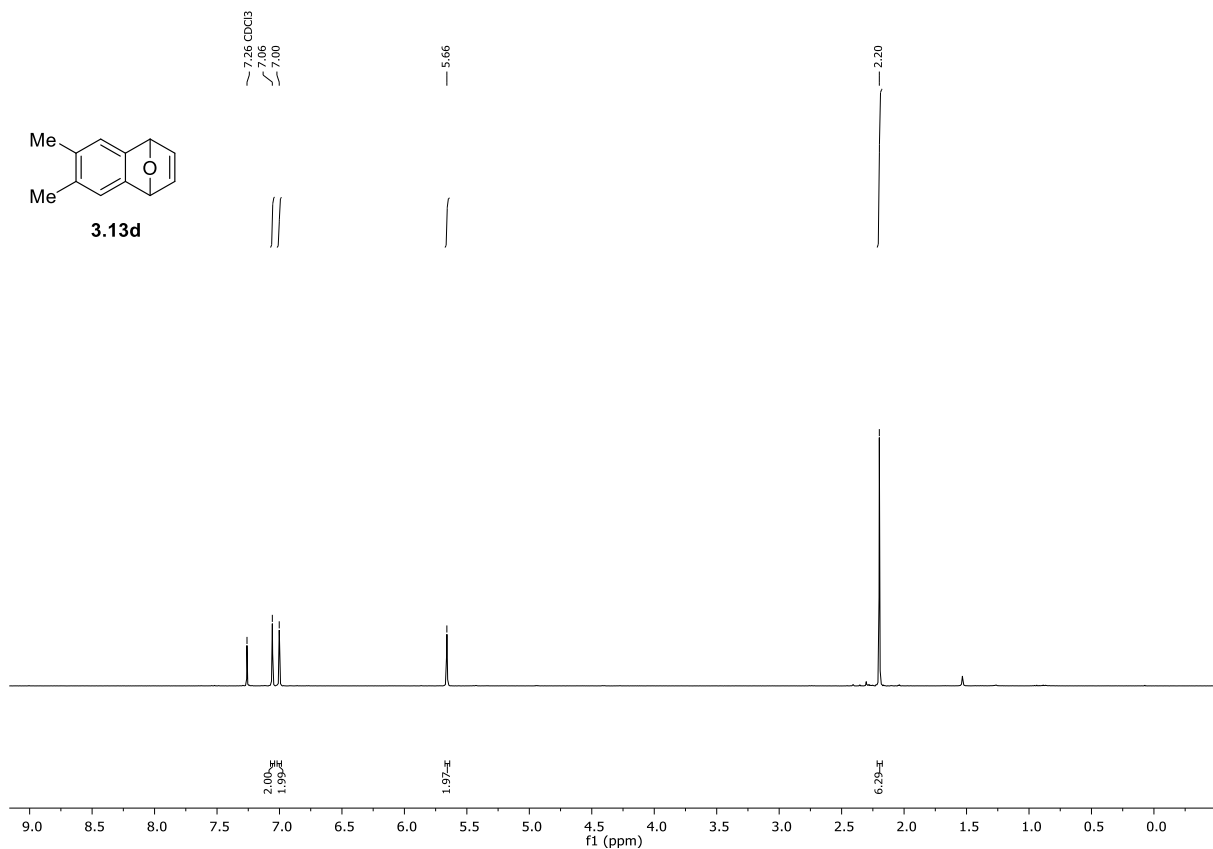


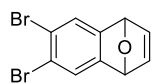


NMR spectra for Chapter 3

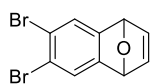
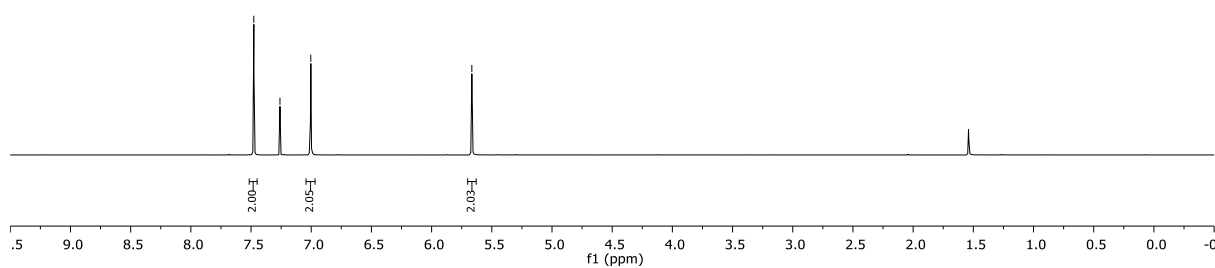
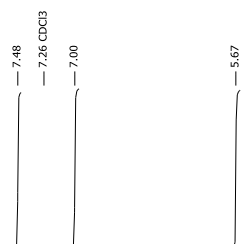




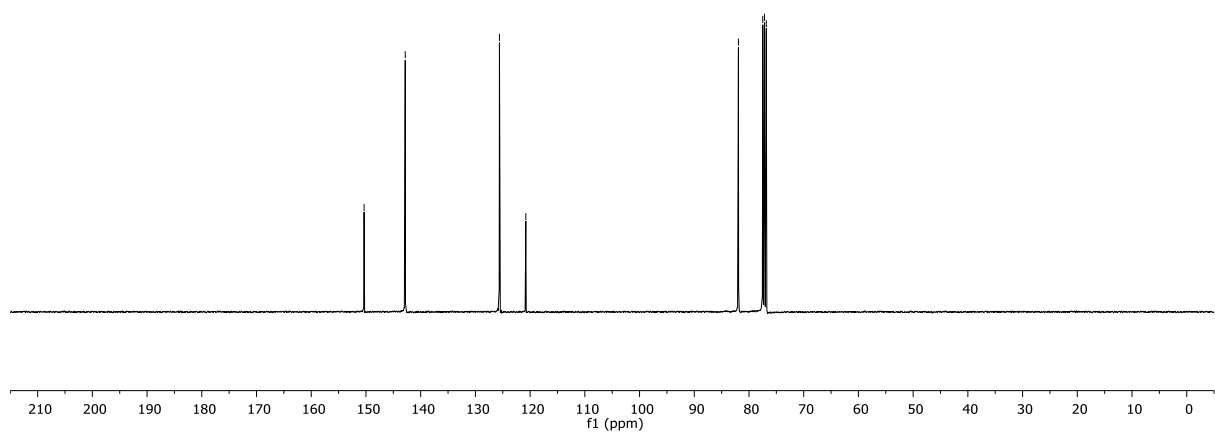


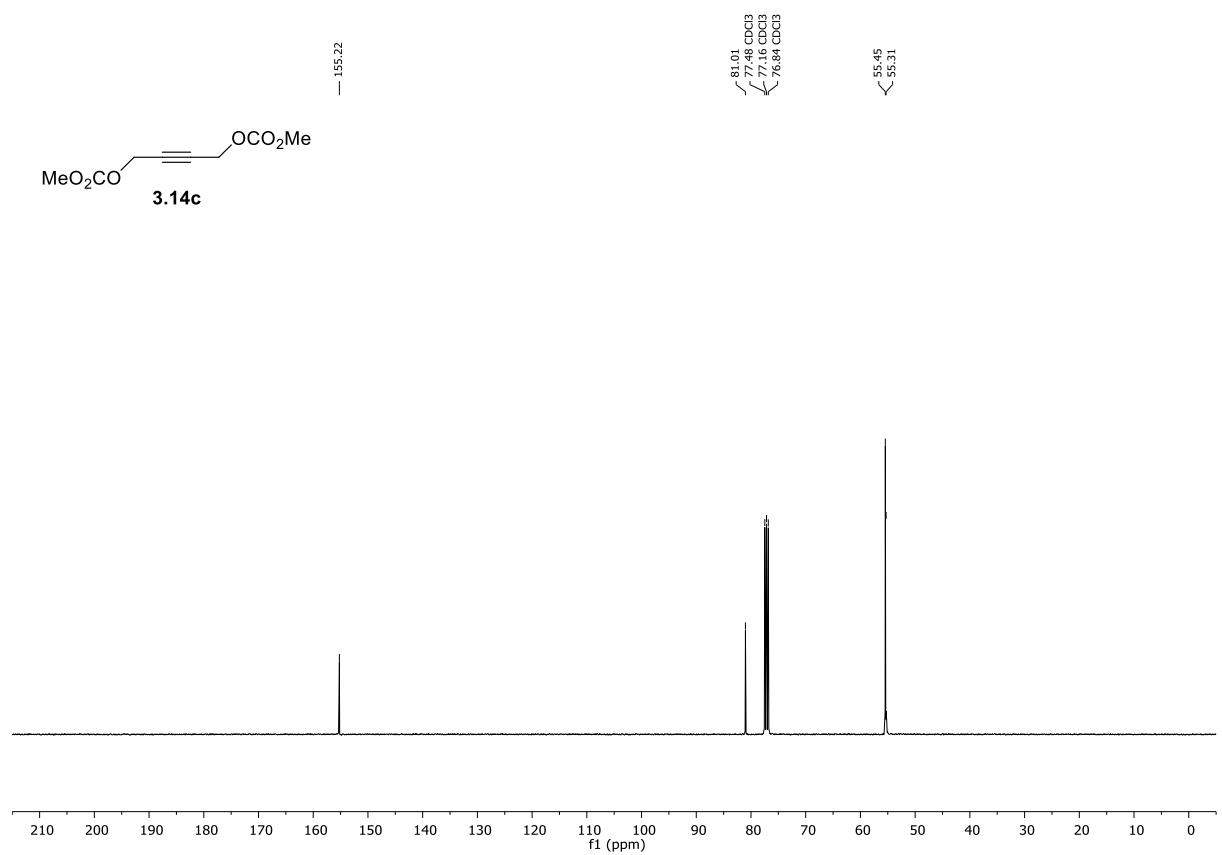
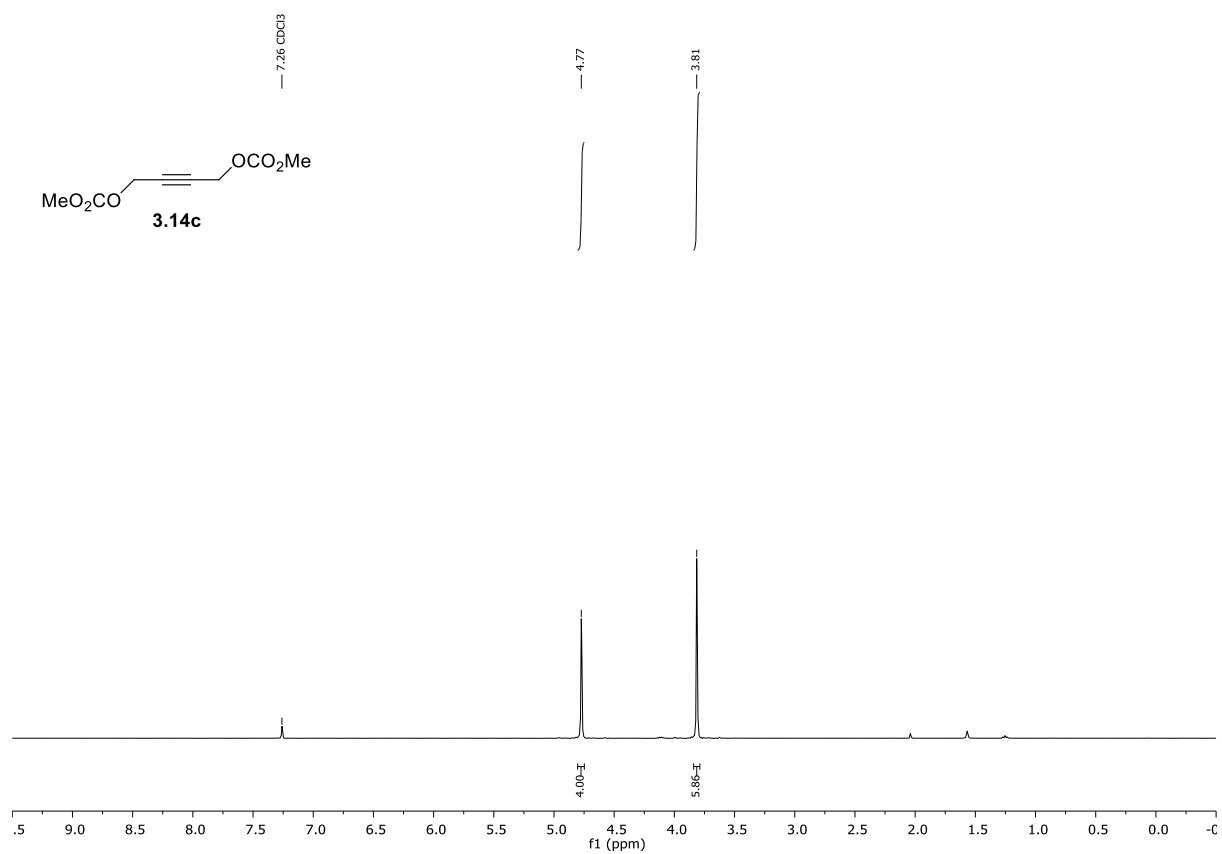


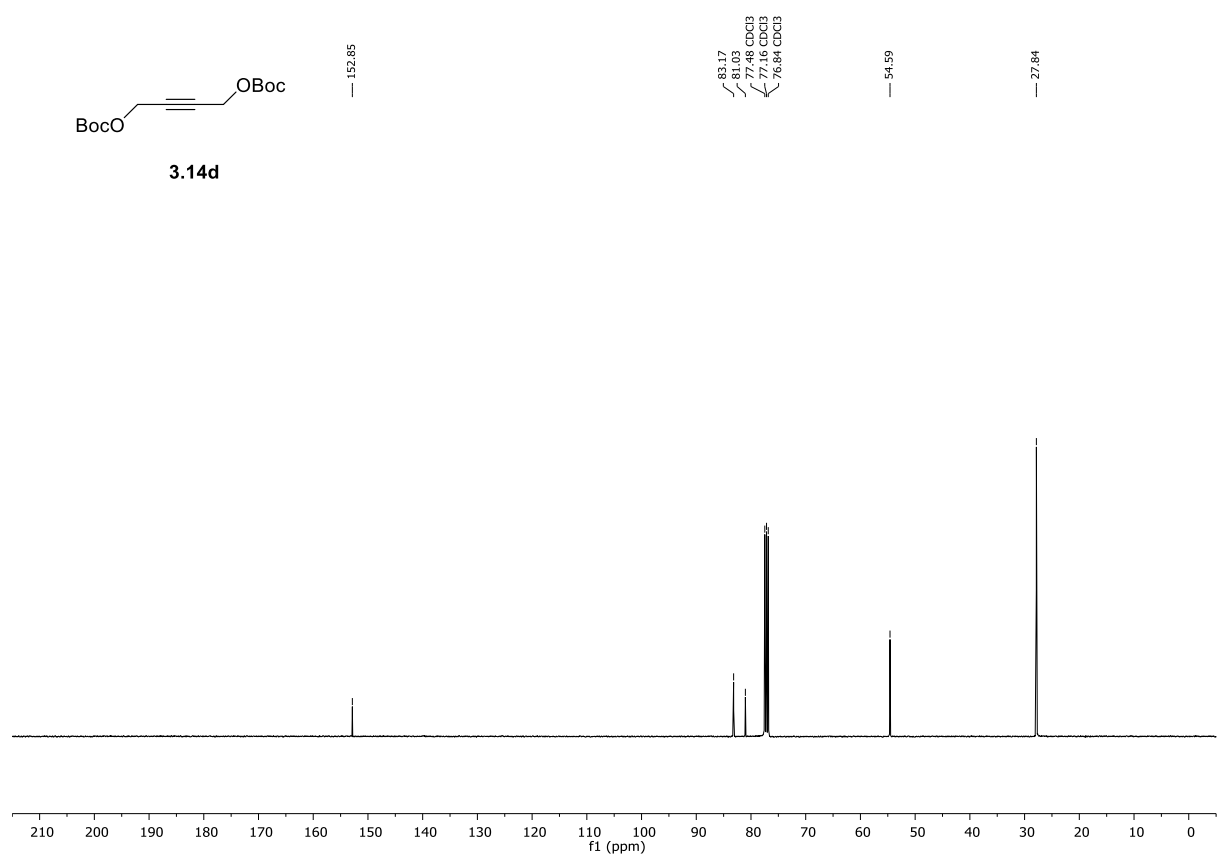
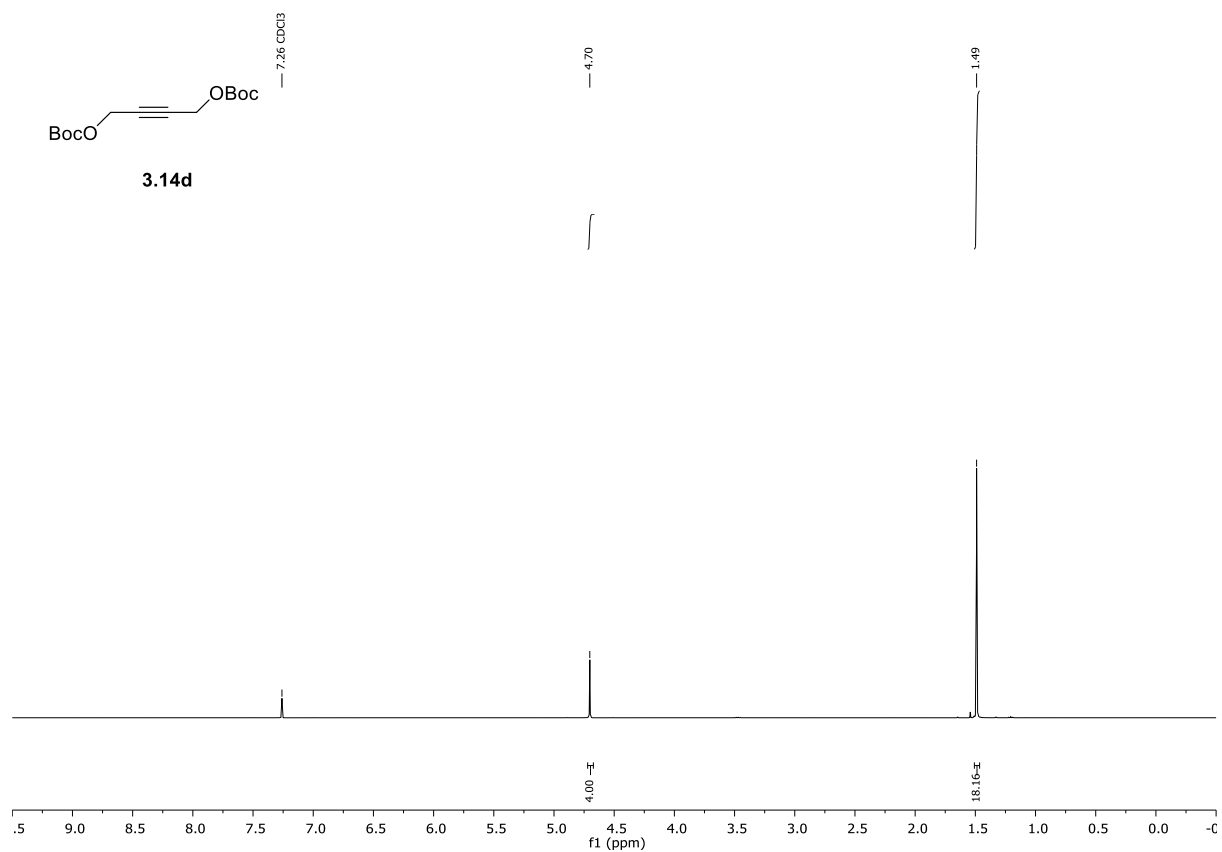
3.13e

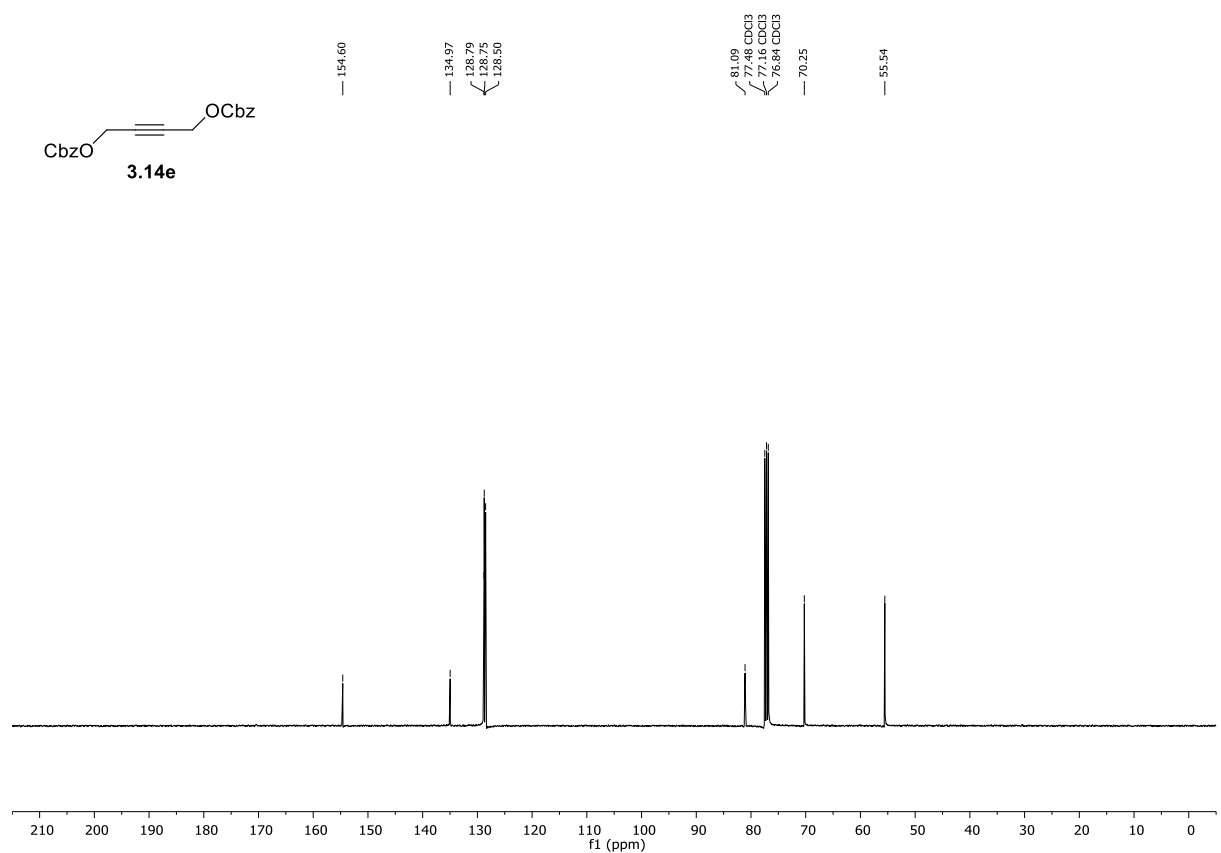
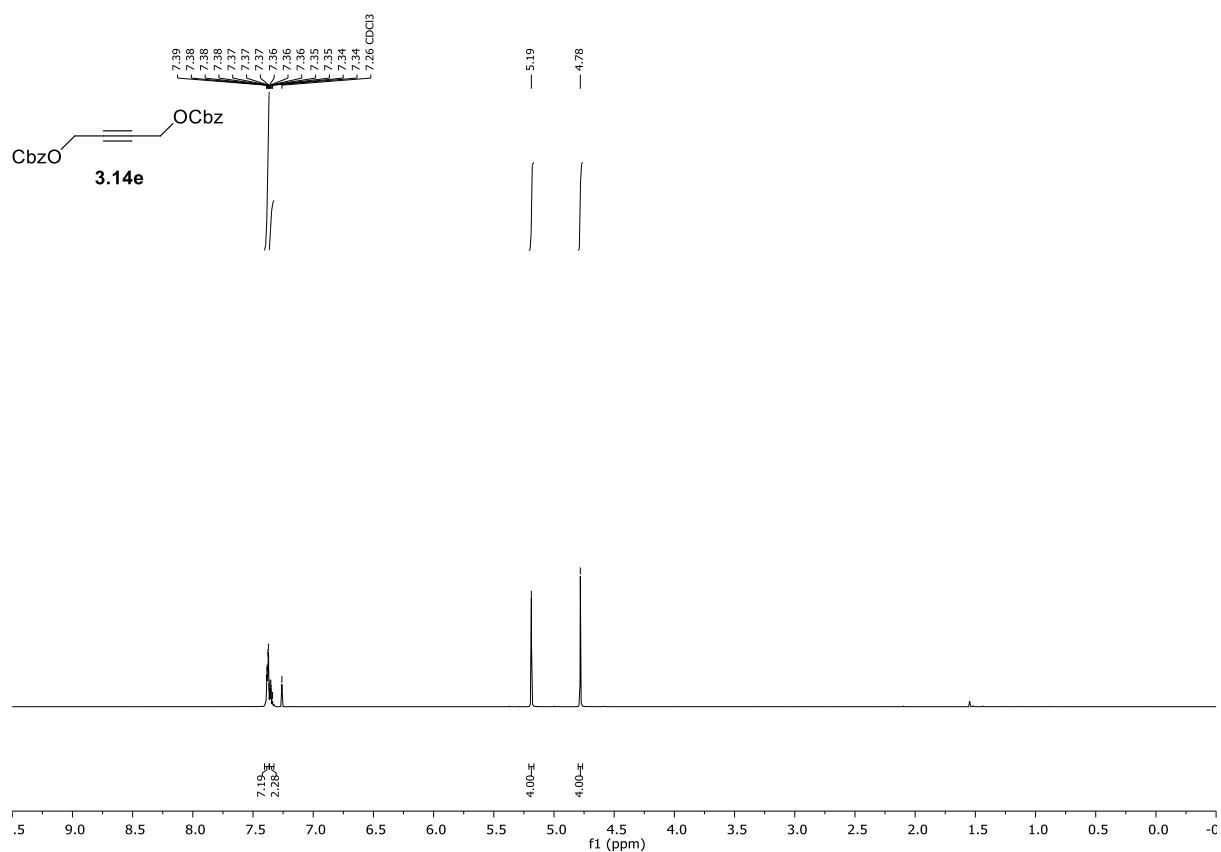


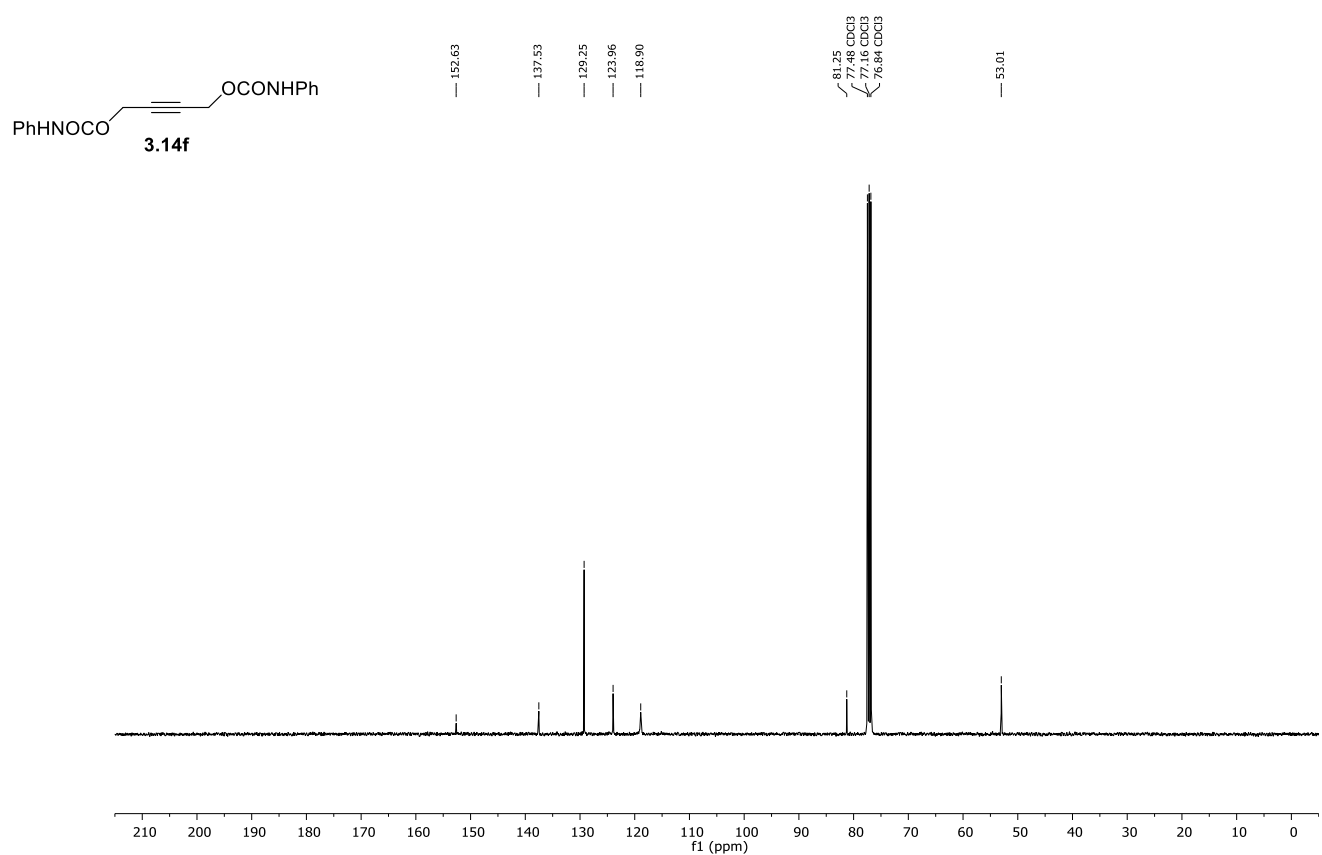
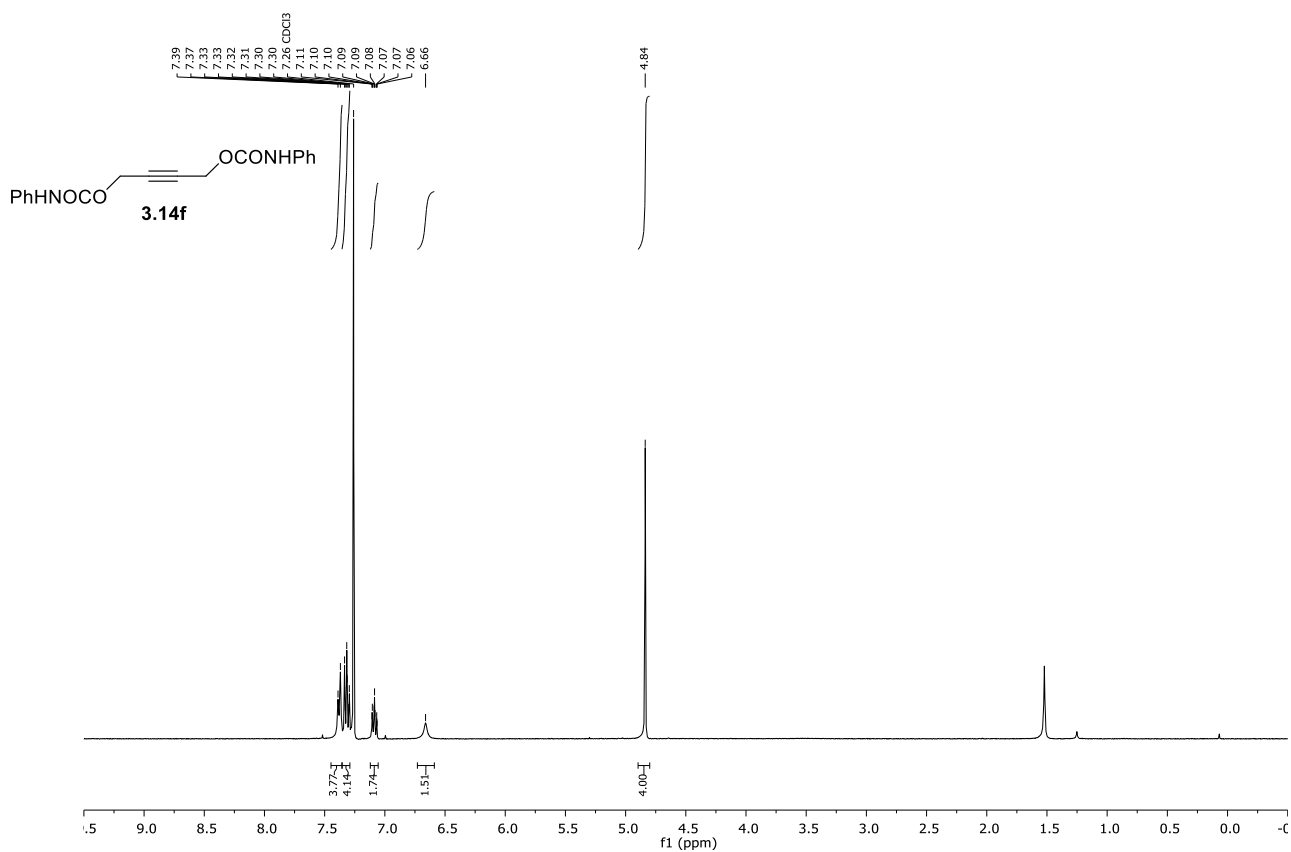
3.13e

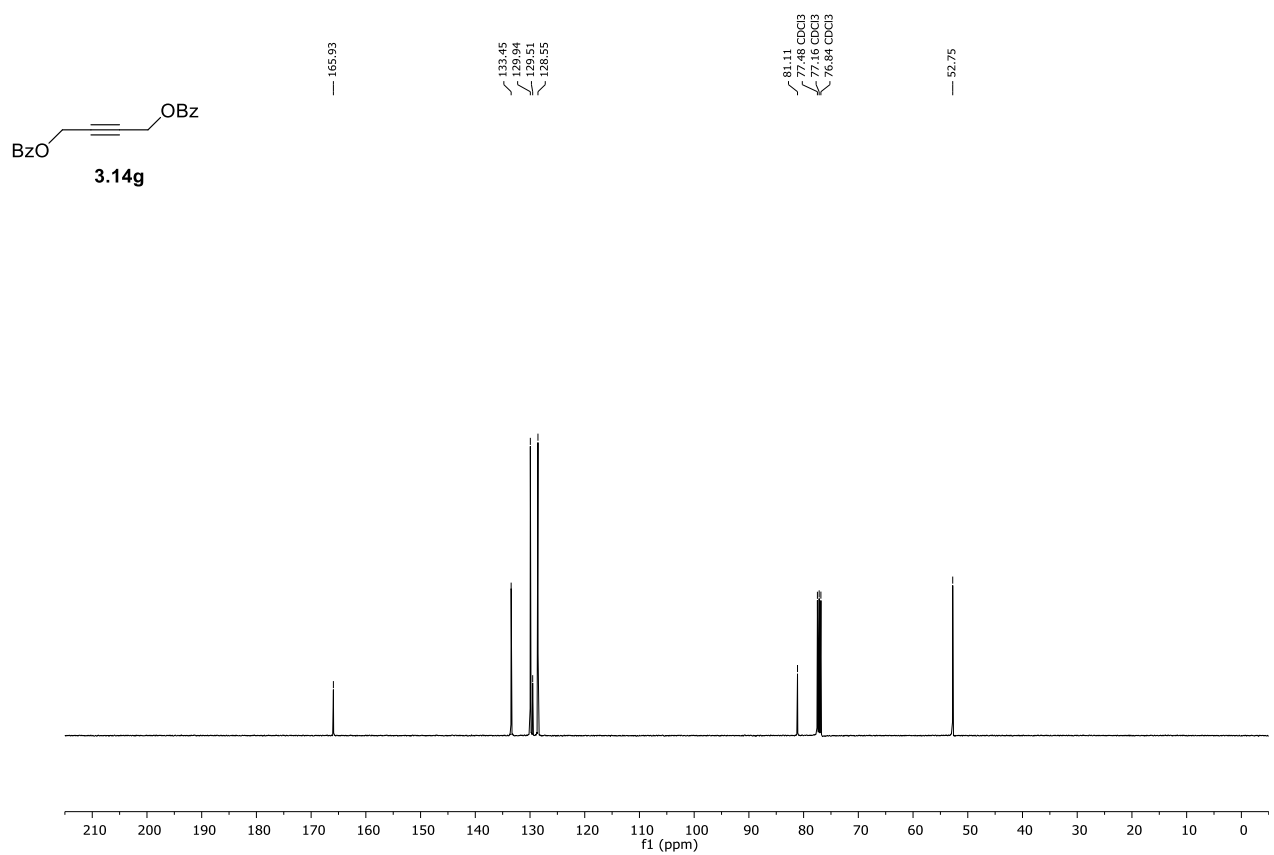
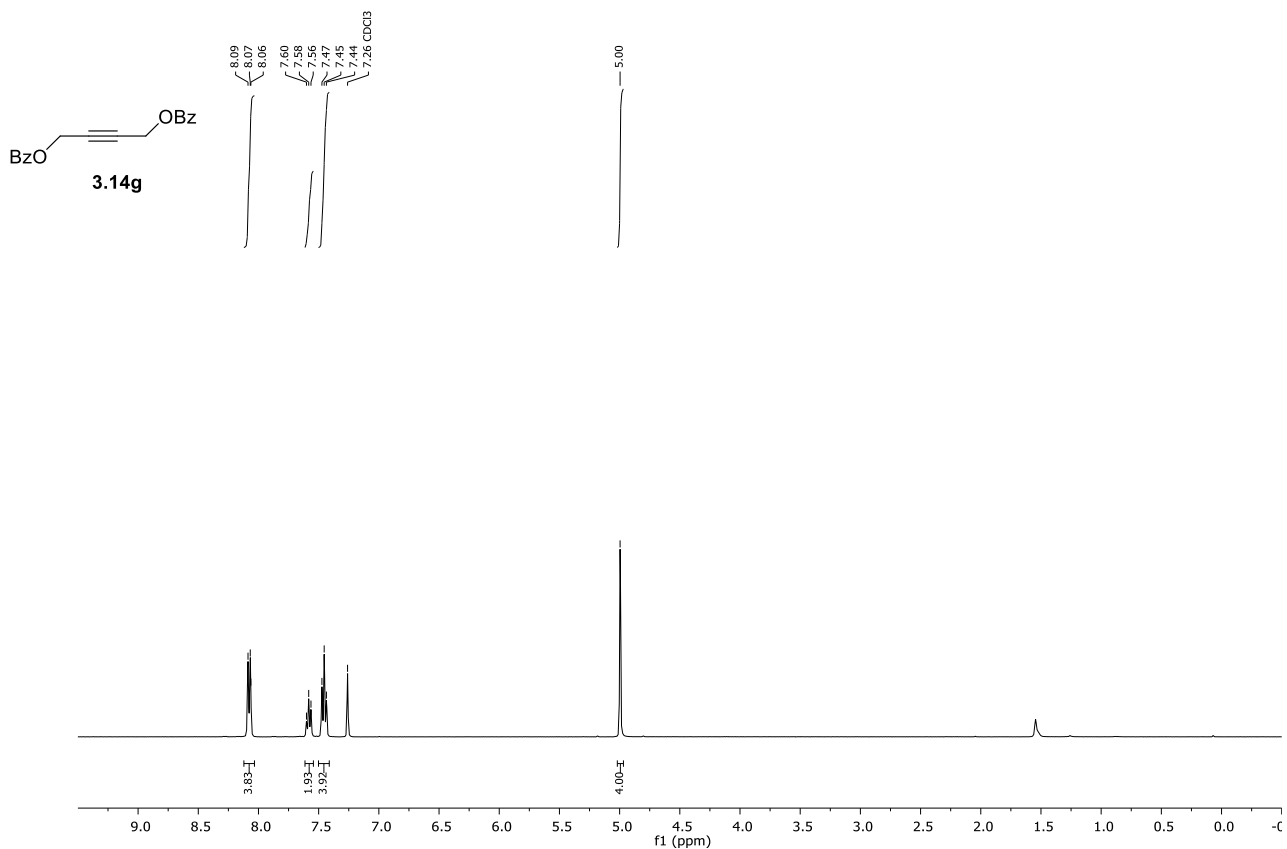


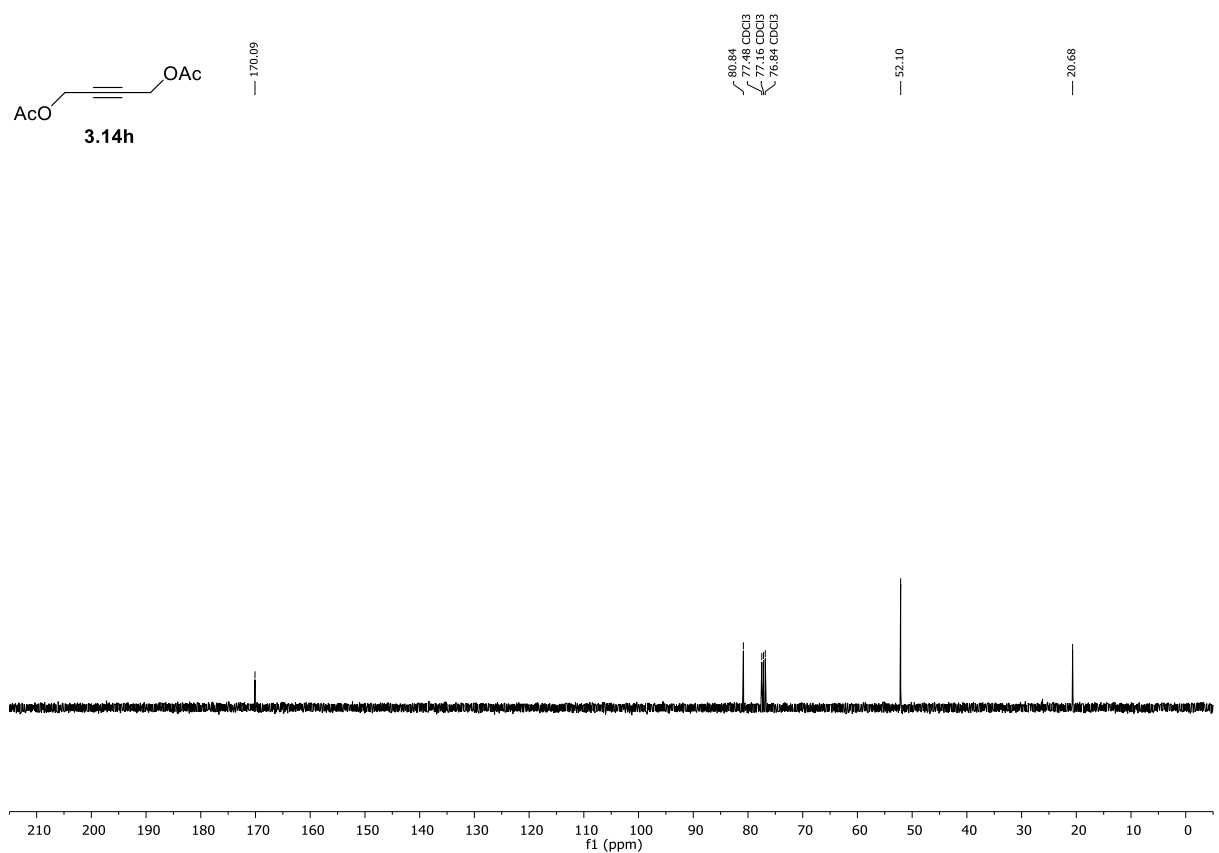
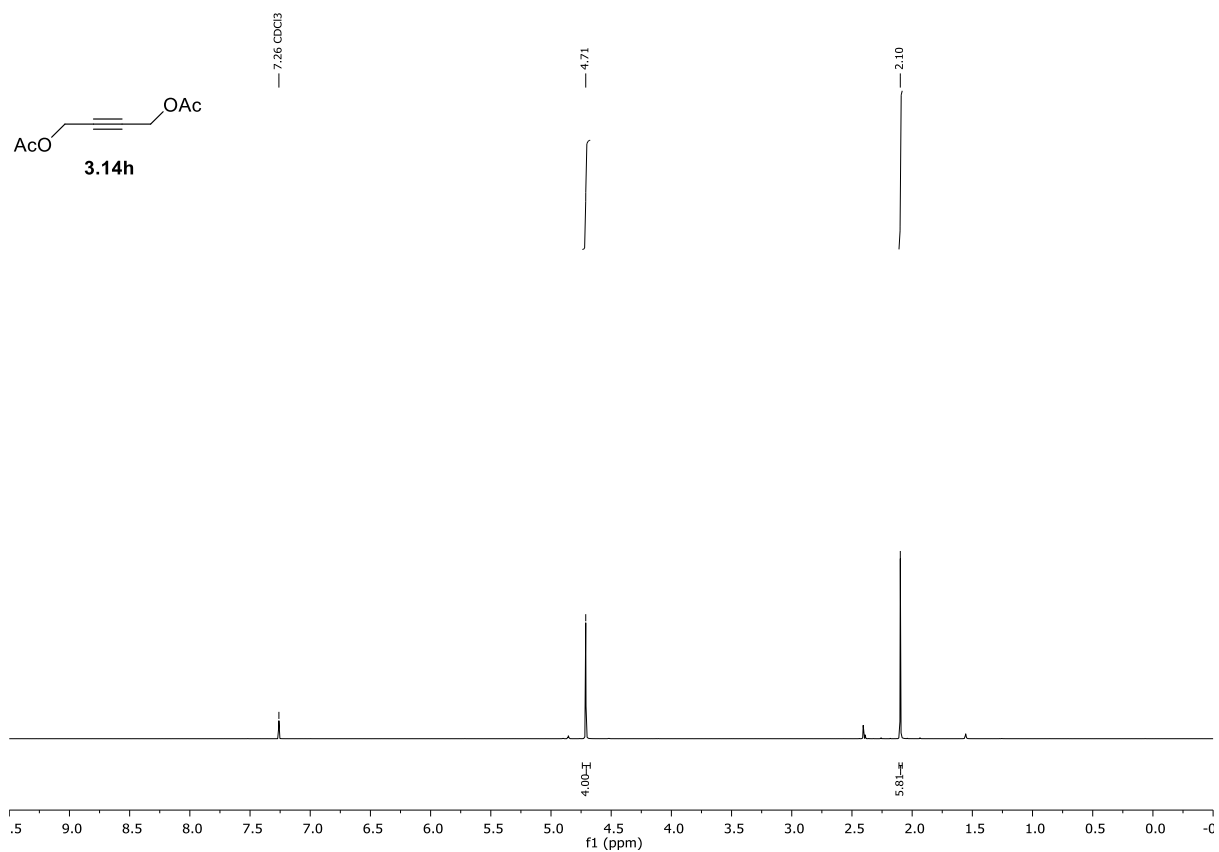


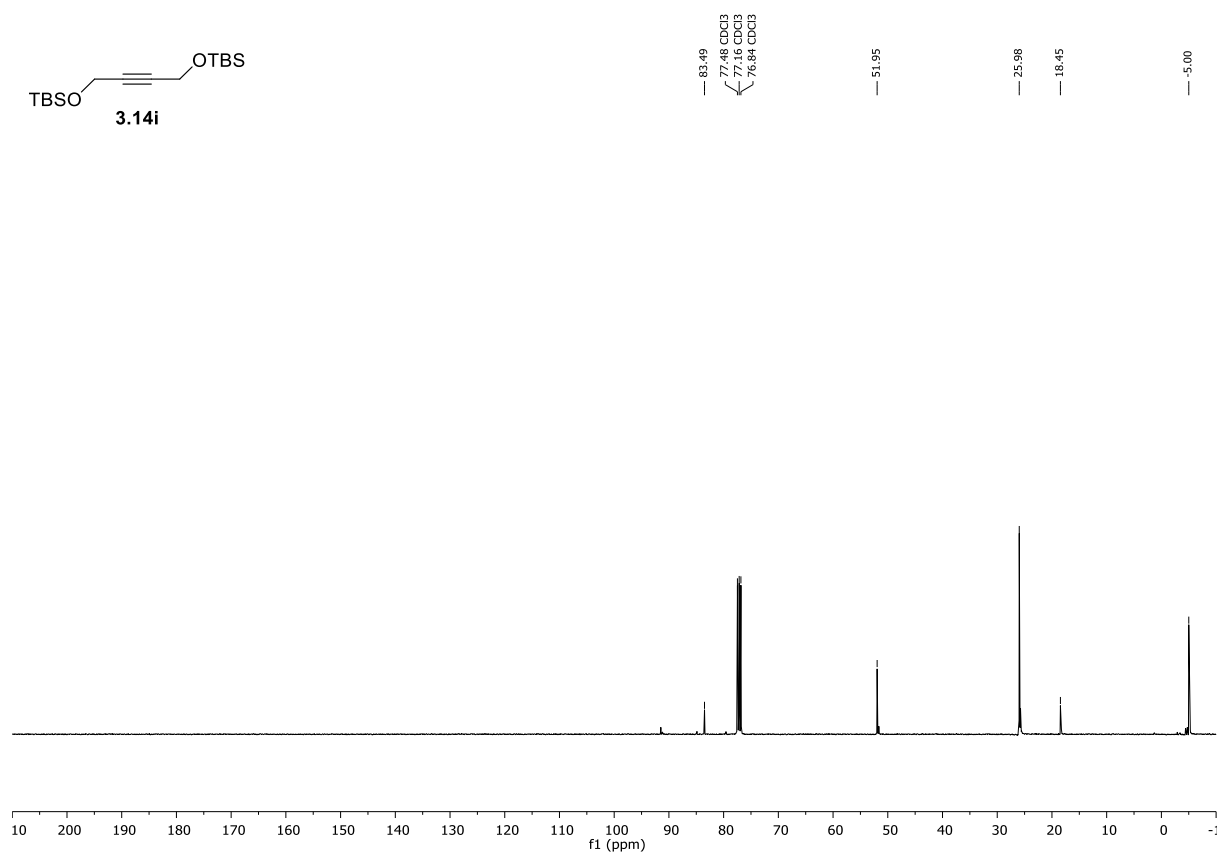
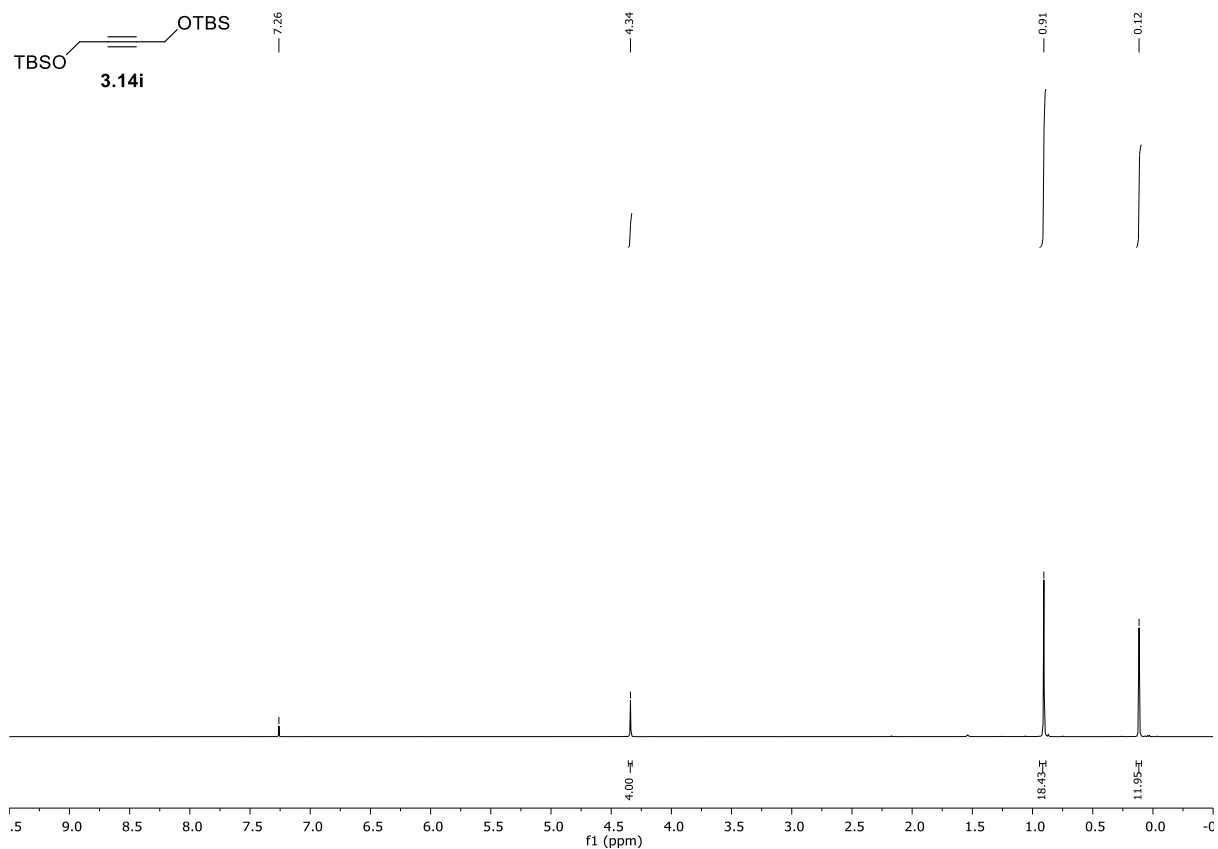


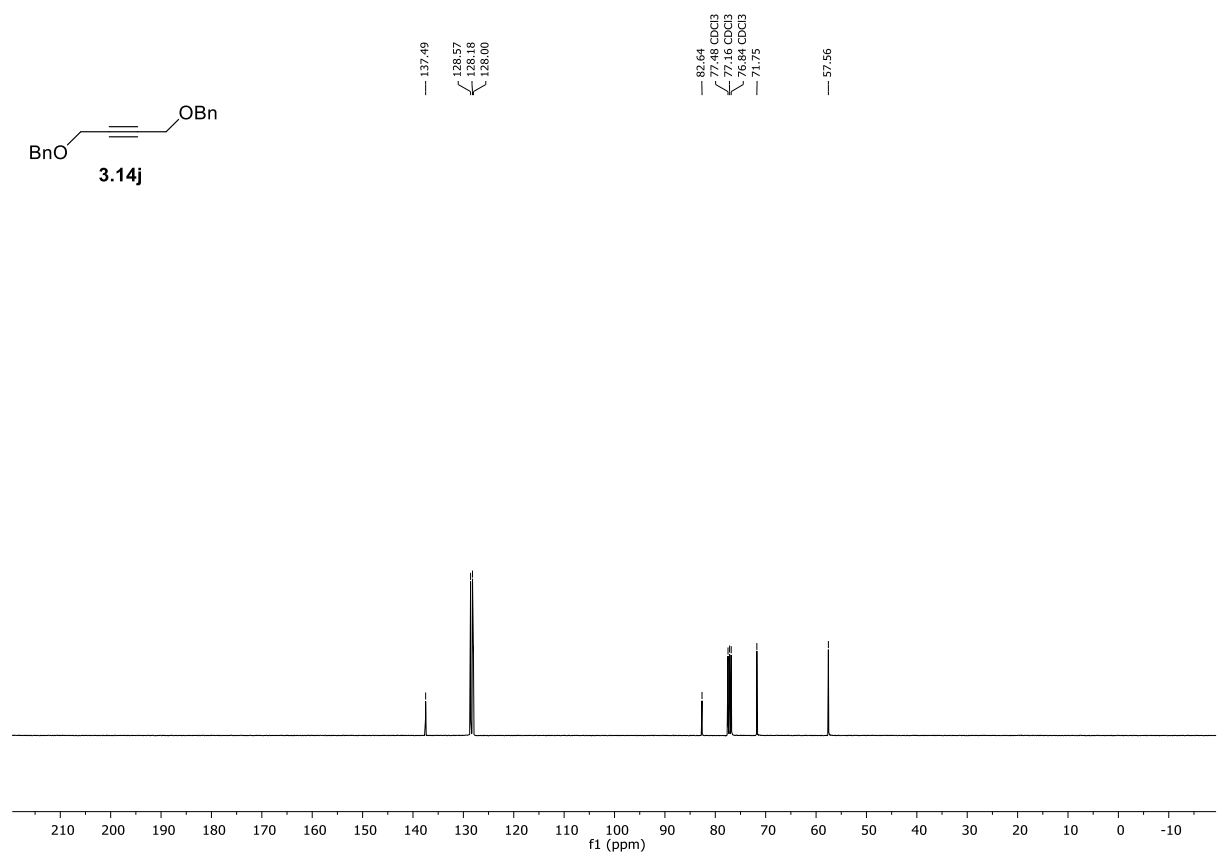
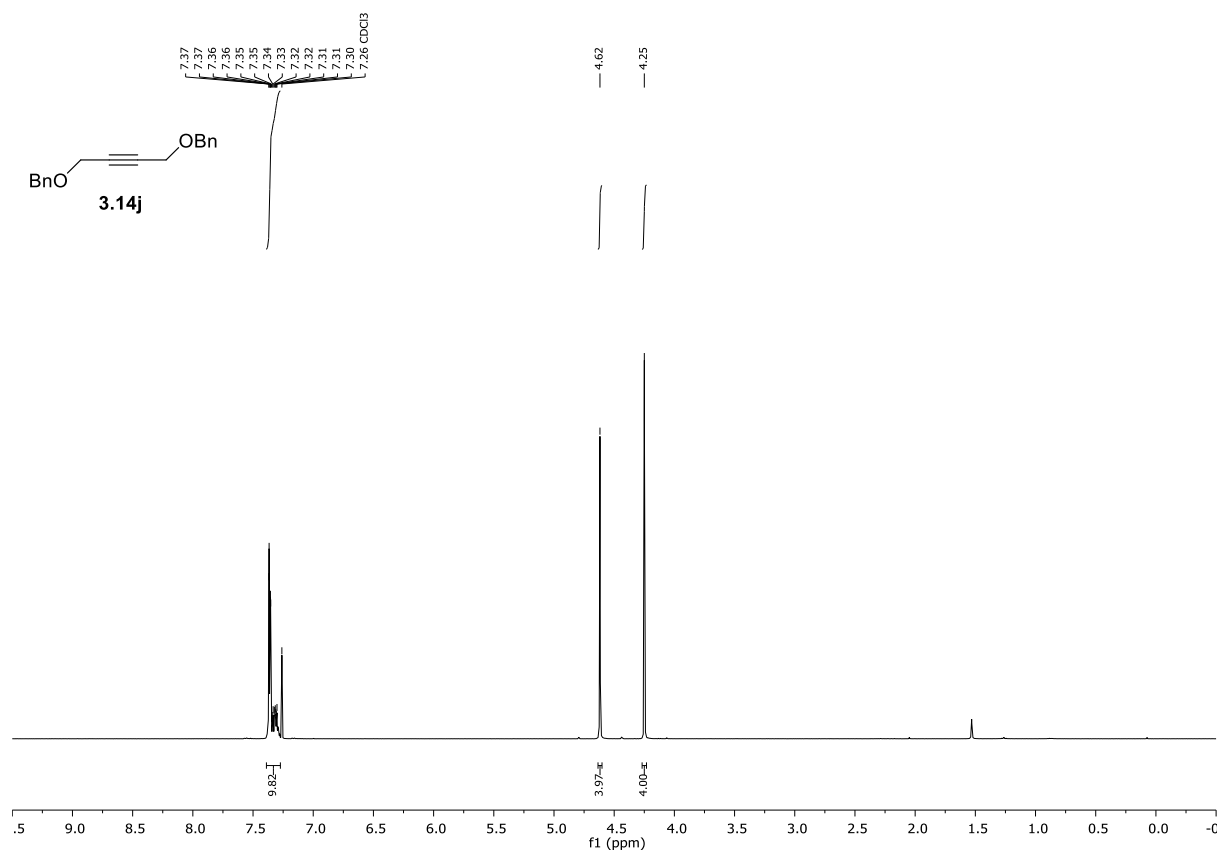


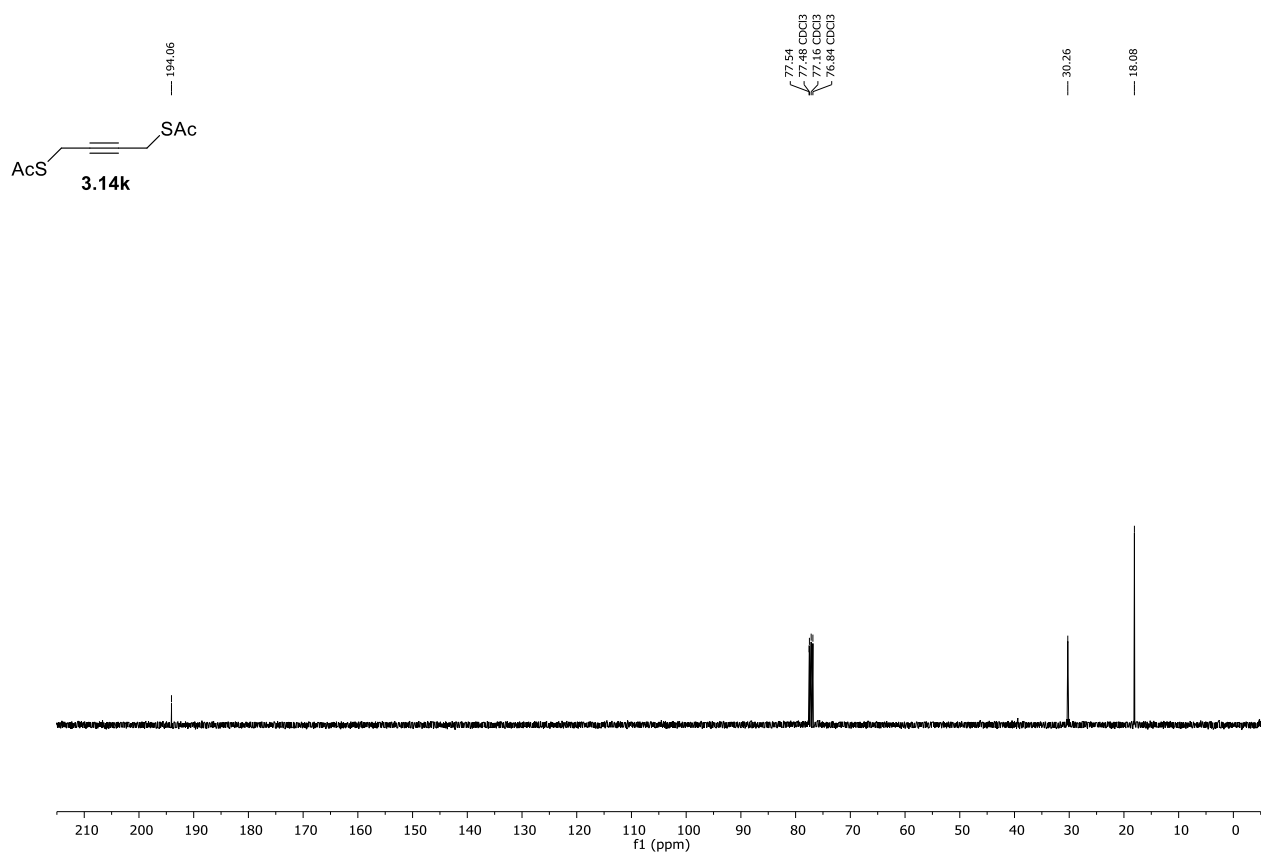
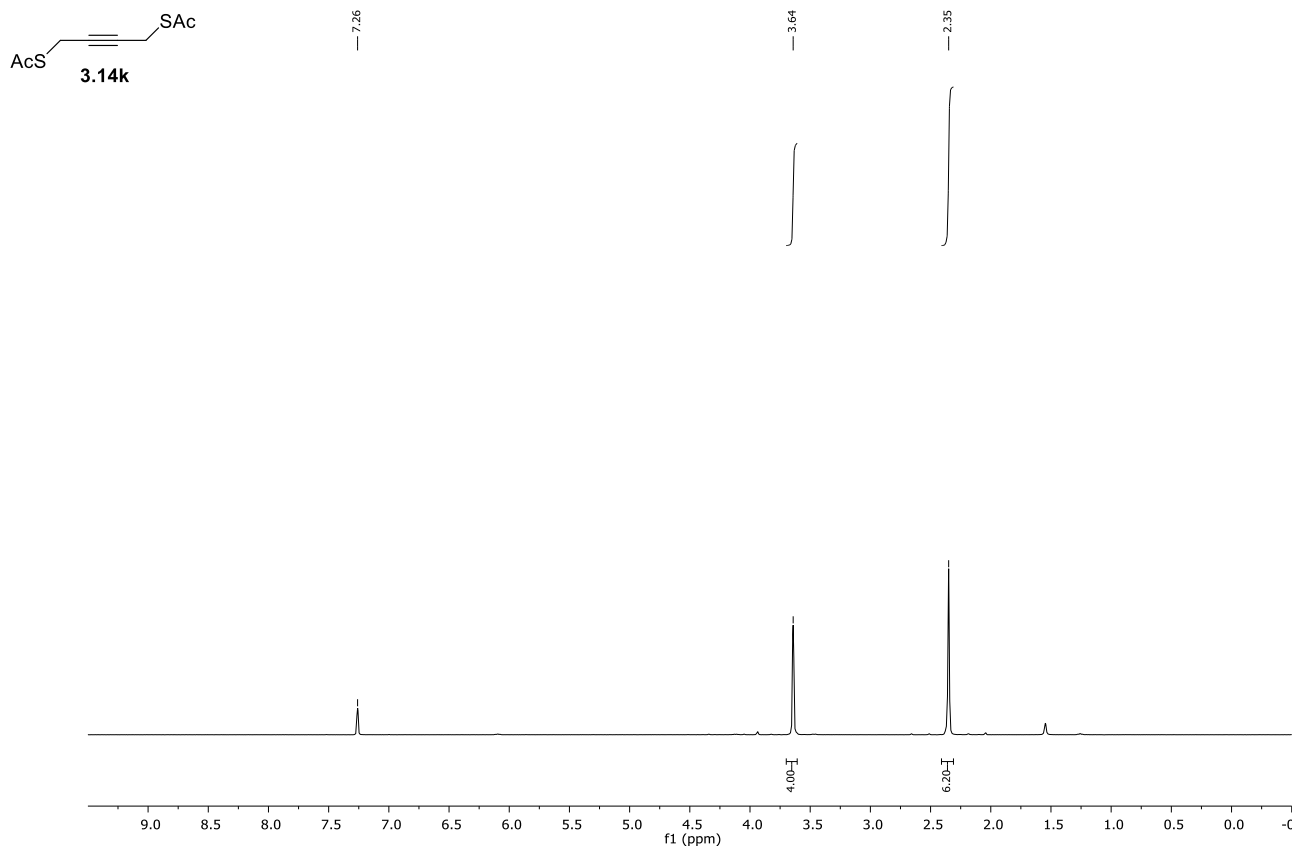


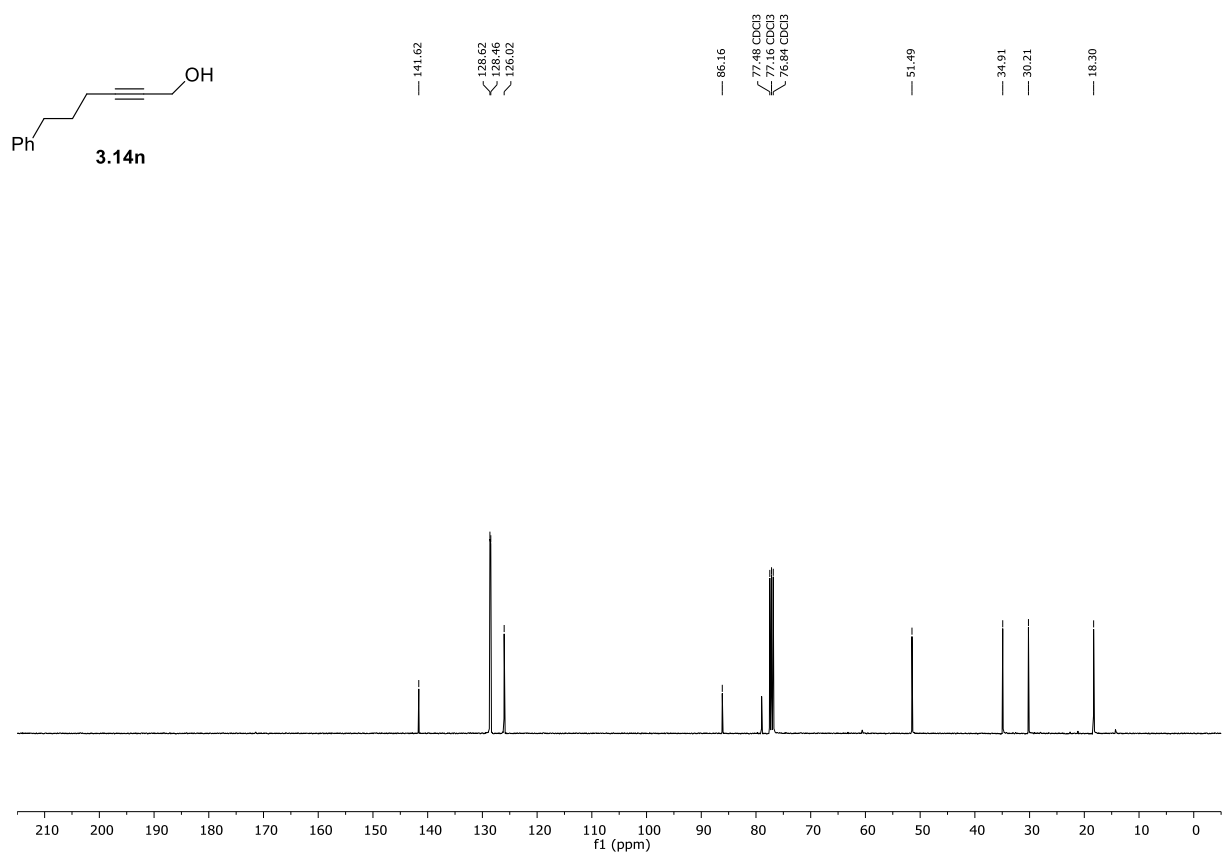
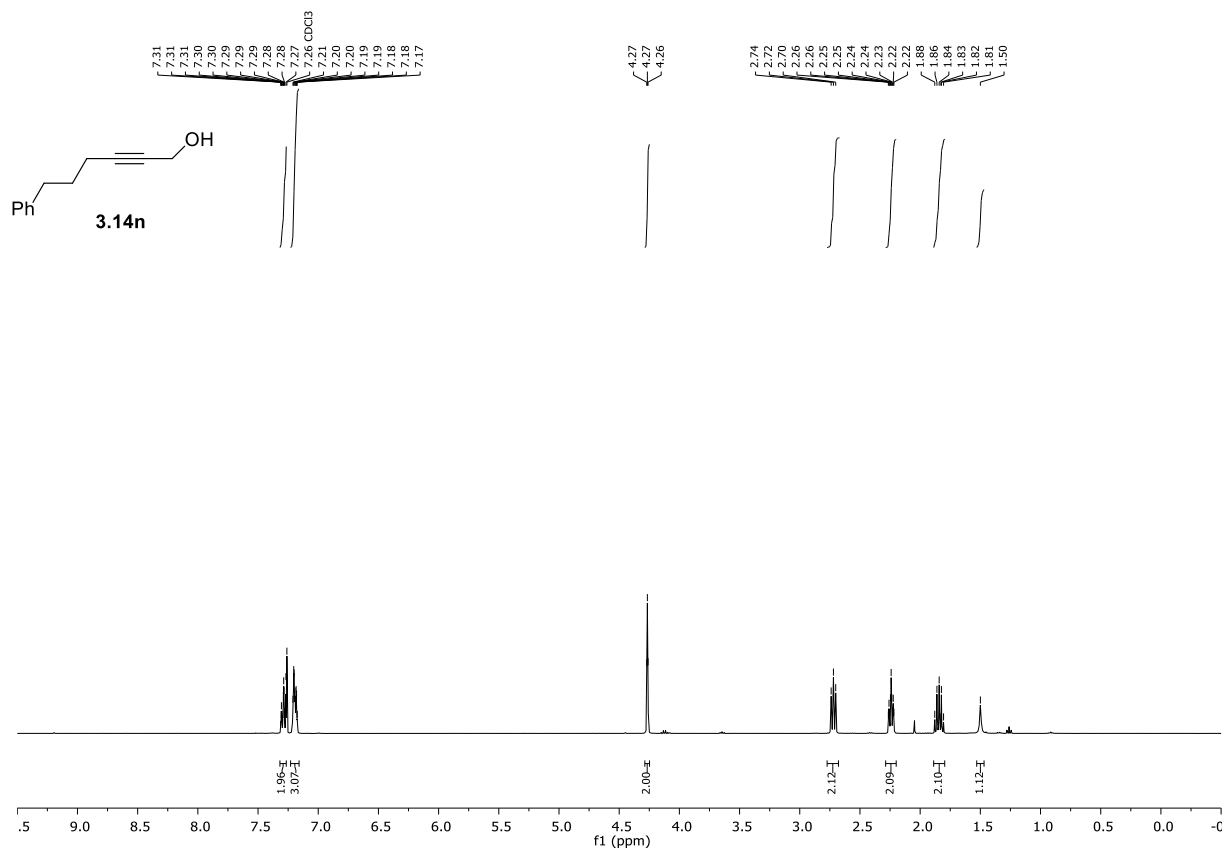


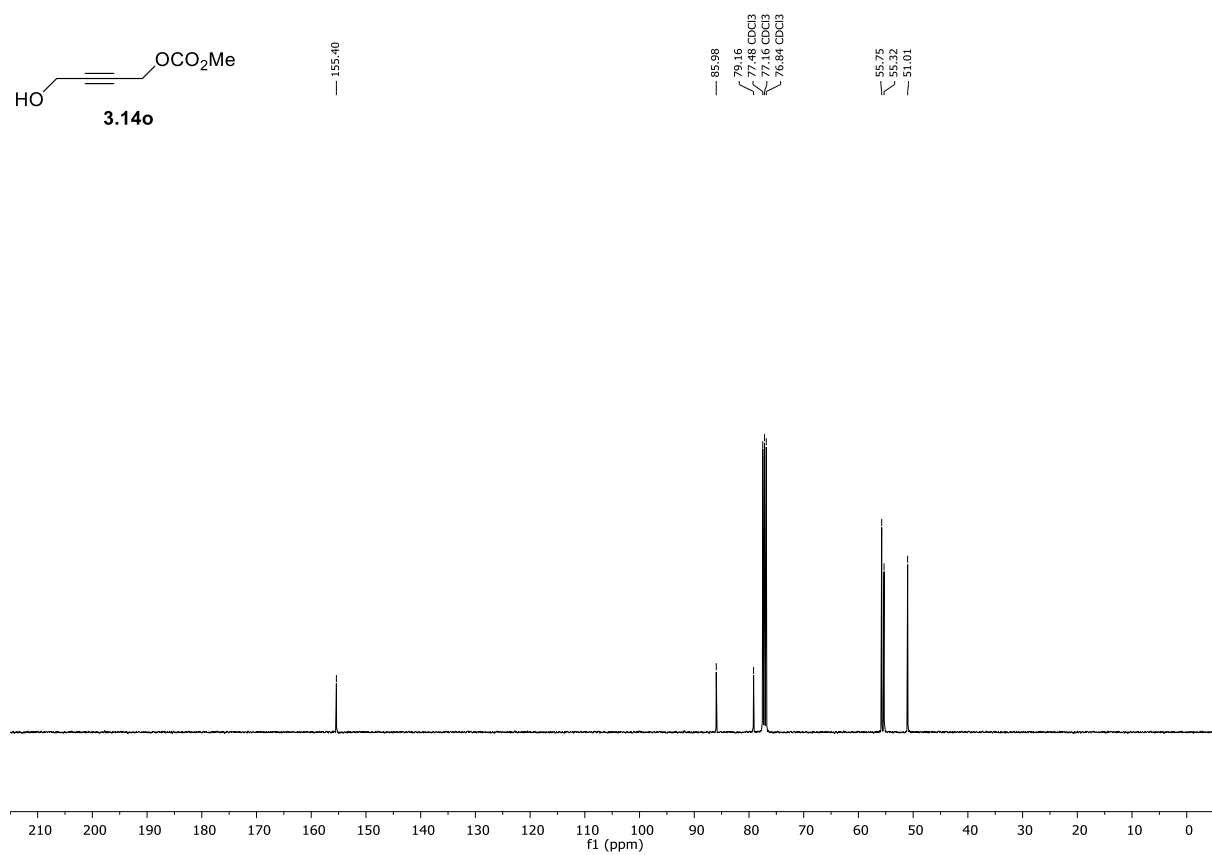
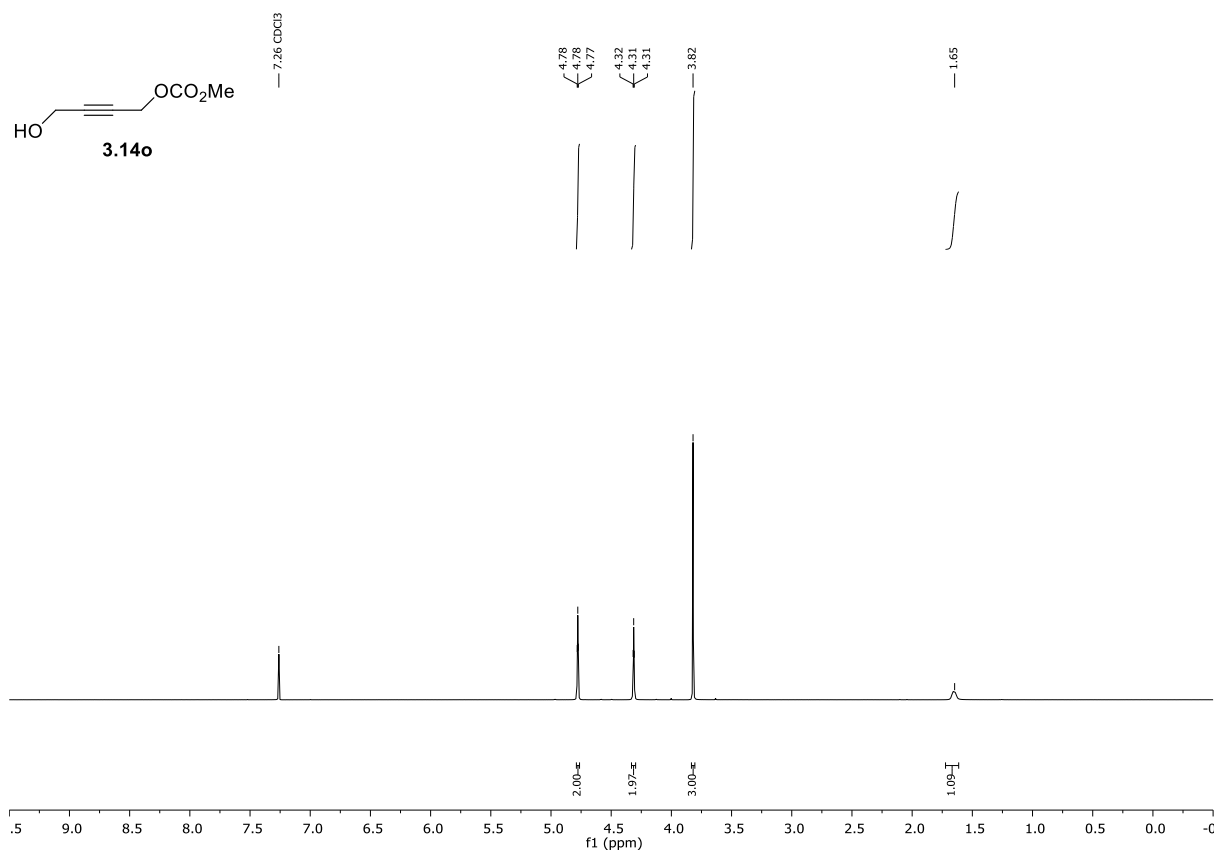


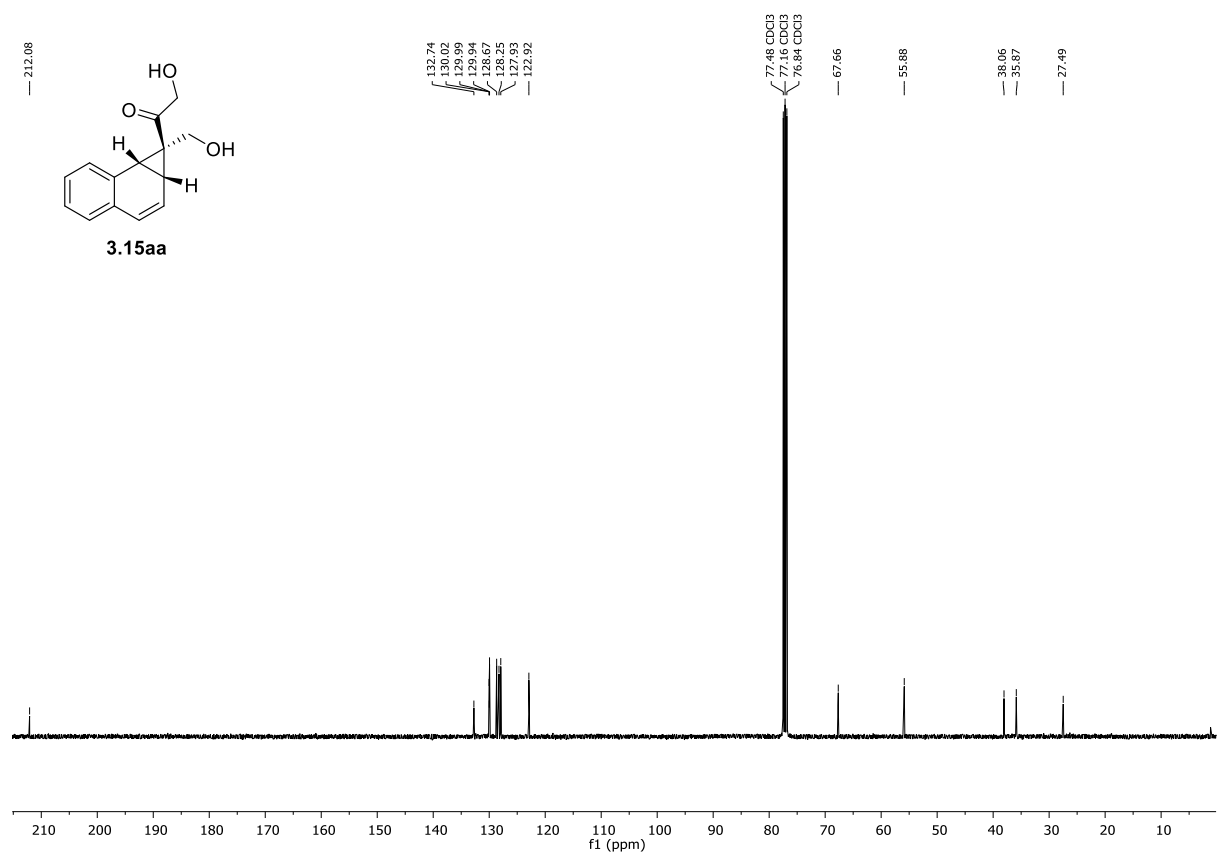
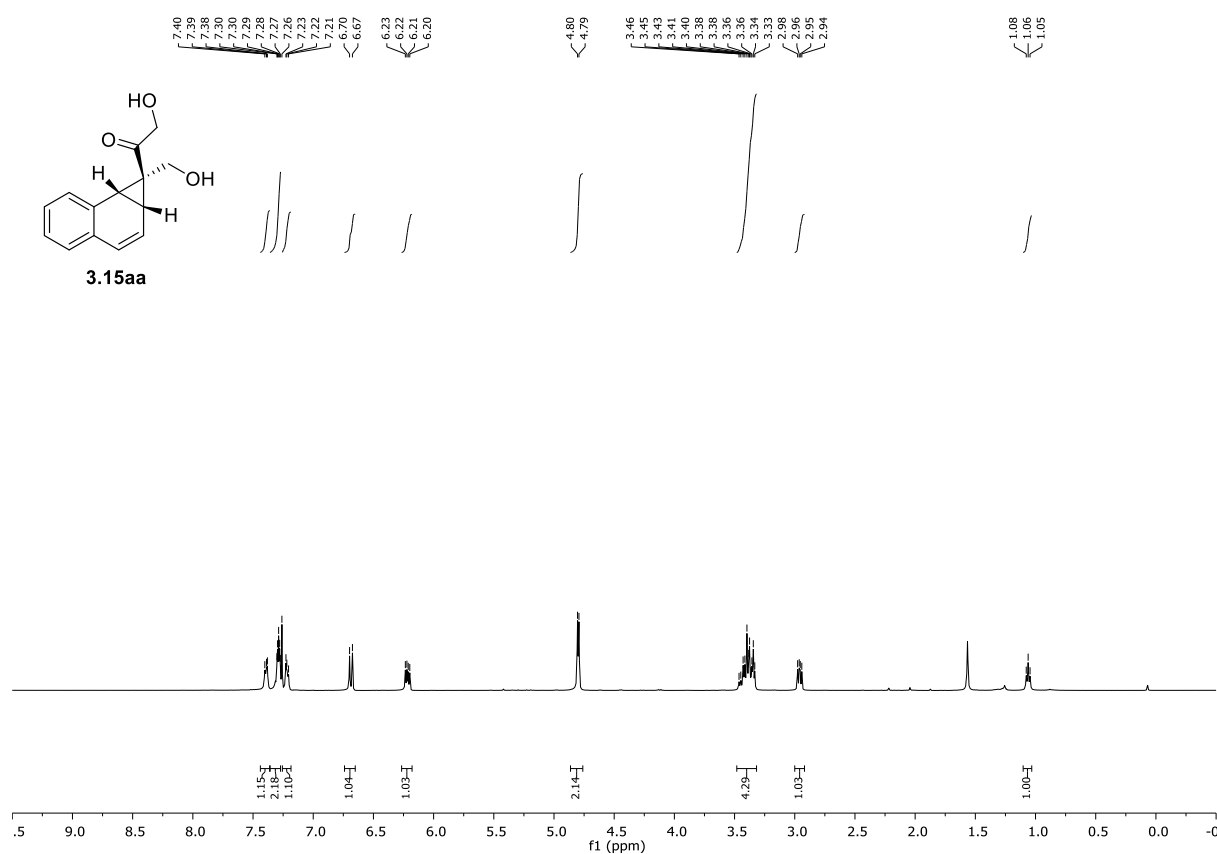


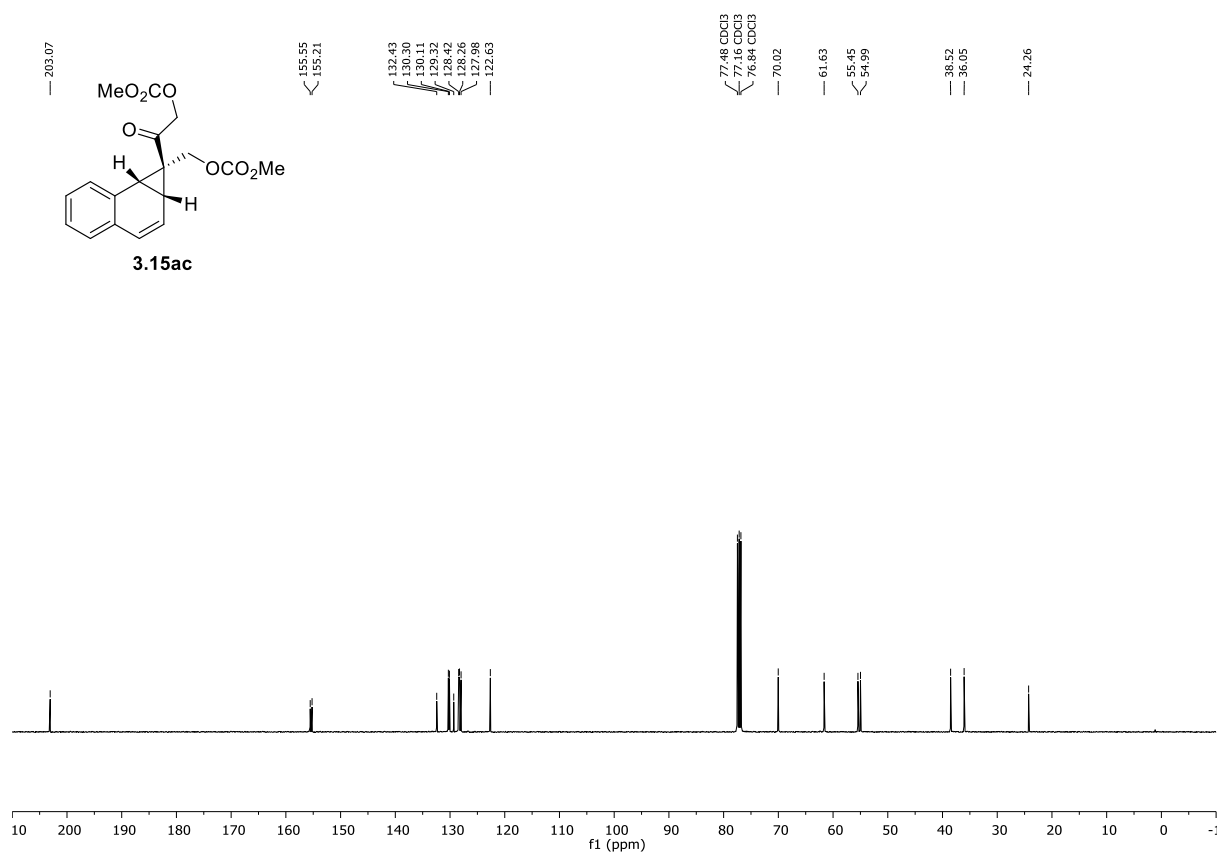
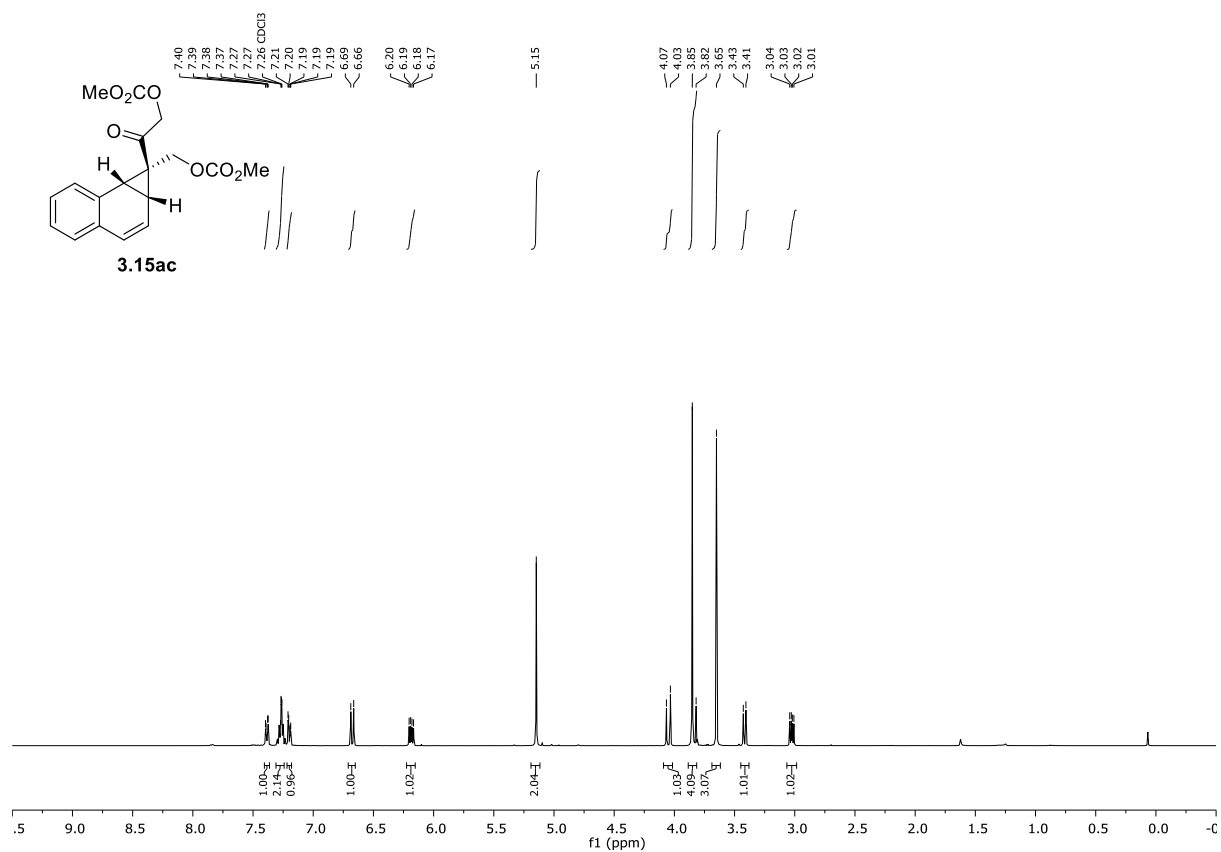


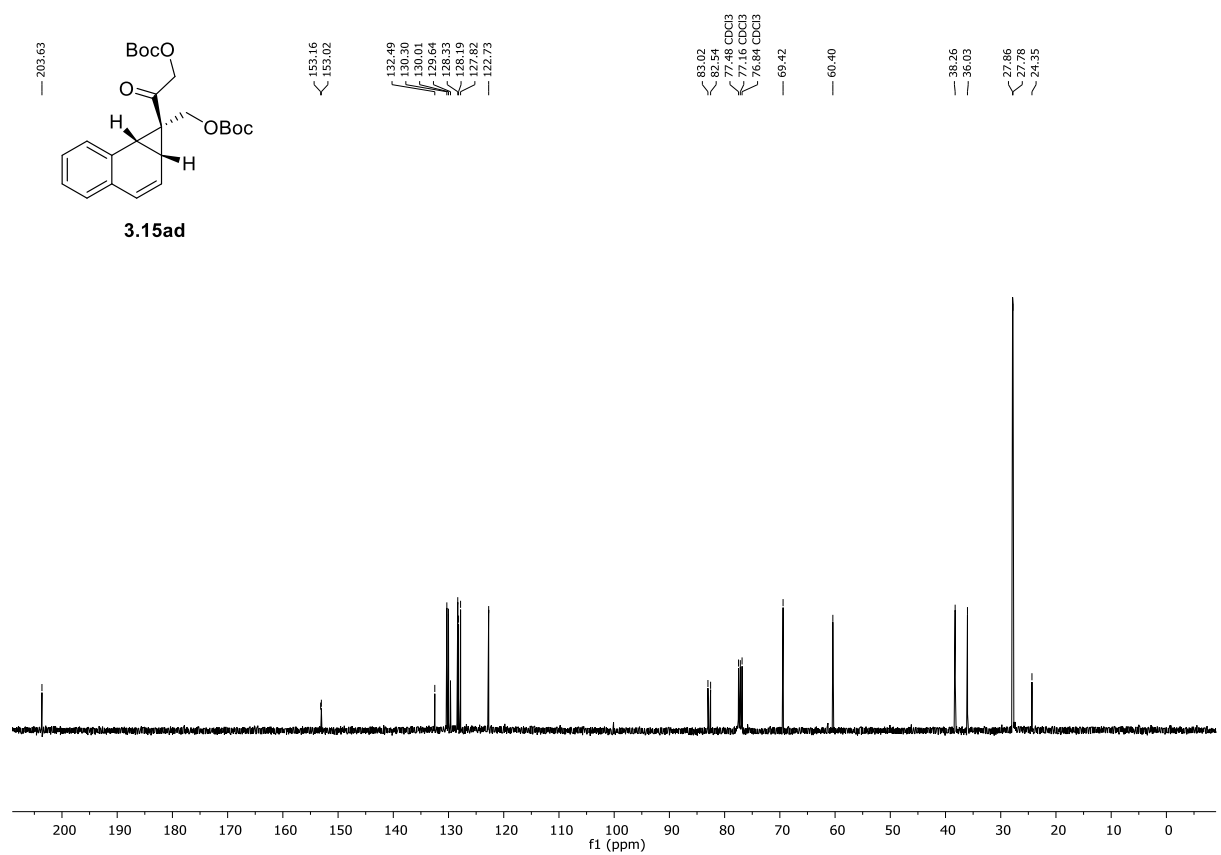
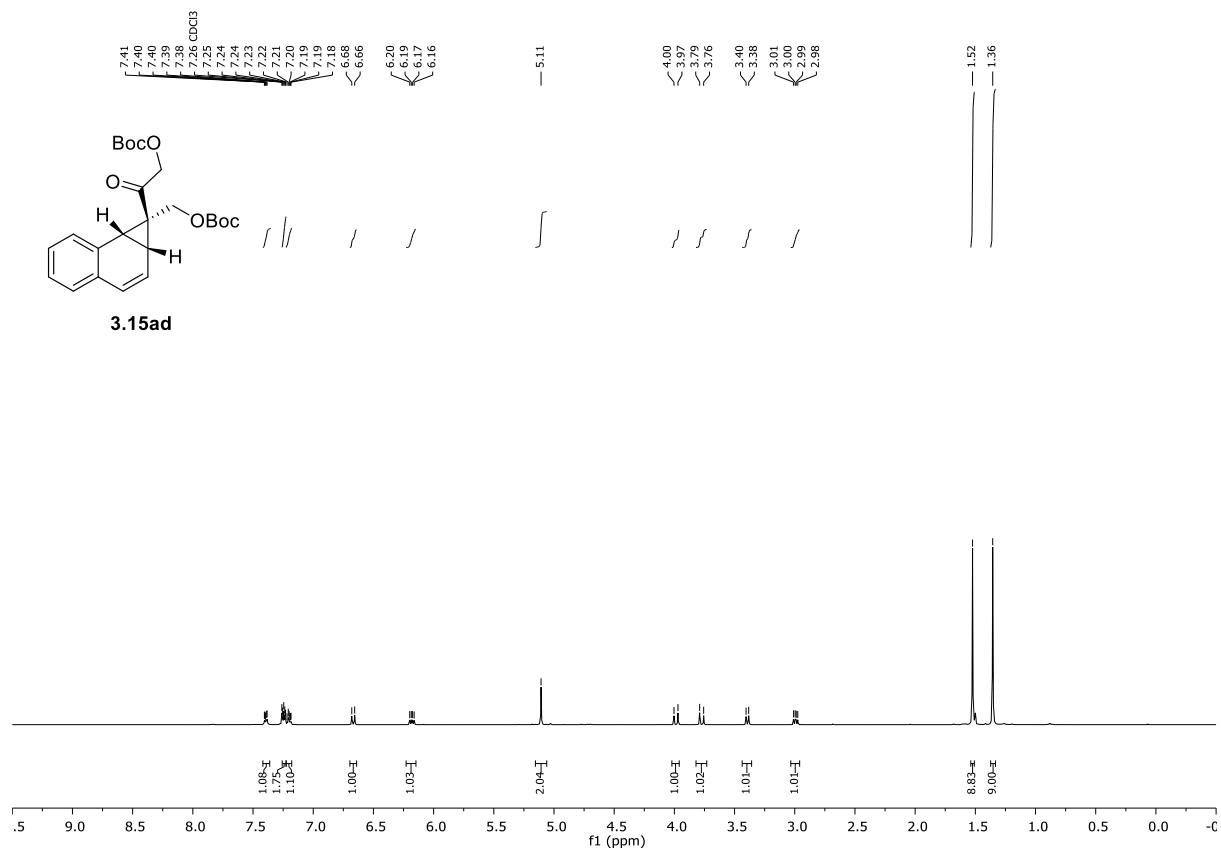


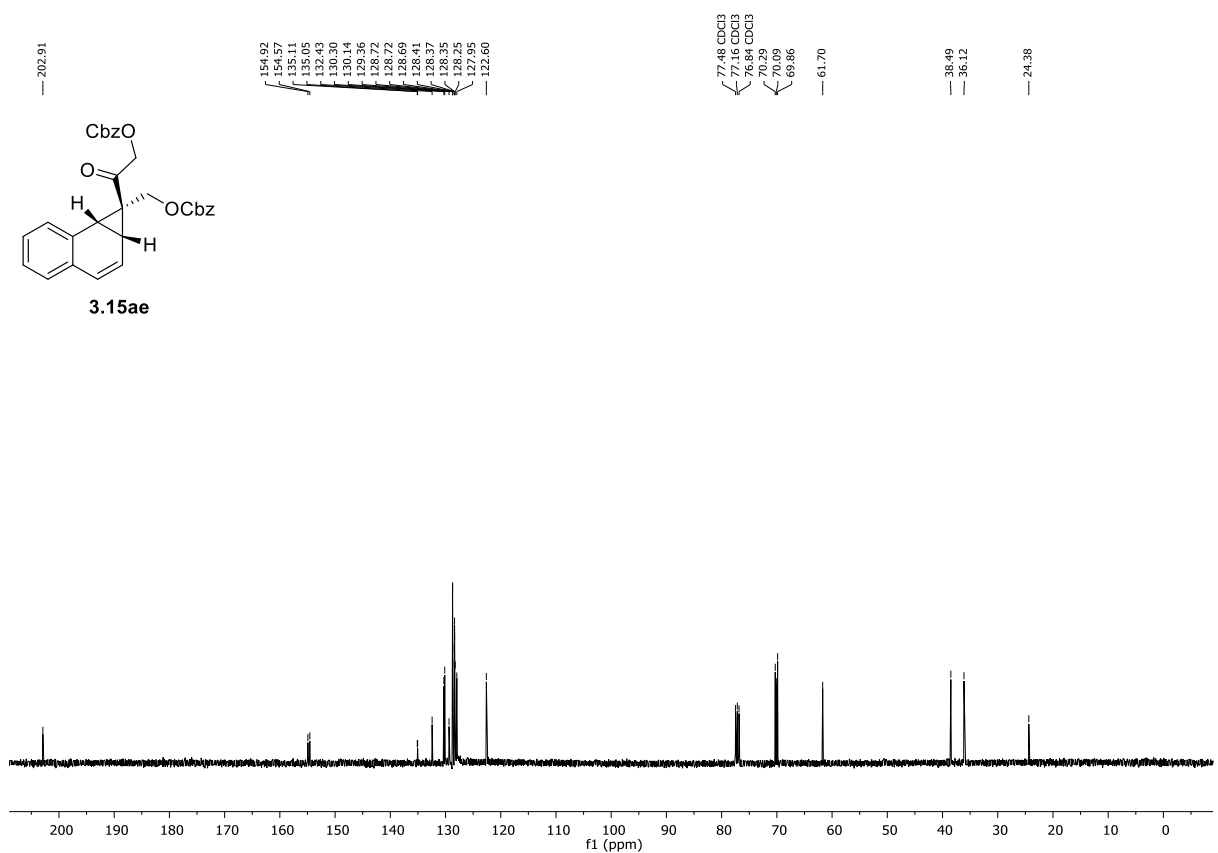
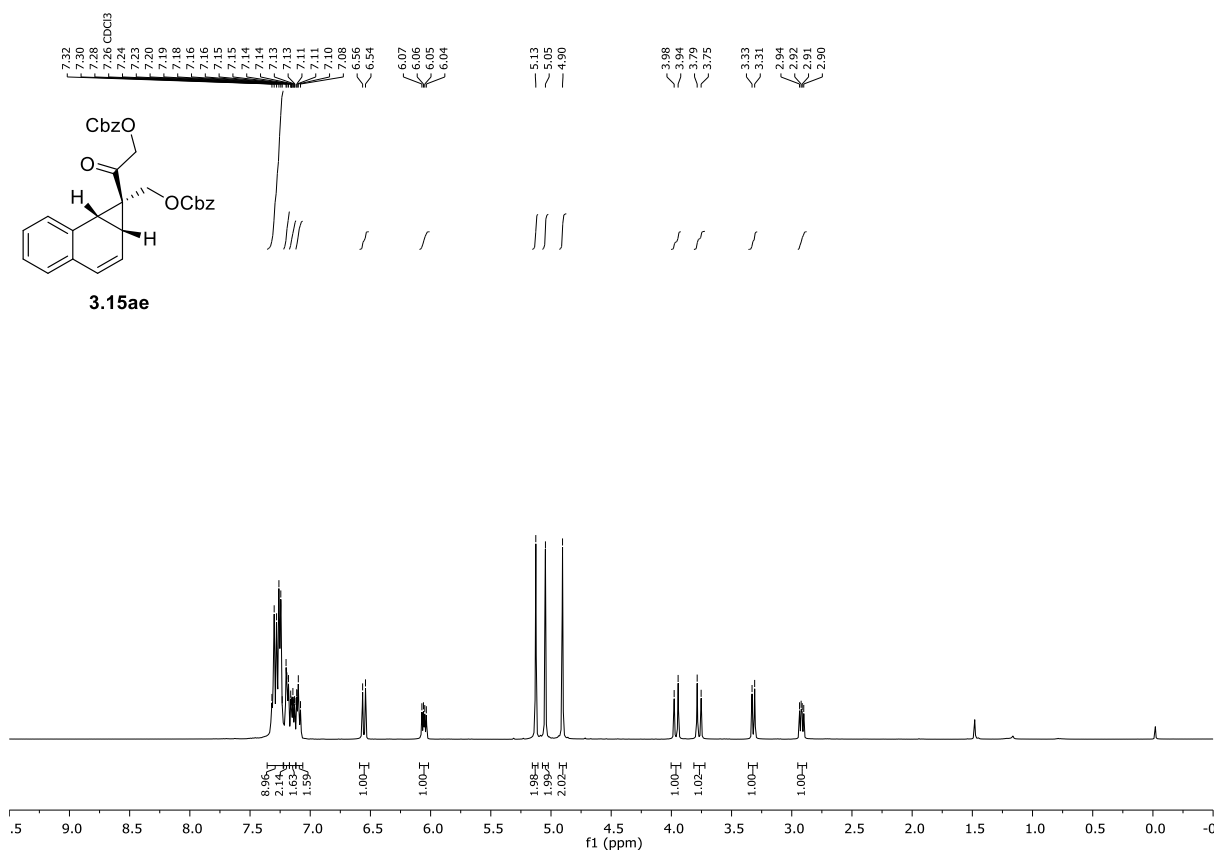


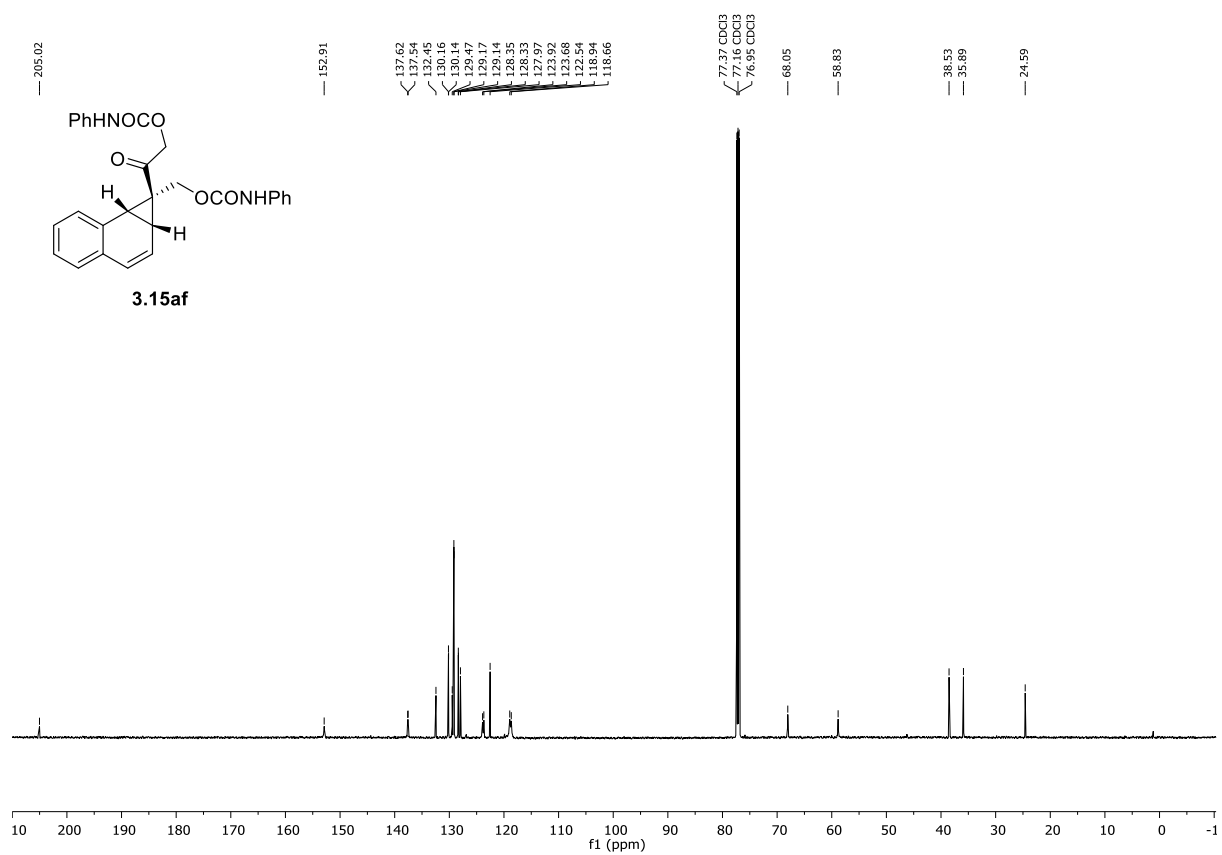
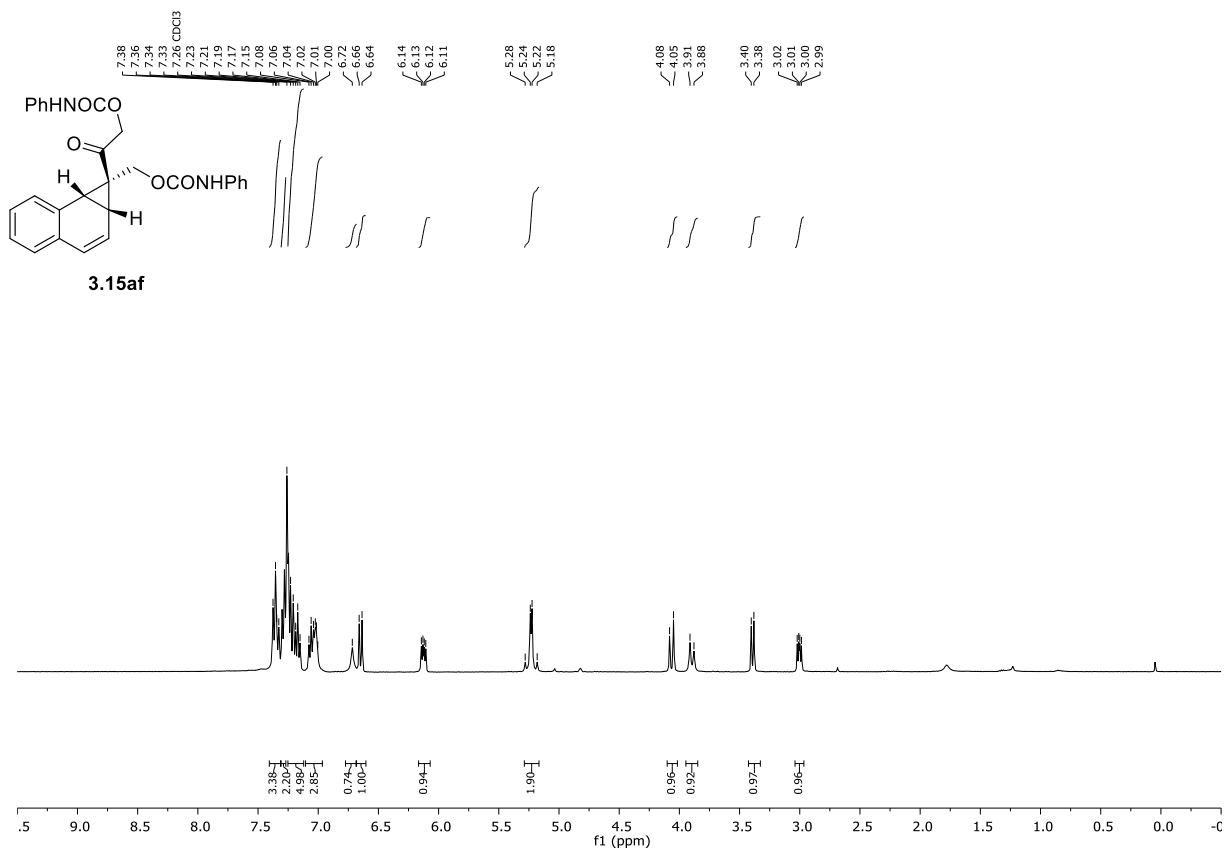


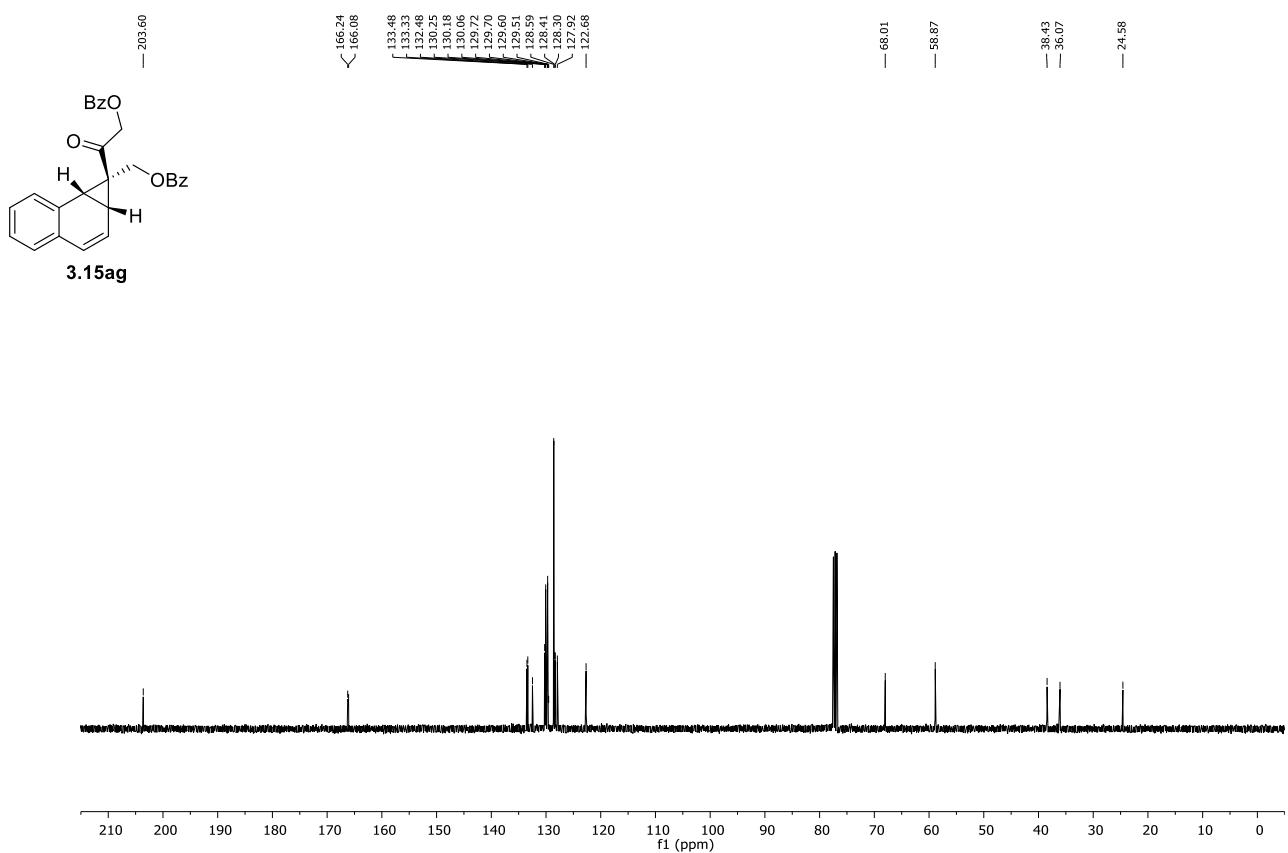
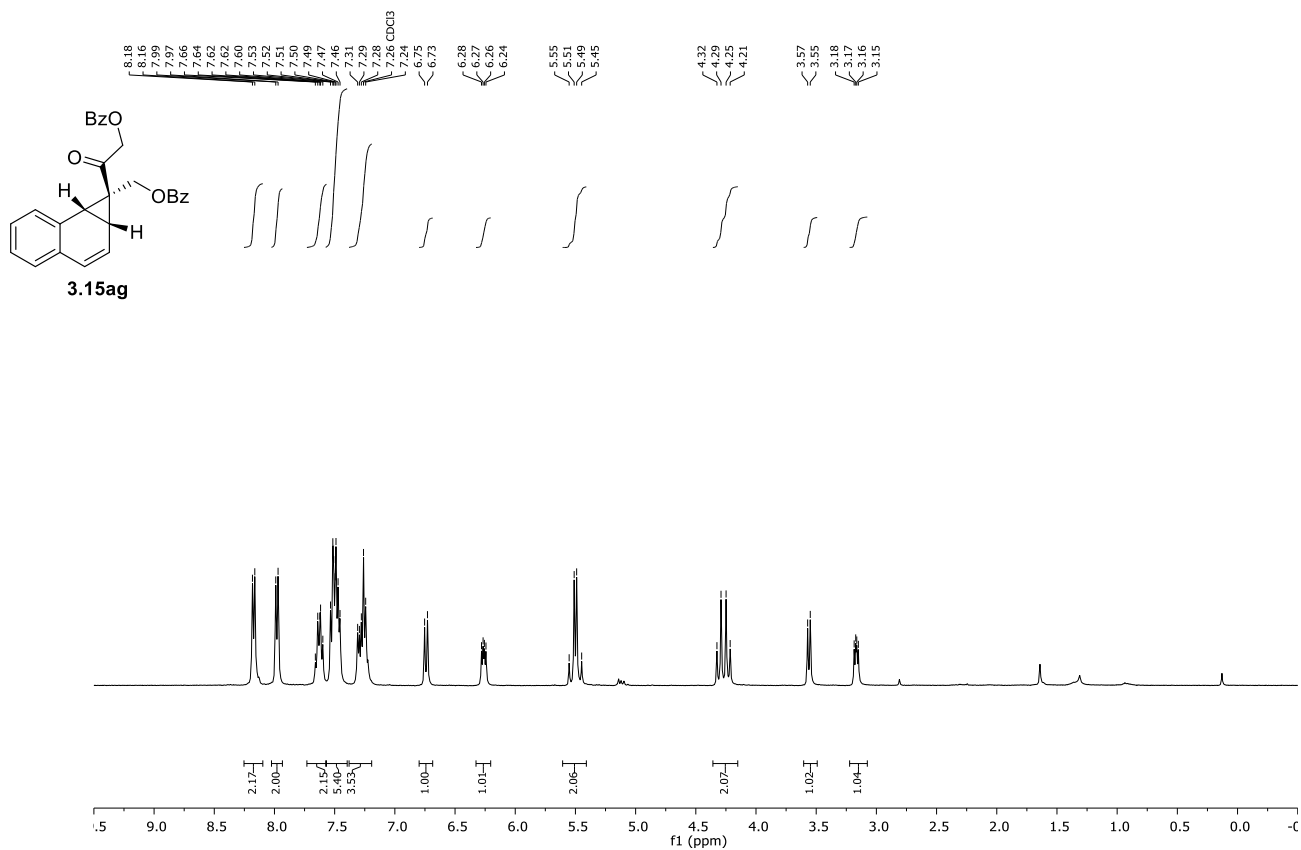


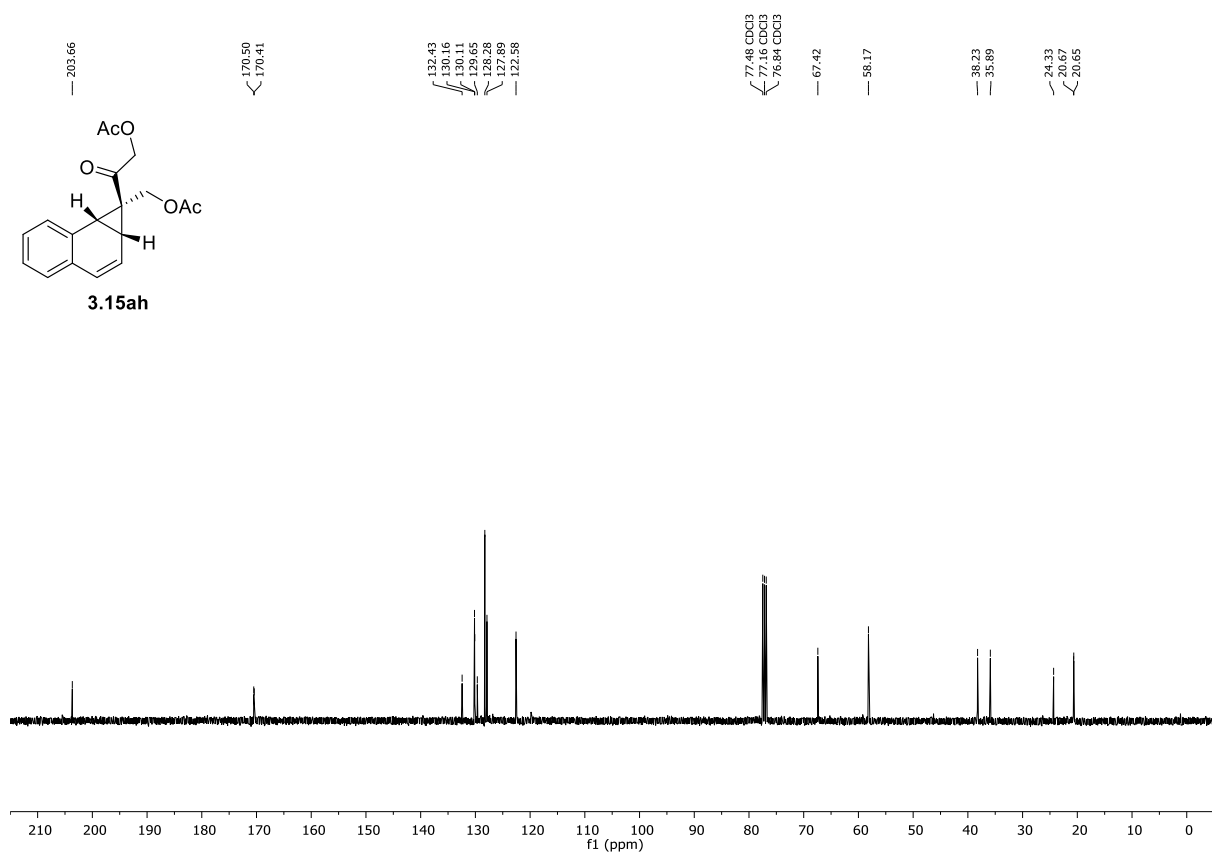
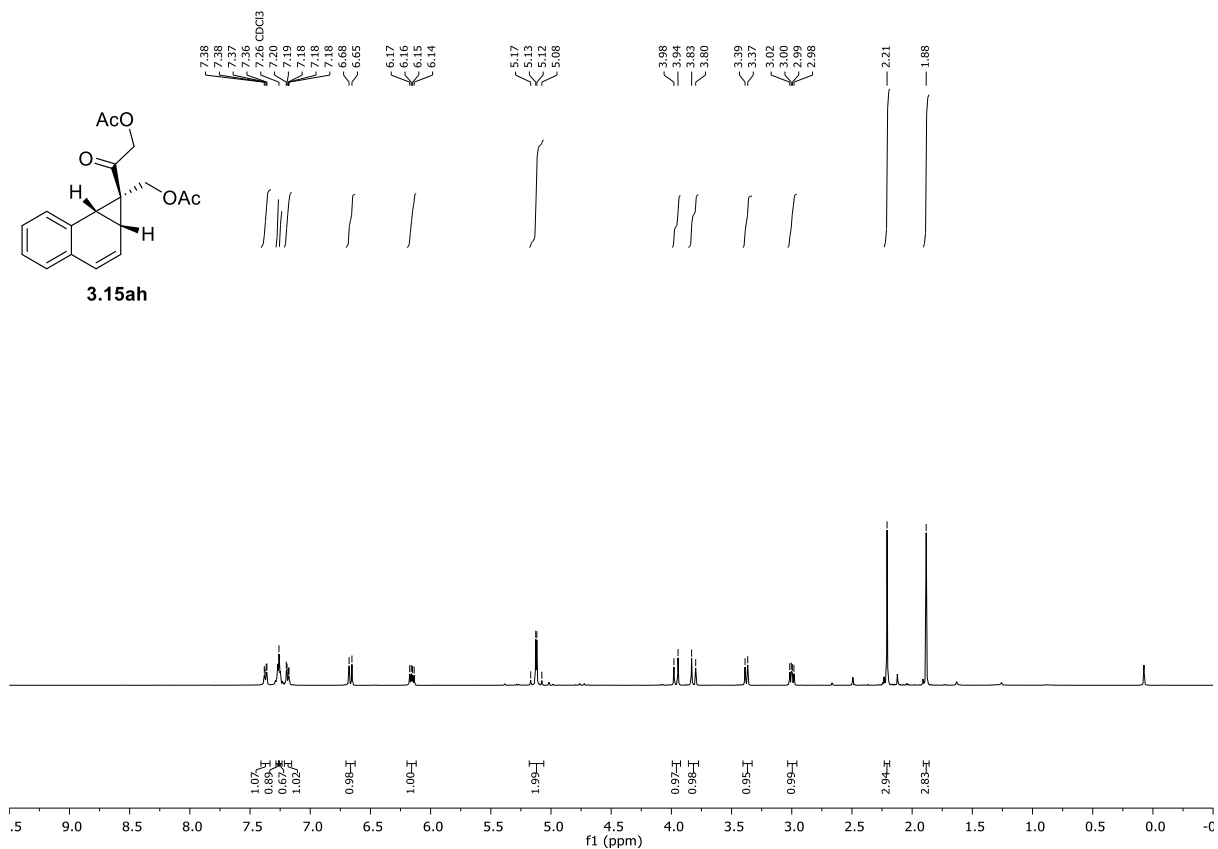


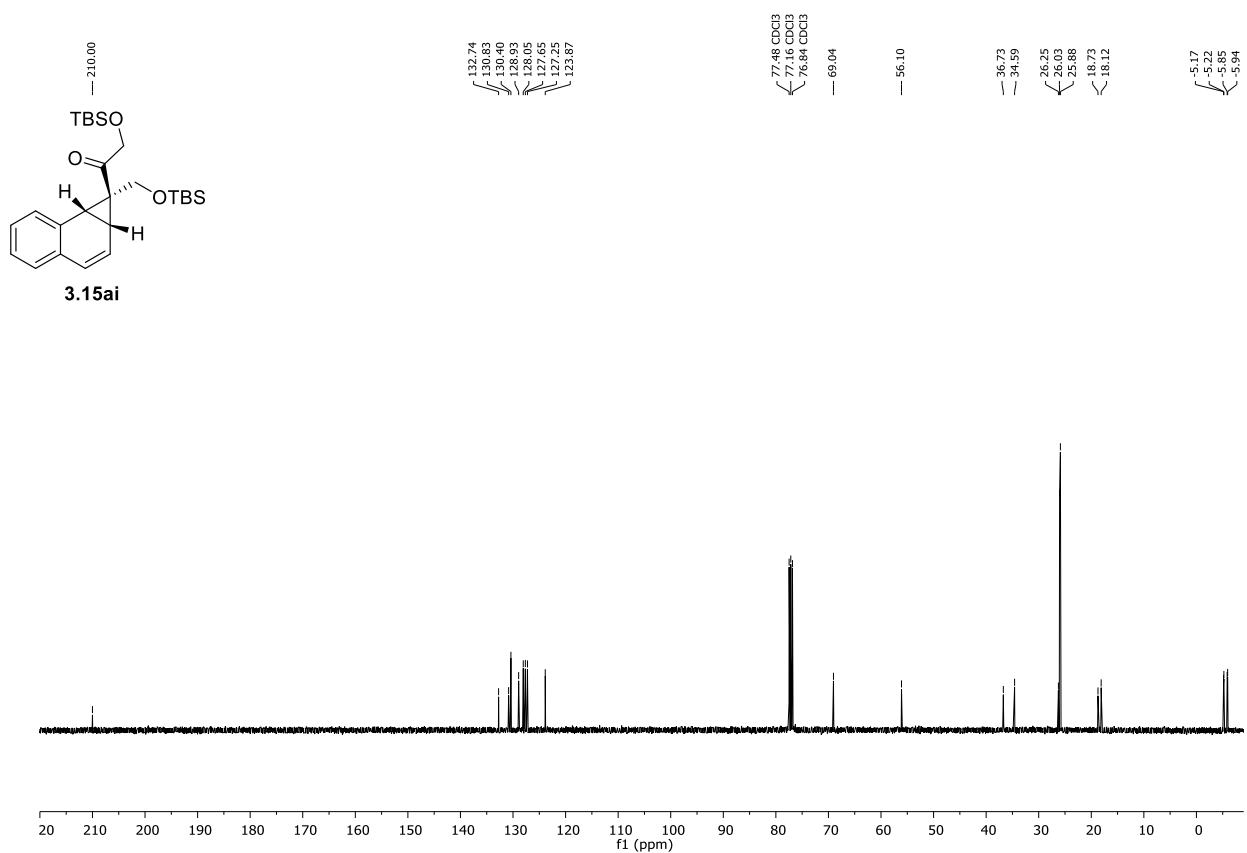
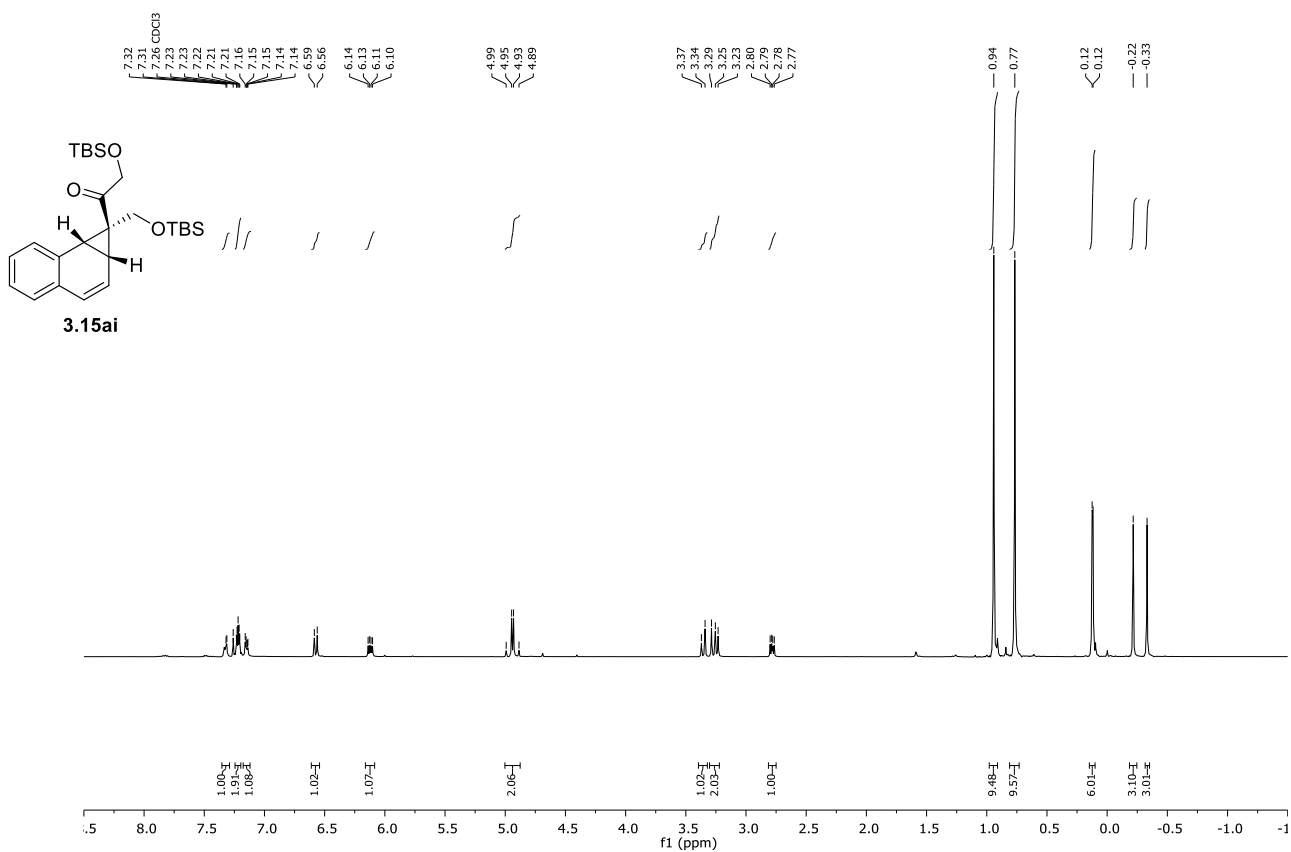


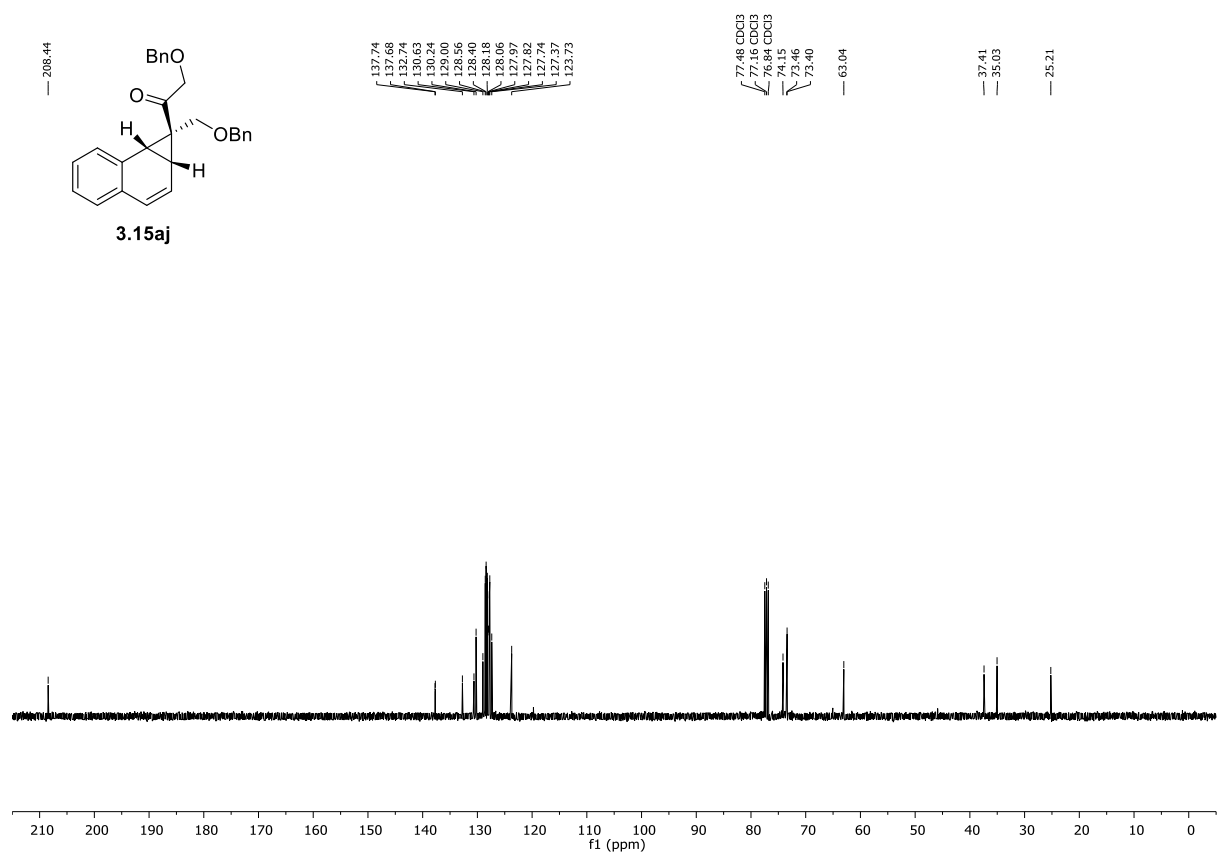
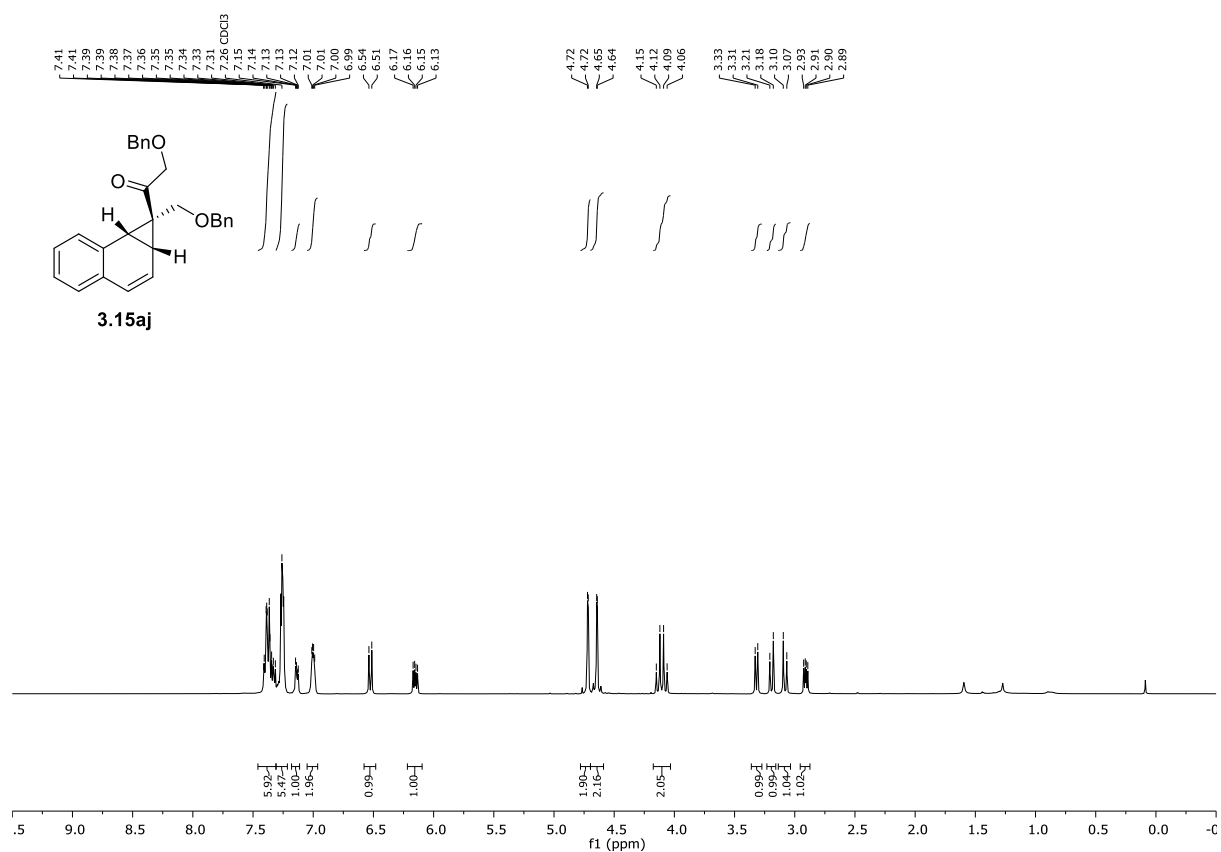


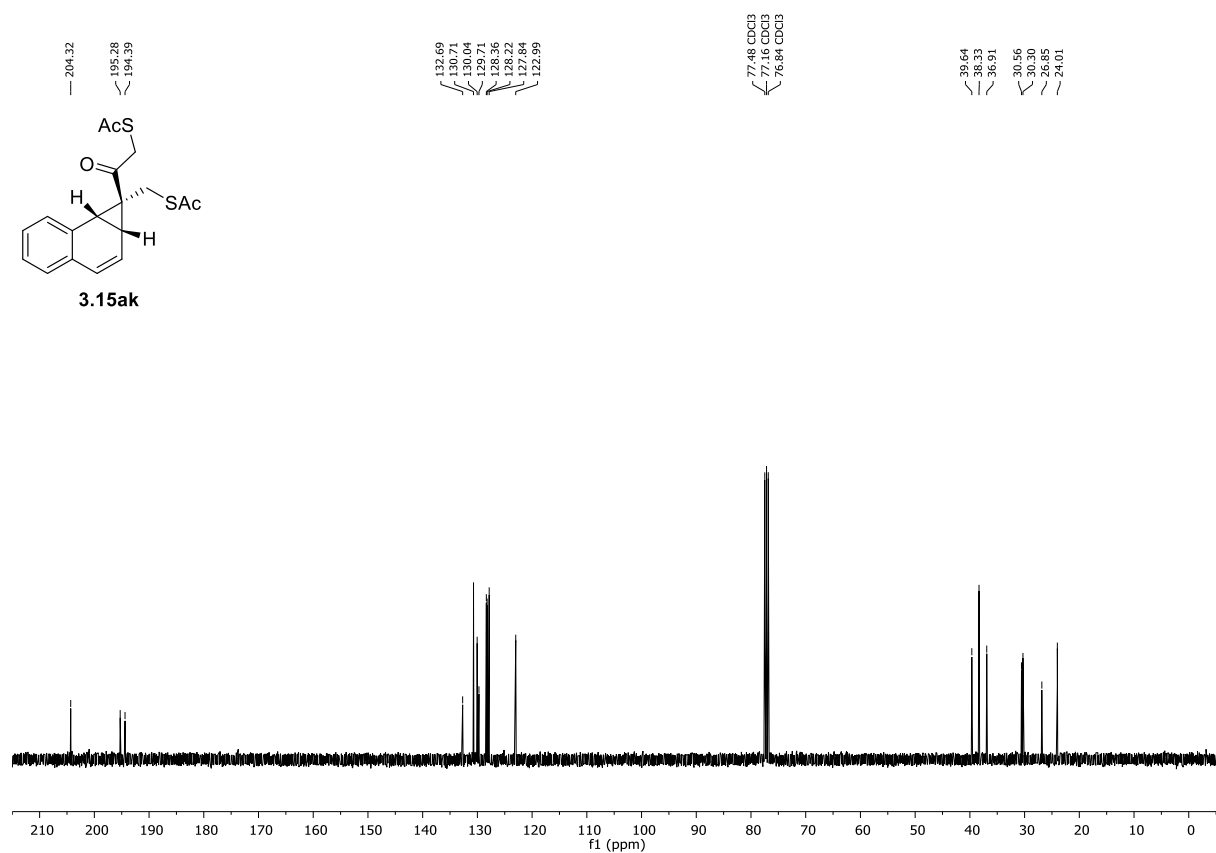
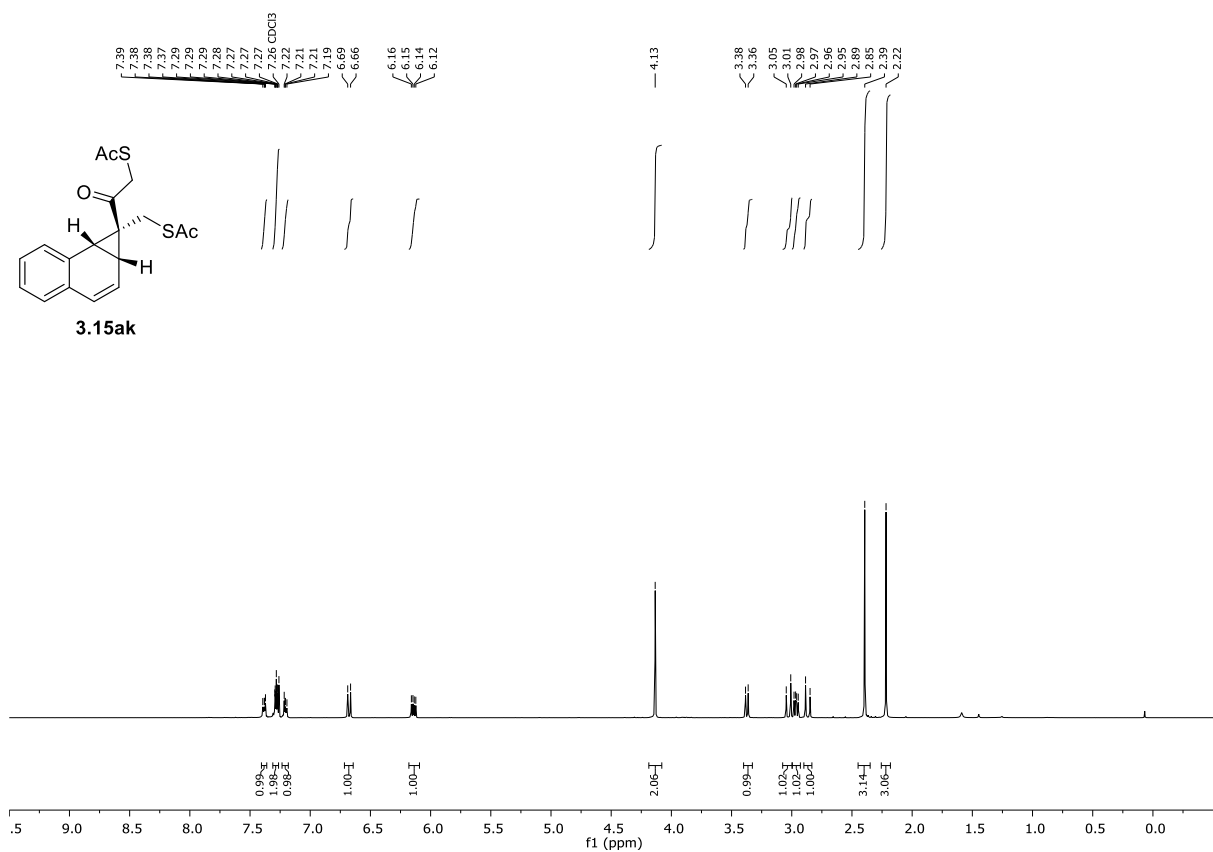


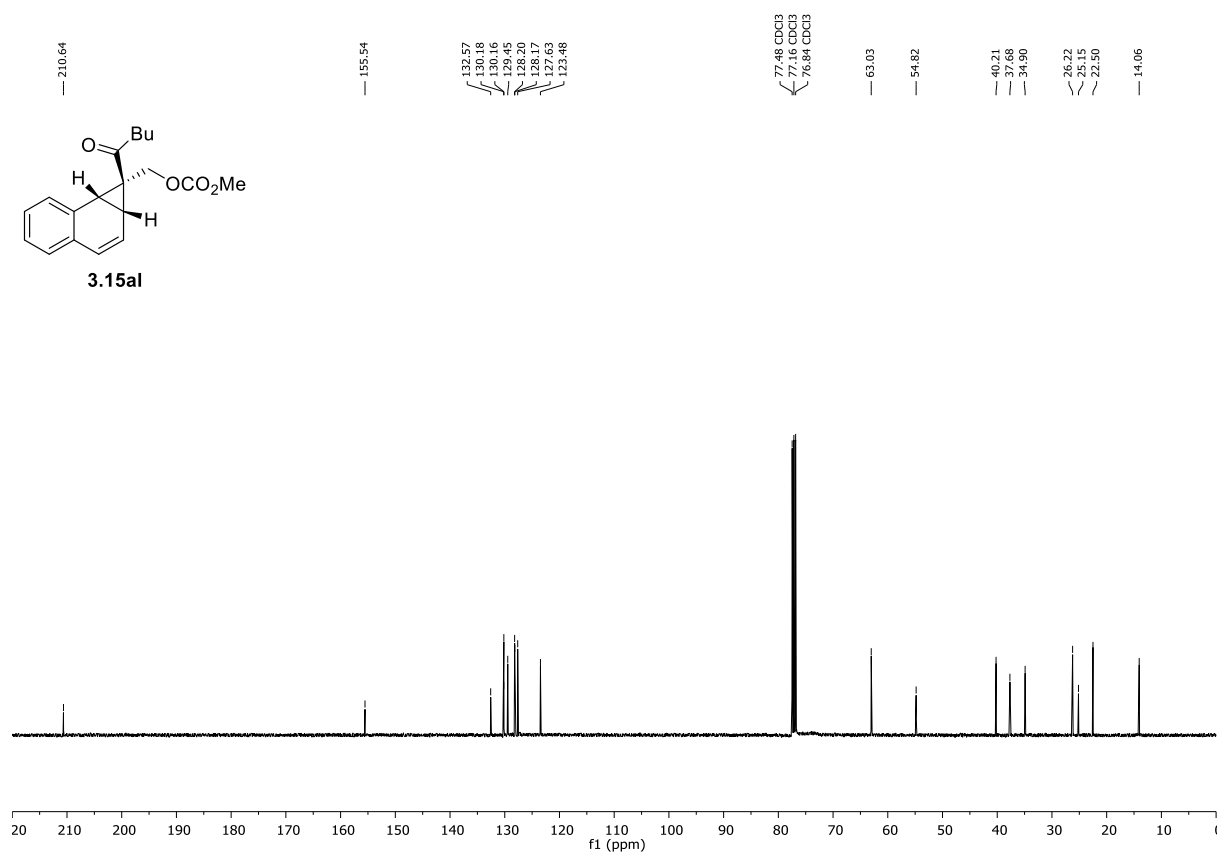
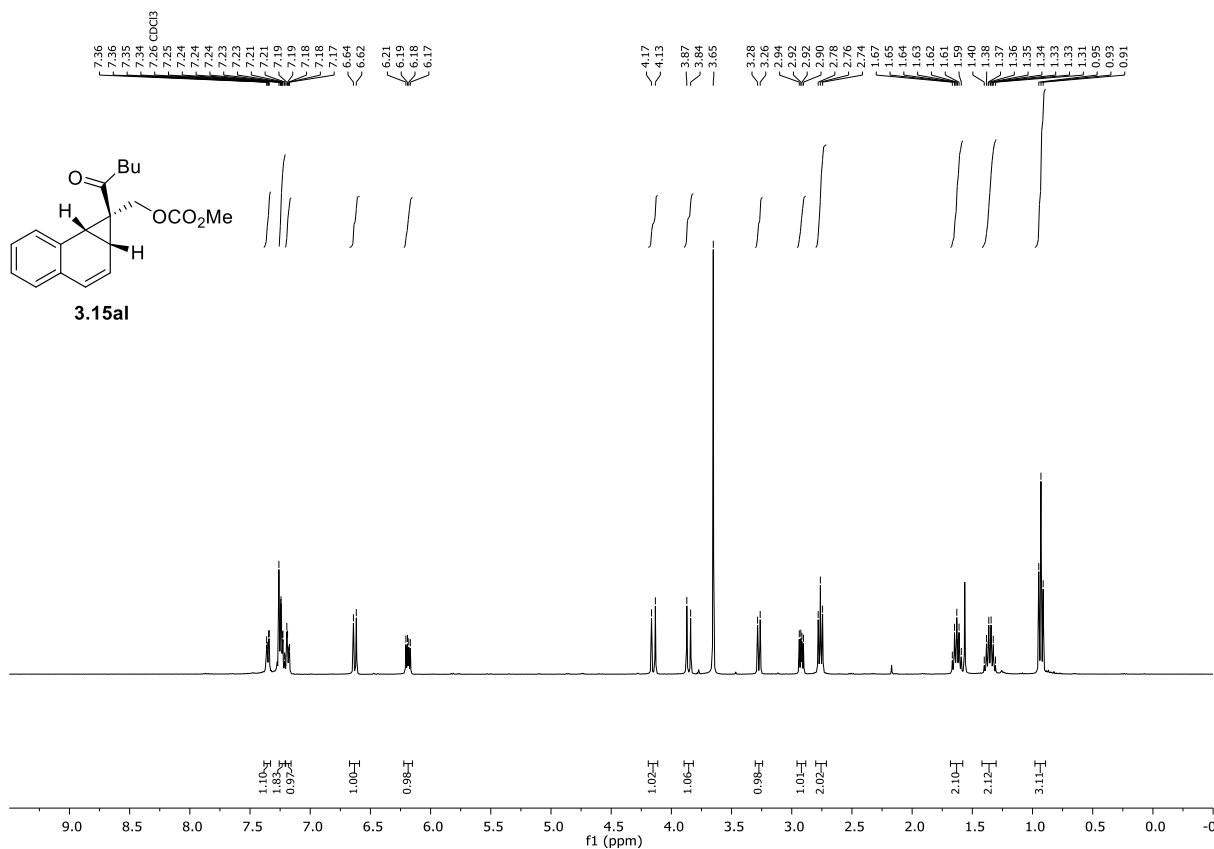


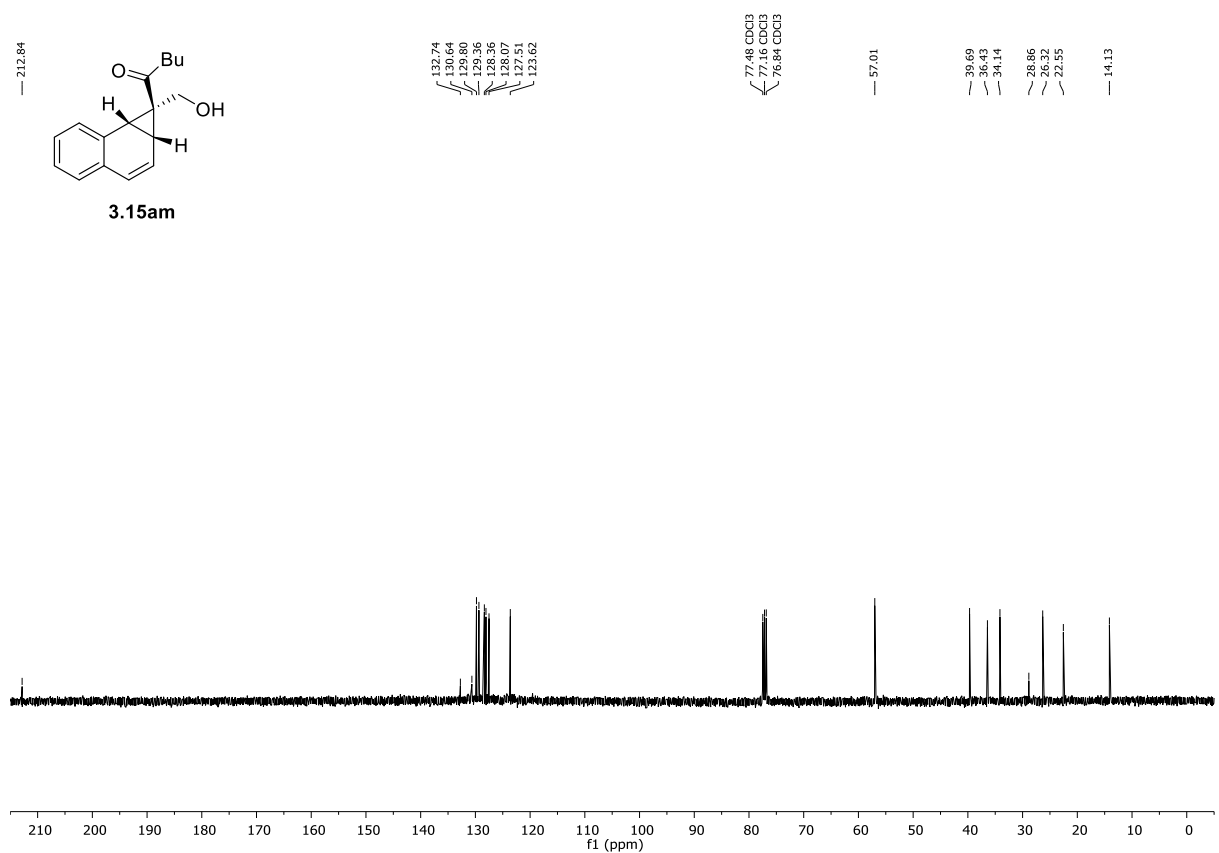
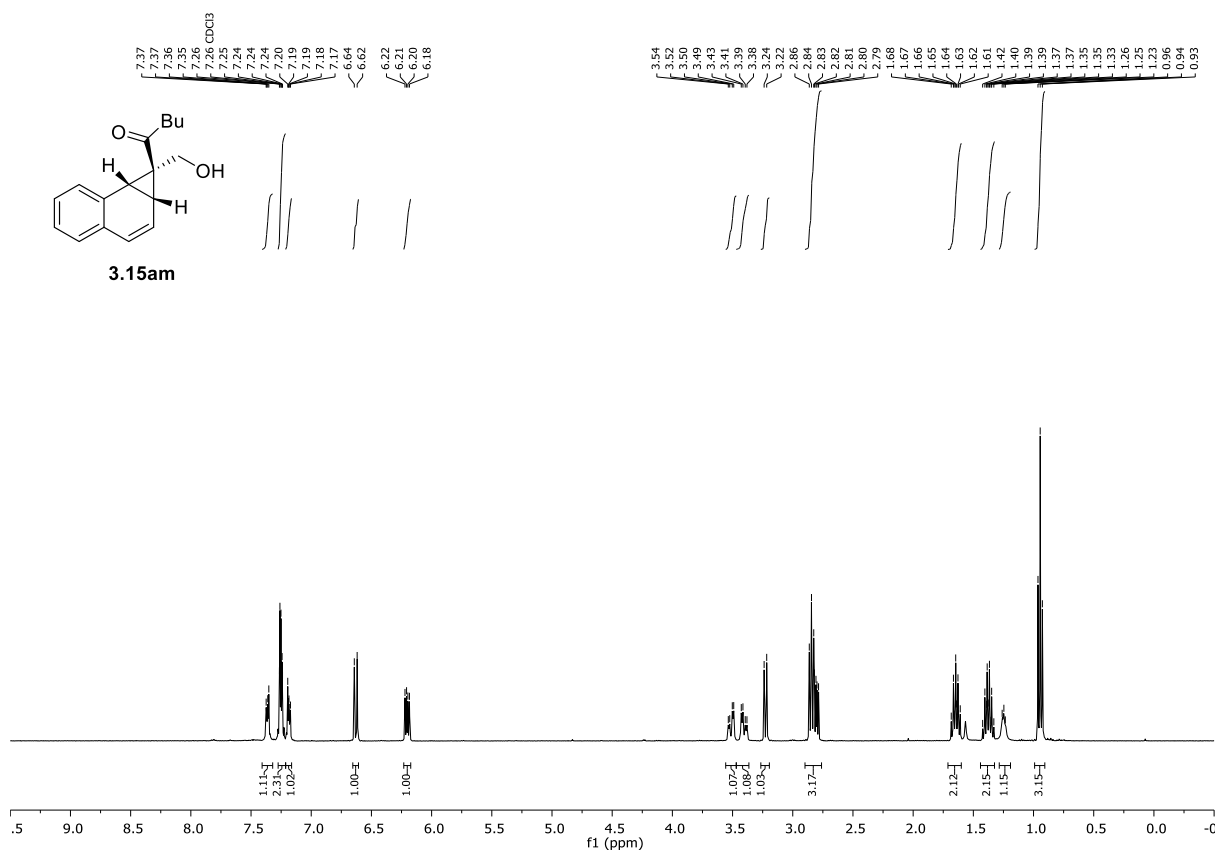


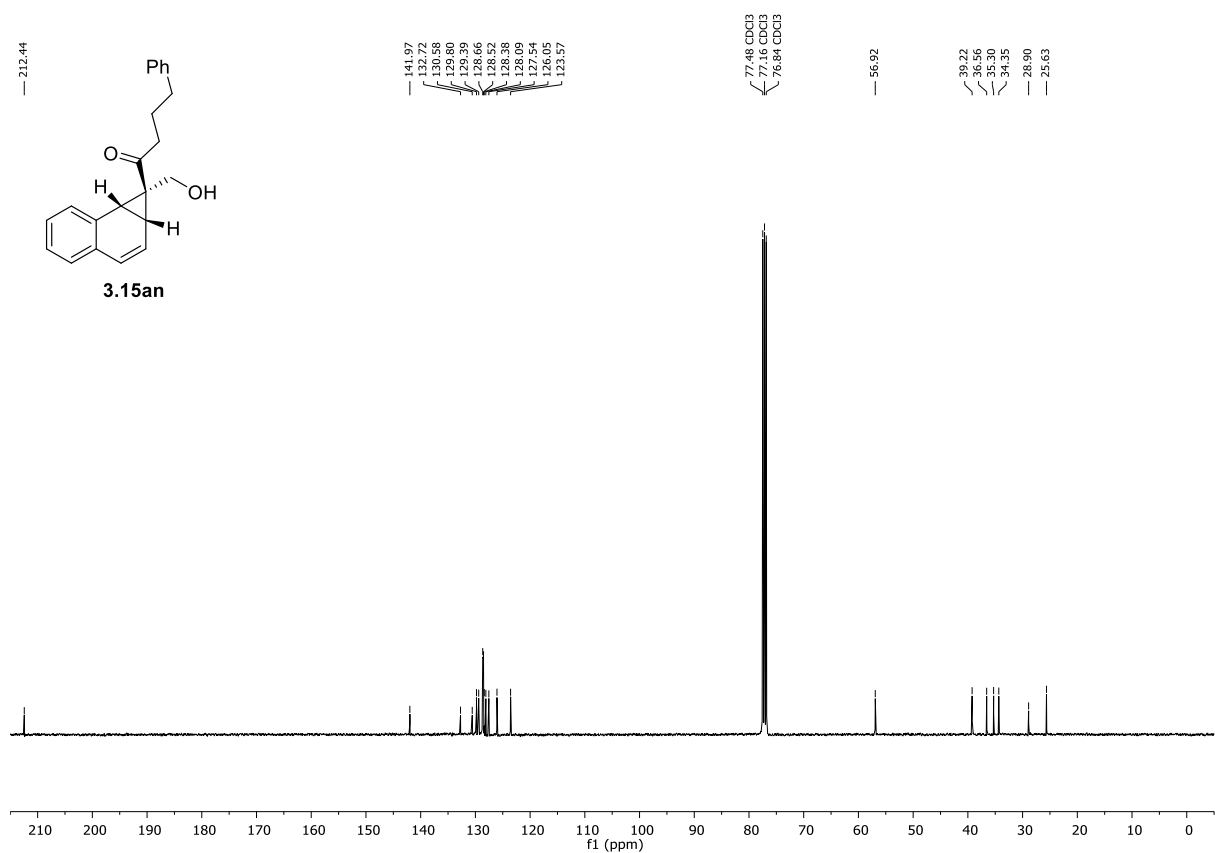
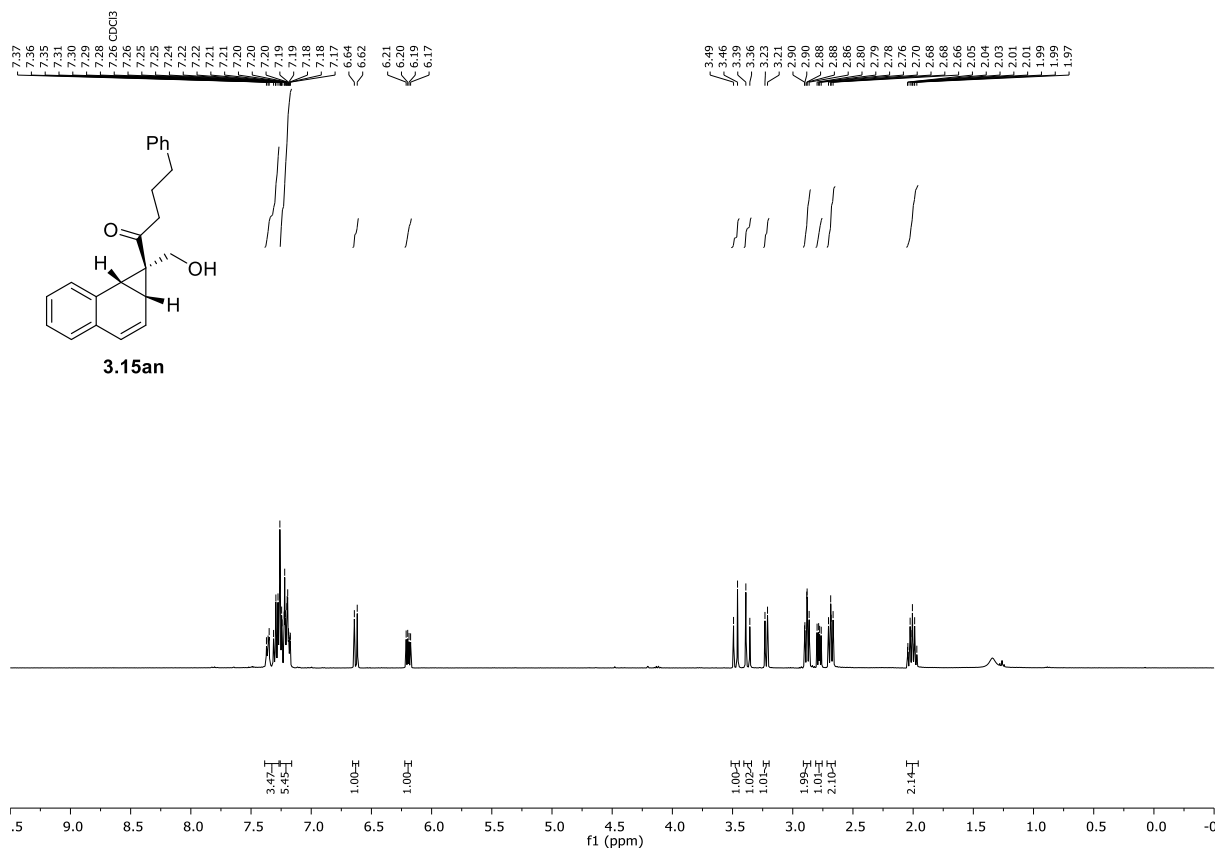


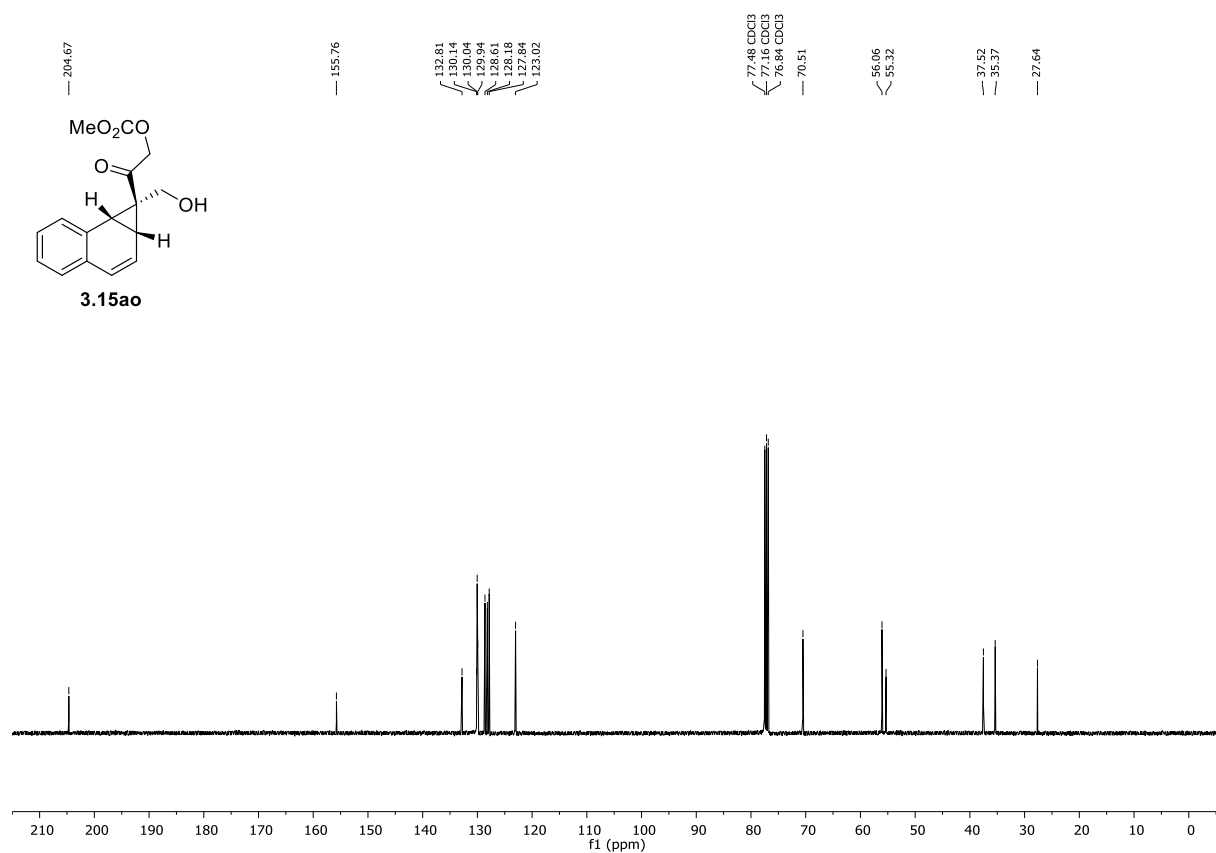
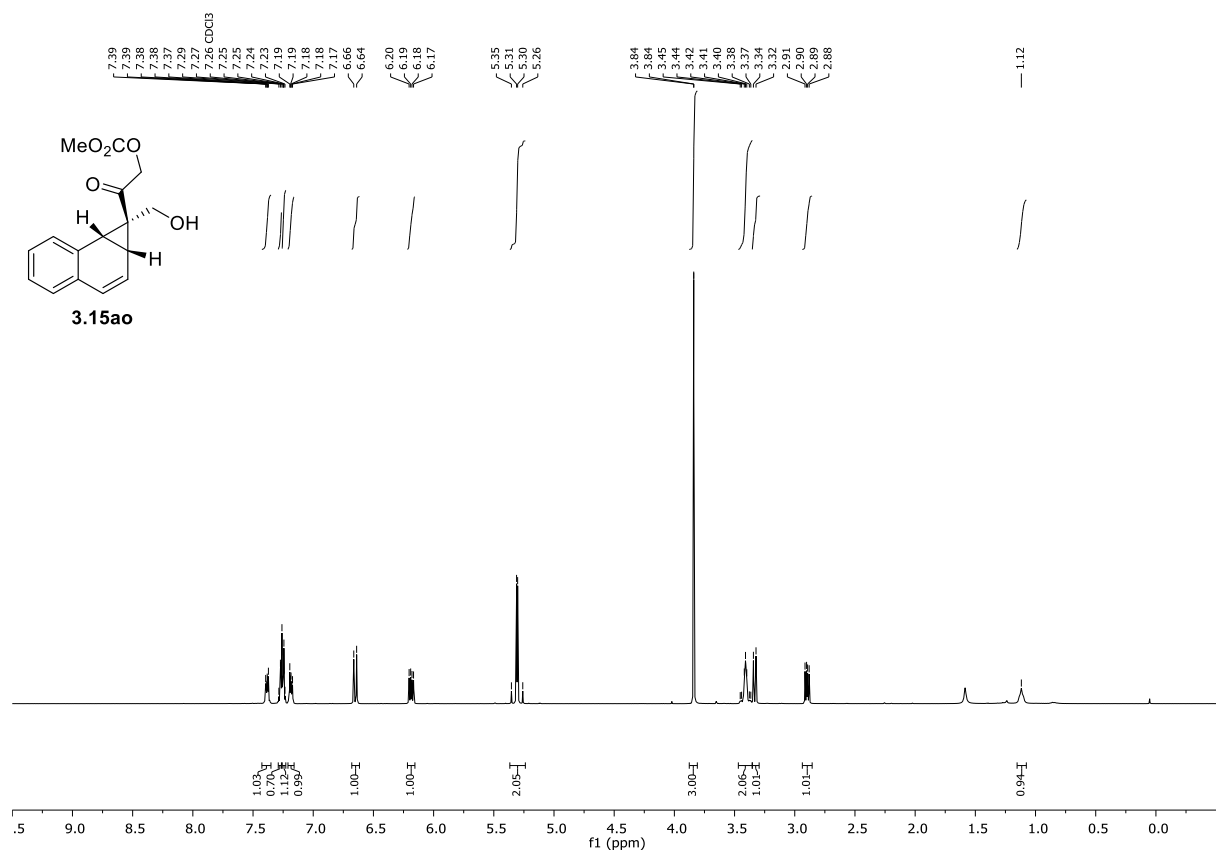


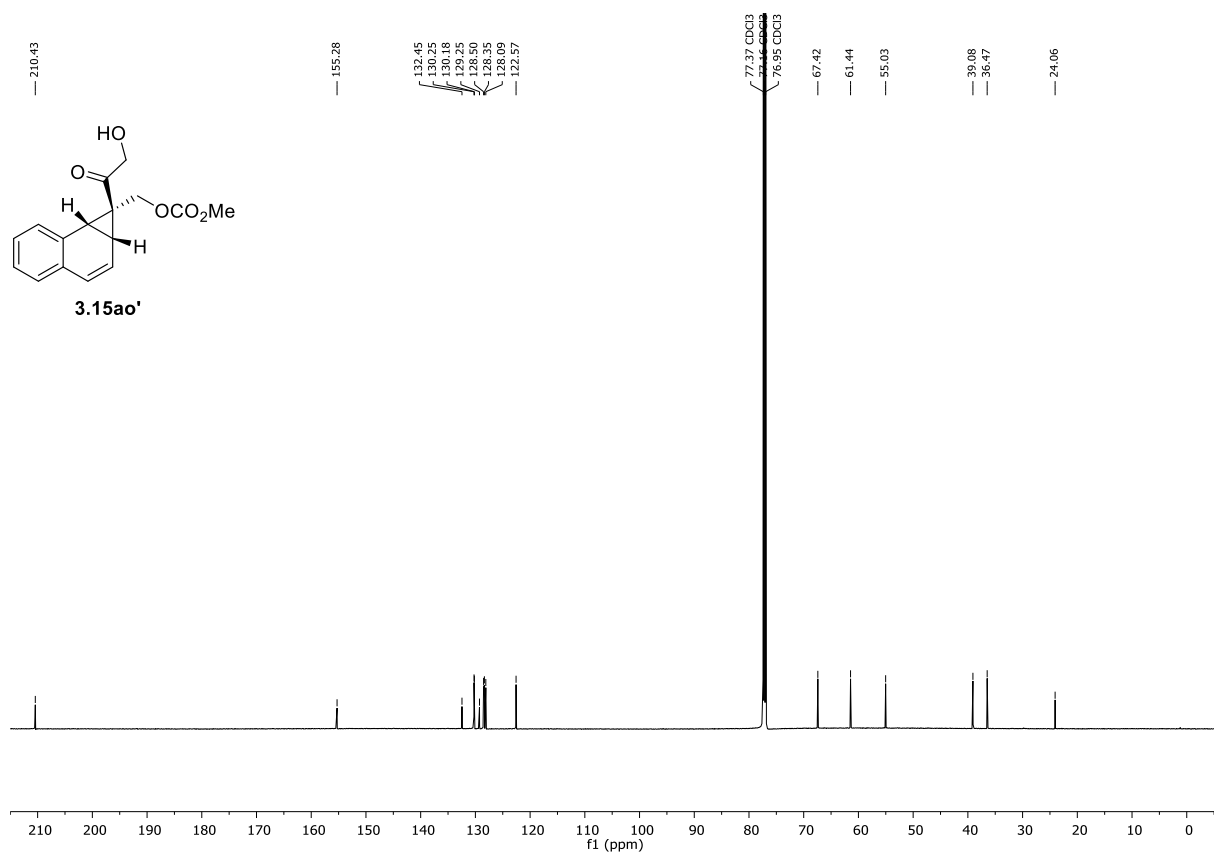
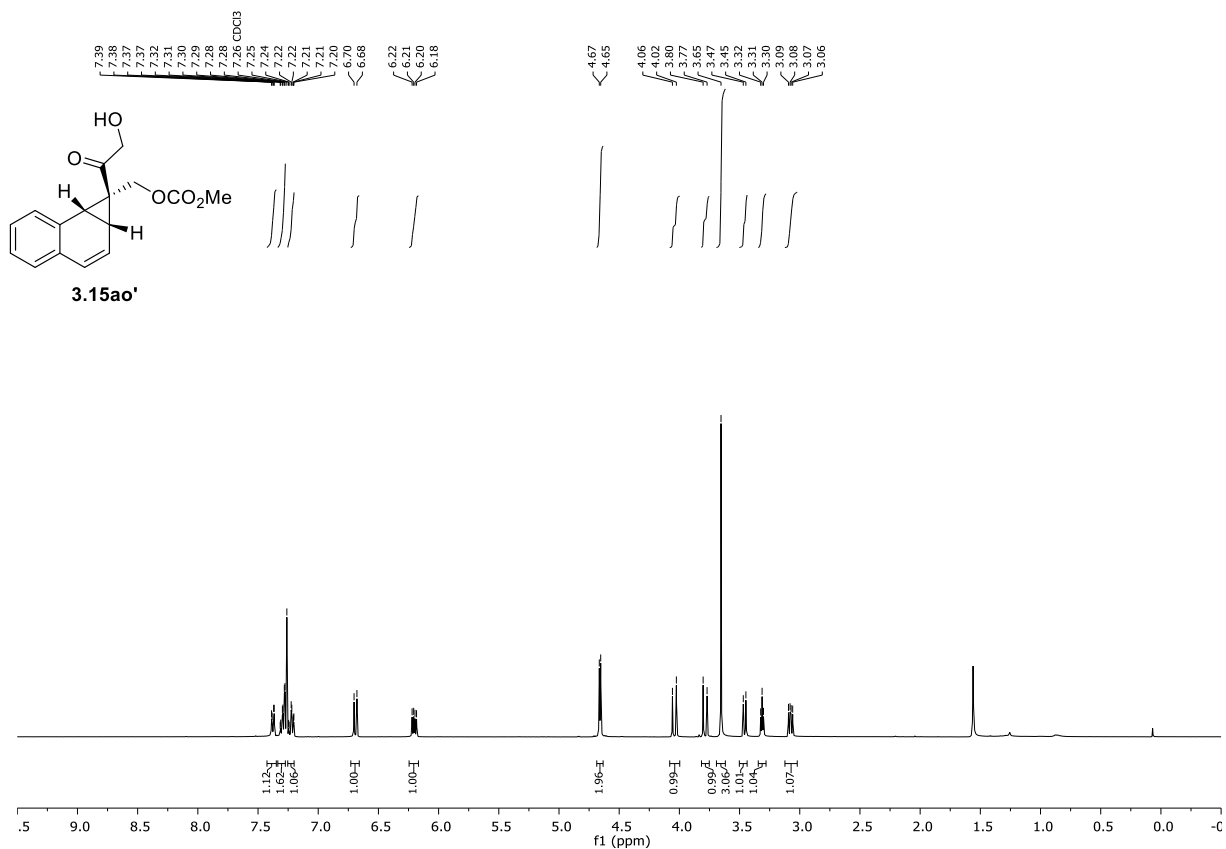


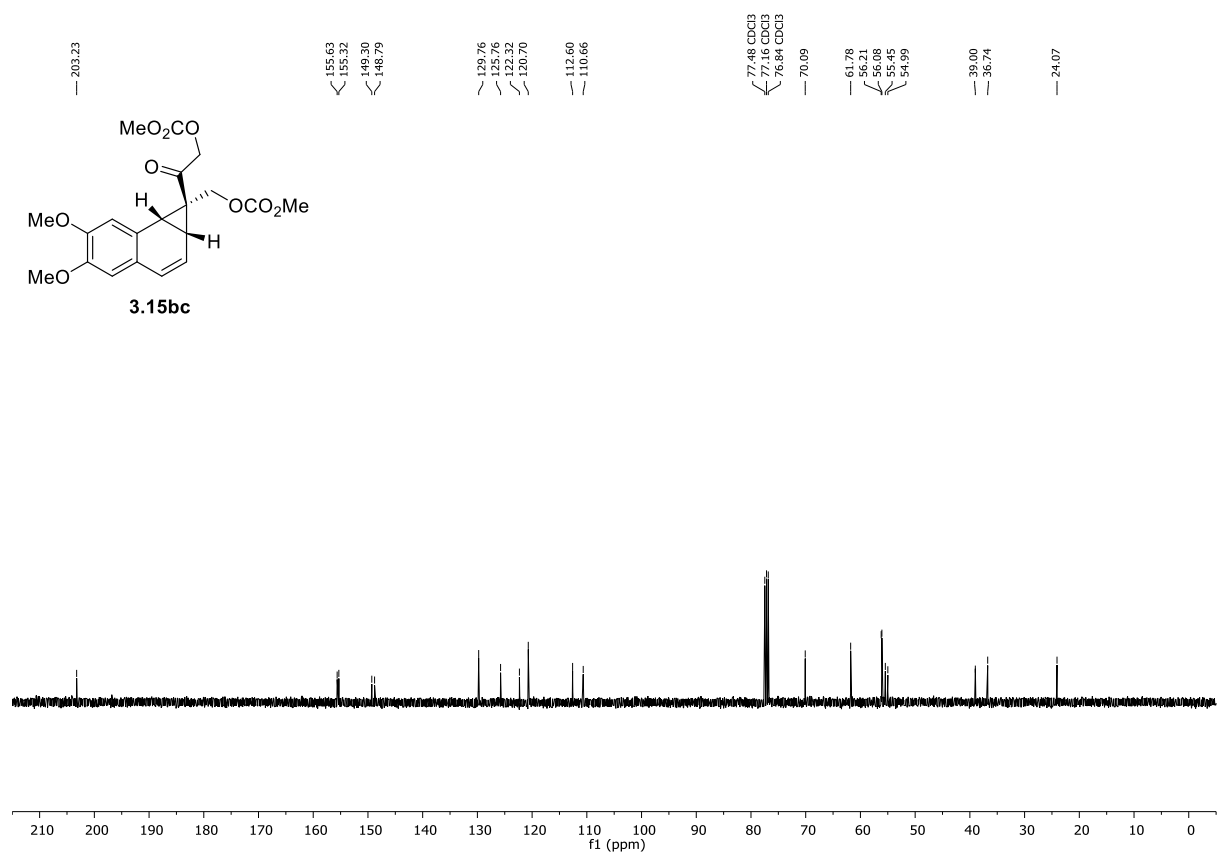
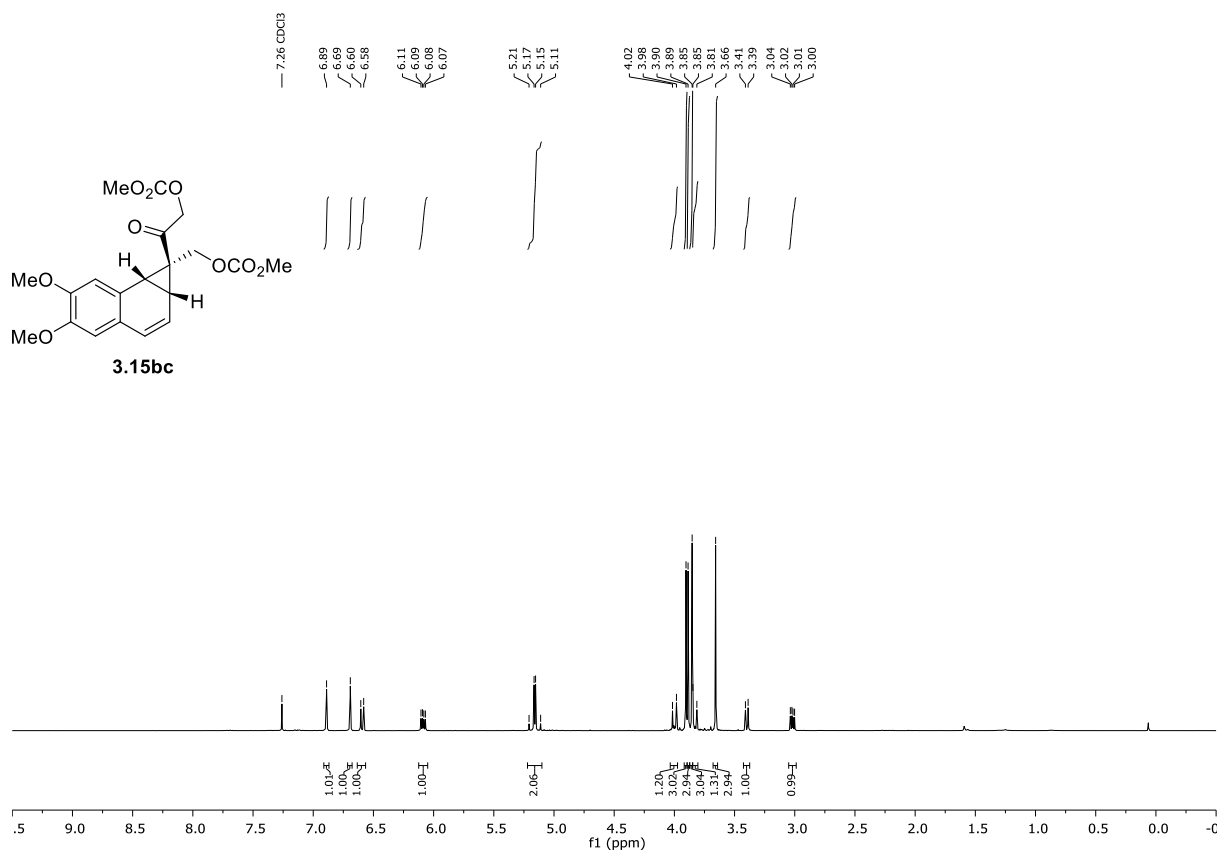


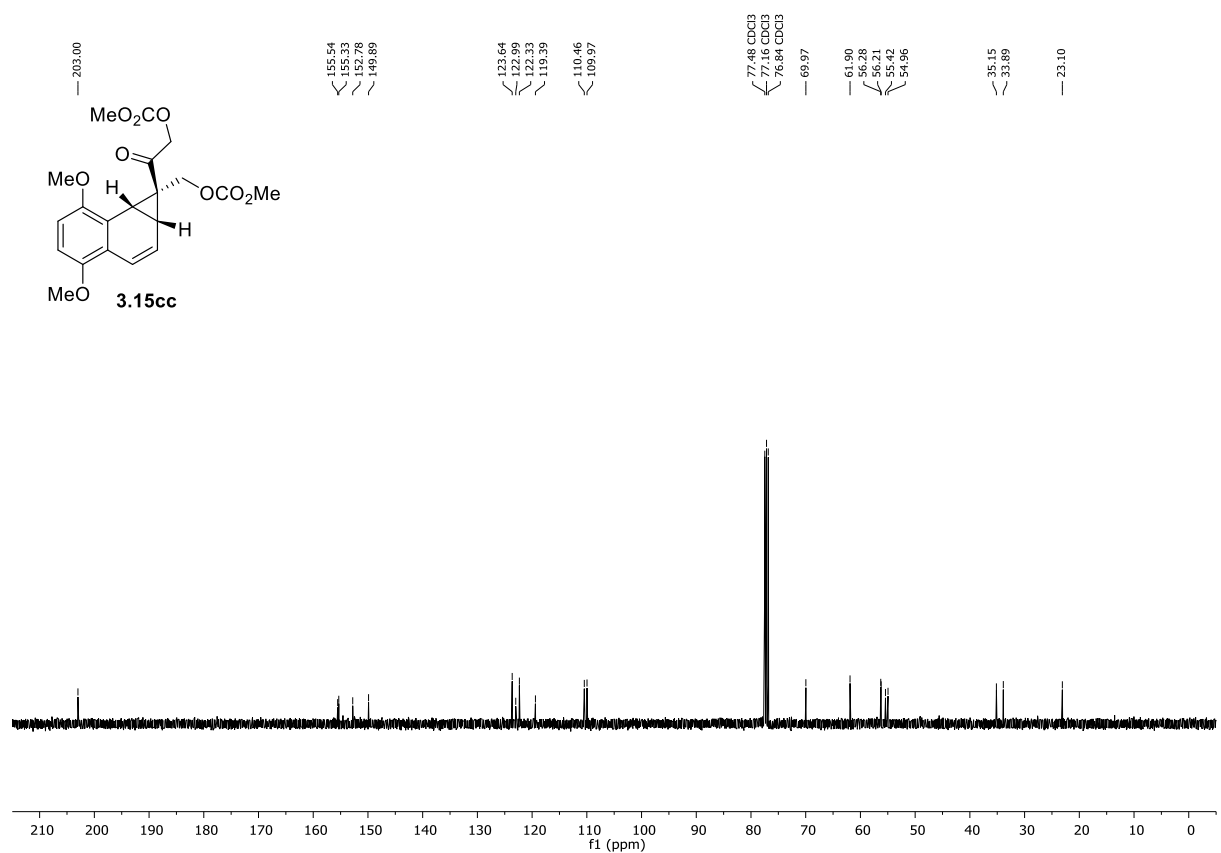
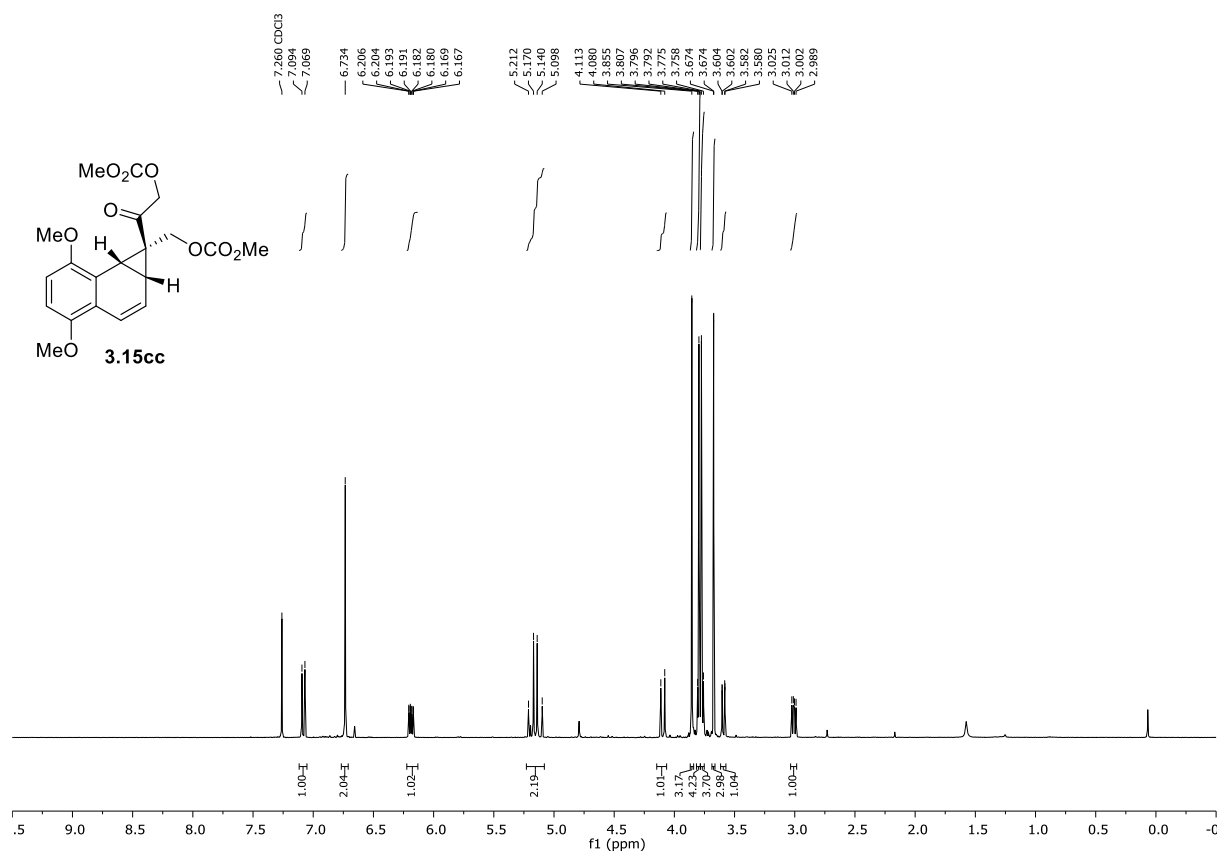


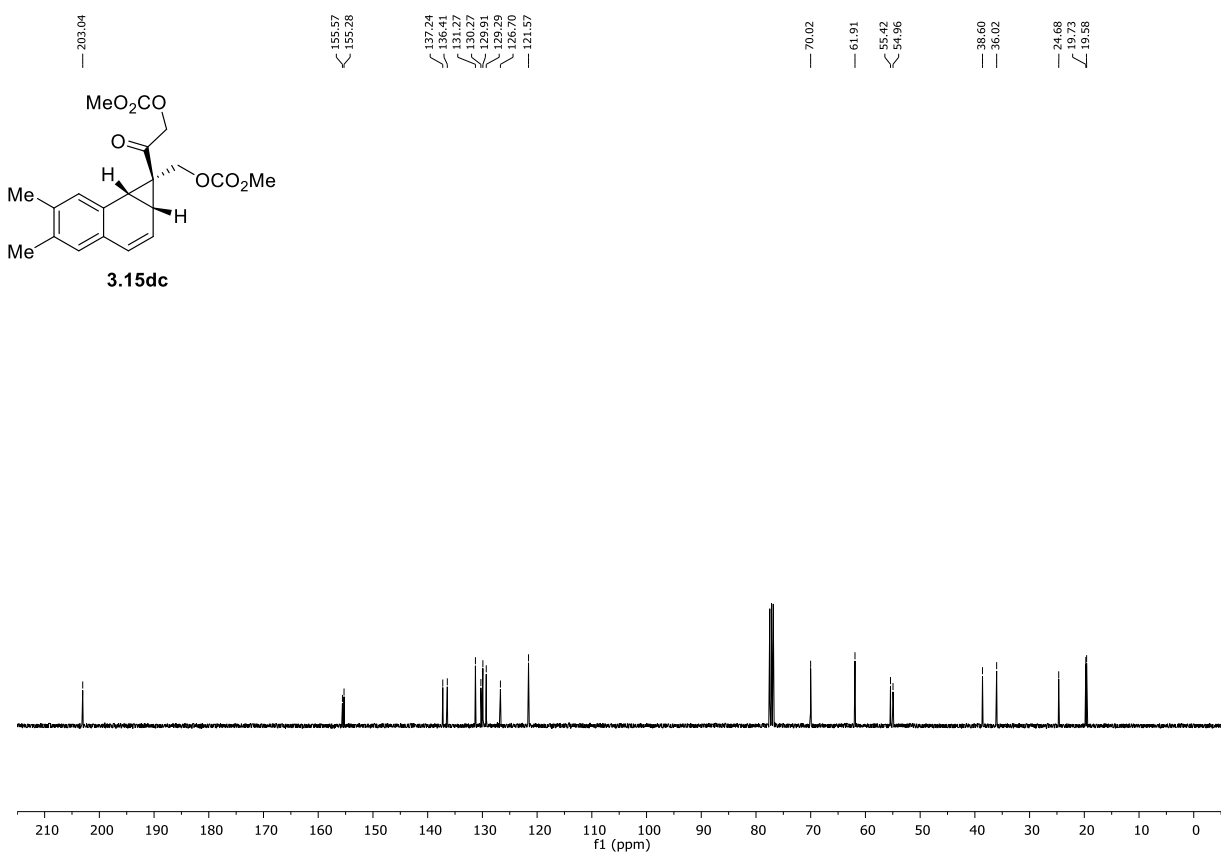
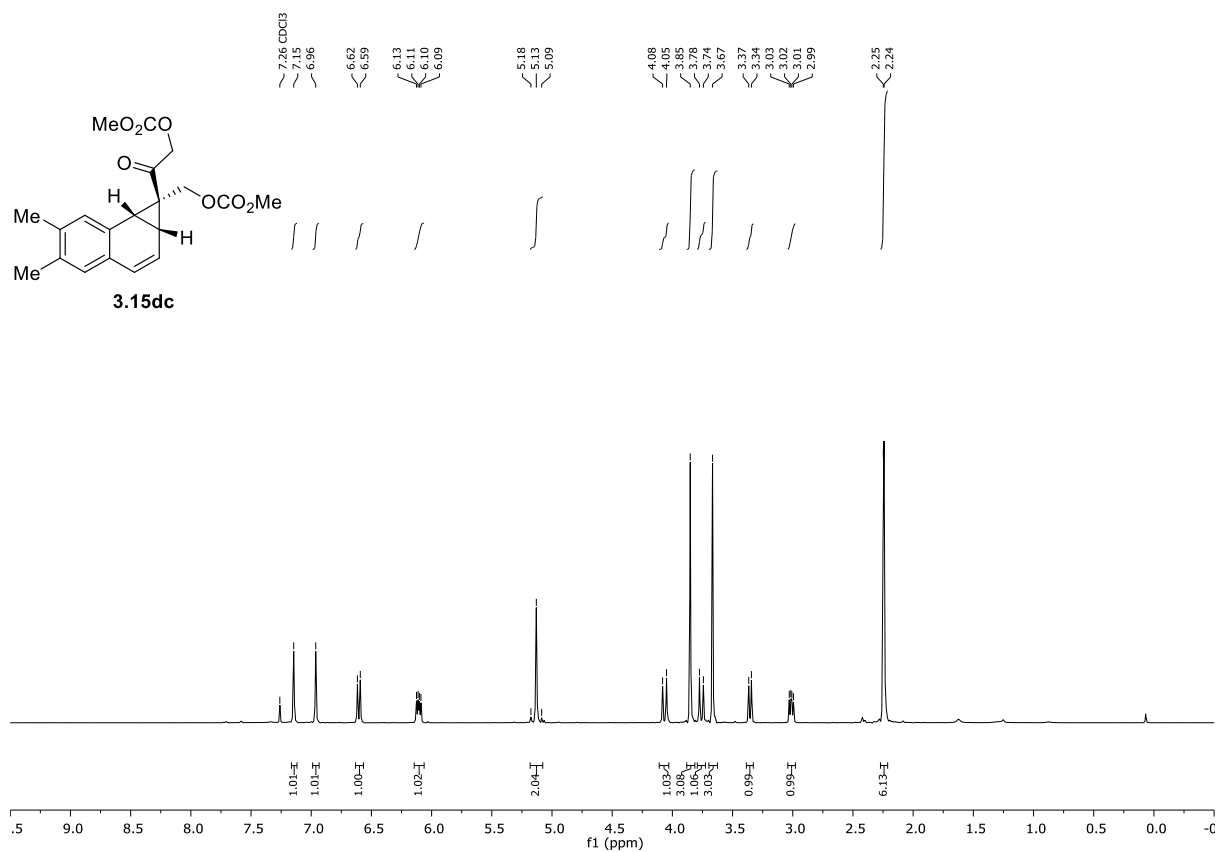


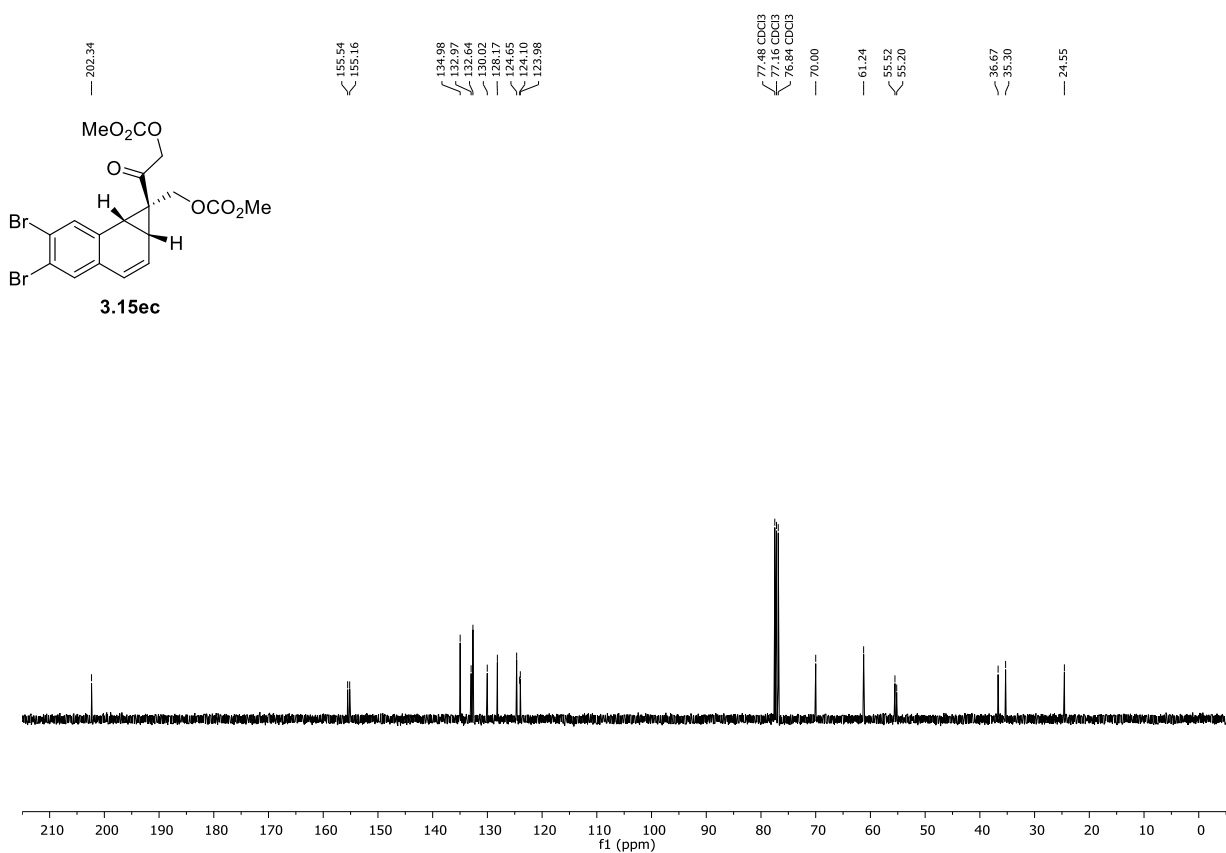
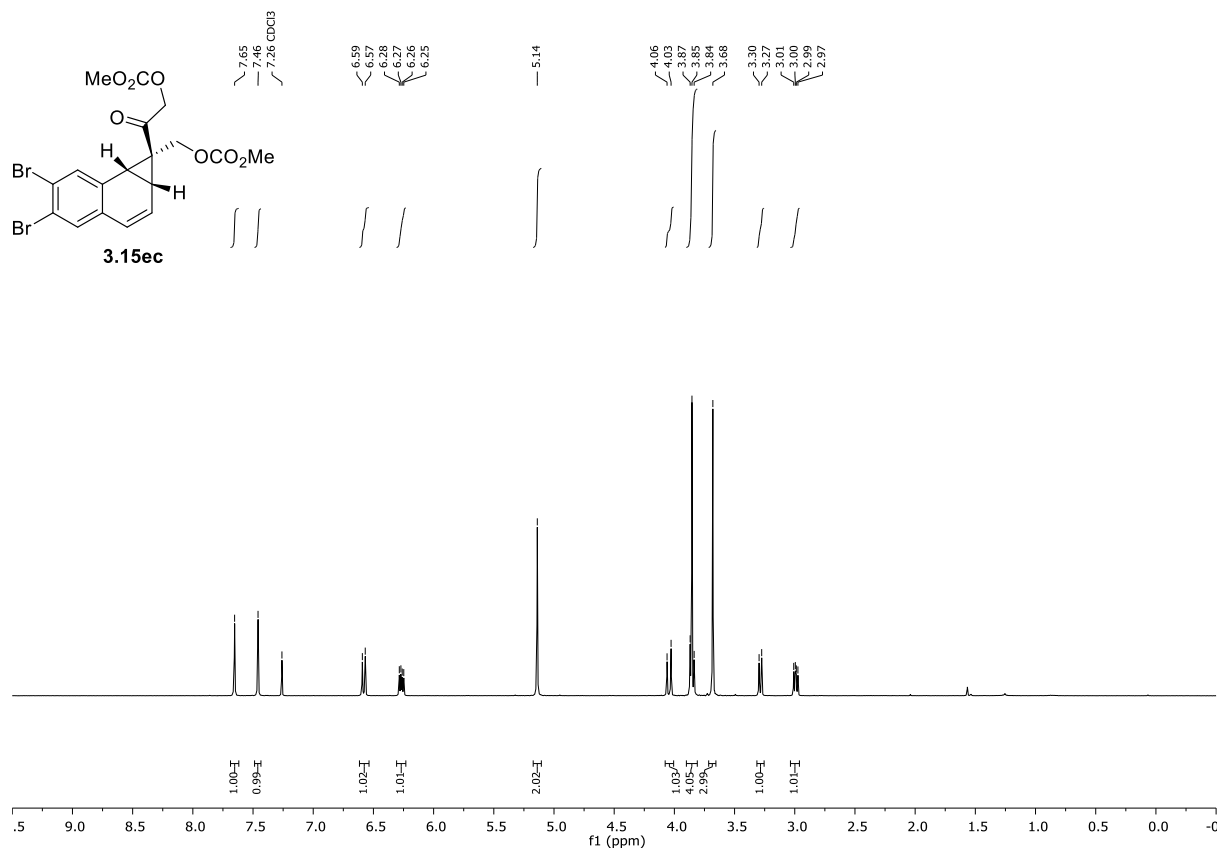


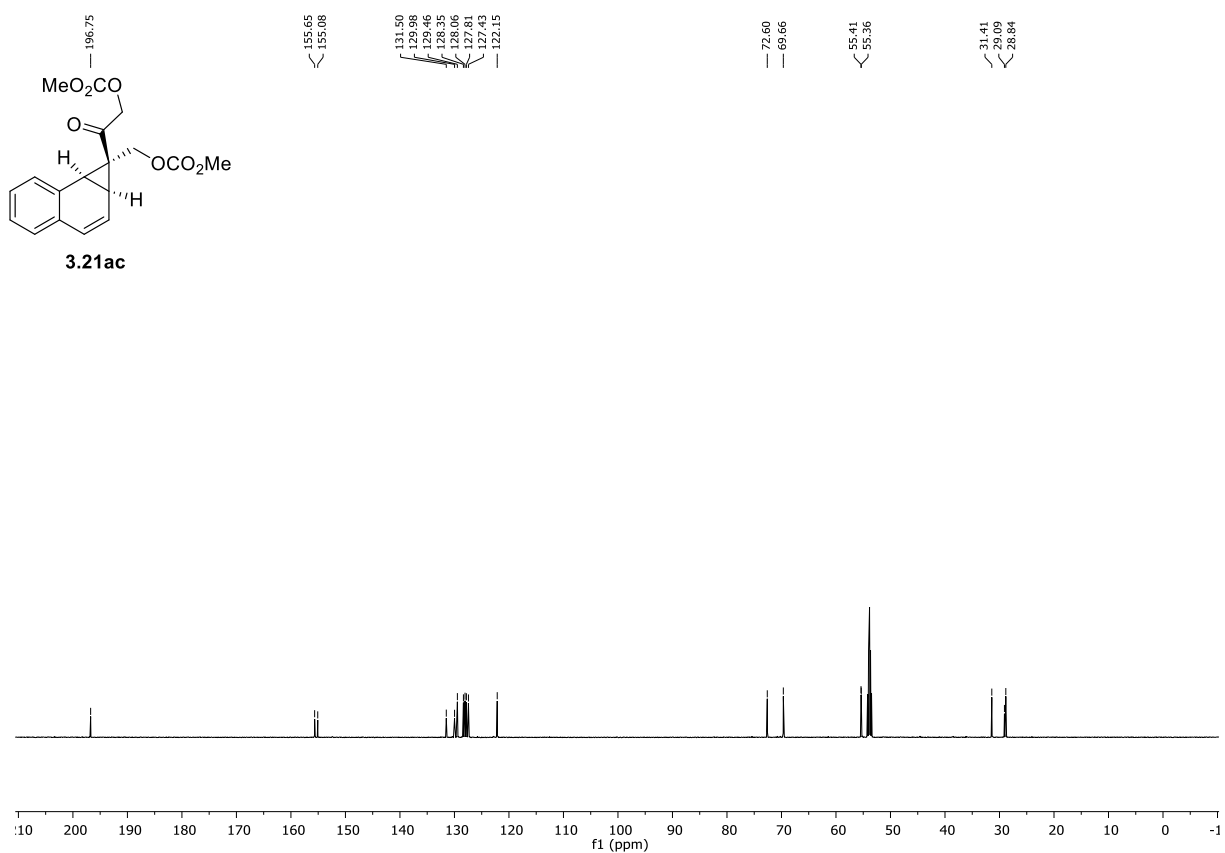
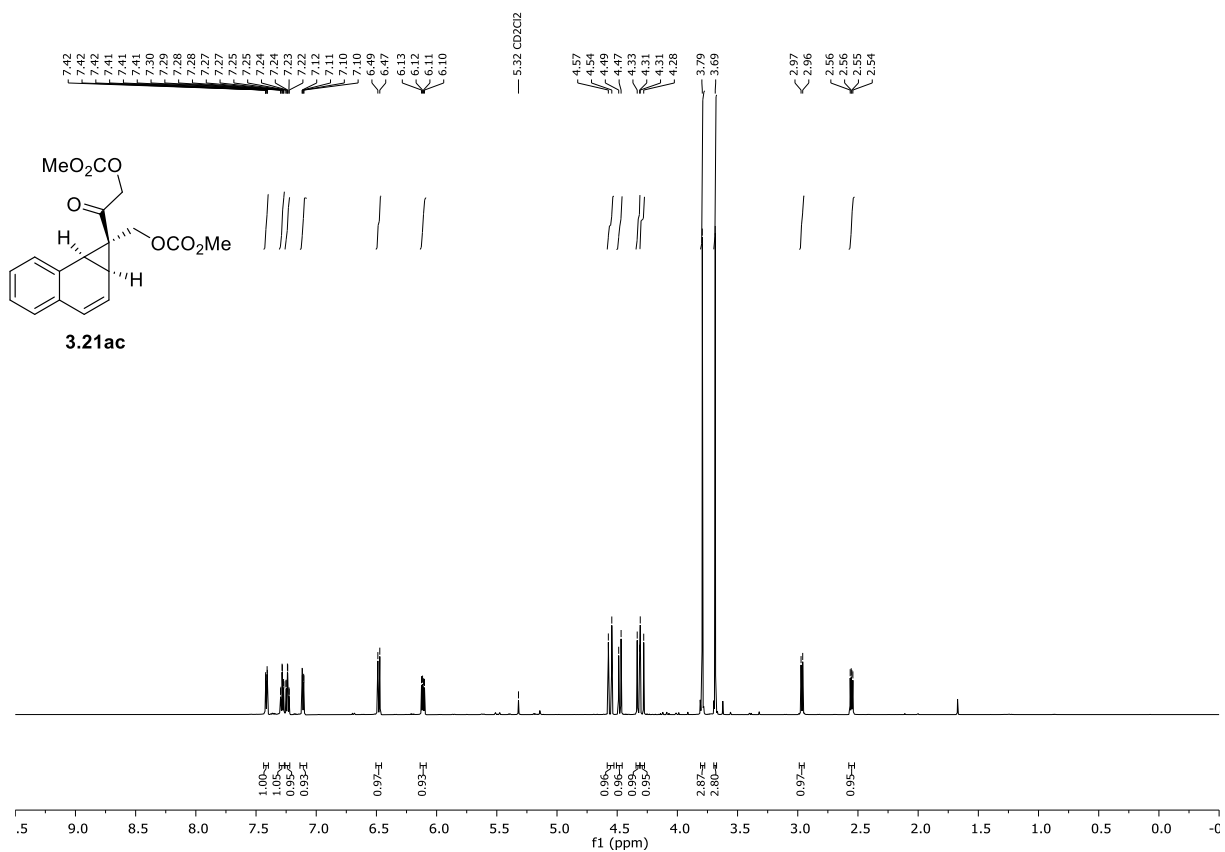




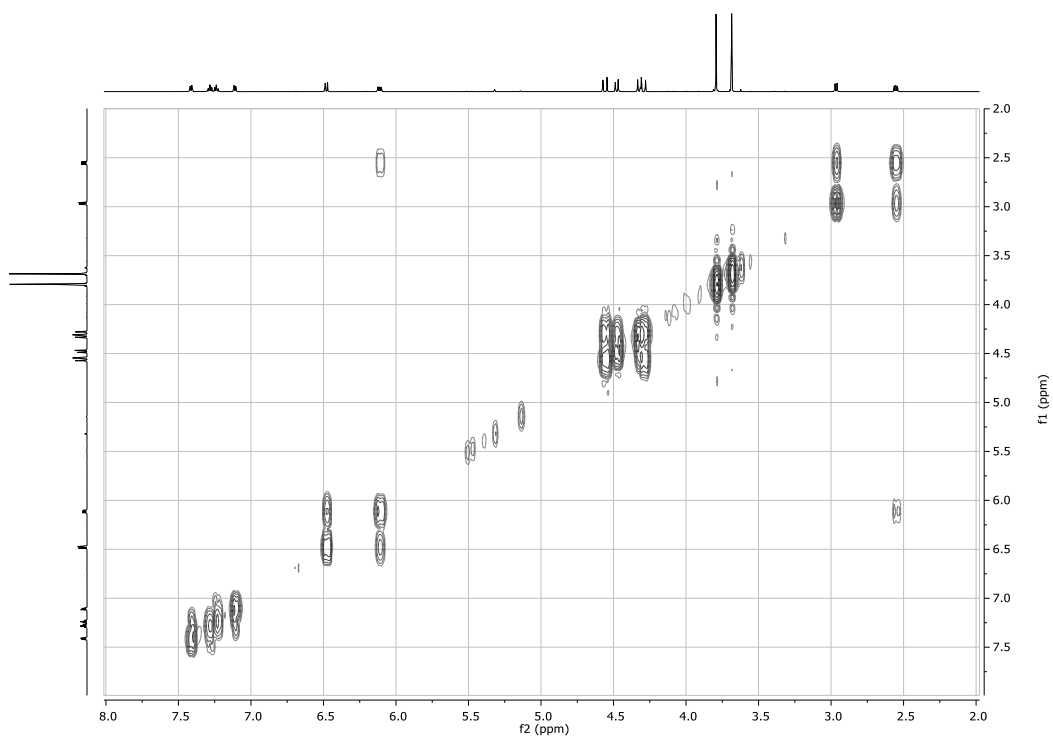




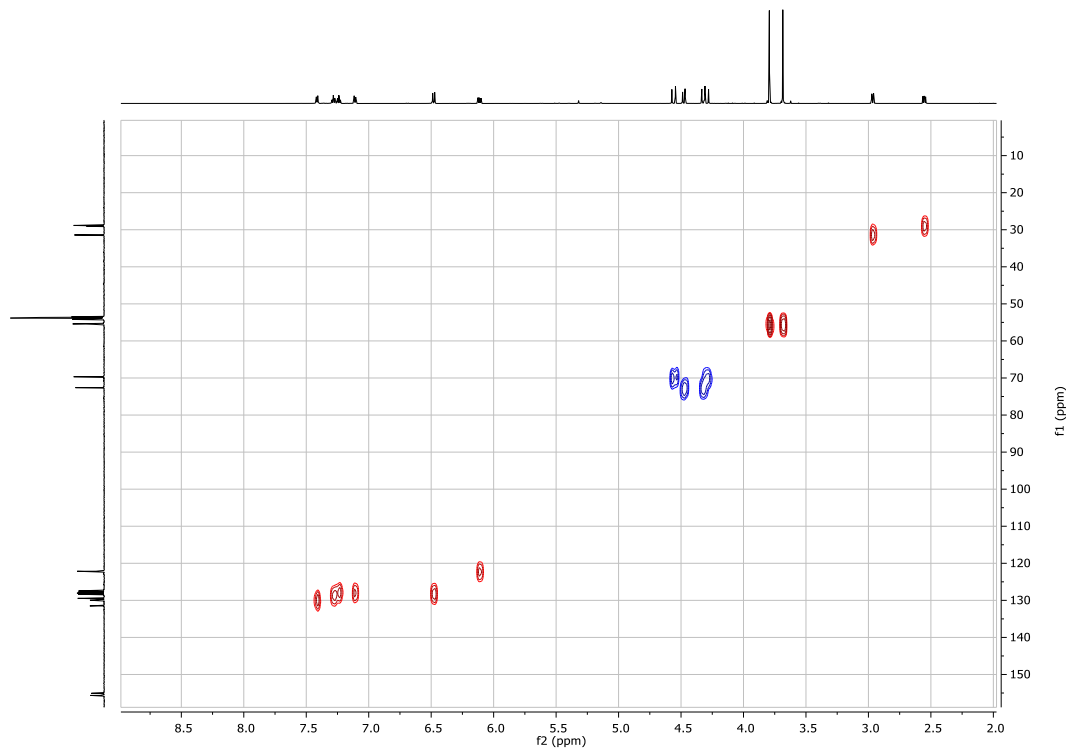




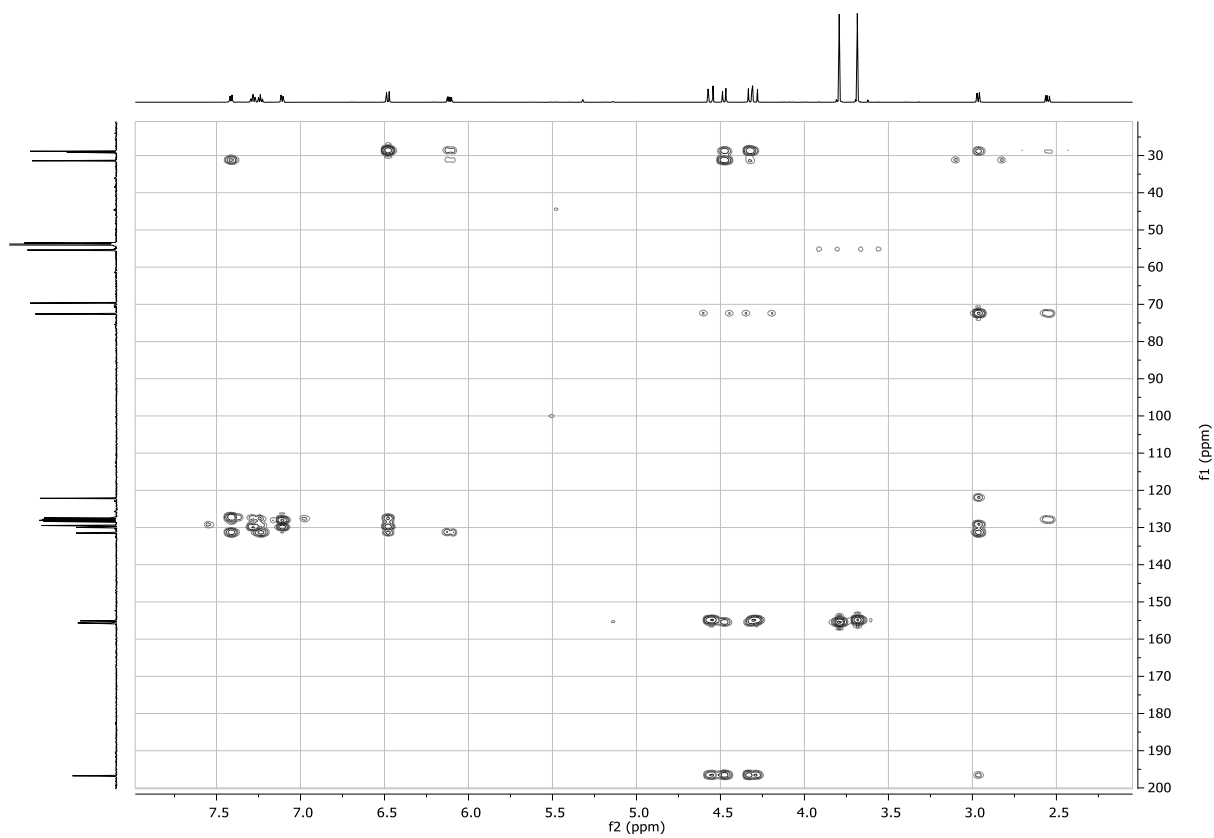
2D NMR of *endo*-product (3.21ac)



COSY spectra

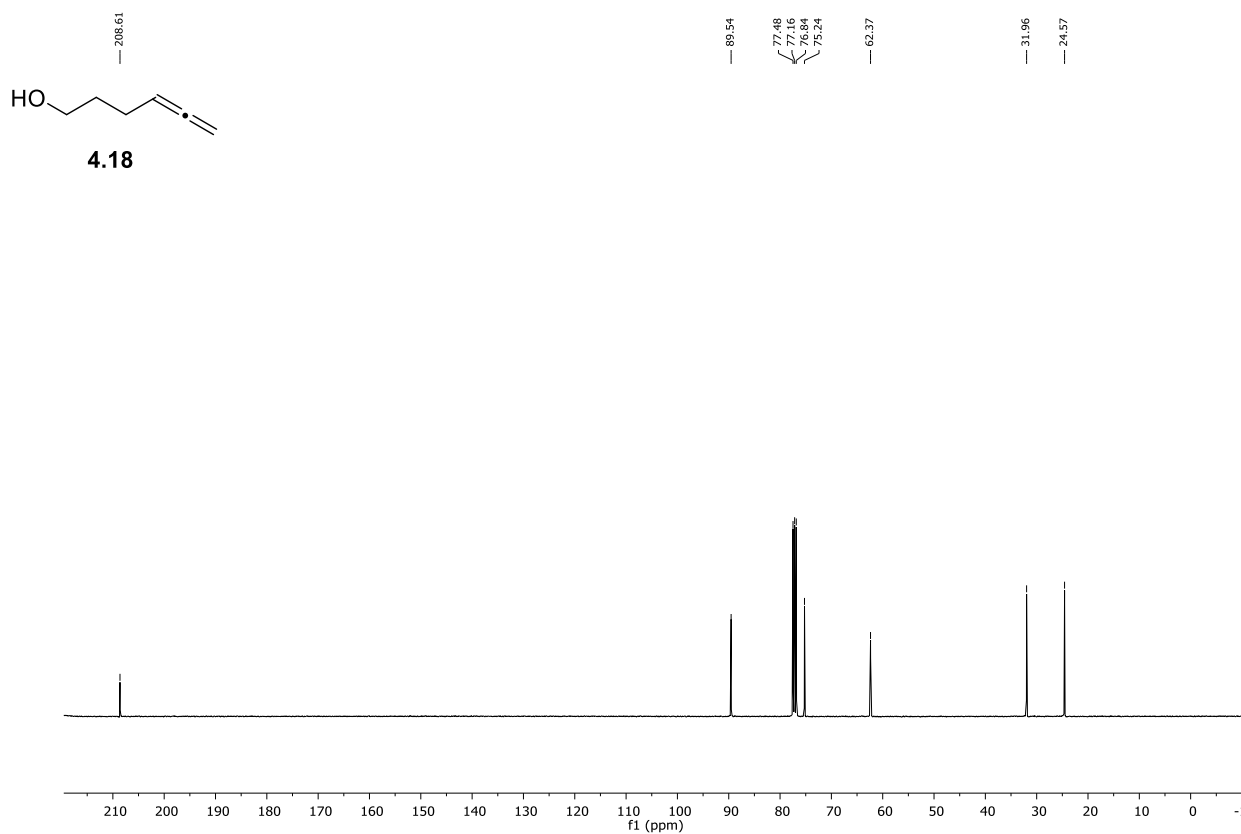
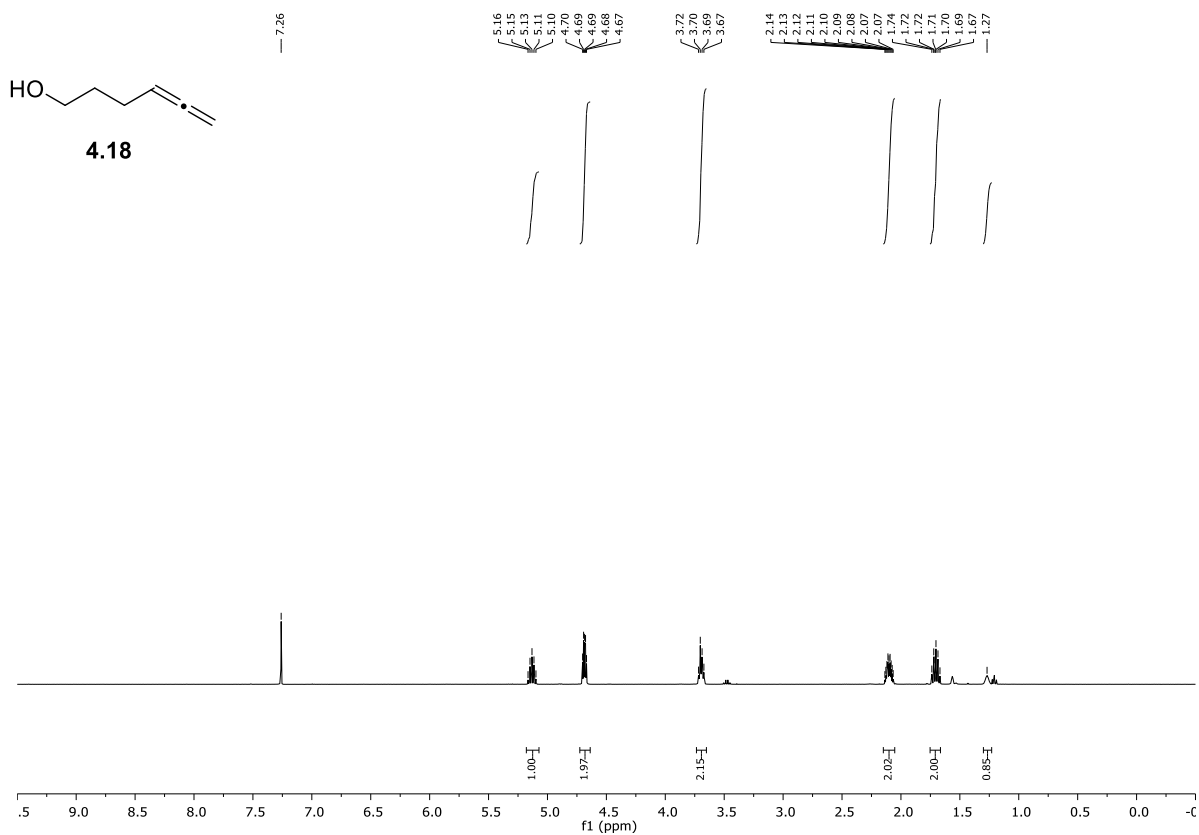


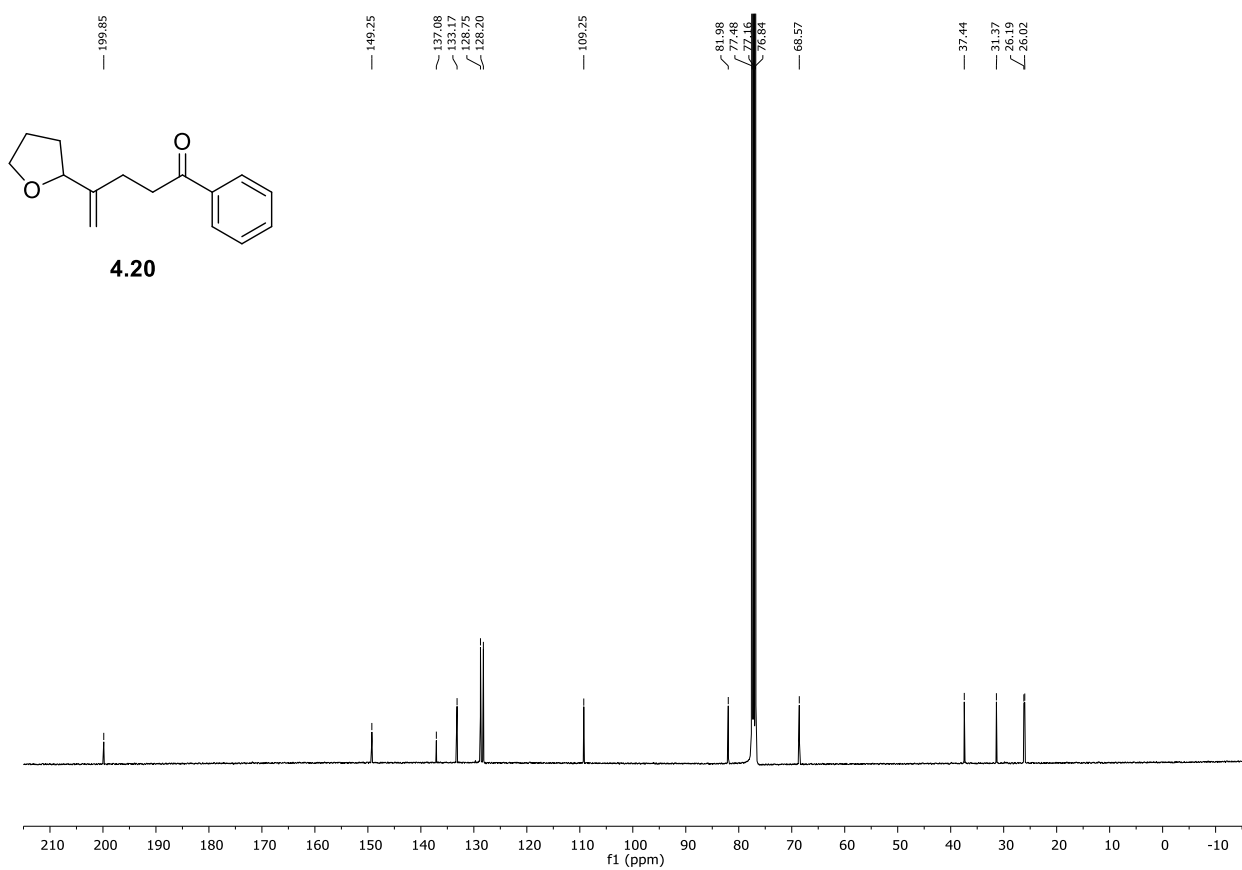
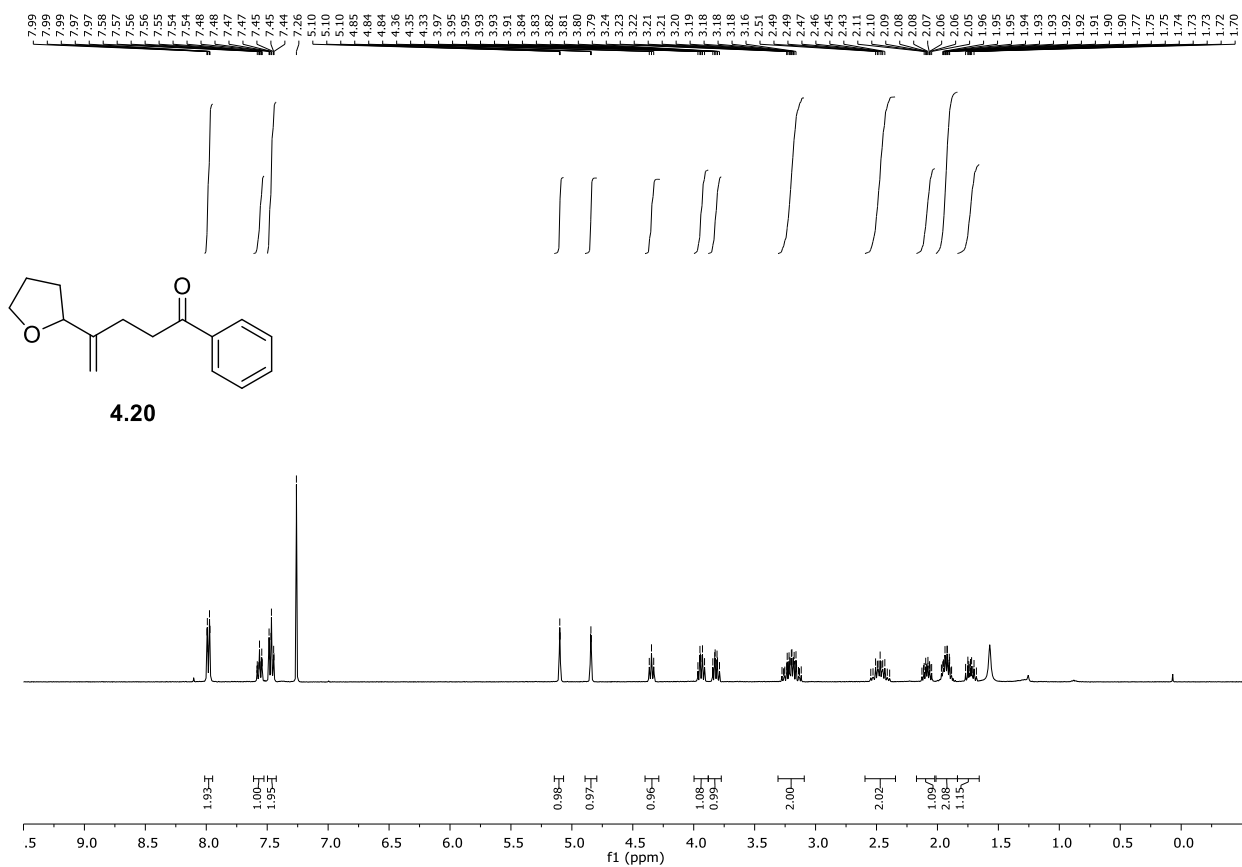
HSQC spectra

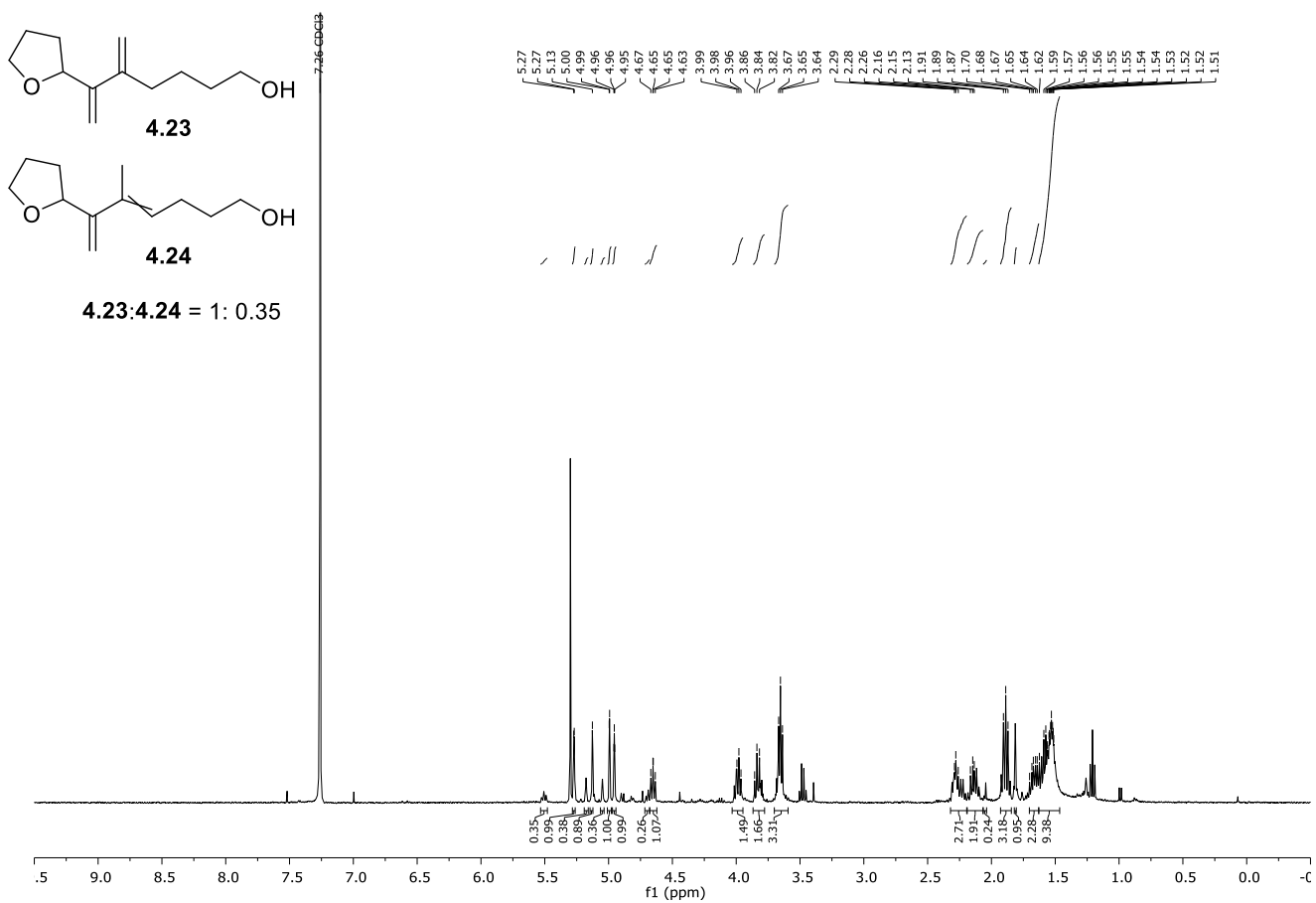


HMBC spectra

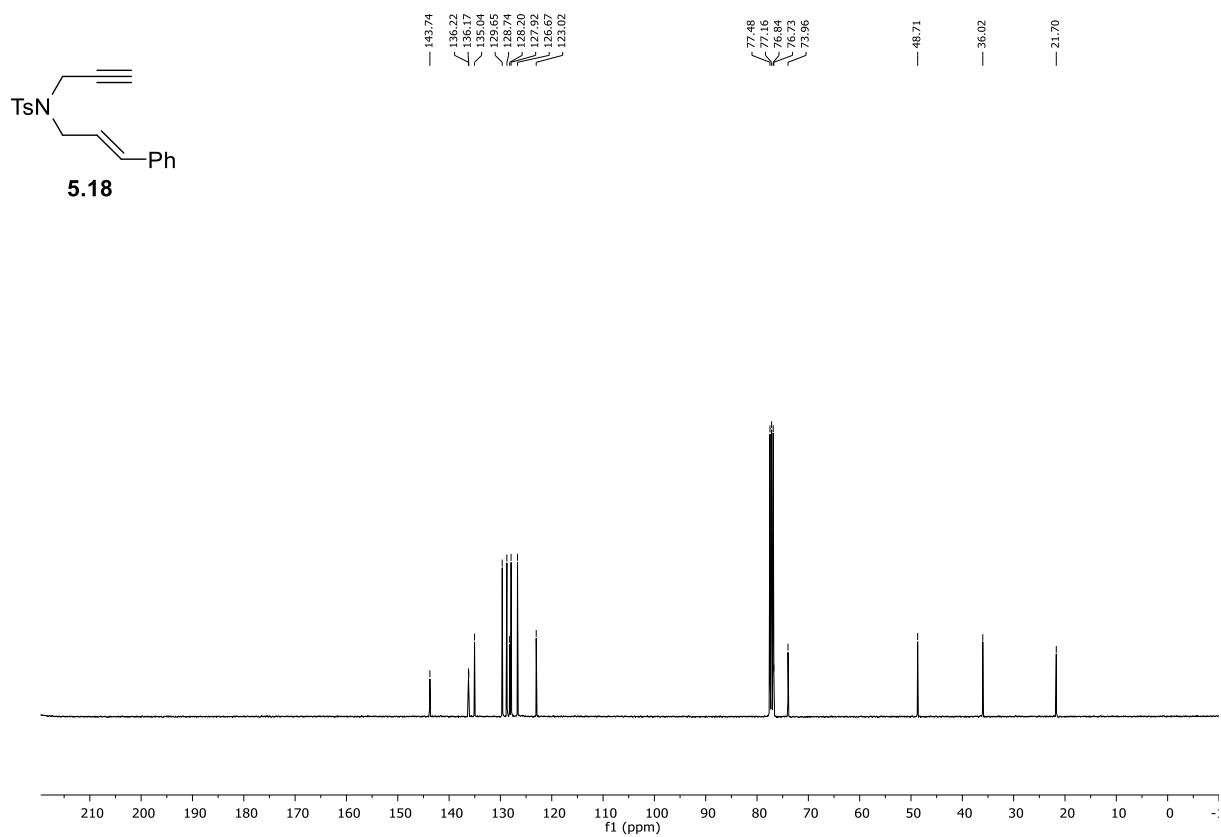
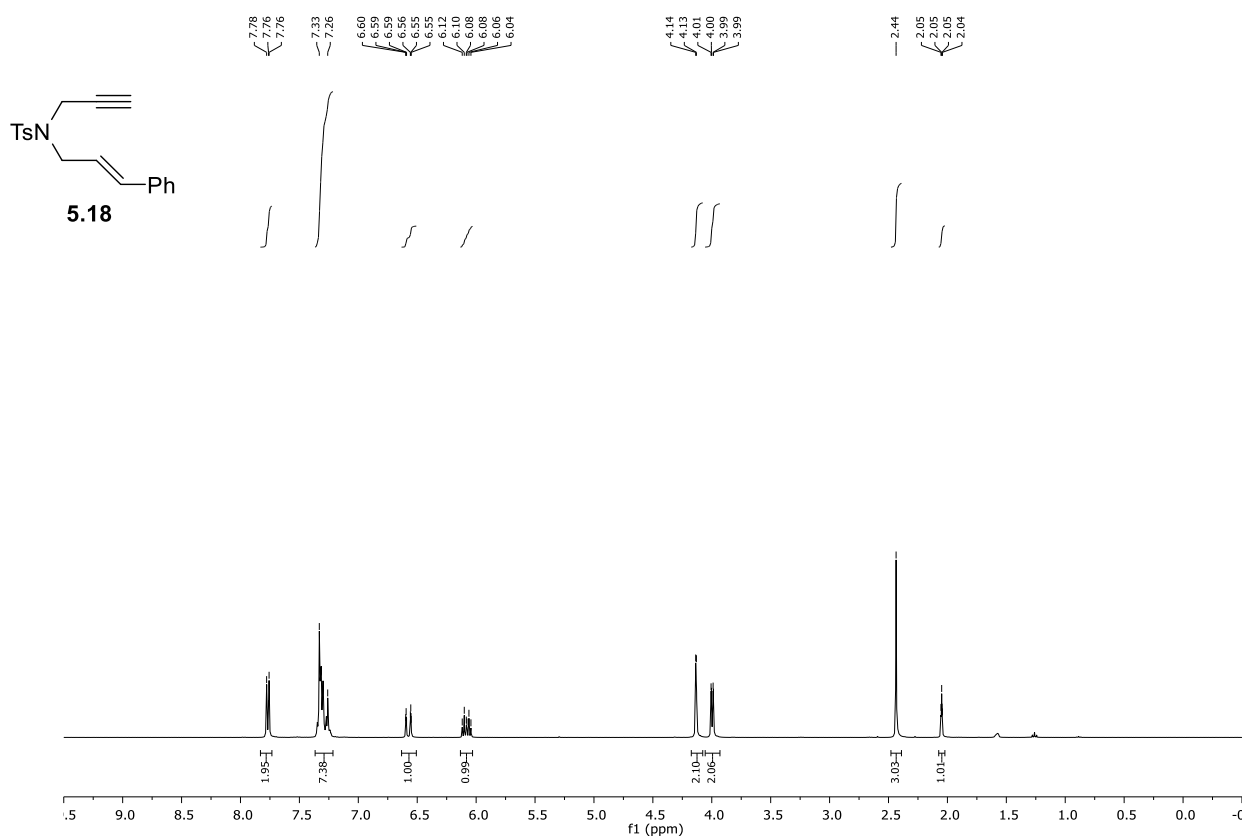
NMR spectra for Chapter 4

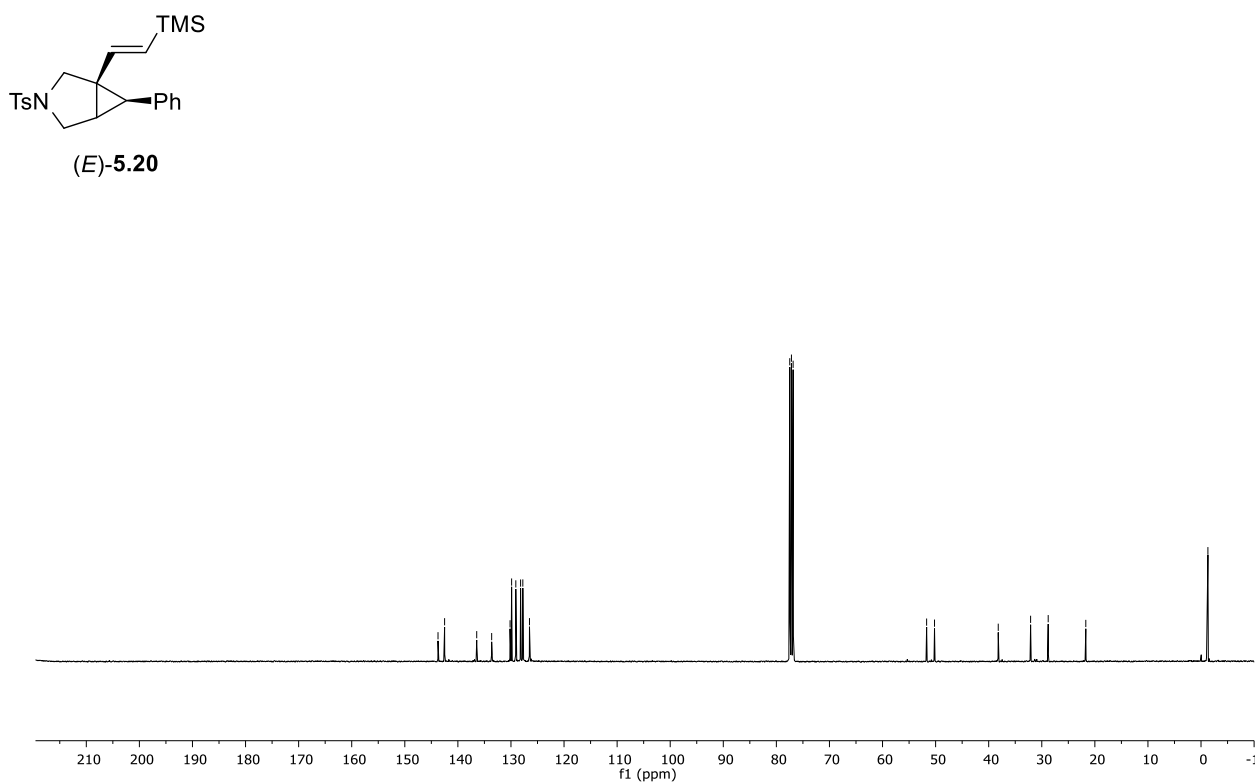
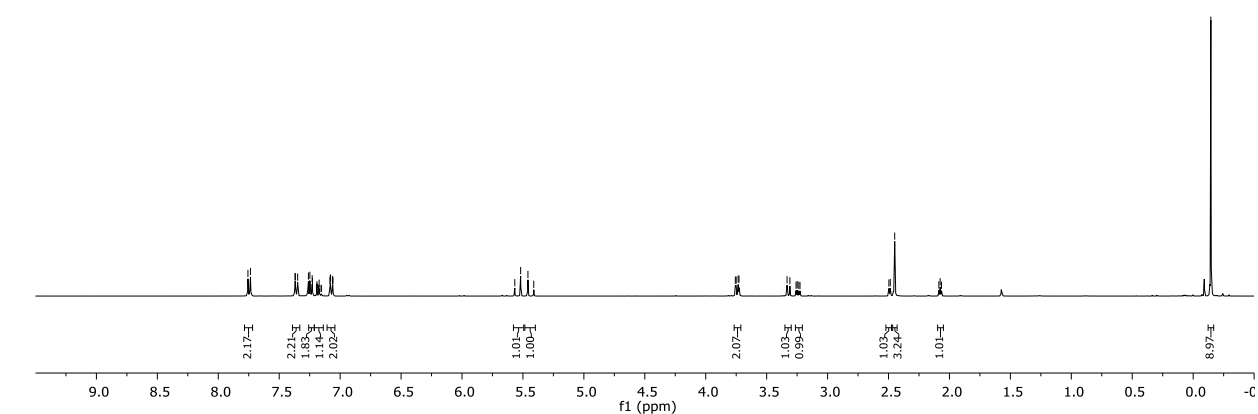
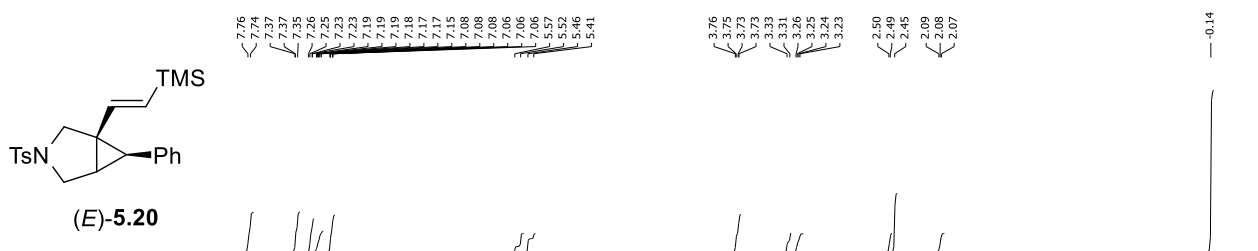


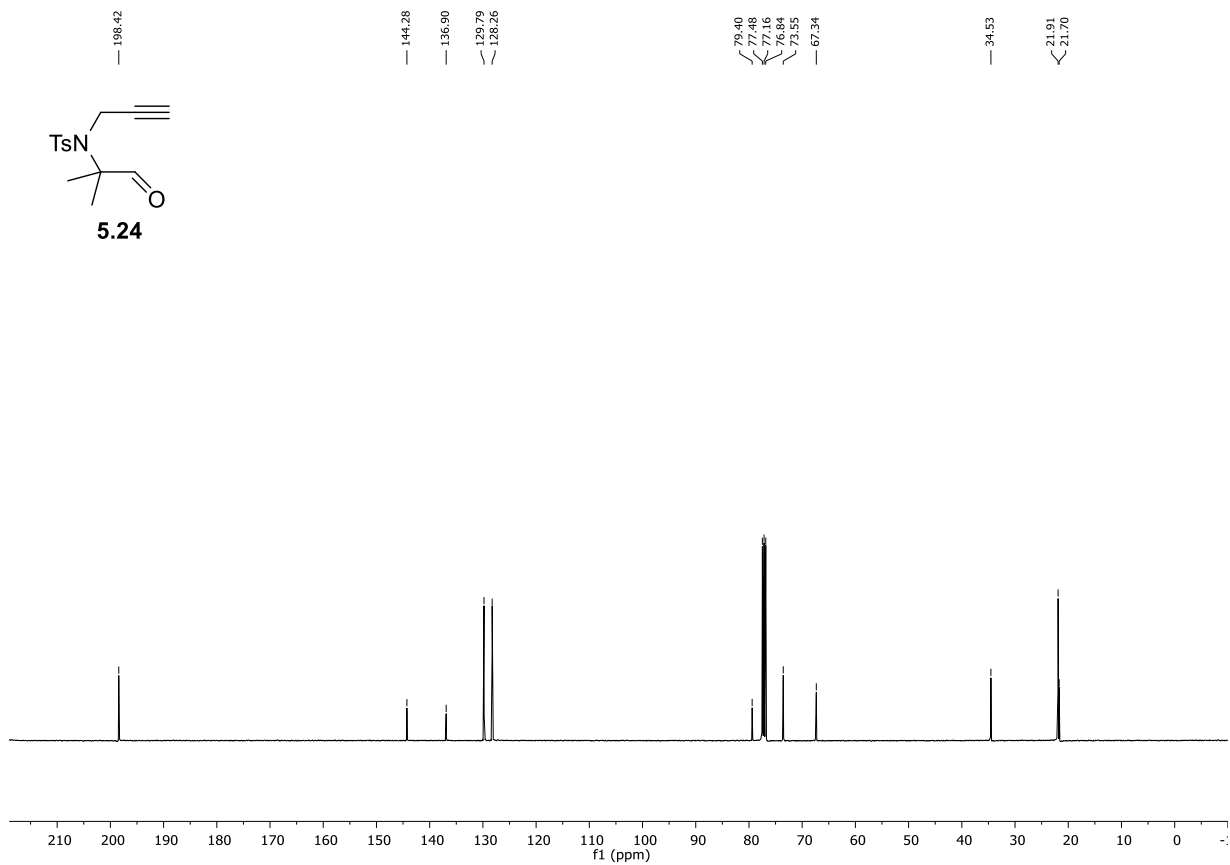
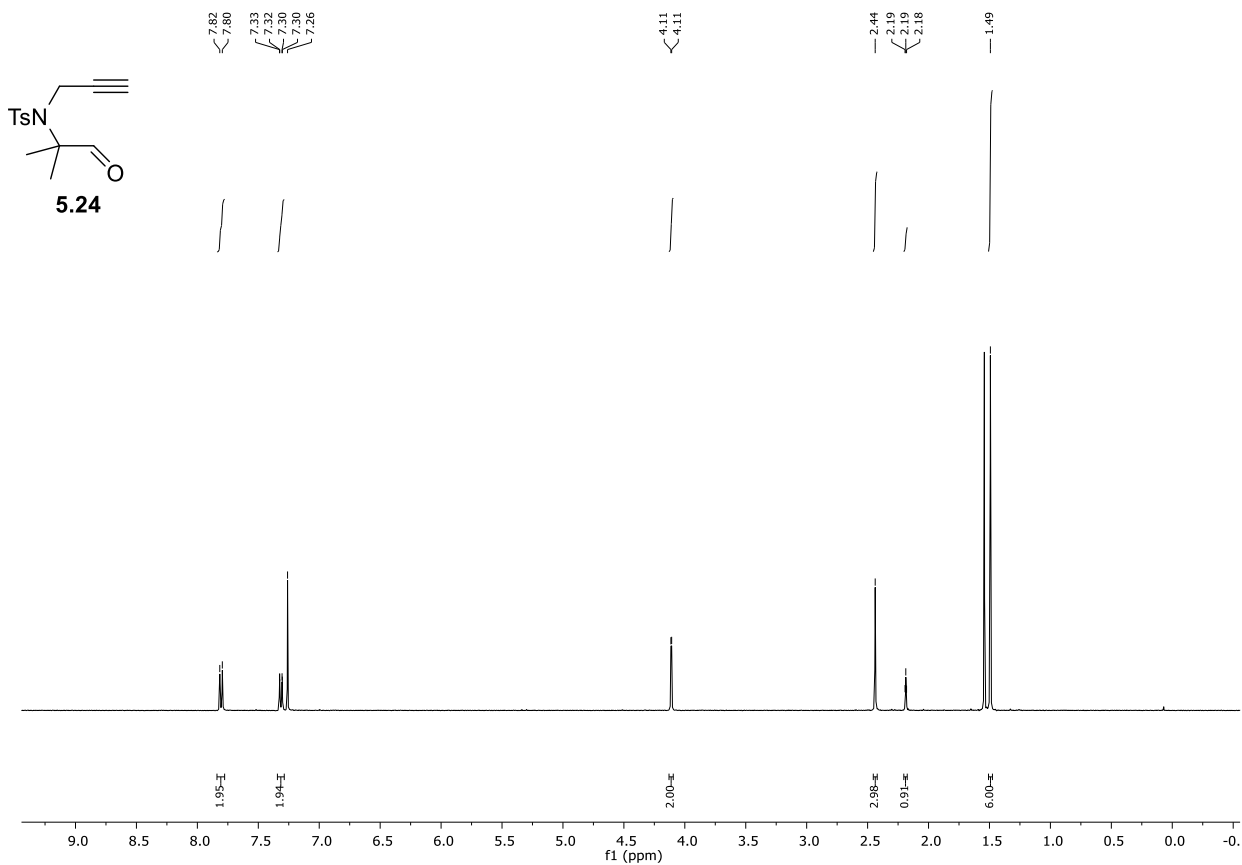


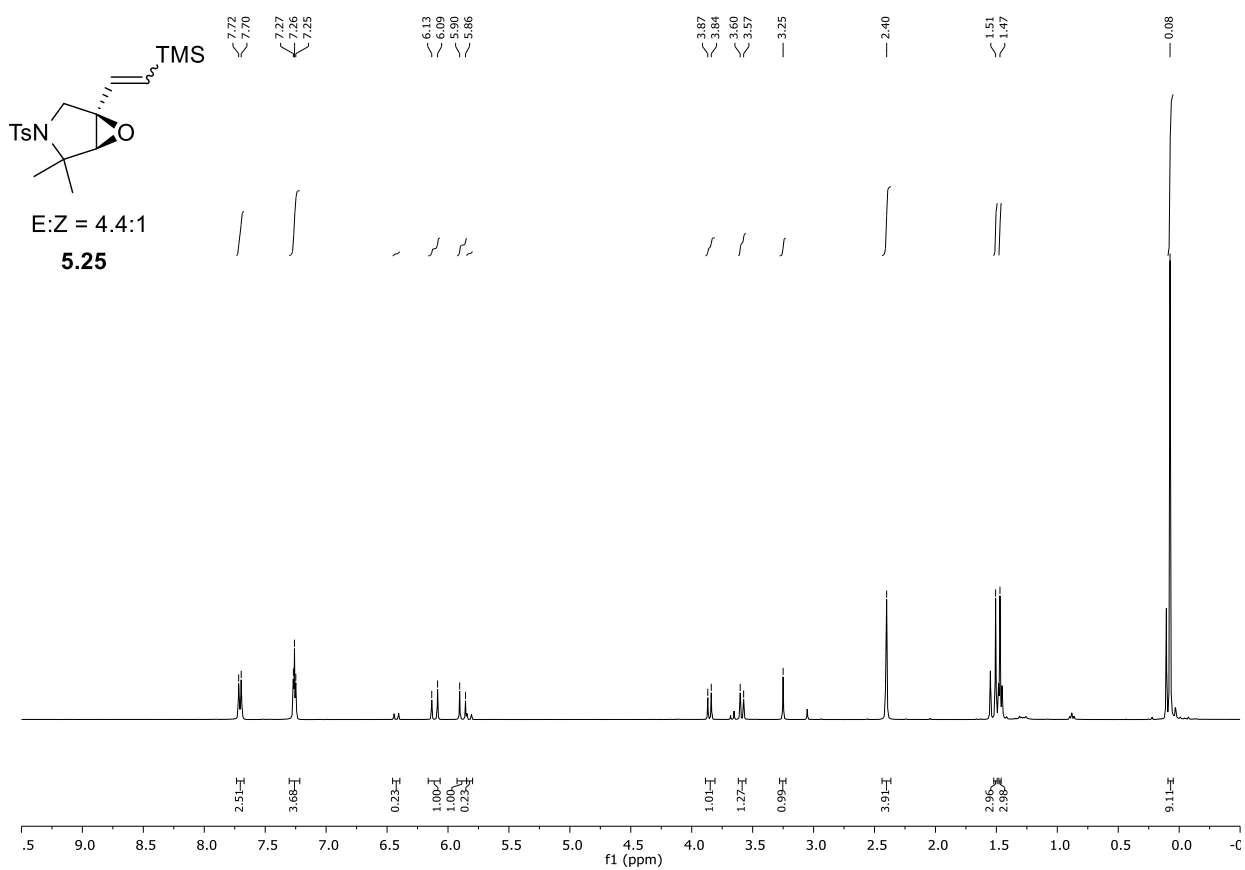
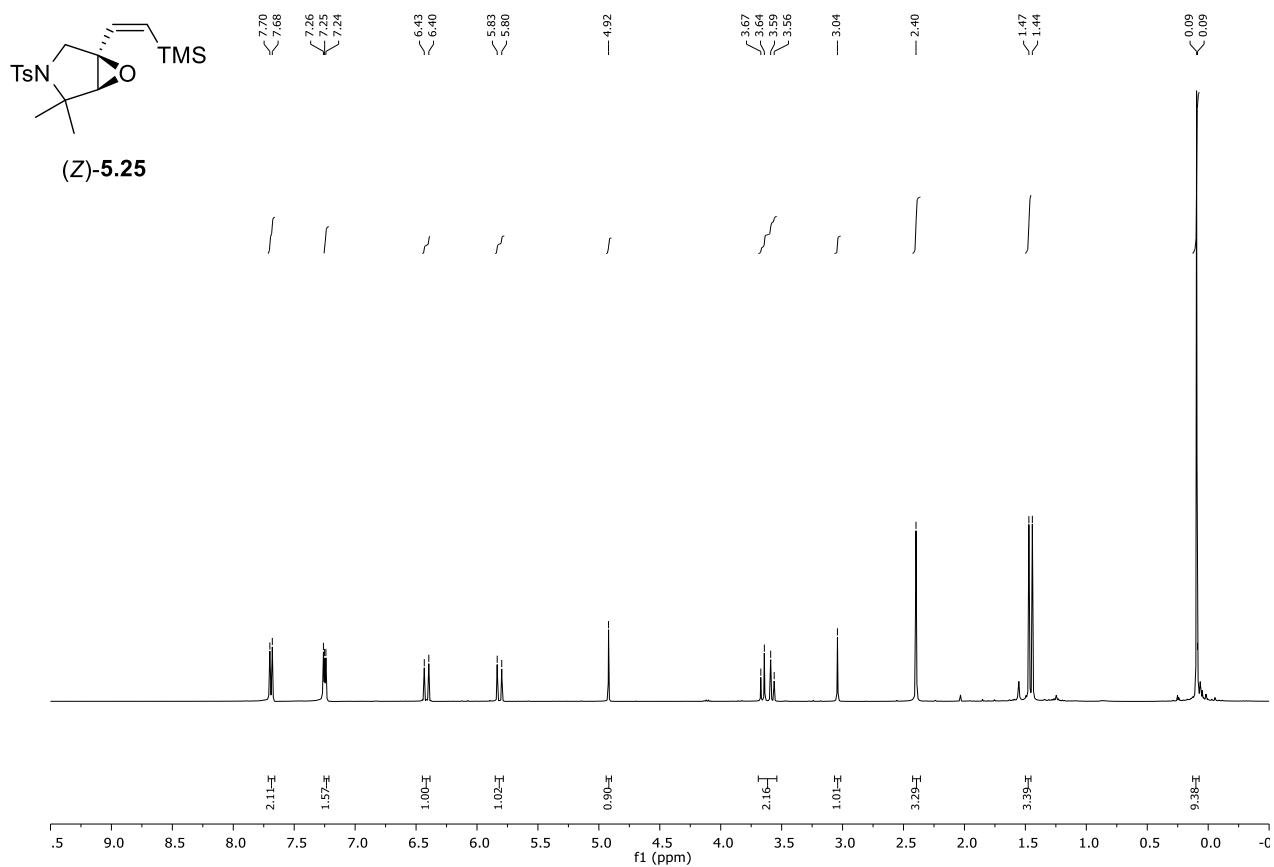


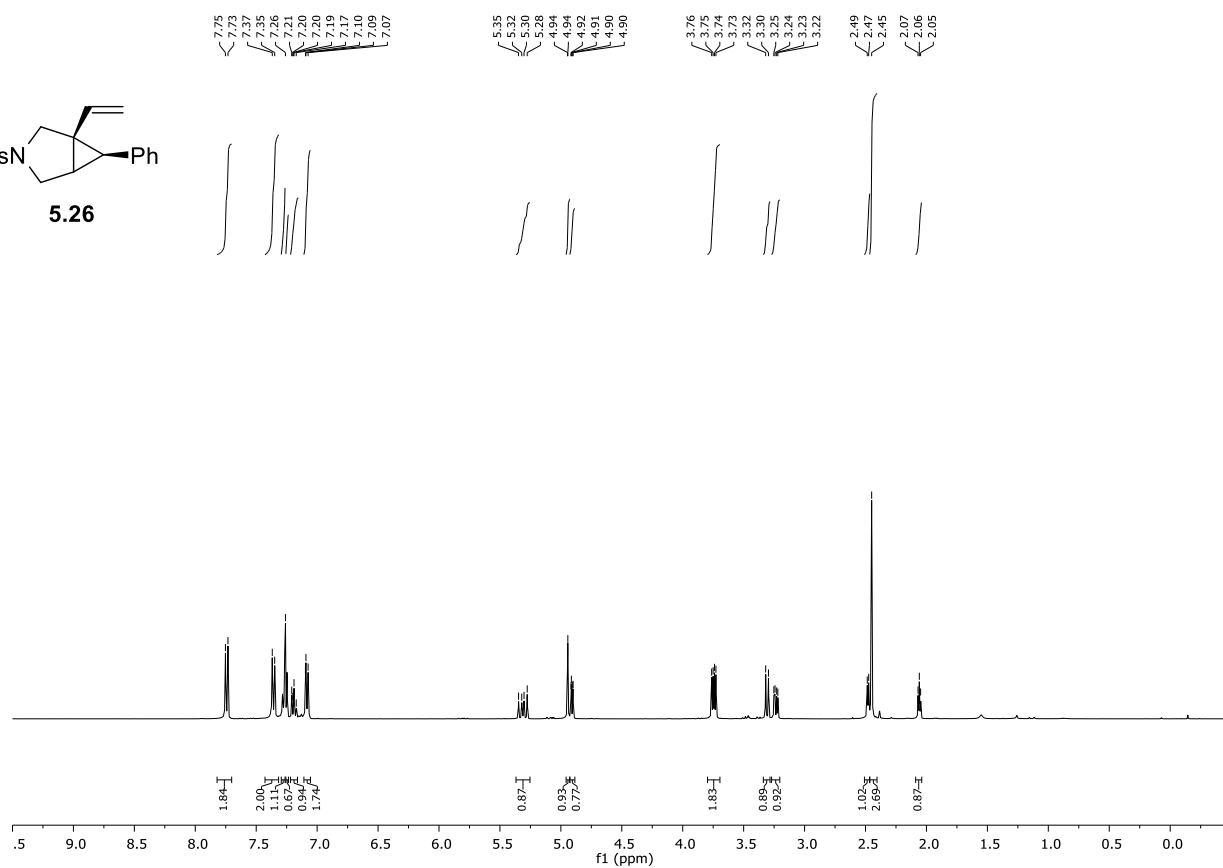
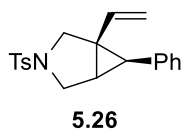
NMR spectra for Chapter 5











Chapter 10 Bibliography

-
- [1] Browne, W. R.; Holder, A. A.; Lawrence, M. A.; Bullock Jr, J. L.; Lilge, L., *Ruthenium Complexes: Photochemical and Biomedical Applications*. 1st ed.; Wiley-VCH Verlag GmbH & Co. KGaA: Weinheim, Germany, 2018.
- [2] Fischer-Gödde, M.; Becker, H.; Wombacher, F., *Chem. Geol.* **2011**, *280* (3), 365-383.
- [3] a) Ley, S. V.; Norman, J.; Wilson, A. J., Tetra-n-propylammonium Perruthenate. In *Encyclopedia of Reagents for Organic Synthesis*, American Cancer Society: 2011; b) Martín, V. S.; Palazón, J. M.; Rodríguez, C. M.; Nevill, C. R., Ruthenium(VIII) Oxide. In *Encyclopedia of Reagents for Organic Synthesis*, American Cancer Society: 2006.
- [4] Murahashi, S.-I., *Ruthenium in Organic Synthesis*. 1st ed.; Wiley-VCH: Weinheim, 2004.
- [5] a) Casey, C. P., *J. Chem. Educ.* **2006**, *83* (2), 192; b) Chauvin, Y., *Angew. Chem. Int. Ed.* **2006**, *45* (23), 3740-3747.
- [6] Novak, B. M.; Grubbs, R. H., *J. Am. Chem. Soc.* **1988**, *110* (22), 7542-7543.
- [7] Nguyen, S. T.; Johnson, L. K.; Grubbs, R. H.; Ziller, J. W., *J. Am. Chem. Soc.* **1992**, *114* (10), 3974-3975.
- [8] Schwab, P.; France, M. B.; Ziller, J. W.; Grubbs, R. H., *Angew. Chem. Int. Ed.* **1995**, *34* (18), 2039-2041.
- [9] Scholl, M.; Ding, S.; Lee, C. W.; Grubbs, R. H., *Org. Lett.* **1999**, *1* (6), 953-956.
- [10] Kingsbury, J. S.; Harrity, J. P. A.; Bonitatebus, P. J.; Hoveyda, A. H., *J. Am. Chem. Soc.* **1999**, *121* (4), 791-799.
- [11] Garber, S. B.; Kingsbury, J. S.; Gray, B. L.; Hoveyda, A. H., *J. Am. Chem. Soc.* **2000**, *122* (34), 8168-8179.
- [12] Bruneau, C.; Dixneuf, P. H., *Ruthenium in Catalysis*. 1st ed.; Springer: New York, 2014.
- [13] Endo, K.; Grubbs, R. H., *J. Am. Chem. Soc.* **2011**, *133* (22), 8525-8527.
- [14] a) Noyori, R., *Angew. Chem. Int. Ed.* **2013**, *52* (1), 79-92; b) Noyori, R.; Ohkuma, T., *Angew. Chem. Int. Ed.* **2001**, *34*.
- [15] Noyori, R.; Ohkuma, T.; Kitamura, M.; Takaya, H.; Sayo, N.; Kumobayashi, H.; Akutagawa, S., *J. Am. Chem. Soc.* **1987**, *109* (19), 5856-5858.
- [16] Ohkuma, T.; Ooka, H.; Hashiguchi, S.; Ikariya, T.; Noyori, R., *J. Am. Chem. Soc.* **1995**, *117* (9), 2675-2676.
- [17] Hashiguchi, S.; Fujii, A.; Takehara, J.; Ikariya, T.; Noyori, R., *J. Am. Chem. Soc.* **1995**, *117* (28), 7562-7563.
- [18] Arockiam, P. B.; Bruneau, C.; Dixneuf, P. H., *Chem. Rev.* **2012**, *112* (11), 5879-5918.
- [19] Murai, S.; Kakiuchi, F.; Sekine, S.; Tanaka, Y.; Kamatani, A.; Sonoda, M.; Chatani, N., *Nature* **1993**, *366* (6455), 529-531.
- [20] Oi, S.; Fukita, S.; Hirata, N.; Watanuki, N.; Miyano, S.; Inoue, Y., *Org. Lett.* **2001**, *3* (16), 2579-2581.
- [21] Simonetti, M.; Cannas, D. M.; Just-Baringo, X.; Vitorica-Yrezabal, I. J.; Larrosa, I., *Nature Chem.* **2018**, *10* (7), 724-731.
- [22] a) Bruin, M. E.; Kündig, E. P., *Chem. Commun.* **1998**, (23), 2635-2636; b) Carmona, D.; Cativiela, C.; García-Correas, R.; Lahoz, F. J.; Lamata, M. P.; López, J. A.; Víu, M. P. L.-R. D.; Oro, L. A.; José, E. S.; Viguri, F., *Chem. Commun.* **1996**, (10), 1247-1248.
- [23] Davies, D. L.; Fawcett, J.; Garratt, S. A.; Russell, D. R., *Chem. Commun.* **1997**, (15), 1351-1352.
- [24] Gunanathan, C.; Milstein, D., *Chem. Rev.* **2014**, *114* (24), 12024-12087.
- [25] Zhang, J.; Leitus, G.; Ben-David, Y.; Milstein, D., *J. Am. Chem. Soc.* **2005**, *127* (31), 10840-10841.
- [26] Nielsen, M.; Alberico, E.; Baumann, W.; Drexler, H.-J.; Junge, H.; Gladiali, S.; Beller, M., *Nature* **2013**, *495* (7439), 85-89.
- [27] a) Trost, B. M.; Frederiksen, M. U.; Rudd, M. T., *Angew. Chem. Int. Ed.* **2005**, *44* (41), 6630-6666; b) Trost, B. M., *Acc. Chem. Res.* **2002**, *35* (9), 695-705; c) Trost, B. M.; Toste, F. D.; Pinkerton, A. B., *Chem. Rev.* **2001**, *101* (7), 2067-2096.
- [28] Trost, B. M.; Toste, F. D., *J. Am. Chem. Soc.* **2002**, *124* (18), 5025-5036.
- [29] Trost, B. M.; Indolese, A., *J. Am. Chem. Soc.* **1993**, *115* (10), 4361-4362.
- [30] Trost, B. M.; Pinkerton, A. B., *J. Am. Chem. Soc.* **1999**, *121* (16), 4068-4069.

- [31] Le Paih, J.; Dérien, S.; Özdemir, I.; Dixneuf, P. H., *J. Am. Chem. Soc.* **2000**, 122 (30), 7400-7401.
- [32] Monnier, F.; Vovard-Le Bray, C.; Castillo, D.; Aubert, V.; Dérien, S.; Dixneuf, P. H.; Toupet, L.; Ienco, A.; Mealli, C., *J. Am. Chem. Soc.* **2007**, 129 (18), 6037-6049.
- [33] Yamamoto, Y., *Tetrahedron Lett.* **2017**, 58 (40), 3787-3794.
- [34] Yamamoto, Y.; Ogawa, R.; Itoh, K., *Chem. Commun.* **2000**, (7), 549-550.
- [35] a) Eckert, M.; Moulin, S.; Monnier, F.; Titanyuk, I. D.; Osipov, S. N.; Roisnel, T.; Dérien, S.; Dixneuf, P. H., *Chem. Eur. J.* **2011**, 17 (34), 9456-9462; b) Paih, J. L.; Bray, C. V.-L.; Dérien, S.; Dixneuf, P. H., *J. Am. Chem. Soc.* **2010**, 132 (21), 7391-7397; c) Vovard-Le Bray, C.; Dérien, S.; Dixneuf, P. H., *Angew. Chem. Int. Ed.* **2009**, 48 (8), 1439-1442.
- [36] Cambeiro, F.; López, S.; Varela, J. A.; Saá, C., *Angew. Chem. Int. Ed.* **2014**, 53 (23), 5959-5963.
- [37] Yamamoto, Y.; Nakagai, Y.-i.; Itoh, K., *Chem. Eur. J.* **2004**, 10 (1), 231-236.
- [38] Tam, W.; Cockburn, N., *Synlett* **2010**, 2010 (08), 1170-1189.
- [39] a) Roh, S. W.; Choi, K.; Lee, C., *Chem. Rev.* **2019**, 119 (6), 4293-4356; b) C. Bruneau, P. H. D., *Metal vinylidenes and allenylidenes in catalysis : from reactivity to applications in synthesis*. 1st ed.; Wiley-VCH: Weinheim, 2008; c) Bruneau, C.; Dixneuf, P. H., *Acc. Chem. Res.* **1999**, 32 (4), 311-323.
- [40] Crabtree, R. H., *The Organometallic Chemistry of the Transition Metals*. 4th ed.; John Wiley & Sons, Inc.: Hoboken, NJ, USA, 2005.
- [41] Hartwig, J., *Organotransition Metal Chemistry: from Bonding to Catalysis*. 1st ed.; 2010.
- [42] Schumann, H.; Meese-Marktscheffel, J. A.; Esser, L., *Chem. Rev.* **1995**, 95 (4), 865-986.
- [43] Kealy, T. J.; Pauson, P. L., *Nature* **1951**, 168 (4285), 1039-1040.
- [44] Miller, S. A.; Tebboth, J. A.; Tremaine, J. F., *J. Chem. Soc.* **1952**, (0), 632-635.
- [45] Wilkinson, G.; Rosenblum, M.; Whiting, M. C.; Woodward, R. B., *J. Am. Chem. Soc.* **1952**, 74 (8), 2125-2126.
- [46] Fischer, E. O.; Pfab, W., *Z. Naturforsch. B* **1952**, 7 (7), 377-379.
- [47] Woodward, R. B.; Rosenblum, M.; Whiting, M. C., *J. Am. Chem. Soc.* **1952**, 74 (13), 3458-3459.
- [48] Kaminsky, W.; Kopf, J.; Sinn, H.; Vollmer, H.-J., *Angew. Chem. Int. Ed.* **1976**, 15 (10), 629-630.
- [49] Jacobsen, E. N.; Pfaltz, A.; Yamamoto, H., *Comprehensive Asymmetric Catalysis*. 1st ed.; Springer-Verlag: Heidelberg, 1999.
- [50] Ye, B.; Cramer, N., *Acc. Chem. Res.* **2015**, 48 (5), 1308-1318.
- [51] Hafner, A.; Duthaler, R. O.; Marti, R.; Rihs, G.; Rothe-Streit, P.; Schwarzenbach, F., *J. Am. Chem. Soc.* **1992**, 114 (7), 2321-2336.
- [52] Murata, K.; Ikariya, T.; Noyori, R., *J. Org. Chem.* **1999**, 64 (7), 2186-2187.
- [53] Kündig, E. P.; Saudan, C. M.; Viton, F., *Adv. Synth. Catal.* **2001**, 343 (1), 51-56.
- [54] a) Matsushima, Y.; Onitsuka, K.; Kondo, T.; Mitsudo, T.-a.; Takahashi, S., *J. Am. Chem. Soc.* **2001**, 123 (42), 10405-10406; b) Dodo, N.; Matsushima, Y.; Uno, M.; Onitsuka, K.; Takahashi, S., *J. Chem. Soc., Dalton Trans.* **2000**, 0 (1), 35-41.
- [55] Trost, B. M.; Rao, M.; Dieskau, A. P., *J. Am. Chem. Soc.* **2013**, 135 (49), 18697-18704.
- [56] Newton, C. G.; Kossler, D.; Cramer, N., *J. Am. Chem. Soc.* **2016**, 138 (12), 3935-3941.
- [57] a) Cesarotti, E.; Ugo, R.; Kagan, H. B., *Angew. Chem. Int. Ed.* **1979**, 18 (10), 779-780; b) Cesarotti, E.; Kagan, H. B.; Goddard, R.; Krüger, C., *J. Organomet. Chem.* **1978**, 162 (3), 297-309.
- [58] a) Halterman, R. L.; Vollhardt, K. P. C., *Organometallics* **1988**, 7 (4), 883-892; b) Halterman, R. L.; Vollhardt, K. P. C., *Tetrahedron Lett.* **1986**, 27 (13), 1461-1464.
- [59] Erker, G.; Aulbach, M.; Knickmeier, M.; Wingbermuehle, D.; Krueger, C.; Nolte, M.; Werner, S., *J. Am. Chem. Soc.* **1993**, 115 (11), 4590-4601.
- [60] a) Gutnov, A.; Drexler, H.-J.; Spannenberg, A.; Oehme, G.; Heller, B., *Organometallics* **2004**, 23 (5), 1002-1009; b) Gutnov, A.; Heller, B.; Fischer, C.; Drexler, H.-J.; Spannenberg, A.; Sundermann, B.; Sundermann, C., *Angew. Chem. Int. Ed.* **2004**, 43 (29), 3795-3797.
- [61] Ye, B.; Cramer, N., *Science* **2012**, 338 (6106), 504.
- [62] Ye, B.; Cramer, N., *J. Am. Chem. Soc.* **2013**, 135 (2), 636-639.

- [63] Ooi, T.; Kameda, M.; Maruoka, K., *J. Am. Chem. Soc.* **2003**, 125 (17), 5139-5151.
- [64] Dieckmann, M.; Jang, Y.-S.; Cramer, N., *Angew. Chem. Int. Ed.* **2015**, 54 (41), 12149-12152.
- [65] a) Kossler, D.; Cramer, N., *Chem. Sci.* **2017**, 8 (3), 1862-1866; b) Kossler, D.; Perrin, F. G.; Suleymanov, A. A.; Kiefer, G.; Scopelliti, R.; Severin, K.; Cramer, N., *Angew. Chem. Int. Ed.* **2017**, 56 (38), 11490-11493; c) Kossler, D.; Cramer, N., *J. Am. Chem. Soc.* **2015**, 137 (39), 12478-12481.
- [66] Ozols, K.; Jang, Y.-S.; Cramer, N., *J. Am. Chem. Soc.* **2019**, 141 (14), 5675-5680.
- [67] a) Teng, H.-L.; Luo, Y.; Nishiura, M.; Hou, Z., *J. Am. Chem. Soc.* **2017**, 139 (46), 16506-16509; b) Teng, H.-L.; Luo, Y.; Wang, B.; Zhang, L.; Nishiura, M.; Hou, Z., *Angew. Chem. Int. Ed.* **2016**, 55 (49), 15406-15410; c) Song, G.; O, W. W. N.; Hou, Z., *J. Am. Chem. Soc.* **2014**, 136 (35), 12209-12212.
- [68] Duchemin, C.; Smits, G.; Cramer, N., *Organometallics* **2019**, 38 (20), 3939-3947.
- [69] Smits, G.; Audic, B.; Wodrich, M. D.; Corminboeuf, C.; Cramer, N., *Chem. Sci.* **2017**, 8 (10), 7174-7179.
- [70] Sun, Y.; Cramer, N., *Chem. Sci.* **2018**, 9 (11), 2981-2985.
- [71] Audic, B.; Wodrich, M. D.; Cramer, N., *Chem. Sci.* **2019**, 10 (3), 781-787.
- [72] Zheng, J.; Cui, W.-J.; Zheng, C.; You, S.-L., *J. Am. Chem. Soc.* **2016**, 138 (16), 5242-5245.
- [73] Xie, J.-H.; Wang, L.-X.; Fu, Y.; Zhu, S.-F.; Fan, B.-M.; Duan, H.-F.; Zhou, Q.-L., *J. Am. Chem. Soc.* **2003**, 125 (15), 4404-4405.
- [74] Jia, Z.-J.; Merten, C.; Gontla, R.; Daniliuc, C. G.; Antonchick, A. P.; Waldmann, H., *Angew. Chem. Int. Ed.* **2017**, 56 (9), 2429-2434.
- [75] Potowski, M.; Bauer, J. O.; Strohmman, C.; Antonchick, A. P.; Waldmann, H., *Angew. Chem. Int. Ed.* **2012**, 51 (38), 9512-9516.
- [76] Trifonova, E. A.; Ankudinov, N. M.; Mikhaylov, A. A.; Chusov, D. A.; Nelyubina, Y. V.; Perekalin, D. S., *Angew. Chem. Int. Ed.* **2018**, 57 (26), 7714-7718.
- [77] Hyster, T. K.; Knorr, L.; Ward, T. R.; Rovis, T., *Science* **2012**, 338 (6106), 500-503.
- [78] Kündig, E. P.; Saudan, C. M.; Bernardinelli, G., *Angew. Chem. Int. Ed.* **1999**, 38 (9), 1219-1223.
- [79] Mbaye, M. D.; Renaud, J.-L.; Demerseman, B.; Bruneau, C., *Chem. Commun.* **2004**, (16), 1870-1871.
- [80] Ghosh, A. K.; Mathivanan, P.; Cappiello, J., *Tetrahedron: Asymmetry* **1998**, 9 (1), 1-45.
- [81] Gotoh, H.; Masui, R.; Ogino, H.; Shoji, M.; Hayashi, Y., *Angew. Chem. Int. Ed.* **2006**, 45 (41), 6853-6856.
- [82] Gill, T. P.; Mann, K. R., *Organometallics* **1982**, 1 (3), 485-488.
- [83] Rüba, E.; Simanko, W.; Mauthner, K.; Soldouzi, K. M.; Slugovc, C.; Mereiter, K.; Schmid, R.; Kirchner, K., *Organometallics* **1999**, 18 (19), 3843-3850.
- [84] Perekalin, D. S.; Karslyan, E. E.; Trifonova, E. A.; Konovalov, A. I.; Loskutova, N. L.; Nelyubina, Y. V.; Kudinov, A. R., *Eur. J. Inorg. Chem.* **2013**, 2013 (4), 481-493.
- [85] a) Le Bideau, F.; Kousara, M.; Chen, L.; Wei, L.; Dumas, F., *Chem. Rev.* **2017**, 117 (9), 6110-6159; b) Rodriguez-Hahn, L.; Esquivel, B.; Sanchez, A. A.; Cardenas, J.; Tovar, O. G.; Soriano-Garcia, M.; Toscano, A., *J. Org. Chem.* **1988**, 53 (17), 3933-3936.
- [86] Hanessian, S.; Schutze, G., *J. Med. Chem.* **1969**, 12 (3), 529-531.
- [87] Layton, M. E.; Pero, J. E.; Fiji, H.; Kelly, M. J., III; De Leon, P.; Rossi, M. A.; Gilbert, K. F.; Roecker, A. J.; Zhao, Z.; Mercer, S. P.; Wolkenberg, S.; Mulhearn, J.; Zhao, L.; Li, D. WO2013/063459, 2013.
- [88] Inaba, T.; Haas, J.; Shiozaki, M.; Littman, N. M.; Yasue, K.; Andrews, S. W.; Sakai, A.; Fryer, A. M.; Matsuo, T.; Laird, E. R.; Suma, A.; Shinozaki, Y.; Hori, Y.; Imai, H.; Negoro, T. WO2005/058884, 2005.
- [89] Marcoux, D.; Bertrand, M. B.; Dhar, T. G. M.; Yang, M. G.; Xiao, Z.; Xiao, H.-Y.; Zhu, Y.; Weigelt, C. A.; Batt, D. G. US 2018/0127368, 2018.
- [90] Mitrenga, M.; Hartmann, R., *Eur. J. Med. Chem.* **1995**, 30 (3), 241-244.
- [91] a) Al-Huniti, M. H.; Sullivan, Z. B.; Stanley, J. L.; Carson, J. A.; Hyatt, I. F. D.; Hairston, A. C.; Croatt, M. P., *J. Org. Chem.* **2017**, 82 (22), 11772-11780; b) Komine, N.; Flores, J. A.; Pal, K.; Caulton, K. G.; Mindiola, D. J., *Organometallics* **2013**, 32 (11), 3185-3191; c) Pérez, P. J.; Díaz-Requejo, M. M.; Rivilla, I., *Beilstein J. Org. Chem.* **2011**, 7, 653-657; d) Barluenga, J.; Andina, F.; Aznar, F.; Valdés, C., *Org. Lett.* **2007**, 9 (21), 4143-4146; e) Müller, P.; Toujas, J.-L.; Bernardinelli,

- G., *Helv. Chim. Acta* **2000**, 83, 1525-1534; f) Anciaux, A. J.; Demonceau, A.; Hubert, A. J.; Noels, A. F.; Petiniot, N.; Teyssié, P., *J. Chem. Soc., Chem. Commun.* **1980**, (16), 765-766; g) Buchner, E.; Hediger, S., *Chem. Ber.* **1903**, 36 (3), 3502-3509.
- [92] a) Saitoh, H.; Ijuin, H. K.; Watanabe, N.; Matsumoto, M., *Helv. Chim. Acta* **2013**, 96 (9), 1704-1713; b) Wijsman, G. W.; van der Veen, L. A.; de Wolf, W. H.; Bickelhaupt, F., *J. Chem. Soc., Perkin Trans. 2* **1997**, (10), 2095-2098; c) Popovici-Müller, J. V.; Spencer, T. A., *Tetrahedron Lett.* **1997**, 38 (47), 8161-8164; d) Adam, W.; Ahrweiler, M.; Balci, M.; Çakmak, O.; Saha-Möller, C. R., *Tetrahedron Lett.* **1995**, 36 (9), 1429-1430.
- [93] a) Kessler, S. N.; Neuburger, M.; Wegner, H. A., *J. Am. Chem. Soc.* **2012**, 134 (43), 17885-17888; b) Kusama, H.; Shiozawa, F.; Shido, M.; Iwasawa, N., *Chem. Lett.* **2002**, 31 (2), 124-125.
- [94] a) Gorin, D. J.; Dubé, P.; Toste, F. D., *J. Am. Chem. Soc.* **2006**, 128 (45), 14480-14481; b) Herlé, B.; Holstein, P. M.; Echavarren, A. M., *ACS Catal.* **2017**, 7 (5), 3668-3675; c) de Orbe, M. E.; Amenós, L.; Kirillova, M. S.; Wang, Y.; López-Carrillo, V.; Maseras, F.; Echavarren, A. M., *J. Am. Chem. Soc.* **2017**, 139 (30), 10302-10311; d) Mato, M.; Martín-Torres, I.; Herlé, B.; Echavarren, A. M., *Org. Biomol. Chem.* **2019**, 17 (17), 4216-4219.
- [95] Tenaglia, A.; Marc, S.; Giordano, L.; De Riggi, I., *Angew. Chem. Int. Ed.* **2011**, 50 (39), 9062-9065.
- [96] a) Crowley, D. C.; Lynch, D.; Maguire, A. R., *J. Org. Chem.* **2018**, 83 (7), 3794-3805; b) Slattery, C. N.; Clarke, L.-A.; O'Neill, S.; Ring, A.; Ford, A.; Maguire, A. R., *Synlett* **2012**, 23 (05), 765-767; c) O'Neill, S.; O'Keeffe, S.; Harrington, F.; Maguire, A. R., *Synlett* **2009**, 2009 (14), 2312-2314; d) O'Keeffe, S.; Harrington, F.; Maguire, A. R., *Synlett* **2007**, 2007 (15), 2367-2370; e) Kennedy, M.; McKervey, M. A.; Maguire, A. R.; Roos, G. H. P., *J. Chem. Soc., Chem. Commun.* **1990**, (5), 361-362.
- [97] Fleming, G. S.; Beeler, A. B., *Org. Lett.* **2017**, 19 (19), 5268-5271.
- [98] a) Doyle, M. P.; Ene, D. G.; Forbes, D. C.; Pillow, T. H., *Chem. Commun.* **1999**, (17), 1691-1692; b) Chen, T.; Gan, L.; Wang, R.; Deng, Y.; Peng, F.; Lautens, M.; Shao, Z., *Angew. Chem. Int. Ed.* **2019**, 58 (44), 15819-15823.
- [99] a) Rummelt, S. M.; Radkowski, K.; Roşca, D.-A.; Fürstner, A., *J. Am. Chem. Soc.* **2015**, 137 (16), 5506-5519; b) Roşca, D.-A.; Radkowski, K.; Wolf, L. M.; Wagh, M.; Goddard, R.; Thiel, W.; Fürstner, A., *J. Am. Chem. Soc.* **2017**, 139 (6), 2443-2455.
- [100] a) Kamer, K. J.; Choudhary, A.; Raines, R. T., *J. Org. Chem.* **2013**, 78 (5), 2099-2103; b) Newberry, R. W.; Raines, R. T., *Acc. Chem. Res.* **2017**, 50 (8), 1838-1846.
- [101] Crystallographic data: CCDC 1947117 contains the supplementary crystallographic data for this paper. These data can be obtained free of charge from The Cambridge Crystallographic Data Centre via www.ccdc.cam.ac.uk/data_request/cif.
- [102] Villeneuve, K.; Tam, W., *J. Am. Chem. Soc.* **2006**, 128 (11), 3514-3515.
- [103] a) Becke, A. D., *Phys. Rev. A* **1988**, 38 (6), 3098-3100; b) Lee, C.; Yang, W.; Parr, R. G., *Phys. Rev. B* **1988**, 37 (2), 785-789; c) Stephens, P. J.; Devlin, F. J.; Chabalowski, C. F.; Frisch, M. J., *J. Phys. Chem.* **1994**, 98 (45), 11623-11627; d) Hertwig, R. H.; Koch, W., *Chem. Phys. Lett.* **1997**, 268 (5), 345-351.
- [104] a) Ditchfield, R.; Hehre, W. J.; Pople, J. A., *J. Chem. Phys.* **1971**, 54 (2), 724-728; b) Hehre, W. J.; Ditchfield, R.; Pople, J. A., *J. Chem. Phys.* **1972**, 56 (5), 2257-2261; c) Hariharan, P. C.; Pople, J. A., *Theoret. Chim. Acta* **1973**, 28 (3), 213-222.
- [105] Merrick, J. P.; Moran, D.; Radom, L., *J. Phys. Chem. A* **2007**, 111 (45), 11683-11700.
- [106] a) Funk, R. L.; Stallman, J. B.; Wos, J. A., *J. Am. Chem. Soc.* **1993**, 115 (19), 8847-8848; b) Mahon, M. F.; Molloy, K.; Pittol, C. A.; Pryce, R. J.; Roberts, S. M.; Ryback, G.; Sik, V.; Williams, J. O.; Winders, J. A., *J. Chem. Soc., Perkin Trans. 1* **1991**, (5), 1255-1263; c) Funk, R. L.; Abelman, M. M.; Munger, J. D., *Tetrahedron* **1986**, 42 (11), 2831-2846; d) Funk, R. L.; Munger, J. D., *J. Org. Chem.* **1985**, 50 (5), 707-709; e) Abelman, M. M.; Funk, R. L.; Munger, J. D., *J. Am. Chem. Soc.* **1982**, 104 (14), 4030-4032.
- [107] Schmidt, M. W.; Baldrige, K. K.; Boatz, J. A.; Elbert, S. T.; Gordon, M. S.; Jensen, J. H.; Koseki, S.; Matsunaga, N.; Nguyen, K. A.; Su, S.; Windus, T. L.; Dupuis, M.; Montgomery, J. A., *J. Comput. Chem.* **1993**, 14 (11), 1347-1363.
- [108] Schneider, T. F.; Werz, D. B., *Org. Lett.* **2011**, 13 (7), 1848-1851.

-
- [109] Marshall, J. A.; Chobanian, H. R., *Org. Lett.* **2003**, 5 (11), 1931-1933.
- [110] Nakajima, H.; Sato, B.; Fujita, T.; Takase, S.; Terano, H.; Okuhara, M., *J. Antibiot.* **1996**, 49 (12), 1196-1203.
- [111] Fujimoto, H.; Nozawa, M.; Okuyama, E.; Ishibashi, M., *Chem. Pharm. Bull.* **2002**, 50 (3), 330-336.
- [112] Sperry, J.; Wilson, Z. E.; Rathwell, D. C. K.; Brimble, M. A., *Nat. Prod. Rep.* **2010**, 27 (8), 1117-1137.
- [113] Trost, B. M.; Pinkerton, A. B., *J. Am. Chem. Soc.* **1999**, 121 (46), 10842-10843.
- [114] a) Krossing, I.; Raabe, I., *Angew. Chem. Int. Ed.* **2004**, 43 (16), 2066-2090; b) Beck, W.; Suenkel, K., *Chem. Rev.* **1988**, 88 (7), 1405-1421.
- [115] Brookhart, M.; Grant, B.; Volpe, A. F., *Organometallics* **1992**, 11 (11), 3920-3922.
- [116] a) Skolnick, P.; Popik, P.; Janowsky, A.; Beer, B.; Lippa, A. S., *Eur. J. Pharmacol.* **2003**, 461 (2), 99-104; b) Xu, F.; Murry, J. A.; Simmons, B.; Corley, E.; Fitch, K.; Karady, S.; Tschaen, D., *Org. Lett.* **2006**, 8 (17), 3885-3888.
- [117] Norris, T.; Braish, T. F.; Butters, M.; DeVries, K. M.; Hawkins, J. M.; Massett, S. S.; Rose, P. R.; Santafianos, D.; Sklavounos, C., *J. Chem. Soc., Perkin Trans. 1* **2000**, (10), 1615-1622.
- [118] Kakeya, H.; Onozawa, C.; Sato, M.; Arai, K.; Osada, H., *J. Med. Chem.* **1997**, 40 (4), 391-394.
- [119] Nicolaou, K. C.; Sun, Y.-P.; Sarlah, D.; Zhan, W.; Wu, T. R., *Org. Lett.* **2011**, 13 (20), 5708-5710.
- [120] a) Eckert, M.; Monnier, F.; Shchetnikov, G. T.; Titanyuk, I. D.; Osipov, S. N.; Toupet, L.; Dérien, S.; Dixneuf, P. H., *Org. Lett.* **2005**, 7 (17), 3741-3743; b) Monnier, F.; Castillo, D.; Dérien, S.; Toupet, L.; Dixneuf, P. H., *Angew. Chem. Int. Ed.* **2003**, 42 (44), 5474-5477.
- [121] Padín, D.; Cambeiro, F.; Fañanás-Mastral, M.; Varela, J. A.; Saá, C., *ACS Catal.* **2017**, 7 (2), 992-996.
- [122] Gotoh, H.; Ogino, H.; Ishikawa, H.; Hayashi, Y., *Tetrahedron* **2010**, 66 (26), 4894-4899.
- [123] Lautens, M.; Fagnou, K.; Yang, D., *J. Am. Chem. Soc.* **2003**, 125 (48), 14884-14892.
- [124] Wang, S.-G.; Park, S. H.; Cramer, N., *Angew. Chem. Int. Ed.* **2018**, 57 (19), 5459-5462.
- [125] Gandeepan, P.; Rajamalli, P.; Cheng, C.-H., *Angew. Chem. Int. Ed.* **2016**, 55 (13), 4308-4311.
- [126] Kirschner, S.; Mewes, J.-M.; Bolte, M.; Lerner, H.-W.; Dreuw, A.; Wagner, M., *Chem. Eur. J.* **2017**, 23 (21), 5104-5116.
- [127] Liu, R.; Giordano, L.; Tenaglia, A., *Chem. Asian J.* **2017**, 12 (17), 2245-2257.
- [128] Horino, Y.; Kimura, M.; Tanaka, S.; Okajima, T.; Tamaru, Y., *Chem. Eur. J.* **2003**, 9 (11), 2419-2438.
- [129] Ye, F.; Haddad, M.; Ratovelomanana-Vidal, V.; Michelet, V., *Catal. Commun.* **2018**, 107, 78-81.
- [130] Yang, C.; Xu, Z.-L.; Shao, H.; Mou, X.-Q.; Wang, J.; Wang, S.-H., *Org. Lett.* **2015**, 17 (21), 5288-5291.
- [131] Wender, P. A.; Deschamps, N. M.; Williams, T. J., *Angew. Chem. Int. Ed.* **2004**, 43 (23), 3076-3079.
- [132] Zhao, T. S. N.; Yang, Y.; Lessing, T.; Szabó, K. J., *J. Am. Chem. Soc.* **2014**, 136 (21), 7563-7566.
- [133] Higashino, M.; Ikeda, N.; Shinada, T.; Sakaguchi, K.; Ohfuné, Y., *Tetrahedron Lett.* **2011**, 52 (3), 422-425.
- [134] Weinstabl, H.; Gaich, T.; Mulzer, J., *Org. Lett.* **2012**, 14 (11), 2834-2837.
- [135] Kuang, J.; Ma, S., *J. Org. Chem.* **2009**, 74 (4), 1763-1765.
- [136] Böhmer, J.; Grigg, R.; Marchbank, J. D., *Chem. Commun.* **2002**, (7), 768-769.